



INTERNATIONAL REVIEW OF CYTOLOGY

A SURVEY OF CELL BIOLOGY

Edited by
Kwang W. Jeon



Volume 243

International Review of

Cytology

A Survey of

Cell Biology

VOLUME 243

SERIES EDITORS

Geoffrey H. Bourne	1949–1988
James F. Danielli	1949–1984
Kwang W. Jeon	1967–
Martin Friedlander	1984–1992
Jonathan Jarvik	1993–1995

EDITORIAL ADVISORY BOARD

Eve Ida Barak	Bruce D. McKee
Peter L. Beech	M. Melkonian
Howard A. Bern	Keith E. Mostov
Dean Bok	Andreas Oksche
William C. Earnshaw	Vladimir R. Pantić
Hiroo Fukuda	Manfred Schliwa
Ray H. Gavin	Teruo Shimmen
Siamon Gordon	Robert A. Smith
Elizabeth D. Hay	Wildred D. Stein
William R. Jeffery	Ralph M. Steinman
Keith Latham	N. Tomilin

International Review of

Cytology

A Survey of

Cell Biology

Edited by

Kwang W. Jeon

Department of Biochemistry
University of Tennessee
Knoxville, Tennessee

VOLUME 243



ELSEVIER
ACADEMIC
PRESS

AMSTERDAM • BOSTON • HEIDELBERG • LONDON
NEW YORK • OXFORD • PARIS • SAN DIEGO
SAN FRANCISCO • SINGAPORE • SYDNEY • TOKYO

Front Cover Photograph: Courtesy of Anthony D. Person,
Scott E. Klewer, and Raymond B. Runyan, University of Arizona.

Elsevier Academic Press
525 B Street, Suite 1900, San Diego, California 92101-4495, USA
84 Theobald's Road, London WC1X 8RR, UK

This book is printed on acid-free paper. 

Copyright © 2005, Elsevier Inc. All Rights Reserved.

No part of this publication may be reproduced or transmitted in any form or by any means, electronic or mechanical, including photocopy, recording, or any information storage and retrieval system, without permission in writing from the Publisher.

The appearance of the code at the bottom of the first page of a chapter in this book indicates the Publisher's consent that copies of the chapter may be made for personal or internal use of specific clients. This consent is given on the condition, however, that the copier pay the stated per copy fee through the Copyright Clearance Center, Inc. (www.copyright.com), for copying beyond that permitted by Sections 107 or 108 of the U.S. Copyright Law. This consent does not extend to other kinds of copying, such as copying for general distribution, for advertising or promotional purposes, for creating new collective works, or for resale. Copy fees for pre-2005 chapters are as shown on the title pages. If no fee code appears on the title page, the copy fee is the same as for current chapters. 0074-7696/2005 \$35.00

Permissions may be sought directly from Elsevier's Science & Technology Rights Department in Oxford, UK: phone: (+44) 1865 843830, fax: (+44) 1865 853333, E-mail: permissions@elsevier.com. You may also complete your request on-line via the Elsevier homepage (<http://elsevier.com>), by selecting "Customer Support" and then "Obtaining Permissions."

For all information on all Academic Press publications
visit our Web site at www.books.elsevier.com

ISBN: 0-12-364647-2

PRINTED IN THE UNITED STATES OF AMERICA

05 06 07 08 9 8 7 6 5 4 3 2 1

Working together to grow
libraries in developing countries

www.elsevier.com | www.bookaid.org | www.sabre.org

ELSEVIER

BOOK AID
International

Sabre Foundation

CONTENTS

Contributors	ix
--------------------	----

Keratins of the Human Hair Follicle

Lutz Langbein and Jürgen Schweizer

I. Introduction	1
II. Human Hair Keratin Family.....	4
III. Hair Keratins and Hair Follicle Pathologies.....	18
IV. Regulation of Hair Keratin Expression	26
V. Epithelial Keratins of the Hair Follicle	39
VI. Keratin Pathologies of the ORS, CL–IRS Unit, and Medulla	55
VII. Regulatory Processes in the CL–IRS Unit and Medulla	60
VIII. Concluding Remarks and Outlook	62
References	65

Calcium Channels and Ca²⁺ Fluctuations in Sperm Physiology

Alberto Darszon, Takuya Nishigaki, Chris Wood, Claudia L. Treviño,
Ricardo Felix, and Carmen Beltrán

I. Introduction	80
II. General Background	80
III. Calcium and Ca ²⁺ Channels	83

IV. Sperm Motility	109
V. Sperm Capacitation and the Acrosome Reaction	120
VI. Single-Cell Measurements in Sperm Physiology.....	137
VII. Concluding Remarks	141
References	142

Genomic Imprinting: *Cis*-Acting Sequences and Regional Control

Bonnie Reinhart and J. Richard Chaillet

I. Introduction.....	173
II. Genomic Imprinting and DNA Methylation.....	176
III. Regional Control at Imprinted Gene Clusters	185
IV. Concluding Remarks	206
References	207

Insulin-Like Growth Factor Signaling in Fish

Antony W. Wood, Cunming Duan, and Howard A. Bern

I. Introduction.....	215
II. General Background.....	216
III. IGFs of Fish.....	228
IV. IGF Receptors and IGF-Binding Proteins.....	244
V. Biological Actions of the IGF System in Fish.....	254
VI. Summary.....	263
References	266

Cell Biology of Cardiac Cushion Development

Anthony D. Person, Scott E. Klewer, and Raymond B. Runyan

I. Introduction.....	288
II. Cardiac Morphology and Cell Biology.....	288

CONTENTS	vii
III. Molecular Mechanisms of Cardiac EMT and Valve Morphogenesis	298
IV. Integration of Molecular Pathways Governing Cardiac EMT	322
V. The Future of Cardiac Cushion Development	323
References	324
Index	337

CONTRIBUTORS

Numbers in parentheses indicate the pages on which the authors' contributions begin.

Carmen Beltrán (79), *Department of Developmental Genetics and Molecular Physiology, Institute of Biotechnology, Universidad Nacional Autónoma de México, Cuernavaca, Morelos, Mexico 62210*

Howard A. Bern (215), *Department of Integrative Biology and Cancer Research Laboratory, University of California, Berkeley, California 94720*

J. Richard Chaillet (173), *Department of Molecular Genetics and Biochemistry, University of Pittsburgh, Pittsburgh, Pennsylvania 15208*

Alberto Darszon (79), *Department of Developmental Genetics and Molecular Physiology, Institute of Biotechnology, Universidad Nacional Autónoma de México, Cuernavaca, Morelos, Mexico 62210*

Cunming Duan (215), *Department of Molecular, Cellular, and Developmental Biology, University of Michigan—Ann Arbor, Ann Arbor, Michigan 48109*

Ricardo Felix (79), *Department of Physiology, Biophysics and Neurosciences, Center for Research and Advanced Studies of the National Polytechnic Institute, Mexico City, Mexico 07300*

Scott E. Klewer (287), *Department of Cell Biology and Anatomy, and Department of Pediatrics, University of Arizona School of Medicine, Tucson, Arizona 85724*

Lutz Langbein (1), *Division of Cell Biology, German Cancer Research Center, Heidelberg, Germany*

- Takuya Nishigaki (79), *Department of Developmental Genetics and Molecular Physiology, Institute of Biotechnology, Universidad Nacional Autónoma de México, Cuernavaca, Morelos, Mexico 62210*
- Anthony D. Person (287), *Department of Cell Biology and Anatomy, University of Arizona School of Medicine, Tucson, Arizona 85724*
- Bonnie Reinhart (173), *Department of Molecular Genetics and Biochemistry, University of Pittsburgh, Pittsburgh, Pennsylvania 15208*
- Raymond B. Runyan (287), *Department of Cell Biology and Anatomy, University of Arizona School of Medicine, Tucson, Arizona 85724*
- Jürgen Schweizer (1), *Section of Normal and Neoplastic Epidermal Differentiation, German Cancer Research Center, Heidelberg, Germany*
- Claudia L. Treviño (79), *Department of Developmental Genetics and Molecular Physiology, Institute of Biotechnology, Universidad Nacional Autónoma de México, Cuernavaca, Morelos, Mexico 62210*
- Antony W. Wood (215), *Department of Molecular, Cellular, and Developmental Biology, University of Michigan—Ann Arbor, Ann Arbor, Michigan 48109*
- Chris Wood (79), *Department of Developmental Genetics and Molecular Physiology, Institute of Biotechnology, Universidad Nacional Autónoma de México, Cuernavaca, Morelos, Mexico 62210*

Keratins of the Human Hair Follicle¹

Lutz Langbein* and Jürgen Schweizer†

*Division of Cell Biology, German Cancer Research Center, Heidelberg, Germany

†Section of Normal and Neoplastic Epidermal Differentiation, German Cancer Research Center, Heidelberg, Germany

Substantial progress has been made regarding the elucidation of differentiation processes of the human hair follicle. This review first describes the genomic organization of the human hair keratin gene family and the complex expression characteristics of hair keratins in the hair-forming compartment. Sections describe the role and fate of hair keratins in the diseased hair follicle, particularly hereditary disorders and hair follicle-derived tumors. Also included is a report on the actual state of knowledge concerning the regulation of hair keratin expression. In the second part of this review, essentially the same principles are applied to outline more recent and, thus, occasionally fewer data on specialized epithelial keratins expressed in various tissue constituents of the external sheaths and the companion layer of the follicle. A closing outlook highlights issues that need to be explored further to deepen our insight into the biology and genetics of the hair follicle.

KEY WORDS: Hair, Keratin, Gene expression, Gene regulation, Hair follicle disease. © 2005 Elsevier Inc.

I. Introduction

Hair is considered a specific acquisition of mammals that developed at the transition from the Triassic Period to the Jurassic Period about 200 million years ago. This great antiquity, together with the striking structural conservation of this anatomical hallmark through evolution, is attested to by a find

¹This article is dedicated with gratitude to Werner W. Franke on the occasion of his 65th birthday. His pioneering work on epithelial and hair keratins has been pivotal to our own investigations in this field.

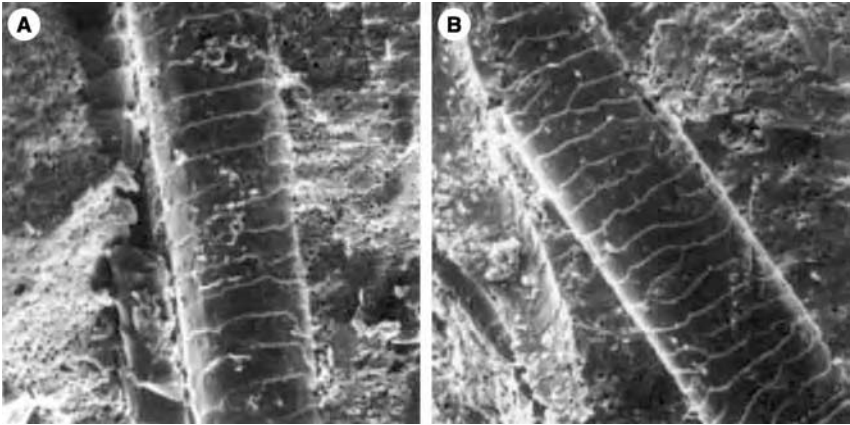


FIG. 1 Scanning electron micrographs of fossilized hairs. The hairs in (A) and (B) originate from ~55-million-year-old late Paleocene mammals and were found in fossil excrements. Note the remarkably well-preserved structure of the hair cuticle. (Reprinted with permission from Meng and Wyss, 1997.)

of ~55-million-year-old fossilized hairs: the surface texture was not only indistinguishable from that of hairs of extant mammals, but the fine structure of the hair cuticle also allowed assignment of the hairs to distinct taxa (Fig. 1) (Meng and Wyss, 1997). Hair is produced in the hair follicle, the major adnexal organ of mammalian skin. The mature hair is the differentiation product of a special type of epithelial cell, called the trichocyte, which assembles with other trichocytes to form the central core of the follicle. This core of living trichocytes, which in this review is designated the “hair-forming compartment” of the follicle (Fig. 2A, B), arises from a germinative matrix, which consists of a population of stem cells and transiently dividing cells located around the opening of the dermal papilla at the base of the hair bulb. The cuboidal matrix cells differentiate into the hair cortex and a central medulla, which, in humans, is not found in all body hairs. Whereas cortical trichocytes become laterally compressed, thereby adopting a spindle-shaped form and a vertical orientation, medullary trichocytes are arranged horizontally and tend to separate from each other, thus creating air-filled insulating spaces.

Both the hair matrix and cortex are concentrically surrounded by a one-layered structure of trichocytes, the hair cuticle, which represents the external protecting coat of the hair. The principle of a concentric architecture is then continued outwardly by the successive addition of further tissue layers, built up by specialized keratinocytes. Adjacent to the hair cuticle is the inner root sheath (IRS), which consists of three independent tissue layers—the IRS cuticle, the Huxley layer, and the Henle layer—the latter being apposed to

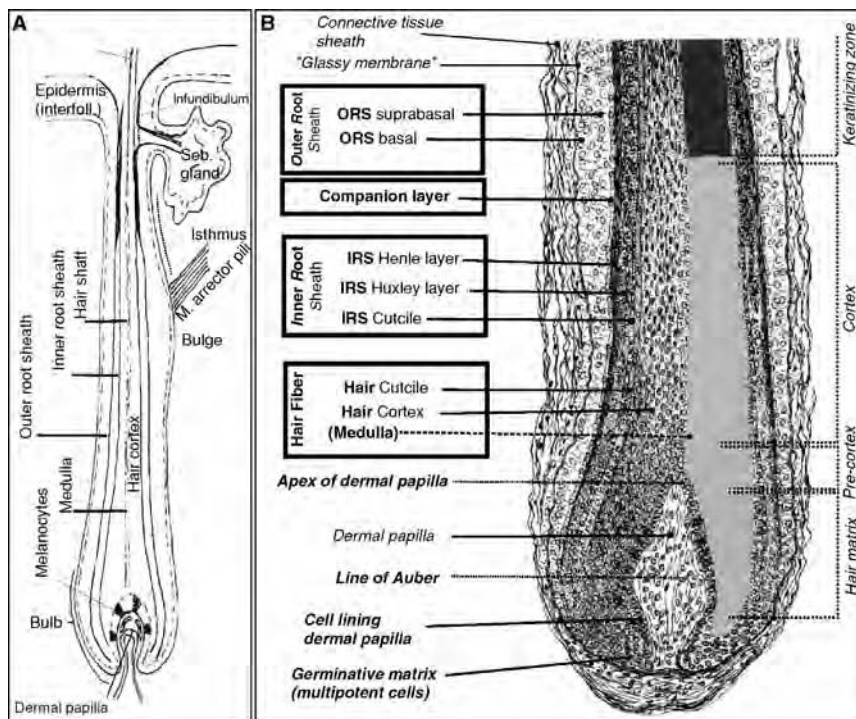


FIG. 2 Hair follicle morphology. (A) Schematic drawing indicating the major structural components of the anagen hair follicle. (B) Detailed illustration of the constituent tissue compartments of the lower portion of the hair follicle. The “hair-forming compartment,” comprising the living cells of the hair matrix, cortex, cuticle, and, if present, the medulla, is shaded in gray in the right half of the follicle. The area shaded in black represents the keratinized portion of the hair shaft. (Figure modified from a precise drawing by Bucher, 1968.)

another single-layered structure, the so-called companion layer (CL), whose nature as an independent compartment of the follicle has been recognized. The most external layer of the hair follicle is the outer root sheath (ORS). Whereas the progenitor cells of both the hair-forming compartment and the IRS and CL layers are all located in the germinative matrix, the ORS is contiguous with the interfollicular epidermis (Fig. 2A, B).

The highly organized tissue architecture and self-renewal features, coupled with its impressive growth rate and easy accessibility, have made the hair follicle a paradigm for investigating the molecular mechanisms that govern its mediolateral cell lineage determination and the subsequent differentiation pathways of the resulting tissue compartments along the long axis of the hair follicle. Our laboratories have focused on the biology and genetics of the major classes of structural proteins that are indispensable for the ultimate

task of the follicle, that is, the production of hair. These protein classes, which are all encoded by large multigene families, comprise the hair keratins and their associated proteins, KAPs, which are constituents of the trichocytes of the hair-forming compartment. Considering the functional association of the hair-forming compartment of the follicle with its external sheaths, we have also begun to investigate the epithelial keratins that are involved in the formation of these highly specialized structures.

The first part of this review describes the genomic organization of the human hair keratin gene family and the complex expression characteristics of the encoded hair keratins in the postnatal anagen hair follicle. By analogy with epithelial keratins (Moll *et al.*, 1982), we also present a two-dimensional catalog of human hair keratin proteins. Sections are devoted to the role and fate of hair keratins in the diseased hair follicle, in particular hereditary disorders and tumors that are derived from the hair follicle. Closely associated with these sections is a report on the actual state of our knowledge on the important aspect of regulation of hair keratin expression. In the second part of this review, essentially the same principles are applied to outline more recent and, thus, occasionally fewer data on the special epithelial keratins that are expressed in the various tissue constituents of the external sheaths of the follicle. The closing section highlights issues that need to be explored further to deepen our insight into the biology and genetics of the hair follicle.

II. Human Hair Keratin Family

It is intriguing to realize that, in a society believing that healthy hair is indispensable for beauty, social recognition, and success, research on the molecular biology and genetics of the structural components of human hair has lagged considerably behind that conducted in mice and, particularly, in sheep, with the latter being generously supported by the wool industry. Indeed, when we began our work on human hair keratins in 1994, a large number of cDNA and gene sequences were available for sheep wool keratins, and a few could be found for mouse hair keratins (Powell and Rogers, 1997), but only one human hair keratin cDNA sequence was known (Yu *et al.*, 1993).

In the mid-1980s, pioneering studies on native hair keratin proteins, performed in the laboratories of W. Franke and H. Sun, had led to the concept that, independent of the species, the hair keratin family consisted of not more than 10 members that could be subdivided into 4 major type I keratins, designated Ha1–Ha4, and four type II members, Hb1–Hb4, as well as a minor keratin pair termed Hax/Hbx. In this nomenclature, *H* stood for hair, and *a* and *b* related to the acidic (type I) or neutral to basic (type II)

nature of these proteins (Heid *et al.*, 1986, 1988a,b; Lynch *et al.*, 1986). The hair keratin family was thus suggested to be distinctly less complex than the large epithelial keratin family. The assumed paucity of hair keratins, and the availability of defined hair/wool keratin cDNA and gene sequences from mice and sheep, encouraged us to undertake the genomic characterization of the human hair keratin family in its entirety. Under the premise that hair keratin sequences are as conserved between species as epithelial keratin sequences, these sheep and mouse sequences were initially used for the screening of a human scalp cDNA library, followed soon thereafter by P1 artificial chromosome and other bacterial cloning methods. This strategy enabled us to successively identify single hair keratin genes and their encoded proteins and, finally, to elucidate the type I and type II gene loci of the human hair keratin family.

A. Physical Organization of Human Hair Keratin Genes

At present we know, that the genes of the human type I and type II hair keratin subfamilies are each clustered in the genome and that both clusters are part of the large type I and type II epithelial keratin gene domains on chromosomes 17q21.2 and 12q13.13, respectively (Rogers *et al.*, 1998, 2000). The clustered type I hair keratin genes are contained within an ~190-kb DNA domain (Fig. 3A). This subfamily alone comprises 10 genes, which are flanked on one side by the *K13* gene. Surprisingly, the other side of the domain is contiguous with seven KAP multigene families, KAP1–3, 4, 9, 16, and 17 (Rogers *et al.*, 2001). While we previously assumed that the KAP genes adjacent to the type I hair keratin gene cluster were followed by a pseudogene and the gene for pancreatic keratin K23, our own investigations, as well as a bioinformatic study on the organization of the human type I and type II keratin/hair keratin gene domains (Hesse *et al.*, 2004), revealed the presence of two further, apparently functional hair keratin genes, tentatively termed *K26* and *K28* (*Ka35* and *Ka36* according to Hesse *et al.*, 2004), which are located between the KAP gene cluster and *K23* (Fig. 3A). The clustered type II hair keratin gene subfamily on chromosome 12q13.13 also comprises 10 genes, which are located on an ~200-kb DNA domain and flanked by the epithelial keratin genes *K6hf* and *K7*, respectively (Fig. 3A).

Both hair keratin gene domains also contain pseudogenes. Whereas there are four pseudogenes within the type II subfamily, the type I subfamily contains only one pseudogene. Collectively, this means that the 2 gene clusters comprise 15 functional genes, 9 type I and 6 type II, as well as 5 pseudogenes. With the exception of the type II *hHb6* gene, the functional genes of both clusters are all arranged in the same orientation (Fig. 3A) (Rogers *et al.*, 1998, 2000). In general, the functional type I hair keratin genes

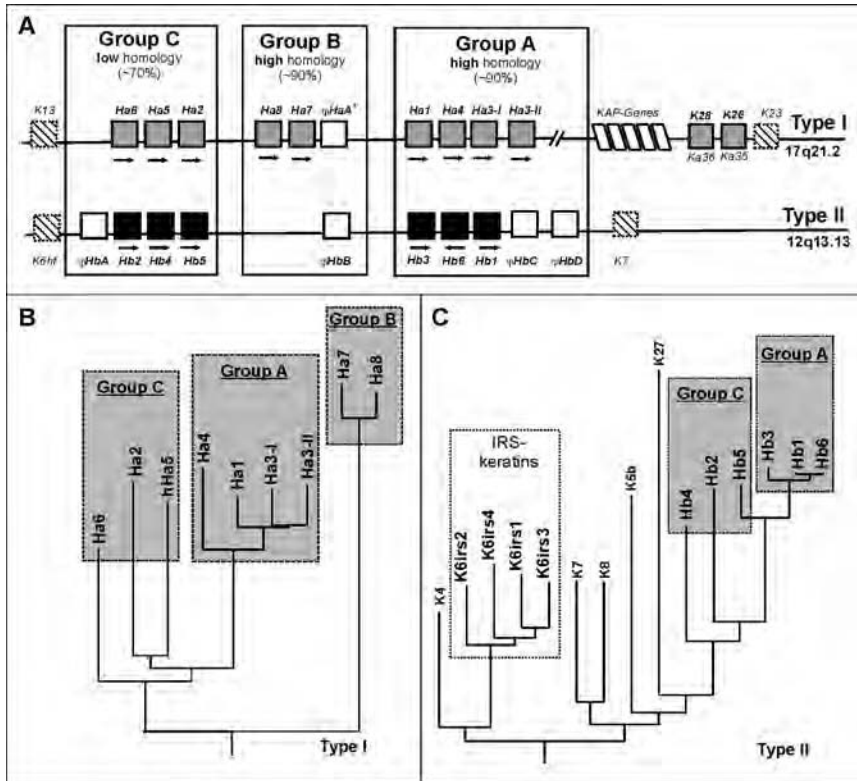


FIG. 3 Organization of human hair keratin gene clusters and evolutionary tree construction. (A) Type I and type II hair keratin gene clusters and their flanking genes. The clustered hair keratin genes are subdivided into gene groups A, B, and C (boxed), according to sequence homologies of the encoded proteins. The transcriptional orientation of the clustered genes is indicated by arrows. Gray rectangles, functional type I genes, including the still uncharacterized *K26* (*Ka35*) and *K28* (*Ka36*) genes (for their designation, see Section II.A), outside the clustered genes (ψ *HaA*¹ is a transcribed pseudogene); black rectangles, functional type II genes; white rectangles, pseudogenes; oblique rectangles, KAP genes; hatched rectangles, epithelial keratin genes. (B and C) Evolutionary tree of (B) type I and (C) type II hair keratins encoded by the clustered hair keratin genes. Note the segregation of the keratins according to the gene grouping indicated in (A). The type II tree also contains branches for some epithelial keratin genes, including those expressed in the IRS (see Section V.C).

are each divided into seven exons and six introns. This is in contrast to the organization of exons and introns of type I epithelial keratin genes, which possess an additional, positionally highly variable intron in the region encoding the tail domain of the keratins. However, both gene families show exceptions to these rules in that the gene of epidermal keratin K9 contains an eighth intron, and hair keratin gene *hHa5* has a seventh intron, both being

located in the 3' noncoding region of the genes. In contrast, type II hair keratin as well as epithelial keratin genes exhibit nine exons and eight introns, with only hair keratin gene *hHb4* deviating from this rule through an additional ninth intron in the 3' noncoding region (Rogers *et al.*, 1998, 2000). Remarkably, comparative analysis of the hair keratin proteins encoded either by the clustered type I or type II genes reveals that on each domain the respective genes can be physically subdivided into distinct groups (Fig. 3A, B). At one end, each domain contains three functional *group C* genes that encode, on a structural basis, only weakly related keratins (<70%). In contrast, the four type I genes, two of which encode hair keratin isoforms hHa3-I and hHa3-II, and the three type II *group A* genes at the other end, encode structurally highly related hair keratins (>90%). Likewise, the three central *group B* genes of the type I gene domain, which (except for pseudo-gene *φhHbB*) have no counterparts in the type II gene domain, contain sequence information for highly homologous keratins (>90%) (Fig. 3A). Evolutionary tree constructions show that the branches leading to the hair keratin genes divided continuously during evolution, first segregating into the type I group B genes, followed by a stepwise generation of the type I and type II group C genes, and culminating in that of the respective group A genes (Fig. 3B).

B. Expression Characteristics of Hair Keratins in the Human Hair Follicle

The manner in which genes are grouped in the two hair keratin gene domains raised questions concerning whether it might be biologically relevant. This question could be answered by means of expression studies of the various hair keratins in the hair follicle. These studies were carried out both on sections of human scalp and plucked beard hair follicles, using specific probes of the 3' noncoding region of the respective hair keratin mRNAs for *in situ* hybridization (ISH) as well as specific antibodies raised against oligopeptides from the carboxy or amino terminus of the individual hair keratins for indirect immunofluorescence (IIF) studies.

Both methods revealed that the structurally related type I and type II group A hair keratins were all expressed in the hair cortex and, thus, represented late differentiation products within the hair-forming compartment. Whereas the expression of hHa1 started early in the precortex region (Fig. 4A, A'), the onset of expression of hair keratins hHa3-I and hHa3-II occurred in the midcortex region (shown for hHa3-I in Fig. 4B, B') and that of hair keratin hHa4 occurred in the upper cortex (Fig. 4C, C'). Conversely, the onset of expression of the type II group A members hHb1, hHb3, and hHb6 uniformly occurred in the midcortex region (Fig. 5A–C').

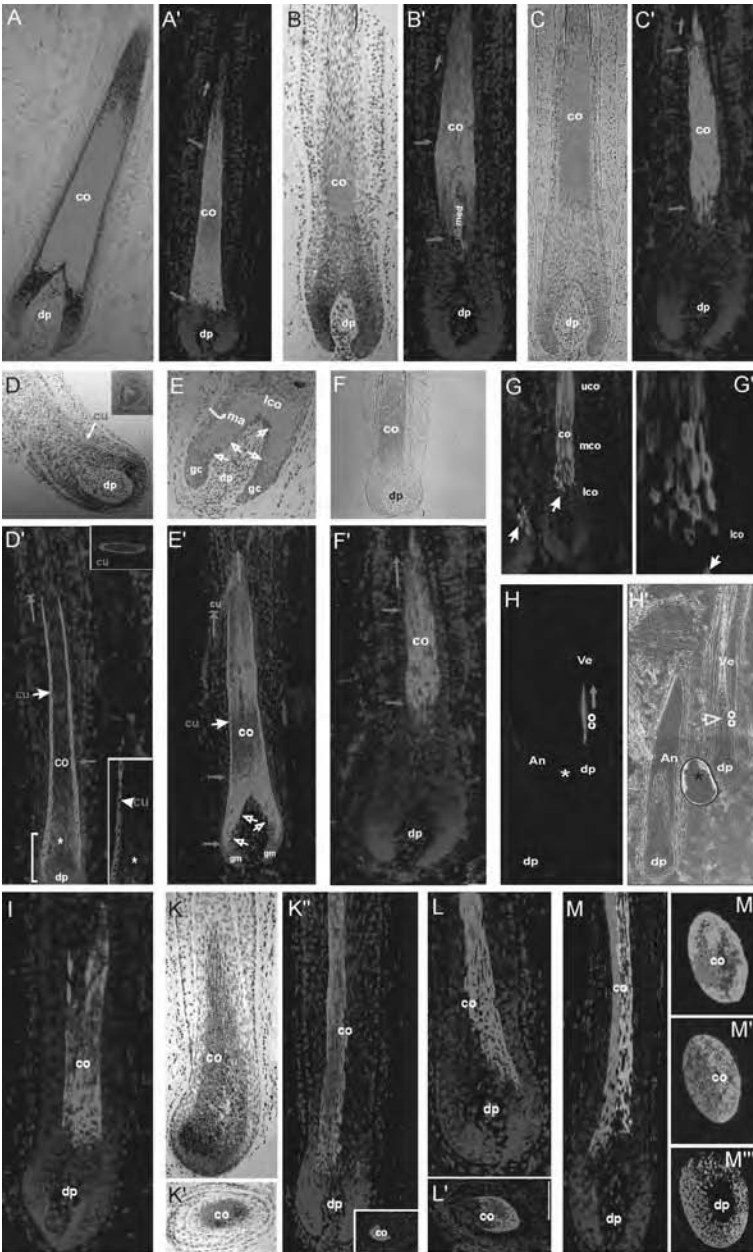


FIG. 4 Expression of human type I hair keratins. (A–H') Human hair follicles. Group A hair keratins: Ha1 [(A) ISH; (A') IIF], Ha3-I [(B) ISH; (B') IIF], and Ha4 [(C) ISH; (C') IIF]. Group C hair keratins: Ha2 [(D) ISH, *inset* shows a cross-section; (D') IIF. *Top inset*: Cross-section.

Thus, type II group A lacked members whose expression began as early as that of hHa1 or as late as that of hHa4 (see Fig. 4A, A', C, C').

In contrast, expression profiles of the structurally less related type I and type II group C members were heterogeneous, with the majority of the keratins being expressed early in the bulb region of the follicle. More precisely, the expression of hair keratins hHa5 and hHb5 uniformly started in both the matrix and cuticle (Figs. 4E, E' and 5E, E'), immediately above the germinative matrix cell compartment of the follicle. Although the majority of cells bordering the dermal papilla were devoid of these keratins, some of them, apparently in transit to the parabasal cell row, were clearly labeled [Fig. 4E, E' (open arrows) and Fig. 5E' (inset, arrowheads)]. In contrast, hair keratins hHa2 and hHb2 were specific for the hair cuticle (Figs. 4D, D' and 5D, D', F). Whereas hHa2 expression began in the lowermost bulb region (Fig. 4D, D'), that of hHb2 was delayed (Fig. 5D, D', G) and shifted to an area slightly above the line of Auber (Auber, 1952; see also Fig. 2B). Consistently, the monoclonal hHa2 antibody also reacted weakly with a 10- to 12-cell layer-thick central area that extended from the upper matrix into the lower cortex [Fig. 4D' (asterisk) and Fig. 5G (green)]. As, however, hHa2 transcripts were virtually restricted to the hair cuticle (Fig. 4D), it appears that the hHa2 antibody cross-reacted with an unknown antigen in the precortex area. The group C type I hair keratin hHa6 represented a cortex keratin whose expression profile in the mid- to upper cortex region (Fig. 4F, F') resembled that of the group A type I hair keratins hHa3-I/II (Fig. 4B, B') and the group A type II hair keratins, respectively (Fig. 5A-C'). Remarkably, the type II hair

Bottom inset: Higher magnification of the lower bulb region. Asterisks denote a cross-reaction of the Ha2 antibody with an unknown antigen in the upper matrix and precortex region], Ha5 [(E) ISH; (E') IIF. Open arrows in (E) and (E') indicate Ha5-positive cells lining the dermal papilla], and Ha6 [(F) ISH; (F') IIF]. Group B hair keratins: Ha8 [(G and G') IIF, solid white arrows indicate isolated hHa8-positive cells at the transition of the matrix and the precortex], Ha7 [(H) IIF; (H') phase-contrast micrograph of (H), showing a terminal anagen hair follicle (An) at the left-hand side and a vellus hair follicle (Ve) at the right-hand side. The yellow arrow in (H') denotes the Ha7-stained area in (H), and the asterisks indicate an air bubble]. Throughout, red arrows demarcate the zones of mRNA expression. Green stop arrows denote the end of demonstrable protein expression. Green arrows indicate that the section went out of plane. (I-M'') Chimpanzee hair follicles. Group B hair keratins: cHa7 [(I) IIF, antiserum against hHa7, cross-reacting with cHa7] and cHaA [(K) ISH, longitudinal section; (K') ISH, cross-section; (K'') IIF, *inset* shows a cross-section]. Group A hair keratin: cHa1 [(L) IIF, longitudinal section; (L') IIF, cross-section; (M) double-label IIF with antisera against cHa1 (red) and cHaA (green) on a longitudinal section; (M'-M'') double-label IIF with antisera against cHa1 (red) and cHaA (green) on cross-sections]. (A'), (B'), (C'), (D'), (E'), (F'), (G), (I), (K''), (L), (L'), and (M) were counterstained with DAPI. Abbreviations: co, cortex; uco, upper cortex; mco, midcortex; lco, lower cortex; cu, cuticle; med, medulla; dp, dermal papilla. (See also color insert.)

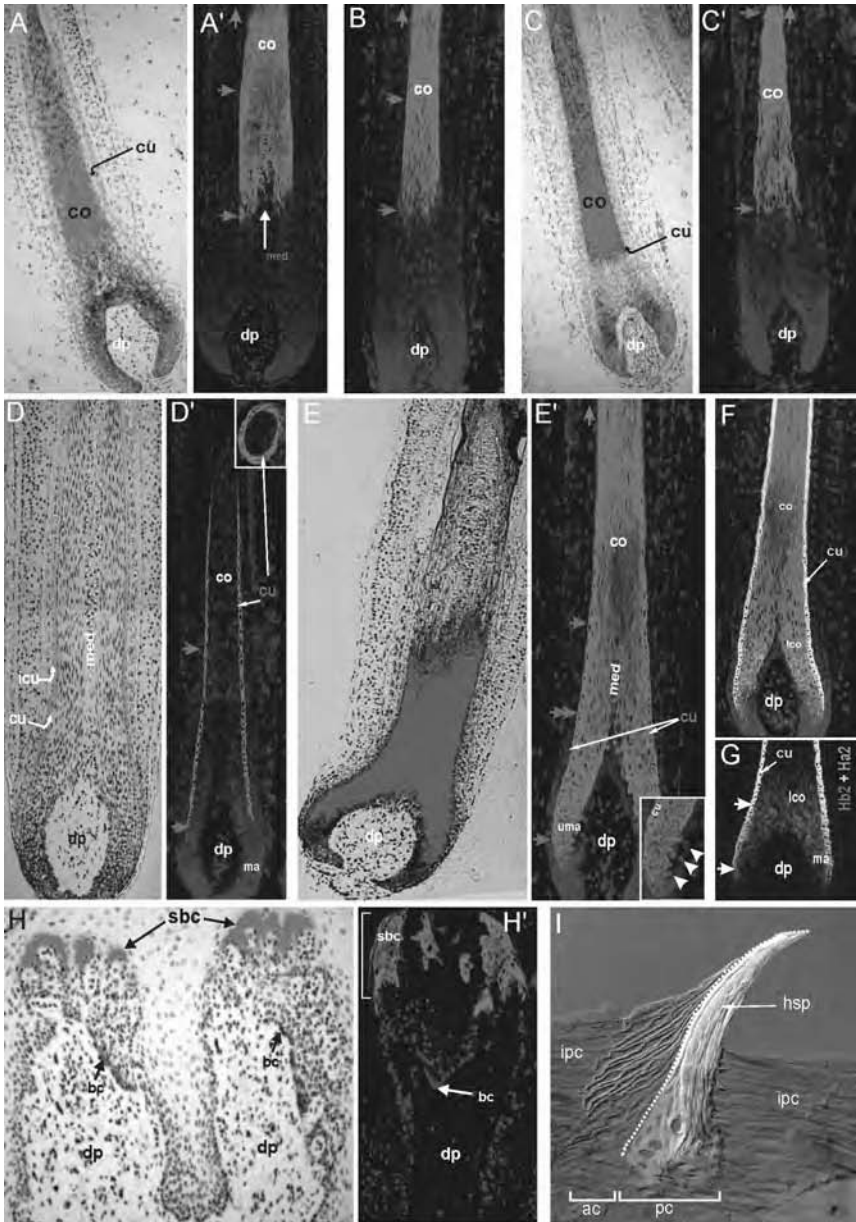


FIG. 5 Expression of human type II hair keratins. (A–G) Human hair follicles. Group A hair keratins: Hb1 [(A) ISH; (A') IIF], hHb3 [(B) IIF], and Hb6 [(C) ISH; (C') IIF]. Group C hair keratins: Hb2 [(D) ISH; (D') IIF, *inset* shows a cross-section through the follicle] and Hb5 [(E) ISH; (E') IIF]. White arrowheads in the *inset* denote hHb5-positive cells lining the dermal

keratin hHb4 could not be demonstrated in scalp or beard hair follicles. However, ISH and IIF on human tongue sections clearly revealed strong hHb4 expression in the dorsal filiform papillae (Fig. 5H, H'). As human filiform papilla units exhibit more than one of the typical hook-shaped spiny protrusions, it was difficult to obtain strictly sagittal sections through the protruding spines. By using mouse tongue, in which the filiform papilla units are preferentially organized into a single, highly compartmentalized spine, hHb4 expression could be precisely assigned to a subregion of the parakeratinizing posterior compartment directly apposed to the base of the adjacent orthokeratinizing anterior compartment of the filiform (Fig. 5I) (Langbein *et al.*, 1999, 2001).

In contrast to the uniform cortical expression patterns of the highly related group A hair keratins of both types, the highly homologous central group B type I hair keratins hHa8 and hHa7 each exhibited highly unusual expression patterns (Langbein *et al.*, 1999). Hair keratin Ha8 was expressed only in single cells, which were randomly scattered throughout the entire cortex region (Fig. 4G, G'). On occasion, hHa8-positive cells could also be observed at the transition of the matrix to the precortex (white arrows in Fig. 4G, G'). Similar to the type II hair keratin hHb4 (Fig. 5H–I), the type I hair keratin hHa7 could not be demonstrated in terminal scalp hairs, but could be readily detected in some, but not all, of the rare vellus hair follicles normally present in the human scalp (Montagna and Parakkal, 1974, pp. 172–258). In these follicles, hHa7 expression was restricted to a column of vertically oriented, spindle-shaped cells in the center of the mid- to upper cortex region (Fig. 4H, H'). Cross-sections showed that the hHa7-positive cortex cells were more or less concentrically arranged around an hHa7-negative core column (results not shown; for further details of hHa7 expression, see Section IV.D).

The most remarkable issue on hair keratin expression was related to the group B type I pseudogene ϕ hHaa (Fig. 3A). On sequencing, the ϕ hHaa gene exhibited a premature stop codon TGA in the center of the region encoding the α -helical rod domain. This TGA codon was found in both

papilla]; (F) Double-label IIF with antibodies against Hb5 (red) and Hb2 (green; merged yellow); (G) Double-label IIF with antibodies against Ha2 (green) and Hb2 (red; merged yellow). The white arrowheads demarcate Ha2 expression without visible Hb2 coexpression. Note the cross-reaction of the Ha2 antibody with an unknown antigen in the upper matrix and precortex (see also Fig. 4D'). (H–I) Human and mouse tongue. Group C hair keratin: Hb4 [(H) ISH, human tongue; (H') IIF, human tongue; (I) IIF, mouse tongue]. Throughout, red arrowheads indicate the zones of mRNA expression. The double-headed arrow in (E') denotes the site of cessation of Hb5 mRNA expression in the hair cuticle. (A'), (B), (C'), (D'), (E'), (F), and (H') were counterstained with DAPI. Abbreviations: ma, matrix; uma, upper matrix; sbc, suprabasal compartment; bc, basal compartment; ipc, interpapillary compartment; ac, anterior compartment; pc, posterior compartment; hsp, horny spine. (For further abbreviations, see caption to Fig. 4.) (See also color insert.)

alleles of the extant human population. Nevertheless, signals for $\phi hHaA$ transcripts could clearly be demonstrated by ISH in the pre- to midcortex region of the hair follicle (results not shown). In contrast, an antiserum generated against an amino-terminal segment of the hypothetical keratin failed to decorate this area, thus indicating that $\phi hHaA$ represents a transcribed pseudogene (Winter *et al.*, 2001). Surprisingly, sequencing of the orthologous genes for $\phi hHaA$ in both chimpanzees and gorillas revealed that these species possessed a homozygous arginine codon, CGA, instead of the human TGA nonsense codon. Indeed, the *cHaA* gene encoded a keratin, cHaA, that was clearly expressed in the hair cortex of chimpanzees, but only in exactly one vertical half of this follicular compartment (Fig. 4K–K''), the other half being occupied by cHa1, that is, the chimpanzee ortholog of hHa1, which cross-reacted with the antibody against hHa1 (Fig. 4L, L'). Double-label IIF, using the antibody against hHa1 (red) and the antiserum against cHaA (green), confirmed this highly unusual cHa1/cHaA expression pattern in chimpanzee hair follicles (Fig. 4M–M'') (Winter *et al.*, 2001).

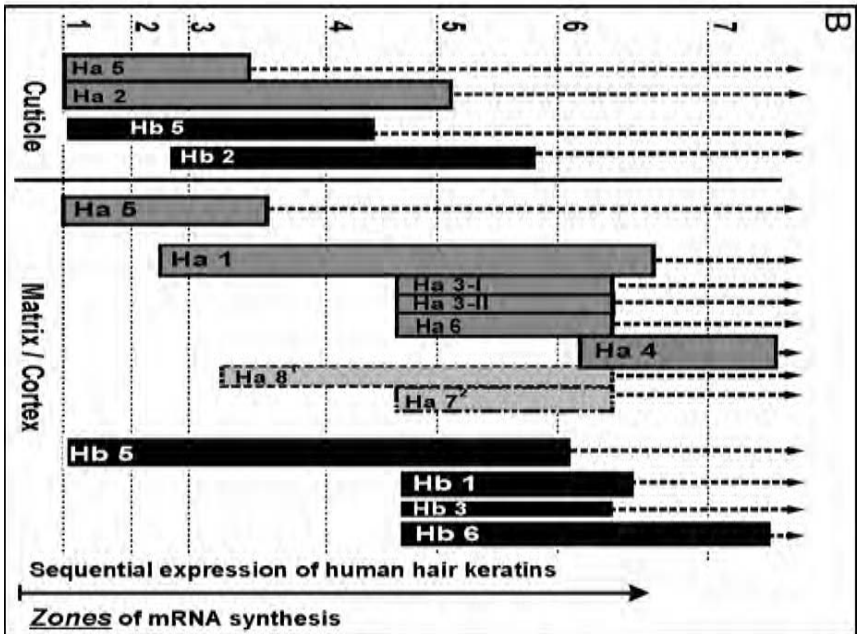
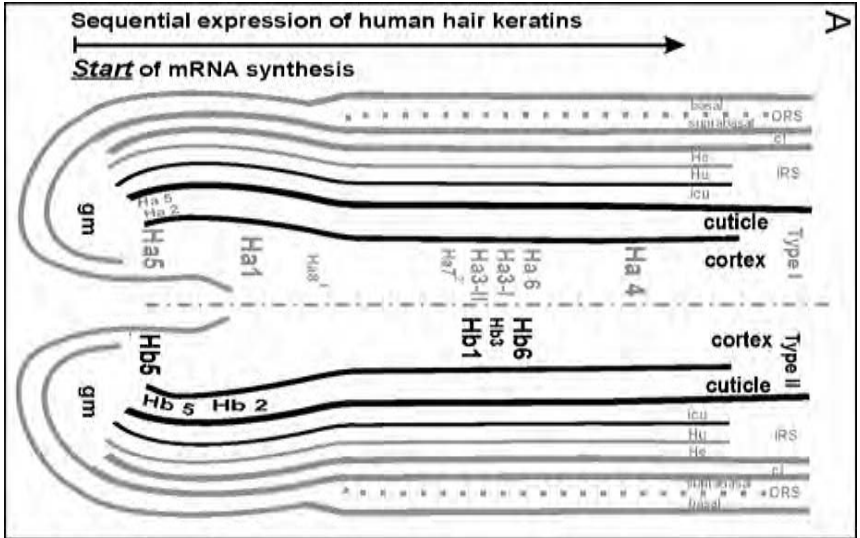
Considering that humans and chimpanzees evolved from a common ancestor after the *Pan–Homo* dichotomy about 5–6 million years ago (Tattersall, 1997), this deviation of the human from the chimpanzee/gorilla hair keratin patterns suggested that the once active form of the present $\phi hHaA$ pseudogene was silenced at some time point during hominid evolution. Obviously, to avoid a loss of function-induced diseased hair phenotype, the inactivation of the *hHaA* gene occurred concomitantly with a shift of *hHa1* gene activity into the adjacent half of the cortex in order to replace the lost hHaA keratin (compare Fig. 4M with Fig. 4A'). On the basis of *HaA* gene comparisons between chimpanzees and humans, and using the respective gorilla sequence as an outgroup, it was possible to calculate that the active form of the present $\phi hHaA$ pseudogene was silenced only about 240,000–200,000 years ago. This implied that all hominids living before this time still possessed a chimp/gorilla pattern of hair keratin expression (Winter *et al.*, 2001). Relative to the suggested 5–6 million years of human evolution, the inactivation of the *hHaA* gene was an amazingly recent event, which in the framework of two opposing hypotheses on the evolution of anatomically modern humans has turned out to be of high relevance, because its history strongly supports the recent African origin of modern humans from a relatively small ancestral population (Stringer and Andrews, 1988).

The complex human hair keratin expression is schematically summarized in Fig. 6A, B. For the sake of a comprehensive interpretation of the data, in both schemes only mRNA expression profiles of the various keratins are indicated. To visualize the sequential expression of the various hair keratins in the hair follicle, the designations of the individual type I (gray letters) and type II (black letters) hair keratins in Fig. 6A stand for the onset of their mRNA synthesis in the hair-forming compartment, with the size of the letters

reflecting their degree of expression. In the scheme shown in Fig. 6B vertical columns indicate the zones of mRNA expression of the individual type I (gray) and type II (black) hair keratins within the hair cuticle and the matrix/cortex, respectively. As IIF studies showed, independent of the onset of mRNA expression, virtually all hair keratin proteins can be demonstrated up to the zone of fiber hardening (vertical dotted arrows in Fig. 6B), where they are no longer accessible to the antibodies. This implies that any cuticle cell that enters terminal differentiation contains 4 different hair keratins, whereas any cortex cell may accumulate the unprecedented high number of up to 10, occasionally 11, different hair keratins. Moreover, each terminally differentiating cuticle cell or cortex cell also contains, impressively, about 20 or 80 individual KAP members, respectively (Rogers *et al.*, 2001, 2002, 2004b; Shibuya *et al.*, 2004; Yahagi *et al.*, 2004).

It is obvious that this complex scenario of hair keratin expression makes it difficult to deduce the formation of distinct type I and type II hair keratin pairs as previously observed for the keratins of various types of epithelia (Fuchs and Weber, 1994; Mischke, 1998; Steinert and Roop, 1988). The hair cuticle, with its less complex keratin expression, may serve as an example for this (Fig. 6B). In its lowermost portion (level 1 in Fig. 6B), the presence of two type I hair keratins, hHa2 and hHa5, versus the presence of only one type II hair keratin, hHb5, suggests a competition of hHa2 with hHa5 for filament formation with hHb5. Higher up (levels 2 and 3 in Fig. 6B), type I hair keratins hHa2 and hHa5 are temporarily coexpressed with type II hair keratins hHb2 and hHb5, before hHa5 expression ceases and, hence, confronts hHa2 with hHb2 and hHb5 (level 4 in Fig. 6B), thus creating an inversion of the situation in the lowermost cuticle. Only in the uppermost region of active cuticular hair keratin expression is hHa2 left to specifically pair with hHb2 (level 5 in Fig. 6B). Collectively, this scenario suggests successive competitive, complex, and unique pairing patterns of cuticular type I and type II hair keratins. The same dynamics hold true for the potential pairing possibilities of matrix and, in particular, cortex keratins (Fig. 6B), whose unprecedented complexity makes it difficult to assume the formation of specific keratin pairs.

We have analyzed hair keratins in the human nail unit and found that their expression was restricted to the different matrix compartments of the nail (Perrin *et al.*, 2004) (Fig. 7). Although the apical matrix clearly expressed a large number of hair keratins in its extended superficial layers, their expression profiles were rather diffuse and patchy, so that it was difficult to pinpoint the onset of expression of a distinct hair keratin. Conversely, the adjacent ventral matrix exhibited hair keratin expression profiles that were similarly well organized as in the hair follicle. The ventral nail matrix is composed of a proliferative, multilayered, up to 10 cell layers thick basal compartment followed by the likewise multilayered so-called keratogenous zone which



ultimately differentiates into the nail plate (Fig. 7). Although the cells of the entire basal compartment are uniformly round, they abruptly adopt both a spindle-shaped form and a vertical orientation as soon as they enter the keratogenous zone. Thus, except for the vertical orientation of the keratogenous cells, the cells in the two compartments of the ventral matrix are morphologically similar to matrix and cortex cells of the hair follicle. As expected, hair cuticle keratins hHa2/hHb2 were absent from the ventral matrix as well as from any other epithelial nail compartment.

In contrast, beginning in the uppermost layers of the basal compartment and extending over the entire keratogenous zone of the ventral matrix, the remaining hair keratins displayed exactly the same complex and sequential expression pattern as observed in the hair-forming compartment of the follicle. One notable exception occurred regarding hair keratins hHa5 and hHb5. In the hair follicle, these keratins are the earliest expressed hair keratins of the matrix (see Figs. 4E, E' and 5E, E'). Accordingly, in the ventral nail matrix hHb5 appeared first in the uppermost layers of the basal compartment and could then be detected in the entire keratogenous

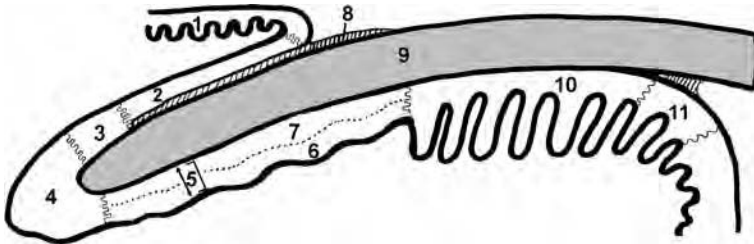


FIG. 7 Histology of the adult human nail unit. (1) dorsal epidermis of the digit; (2) eponychium; (3) dorsal matrix; (4) apical matrix; (5) ventral matrix; (6) multilayered basal compartment of the ventral matrix; (7) keratogenous zone of the ventral matrix; (8) cuticle; (9) nail plate; (10) nail bed; (11) hyponychium.

FIG. 6 Patterns of hair keratin expression in the human hair follicle. (A) Schematic presentation of an anagen hair follicle and its constituent tissue compartments. The positions at which the individual type I (gray) and type II hair keratins (black) are indicated denote the onset of their mRNA expression in the respective compartment, with the size of the letters and numbers mirroring the degree of expression of the individual keratins. (B) mRNA expression zones of major type I (gray columns) and type II hair keratins (black columns) in the hair cuticle, matrix, and cortex. mRNA expression profiles of minor hair keratins are indicated by dotted columns. The vertical dotted arrows indicate that the hair keratin proteins can be demonstrated up to the level of fiber hardening by their respective antibodies. Numbers 1–7 at the left-hand site denote levels of the hair follicle referred to in text (see Section II.B). Ha8¹, expression occurring only in single cortex cells; Ha7², expression in vellus hairs; for medullary Ha7 expression, see Section V.D.

zone. Remarkably, its follicular type I partner hHa5 was completely absent from the ventral matrix epithelium. As cortex keratins of both types were sequentially expressed in the keratogenous zone, there was no lack of potential type I hair keratins acting as partners for hHb5 in this compartment. However, no further hair keratins were present in the uppermost layers of the basal compartment, thus leaving hHb5 without a type I hair keratin partner in this region. In summary, our study of the nail unit did not provide conclusive information about specific hair keratin pairing; rather, it raised new questions. Therefore, it remains to be seen whether, for instance, the viscosity of intermediate filaments (IFs) assembled *in vitro* from various recombinant type I and type II hair keratins, or biophysical investigations on the affinity strengths between various *in vitro* combinations of type I and type II hair keratins, may be suitable approaches to ultimately solve the problem of specific or “promiscuous” *in vivo* hair keratin pairing.

C. Catalog of Human Hair Keratins

On the basis of our IIF studies on hair keratin expression, the previously observed two-dimensional electrophoretic (2-DE) gel resolution of hair keratin extracts into only four type I and four type II Coomassie-stained protein spots (Heid *et al.*, 1986, 1988a,b), can now be explained by the highly variable degree of expression of the various hair keratins in the follicle. Most probably, this pattern originated from the most strongly expressed matrix and cortex keratins of both types (e.g., hHa5, hHa1, hHa3-I, hHa3-II, hHa6 and hHb5, hHb1, hHb3, hHb6), while keratins hHa2 and hHb2 of the single-layered cuticle or the minor cortex keratins hHa4 and hHa8 escaped detection by the dye. This drawback could, however, be overcome by successively subjecting two-dimensionally resolved hair keratins to considerably more sensitive Western blots using specific hair keratin antibodies (Langbein *et al.*, 1999, 2001). Two exceptions, both related to the use of terminal scalp hairs as a source for hair keratins, are worth mentioning. As expected from the IIF studies, the type II hair keratin hHb4 could not be detected in hair follicle cytoskeletal extracts and required the use of extracts of human dorsal tongue for its demonstration as the largest and most alkaline member of the type II hair keratin subfamily (Langbein *et al.*, 2001). Moreover, the type I hair keratin hHa7, which was not found by IIF in terminal scalp hair follicles, could be detected in Western blots of keratin extracts of beard hairs (Langbein *et al.*, 1999). The reason for this property of hHa7 is given below (see Section IV.D). Whereas for some members of the type I hair keratin subfamily considerable discrepancies occurred between their calculated molecular mass values and their position in gels (Langbein *et al.*, 1999), the

mass calculations and migration properties of the type II hair keratins agreed much better (Langbein *et al.*, 2001).

Figure 8 shows the resulting catalog of human type I (gray squares) and type II (black squares) hair keratins, combined with the catalog of human type I and type II epithelial keratins (open circles) of Moll *et al.* (1982). It should be emphasized that hair keratins hHa1–4 and hHb1–4 of the present catalog do not correspond to hair keratins with the same designation in the previously published hair keratin catalog (Heid *et al.*, 1986). *A priori*, this could not be expected because the earlier nomenclature relied on a counterclockwise numerical designation of Coomassie-stainable hair keratins, whereas the present designation is based on the immunodetection of defined hair keratin gene products. Regarding the earlier “minor hair keratins” Hax and Hbx (Heid *et al.*, 1988a,b), their current designation is hHa6 and hHb4, respectively (Fig. 8).

The human hair keratin catalog reveals a numerical imbalance between type I and type II members. A similar excess of type I keratins over type II

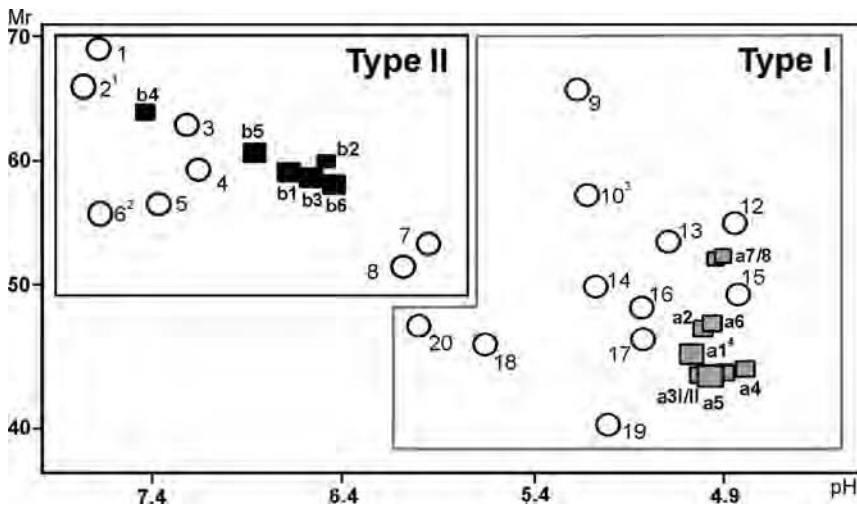


FIG. 8 The catalog of human hair keratins. The type I and II hair keratins, indicated by gray and black squares, respectively, have been combined with the catalog of human epithelial keratins (open circles) according to Moll *et al.* (1982). Epithelial keratins are indicated by their number (i.e., 1 = K1), and hair keratins are indicated by *a* or *b* and their number (i.e., a2 = Ha2). Abscissa, isoelectric pH; ordinate, molecular mass values. 2¹, two keratins, K2e and K2p, which exhibit highly similar migration properties in SDS-PAGE (Collin *et al.*, 1992a,b); 6², three isoforms of K6 (for details, see Section V.A), as well as type II keratin K6hf and the type II IRS keratins, which migrate similarly (for details, see Section V.B and V.C); 10³, a previously described K11 keratin representing a polymorphic form of K10 that arises through the loss of glycine-rich repeats in the head or tail domains of the keratin (Mischke, 1998); a1⁴, a low molecular weight isoform, hHa1-t, which lacks the complete tail domain (for details, see Section III.A.2).

keratins has also been observed in the teleost fish *Fugu rubripes* (Zimek *et al.*, 2003). The still uncharacterized human type I hair keratins encoded by genes *K26* (*Ka35*) and *K28* (*Ka36*) aside (see Fig. 3A), the observed imbalance is due to the occurrence of two isoforms of the type I hair keratin gene *hHa3* as well as the fact that the type II hair keratin gene domain lacks counterparts of the two functional type I group B hair keratin genes *hHa7* and *hHa8* (Fig. 3A). In human scalp hairs, the *hHa7* and *hHa8* keratins show a highly unusual restriction of their expression to distinct hair cortex cells (Fig. 4G–H') (Langbein *et al.*, 1999), whereas their chimpanzee orthologs are both expressed as major keratins in the entire hair cortex (shown for *cHa7* in Fig. 4I) (L. Langbein and J. Schweizer, unpublished data). In addition, as outlined above, chimpanzees express a functional ortholog of the human type I hair keratin pseudogene ϕ *hHaA* in half of their hair cortex (Fig. 4K–K'') (Winter *et al.*, 2001). Thus, the strong expression of three additional type I hair keratins in the cortex raises a question as to whether the hairs of our closest relatives may possess a greater strength and resilience than human hairs. In this context, it should also be noted that the type I group B hair keratin gene subcluster (Fig. 3A) seems to be a specific evolutionary acquisition of primates, as both the mouse and rat type I keratin gene domains do not possess this subcluster in their genome (Hesse *et al.*, 2004). Considering that the expression profiles of the members of human group B subcluster underwent conspicuous alterations after the *Pan–Homo* divergence, it might be speculated that in humans, the cluster is under low evolutionary pressure and, in the long run, on its way to being completely eliminated from the genome, thus reestablishing an evolutionarily older genotype. All in all, these observations support the evidence that, besides alternative gene use as a major principle, the manifold differences between chimpanzees and humans are not basically due to the acquisition of new genes in the human lineage, but rather to the loss of genes, especially from multigene families (Olson, 1999).

III. Hair Keratins and Hair Follicle Pathologies

A. Hereditary Hair Disorders

Since the early 1990s, a large number of autosomal dominantly transmitted diseases of the skin and various internal epithelia have been found to be caused by mutations in keratin genes. The resulting autosomal dominant pathologies are primarily due to the inability of the mutated keratin protein to form stable IF with its intact endogenous partner of the opposite type. This leads to an accumulation of disorganized IF bundles, entailing a cascade-like

series of events that eventually culminate in failure of tissue integrity, in particular on exposure to mechanical stress. In the majority of cases, the mutations result in inappropriate amino acid substitutions at the beginning of subdomain 1A or at the end of subdomain 2B of the α -helical rod of either type I or type II keratins, although in type II keratins, deleterious mutations have also been found in distinct regions of the head and tail domains (for reviews, see Herrmann *et al.*, 2003; Smith, 2003).

It is obvious that the extrapolation of the rules underlying epithelial keratin diseases to inherited hair disorders would limit the large number of hair anomalies to those with autosomal dominant transmission, and restrict the phenotype to the structure of hairs and, possibly other hair keratin-expressing tissues, such as the nail unit, although hair keratin disorders with autosomal recessive transmission cannot *a priori* be excluded (for an example, see Section VI). This means that potential disease candidates encompass disorders such as *pili annulati*, *pili trianguli et canaliculi* (spun glass or uncombable hair), woolly hair, monilethrix, as well as numerous forms of hypotrichoses and nail diseases. Among these, monilethrix was a prime candidate, as previous ultrastructural studies of moniliform hair suggested a local degeneration of matrix cells of the hair bulb along with cytolysis and structural alterations of hair cortex cells, including disrupted keratin filament packing (De Berker *et al.*, 1993; Ito *et al.*, 1990). More importantly, several pedigrees of this disease had independently been linked to the type II epithelial and hair keratin gene domain on chromosome 12q13.13 (Healy *et al.*, 1995; Stevens *et al.*, 1996).

1. Monilethrix

Monilethrix (Latin/Greek, necklace hair; OMIM 158000 and 252200) was first described in 1879 as a new disease entity (Smith, 1879). The autosomal dominant transmission with high penetrance but variable expression of the disease was recognized soon after the condition was first identified, although in some cases evidence of autosomal recessive transmission has been reported (Baker, 1962). The hairs in monilethrix have a beaded appearance because of a periodic decrease in the diameter along the hair shaft. At the internodes the hairs easily break, leading to dystrophic alopecia, frequently associated with keratosis follicularis. Although the occiput is most frequently and severely affected, moniliform hairs have also been observed in the entire scalp, eyebrows, eyelashes, and body hairs. In addition, nail changes such as koilonychia have been described (Heydt, 1963).

Relying on the linkage of monilethrix to the type II keratin/hair keratin locus (Healy *et al.*, 1995; Stevens *et al.*, 1996), the gene regions encoding the helix initiation motif (HIM) and the helix termination motif (HTM) of type II matrix keratin hHb5 as well as type II cortex keratins hHb1, hHb3, and

hHb6 were analyzed for possible mutations. Indeed, in three unrelated families, two different types of causal mutations, E413K and E413D, in the HTM of type II hair keratin hHb6, as well as an HTM E413K mutation in type II hair keratin hHb1, could be detected (Winter *et al.*, 1997c). Due to discrepancies in the reported *hHb6* and *hHb1* gene sequences, these mutations were originally designated E410K (hHb6) and E403K (hHb1) (Winter *et al.*, 1998a).

After this, numerous families were investigated in which causative mutations were invariably restricted to the hHb6 and hHb1 keratins, thus indicating that monilethrix is a disease of the hair cortex. In both keratins, the HTM was the most mutated region (~87% in hHb6, 100% in hHb1), with a few HIM mutations (~13%) occurring only in the hHb6 keratin (Smith, 2003). Among the hHb6 mutations found, the nonconservative E413K substitution was by far the most frequent mutation, followed by the conservative E413D and the nonconservative E402K substitutions (Table I and references in Smith, 2003). Conversely, in the hHb1 keratin, mostly E402K mutations were found. Most probably, the change at the gene level responsible for the two E-K substitutions is promoted by a methylated CpG deamination mutation of a 5-methyl cytosine on the antisense strand of both genes, leading to a CG-to-CA transition in the sense strand (Winter *et al.*, 1997b).

Notwithstanding initial evidence (Winter *et al.*, 1997c), later investigations clearly excluded a genotype-phenotype correlation for any of the monilethrix mutations observed. One of the most impressive examples of the interfamilial

TABLE I
Hair Keratin Mutations Involved in Monilethrix^a

Gene	Mutation	α -Helical subdomain (mutation site)	Frequency
<i>hHb6</i>	E413K	1B	Most frequent
	E402K	1B	Frequent
	E413D	1B	Frequent
	E402Q	1B	Rare
	N114D	1A	Rare
	N114H	1A	Rare
	N118E	1A	Rare
<i>hHb1</i>	E402K	1B	Frequent
	E413K	1B	Rare

^aData are from Djabali *et al.* (2003), Horev *et al.* (2000, 2003), Korge *et al.* (1998, 1999), Muramatsu *et al.* (2003), Pearce *et al.* (1999), Winter *et al.* (1997b,c, 1998a, 1999, 2000), and Zlotogorski *et al.* (1998).

variability of the disease was noted in a pedigree in which the nonconservative hHb1 E402K mutation was associated in one child with a pronounced dystrophic alopecia, follicular keratosis, and clear-cut moniliform hair visible to the naked eye, whereas in another child, moniliform hair were detectable only by electron microscopy (Winter *et al.*, 1998a). Moreover, despite the presence of the E402K mutation, the mother's hairs virtually lacked moniliform symptoms even on electron microscopic inspection. However, the microscopic analysis of archival hairs, removed from the mother during early childhood, clearly revealed the beaded hair type (Winter *et al.*, 1998a). The epigenetic events underlying the highly variable expression of monilethrix are, at present, unknown. Interestingly, in a large 3-generation monilethrix family (comprising a total of 33 members, of which 22 were affected), Horev *et al.* (2000) observed 3 affected individuals who clearly exhibited the most severe clinical picture consisting of universal cicatricial alopecia and erythematous papules on the occipital scalp, arms, shins, back, and abdomen (especially around the navel). Mutational analysis revealed that in these cases the underlying conservative hHb6 E402D substitution occurred in both alleles, suggesting that the homozygous mutation in these individuals acted in a codominant manner.

Remarkably, up to now, no disease-related mutations in type I hair keratins could be detected. Moreover, a rough estimate of the monilethrix families investigated so far for hair keratin mutations revealed that about one-third of the families did not contain mutations in the *hHb6* and *hHb1* genes. In one monilethrix family that did not map to the 12q13.13 locus, analysis of the genes of a variety of other structural proteins or enzymes playing a role in hair shaft differentiation, such as type I keratins, trichohyalin, involucrin, ultrahigh sulfur KAPs, and transglutaminases, did not provide evidence of genetic linkage (Richard *et al.*, 1996). These data point to a genetic heterogeneity in monilethrix and imply that aberrations in genes other than type II cortex keratin genes can result in a similar hair phenotype. Conceptually, the most promising candidate genes should be found among members of the various KAP multigene families. The previous exclusion of the ultrahigh sulfur KAP genes on the two chromosome 11 loci (Richard *et al.*, 1996; Yahagi *et al.*, 2004) is not contradictory to this assumption, as these KAPs are all expressed in the hair cuticle (Rogers *et al.*, 2005). Similarly, genes of the numerous KAP families located on chromosome 17 can also be excluded, because their gene loci are part of the type I keratin/hair keratin gene domain (Rogers *et al.*, 2001). In contrast, those members of the KAP families on chromosome 21q22.1, which are expressed in the hair cortex (Rogers *et al.*, 2002), should be taken into consideration.

Whereas the typical intraepithelial blistering and tissue fragility of the large number of keratin diseases could ultimately be traced back to defects in the strength and resilience of IFs assembled from mutated keratins, it is

still completely unknown how mutations in hair cortex keratins are related to the striking periodicity of the node–internode formation along moniliform hair. There is no evidence of a similar periodicity in the growth rate or daily rhythm of normal and monilethrix hairs (Comaish, 1969) that could interfere with the expression of hair keratins. Likewise, the assumption that dystrophic cortical trichocytes, caused by the mutated hHb1 and hHb6 keratins, may give rise to a cytokine response that periodically modulates hair growth and a subsequent corrective response (Korge *et al.*, 1999) lacks experimental evidence.

2. Truncated Hair Keratin hHa1-t

Another mutational event that entailed dramatic changes in the structure of a hair keratin without, however, being associated with a visible hair phenotype, is worth mentioning. The issue, which was first reported in the late 1970s, relates to the observation that, sporadically, the one-dimensional electrophoretic resolution of keratin extracts of hairs from different individuals led to the occurrence of a small protein component appearing about 3–4 kDa below the type I hair keratin proteins, which collectively migrated at 48–44 kDa. A systematic analysis of this enigmatic 41-kDa protein revealed that it occurred in about 5% of the human population and that it was inherited by autosomal dominant transmission, thus indicating that the protein was encoded by a gene of its own (Winter *et al.*, 1997a). Our assumption that the 41-kDa protein might originate from a mutated type I hair keratin could be confirmed by analyzing the two most promising candidate genes, *hHa5* and *hHa1*, in individuals either positive or negative for the 41-kDa protein. Whereas the *hHa5* gene was unchanged, solely 41 kDa-positive individuals contained a heterozygous G → A mutation in the *hHa1* gene, which destroyed the 5' donor splice site of intron 6 and, instead, created a premature stop codon. The amino acid translation of the resulting aberrant hHa1 mRNA species yielded a truncated 42,290-Da hHa1 keratin that lacked the last amino acid leucine of the 2B α -helical subdomain as well as the complete nonhelical tail domain of hHa1. A recombinant hHa1-t protein clearly comigrated in sodium dodecyl sulfate (SDS) gels with the authentic 41-kDa protein. Moreover, *in situ* hybridization, using a riboprobe that contained hHa1-t-specific sequences from a retained intron 6 sequence stretch, clearly showed that the hHa1-t mRNA was expressed in the hair cortex of 41 kDa-positive, but not 41 kDa-negative, individuals. These data confirmed that the 41-kDa protein corresponded to the tailless hHa1-t hair keratin (Winter *et al.*, 1997a).

When both recombinant normal and truncated hHa1 proteins were assembled *in vitro*, using hair keratin hHb3 as a type II partner, the resulting filaments turned out to be indistinguishable. This indicated that the loss of

the hHa1 tail domain did not compromise the capacity of the truncated keratin to correctly assemble with a type II cortex keratin and thus helped to explain the absence of a hair phenotype in hHa1-t-positive individuals. Generally, this finding is in line with the notion that tail domains of type I keratins are not essential for proper filament formation (Winter *et al.*, 1997a). The absence of a visible hair phenotype in hHa1-t-positive individuals also speaks against a crucial role of the tail domain regarding lateral intermolecular interactions of the cysteine residues with both other hair keratin IFs or KAPs (Wang *et al.*, 2000).

B. Hair Follicle-Derived Tumors

Skin tumors of epidermal appendages can be divided into those originating from hair follicles, sebaceous glands, and apocrine or eccrine sweat glands. Basically, the numerous neoplastic proliferations with hair type differentiation arise either from the primary hair germ during embryogenesis or the secondary or telogen hair germ in the adult, that is, during conditions in which pluripotential cells set out to differentiate into the various cell lineages that built up the seven or eight tissue compartments of the mature anagen hair follicle. As each of the progenitor cells of these compartments may be a target for neoplastic transformation, a multitude of tumors potentially exhibiting morphological signs of a distinct follicular differentiation pathway can arise (Ackermann *et al.*, 1993; Schaumburg-Lever, 1975).

1. Hair Keratin Expression in Pilomatricomas

One of these tumors is the so-called pilomatricoma, a benign cystic neoplasm located mostly in the mid- to lower dermis with no obvious contact to the surface epidermis. Originally, this neoplasm was designated “calcifying epithelioma of Malherbe” and was thought to arise from sebaceous glands (Malherbe, 1880). After a convoluted histopathological path regarding its classification, the tumor is now considered to originate from the matrix cell compartment of the hair follicle. In its fully developed stage, a pilomatricoma consists mainly of peripheral basaloid cells, said to resemble matrical follicular cells through their monomorphous round nuclei with one or more distinctive nucleoli and variable numbers of mitotic figures. More inwardly, the basaloid cells transform into larger polygonal and less densely packed nonproliferative “transitional cells,” which eventually lose their nuclei and differentiate into cornified eosinophilic masses made up of “ghost” or “shadow” cells (Ackermann *et al.*, 1993; Forbis and Helwig, 1961). Collectively, the whole process is thought to reflect a faulty cortical differentiation toward hair, a view supported by similarities in the intensity and distribution of –SH

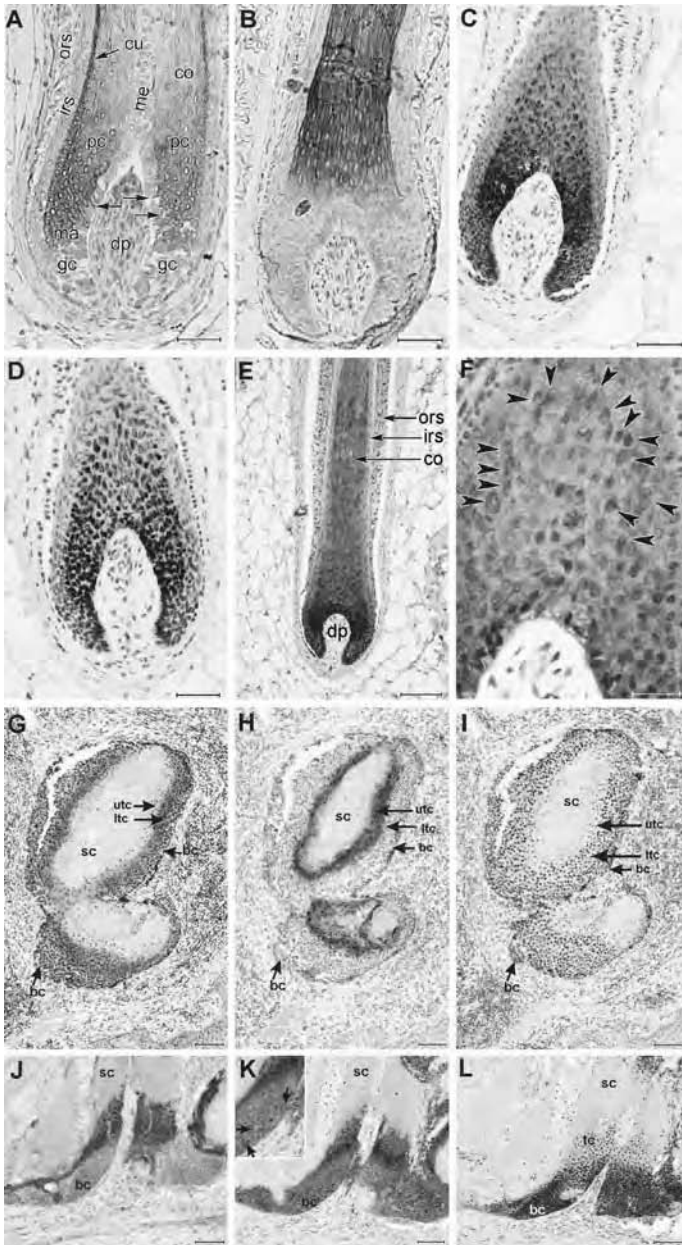


FIG. 9 Expression of hair keratins and transcription factors HOXC13, LEF1, and β -catenin in normal adult hair follicles and pilomatricomas. (A–F) Sections of formalin-fixed and paraffin-embedded normal scalp hair follicles and (G–L) pilomatricomas were stained with antibodies against (A) hHa5, (B) hHa1, (C) HOXC13, (D) LEF1, (E and F) β -catenin, (G) hHa5,

and –SS groups between shadow cell precursors and normal cells of the hair cortex (Hashimoto *et al.*, 1966). A particular feature of advanced pilomatricomas is the propensity of the shadow cell compartment to undergo calcification, eventually leading to a calcified and ossified nodule with no viable epithelial component being left (Ackermann *et al.*, 1993; Forbis and Helwig, 1961).

In line with the histopathological classification, out of a large collection of hair follicle-derived tumors (i.e., trichoepitheliomas, desmoplastic trichoepitheliomas, trichoblastomas, pilomatricomas, and basal cell carcinomas), only pilomatricomas turned out to express hair keratins. Whereas hair keratins were virtually absent from both the entire basaloid cell compartment and the shadow cell areas, they were strongly present in the intermittent transitional cell compartment. Remarkably, when hair keratins exhibiting sequential expression in the hair-forming compartment of the follicle, for example, hHa5 and hHa1 (Fig. 9A, B), were investigated in pilomatricomas, they strictly maintained the same sequence of expression in the transitional cell compartment of the tumors (Cribier *et al.*, 2001, 2004). Thus, the lowermost transitional cells above the basaloid compartment were positive for keratin hHa5 (Fig. 9G), the synthesis of which was followed by or slightly overlapped that of hHa1 in advanced transitional cells, up to their transformation into shadow cells (Fig. 9H). In pilomatricomas showing a particularly prominent transitional cell compartment, the late cortex keratin hHa4 could occasionally be demonstrated in the uppermost transitional cells in transit to shadow cell differentiation (Cribier *et al.*, 2001). Moreover, involucrin, which like hair keratin hHa1 is expressed in cortex cells of the hair follicle, specifically occurred in advanced transitional cells of pilomatricomas (Hashimoto *et al.*, 1987; Murthy *et al.*, 1993; Watanabe *et al.*, 1994).

All in all, a comparison of the expression sites of structural proteins in hair follicles and pilomatricomas suggests that lower transitional cells correspond to mid- to upper matrix cells of the hair follicle, whereas upper transitional cells represent cortex cell counterparts. This molecular assignment is clearly different from the traditional histological assignment of the various cell compartments in pilomatricomas and hair follicles, which correlated the cells of the basaloid compartment generally to hair matrix cells and the transitional cells to hair cortex cells (Ackermann *et al.*, 1993; Schaumburg-Lever, 1975). In our opinion, basaloid tumor cells represent the counterparts

(H) hHa1, (I) HOXC13, (J) hHa1, (K) β -catenin and (L) LEF1. Arrowheads in (F) indicate trichocytes in the precortex region exhibiting nuclear β -catenin expression. The small arrows in the *inset* of (K) denote basaloid cells of a pilomatricoma that express nuclear β -catenin. Abbreviations: ors, outer root sheath; irs, inner root sheath; co, cortex; cu, hair cuticle; ma, matrix; gc, germinative matrix compartment; dp, dermal papilla; me, medulla; bc, basaloid cells; tc, transitional cells; ltc, lower transitional cells; utc, upper transitional cells; sc, shadow cells. For further details, see Section III.B.1 and Cribier *et al.* (2004). (See also color insert.)

of the lowermost and keratin-free germinative cells of the hair matrix. This assumption is strengthened by the demonstration of both p63 and Ki67 expression in the highly proliferative germinative matrix cells of the hair follicle as well as in basaloid pilomatricoma cells (Tsujiya-Kyutoku *et al.*, 2003). Further evidence supporting this revised tissue correlation between the hair forming compartment and pilomatricomas is provided in Section IV.E.

2. Hair Keratin Expression in a Malignant Pilomatricoma

In addition to benign pilomatricomas, we also investigated the expression of keratins in a rare case of malignant pilomatricoma (Cribier *et al.*, 2005). This tumor was composed predominantly of basaloid cells exhibiting both extraordinarily high mitotic activity and prominent nuclear labeling for Ki67. Scattered throughout the mass of basaloid cells were numerous circular whorls and eddies of strongly varying size. These were surrounded by more or less broad areas of peripheral cell layers whose cells were distinctly less densely packed than the adjacent basophilic cells and thus resembled transitional cells of benign pilomatricomas. In contrast, typical shadow cells were only rarely seen as small foci; rather, the entire inner mass of the whorls consistently showed a massive and concentric parakeratotic keratinization. As expected, antibodies against hHa5 and hHa1 clearly reacted with the peripheral cells of the whorls, thus confirming their nature as transitional cells. Surprisingly, however, and in clear contrast to transitional cells of benign pilomatricomas, the same cells were also stained by antibodies against epidermal keratins K5, K14, and (most strongly) K17, with the latter also decorating the inner mass of the whorls. As there was also evidence of weak K1 expression in some peripheral cells, it appears that in this malignant pilomatricoma, the shadow cell differentiation pathway is almost entirely suppressed in favor of an epithelial-type keratinization pathway (Cribier *et al.*, 2005). Conceptually, the conspicuously changed differentiation process in the malignant pilomatricoma may represent a pathway that circumvents calcification of shadow cells and thus avoids “suicide differentiation,” which is generally the fate of untreated benign pilomatricomas (Ackermann *et al.*, 1993; Forbis and Helwig, 1961).

IV. Regulation of Hair Keratin Expression

In the preceding sections we have shown that differentiation of the hair involves the consecutive activation of an unprecedented high number of hair keratin genes from the lowermost up to the uppermost regions of the hair-forming compartment, and includes also extreme situations such as gene activation in only single cells. It is obvious that the regulatory control

mechanisms underlying this scenario must be of similar complexity, requiring the intervention of numerous, possibly interconnected, but also distinct signaling cascades. In the following sections, those factors for which at present evidence of a direct regulatory interaction with hair keratin genes exists, are presented in chronological order.

A. *Foxn1*

In 1962 and in more detail in 1966, an autosomal recessive mouse mutant, *nude* (symbol *nu*), was described, which failed to develop a postnatal hair coat and remained almost completely hairless in adulthood (Issacson and Cattanaach, 1962). Later it was shown that *nude* mice also suffered from thymic aplasia and severe immunodeficiency (Pantelouris, 1973). The *nude* locus could be mapped to chromosome 11 (Nehls *et al.*, 1994a) and the responsible gene was shown to belong to the winged-helix or forkhead family of transcription factors (Nehls *et al.*, 1994b). Originally designated *whn* (winged-helix-nude) or *hfh11* (hepatocyte nuclear factor 3/forkhead homolog 11), the gene has been renamed *Foxn1* (Forkhead box n1), according to a revised nomenclature of the members of the winged-helix/forkhead family (Carlsson and Mahlapuu, 2002; Kaestner *et al.*, 2000). The mutated *Foxn1* gene was shown to encode a protein that lacked both the DNA-binding and transcriptional activation domains (Schorpp *et al.*, 2000). Confirming its causal involvement in the hair anomaly, the *nude* phenotype could be completely rescued by a wild-type *Foxn1* gene (Cunliffe *et al.*, 2002). Moreover, the hairlessness of *nude* mice could be partly reverted by oral application of cyclosporin A (Sawada *et al.*, 1987) or, more efficiently, by subcutaneous or intraperitoneal administration of recombinant keratinocyte growth factor 7, KGF-7 (Buhl *et al.*, 1990; Danilenko *et al.*, 1995), as well as by oral, topic, or systemic application of the nontoxic tellurium compound AS101 (Sredni *et al.*, 2004). The human and murine *Foxn1* protein sequences are highly conserved (Schorpp *et al.*, 1997), and a homozygous loss-of-function mutation in the human *FOXN1* gene (the human *FOX* genes and proteins are usually given in capital letters) on chromosome 17 has been found to be linked with congenital alopecia, nail dystrophy, and severe T cell deficiency (Adriani *et al.*, 2004; Frank *et al.*, 1999).

Notwithstanding their apparent hairlessness, *nude* mice contain the same number of hair follicles as wild-type mice. However, these follicles form only thin hairs that tend to form coils in the isthmus of the follicle just below the epidermis, which they fail to penetrate. In the lower follicle, the hair cortex and, apparently, also the hair cuticle and the IRS are not formed properly and are much reduced in size (Flanagan, 1966; Köpf-Maier *et al.*, 1990). Together with the demonstration of weak *Foxn1* expression in uppermost

matrical and precortex cells, but strong expression in the lower to mid-cortex region as well as in the hair cuticle and the IRS of anagen hair follicles of normal mice (Lee *et al.*, 1999; Schlake and Boehm, 2001), this scenario suggested that the defects seen in *nude* mouse follicles might be due to failure of the mutated *Foxn1* to activate genes involved in cortex and IRS differentiation.

The first putative *Foxn1* target gene discovered was that encoding the type I hair keratin mHa3, whose mRNA was found to be virtually absent from pelage hair follicles of *nude* mice. In contrast, the extent of mRNA expression of the type I hair keratins mHa1 and mHa4 was reduced only by about 10–20% of normal levels (Meier *et al.*, 1999). A later study that included more members of the murine hair keratin family (mHa1, mHa2, mHa3, mHa4, and mHa5, and mHb3, mHb5, and mHb6) revealed that in *nude* mice, the expression of hair keratin mHa5 remained unaffected, that of mHa2, mHa1, and mHa4 was moderately reduced, and that of mHa3 and the three type II hair keratins was suppressed by the loss of *Foxn1* function (Schlake *et al.*, 2000). In line with this, using human HeLa cells which expressed *Foxn1* under the control of a tetracycline-sensitive promoter, Schlake *et al.* (2000) were able to show that the human type I hair keratin hHa3-II (but not its isoform hHa3-I), as well as the type II hair keratins hHb1, 3, 5, 6 were specifically activated in Foxn1-expressing cells.

On the basis of the expression patterns of the human orthologs of these keratins in the normal hair follicle (see Section II.B), the Foxn1-mediated hair keratin gene suppression characteristics of *nude* mice indicated that the completely suppressed hair keratins, that is, mHa3, mHb1, mHb3, and mHb6, were indeed those showing maximal overlap of expression with Foxn1 in the midcortex region, whereas those exhibiting partial suppression, that is, precortex keratin mHa1, cuticular keratin mHa2 and the late cortex keratin mHa4, displayed only partial overlap with Foxn1 expression. Although the strong suppression observed for the matrix to midcortex keratin mHb5 (Schlake *et al.*, 2000) would be an exception to this rule, the undisturbed expression of mHa5 in *nude* mouse follicles (Schlake *et al.*, 2000) would be particularly in line with the restriction of its active mRNA synthesis essentially to the matrix (Fig. 4E) (Langbein *et al.*, 1999). From this, it might be concluded that hair keratin genes *mHa3*, *mHb1*, *mHb3*, and *mHb6* represent true Foxn1 target genes in the hair follicle. In support of this, Schlake *et al.* (2000) were able to show that the human *hHa3-II* gene, which is the ortholog of *mHa3*, and which was upregulated in the inducible HeLa cell system, harbored an extended 10-bp Foxn1-binding element (core sequence, 5'-ACGC-3') in the first intron (Schlake *et al.*, 2000), which, however, deviated substantially from other Foxn1-binding sites (Kaufmann *et al.*, 1995; Overdier *et al.*, 1994; Pierrou *et al.*, 1994). The availability of the murine type I and type II hair keratin genes (Hesse *et al.*, 2004) now allows

investigation of whether the promoters of the type II cortex keratin genes *mHb1*, *mHb3*, and *mHb6* are also responsive to Foxn1.

B. LEF1/ β -catenin

Undoubtedly, the canonical Wnt signaling cascade represents one of the major regulatory pathways involved in the formation of the various types of epithelial appendages, that is, hair follicles, filiform tongue papillae, and teeth. Wnt signaling, which involves a series of membrane-bound as well as cytosolic intermediates, ultimately results in the stabilization of β -catenin, the mammalian homolog of *armadillo*, a segment polarity gene involved in the wingless signaling pathway in *Drosophila*. Most functions of β -catenin are supported by the structural organization of the protein: an amino-terminal domain that regulates protein stability through several serine-threonine phosphorylation sites; a central domain composed of armadillo repeats responsible for the interactions with various transcription factors, tumor suppressor genes, and signaling molecules; as well as amino- and carboxy-terminal domains with transcriptional regulation capacity. The lack of a defined DNA-binding domain in the β -catenin molecule is compensated for by binding to members of the Tcf/LEF1 family, thus leading to Tcf/LEF1 target gene activation (Cadigan and Nusse, 1997; Eastman and Grosschedl, 1999; Morin, 1999). It is a characteristic of the Wnt signaling cascade that its role in the formation of appendages is essentially 2-fold. During embryonic development, its multiple members are key players in the framework of the complex initiation phase of appendageal morphogenesis, but later they are also indispensable for the maintenance of the differentiated state of respective adnexal organ (Andl *et al.*, 2002; Fuchs *et al.*, 2001; Millar *et al.*, 1999; Nelson and Nusse, 2004; Niemann and Watt, 2002; Shimizu and Morgan, 2004; Thesleff, 2003).

In the literature, there are conflicting data regarding the experimental conditions ensuring the visualization of nuclear β -catenin in cells. Although there is evidence that, independent of the antibody used, nuclear β -catenin expression can best be revealed in formalin-fixed paraffin sections (Munné *et al.*, 1999), there are also a variety of reports demonstrating nuclear β -catenin expression in frozen tissue sections (DasGupta *et al.*, 2002; Merrill *et al.*, 2001; Niemann *et al.*, 2002). However, up to now, no protocols have been worked out that ensure reliable nuclear β -catenin demonstration either in paraffin or frozen sections.

Antibody studies in the adult human anagen hair follicle showed that membrane-bound β -catenin occurred in the entire ORS but not in the IRS, whereas it was both membranous and cytoplasmic in the entire hair-forming compartment from the germinative matrix area up to the late cortex (Fig. 9E).

An exception to this rule was a small population of precortex cells generally arranged in an arc or triangle above the dermal papilla, in which β -catenin was nuclear (Fig. 9F) (DasGupta *et al.*, 2002; Merrill *et al.*, 2001; Niemann *et al.*, 2002). Compared with β -catenin, its transcriptional activation partner LEF1 exhibited a rather uniform expression pattern in the anagen follicle that was virtually restricted to the nuclei of cells of the matrix (including those lining the dermal papilla), lower cuticle, and precortex. Characteristically, cells of the germinative matrix compartment of the follicle did not express visible amounts of LEF1 (Fig. 9D) (DasGupta and Fuchs, 1999; DasGupta *et al.*, 2002; Kobiela *et al.*, 2003; Merrill *et al.*, 2001).

From the resulting nuclear coexpression of LEF1 and β -catenin only in precortex cells (compare Fig. 9D and F), it was concluded that these downstream effectors of the Wnt signaling pathway are involved in the commitment of late hair matrix cells toward cortex differentiation by inducing the expression of precortical genes (DasGupta and Fuchs, 1999; Merrill *et al.*, 2001). Typically, most hair keratin genes as well as a variety of genes encoding hair keratin-associated proteins (KAPs) contain a LEF1 consensus binding site, 5'-CTTTGAAG-3', in their proximal promoter region (Rogers *et al.*, 1998, 2000; Zhou *et al.*, 1995). Moreover, studies in transgenic mice revealed that mutation of the LEF1-binding site in an ovine type II cortex keratin gene resulted in an apparent reduction of promoter activity (Dunn *et al.*, 1998). Further proof for precortex keratins being potential β -catenin/LEF1 target genes was provided by the demonstration that the promoter of the murine precortical keratin gene *mHal* could be activated *in vitro* by β -catenin and LEF1 in epidermal keratinocytes (Merrill *et al.*, 2001).

C. HOXC13

Another factor that was shown to be directly involved in the control of hair keratin expression belonged to the phylogenetically highly conserved *Hox* multigene family. The mammalian *Hox* genes, which are related to the *Drosophila* homeotic genes (the HOM-C complex) through a central 180-bp sequence encoding the so-called homeodomain, exhibit unusual features regarding both their genomic organization and their activation patterns during embryonic development. The 39 *Hox* genes in mouse and human are organized into four separate chromosomal clusters, *Hoxa* through *Hoxd*. On the basis of sequence homology and location within a cluster, the genes are further divided into 13 paralogous groups (Capecchi, 1997; Gehring *et al.*, 1994; Maconochie *et al.*, 1996). Besides sequence similarities, the temporal and spatial expression patterns of paralogous *Hox* genes are often similar. During embryogenesis, paralogous genes located at the 3' end of each cluster are activated first, whereas genes located nearer the 5' end are transcribed

progressively later. In addition, there is a spatial colinearity of position in a cluster such that members of successive paralogous groups display increasingly posterior limits of expression (Peterson *et al.*, 1994).

Thus, Hox proteins are transcription factors that are primarily involved in embryonic cell fate determination along the anterior–posterior body axis, but they also participate in patterning functions in structures such as limbs and epithelial appendages. Studies on the expression of *Hoxc13* during mouse embryogenesis showed that transcripts of this 5'-most gene of the *Hoxc* gene cluster were first seen on embryonic day 10.5 (E10.5) in the tail bud and the epithelia of the wrist and ankle regions of the limbs as well as in the developing foot pads and nails (Awgulewitsch, 2003; Godwin and Capecchi, 1998). Remarkably, however, at later embryonic stages, *Hoxc13* mRNA expression deviated from the concept of colinearity, as it also appeared in both vibrissae and all body hair follicles, in the filiform papillae of tongue epithelium, and in footpad epidermis. On postnatal day 7, as well as during each of the later hair cycles, *Hoxc13* transcripts occurred in the matrix and the precortical region of growing anagen hair follicles and could also be demonstrated at the base of the posterior unit of the filiform tongue papillae. Accordingly, besides defects in caudal tail vertebrae, *Hoxc13* null mice showed malformation of nails and filiform tongue papillae, and, notwithstanding normal-looking hair follicles, lacked vibrissae and pelage hairs because of the premature fracture of the hairs at the surface of the skin (Duboule, 1998; Godwin and Capecchi, 1998, 1999).

As in the mouse, most of these *Hoxc13*-expressing anatomical regions are also known sites of hair keratin synthesis (Dhouailly *et al.*, 1989; Winter *et al.*, 1994), and it has been hypothesized that *Hoxc13* might possess special functions in hair and filiform papilla development by being involved in the control of hair keratin gene expression (Duboule, 1998; Godwin and Capecchi, 1998). In line with this assumption, investigations in *Hoxc13*-overexpressing mice showed that a variety of hair follicle-specific genes were deregulated in these animals (Tkatchenko *et al.*, 2001). Our assessment of HOXC13 protein expression in human hair follicles confirmed its presence in cell nuclei of the hair matrix, cuticle, precortex, and, if present, the lowermost medulla. Outside the hair-forming compartment, HOXC13 occurred in the cuticle of the IRS and the companion layer (Jave-Suarez *et al.*, 2002). This study showed further that the onset of HOXC13 expression in the hair bulb occurred above the HOXC13-free germinative matrix cell compartment, that is, slightly below the midmatrix, including the cells lining the upper portion of the dermal papilla (Fig. 9C) (Jave-Suarez *et al.*, 2004). Thus, nuclear HOXC13 expression in the hair follicle completely overlapped with that of LEF1 (Fig. 9D). As these HOXC13 expression sites essentially matched those of hair keratins hHa5/hHb5 and hHa2/hHb2 (see Section II.B), the assumption that these genes might be HOXC13 target

genes appeared justified. Indeed, transient cotransfection experiments on *hHa5* and *hHa2* promoter constructs of decreasing length with a human HOXC13 expression vector showed that the proximal promoter region (~0.3 kb) of both genes was sufficient for optimal reporter gene activation. In contrast, no reporter gene activation occurred on cotransfection with a homeobox-deleted HOXC13 expression vector (Jave-Suarez *et al.*, 2002). It should be emphasized that the expression profiles of HOXC13 and its target keratin genes do not completely match, in that HOXC13 is already expressed in the K5/K14-positive ORS cells lining the dermal papilla (Fig. 9C), which, with the exception of a few positive cells, do not express hair keratin hHa5 (Figs. 9A and 4E, E'). It might be speculated that in line with the general property of *Hox* genes to determine cell fate during embryogenesis, in the adult hair follicle HOXC13 might commit the basal keratinocytes along the upper part of the dermal papilla to the trichocyte differentiation pathway.

While previous studies indicated that monomeric Hox1–8 protein preferentially binds to the DNA core motif TAAT, apparently Hox9–10 and in particular Hox11–13 proteins seemed to display a higher affinity for the TTAT or TTAC core motif (Ekker *et al.*, 1994; Shen *et al.*, 1997, 1999). The proximal *hHa5* and *hHa2* promoters contained copies of each of the three motifs. Electrophoretic mobility shift assay (EMSA) studies, combined with appropriate control experiments (use of a homeodomain-deleted HOXC13, specific/unspecific competition, and HOXC13 antibody-driven supershifts), clearly revealed that HOXC13 bound to TTAT but not to TTAC whereas, unexpectedly, the most frequent binding motif was TAAT (Jave-Suarez *et al.*, 2002). As the human HOXA13 protein also formed strong complexes with TAAT-containing oligonucleotides (J. Schweizer, unpublished data), this indicated that the DNA-binding specificity of *Hox9-13* members is obviously more variable than previously thought. A closer inspection of all HOXC13-binding TAAT and TTAT core motifs revealed that both required distinct flanking sequence conditions that ultimately allowed the deduction of an extended 8-bp consensus binding site $TT(A/T)ATN(A/G)(A/G)$ for HOXC13. While the T in position 1 and the A/G in position 8 were as mandatory as the two core motifs for HOXC13 binding, in one case a tolerance for T in position 7 was noted (Jave-Suarez *et al.*, 2002). All in all, the proximal *hHa5* and *hHa2* promoters contained four and two extended HOXC13 consensus sequences, respectively (core sequence frequency: *hHa5*, 3 × TAAT and 1 × TTAT; *hHa2*, 1 × TAAT and 1 × TTAT) (Fig. 10). Although it is not yet known whether there is a distinct hierarchy regarding the contribution of the four HOXC13-binding sites to activation of the *hHa5* gene, preliminary transfection data indicate that, independent of their core motifs, the two HOXC13-binding sequences of the *hHa2* promoter contribute equally to activation of the *hHa2* gene (J. Schweizer, unpublished results).

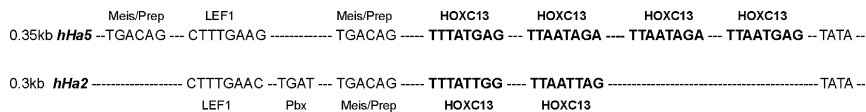


FIG. 10 Binding sites for HOXC13, Meis/Prep, Pbx, and LEF1 in the proximal promoters of type I hair keratin genes *hHa5* and *hHa2*. For details, see text (Section IV.C).

It has been shown that one way by which Hox proteins gain both affinity and functional specificity consists of their binding DNA together with distinct cofactors. At present, three Hox cofactors, Pbx, Meis, and Prep, all belonging to the so-called TALE (*three amino acid loop extension*) class of homeoproteins, have been identified (Berthelsen *et al.*, 1998; Fognani *et al.*, 2002; Haller *et al.*, 2002; Imoto *et al.*, 2001; Mann and Affolter, 1998; Moskow *et al.*, 1995; Nakamura *et al.*, 1996; Salzberg *et al.*, 1999; Smith *et al.*, 1997). Interestingly, the *hHa5* and *hHa2* promoters contain binding sites for both Meis and Prep, which are located upstream of the HOXC13 response elements (Fig. 10). Reverse transcription-polymerase chain reaction (RT-PCR) studies using mRNA from human anagen hair bulbs showed that transcripts of the *Pbx1-4*, *Meis1a*, *Meis1b*, and *Meis2* genes, as well as the *Prep1* and *Prep2* genes, were all present in the lower hair follicle. Preliminary IIF studies, using specific antibodies against these TALE proteins, revealed, however, that none of them exhibited nuclear coexpression with HOXC13 in the cuticle, matrix, and precortex of the human hair follicle. Instead, all of them were expressed in the IRS, except Prep1, which was found in nuclei of dermal papilla cells (J. Schweizer, unpublished data). It therefore appears that the Meis and Prep sites in the two hair keratin promoters are not functional.

D. Androgen Receptor

Of all the hair keratins, only type II hair keratin hHb4 and type I hair keratin hHa7 could not be detected by IIF in terminal scalp hairs (see Section II.B). Whereas hHb4 was found in the filiform tongue papilla (Fig. 5H-I), hair keratin hHa7 occurred in the center of the cortex of some of the small vellus hairs (Fig. 4H, H'), which constitute a minor hair population of the healthy human scalp (Montagna and Parakkal, 1974, pp. 172-258). In accordance with these tissue expression data, the hHa7 protein could initially not be demonstrated in a keratin extract of a terminal scalp hair sample by Western blotting. Surprisingly, however, the keratin was clearly demonstrable as an ~54-kDa protein in extracts of beard hairs (Langbein *et al.*, 1999), as well as in pubic or axillary hairs from both sexes (L. Langbein, unpublished data). Sexual hairs represent particularly coarse, strongly pigmented hairs, which all contain a medulla (Randall, 1994). IIF studies using the hHa7

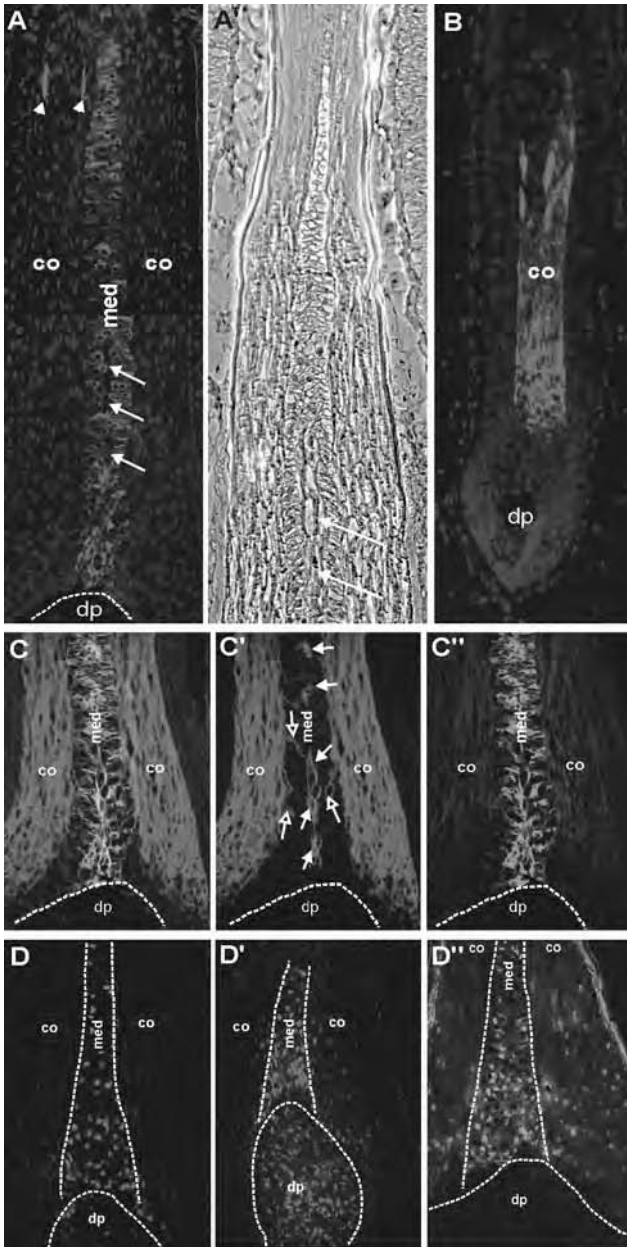


FIG. 11 Expression of hair keratin hHa7 and the androgen receptor (AR) in the medulla of hair follicles. Longitudinal cryosections of (A, A', and C'-D'') plucked human beard hair follicles and (B) a chimpanzee body hair. (A) IIF study with antiserum against hHa7. Note hHa7 expression in the entire medulla. The arrowheads indicate rare hHa7-positive cortex cells. The white arrows

antibody showed that this keratin was expressed—besides in the vellus hair cortex—in the medulla of sexual hairs (Jave-Suarez *et al.*, 2004). Its expression began directly above the dermal papillae, where the lowermost medulla cells have not yet adopted the typical horizontal orientation of later medulla cells, and continued to be expressed up to the height of the upper cortex region (Fig. 11A). Double-label IIF, using antisera against hHa7 and the cortex keratin hHa1, revealed that expression of the two keratins was mutually exclusive in the two tissue compartments (Fig. 11C, C'') (for further details of hHa7 and hHa1 expression in the medulla, see Section V.D). In humans, the coarse, strongly pigmented and medullated sexual hairs arise gradually during puberty from fine, uncolored vellus hairs that are devoid of a medulla. This “vellus-terminal hair switch” is precipitated by an increase in circulating androgens bound either to sex hormone-binding globulin or albumin (Kaufman, 1996; Randall, 1994; Stenn *et al.*, 1996). The intimate relationship between the androgen-dependent development of terminal sexual hairs and the concomitant formation of a medulla is exemplified by the observation that antiandrogenic steroid treatment of women suffering from idiopathic hirsutism drastically reduced the abnormal size of facial and body hairs, and also reduced their extent of medullation (Ebling, 1987). Collectively, this scenario suggested that the medulla-specific hHa7 expression in sexual hairs might be controlled by androgens.

Androgen-mediated gene expression implies the binding of the androgen to the androgen receptor (AR). Indeed, IIF studies on beard hair sections showed that this steroid hormone receptor was expressed in the nuclei of medulla cells (Fig. 11D–D''). A further prerequisite for AR-mediated gene expression is the presence of AR-responsive elements in the promoters of target genes, to which the receptor binds in dimeric form. A homology search for the semipalindromic AR consensus binding sequence 5'-GG (A/T)ACAnnnTGTTCT-3' (Roche *et al.*, 1992) revealed the presence of three putative androgen-responsive elements (ARE-1, ARE-2, and ARE-3)

denote vertically oriented hHa7-negative cells in the center of the medulla. These cells can also be seen in the phase-contrast micrograph of a beard hair follicle (A', white arrows). (B) Chimpanzee hair follicle stained for hHa7. Note the strong staining over the entire cortex. (A) and (B) were counterstained with DAPI. (C–C'') Double-label IIF study with antiserum against hHa7 (green) and antiserum against the cortex keratin hHa1 (red). Note the laterally oriented hHa1-positive cortex cells extending into the medulla [open arrows in (C')]. Also note that the vertically oriented cells in the center of the medulla exhibit strong hHa1 expression (closed arrows), but faintly coexpress hHa7 in a patchy manner [merged yellow in (C)]. (D and D') IIF study with an antibody against the AR on two different beard hair follicles. Note the strong nuclear AR expression in medullary cells, variable expression in the dermal papilla cells, and faint background staining in cortex cells. (D'') Double-label IIF study with antibody against the AR (green) and antibody against hHa7 (red). For abbreviations, see the caption to Fig. 4. For further details, see Section IV.D and Jave-Suarez *et al.* (2004). (See also color insert.)

in the *hHa7* promoter. Compared with the ARE consensus sequence, the putative *hHa7* AREs deviated mainly in their second half: ARE-3 differed in three positions, whereas ARE-1 and ARE-2 differed in four positions. In addition, ARE-1 exhibited a G → A change in the second position of the first half. EMSA studies, combined with appropriate control experiments (use of oligonucleotides containing mutated versions of the three AREs, specific/unspecific competition, and AR antibody-driven supershifts), clearly demonstrated AR binding to each of the *hHa7* AREs (Jave-Suarez *et al.*, 2004). Their function as AR-responsive elements, either individually or in concert within the *hHa7* promoter, could be further established by transfection studies with or without an AR expression vector in the presence or absence of a synthetic androgen. Both types of transfections confirmed that the most distal element, ARE-3, exhibiting the least deviation from the ARE consensus sequence, contributed most to gene activation. Furthermore, the complete insensitivity of the *hHa7* promoter to androgens in AR-transfected cells, observed after the specific deletion of the three ARE sequences, definitely characterized them as functional AR regulatory elements (Jave-Suarez *et al.*, 2004).

The identification of *hHa7* as an androgen-regulated gene in medullary cells of human sexual hairs bears several consequences. Although previous investigations on AR expression in human hair follicles of various body sites differed considerably regarding the occurrence of the receptor in the ORS, they were generally consistent about its expression in the specialized fibroblasts of the dermal papillae (Blauer *et al.*, 1991; Choudhry *et al.*, 1992; Hodgins *et al.*, 1998; Kimura *et al.*, 1993; Liang *et al.*, 1993). This particular AR expression pattern has led to the current concept that androgen actions in the hair follicle proceed predominantly via hormone–receptor complex-mediated alterations of gene expression in dermal papilla cells, leading to paracrine factors that appropriately modify gene expression and properties of both follicular trichocytes of the hair-forming compartment and keratinocytes of the root sheaths. Examples for such paracrine factors are insulin-like growth factor (IGF-I) and transforming growth factor β_1 (TGF- β_1) (Inui *et al.*, 2003; Itami *et al.*, 1995; Philpott *et al.*, 1994). Our study has, however, clearly shown that androgen-controlled gene expression in sexual hairs is not limited to the dermal papilla, but that androgens can also affect target genes in a subpopulation of follicular trichocytes that during puberty are committed to embark on the medullary pathway.

It cannot be excluded that after AR induction, further transcription factors might be involved in the control of medullary *hHa7* expression. We were able to show that in beard hairs, HOXC13 was present in the nuclei of matrix, precortex, and also lower medulla cells. Besides the *hHa2* and *hHa5* genes, this transcription factor also activated the *hHa7* gene through binding to a HOXC13 response element in its proximal promoter (Jave-Suarez *et al.*,

2002). Whether an LEF1 site in the *hHa7* promoter (Rogers *et al.*, 1998) is functional *in vivo* is questionable, as there is no evidence of LEF1 expression in the medulla of human hair elements (Jave-Suarez *et al.*, 2004). Moreover, although the three *hHa7* AREs were fully preserved in the promoter of the chimpanzee ortholog of the *hHa7* gene, its expression in the mid- to upper cortex of androgen-independent body hairs of this species (Fig. 11B) showed that the gene is not necessarily androgen dependent and that, obviously, its sensitivity to androgens has been acquired during the evolution of the human lineage.

The identification of medullary hHa7 as a molecular marker for androgen action on human hairs requires comment on the initial observation of sporadic hHa7 expression in a medulla-like structure within the cortex of vellus hairs of the human scalp (see Fig. 4H). These vellus hairs constitute a minor hair population of the healthy human adult, and also the infant scalp. It has been observed that juvenile vellus hairs become rare in late puberty, suggesting that they are transformed into terminal hairs. Indicating the reverse pathway, vellus hairs slowly reappear in the twenties and then seem to remain constant in the healthy adult scalp (Montagna and Parakkal, 1974). On the basis of their timing, it is reasonable to assume that these processes occur under the influence of androgens. This would imply that, besides in vellus hairs, hHa7 expression should also be sporadically seen in adult terminal scalp hairs, either originating from the observed vellus–terminal hair switch or representing the targets of its later reversal. Indeed, contrary to our initial findings in a few adult terminal hair samples, we were able to show by a large-scale hHa7 Western blot analysis of keratin extracts of 70 terminal hair samples, including those removed from the occiput of individuals of both sexes, that hHa7 was present in variable amounts in about 10% of these hair samples (L. Langbein and J. Schweizer, unpublished data). The presence of a small vellus and terminal hair population in the normal human scalp, apparently kept in equilibrium by androgens, bears considerable significance regarding the gradual follicular miniaturization during androgenetic alopecia. It would therefore be interesting to further investigate hHa7 expression patterns in the various hair types of the scalp during and after puberty as well as in various stages of androgenetic alopecia.

E. Synopsis

The proper formation of hair in the postnatal hair follicle requires not only that the various spatially defined cell lineages leading to the development of the hair shaft be specified correctly according to a mediolateral positioning in the hair matrix, but also that the subsequent proliferation and differentiation processes be coordinated along the proximal–distal axis of the follicle. In the

following, the function of the chronologically described transcription factors is considered in the framework of a model that, on the basis of investigations in mice carrying a conditional ablation of the bone morphogenetic protein (BMP) receptor 1A (Andl *et al.*, 2004; Kobiela *et al.*, 2003; Kwan *et al.*, 2004), proposes a highly orchestrated network of signaling pathways intended to control hair shaft differentiation in the postnatal hair follicle. Central to this model is the assumption that after the dermal papilla-induced formation of hair shaft progenitor cells, a paracrine noggin signal from the dermal papilla leads to an inhibition gradient of BMP signaling along the proximal–distal axis of the lower hair follicle. This gradient is thought to induce nuclear LEF1 expression, probably along with that of other transcription factors, but by still unknown mechanisms, prevents matrix cells from becoming sensitive to Wnt signaling through the LEF1/ β -catenin complex, thus keeping them in an undifferentiated state (Kobiela *et al.*, 2003; Kwan *et al.*, 2004; Plikus *et al.*, 2004).

Although this concept is consistent with our finding that matrix and lower cuticle cells coexpress nuclear LEF1 and, in addition, HOXC13 (see Fig. 9C, D), the concomitant strong expression of hair keratins hHa2/hHb2 and hHa5/hHb5 in these cells (see Figs. 4D', E' and 5D', E') unequivocally speaks against an undifferentiated state of these cells. Rather, it clearly demonstrates the early onset of a first phase of hair shaft differentiation in matrix and cuticle cells. Despite the presence of LEF1-binding sites in the promoters of the early hair cuticle and matrix keratin genes (Fig. 10) (Rogers *et al.*, 1998, 2000), the apparent absence of nuclear β -catenin makes it unlikely that canonical Wnt signaling is involved in their expression control. Rather, we have provided strong evidence that the expression of these hair keratins is under the control of *Hoxc13* (Jave-Suarez *et al.*, 2002), which seems to regulate its own expression by a negative feedback mechanism, substantiated by the presence of *Hoxc13*-binding sites in its proximal promoter (Sander and Powell, 2004; Tkatchenko *et al.*, 2001).

According to the proposed model, the gradual attenuation of the noggin-mediated BMP signaling inhibition during the upward movement of matrix cells is accompanied by a likewise gradual decrease in LEF1 expression (Kobiela *et al.*, 2003). On the basis of immunohistochemical data (DasGupta *et al.*, 2002; Merrill *et al.*, 2001; Niemann *et al.*, 2002), the authors argue that, obviously, a window of differentiation exists in the precortex region where cells become able to stabilize nuclear β -catenin and still contain sufficient amounts of LEF1 to activate Wnt-mediated genes such as *hHal* (Merrill *et al.*, 2001). Therefore, the present data suggest that, basically, a noggin-mediated and subtly orchestrated interplay between BMP and Wnt signaling leads to the sequential activation of transcription factors, which in turn regulate the sequential expression of differentiation markers in the hair-forming compartment of the postnatal hair follicle.

Whereas *Hoxc13* seems to play a crucial role in early differentiation events in the matrix, Wnt signaling apparently initiates both a second wave of differentiation in the precortex region, that is, hHa1 induction, as well as the activation of further transcription factors such as *Foxn1* (Balciunaite *et al.*, 2002), *Hoxc12* (Shang *et al.*, 2002), and *movo1* (Li *et al.*, 2002), which then drive cortical cells into terminal differentiation. In keeping with this, binding sites for LEF1, *Foxn1*, and Hox proteins have been identified in the genes of both type I and type II cortex keratins as well as in a large number of hair keratin-associated proteins (KAPs) expressed in the cortex (Rogers *et al.*, 1998, 2000, 2001, 2002; Schlake *et al.*, 2000; Zhou *et al.*, 1995).

We noticed that in pilomatricomas, the conservation of sequential expression of matrix keratin hHa5 and precortex keratin hHa1 in lower and upper transitional cells, respectively (Section III.B.1 and Fig. 9G, H), appears to be only partially regulated according to the model proposed for the postnatal hair follicle. While the matrix keratin hHa5 remained strictly coexpressed with nuclear HOXC13 in lower transitional cells (compare Fig. 9G, I), the subsequent onset of hHa1 expression in upper transitional cells (Fig. 9H) no longer coincided with the nuclear localization of LEF1 and β -catenin, seen in the normal hair follicle (compare Fig. 9C, D). Instead, β -catenin was essentially cytoplasmic in upper transitional cells (Fig. 9K), in which it was coexpressed with hHa1 (Fig. 9J), while nuclear LEF1 was specifically shifted into the hair keratin-free basaloid cell compartment (Fig. 9L), where nuclear coexpression of β -catenin/LEF1 was visible in only a small population of the basaloid cells of the tumors (*inset* in Fig. 9K). These data imply that, unlike in the hair follicle, in pilomatricomas both cortex-like differentiation and sequentially correct hHa1 expression are no longer under the control of Wnt signaling. As the vast majority of pilomatricomas contain mutations in the *CTNNB* gene (Chan *et al.*, 1999; Kajino *et al.*, 2001; L. Langbein and J. Schweizer, unpublished results), the function of Wnt signaling in the tumors has most probably been changed from differentiation control to the maintenance of autonomous tumor growth, thus disrupting the noggin-mediated fine tuning with BMP signaling, operating in the normal follicle (Kobielak *et al.*, 2003). At present, it is not known which mechanisms keep hHa5 expression under HOXC13 control in pilomatricomas and how spatially correct hHa1 expression is maintained in the absence of nuclear β -catenin and LEF1.

V. Epithelial Keratins of the Hair Follicle

The central hair-forming compartment of the hair follicle, which has been the topic of the preceding sections, is concentrically surrounded by several epithelial layers that are clearly distinguishable from each other by their

morphology and type of differentiation. From outward to inward, these layers have classically been divided into the outer root sheath (ORS), which is contiguous with the epidermis, and the inner root sheath (IRS), which by itself consists of three morphologically well-defined tissue layers, the Henle layer, the Huxley layer, and the cuticle of the IRS, the latter being apposed to the hair cuticle (Fig. 2B). The ORS constitutes a single-layered epithelial sheath as long as it surrounds the lowermost hair bulb and encases the dermal papilla, but slightly above the height of the line of Auber (Auber, 1952), that is, the greatest width of the hair bulb, it becomes gradually multilayered along the proximal–distal axis. The mostly cuboidal cells of this multilayered portion of the ORS, which usually contain large amounts of glycogen deposits in their cytoplasm, exhibit horizontal differentiation without, however, showing signs of keratinization. An exception to this rule is the uppermost ORS at the height of the isthmus and the infundibulum, which exhibit trichilemmal- and epidermal-type differentiation, respectively (Hashimoto, 1988; Ito, 1988; Pinkus, 1969; Sperling, 1991). Of the three tissue components of the IRS, the outermost Henle layer and the innermost IRS cuticle are essentially a one-cell layer, whereas the central Huxley layer comprises two or even three rather unstructured layers, depending on the size of the follicle. In the hair bulb region, the progenitor cells of all three layers are morphologically similar, but slightly above; both Henle cells and IRS cuticle cells gradually adopt a vertically elongated form while Huxley cells remain essentially cuboidal. In this region, first the Henle layer and soon after the Huxley layer, but not the IRS cuticle, show signs of differentiation as revealed by the production of numerous trichohyalin granules. Subsequently, the Henle layer is the first to abruptly keratinize from one cell to the next at the suprabulbar level, followed by the IRS cuticle in the midcortex region and the Huxley layer above the level of the keratogenous zone. In human hair follicles, the three layers are gradually sloughed off into the hair canal at the level of the isthmus, with the IRS cuticle and the Huxley layer being lost in the midportion and the Henle layer in the upper portion of the isthmus (Hashimoto, 1988; Ito, 1988, 1990; Langbein *et al.*, 2002b; Montagna and Parakkal, 1974; Sperling, 1991).

On the basis essentially of electron microscopic studies, a number of earlier studies doubted this classic division of follicular epithelial sheaths by questioning the homogeneous nature of ORS cells. Indeed, in contrast to the bulk of the cuboidal ORS cells, which exhibit a homogeneous cytoplasmic distribution of IFs, the innermost ORS cells, apposed to the Henle layer, generally display a flattened appearance and strongly accumulate IFs in the portion of the cytoplasm that faces Henle cells. These IFs always run transversely against the long axis of the hair follicle, thus surrounding the IRS like the hoops of a barrel. Further studies led Orwin and Ito, respectively, to dub this particular layer the “companion layer” or “innermost cell layer of the ORS,”

with “companion layer” being the currently used designation (Ito, 1986; Orwin, 1971; Rogers, 1964). In the following sections, the epithelial keratins that are expressed in the ORS, the companion layer (CL), and the three layers of the IRS of the human anagen hair follicle are described. Although it might appear misplaced at first glance, as a special case, this description also includes mixed epithelial and hair keratin expression in the medulla, that is, the innermost trichocyte structure of the hair-forming compartment, which, unlike the other tissue components, distinguishes itself by its variable occurrence in human hair follicles.

A. Keratins of the ORS

In line with being a continuation of the interfollicular epidermis, the keratin pattern in the orthokeratinizing infundibular ORS is similar to that of the latter, except that it first loses suprabasal K2e expression, followed by that of K1/K10 (L. Langbein, unpublished data), but instead acquires suprabasal K6 and K17 expression (Kurokawa *et al.*, 2002).

In this context it should be mentioned that K6 is unique among keratins in that several active *K6* genes have been described in humans, mice, and bovines. Initially, evidence was provided that humans may have as many as seven active *K6* isoforms (Takahashi *et al.*, 1995), but more recent studies have clearly shown that the human genome contains only three active *K6* genes, *K6a*, *K6b*, and another gene, tentatively termed *K6e* or *K6h*, whose final designation has yet to be agreed on (Hesse *et al.*, 2004; Rogers *et al.*, 2004b). Whereas K6a is the major keratin of the ORS, K6b is apparently expressed only in reduced amounts and has been found mainly in the sebaceous duct epithelium (Smith *et al.*, 1998).

A K5/K14 and K6/K16, K17 pattern is found in the isthmus and the entire portion of the lower, multilayered ORS of the human hair follicle with K5/K14 being, however, found throughout the full thickness and length of the ORS. This pattern changes below the suprabulbar level when the ORS loses its multilayered structure and, together with the loss of K6/K16/K17 expression, is converted into a K5/K14-positive one-layered sheath (Heid *et al.*, 1988b; Kopan and Fuchs, 1989; Lynch *et al.*, 1986; Stark *et al.*, 1987; Winter *et al.*, 1998b).

It should be noted that the expression of K6, K16, and K17 in mouse hair follicles is different from that in human hair follicles. Whereas whisker follicles exhibit the same ORS keratin pattern as human hair follicles, the ORS of pelage hair follicles below the infundibulum completely lacks expression of the K6, K16, and K17 keratins (Bernot *et al.*, 2002; McGowan and Coulombe, 2000; Panteleyev *et al.*, 1997; Rothnagel *et al.*, 1999; Tong and Coulombe, 2004). Instead, these keratins are found only in the companion

layer of these hair follicles (see below). A further difference between mouse and human is the existence of an mK17-related keratin, mK17n, whose gene is located immediately 5' to the *mK17* gene at one end of the murine type I keratin gene domain and whose human counterpart appears to be a pseudo-gene. mK17n is only weakly expressed in the companion layer of both mouse vibrissae and pelage hair follicles; its main expression site has been found in the ventral nail matrix and the nail bed, in which mK17 is expressed to a much lesser degree (Hesse *et al.*, 2004; Tong and Coulombe, 2004).

Further keratins expressed in the ORS of human hair follicles are K15 and K19. Investigations with various K15 antibodies were slightly inconsistent in that some detected the keratin mainly in stem cells of the bulge whereas others decorated the entire basal layer of the ORS, except for the isthmus, but including the infundibulum and continuing in the basal layer of the interfollicular epidermis (Lloyd *et al.*, 1995; Lyle *et al.*, 1998; Porter *et al.*, 2000). The isthmus was also K15 negative in sheep wool follicles analyzed by *in situ* hybridization (Whitbread and Powell, 1998). The *mK15* promoter has been used to target mouse bulge cells with the enhanced green fluorescent protein (EGFP) in order to isolate hair follicle stem cells (Morris *et al.*, 2004). Except for a patchy reaction in the interfollicular epidermis, various antibodies against K19 led to a similar expression pattern in the outermost layers of the lower ORS around the hair bulb and in the region below the isthmus and the sebaceous gland duct (Asada *et al.*, 1990 (in Japanese); Commo *et al.*, 2000; Gho *et al.*, 2004; Heid *et al.*, 1988b; Michel *et al.*, 1996; Stasiak *et al.*, 1989).

In contrast to the ORS, considerable time passed before special keratins of the companion layer (CL) and the IRS were revealed. Although it had been shown that a monoclonal antibody, HKN-5, raised against total proteins of human hair follicles, reacted specifically with the upper portion of the CL, the nature of the antigen remained obscure, in particular as further down the antibody lost its specificity and also decorated the cells of the IRS and the hair cortex (Ito *et al.*, 1986a,b). The first evidence of a defined keratin expressed in the CL came from investigations in mouse pelage hairs, in which an antibody against murine K6a reacted specifically with CL cells, but not with ORS cells (Rothnagel and Roop, 1995; Rothnagel *et al.*, 1994). Considerable progress has, however, been made regarding the identification of CL and IRS keratins.

B. Keratins of the Companion Layer

In an attempt to elucidate new members of the human type II human hair keratin subfamily, we identified a novel type II epithelial keratin that comprised 251 amino acids and showed the highest sequence homology with K5,

but shared an almost identical calculated molecular weight with K6a/b. Using an antibody against the novel keratin, we could show by one- and two-dimensional Western blots that the protein was specifically present in keratin extracts of the ORS–CL–IRS fraction and indeed migrated at the same height as K6, but clearly exhibited a distinctly more acidic isoelectric point on two-dimensional separation (Winter *et al.*, 1998b). In a precedent case, in which a newly characterized keratin of the human palate epithelium, exhibiting the highest sequence homology with corneal keratin K3, but almost identical gel mobility with epidermal keratin K2e, was designated K2p (Collin *et al.*, 1992b), we named the new keratin K6hf, with *hf* indicating its specificity for the hair follicle (Winter *et al.*, 1998b), ignoring at that time the existence of further hair follicle-specific keratins. The gene for human K6hf was found to be located between the *K6b* gene and the hair keratin pseudogene ϕHbA of the type II keratin gene domain on 12q13.13 (Rogers *et al.*, 2000). mK6hf, the murine ortholog of hK6hf, has also been characterized (Wojcik *et al.*, 2001).

Both *in situ* hybridization and IIF studies showed that K6hf was specifically expressed in the CL of anagen hair follicles. The onset of K6hf mRNA and protein expression clearly occurred in the lowermost outer matrix cells, in which both K6hf transcripts and protein could virtually be demonstrated almost down to the beginning of the invagination of the dermal papilla (Fig. 12A, A'). Unlike K6hf mRNA, K6hf protein could be visualized along the entire CL up to the lower isthmus of the hair follicle (Winter *et al.*, 1998b), thus confirming earlier ultrastructural studies on the differentiation of the CL (Ito, 1986). In accordance with the previous demonstration of K6 expression in the CL of the murine hair follicle (Rothnagel and Roop, 1995; Rothnagel *et al.*, 1994), human K6 (results not shown) as well as the type I keratins K17 and K16 could also be localized in the human CL. Whereas the onset of K17 expression was demonstrable down to the line of Auber (Fig. 12B) (Auber, 1952), that of K16 occurred slightly above the height at which the ORS widens (*merged yellow* in Fig. 12C). Initially, the apparent absence of type I keratin synthesis in the CL below the line of Auber raised a question concerning whether K6hf might have a specific type I partner of its own. However, completion of the human type I epithelial and hair keratin domain on 17q21.2 did not provide evidence of the existence of a novel CL-specific type I keratin (Hesse *et al.*, 2004; L. Langbein and J. Schweizer, unpublished results). Therefore, there is every reason to believe that K17, whose presently available antibodies are obviously not sensitive enough to reveal its entire expression pattern along the CL, represents the type I partner of K6hf in the CL. Thus the assymmetrically located IFs accumulating in CL cells are formed by four keratins, with K6hf identifying this single-layered structure (which does not express the typical ORS keratins K5 and K14) as an independent tissue compartment of the hair follicle

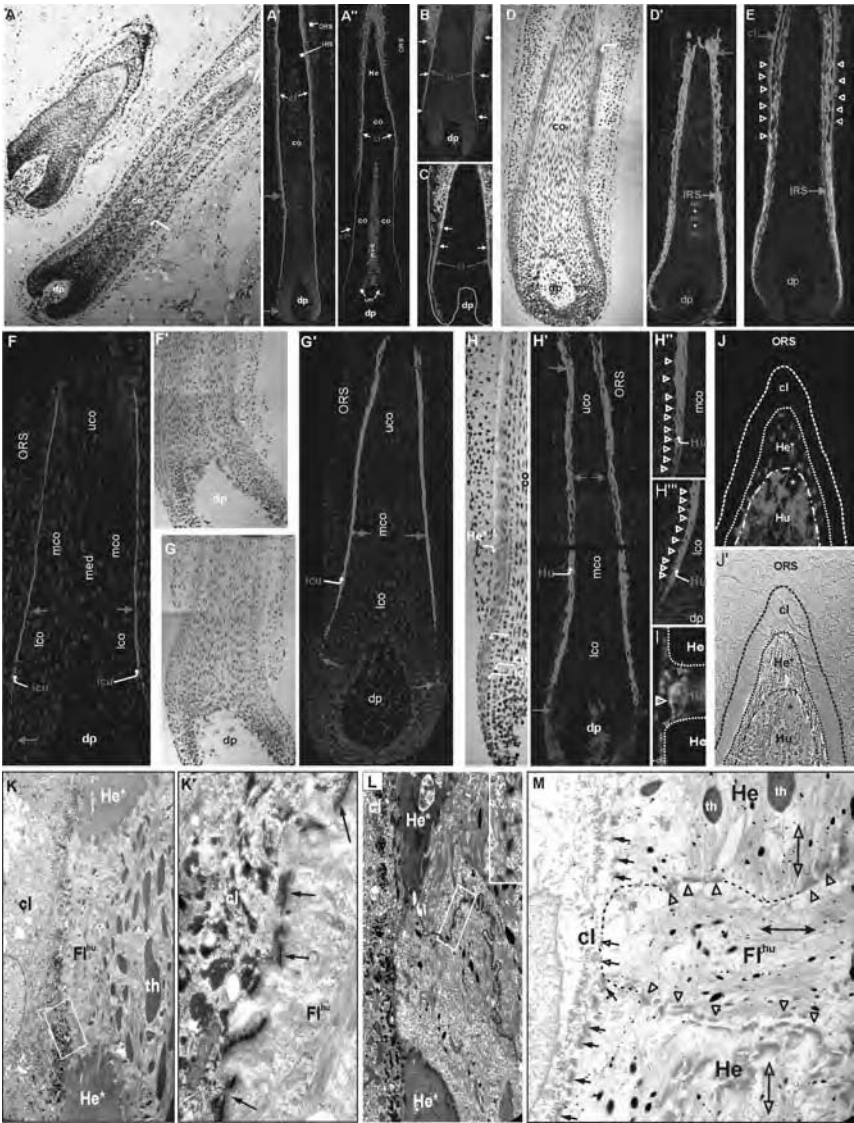


FIG. 12 Keratin expression in the companion layer and the IRS of the hair follicle. (A–C) Expression of K6hf, K16, and K17 in the companion layer, CL. (A) K6hf (ISH); (A') K6hf (IIF, scalp follicle); (A'') K6hf (IIF, beard hair); (B) K17 (IIF; note the expression in the CL and suprabasal cells of the multilayered ORS); (C) double-label IIF with antibodies against K6hf (red) and K16 (green, merged yellow). (D–J') Expression of type II IRS keratins. (D) K6irs1 (ISH); (D') K6irs1 (IIF); (E) double-label IIF with antibodies against K6hf (red) and K6irs1 (green). The arrowheads indicate *Flügelzellen* abutting on the CL. (F) K6irs3 (IIF); (F') K6irs3 (ISH); (G) K6irs2 (ISH); (G') K6irs2 (IIF); (H) K6irs4 (ISH); (H') K6irs4 (IIF); (H'') K6irs4

(Winter *et al.*, 1998b), instead of being the “innermost layer of the ORS” as assumed previously.

Subsequent studies showed that besides being expressed in the hair follicle, K6hf, together with K17, is also expressed in the nail bed of the murine and human nail unit (Rogers *et al.*, 2004c; Wang *et al.*, 2003; Wojcik *et al.*, 2001). Moreover, K6hf has been found in mouse tongue epithelium, in which, unexpectedly, it was not present in the filiform papillae, but instead occurred in lateral portions of the fungiform papillae (Wang *et al.*, 2003). Collectively, these data indicate that K6hf expression, apparently together with K17, is generally restricted to highly specialized subcompartments of epithelial appendages. A further, unusual expression site of the K6hf–K17 pair in the medulla of the hair follicle is discussed in Section V.D.

C. Keratins of the IRS

Although evidence of the presence of IFs in IRS cells of sheep wool follicles had already been provided in 1959 (Rogers, 1959), the long-lasting uncertainty and confusion regarding the constituent keratin proteins is mirrored by the striking number of quite heterogeneous keratins (i.e., K1, K4, K5, K6,

(IIF, height of the keratinized Henle layer); (H^{'''}) K6irs4 [IIF, height of the unkeratinized Henle layer; the arrowheads in (H^{''}) and (H^{'''}) indicate *Flügelzellen*]. (J) K6irs4 (IIF, oblique cross-section through a hair follicle). Note the rather uniform staining of the cells of the Huxley layer (Hu) and the occurrence of multiple K6irs4-positive, mostly oval structures in the differentiated Henle layer (He*), representing extensions of *Flügelzellen*. (J') Phase-contrast micrograph of (J). Asterisks in (J) and (J') indicate focal loss of tissue during sectioning. Red arrows in (A'), (F), and (G') indicate the zone of mRNA synthesis of the respective keratin. (I) Double-label IIF with antibodies against K6irs4 (red) and ezrin (green). The arrowhead denotes the tip of a *Flügelzell* process, actively passing through the Henle layer and abutting on the CL. (K–M) Electron microscopic study of *Flügelzellen*. (K) *Flügelzell* process (F^{1hu}) between two fully keratinized Henle cells (He*), contacting a CL cell (cl); (K') higher magnification of the boxed area in (K), showing numerous desmosomal connections (arrows) between a *Flügelzell* process (F^{1hu}) and a CL cell (cl); (L) two *Flügelzellen* (F¹ and F²) between two fully keratinized Henle cells (He*), both contacting a CL cell (cl). *Inset* at top: A higher magnification of the boxed area, showing numerous desmosomal connections between the two *Flügelzellen*. (M) A *Flügelzell* process (F^{1hu}, dotted line) that extends through two incompletely keratinized Henle cells (He) and has reached a companion layer cell (cl). Note the numerous desmosomal connections between the *Flügelzell* process and the Henle cells (triangles) as well as between Henle and CL cells (small closed arrows), whereas only rare desmosomal connections are visible between the *Flügelzell* process and the Cl cell (small open arrows). Also note the vertically oriented IF bundles in the Henle cells (open double arrows) compared with the horizontally oriented IF bundles in the *Flügelzell* process (closed double arrow). (A), (B), (D'), (E), (F), (G'), and (H'–H^{'''}) were counterstained with DAPI. Abbreviations: lco, lower cortex; mco, midcortex; uco, upper cortex; th, trichohyalin; for other abbreviations, see the caption to Fig. 4. (See also color insert.)

K7, K10, K13, K16, and K18) that, essentially on the basis of early immunohistochemical studies, have all tentatively been assigned to the IRS (Heid *et al.*, 1988b; Kopan and Fuchs, 1989; Krüger *et al.*, 1996; Lynch *et al.*, 1986; Schirren *et al.*, 1997; Stark *et al.*, 1990; Wilson *et al.*, 1994). With the possible exception of K7 (Schon *et al.*, 1999; Smith *et al.*, 2002), these data have, however, not been substantiated.

The first report on IRS-specific keratins was provided in 2001 by Bawden *et al.*, who described four type I keratin genes named *oIRSa1*, *oIRSa2*, *oIRSa3.1*, and *oIRSa3.2*, as well as three functional orthologs *hIRSa1*, *hIRSa2*, and *hIRSa3.1* in humans. *In situ* hybridization studies clearly showed that the genes were expressed in the IRS of sheep wool and human hair follicles, with the respective transcripts being visible from the lowermost bulb up to a region fairly beyond the keratogenous zone of the follicle. The method did not, however, allow any determination concerning whether the various keratins were specific for distinct layers of the IRS (Bawden *et al.*, 2001). The murine orthologs of *oIRSa1*, *oIRSa2*, and *oIRSa3.1* have been elucidated, and antibodies raised against *mIRSa2* and *mIRSa3-1* demonstrated the expression of these keratins in all three layers of the IRS (Porter *et al.*, 2004).

Also in 2001, Aoki *et al.* reported on the identification of a mouse type II IRS keratin, which seemed to be specific for the Henle and Huxley layers of the IRS (Aoki *et al.*, 2001). Like the companion layer keratin K6hf (Winter *et al.*, 1998b), the murine IRS keratin also ran at the height of K6 in one-dimensional gels, and was designated *mK6irs* (Aoki *et al.*, 2001). In 2002, our group identified the human ortholog of *mK6irs*, which we named *hK6irs1* (Langbein *et al.*, 2002b) and 1 year later, we characterized three further human IRS keratins, *hK6irs2*, *hK6irs3*, and *hK6irs4* (Langbein *et al.*, 2003). It should be noted that *hK6irs2* had already been discovered in 2001 by Porter *et al.*, who, at that time, however, assumed this keratin to be the human ortholog of *K6irs1* (Porter *et al.*, 2001). The *hK6irs1*, *hK6irs2*, *hK6irs3*, and *hK6irs4* genes are subclustered within the type II keratin gene domain on chromosome 12q13.13 (see also Fig. 3B) and flanked by the genes for keratins K2e and K5, respectively (Langbein *et al.*, 2003).

Although the head and rod domains as well as the H2 regions of all four type II IRS keratins were highly homologous, each of them exhibited a specific penultimate tail sequence from which suitable peptide sequences could be used to raise keratin-specific antibodies. Detailed ISH and IIF studies revealed that each of the human type II IRS keratins displayed an expression pattern of its own. Thus, *hK6irs1* was clearly expressed in all three IRS layers (Fig. 12D, D') (Langbein *et al.*, 2002b), and thus differed from its murine counterpart, which could be detected only in the Henle and Huxley layers (Aoki *et al.*, 2001). In contrast, both *hK6irs3* (Fig. 12F, F') and *hK6irs2* (Fig. 12G, G') were sequentially expressed in the IRS cuticle, whereas *hK6irs4* was strictly confined to Huxley cells (Fig. 12H, H') (Langbein

et al., 2003). Remarkably, both hK6irs1 mRNA and protein expression in the three IRS layers began simultaneously in three adjacent, well-discernible cells of the lower matrix region and also terminated simultaneously in the suprabulbar region, exactly at those sites that, morphologically, corresponded to the sharply demarcated areas of terminal differentiation in the three layers (Langbein *et al.*, 2002b). Also, synthesis of the cuticular hK6irs2 and hK6irs3 proteins, as well as the Huxley layer-specific hKirs4 protein, could generally be discerned up to the zone of terminal differentiation; however, each of them exhibited a different onset of expression along the lower IRS. Thus, similar to hK6irs1, hK6irs3 synthesis began low down in a single cell of the matrix region (Fig. 12F, F'), followed by hK6irs4 at the height of the line of Auber (Fig. 12H, H') and finally by hK6irs2 slightly above (Fig. 12G, G'). On the basis of the data on type II IRS keratins, it is interesting to note that, compared with Henle and Huxley cells, the distinctly smaller IRS cuticle cells expressed the highest number of IRS keratins. This appears plausible considering that these cells are subject to considerable mechanical constraints when tightly interacting with the cells of the hair cuticle during the upward journey of the growing hair.

The hK6irs1 antibody revealed a striking feature of Huxley cells, which faced the fully keratinized and thus unstained Henle cells. At seemingly regular intervals, we observed Huxley cells that exhibited externally directed cell extensions through adjacent terminally differentiated Henle cells along the upper portion of the hair follicle. Double-label IIF studies (Fig. 12E), using the hK6irs1 antibody (*green*) and the antibody against the CL-specific keratin K6hf (*red*), clearly demonstrated that the hK6irs-positive Huxley cell extensions abutted on CL cells (*arrowheads* in Fig. 12E) as long as Huxley cells were accessible to the hK6irs1 antibody (Langbein *et al.*, 2002b).

The history of this particular type of Huxley cell goes back to 1840, when Henle discovered regularly spaced "slits and holes" in carefully prepared sheets of the outermost IRS layer (Henle, 1840). Subsequently, it was found that these openings were due to cell extensions of neighboring Huxley cells, which at that time were thought to end at cells of the ORS (Ebner, 1876). Relying on a proposal by Waldeyer (1882), Hoepke (1927) coined the name *Flügelzellen* (i.e., *winged cells*) for these Huxley cells.

The K6irs1 antibody did not allow the visualization of *Flügelzellen* in the undifferentiated and therefore K6irs1-positive lower portion of the Henle layer (Fig. 12E). This handicap could, however, be overcome by means of the Huxley layer-specific K6irs4 antibody (Fig. 12H, H'), which clearly revealed the typical cell processes of *Flügelzellen* not only in the differentiated Henle layer (*arrowheads* in Fig. 12H''), but also along its undifferentiated portion down to the level of the line of Auber (*arrowheads* in Fig. 12H'''). The demonstration of *Flügelzellen* in the differentiated portion of the Henle layer could also be achieved by means of the hK6irs4 antibody, using sections

from weakly oblique cuts through the hair follicle; as long as the cut went through the Huxley layer, the antibody produced homogeneous staining of the cells, but once the differentiated Henle layer was traversed this homogeneous staining was abruptly replaced by a multitude of mostly spindle-shaped, K6irs4-positive structures of varying size, which undoubtedly represented the sectioned protrusions of *Flügelzellen* passing through the Henle layer (Fig. 12J, J'). It is obvious that the K6irs-positive structures corresponded to the "holes" previously observed by Henle (1840) in separated sheets of the outermost IRS layer. All in all, our data indicated the existence of an extremely dense and regular network of *Flügelzell* protrusions intercalated into the entire Henle cell layer.

Earlier ultrastructural studies suggested the formation of "gap junction-like" structures between the trichohyalin-containing cell processes of *Flügelzellen* and the Henle cells between which they pass (Clemmensen *et al.*, 1991). More recently, however, we showed that most of these structures were positive for occludin and claudins, thus indicating that they represent functional tight junctions or tight junction-related structures that, as such, are part of the skin barrier system (Langbein *et al.*, 2002a). Moreover, we could unambiguously demonstrate that particularly prominent desmosomes were also formed between the *Flügelzellen* and CL cells (Fig. 12K), where dense IF bundles, concentrated at the side facing Henle cells and running perpendicular to the long axis of the hair follicle, terminated at particularly thick desmosomal plaques, whose counterparts in *Flügelzellen* were much less developed and hooked to a less prominent, vertically oriented IF network (Fig. 12K').

Remarkably, we frequently noticed protrusions of two or even more *Flügelzellen* actively passing through the Henle layer (Fig. 12L). As there was evidence that some of these composed cell extensions originated from Huxley cells that were located more internally toward the IRS cuticle, it cannot be excluded that the propensity to develop these structures may be a general feature of all Huxley cells (Langbein *et al.*, 2002b). On occasion, however, we observed below the differentiated Henle layer *Flügelzellen* that had formed desmosomal connections with Henle cells between which they were sandwiched, but not or not yet with the facing CL cells. Because in those cases the cell processes contained horizontally oriented streams of IF bundles (Fig. 12M), most probably these cell processes were just beginning to extend. In general, cell motility and the formation of cell processes are based on activities of local assemblies of actin and actin-binding proteins, such as ezrin, profilin, and debrin, which accumulate at the leading edges of lamellipodia and filopodia as well as in cytoplasmic processes of a variety of other cells (Peitsch *et al.*, 2001). Indeed, a double-label IIF study (Fig. 12I) with the K6irs4 antibody (*red*) and an antibody against ezrin (*green*) showed that ezrin was most strongly expressed at the very tips of the *Flügelzell* processes.

What is the function of *Flügelzellen*? We and others have previously proposed that the CL and the three IRS compartments form, around the hair-forming compartment and the hair shaft, a functional tissue unit that is aimed at properly molding and guiding the growing hair (Ito, 1989; Langbein *et al.*, 2002b, 2003; Winter *et al.*, 1998b). To fulfill this task, this CL–IRS unit not only must be strong enough, but also flexible enough to respond to, and to withstand, both vertical and lateral forces constantly exerted on the skin and transmitted to the adnexal organs. Because of its comparatively early and strong terminal differentiation, most of the Henle layer would be composed of heavily keratinized, rigid cells, whereas the surrounding CL as well as the Huxley and IRS cuticle layers still contain fully viable and flexible cells. It is evident that such an immobile central layer would considerably reduce the overall flexibility of the proposed unit, if its rigidity were not substantially attenuated by the intercalation of a myriad of viable, firmly anchored, hinge-like structures. Most probably, the active penetration of *Flügelzellen* into the Henle layer occurs as long as Henle cells are still undifferentiated and exert less resistance to their separation. It cannot be excluded that this early process represents a highly dynamic scenario that is subject to a continual opening and reforming of cell connections during the ascendance of the cells. However, once the Henle layer becomes terminally differentiated, the desmosomal connections of *Flügelzellen* might become sealed, thus optimally adapting the CL–IRS unit to its supposed function until its degradation in the isthmus. Provided that *Flügelzellen* also serve to enable the selective diffusion of nutrients through tight junctions along the upper part of the hair shaft (Clemmensen *et al.*, 1991; Langbein *et al.*, 2002a; Zaun, 1968), their cell processes undoubtedly would represent one of the most remarkable devices of the hair follicle.

D. Keratins of the Medulla

The medulla of mammalian hair represents a vertical cell column in the center of the hair cortex, which begins directly above the apex of the dermal papilla. Morphologically, it consists of large, loosely connected cells that are arranged horizontally in a ringlike fashion between the vertically oriented cortex cells. Moreover, medullary cells become wedged between lateral cell projections obviously originating from the adjacent cortical cells (Mahrle and Orfanos, 1971 [in German]; Montagna and Parakkal, 1974). Indeed, we were able to show that these lateral cells express cortex keratin hHa1, but not medullary hair keratin hHa7 (Section IV.D; Fig. 11C, C').

It should, however, be noted that, in addition to hHa1-positive cortex cells that extend laterally into the medulla of beard hairs, the latter also contains hHa1-positive cells in its center, which, in addition, show a weak and patchy

hHa7 expression (Section IV.D; Fig. 11C, C'). In contrast to the horizontally oriented cortex cells, these particular cells are arranged vertically and exhibit the typical spindle-shaped form of cortex cells. It is most probable that these cells with essentially cortical properties have partially escaped the molecular signals that, in the course of the gradual transformation of facial vellus hairs into terminal beard hairs during puberty, switched the commitment of the basal trichocytes above the apex of the dermal papillae from a cortical to a medullary program of differentiation (Jave-Suarez *et al.*, 2004).

When almost fully formed, cells of the medulla develop large intra- and intercellular spaces filled with air, which provide insulating capacities to animal hairs. This function has largely been lost in humans, who invariably possess medullated hairs only in the bearded face area as well as in the axillary and pubic regions. In contrast, the frequency of medullated scalp hairs varies considerably depending on gender, age, and ethnicity, with Caucasian scalp hairs being consistently less medullated than Negroid or Asian hairs (Montagna and Parakkal, 1974; see also Section IV.D).

It is remarkable that early electron microscopic studies, as well as X-ray and biochemical analyses, suggested the occurrence of only a few, if any, α -keratins in medullary cells of human hair (Mahrlé and Orfanos, 1971; Rudall, 1947; Swift, 1969). Rather surprisingly, subsequent IIF studies, aimed at investigating the presence of epithelial keratins in the hair follicle by means of antibodies recognizing a broad range of these keratins, suggested the presence of both types of epithelial keratins in medullary trichocytes of human hair. Whereas an antibody against keratin K19, which clearly reacted with the basal layer of the ORS (see Section V.A), also detected single cells in the medulla of human hairs (Heid *et al.*, 1988b), the presence of K19 could not be confirmed in the strongly medullated mouse hairs (Stasiak *et al.*, 1989). In later studies, however, keratins K17 and (to a lesser extent) K16 were shown to represent type I epithelial keratins in the medulla of murine hair (Bernot *et al.*, 2002; McGowan and Coulombe, 1998, 2000, 2002; Panteleyev *et al.*, 1997). As, however, neither K5 nor, more importantly, K6 could be found (McGowan and Coulombe, 2000), the nature of the corresponding type II keratin(s) in the medulla remained unelucidated. This question could be solved by the unexpected finding that keratin K6hf, originally thought to be specific for the keratinocytes of the companion layer of the hair follicle (Winter *et al.*, 1998b), was strongly coexpressed with K17 in the medulla of murine pelage hairs and human beard hairs (Fig. 12A') (Wang *et al.*, 2003; L. Langbein and J. Schweizer, unpublished data).

Only more recently could the impression be corrected that the medulla, as an intrinsic structure of the hair-forming compartment, might express only epithelial keratins. The first trichocytic keratin explicitly expressed in the hair medulla is the androgen-dependent type I hair keratin hHa7 of human

sexual hairs (Jave-Suarez *et al.*, 2004). As already mentioned in Section IV.D, the medullary expression of hHa7 in sexual hairs represents a special property of humans, whereas other primate species, which do not develop androgen-dependent hairs, express this keratin in the hair cortex (Fig. 11B) (Jave-Suarez *et al.*, 2004). However, a careful rescreening of our studies on hair keratin expression in human hairs provided evidence that, besides hHa7, beard hairs expressed type I hair keratins hHa3, hHa4, and hHa6 as well as type II hair keratins hHb1, hHb3, hHb5, and hHb6 in their medulla (Table II) (Langbein *et al.*, 1999, 2001; L. Langbein, unpublished results). It is, however, clear that a separate study is needed to gain insight into the full spectrum of medullary hair keratins.

Collectively, these data show that, of the multiple tissue compartments of the hair follicle, the medulla is unique in that its constituent cells coexpress epithelial and hair keratins. The reason for this particular property is unknown, although it may be speculated that the presence of “soft” keratins in medullary trichocytes could facilitate the typical septation of this tissue compartment. It has not yet been investigated whether epithelial and hair keratins in medullary cells form separate IF networks. Previous studies have, however, shown that at least *in vitro*, hHa1 as well as its tailless version hHa1-t (see Section III.A.2) are able to form normal-looking IFs with epithelial type II keratin K8 (Hofmann *et al.*, 2002; Winter *et al.*, 1997a). Moreover, the forced expression of either a murine type I or type II hair keratin in HeLa cells led to their incorporation into the existing soft IF network of epithelial keratins, provided the hair keratins were not overexpressed (Yu *et al.*, 1991).

E. Synopsis

In the preceding sections we have described the expression of epithelial and hair keratins in the various tissue compartments of the anagen hair follicle. Whereas the ORS as the outermost layer is continuous with the interfollicular epidermis, the seven inner layers or compartments (CL, Henle and Huxley layers, and IRS, and hair cuticle, cortex, and medulla) all arise in the lower half of the hair matrix, the so-called germinative matrix, which contains a population of keratin-free, rapidly dividing cells (Fig. 13A), although it is not uncommon to detect dividing cells also higher up, mainly in the region ascending along the boundary to the dermal papilla (Wang *et al.*, 2003; Weinstein and Mooney, 1980). The epithelial and hair keratins synthesized in the various tissue layers enabled the localization of the respective precursor cells at their transition in the germinative matrix to their destined differentiation pathway. Thus the antibody against K6hf detects the precursor

TABLE II
Preliminary Data on Keratins Expressed in Hair Medulla^a

Epithelial keratins			
Type I		Type II	
Name	Area of expression	Name	Area of expression
K16	Lower medulla	K6	Lower medulla
K17	Entire medulla	K6hf	Entire medulla
Hair keratins			
Name	Area of expression	Name	Area of expression
hHa1	Vertical cells in the center of the medulla and in cortex cells extending laterally into the medulla ^b	hHb1	Upper medullary cells
Ha3	Upper medullary cells	hHb3	Expression similar to hHa1, but only in upper medullary cells
Ha4	Entire medulla	hHb5	Lowermost medullary cells and in upper cortex cells extending into the medulla
Ha6	Entire medulla	hHb6	Upper medullary cells
hHa7	Entire medulla		

^aStrongly expressed keratins are given in boldface letters.

^bSee Fig. 11C, C'.

cells of the single-layered CL low down, near the invagination of the dermal papilla (Fig. 13A). Internally apposed to the CL, but visibly displaced outwardly, the clearly staggered origin of the three IRS layers can be detected by the antibodies for K6irs1, K6irs4, and K6irs3. The precursor cells of both the single-layered IRS cuticle, specifically revealed by the antibody against K6irs3, and the likewise single-layered hair cuticle, detected by the antibodies against hair keratins hHa2 or hHb2, are the first that, relative to those of the Henle and Huxley layers, tend to be located more inwardly. This change of direction is continued by the precursor cells of the hHa5- and hHb5-expressing midmatrix cells, which extend inwardly and then ascend along the single-layered ORS lining the dermal papilla (Fig. 13A).

Finally, in sexual hairs, antibodies against hHa7, K6hf, and K17 detect the precursor cells of the medulla around the apex of the dermal papilla

(Fig. 13A). Collectively, these data indicate that the progenitor cells of the various concentric tissue compartments circumscribe an essentially S-shaped germinative matrix that, however, does not completely overlap with the area of mitotically active cells in this area (Wang *et al.*, 2003; Weinstein and Mooney, 1980), suggesting that the earliest progenitor cells of each layer still possess the capacity to divide. This elaborate and dynamic scenario of cell fate determination and specific tissue differentiation in the lower bulb region of the postnatal hair follicle is continuously sustained by stem cells originating from the bulge region and migrating downward through the ORS (Alonso and Fuchs, 2003; Turksen, 2004) (Fig. 13A). Conceptually, it is assumed that once the stem cells contained in the single-layered lower ORS reach the lowest point of the bulb, their daughter cells migrate into the germinative matrix and establish a pool of transiently amplifying cells in the germinative matrix as demonstrated by the expression of transcription factor p63, which is thought to be associated with stem cells and their conversion into transiently amplifying cells (Alonso and Fuchs, 2003; Parsa *et al.*, 1999; Pellegrini *et al.*, 2001; Tsujita-Kyutoku *et al.*, 2003). Remarkably, unlike stem cells, this transiently dividing cell reservoir remains unstained with virtually any of the known epithelial and hair keratin antibodies, suggesting that whatever keratins are expressed in stem cells, their synthesis is obviously arrested and their IF network is degraded among the “dedifferentiated” stem cell progeny.

There is, however, a critical region that ascends along the wall of the dermal papilla (*black arrow* in Fig. 13A). As shown in the inset of Fig. 5E' and in Fig. 9A, in this area, hHa5/hHb5-expressing matrix cells arise directly from the K5/K14-positive ORS layer (Fig. 13A) without the demonstrable occurrence of a keratin-free transitional cell population. The same observation holds true for the area around the apex of the dermal papilla (*open arrows* in Fig. 13A), out of which the precursor cells of the medulla arise. A plausible explanation for this may be that a rather large population of transiently dividing cells in the germinative matrix cell compartment is needed in order to allow the generation of the CL-IRS unit, the hair cuticle, and the prominent differentiated matrix, whereas the vertically ascending stem cell reservoir in the ORS lining the dermal papilla, as well as that around the apex of the dermal papilla, contributes only to the lateral supply with differentiating matrix cells and the vertical generation of medulla cells, respectively (Fig. 13A), so that its transiently dividing cell population may remain essentially undetectable.

Last, but not least, our detailed analysis of keratin expression in the various tissue compartment of the hair follicle made it possible to define all of them at the molecular level by means of specific members of the epithelial or hair keratin families (Fig. 13B).

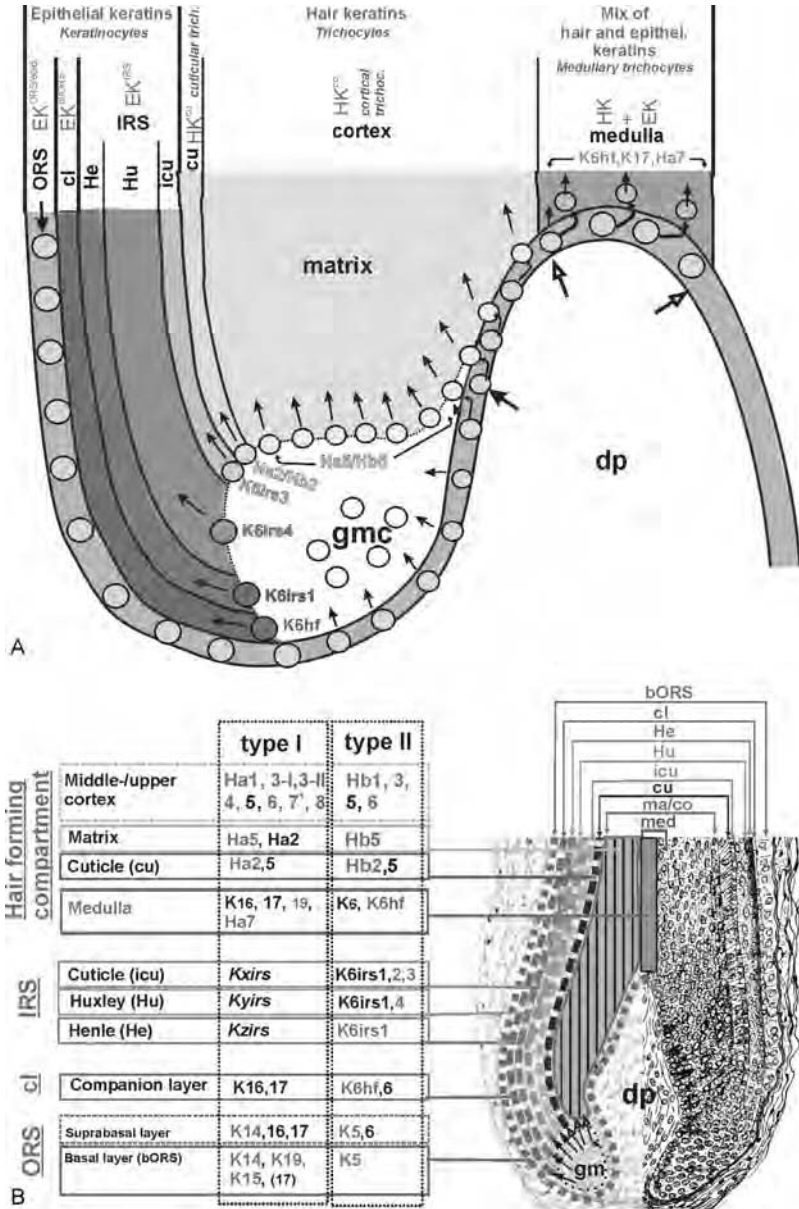


FIG. 13 Cell lineage differentiation and summary of epithelial and hair keratin expression in the hair bulb. (A) Cell lineage differentiation. The various tissue compartments are indicated by different colors. Stem cells in the single-layered lower ORS (green) are marked in light green. Transiently dividing cells in the germinative matrix compartment (gmc), which are negative for keratins, are given in white. Keratins whose antibodies specifically detect the precursor cells of

VI. Keratin Pathologies of the ORS, CL-IRS Unit, and Medulla

As indicated in Section V.A, all ORS cells of the human hair follicle express the keratin pairs K5/K14 and K6a,b/K16, and K17 in the multilayered ORS portion. Intriguingly, however, even strongly disruptive mutations in *K5* or *K14*, leading to epidermolysis bullosa simplex (EBS), do not produce a visible hair phenotype. Similarly, mutations in the *K6a/K16* or *K6b/K17* genes are primarily causal for the nail bed disorders pachyonychia congenita (PC) type 1 and type 2, respectively, with only PC-2 patients exhibiting occasional signs of twisted hairs (*pili torti*) in the presence of *K17* mutations (Smith, 2003). Remarkably, while *mK17* null mice develop a severe, but reversible, hair loss in a strain-dependent fashion, nail lesions have not been observed in these mice (McGowan *et al.*, 2002). Most probably this is due to the presence of an additional keratin gene, *mK17n*, in the mouse genome (Hesse *et al.*, 2004), which is strongly expressed in the nail matrix and bed and may compensate for the loss of mK17 (Tong and Coulombe, 2004). At present, the reason why the ORS of the human hair follicle pertinaciously withstands keratin mutations that are fatal for other epidermal locations remains unclear.

On the other hand, shortly after elucidation of the IRS-specific keratins (see Section V.C), hereditary hair disorders were found that could be attributed to mutations in one of these keratins. Thus, Peters *et al.* (2003) described a new autosomal recessive mouse mutation, RCO3, which was characterized by severe alopecia in homozygotes, whereas heterozygous animals were phenotypically normal. The disorder developed postnatally and the alopecia became apparent by the time of the second hair cycle. All types of body hairs were malformed and could be plucked without force. Ultrastructurally, normal IF bundles were absent from the severely disturbed Henle and Huxley layers, whereas those of the cells of the IRS cuticle appeared normal. Positional cloning revealed a 10-bp deletion in exon 1 of the type II *mK6irs1* gene, which in mice is expressed in these layers of the IRS (Aoki *et al.*, 2001; Porter *et al.*, 2001). The resulting protein would consist of 58 amino acids of the mK6irs1 head domain plus 76 amino acids with no sequence homology to keratins, thus prohibiting its ability to participate in IF assembly. Because of the lack of an appropriate antibody, it could not be excluded that the

the various tissue compartments in the gmc are indicated. For the meaning of the closed and open arrows, see text (Section V.E). (B) Summary of epithelial and hair keratins of the hair follicle. Keratins expressed in the various tissue compartments are indicated on the left-hand side. Keratins that are specific for a given tissue compartment are given in red. ⁷¹, expression of the hair keratin in Ha7 vellus hairs. The drawing of the follicle was modified from Bucher (1968). (See also color insert.)

truncated mK6irs1 protein might exert a concentration-dependent effect on IF formation, but taking into account the recessive inheritance of the ROC3 phenotype and the normal appearance of RCO3 heterozygotes, the authors favored the theory that RCO3 represents a loss of function owing to mK6irs1 deficiency. Although mK6irs1 represents the only type II keratin in the Henle layer, apparently, the absence of mK6irs1 protein in the Huxley layer (Fig. 12D') could not be compensated for by the concomitant expression of mK6irs4 (Fig. 12H'). The observation of a morphologically undisturbed IRS cuticle would be in line with the finding that, unlike human K6irs1, its murine counterpart is not expressed in the IRS cuticle (Aoki *et al.*, 2001).

Further mutations in the *mK6irs1* gene with, however, autosomal dominant transmission, and entailing a quite different hair phenotype, were described in mouse mutant *Ca^{Rin}*, whose hairs resembled those of the classic wavy coat mutation *caracul* (*Ca*). Ultrastructurally, the mutant follicles showed severe disturbances of the IRS structure and keratinization. Analysis of the *mK6irs1* gene in *Ca^{Rin}* mice as well as in five independent *Ca* alleles revealed two mutational hot spots consisting of either a 3-bp deletion in the first exon leading to an Asp deletion in the 1A helix, or to a point mutation generating a Leu → Trp substitution in the 2B helix of the mK6irs1 keratin (Kikkawa *et al.*, 2003). Both studies demonstrated that K6irs1 is indispensable for the proper formation of the IRS and that its loss or mutation compromises the correct molding and guidance of the growing hair.

Up to now, *K6irs1* mutations or mutations in other IRS keratin genes have not yet been reported in humans. Interestingly, however, it has been found that the human hair disorder hypotrichosis simplex of the scalp (HSS), an autosomal dominant form of isolated alopecia, is also due to IRS damage. HSS patients exhibit normal scalp hair early in childhood but gradually lose them in the middle of the first decade and experience almost complete baldness in later life. In contrast, body hair, beard, eyebrows, axillary hair, pubic hair, and nails are not visibly affected. Causative mutations for HSS were found in the corneodesmosin gene (Levy-Nissenbaum *et al.*, 2003), which encodes a protein expressed in the corneodesmosomes of the late stages of epidermal differentiation as well as in the Henle and Huxley layers of the IRS and, if present, the medulla of hair follicles (Gallinaro *et al.*, 2004).

In view of the tight connection of the IRS with the companion layer (see Section V.B and V.C), conceptually, mutations in the CL keratin K6hf should *a priori* also produce a hair phenotype. It is evident that the loose anagen hair syndrome (LAH) might be one of the candidate diseases, as mutations in the *K6hf* gene might affect the strength by which the hair is anchored in the follicle and thus explain the painless and easy extraction of LAH hairs (Price and Gummer, 1989; Sinclair *et al.*, 1999). Our analysis of LAH patients of several two-generation families revealed the sporadic presence of a heterozygous Glu → Lys mutation in the short L2 linker region of

K6hf in some patients. Investigations have emphasized the importance of the highly conserved L2 linker for the correct axial alignment of keratin molecules (Wang *et al.*, 2000). However, this defect in K6hf did not reliably segregate with the LAH phenotype in the families and its significance in the disease process remained unclear (Chapalain *et al.*, 2002).

However, we detected a mutation in the *K6hf* gene that appears to be a risk factor for the common hair disorder pseudofolliculitis barbae (PFB) (Winter *et al.*, 2004). PFB, also termed *pili incarnati* or “ingrown hairs,” is a human hair disorder that occurs predominantly on the neck and the submental region of the face. Regular shaving, in particular “against the grain,” which produces short and pointed hairs that penetrate the skin and leads to erythematous papules and pustules, represents the *conditio sine qua non* for the disease. Because of a genetic predisposition for strongly curled hair, PFB occurs predominantly in Black individuals; it is rather rare and usually far less severe in Caucasian individuals with straight or wavy hair. The disease is, however, not gender dependent or restricted to the face, but can occur in any hairy skin region on regular shaving or other traumatic means of hair removal (Crutchfield, 1998; Kligman and Strauss, 1956).

To investigate the potential of mutated keratins that are expressed in the CL and the IRS, K6irs1 and K6hf keratins were analyzed in a three-generation Caucasian family whose male members suffered from relatively severe PFB symptoms. Although no alterations were found in the *K6irs1* gene, affected males of the family exhibited a heterozygous point mutation in the *K6hf* gene that led to a conservative Ala12Thr substitution in the 1A segment of the protein. As an Ala12Glu mutation in the hair keratin hHb6 had previously been found to be causal for monilethrix (Winter *et al.*, 2000), this showed that the highly conserved Ala-12 residue is crucial for correct IF formation. Indeed, cotransfection of expression vectors for K17 and the Ala12Thr-mutated K6hf into cultured cells resulted in disrupted IFs. It must, however, be emphasized that analysis of the family revealed a general problem that was inherently associated with the search for *K6hf* gene alterations in PFB. Our study showed that the mutation was also present in a female member of the family. As, however, this individual did not shave or remove hairs by other means, it could not be said whether the mutation would have been deleterious in the case of shaving.

On the basis of these observations, the frequency of the Ala12Thr substitution was investigated in representative groups of phenotypically affected and unaffected individuals. Typically, the affected group comprised mainly Black Americans, whereas the unaffected group consisted essentially of white individuals, with both groups containing also a small number of females who noted PFB symptoms after shaving in the groin and/or the axilla. The frequency of the Ala12Thr substitution was found to be 9% in the unaffected group and 36% in the affected group. It is clear that in view of the observed

frequencies of the underlying gene alteration in the two groups, the latter must be considered a single-nucleotide polymorphism (SNP). To our knowledge, this is the first example of a deleterious base substitution in a keratin gene that has passed beyond the 1% margin through which mutations are, per definition, distinguished from SNPs (Brookes, 1999). Several reasons may account for this unusual spread of the *K6hf* gene defect and its maintenance in the human population. Compared with the majority of disfiguring keratinopathies, PFB certainly represents a minor health problem, which in males can either be completely suppressed by growing a beard or be minimized by improvising less traumatic shaving methods. More importantly, in the female population, with a generally low shaving rate, the gene defect remains essentially dormant and is thus propagated without knowledge.

Notwithstanding the occurrence of K6hf in both the companion layer and the medulla of beard hairs (described in Sections V.B and V.D, respectively), the latter appear completely normal in bearded PFB patients having the Ala12Thr polymorphism. This is certainly due to the fact that in males who do not shave, the *K6hf* gene defect remains dormant. It is, however, conceivable that both pressure and traction exerted on the skin by regular and close shaving may activate the deleterious nature of the *K6hf* gene defect and result in a destabilization of the CL-IRS unit, which may no longer be able to correctly guide the pointed hairs on their way to the skin surface. While this may augment the existing tendency of curled hairs to grow back into the concave skin areas of the submental skin of Black males, the combination K6hf Ala12Thr/straight hair in Caucasians may remain phenotypically unremarkable, in particular if the submental skin exhibits horizontally instead of caudally growing hairs. These apparently not unusual facial hair patterns (Pinkus, 1927; Ross *et al.*, 1993), may partially account for the relatively high number of Caucasian individuals having the *K6hf* gene defect in the absence of PFB symptoms. Collectively, it appears that PFB represents an unusually complex disease promoted by curly hair and/or a defective K6hf protein, but requiring shaving as a precipitating factor. Apparently, the effects of the two genetic risk factors can be modulated by likewise genetically determined hair types and growth patterns that may lead to either an aggravation or an attenuation of the PFB phenotype (Winter *et al.*, 2004).

It should be noted that the rather subtle effect of the mutated K6hf keratin in PFB patients strongly contrasts with findings in transgenic mice that expressed a modified keratin K6a in which the C-terminal E2 domain was replaced by a human K1 epitope tag. As outlined in Section V.A, mouse pelage hairs do not express K6a in the ORS but only in the CL. Although the hair coat of these mice appeared completely unremarkable for the first months of life, at about 6 months the animals developed signs of alopecia over the entire body together with a highly keratotic skin prone to infection. Thus, in this case, disturbances in the K6a/K16 filament system of cells of the

CL obviously resulted in the destruction of this layer and ultimately led to hair loss (Rothnagel and Roop, 1995).

As described in Section V.D, the medulla of human hairs contains a large number of hair and epithelial keratins that are also expressed elsewhere in the various compartments of the hair follicle, and some have been shown to be involved in the etiology of hereditary skin and hair disorders. Thus in scalp hairs, which are usually only rarely medullated, mutations in the cortex keratins hHb1 and hHb6 are causal for monilethrix (see Section III.B). However, despite the expression of mutated hHb1 and hHb6 keratins in both the cortex and their prominent medulla (see Table II), sexual hairs of monilethrix patients are only rarely affected. Similarly, mutations in K6hf, which besides being expressed in the CL, is expressed in the medulla of beard hairs, do not seem to alter the medullary structure of beard hairs of PFB patients. A further example outside the keratin field is hypotrichosis simplex of the scalp (HSS), for which the mutated desmosomal protein corneodesmosin is the causative factor (Levy-Nissenbaum *et al.*, 2003). Besides the IRS, corneodesmosin is strongly expressed in the medulla of sexual hairs (Gallinaro *et al.*, 2004), but these hairs are not visibly affected in HSS patients (Levy-Nissenbaum *et al.*, 2003). The only medullary keratin for which evidence of involvement in a hair phenotype exists is K17, which is, however, also expressed in the ORS and the companion layer (Wang *et al.*, 2003). The mutated form of this keratin is known to be causal for the type 2 form of pachyonychia congenita (see above), but occasionally, PC-2 patients have been found to exhibit twisted hairs (*pili torti*), preferentially in medullated eyebrow and facial hairs (McLean and Lane, 1995). Collectively, these data suggest that deleterious mutations in structural proteins of the medulla seem to remain essentially silent. A plausible explanation for this phenomenon would be that this innermost structure of hairs is so strongly protected by the surrounding cohesive cortex compartment that mechanical forces exerted on hair follicles are prevented from being translocated to the hair medulla and initiating disturbances of its cellular IF network.

Interestingly, it has been shown that in addition to the transcription factor Foxn1, which plays a role in cortex differentiation (see Section IV.A), another member of the forkhead family of transcription factors, Foxq1, appears to be essential for the differentiation of the medulla of hairs. Investigations in Satin mice, whose hairs exhibit a particularly high sheen, revealed a missense mutation in the *Foxq1* gene that led to a highly disorganized medulla lacking the characteristic septation of medullary cells and showing clumping of trichohyalin granules. However, besides altered refractive properties, macroscopically hairs of Satin mice appeared completely normal except for a reduction in diameter due to the collapsed medulla (Hong *et al.*, 2001). These data convincingly show that even strong damage to the medulla does

not seem to have far-reaching repercussions on the external appearance and mechanical properties of hairs, thus underscoring that even mutated medullary keratins may remain essentially unremarkable.

VII. Regulatory Processes in the CL-IRS Unit and Medulla

Despite significant advances in our understanding of the molecular mechanisms controlling the differentiation of the hair shaft (see Section IV.E), the control mechanisms governing the specification and differentiation of the CL-IRS unit are just beginning to be understood; there are only poor data regarding those operating in the medulla. Although a variety of transcription factors, such as hairless (Cachon-Gonzalez *et al.*, 1994); Foxn1 and Hoxc13, which play a major regulatory role in the central hair-forming compartment of the hair follicle; as well as members of the TALE protein family (see Section IV.C), also show differential expression in the CL-IRS unit, their putative function in the latter is still unknown. However, two further transcription factors have been uncovered that seem to be more specifically linked to the development and differentiation of the CL-IRS unit.

In 2001, Ellis *et al.* reported on a hair phenotype in mice carrying a null mutation of the transcriptional repressor CDP (CCAAT displacement protein), encoded by the *Cutl1* gene, which represses genes regulated by CCAAT sequence motifs (Ellis *et al.*, 2001). Investigations in wild-type mice showed that besides the nuclei of cells of the lowermost ORS and the portion of the matrix supposed to harbor the progenitor cells of the CL-IRS unit, CDP was also strongly expressed in virtually all tissue layers of the CL-IRS unit itself. Apparently, nuclear CDP was maintained along the entire undifferentiated portions of the four layers, clearly visible by the abrupt lack of nuclear CDP in the fully keratinized cells of the early differentiating Henle layer. Ultrastructurally, hair follicles of homozygous CDP null mice showed a rather undisturbed hair bulb in which, however, the developing CL-IRS unit soon became strongly compressed and, beginning in the precortex region, was reduced to only one barely discernible, discontinuous cell layer, sandwiched between a drastically enlarged ORS and hair cortex, which exhibited a desintegrated medulla. At the molecular level, the loss of CDP function led to the ectopic and irregular expression of the CL-IRS-specific genes for K6hf, K6irs1, and trichohyalin in the expanded hair cortex (Ellis *et al.*, 2001). It should be mentioned that an earlier transgenic study, in which a mutant form of CDP was homozygously expressed in mice, reported on the formation of curly vibrissae and wavy body hair. The hair follicles showed spatial disorganization and were more deeply rooted than wild-type follicles,

but morphologically did not reveal obvious differences from normal hair follicles (Tufarelli *et al.*, 1998).

The second factor involved in the specification and differentiation of the CL–IRS unit is GATA-3, a protein belonging to the GATA family of zinc finger transcription factors, which are normally involved in lineage specification of hematopoietic cells. In skin, GATA-3 exhibited a highly restricted expression pattern in both the differentiating layers of the epidermis as well as the Huxley layer and the cuticle of the IRS of the hair follicle (Kaufman *et al.*, 2003). Mutations in the *GATA-3* gene have been found to be causal for the hypoparathyroidism, deafness, and renal dysplasia (HDR) syndrome; but curiously enough, hair follicle defects in HDR patients have not been reported (Nesbit *et al.*, 2004). In contrast, investigations of both whisker and pelage hairs in GATA-3 null mice showed that similar to CDP null mice, the lower bulb region of the follicles appeared grossly normal but higher up displayed a disorganized mass of cortical, cuticular, and medullary cells. The use of the trichohyalin-specific antibody AE15 revealed only reduced amounts or the complete absence of IRS cells, indicating that the formation of the GATA-3-free Henle layer had also been suppressed.

In contrast, the K6a-positive CL appeared grossly normal but was directly apposed to cortex cells, which stained positive for the hair keratin antibody AE13. Further studies applying antibodies against LEF1 and another zinc finger protein, Friend of GATA1 (FOG1), which often functions together with GATA factors, as well as immunolocalization studies for a LacZ-coding sequence inserted downstream from the GATA-3 promoter in knockout animals, revealed a strong and compartmentalized accumulation of both IRS and precortical precursor cells in the hair matrix of GATA-3 null mouse hair follicles. Remarkably, the first also exhibited a local misexpression of cortical genes whereas in the latter, regional GATA-3 promoter activity could be demonstrated (Kaufman *et al.*, 2003). Collectively, the data in CDP and GATA-3 null mice suggest that both factors play a major role as *trans*-activators during the differentiation of either the entire CL–IRS unit or only distinct layers of it. In addition, the accumulation of IRS precursor cells in the matrix of GATA null mice follicles, which are obviously inhibited from developing further, indicates that GATA-3 may also be involved in the lineage specification of the Huxley layer and the IRS cuticle (Kaufman *et al.*, 2003). As CDP is normally also expressed in what is considered to be the matrical compartment of CL–IRS precursor cells (Ellis *et al.*, 2001), it cannot be excluded that CDP and GATA-3 function along the same pathway to regulate IRS specification and differentiation, although their target genes may not necessarily overlap.

In contrast to this progress in our understanding of the regulatory processes involved in the formation of the CL–IRS unit, the factors controlling the morphogenesis, and the complex and unusual expression, of structural

proteins of the medulla, remain largely unknown. Despite its regulatory role for the genes of the surrounding precortex (see Section IV.B), it is clear that Wnt signaling is not involved in the control of medullary specification and the expression of early medullary genes, as LEF1 as well as its target genes *hHal* and *Foxn1* are not expressed in medullary trichocytes (DasGupta and Fuchs, 1999; Dunn *et al.*, 1998; Lee *et al.*, 1999; Schlake and Boehm, 2001; Winter *et al.*, 1997a). In contrast, besides the matrix and precortex, HOXC13 is expressed in the lower medulla of human sexual hairs, in which it might participate in the expression control of the otherwise androgen-regulated hair keratin hHa7, as well as other medullary hair keratins (see Section IV.D). Moreover, the transcription factor Foxq1 (Hong *et al.*, 2001) (see Section IV) may represent another promising player. As, however, the loss of Foxq1 function results in a strongly disorganized but not suppressed medulla, it appears that this factor may primarily govern the differentiation pathway of this hair compartment. Which of the genes for the large number of epithelial and hair keratins, as well as of a variety of further constituents of the medulla, such as trichohyalin, transglutaminases 1 and 3 (Tarcza *et al.*, 1997), peptidyl-arginine deaminase III (Nishijyo *et al.*, 1997), involucrin (de Viragh *et al.*, 1994), and corneodesmosin (Gallinaro *et al.*, 2004), may represent Hoxc13 or Foxq1 target genes remains to be seen.

VIII. Concluding Remarks and Outlook

Initially, our studies on the genomic organization of the human hair keratin genes had led to the attractive notion that the type I as well as the type II genes occurred as well-demarcated clusters, each containing virtually all genes intercalated into the respective gene domains of epithelial keratins on chromosomes 17q21.2 and 12q13.13. Although this appears to hold true for the numerically smaller type II hair keratin gene domain, bioinformatic investigations and studies in our laboratory demonstrated that the numerically larger type I gene domain is not clustered, as we thought, but rather interrupted on one side by a large KAP gene locus that is then followed by two newly discovered hair keratin genes, *K26* (*Ka36*) and *K28* (*Ka35*) (see Fig. 3A) (Hesse *et al.*, 2004; Rogers *et al.*, 2004c). Thus, the complete description of the two hair keratin gene domains as well as the expression patterns of their members and the location of the latter within the hair keratin catalog must still await the characterization of these novel, apparently functional type I hair keratin genes. Preliminary data suggest that, structurally, the hair keratin encoded by the *K28* (*Ka35*) gene is quite different from the highly related group A members hHa3-I, hHa3-II, hHa4, and hHa1 (see Fig. 3A), from which it is separated by the KAP genes, suggesting that its

gene did not arise from the duplication of one of the group A genes. Regarding the collective of epithelial keratins expressed in the ORS, the CL-IRS unit, and the medulla of the human hair follicle, apparently only the type I IRS keratins still need to be fully characterized, although it cannot be excluded that a novel type II epithelial gene, *K27 (Kb20)*, representing one of the physical boundaries of the type II hair and epithelial keratin gene domain (Hesse *et al.*, 2004; Rogers *et al.*, 2004b), might be expressed in the hair follicle. Likewise, the exact number of hair and epithelial keratins expressed in the medulla remains to be determined.

Considering the large number of hair keratins in the human genome, the conspicuous restriction of disease-causing mutations to only the group A type II cortex keratins hHb1 and hHb6, associated with monilethrix, is highly intriguing, all the more as the gene of the third cortex keratin, hHb3, of this group (see Fig. 3) possesses an identical nucleotide sequence around the mutational hot spots leading to the Glu-402 and Glu-413 substitutions in the *hHb1* and *hHb6* genes. More importantly, keratin diseases are generally due to mutations in either the type I or the type II member of a given keratin pair. Although in the case of hair keratins, the specific pairing of distinct type I and type II members is difficult to assess (see Section II.B), a variety of type I hair keratins, such as hHa1, hHa3-I/II, hHa6, and hHa4, are all expressed in the hair cortex (Langbein *et al.*, 1999, 2001). Yet, among the large number of autosomal dominant hair disorders, at present none can be causally associated with a mutated type I hair keratin. It is clear that the potential of hHb3 and the type I cortex keratins, as well as of the members of the matrical and cuticular keratin pairs hHa5/hHb5 and hHa2/hHb2, to induce a disease phenotype can be assessed only by introducing disruptive mutations into the corresponding genes, followed by their transgenic expression in mice. It can be predicted that if mutations in type I hair keratin genes (that are disruptive in other keratins) do not lead to a hair phenotype, this may have profound consequences regarding the role of type I hair keratins in the assembly of IFs.

Despite considerable progress in our understanding of the control mechanisms governing the specific expression of both hair keratins and epithelial keratins in the postnatal hair follicle, this issue remains one of the most captivating and compelling challenges in hair follicle biology. Although it appears that the main avenues along which the control of keratin expression in both the hair-forming compartment and the surrounding tissue compartments of the hair follicle proceeds have essentially been paved, the fine tuning and interactions of the various players still need to be substantiated and consolidated, with (remembering GATA-3 and CDP as well as the orphan G protein-coupled receptor GPRC5D) (Inoue *et al.*, 2004) the surfacing of novel factors being more expected than excluded.

The present nomenclature of human hair keratins used throughout this review relies on the early proposal by Heid *et al.* (1986), whose underlying rules were different from those applied since 1982 for the designation of epithelial keratins (Moll *et al.*, 1982; see also Section II). At present, there is every reason to believe that, by and large, most of the human epithelial and hair keratins are known, so that the establishment of a unifying nomenclature according to the principles proposed by the Hugo Gene Nomenclature Committee (HGNC) for multigene families becomes more than mandatory. As it stands, the Moll catalog of epithelial keratins represents an open system only for type I keratins (i.e., from K9 upward), whereas the type II keratin numbering is blocked at K8. However, the nomenclature can easily be transformed into an open system for all keratins by changing the designation of the members of the type II epithelial keratin family to K2.1–K2.8 (as previously proposed by Powell and Rogers, 1997), or Kb1–Kb8 (according to a proposal by Hesse *et al.*, 2004), with the number 2 or the letter *b* indicating the type II or basic-to-neutral nature of the keratins. The numbering of type I keratins would then range from K1.9 or Ka9 upward and, in both cases, the species could be indicated by a prefix. The Ka9-to-KaX and Kb1-to-KbY version of the nomenclature has been used in a bioinformatic study on the organization of the human type I and type II epithelial and hair keratin gene domains on chromosomes 17q12.2 and 12q13.13, respectively (Hesse *et al.*, 2004), in which all keratins described subsequent to those contained in the original Moll catalog received numbers accordingly. The new designations for hair keratins according to this system are indicated in Table III. Pending the

TABLE III
Hair Keratin Nomenclature^a

Type I hair keratin		Type II hair keratin	
Current name	Proposed name	Current name	Proposed name
Ha1	Ka25	Hb1	Kb21
Ha2	Ka26	Hb2	Kb22
Ha3-I	Ka27	Hb3	Kb23
Ha3-II	Ka28	Hb4	Kb24
Ha4	Ka29	Hb5	Kb25
Ha5	Ka30	Hb6	Kb26
Ha6	Ka31		
hHa7	Ka32		
hHa8	Ka33		

^aThe new designation of hair keratins is indicated according to a proposal by Hesse *et al.* (2004).

approval of this nomenclature, in which the letter *K* might be changed to *KRT*, by the HGNC, it appears a reasonable and practicable solution to be used in future for the definite designation of keratins.

Note Added in Proofs

In Sections III.A.1 and VIII, we stated that the vast majority of mutations causing the inherited hair disorder monilethrix were restricted to two type II hair-cortex keratins, hHb1 and hHb6, in which two mutational hot spots, E402K and E413K, occurred in the helix termination motif of the keratins. In this context we stressed that at the writing of this article, no monilethrix-associated mutations had been found in a third hair keratin, hHB3, although this keratin is also expressed in the hair cortex and exhibits a complete α -helical sequence identity with hHb1 and hHb6. Recently, however, one of the hHb1/hHb6 mutations, E402K, was reported in the hHb3 keratin of a monilethrix family. As compared to hHb1 and hHb6, the hHb3 keratin possesses five additional amino acid residues in the head domain (Rogers *et al.*, 2000), and the mutation occurred at position E407K of its helix termination motif. The finding was published as a meeting abstract (Van Geel *et al.*, 2004).

Acknowledgments

We are grateful to our colleagues Hermelita Winter, Michael A. Rogers, Luis-Felipe Jave-Suarez, Silke Praetzel, and Herbert Spring. Over the years, each of them contributed essentially to the work reported here. We also enjoyed fruitful cooperations with the laboratories of Brigitte Lane (Dundee), Irene M. Leigh (London), Pierre A. Coulombe (Baltimore), Bernard Cribrier (Strasbourg), Alain Taieb (Bordeaux), and Christophe Perrin (Nice). We thank Michael A. Rogers for helpful discussions during the preparation of this review and for critically reading the manuscript.

References

- Ackermann, A. B., de Viragh, P. A., and Chongchitnant, N. (1993). "Neoplasms with Follicular Differentiation." Lea & Febiger, Philadelphia, PA.
- Adriani, M., Martinez-Mir, A., Fusco, F., Busiello, R., Frank, J., Telese, S., Matrecano, E., Ursini, M. V., Christiano, A. M., and Pignata, C. (2004). Ancestral founder mutations of the *nude* (*FOXNI*) gene in congenital severe combined immunodeficiency associated with alopecia in southern Italy population. *Ann. Hum. Genet.* **68**, 365–368.
- Alonso, L., and Fuchs, E. (2003). Stem cells of the skin epithelium. *Proc. Natl. Acad. Sci. USA* **100**, 11830–11835.
- Andl, T., Reddy, S. T., Gaddapara, T., and Millar, S. E. (2002). Wnt signals are required for the initiation of hair follicle development. *Dev. Cell* **2**, 643–653.
- Andl, T., Ahn, K., Kairo, A., Chu, E. Y., Wine-Lee, L., Reddy, S. T., Croft, N. J., Cebra-Thomas, J. A., Metzger, D., Chambon, P., Lyons, K. M., Mishina, Y., Seykora, J. T., Crenshaw, E. B.,

- III, and Millar, S. E. (2004). Epithelial *Bmpr1a* regulates differentiation and proliferation in postnatal hair follicles and is essential for tooth development. *Development* **131**, 2257–2268.
- Aoki, N., Sawada, S., Rogers, M. A., Schweizer, J., Shimomura, Y., Tsujimoto, T., Ito, K., and Ito, M. (2001). A novel type II cytokeratin, mK6irs, is expressed in the Huxley and Henle layers of the mouse inner root sheath. *J. Invest. Dermatol.* **116**, 359–365.
- Asada, M., Kurokawa, I., Nishijima, S., and Asada, Y. (1990). An immunohistochemical study on cell differentiation in the outer root sheath of the normal human anagen hair follicles with antikeratin monoclonal antibodies [in Japanese]. *Nippon Hifuka Gakkai Zasshi* **100**, 1423–1430.
- Auber, L. (1952). The anatomy of follicles producing wool-fibres with special reference to keratinization. *Trans. R. Soc. Edinburgh* **62**, 191–254.
- Awgulewitsch, A. (2003). Hox in hair growth and development. *Naturwissenschaften* **90**, 193–211.
- Baker, H. (1962). An investigation of monilethrix. *Br. J. Dermatol.* **74**, 24–30.
- Balciunaite, G., Keller, M. P., Balciunaite, E., Piali, L., Zuklys, S., Mathieu, Y. D., Gill, J., Boyd, R., Sussman, D. J., and Hollander, G. A. (2002). Wnt glycoproteins regulate the expression of *Foxn1*, the gene defective in nude mice. *Nat. Immunol.* **3**, 1102–1108.
- Bawden, C. S., McLaughlan, C., Nesci, A., and Rogers, G. (2001). A unique type I keratin intermediate filament gene family is abundantly expressed in the inner root sheaths of sheep and human hair follicles. *J. Invest. Dermatol.* **116**, 157–166.
- Bernot, K. M., Coulombe, P. A., and McGowan, K. M. (2002). Keratin 16 expression defines a subset of epithelial cells during skin morphogenesis and the hair cycle. *J. Invest. Dermatol.* **119**, 1137–1149.
- Berthelsen, J., Zappavigna, V., Mavilio, F., and Blasi, F. (1998). Prepl, a novel functional partner of Pbx proteins. *EMBO J.* **17**, 1423–1433.
- Blauer, M., Vaalasti, A., Pauli, S. L., Ylikomi, T., Joensuu, T., and Tuohimaa, P. (1991). Location of androgen receptor in human skin. *J. Invest. Dermatol.* **97**, 264–268.
- Brookes, A. J. (1999). The essence of SNPs. *Gene* **234**, 177–186.
- Bucher, O. (1968). "Cytologie, Histologie und mikroskopische Anatomie des Menschen." Verlag Huber, Bern, Switzerland.
- Buhl, A. E., Waldon, D. J., Miller, B. F., and Brunden, M. N. (1990). Differences in activity of minoxidil and cyclosporin A on hair growth in nude and normal mice: Comparisons of *in vivo* and *in vitro* studies. *Lab. Invest.* **62**, 104–107.
- Cachon-Gonzalez, M. B., Fenner, S., Coffin, J. M., Moran, C., Best, S., and Stoye, J. P. (1994). Structure and expression of the hairless gene of mice. *Proc. Natl. Acad. Sci. USA* **91**, 7717–7721.
- Cadigan, K. M., and Nusse, R. (1997). Wnt signaling: A common theme in animal development. *Genes Dev.* **11**, 3286–3305.
- Capecchi, M. R. (1997). Hox genes and mammalian development. *Cold Spring Harb. Symp. Quant. Biol.* **62**, 273–281.
- Carlsson, P., and Mahlapuu, M. (2002). Forkhead transcription factors: Key players in development and metabolism. *Dev. Biol.* **250**, 1–13.
- Chan, E. F., Gat, U., McNiff, J. M., and Fuchs, E. (1999). A common human skin tumour is caused by activating mutations in β -catenin. *Nat. Genet.* **21**, 410–413.
- Chapalain, V., Winter, H., Langbein, L., Le Roy, J. M., Labreze, C., Nikolic, M., Schweizer, J., and Taieb, A. (2002). Is the loose anagen hair syndrome a keratin disorder? A clinical and molecular study. *Arch. Dermatol.* **138**, 501–506.
- Choudhry, R., Hodgins, M. B., Van der Kwast, T. H., Brinkmann, A. O., and Boersma, W. J. (1992). Localization of androgen receptors in human skin by immunohistochemistry: Implications for the hormonal regulation of hair growth, sebaceous glands and sweat glands. *J. Endocrinol.* **133**, 467–475.

- Clemmensen, O. J., Hainau, B., and Hansted, B. (1991). The ultrastructure of the transition zone between specialized cells ("Flugelzellen") of Huxley's layer of the inner root sheath and cells of the outer root sheath of the human hair follicle. *Am. J. Dermatopathol.* **13**, 264–270.
- Collin, C., Moll, R., Kubicka, S., Ouhayoun, J. P., and Franke, W. W. (1992a). Characterization of human cytokeratin 2, an epidermal cytoskeletal protein synthesized late during differentiation. *Exp. Cell Res.* **202**, 132–141.
- Collin, C., Ouhayoun, J. P., Grund, C., and Franke, W. W. (1992b). Suprabasal marker proteins distinguishing keratinizing squamous epithelia: Cytokeratin 2 polypeptides of oral masticatory epithelium and epidermis are different. *Differentiation* **51**, 137–148.
- Comaish, S. (1969). Autoradiographic studies of hair growth in various dermatoses: Investigation of a possible circadian rhythm in human hair growth. *Br. J. Dermatol.* **81**, 283–288.
- Commo, S., Gaillard, O., and Bernard, B. A. (2000). The human hair follicle contains two distinct K19 positive compartments in the outer root sheath: A unifying hypothesis for stem cell reservoir? *Differentiation* **66**, 157–164.
- Cribier, B., Peltre, B., Langbein, L., Winter, H., Schweizer, J., and Grosshans, E. (2001). Expression of type I hair keratins in follicular tumours. *Br. J. Dermatol.* **144**, 977–982.
- Cribier, B., Peltre, B., Grosshans, E., Langbein, L., and Schweizer, J. (2004). On the regulation of hair keratin gene expression: Lessons from studies in pilomatricomas. *J. Invest. Dermatol.* **122**, 1078–1083.
- Cribier, B., Worret, W. I., Braun-Falco, M., Peltre, B., Langbein, L., and Schweizer, J. (2005). Expression patterns of hair and epithelial keratins and transcription factors HOXC13, LEF1, and β -catenin in a malignant pilomatricoma: A histological and immunohistochemical study. *J. Cutan. Pathol.* In press.
- Crutchfield, C. E., III (1998). The causes and treatment of pseudofolliculitis barbae. *Cutis* **61**, 351–356.
- Cunliffe, V. T., Furley, A. J., and Keenan, D. (2002). Complete rescue of the nude mutant phenotype by a wild-type Foxn1 transgene. *Mamm. Genome* **13**, 245–252.
- Danilenko, D. M., Ring, B. D., Yanagihara, D., Benson, W., Wiemann, B., Starnes, C. O., and Pierce, G. F. (1995). Keratinocyte growth factor is an important endogenous mediator of hair follicle growth, development, and differentiation. *Am. J. Pathol.* **147**, 145–154.
- DasGupta, R., and Fuchs, E. (1999). Multiple roles for activated LEF/TCF transcription complexes during hair follicle development and differentiation. *Development* **126**, 4557–4568.
- DasGupta, R., Rhee, H., and Fuchs, E. (2002). A developmental conundrum: A stabilized form of β -catenin lacking the transcriptional activation domain triggers features of hair cell fate in epidermal cells and epidermal cell fate in hair follicle cells. *J. Cell Biol.* **158**, 331–344.
- De Berker, D. A. R., Ferguson, D. J. P., and Dawber, R. P. R. (1993). Monilethrix: A clinicopathological illustration of a cortical defect. *Br. J. Dermatol.* **128**, 327–331.
- de Viragh, P. A., Huber, M., and Hohl, D. (1994). Involucrin mRNA is more abundant in human hair follicles than in normal epidermis. *J. Invest. Dermatol.* **103**, 815–819.
- Dhouailly, D., Xu, C., Manabe, M., Schermer, A., and Sun, T.-T. (1989). Expression of hair-related keratins in a soft epithelium: Subpopulations of human and mouse dorsal tongue keratinocytes express keratin markers for hair-, skin- and esophageal-types of differentiation. *Exp. Cell Res.* **181**, 141–158.
- Djabali, K., Panteleyev, A. A., Lalin, T., Garzon, M. C., Longley, B. J., Bickers, D. R., Zlotogorski, A., and Christiano, A. M. (2003). Recurrent missense mutations in the hair keratin gene hHb6 in monilethrix. *Clin. Exp. Dermatol.* **28**, 206–210.
- Duboule, D. (1998). Hox is in the hair: A break in colinearity? *Genes Dev.* **12**, 1–4.
- Dunn, S. M., Keough, R. A., Rogers, G. E., and Powell, B. C. (1998). Regulation of a hair follicle keratin intermediate filament gene promoter. *J. Cell Sci.* **111**, 3487–3496.
- Eastman, Q., and Grosschedl, R. (1999). Regulation of LEF-1/TCF transcription factors by Wnt and other signals. *Curr. Opin. Cell Biol.* **11**, 233–240.

- Ebling, F. J. (1987). The biology of hair. *Dermatol. Clin.* **5**, 467–481.
- Ebner, V. V. (1876). Mikroskopische Studien über Wachstum und Wechsel der Haare. *Sitzungsber. Kaiserl. Acad. Wiss. Wien Math. Nat. Classe Abt. III* **73**, 339–394.
- Ekker, S. C., Jackson, D. G., von Kessler, D. P., Sun, B. I., Young, K. E., and Beachy, P. A. (1994). The degree of variation in DNA sequence recognition among four *Drosophila* homeotic proteins. *EMBO J.* **13**, 3551–3560.
- Ellis, T., Gambardella, L., Horcher, M., Tschanz, S., Capol, J., Bertram, P., Jochum, W., Barrandon, Y., and Busslinger, M. (2001). The transcriptional repressor CDP (Cut1) is essential for epithelial cell differentiation of the lung and the hair follicle. *Genes Dev.* **15**, 2307–2319.
- Flanagan, S. P. (1966). “Nude,” a new hairless gene with pleiotropic effects in the mouse. *Genet. Res.* **8**, 295–309.
- Fognani, C., Kilstrup-Nielsen, C., Berthelsen, J., Ferretti, E., Zappavigna, V., and Blasi, F. (2002). Characterization of PREP2, a paralog of PREP1, which defines a novel sub-family of the MEINOX TALE homeodomain transcription factors. *Nucleic Acids Res.* **30**, 2043–2051.
- Forbis, R., Jr., and Helwig, E. B. (1961). Pilomatrixoma (calcifying epithelioma). *Arch. Dermatol.* **83**, 606–618.
- Frank, J., Pignata, C., Panteleyev, A. A., Prowse, D. M., Baden, H., Weiner, L., Gaetaniello, L., Ahmad, W., Pozzi, N., Cserhalmi-Friedman, P. B., Aita, V. M., Uyttendaele, H., Gordon, D., Ott, J., Brissette, J. L., and Christiano, A. M. (1999). Exposing the human *nude* phenotype. *Nature* **398**, 473–474.
- Fuchs, E., and Weber, K. (1994). Intermediate filaments: Structure, dynamics, function and disease. *Annu. Rev. Biochem.* **63**, 345–382.
- Fuchs, E., Merrill, B. J., Jamora, C., and DasGupta, R. (2001). At the roots of a never-ending cycle. *Dev. Cell* **1**, 13–25.
- Gallinaro, H., Jonca, N., Langbein, L., Vincent, C., Simon, M., Serre, G., and Guerrin, M. (2004). A 4.2kb upstream region of the human corneodesmosin gene directs site-specific expression in hair follicles and hyperkeratotic epidermis of transgenic mice. *J. Invest. Dermatol.* **122**, 730–738.
- Gehring, W. J., Affolter, M., and Burglin, T. (1994). Homeodomain proteins. *Annu. Rev. Biochem.* **63**, 487–526.
- Gho, C. G., Braun, J. E., Tilli, C. M., Neumann, H. A., and Ramaekers, F. C. (2004). Human follicular stem cells: Their presence in plucked hair and follicular cell culture. *Br. J. Dermatol.* **150**, 860–868.
- Godwin, A. R., and Capecchi, M. R. (1998). *Hoxc13* mutant mice lack external hair. *Genes Dev.* **12**, 11–20.
- Godwin, A. R., and Capecchi, M. R. (1999). Hair defects in *Hoxc13* mutant mice. *J. Invest. Dermatol. Symp. Proc.* **4**, 244–247.
- Haller, K., Rambaldi, I., Kovacs, E. N., Daniels, E., and Featherstone, M. (2002). Prep2: Cloning and expression of a new prep family member. *Dev. Dyn.* **225**, 358–364.
- Hashimoto, K. (1988). The structure of human hair. *Clin. Dermatol.* **6**, 7–21.
- Hashimoto, K., Nelson, R. G., and Lever, W. F. (1966). Calcifying epithelioma of Malherbe: Histochemical and electron microscopic studies. *J. Invest. Dermatol.* **46**, 391–408.
- Hashimoto, T., Inamoto, N., Nakamura, K., and Harada, R. (1987). Involucrin expression in skin appendage tumors. *Br. J. Dermatol.* **117**, 325–332.
- Healy, E., Holmes, S. C., Belgaid, C. E., Stephenson, A. M., McLean, W. H. I., Rees, J., and Munro, C. S. (1995). A gene for monilethrix is closely linked to the type II keratin gene cluster at 12q13. *Hum. Mol. Genet.* **4**, 2399–2402.
- Heid, H. W., Werner, E., and Franke, W. W. (1986). The complement of native α -keratin polypeptides of hair-forming cells: A subset of eight polypeptides that differ from epithelial cytokeratins. *Differentiation* **32**, 101–119.

- Heid, H. W., Moll, I., and Franke, W. W. (1988a). Pattern of expression of trichocytic and epithelial cytokeratins in mammalian tissues. II. Concomitant and mutually exclusive synthesis of trichocytic and epithelial cytokeratins in diverse human and bovine tissues (hair follicle, nail bed and matrix, lingual papilla and thymic reticulum). *Differentiation* **37**, 215–230.
- Heid, H. W., Moll, I., and Franke, W. W. (1988b). Patterns of expression of trichocytic and epithelial cytokeratins in mammalian tissues. I. Human and bovine hair follicles. *Differentiation* **37**, 137–157.
- Henle, J. (1840). Über die Structur und die Bildung der menschlichen Haare. *Neue Notizen Gebiet Natur Heilkunde* **14**, 113–119.
- Herrmann, H., Hesse, M., Reichenzeller, M., Aebi, U., and Magin, T. M. (2003). Functional complexity of intermediate filament cytoskeletons: From structure to assembly to gene ablation. *Int. Rev. Cytol.* **223**, 83–175.
- Hesse, M., Zimek, A., Weber, K., and Magin, T. M. (2004). Comprehensive analysis of keratin gene clusters in humans and rodents. *Eur. J. Cell Biol.* **83**, 19–26.
- Heydt, G. E. (1963). Zur Kenntnis des Monilethrix-Syndroms. *Arch. Klein. Exp. Derm.* **217**, 15–29.
- Hodgins, M. B., Spike, R. C., Mackie, R. M., and MacLean, A. B. (1998). An immunohistochemical study of androgen, oestrogen and progesterone receptors in the vulva and vagina. *Br. J. Obstet. Gynaecol.* **105**, 216–222.
- Hoepke, H. (1927). Die Haare. In “Handbuch der mikroskopischen Anatomie” (W. V. Moellendorf, Ed.), pp. 68–88. Springer-Verlag, Berlin.
- Hofmann, I., Winter, H., Mücke, N., Langowski, J., and Schweizer, J. (2002). The *in vitro* assembly of hair follicle keratins: Comparison of cortex and companion layer keratins. *Biochem. J.* **383**, 1373–1381.
- Hong, H. K., Noveroske, J. K., Headon, D. J., Liu, T., Sy, M. S., Justice, M. J., and Chakravarti, A. (2001). The winged helix/forkhead transcription factor Foxq1 regulates differentiation of hair in satin mice. *Genesis* **29**, 163–171.
- Horev, L., Glaser, B., Metzker, A., Ben Amitai, D., Vardy, D., and Zlotogorski, A. (2000). Monilethrix: Mutational hotspot in the helix termination motif of the human hair basic keratin 6. *Hum. Hered.* **50**, 325–330.
- Horev, L., Djabali, K., Green, J., Sinclair, R., Martinez-Mir, A., Ingber, A., Christiano, A. M., and Zlotogorski, A. (2003). *De novo* mutations in monilethrix. *Exp. Dermatol.* **12**, 882–885.
- Imoto, I., Sponoda, I., Yuki, Y., and Inazawa, J. (2001). Identification and characterization of human PKNOX2, a novel homeobox-containing gene. *Biochem. Biophys. Res. Commun.* **287**, 270–276.
- Inoue, S., Nambu, T., and Shimomura, T. (2004). The RAIG family member, GPRC5D, is associated with hard-keratinized structures. *J. Invest. Dermatol.* **122**, 565–573.
- Inui, S., Fukuzato, Y., Nakajima, T., Yoshikawa, K., and Itami, S. (2003). Identification of androgen-inducible TGF- β_1 derived from dermal papilla cells as a key mediator in androgenetic alopecia. *J. Invest. Dermatol. Symp. Proc.* **8**, 69–71.
- Issacson, J. H., and Cattanach, B. M. (1962). Report. *Mouse News Lett.* **27**, 31.
- Itami, S., Kurata, S., and Takayasu, S. (1995). Androgen induction of follicular epithelial cell growth is mediated via insulin-like growth factor-I from dermal papilla cells. *Biochem. Biophys. Res. Commun.* **212**, 988–994.
- Ito, M. (1986). The innermost cell layer of the outer root sheath in anagen hair follicle: Light and electron microscopic study. *Arch. Dermatol. Res.* **279**, 112–119.
- Ito, M. (1988). Electron microscopic study on cell differentiation in anagen hair follicles in mice. *J. Invest. Dermatol.* **90**, 65–72.
- Ito, M. (1989). Biologic roles of the innermost cell layer of the outer root sheath in human anagen hair follicle: Further electron microscopic study. *Arch. Dermatol. Res.* **281**, 254–259.

- Ito, M. (1990). The morphology and cell biology of the hair apparatus: Recent advances. *Acta Med. Biol.* **38**, 51–67.
- Ito, M., Tazawa, T., Ito, K., Shimizu, N., Katsuumi, K., and Sato, Y. (1986a). Immunological characteristics and histological distribution of human hair fibrous proteins studied with anti-hair keratin monoclonal antibodies HKN-2, HKN-4, and HKN-6. *J. Histochem. Cytochem.* **34**, 269–275.
- Ito, M., Tazawa, T., Shimizu, N., Ito, K., Katsuumi, K., Sato, Y., and Hashimoto, K. (1986b). Cell differentiation in human anagen hair and hair follicles studied with anti-hair keratin monoclonal antibodies. *J. Invest. Dermatol.* **86**, 563–569.
- Ito, M., Hashimoto, K., and Sato, Y. (1990). Pathogenesis of monilethrix: Computer stereography and electron microscopy. *J. Invest. Dermatol.* **95**, 186–194.
- Jave-Suarez, L. F., Winter, H., Langbein, L., Rogers, M. A., and Schweizer, J. (2002). HOXC13 is involved in the regulation of human hair keratin gene expression. *J. Biol. Chem.* **277**, 3718–3726.
- Jave-Suarez, L. F., Langbein, L., Winter, H., Praetzel, S., Rogers, M. A., and Schweizer, J. (2004). Androgen regulation of the human hair follicle: The type I hair keratin hHa7 is a direct target gene in trichocytes. *J. Invest. Dermatol.* **122**, 555–564.
- Kaestner, K. H., Knochel, W., and Martinez, D. E. (2000). Unified nomenclature for the winged helix/forkhead transcription factors. *Genes Dev.* **14**, 142–146.
- Kajino, Y., Yamaguchi, A., Hashimoto, N., Matsuura, A., Sato, N., and Kikuchi, K. (2001). β -Catenin gene mutation in human hair follicle-related tumors. *Pathol. Int.* **51**, 543–548.
- Kaufman, C. K., Zhou, P., Pasolli, H. A., Rendl, M., Bolotin, D., Lim, K. C., Dai, X., Alegre, M. L., and Fuchs, E. (2003). GATA-3: An unexpected regulator of cell lineage determination in skin. *Genes Dev.* **17**, 2108–2122.
- Kaufman, K. D. (1996). Androgen metabolism as it affects hair growth in androgenetic alopecia. *Dermatol. Clin.* **14**, 697–711.
- Kaufmann, E., Muller, D., and Knochel, W. (1995). DNA recognition site analysis of *Xenopus* winged helix proteins. *J. Mol. Biol.* **248**, 239–254.
- Kikkawa, Y., Oyama, A., Ishii, R., Miura, I., Amano, T., Ishii, Y., Yoshikawa, Y., Masuya, H., Wakana, S., Shiroishi, T., Taya, C., and Yonekawa, H. (2003). A small deletion hotspot in the type II keratin gene mK6irsl/Krt2-6g on mouse chromosome 15, a candidate for causing the wavy hair of the caracul (Ca) mutation. *Genetics* **165**, 721–733.
- Kimura, N., Mizokami, A., Oonuma, T., Sasano, H., and Nagura, H. (1993). Immunocytochemical localization of androgen receptor with polyclonal antibody in paraffin-embedded human tissues. *J. Histochem. Cytochem.* **41**, 671–678.
- Kligman, A. M., and Strauss, J. S. (1956). Pseudofolliculitis of the beard. *Arch. Dermatol.* **74**, 533–542.
- Kobiela, K., Pasolli, H. A., Alonso, L., Polak, L., and Fuchs, E. (2003). Defining BMP functions in the hair follicle by conditional ablation of BMP receptor 1A. *J. Cell Biol.* **163**, 609–623.
- Kopan, R., and Fuchs, E. (1989). A new look into an old problem: Keratins as tools to investigate determination, morphogenesis, and differentiation in skin. *Genes Dev.* **3**, 1–15.
- Köpf-Maier, P., Mboneko, V. F., and Merker, H. J. (1990). Nude mice are not hairless. *Acta Anat.* **139**, 178–190.
- Korge, B. P., Healy, E., Munro, C. S., Plünter, C., Birch-Machin, M. A., Holmes, S. C., Darlington, S., Hamm, H., Messenger, A. G., Rees, J. L., and Traupe, H. (1998). A mutational hotspot in the 2B domain of human hair basic keratin 6 (hHb6) in monilethrix patients. *J. Invest. Dermatol.* **111**, 896–899.
- Korge, B. P., Hamm, H., Jury, C. S., Traupe, H., Irvine, A. D., Healy, E., Birch-Machin, M. A., Rees, J. L., Messenger, A. G., Holmes, S. C., Parry, D. A. D., and Munro, C. S. (1999).

- Identification of novel mutations in basic hair keratins hHb1 and hHb6 in monilethrix: Implications for protein structure and clinical phenotype. *J. Invest. Dermatol.* **113**, 607–612.
- Krüger, K., Blume-Petavi, U., and Orfanos, C. E. (1996). Morphological and histochemical characterization of the human vellus hair follicle. In “Hair Research for the Next Millennium” (D. Van Desk and V. A. Randall, Eds.), pp. 157–160. Elsevier, Amsterdam.
- Kurokawa, I., Nishijima, S., Suzuki, K., Kusumoto, K., Sensaki, H., Shikata, N., and Tsubura, A. (2002). Cytokeratin expression in pilonidal sinus. *Br. J. Dermatol.* **146**, 409–413.
- Kwan, K. M., Li, A. G., Wang, X. L., Wurst, W., and Behringer, R. R. (2004). Essential roles of BMPR-1A signaling in differentiation and growth of hair follicles and in skin tumorigenesis. *Genesis* **39**, 10–25.
- Langbein, L., Rogers, M. A., Winter, H., Praetzel, S., Beckhaus, U., Rackwitz, H.-R., and Schweizer, J. (1999). The catalog of human hair keratins. I. Expression of the nine type I members in the hair follicle. *J. Biol. Chem.* **274**, 19874–19884.
- Langbein, L., Rogers, M. A., Winter, H., Praetzel, S., and Schweizer, J. (2001). The catalog of human hair keratins. II. Expression of the six type II members in the hair follicle and the combined catalog of human type I and II keratins. *J. Biol. Chem.* **276**, 35123–35132.
- Langbein, L., Grund, C., Kuhn, C., Praetzel, S., Kartenbeck, J., Brandner, J. M., Moll, I., and Franke, W. W. (2002a). Tight junctions and compositionally related junctional structures in mammalian stratified epithelia and cell cultures derived therefrom. *Eur. J. Cell Biol.* **81**, 419–435.
- Langbein, L., Rogers, M. A., Praetzel, S., Aoki, N., Winter, H., and Schweizer, J. (2002b). A novel epithelial keratin, hK6irs1, is expressed differentially in all layers of the inner root sheath, including specialized Huxley cells (Flügelzellen) of the human hair follicle. *J. Invest. Dermatol.* **118**, 789–799.
- Langbein, L., Rogers, M. A., Praetzel, S., Winter, H., and Schweizer, J. (2003). K6irs1, K6irs2, K6irs3, and K6irs4 represent the inner-root-sheath-specific type II epithelial keratins of the human hair follicle. *J. Invest. Dermatol.* **120**, 512–522.
- Lee, D., Prowse, D. M., and Brissette, J. L. (1999). Association between mouse nude gene expression and the initiation of epithelial terminal differentiation. *Dev. Biol.* **208**, 362–374.
- Levy-Nissenbaum, E., Betz, R. C., Frydman, M., Simon, M., Lahat, H., Bakhan, T., Goldman, B., Bygum, A., Pierick, M., Hillmer, A. M., Jonca, N., Toribio, J., Kruse, R., Dewald, G., Cichon, S., Kubisch, C., Guerrin, M., Serre, G., Nöthen, M. M., and Pras, E. (2003). Hypotrichosis simplex of the scalp is associated with nonsense mutations in *CDSN* encoding corneodesmosin. *Nat. Genet.* **34**, 151–153.
- Li, B., Mackay, D. R., Dai, Q., Li, T. W., Nair, M., Fallahi, M., Schonbaum, C. P., Fantes, J., Mahowald, A. P., Waterman, M. L., Fuchs, E., and Dai, X. (2002). The LEF1/ β -catenin complex activates *moval*, a mouse homolog of *Drosophila ovo* required for epidermal appendage differentiation. *Proc. Natl. Acad. Sci. USA* **99**, 6064–6069.
- Liang, T., Hoyer, S., Yu, R., Soltani, K., Lorincz, A. L., Hiiipakka, R. A., and Liao, S. (1993). Immunocytochemical localization of androgen receptors in human skin using monoclonal antibodies against the androgen receptor. *J. Invest. Dermatol.* **100**, 663–666.
- Lloyd, C., Yu, Q.-C., Chen, J., Turksen, K., Degenstein, L., Hutton, E., and Fuchs, E. (1995). The basal keratin network of stratified squamous epithelia: Defining K15 function in the absence of K14. *J. Cell Biol.* **129**, 1329–1344.
- Lyle, S., Christofidou-Solomidou, M., Liu, Y., Elder, D. E., Albelda, S., and Cotsarelis, G. (1998). The C8/144B monoclonal antibody recognizes cytokeratin 15 and defines the location of human hair follicle stem cells. *J. Cell Sci.* **111**, 3179–3188.
- Lynch, M. H., O’Guin, W. M., Hardy, C., Mak, L., and Sun, T. T. (1986). Acidic and basic hair/nail (“hard”) keratins: Their colocalization in upper cortical and cuticle cells of the human hair follicle and their relationship to “soft” keratins. *J. Cell Biol.* **103**, 2593–2606.

- Maconochie, M., Nonchev, S., Morrison, A., and Krumlauf, R. (1996). Paralogous Hox genes: Function and regulation. *Annu. Rev. Genet.* **30**, 529–556.
- Mahrle, G., and Orfanos, C. E. (1971). The spongy keratin and the medulla of the human scalp hair. Scanning and transmission electromicroscopical observations [in German]. *Arch. Dermatol. Forsch.* **241**, 305–316.
- Malherbe, A. (1880). Note sur l'épithéliome calcifié des glandes sebacées. *Bull. Soc. Anat. Paris* **5**, 169–176.
- Mann, R. S., and Affolter, M. (1998). Hox proteins meet more partners. *Curr. Opin. Genet. Dev.* **8**, 423–429.
- McGowan, K. M., and Coulombe, P. A. (1998). Onset of keratin 17 expression coincides with the definition of major epithelial lineages during skin development. *J. Cell Biol.* **143**, 469–486.
- McGowan, K. M., and Coulombe, P. A. (2000). Keratin 17 expression in the hard epithelial context of the hair and nail, and its relevance for the pachyonychia congenita phenotype. *J. Invest. Dermatol.* **114**, 1101–1107.
- McGowan, K. M., Tong, X., Colucci-Guyon, E., Langa, F., Babinet, C., and Coulombe, P. A. (2002). Keratin 17 null mice exhibit age- and strain-dependent alopecia. *Genes. Dev.* **16**, 1412–1422.
- McLean, W. H. I., and Lane, E. B. (1995). Intermediate filaments in disease. *Curr. Opin. Cell Biol.* **7**, 118–125.
- Meier, N., Dear, T. M., and Boehm, T. (1999). *Whn* and *mHa3* are components of the genetic hierarchy controlling hair follicle differentiation. *Mech. Dev.* **89**, 215–221.
- Meng, J., and Wyss, A. R. (1997). Multituberculate and other mammal hair recovered from Palaeogene excreta. *Nature* **385**, 712–714.
- Merrill, B. J., Gat, U., DasGupta, R., and Fuchs, E. (2001). Tcf3 and Lef1 regulate lineage differentiation of multipotent stem cells in skin. *Genes Dev.* **15**, 1688–1705.
- Michel, M., Torok, N., Godbout, M. J., Lussier, M., Gaudreau, P., Royal, A., and Germain, L. (1996). Keratin 19 as a biochemical marker of skin stem cells *in vivo* and *in vitro*: Keratin 19 expressing cells are differentially localized in function of anatomic sites, and their number varies with donor age and culture stage. *J. Cell Sci.* **109**, 1017–1028.
- Millar, S. E., Willert, K., Salinas, P. C., Roelink, H., Nusse, R., Sussman, D. J., and Barsh, G. S. (1999). WNT signaling in the control of hair growth and structure. *Dev. Biol.* **207**, 133–149.
- Mischke, D. (1998). The complexity of gene families involved in epithelial differentiation: Keratin genes and the epidermal differentiation complex. *Subcell. Biochem.* **31**, 71–104.
- Moll, R., Franke, W. W., Schiller, D. L., Geiger, B., and Krepler, R. (1982). The catalog of human cytokeratins: Patterns of expression in normal epithelia, tumors and cultured cells. *Cell* **31**, 11–24.
- Montagna, W., and Parakkal, P. (1974). “The Structure and Function of Skin.” Academic Press, New York.
- Morin, P. J. (1999). β -Catenin signaling and cancer. *Bioessays* **21**, 1021–1030.
- Morris, R. J., Liu, Y., Marles, L., Yang, Z., Trempus, C., Li, S., Lin, J. S., Sawicki, J. A., and Cotsarelis, G. (2004). Capturing and profiling adult hair follicle stem cells. *Nat. Biotechnol.* **22**, 411–417.
- Moskow, J. J., Bullrich, F., Huebner, K., Daar, I. O., and Buchberg, A. M. (1995). Meis1, a Pbx1-related homeobox gene involved in myeloid leukemia in BXH-2 mice. *Mol. Cell. Biol.* **15**, 5434–5443.
- Munné, A., Fabre, M., Marinoso, M. L., Gallen, M., and Real, F. X. (1999). Nuclear β -catenin in colorectal tumors: To freeze or not to freeze? *J. Histochem. Cytochem* **47**, 1089–1094.
- Muramatsu, S., Kimura, T., Ueki, R., Tsuboi, R., Ikeda, S., and Ogawa, H. (2003). Recurrent E413K mutation of hHb6 in a Japanese family with monilethrix. *Dermatology* **206**, 338–340.

- Murthy, S., Crish, J. F., Zaim, T. M., and Eckert, R. L. (1993). A dual role for involucrin in the epidermis: Ultrastructural localization in epidermis and hair follicle in humans and transgenic mice. *J. Struct. Biol.* **111**, 68–76.
- Nakamura, T., Jenkins, N. A., and Copeland, N. G. (1996). Identification of a new family of Pbx-related homeobox genes. *Oncogene* **13**, 2235–2242.
- Nehls, M., Luno, K., Schorpp, M., Krause, S., Matysiak-Scholze, U., Prokop, C. M., Hedrich, H. J., and Boehm, T. (1994a). A yeast artificial chromosome contig on mouse chromosome 11 encompassing the *nu* locus. *Eur. J. Immunol.* **24**, 1721–1723.
- Nehls, M., Pfeifer, D., Schorpp, M., Hedrich, H., and Boehm, T. (1994b). New member of the winged-helix protein family disrupted in mouse and rat nude mutations. *Nature* **372**, 103–107.
- Nelson, W. J., and Nusse, R. (2004). Convergence of Wnt, β -catenin, and cadherin pathways. *Science* **303**, 1483–1487.
- Nesbit, M. A., Bowl, M. R., Harding, B., Ali, A., Ayala, A., Crowe, C., Dobbie, A., Hampson, G., Holdaway, I., Levine, M. A., McWilliams, R., Rigden, S., Sampson, J., Williams, A. J., and Thakker, R. V. (2004). Characterization of GATA-3 mutations in the hypoparathyroidism, deafness and renal dysplasia (HDR) syndrome. *J. Biol. Chem.* **279**, 22624–22634.
- Niemann, C., Owens, D. M., Hulsken, J., Birchmeier, W., and Watt, F. M. (2002). Expression of Δ NLef1 in mouse epidermis results in differentiation of hair follicles into squamous epidermal cysts and formation of skin tumours. *Development* **129**, 95–109.
- Niemann, C., and Watt, F. M. (2002). Designer skin: Lineage commitment in postnatal epidermis. *Trends Cell Biol.* **12**, 185–192.
- Nishijyo, T., Kawada, A., Kanno, T., Shiraiwa, M., and Takahara, H. (1997). Isolation and molecular cloning of epidermal- and hair follicle-specific peptidylarginine deiminase (type III) from rat. *J. Biochem. (Tokyo)* **121**, 868–875.
- Olson, M. V. (1999). When less is more: Gene loss as an engine of evolutionary change. *Am. J. Hum. Genet.* **64**, 18–23.
- Orwin, D. F. G. (1971). Cell differentiation in the lower outer sheath of the Romney wool follicle: A companion layer. *Aust. J. Biol. Sci.* **24**, 989–999.
- Overdier, D. G., Porcella, A., and Costa, R. H. (1994). The DNA-binding specificity of the hepatocyte nuclear factor 3/forkhead domain is influenced by amino-acid residues adjacent to the recognition helix. *Mol. Cell. Biol.* **14**, 2755–2766.
- Panteleyev, A. A., Paus, R., Wanner, R., Nurnberg, W., Eichmuller, S., Thiel, R., Zhang, J., Henz, B. M., and Rosenbach, T. (1997). Keratin 17 gene expression during the murine hair cycle. *J. Invest. Dermatol.* **108**, 324–329.
- Pantelouris, E. M. (1973). Athymic development in the mouse. *Differentiation* **1**, 437–450.
- Parsa, R., Yang, A., McKeon, F., and Green, H. (1999). Association of p63 with proliferative potential in normal and neoplastic human keratinocytes. *J. Invest. Dermatol.* **113**, 1099–1105.
- Pearce, E. G., Smith, K., Lanigan, S. W., and Bowden, P. E. (1999). Two different mutations in the same codon of a type II hair keratin (hHb6) in patients with monilethrix. *J. Invest. Dermatol.* **113**, 1123–1127.
- Peitsch, W. K., Hofmann, I., Praetzel, S., Grund, C., Kuhn, C., Moll, I., Langbein, L., and Franke, W. W. (2001). Drebrin particles: Components in the ensemble of proteins regulating actin dynamics of lamellipodia and filopodia. *Eur. J. Cell Biol.* **80**, 567–579.
- Pellegrini, G., Dellambra, E., Golisano, O., Martinelli, E., Fantozzi, I., Bondanza, S., Ponzin, D., McKeon, F., and De Luca, M. (2001). p63 identifies keratinocyte stem cells. *Proc. Natl. Acad. Sci. USA* **98**, 3156–3161.
- Perrin, C., Langbein, L., and Schweizer, J. (2004). Expression of hair keratins in the adult human nail unit: An immunohistochemical analysis of the onychogenesis in the proximal nail fold, matrix and nail bed. *Br. J. Dermatol.* **151**, 362–371.
- Peters, T., Sedlmeier, R., Bussow, H., Runkel, F., Luers, G. H., Korthaus, D., Fuchs, H., Hrabe, D. A., Stumm, G., Russ, A. P., Porter, R. M., Augustin, M., and Franz, T. (2003).

- Alopecia in a novel mouse model RCO3 is caused by mK6irs1 deficiency. *J. Invest. Dermatol.* **121**, 674–680.
- Peterson, R. L., Papenbrock, T., Davda, M. M., and Awgulewitsch, A. (1994). The murine Hoxc cluster contains five neighboring AbdB-related Hox genes that show unique spatially coordinated expression in posterior embryonic subregions. *Mech. Dev.* **47**, 253–260.
- Philpott, M. P., Sanders, D. A., and Kealey, T. (1994). Effects of insulin and insulin-like growth factors on cultured human hair follicles: IGF-I at physiological concentrations is an important regulator of hair follicle growth *in vitro*. *J. Invest. Dermatol.* **102**, 857–861.
- Pierrou, S., Hellqvist, M., Samuelsson, L., Enerback, S., and Carlsson, P. (1994). Cloning and characterization of seven human forkhead proteins: Binding site specificity and DNA bending. *EMBO J.* **13**, 5002–5012.
- Pinkus, F. (1927). Die normale Anatomie der Haut. In “Handbuch der Haut- und Geschlechtskrankheiten: Anatomie der Haut” (J. Jadason, Ed.), p. 116. Springer-Verlag, Berlin.
- Pinkus, H. (1969). “Sebaceous cysts” are trichilemmal cysts. *Arch. Dermatol.* **99**, 544–555.
- Plikus, M., Wang, W. P., Liu, J., Wang, X., Jiang, T. X., and Chuong, C. M. (2004). Morphoregulation of ectodermal organs: Integument pathology and phenotypic variations in K14-Noggin engineered mice through modulation of bone morphogenic protein pathway. *Am. J. Pathol.* **164**, 1099–1114.
- Porter, R. M., Lunny, D. P., Ogden, P. H., Morley, S. M., McLean, W. H., Evans, A., Harrison, D. L., Rugg, E. L., and Lane, E. B. (2000). K15 expression implies lateral differentiation within stratified epithelial basal cells. *Lab. Invest.* **80**, 1701–1710.
- Porter, R. M., Corden, L. D., Lunny, D. P., Smith, F. J., Lane, E. B., and McLean, W. H. (2001). Keratin K6irs is specific to the inner root sheath of hair follicles in mice and humans. *Br. J. Dermatol.* **145**, 558–568.
- Porter, R. M., Gandhi, M., Wilson, N. J., Wood, P., McLean, W. H., and Lane, E. B. (2004). Functional analysis of keratin components in the mouse hair follicle inner root sheath. *Br. J. Dermatol.* **150**, 195–204.
- Powell, B. C., and Rogers, G. E. (1997). The role of keratin proteins and their genes in the growth, structure and properties of hair. In “Formation and Structure of Human Hair” (P. Jolles, H. Zahn, and H. Höcker, Eds.), pp. 59–148. Birkhäuser-Verlag, Basel.
- Price, V. H., and Gummer, C. L. (1989). Loose anagen syndrome. *J. Am. Acad. Dermatol.* **20**, 249–256.
- Randall, V. A. (1994). Androgens and human hair growth. *Clin. Endocrinol.* **40**, 439–457.
- Richard, G., Itin, P., Lin, J. P., Bon, A., and Bale, S. J. (1996). Evidence for genetic heterogeneity in monilethrix. *J. Invest. Dermatol.* **107**, 812–814.
- Roche, P. J., Hoare, S. A., and Parker, M. G. (1992). A consensus DNA-binding site for the androgen receptor. *Mol. Endocrinol.* **6**, 2229–2235.
- Rogers, G. E. (1959). Newer findings on the enzymes and proteins of hair follicles. *Ann. N. Y. Acad. Sci.* **83**, 408–428.
- Rogers, G. E. (1964). In “Structural and Biochemical Features of the Hair Follicle” (W. Montagna and W. C. Lobitz, Eds.), pp. 179–236. Academic Press, New York.
- Rogers, M. A., Winter, H., Wolf, C., Heck, M., and Schweizer, J. (1998). Characterization of a 190-kilobase pair domain of human type I hair keratin genes. *J. Biol. Chem.* **273**, 26683–26691.
- Rogers, M. A., Winter, H., Langbein, L., Wolf, C., and Schweizer, J. (2000). Characterization of a 300 kbp region of human DNA containing the type II hair keratin gene domain. *J. Invest. Dermatol.* **114**, 464–472.
- Rogers, M. A., Langbein, L., Winter, H., Ehmann, C., Praetzel, S., Korn, B., and Schweizer, J. (2001). Characterization of a cluster of human high/ultrahigh sulfur keratin associated protein (KAP) genes imbedded in the type I keratin gene domain on chromosome 17q12–21. *J. Biol. Chem.* **276**, 19440–19451.

- Rogers, M. A., Langbein, L., Winter, H., Ehmann, C., Praetzel, S., and Schweizer, J. (2002). Characterization of a first domain of human high glycine-tyrosine and high sulfur keratin-associated protein (KAP) genes on chromosome 21q22.1. *J. Biol. Chem.* **277**, 48993–49002.
- Rogers, M. A., Langbein, L., Winter, H., Beckmann, I., Praetzel, S., and Schweizer, J. (2004a). Hair keratin associated proteins: Characterization of a second high sulfur KAP gene domain on human chromosome 21. *J. Invest. Dermatol.* **122**, 147–158.
- Rogers, M. A., Edler, L., Winter, H., Langbein, L., Beckmann, I., and Schweizer, J. (2004b). Characterization of new members of the human type II keratin gene family and a general evaluation of the keratin gene domain on chromosome 12q13.13. *J. Invest. Dermatol.* In press and online.
- Rogers, M. A., Winter, H., Langbein, L., Bleiler, R., and Schweizer, J. (2004c). The human type I keratin gene family: Characterization of new hair follicle-specific members and evaluation of the chromosome 17q21.2 gene domain. *Differentiation* **72**, 527–540.
- Rogers, M. A., Langbein, L., Winter, H., and Schweizer, J. (2005). In preparation.
- Ross, E. V., Evans, L. A., and Yeager, J. K. (1993). Pseudofolliculitis barbae associated with an unusual hair whorl. *Cutis* **51**, 107–108.
- Rothnagel, J. A., and Roop, D. R. (1995). Hair follicle companion layer: Reacquainting an old friend. *J. Invest. Dermatol.* **104**, 42S–43S.
- Rothnagel, J. A., Longley, M. A., Holder, R. A., Bundman, D. S., Seki, T., Bickenbach, J. R., and Roop, D. R. (1994). Genetic disorders of keratin: Are scarring alopecias a sub-set? *J. Dermatol. Sci.* **7**, s164–s169.
- Rothnagel, J. A., Seki, T., Ogo, M., Longley, M. A., Wojcik, S. M., Bundman, D. S., Bickenbach, J. R., and Roop, D. R. (1999). The mouse keratin 6 isoforms are differentially expressed in the hair follicle, footpad, tongue and activated epidermis. *Differentiation* **65**, 119–130.
- Rudall, K. M. (1947). Studies of the distribution of protein chain types in the vertebrate epidermis. *J. Ultrastruct. Res.* **11**, 33–51.
- Salzberg, A., Elias, S., Nachaliel, N., Bonstein, L., Henig, C., and Frank, D. (1999). A Meis family protein caudalizes neural cell fates in *Xenopus*. *Mech. Dev.* **80**, 3–13.
- Sander, G. R., and Powell, B. C. (2004). Structure and expression of the ovine *Hoxc13* gene. *Gene* **327**, 107–116.
- Sawada, M., Terada, N., Taniguchi, H., Tateishi, R., and Mori, Y. (1987). Cyclosporin A stimulates hair growth in nude mice. *Lab. Invest.* **56**, 684–686.
- Schaumburg-Lever, G. (1975). Tumors of the epidermal appendages. In “Histopathology of the Skin” (W. F. Schaumburg and G. Schaumburg-Lever, Eds.), vol. 2. Lippincott, Philadelphia, PA.
- Schirren, C. G., Burgdorf, W. H., Sander, C. A., and Plewig, G. (1997). Fetal and adult hair follicle: An immunohistochemical study of anticytokeratin antibodies in formalin-fixed and paraffin-embedded tissue. *Am. J. Dermatopathol.* **19**, 335–340.
- Schlake, T., and Boehm, T. (2001). Expression domains in the skin of genes affected by the nude mutation and identified by gene expression profiling. *Mech. Dev.* **109**, 419–422.
- Schlake, T., Schorpp, M., Maul-Pavicic, A., Malashenko, A. M., and Boehm, T. (2000). Forkhead/winged-helix transcription factor whn regulates hair keratin gene expression: Molecular analysis of the nude skin phenotype. *Dev. Dyn.* **217**, 368–376.
- Schon, M., Benwood, J., O’Connell-Willstaedt, T., and Rheinwald, J. G. (1999). Human sweat gland myoepithelial cells express a unique set of cytokeratins and reveal the potential for alternative epithelial and mesenchymal differentiation states in culture. *J. Cell. Sci.* **112**, 1925–1936.
- Schorpp, M., Hofmann, M., Dear, T. N., and Boehm, T. (1997). Characterization of mouse and human nude genes. *Immunogenetics* **46**, 509–515.
- Schorpp, M., Schlake, T., Kreamalmeyer, D., Allen, P. M., and Boehm, T. (2000). Genetically separable determinants of hair keratin gene expression. *Dev. Dyn.* **218**, 537–543.

- Shang, L., Pruett, N. D., and Awgulewitsch, A. (2002). Hoxc12 expression pattern in developing and cycling murine hair follicles. *Mech. Dev.* **113**, 207–210.
- Shen, W. F., Rozenfeld, S., Lawrence, H. J., and Largman, C. (1997). The Abd-B-like Hox homeodomain proteins can be subdivided by the ability to form complexes with Pbx1a on a novel DNA target. *J. Biol. Chem.* **272**, 8198–8206.
- Shen, W. F., Rozenfeld, S., Kwong, A., Kom ves, L. G., Lawrence, H. J., and Largman, C. (1999). HOXA9 forms triple complexes with PBX2 and MEIS1 in myeloid cells. *Mol. Cell. Biol.* **19**, 3051–3061.
- Shibuya, K., Obayashi, I., Asakawa, S., Minoshima, S., Kudoh, J., and Shimizu, N. (2004). A cluster of 21 keratin-associated protein genes within introns of another gene on human chromosome 21q22.3. *Genomics* **83**, 679–693.
- Shimizu, H., and Morgan, B. A. (2004). Wnt signaling through the β -catenin pathway is sufficient to maintain, but not restore, anagen-phase characteristics of dermal papilla cells. *J. Invest. Dermatol.* **122**, 239–245.
- Sinclair, R., Cargnello, J., and Chow, C. W. (1999). Loose anagen syndrome. *Exp. Dermatol.* **8**, 297–298.
- Smith, F. J. D. (2003). The molecular genetics of keratin disorders. *Am. J. Clin. Dermatol.* **4**, 347–364.
- Smith, F. J. D., Steijlen, P. M., McKenna, K. E., van Goor, H., Coleman, C. M., Covello, S. P., Uitto, J., and McLean, W. H. I. (1998). A mutation in human keratin K6b produces a phenocopy of the K17 disorder pachyonychia congenita type 2. *Hum. Mol. Genet.* **7**, 1143–1148.
- Smith, F. J. D., Porter, R. M., Corden, L. D., Lunny, D. P., Lane, E. B., and McLean, W. H. I. (2002). Cloning of human, murine, and marsupial keratin 7 and a survey of K7 expression in the mouse. *Biochem. Biophys. Res. Commun.* **297**, 818–827.
- Smith, J. E., Jr., Bollekens, J. A., Inghirami, G., and Takeshita, K. (1997). Cloning and mapping of the *MEIS1* gene, the human homolog of a murine leukemogenic gene. *Genomics* **43**, 99–103.
- Smith, W. G. (1879). A rare nodose condition of the hair. *Br. Med. J.* **2**, 291–296.
- Sperling, L. C. (1991). Hair anatomy for the clinician. *J. Am. Acad. Dermatol.* **25**, 1–17.
- Sredni, B., Gal, R., Cohen, I. J., Dazard, J. E., Givol, D., Gafter, U., Motro, B., Eliyahu, S., Albeck, M., Lander, H. M., and Kalechman, Y. (2004). Hair growth induction by the tellurium immunomodulator AS101: Association with delayed terminal differentiation of follicular keratinocytes and ras-dependent up-regulation of KGF expression. *FASEB J.* **18**, 400–402.
- Stark, H.-J., Breitkreuz, D., Limat, A., Bowden, P. E., and Fusenig, N. E. (1987). Keratins of the human hair follicle: “Hyperproliferative” keratins consistently expressed in outer root sheath cells *in vivo* and *in vitro*. *Differentiation* **35**, 236–248.
- Stark, H.-J., Breitkreutz, D., Limat, A., Ryle, C. M., Roop, D. R., Leigh, I., and Fusenig, N. E. (1990). Keratins 1 and 10 or homologues as regular constituents of inner root sheath and cuticle cells in the human hair follicle. *Eur. J. Cell Biol.* **52**, 359–372.
- Stasiak, P. C., Purkis, P. E., Leigh, I. M., and Lane, E. B. (1989). Keratin 19: Predicted amino acid sequence and broad tissue distribution suggest it evolved from keratinocyte keratins. *J. Invest. Dermatol.* **92**, 707–716.
- Steinert, P. M., and Roop, D. R. (1988). Molecular and cellular biology of intermediate filaments. *Annu. Rev. Biochem.* **57**, 593–625.
- Stenn, K. S., Combates, N. J., Eilertsen, K. J., Gordon, J. S., Pardinas, J. R., Parimoo, S., and Prouty, S. M. (1996). Hair follicle growth controls. *Dermatol. Clin.* **14**, 543–558.
- Stevens, H. P., Keisell, D. P., Bryant, S. P., Bishop, D. T., Dawber, R. P. R., Spurr, N. K., and Leigh, I. M. (1996). Linkage of monilethrix to the trichocyte and epithelial keratin gene cluster on 12q11–13. *J. Invest. Dermatol.* **106**, 795–805.

- Stringer, C. B., and Andrews, P. (1988). Genetic and fossil evidence for the origin of modern humans. *Science* **239**, 1263–1268.
- Swift, J. A. (1969). The electron histochemical demonstration of cystine-containing proteins in the guinea pig hair follicle. *Histochemie* **19**, 88–98.
- Takahashi, K., Paladini, R. D., and Coulombe, P. A. (1995). Cloning and characterization of multiple human genes and cDNAs encoding highly related type II keratin 6 isoforms. *J. Biol. Chem.* **270**, 18581–18592.
- Tarcsa, E., Marekov, L. N., Andreoli, J., Idler, W. W., Candi, E., Chung, S. I., and Steinert, P. M. (1997). The fate of trichohyalin: Sequential post-translational modifications by peptidyl-arginine deiminase and transglutaminases. *J. Biol. Chem.* **272**, 27893–27901.
- Tattersall, I. (1997). Out of Africa again . . . and again? *Sci. Am.* **276**, 60–67.
- Thesleff, I. (2003). Epithelial–mesenchymal signalling regulating tooth morphogenesis. *J. Cell Sci.* **116**, 1647–1648.
- Tkatchenko, A. V., Visconti, R. P., Shang, L., Papenbrock, T., Pruett, N. D., Ito, T., Ogawa, M., and Awgulewitsch, A. (2001). Overexpression of Hoxc13 in differentiating keratinocytes results in downregulation of a novel hair keratin gene cluster and alopecia. *Development* **128**, 1547–1558.
- Tong, X., and Coulombe, P. A. (2004). A novel mouse type I intermediate filament gene, keratin 17n (K17n), exhibits preferred expression in nail tissue. *J. Invest. Dermatol.* **122**, 965–970.
- Tsujita-Kyutoku, M., Kiuchi, K., Danbara, N., Yuri, T., Senzaki, H., and Tsubura, A. (2003). p63 expression in normal human epidermis and epidermal appendages and their tumors. *J. Cutan. Pathol.* **30**, 11–17.
- Tufarelli, C., Fujiwara, Y., Zappulla, D. C., and Neufeld, E. J. (1998). Hair defects and pup loss in mice with targeted deletion of the first cut repeat domain of the Cox/CDP homeoprotein gene. *Dev. Biol.* **200**, 69–81.
- Turksen, K. (2004). Revisiting the bulge. *Dev. Cell* **6**, 454–456.
- Waldeyer, W. (1882). Untersuchungen über die Histogenese der Horngebilde, insbesondere der Haare und Federn. In “Beitr. z. Anatomie u. Embryologie,” pp. 141–163. Bonn, Germany.
- Wang, H., Parry, D. A., Jones, L. N., Idler, W. W., Marekov, L. N., and Steinert, P. M. (2000). *In vitro* assembly and structure of trichocyte keratin intermediate filaments: A novel role for stabilization by disulfide bonding. *J. Cell Biol.* **151**, 1459–1468.
- Wang, Z., Wong, P., Langbein, L., Schweizer, J., and Coulombe, P. A. (2003). Type II epithelial keratin 6hf (K6hf) is expressed in the companion layer, matrix, and medulla in anagen-stage hair follicles. *J. Invest. Dermatol.* **121**, 1276–1282.
- Watanabe, S., Wagatsuma, K., and Takahashi, H. (1994). Immunohistochemical localization of cytokeratins and involucrin in calcifying epithelioma: Comparative studies with normal skin. *Br. J. Dermatol.* **131**, 506–513.
- Weinstein, G. D., and Mooney, K. M. (1980). Cell proliferation kinetics in the human hair root. *J. Invest. Dermatol.* **74**, 43–46.
- Whitbread, L. A., and Powell, B. C. (1998). Expression of the intermediate filament keratin gene, *K15*, in the basal cell layers of epithelia and the hair follicle. *Exp. Cell Res.* **244**, 448–459.
- Wilson, C. L., Dean, D., Lane, E. B., Dawber, R. P., and Leigh, I. M. (1994). Keratinocyte differentiation in psoriatic scalp: Morphology and expression of epithelial keratins. *Br. J. Dermatol.* **131**, 191–200.
- Winter, H., Siry, P., Tobiasch, E., and Schweizer, J. (1994). Sequence and expression of murine type I hair keratins mHa2 and mHa3. *Exp. Cell Res.* **212**, 190–200.
- Winter, H., Hoffman, I., Langbein, L., Rogers, M. A., and Schweizer, J. (1997a). A splice site mutation in the gene of the human type I hair keratin hHa1 results in the expression of a tailless keratin isoform. *J. Biol. Chem.* **272**, 32345–32352.

- Winter, H., Rogers, M. A., Gebhardt, M., Wollina, U., Boxall, L., Chitayat, D., Babul-Hirji, R., Stevens, H. P., Zlotogorski, A., and Schweizer, J. (1997b). A new mutation in the type II hair cortex keratin hHb1 involved in the inherited hair disorder monilethrix. *Hum. Genet.* **101**, 165–169.
- Winter, H., Rogers, M. A., Langbein, L., Stevens, H. P., Leigh, I. M., Labreze, C., Roul, S., Taieb, A., Krieg, T., and Schweizer, J. (1997c). Mutations in the hair cortex keratin hHb6 cause the inherited hair disease monilethrix. *Nat. Genet.* **16**, 372–374.
- Winter, H., Labrèze, C., Chapalain, V., Surlève-Bazeille, J., Mercier, M., Rogers, M. A., Taieb, A., and Schweizer, J. (1998a). A variable monilethrix phenotype associated with a novel mutation, Glu402Lys, in the helix termination motif of the type II hair keratin hHb1. *J. Invest. Dermatol.* **111**, 169–172.
- Winter, H., Langbein, L., Praetzel, S., Jacobs, M., Rogers, M. A., Leigh, I. M., Tidman, N., and Schweizer, J. (1998b). A novel human type II cytokeatin, K6hf, specifically expressed in the companion layer of the hair follicle. *J. Invest. Dermatol.* **111**, 955–962.
- Winter, H., Clark, R. D., Tarras-Wahlberg, C., Rogers, M. A., and Schweizer, J. (1999). Monilethrix: A novel mutation (Glu402Lys) in the helix termination motif and the first causative mutation (Asn114Asp) in the helix initiation motif of the type II hair keratin hHb6. *J. Invest. Dermatol.* **113**, 263–266.
- Winter, H., Vabres, P., Larrègue, M., Rogers, M. A., and Schweizer, J. (2000). A novel missense mutation, A118E, in the helix initiation motif of the type II hair cortex keratin hHb6, causing monilethrix. *Hum. Hered.* **50**, 322–324.
- Winter, H., Langbein, L., Krawczak, M., Cooper, D. N., Jave-Suarez, L. F., Rogers, M. A., Praetzel, S., Heidt, P. J., and Schweizer, J. (2001). Human type I hair keratin pseudogene ϕ hHaA has functional orthologs in the chimpanzee and gorilla: Evidence for recent inactivation of the human gene after the *Pan-Homo* divergence. *Hum. Genet.* **108**, 37–42.
- Winter, H., Schissel, D., Parry, D. A., Smith, T. A., Liovic, M., Birgitte, L. E., Edler, L., Langbein, L., Jave-Suarez, L. F., Rogers, M. A., Wilde, J., Peters, G., and Schweizer, J. (2004). An unusual Ala12Thr polymorphism in the 1A α -helical segment of the companion layer-specific keratin K6hf: Evidence for a risk factor in the etiology of the common hair disorder pseudofolliculitis barbae. *J. Invest. Dermatol.* **122**, 652–657.
- Wojcik, S. M., Longley, M. A., and Roop, D. R. (2001). Discovery of a novel murine keratin 6 (K6) isoform explains the absence of hair and nail defects in mice deficient for K6a and K6b. *J. Cell Biol.* **154**, 619–630.
- Yahagi, S., Shibuya, K., Obayashi, I., Masaki, H., Kurata, Y., Kudoh, J., and Shimizu, N. (2004). Identification of two novel clusters of ultrahigh-sulfur keratin-associated protein genes on human chromosome 11. *Biochem. Biophys. Res. Commun.* **318**, 655–664.
- Yu, D.-W., Pang, S. Y. Y., Checkla, D. M., Freedberg, I. M., Sun, T.-T., and Bertolino, A. P. (1991). Transient expression of mouse hair keratin in transfected HeLa cells: Interactions between “hard” and “soft” keratins. *J. Invest. Dermatol.* **97**, 354–363.
- Yu, J., Yu, D.-W., Checkla, D. M., Freedberg, I. M., and Bertolino, A. P. (1993). Human hair keratins. *J. Invest. Dermatol.* **101**, 56s–59s.
- Zaun, H. (1968). Histologie, Histochemie und Wachstumsdynamik des Haarfollikels. In “Handbuch der Haut- und Geschlechtskrankheiten” (O. Gans and G. K. Steigleder, Eds.), pp. 143–157. Springer-Verlag, New York.
- Zhou, P., Byrne, C., Jacobs, J., and Fuchs, E. (1995). Lymphoid enhancer factor 1 directs hair follicle patterning and epithelial cell fate. *Genes Dev.* **9**, 700–713.
- Zimek, A., Stick, R., and Weber, K. (2003). Genes coding for intermediate filament proteins: Common features and unexpected differences in the genomes of humans and the teleost fish *Fugu rubripes*. *J. Cell Sci.* **116**, 2295–2302.
- Zlotogorski, A., Horev, L., and Glaser, B. (1998). Monilethrix: A keratin hHb6 mutation is co-dominant with variable expression. *Exp. Dermatol.* **7**, 268–272.

Calcium Channels and Ca^{2+} Fluctuations in Sperm Physiology

Alberto Darszon,* Takuya Nishigaki,* Chris Wood,* Claudia L. Treviño,* Ricardo Felix,† and Carmen Beltrán*

*Department of Developmental Genetics and Molecular Physiology, Institute of Biotechnology, Universidad Nacional Autónoma de México, Cuernavaca, Morelos, Mexico 62210

†Department of Physiology, Biophysics and Neurosciences, Center for Research and Advanced Studies of the National Polytechnic Institute, Mexico City, Mexico 07300

Generating new life in animals by sexual reproduction depends on adequate communication between mature and competent male and female gametes. Ion channels are instrumental in the dialogue between sperm, its environment, and the egg. The ability of sperm to swim to the egg and fertilize it is modulated by ion permeability changes induced by environmental cues and components of the egg outer layer. Ca^{2+} is probably the key messenger in this information exchange. It is therefore not surprising that different Ca^{2+} -permeable channels are distinctly localized in these tiny specialized cells. New approaches to measure sperm currents, intracellular Ca^{2+} , membrane potential, and intracellular pH with fluorescent probes, patch-clamp recordings, sequence information, and heterologous expression are revealing how sperm channels participate in fertilization. Certain sperm ion channels are turning out to be unique, making them attractive targets for contraception and for the discovery of novel signaling complexes.

KEY WORDS: Sperm Ca^{2+} channels, Acrosome reaction, Spermatogenesis, Sperm motility, Chemotaxis, Sperm capacitation, Ion channels, Single-cell imaging. © 2005 Elsevier Inc.

I. Introduction

The male gamete (spermatozoon or sperm) must reach, recognize, and fuse with the female gamete (egg) for fertilization to occur, thus initiating the development of a new individual. Amazingly, the unique sperm is able to do this even though it cannot transcribe genes or synthesize proteins. This meticulously orchestrated process requires fully mature and competent gametes and a complex dialogue between sperm and egg. We are still far from fully understanding this molecular conversation. The importance of ion channels in sperm physiology, particularly those permeable to Ca^{2+} , has become evident. These ion channels are key players in gamete signaling. For instance, sperm motility and the acrosome reaction (AR), an exocytotic process required for fertilization in many species, are inhibited by ion channels blockers (Darszon *et al.*, 1999, 2001; Yoshida *et al.*, 2003).

Ion channels perform essential transport and signaling functions in all cells. It is no wonder that hundreds of channels are encoded in the genomes of fruit fly, worm, zebra fish, mouse, and human. Cells spend considerable energy building and maintaining ion concentration gradients across the membrane through the use of pumps. These resources are utilized by ion channels, which on activation can change the electrical potential of the cell and the concentrations of second messengers within a wide time range, depending on the modes of channel regulation. Ion channels can be opened by small conformational changes induced by voltage, ligands, phosphorylation changes, membrane pressure, and so on. Channel opening leads to the flow of millions of ions per second across the membrane, down their electrochemical gradient (Hille, 2001).

The main theme of this review is the participation of Ca^{2+} channels in sperm function. It is regrettably impossible to surmount the authors' limitations and biases, which result in omissions of some important contributions. An apology is offered together with reference to several reviews that directly or indirectly deal with the subject of the review (Baker and Aitken, 2004; Baldi *et al.*, 2000, 2002; Benoff, 1998b; Benoff *et al.*, 2000; Breitbart, 2003; Jagannathan *et al.*, 2002a; Neill and Vacquier, 2004; Patrat *et al.*, 2000; Vacquier, 1998; Wassarman *et al.*, 2001).

II. General Background

A. Spermatogenesis

The process of germ cell differentiation and proliferation to yield haploid sperm takes place in the seminiferous tubules and is called spermatogenesis. In addition to being under paracrine control, spermatogenesis is regulated by

a complex communication scheme achieved by cell–cell interactions involving enzymes, cytokines, transport proteins, growth factors, and so on. However, the molecular mechanisms utilized during this process are not well understood. Testis differentiation occurs early in gestation as primordial germ cells reach the gonad and somatic cells begin to express the testis-determining *Syr* gene (McLaren, 1998). *Syr* induces the differentiation of somatic cells to Sertoli cells and later on directs the production of Leydig cells, which in turn produce testosterone and favor the production of peritubular cells. Sertoli and peritubular cells form the basement membrane of seminiferous tubules. Sertoli cells interact directly with germ cells, performing critical functions such as the secretion of a complex fluid containing many essential proteins and factors that are necessary for germ cell viability, maturation, and differentiation. Peritubular cells interact both indirectly (via Sertoli cells) and directly with germ cells, also secreting factors essential for the self-renewal and propagation of stem cells.

There are three basic phases during spermatogenesis (Parks *et al.*, 2003):

1. Spermatocytogenesis: The differentiation and proliferation of germ stem cells to generate spermatogonia and finally preleptotene primary spermatocytes.
2. Meiosis: A process, which includes two divisions, that converts primary spermatocytes ($4N$) to secondary spermatocytes ($2N$) and the latter into round haploid ($1N$) spermatids.
3. Spermiogenesis: A differentiation process with no further division, to render a differentiated sperm cell.

In mammals this process takes several weeks and varies according to species; several stages of differentiation can be identified in each phase. Regulation of cellular processes often involves changes in membrane permeability and spermatogenesis is not an exception. The precise control required for cell division and differentiation in the seminiferous tubules must involve complex signaling mechanisms. Changes in intracellular Ca^{2+} ($[\text{Ca}^{2+}]_i$), intracellular pH (pH_i), and membrane potential (E_m) are likely to be involved in sperm development. However, little is known about the role of specific ion channels during this important process. The presence of several ion channels has been determined in spermatogenic cells at distinct stages of differentiation, although their specific function during spermatogenesis remains to be established. Members of the voltage-dependent Ca^{2+} (Ca_v) channels (Serrano *et al.*, 1999a; Son *et al.*, 2002; Treviño *et al.*, 2004) as well as several K^+ channels have been localized to spermatogenic cells (Chan *et al.*, 1998; Felix *et al.*, 2002; Munoz-Garay *et al.*, 2001). In addition, transcripts and proteins of other ion channels have been identified in spermatogenic cells, such as the glycine receptor/ Cl^- channel (Sato *et al.*, 2002), aquaporin-8 (AQP8) (Elkjaer *et al.*, 2001), and the inositol-1,4,5-trisphosphate (IP_3) and ryanodine receptors (Treviño *et al.*, 1998). AQP8 may

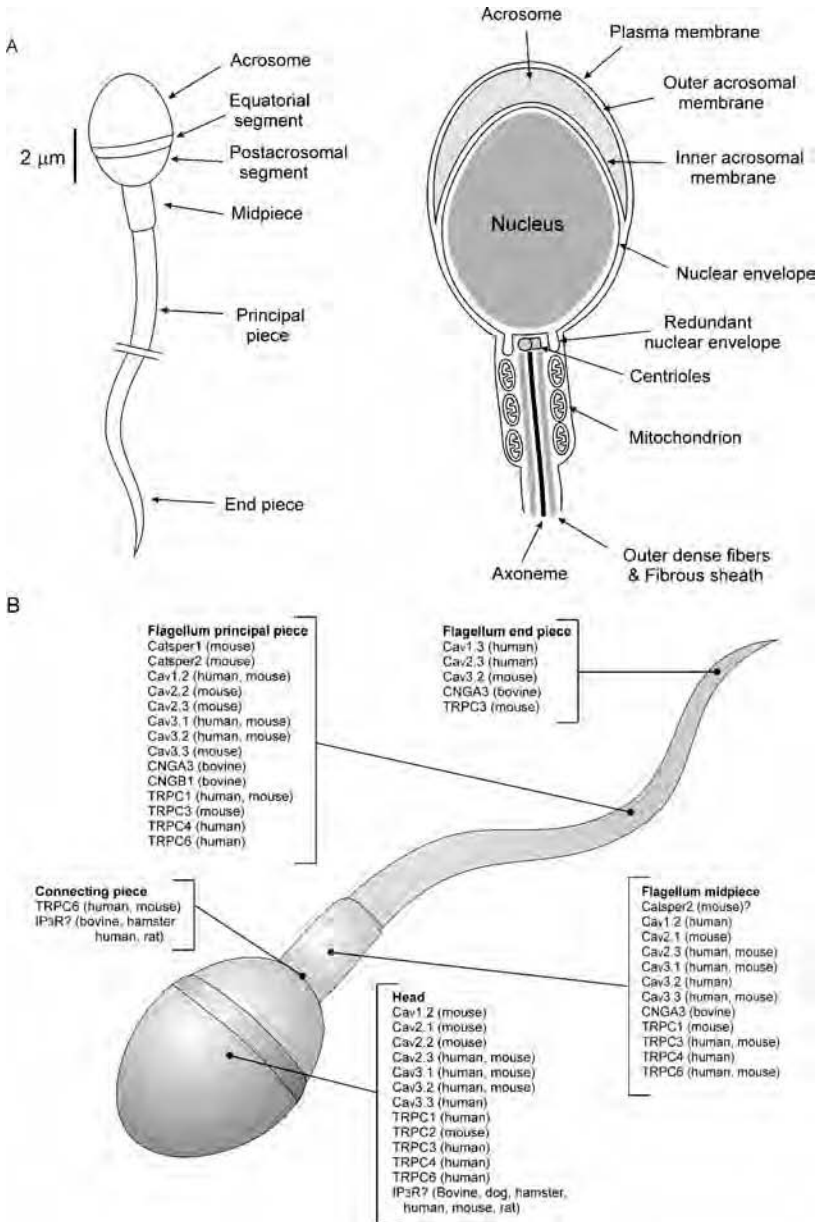


FIG. 1 (A) Diagram of human sperm. Sperm head and flagellum are composed of several segments (*left*). Structure of the sperm head and midpiece region (*right*). (B) Distribution of Ca^{2+} -permeable channels in mammalian sperm. The location of the channels is approximate, considering morphological differences between species.

participate in water secretion to form a fluid-filled seminiferous tubular lumen, an event that starts spermatogenesis. It also participates in tubular fluid secretion, which contributes to sperm transport and possibly to further sperm maturation (Cho *et al.*, 2003; Ishibashi *et al.*, 1997). AQP8 and/or AQP7 are presumed to be responsible for most of the cell volume reduction by which spermatids differentiate into sperm during spermiogenesis (Calamita *et al.*, 2001; Cho *et al.*, 2003; Kageyama *et al.*, 2001).

B. Basic Characteristics of Sperm

Nearly all animal sperm conform to a similar general design (Fig. 1). These specialized cells are quite small and mainly constituted by: (1) the head (2–5 μm in diameter), containing condensed packages of chromosomes in the nucleus (which occupies a significant proportion of the head), two centrioles, and in many species the acrosome, a membranous structure overlying the nucleus in the anterior part of the sperm head; (2) the flagellum or tail, which varies in length, depending on the species (10–100 μm), and contains the axoneme, the machinery that propels sperm. The great majority of axonemes have a characteristic structure comprising nine microtubule doublets arranged in a ring around two central singlet microtubules. The doublet microtubules are sliding units containing radial spokes, dynein arms, and dynein docking and regulatory complexes. The nine doublets are interconnected and the central pair bridge joins the inner microtubules. The total number of proteins present in the axoneme is about 250, but the exact composition varies according to species (Inaba, 2003). Dyneins are ATPases producing the motility force and phosphorylation is important in regulation of axonemal movement; and (3) mitochondria at the base of the tail, contributing to power its movement. They can be inside the sperm head as in sea urchins, or spirally arranged in the flagellar midpiece, as in mammals. Sperm have a reduced cytoplasmic volume and are incapable of synthesizing proteins or nucleic acids. The singular purpose of these dedicated cells is to find, fuse, and deliver their genetic information to the egg.

III. Calcium and Ca^{2+} Channels

A. Calcium

Ca^{2+} is the most widely used intracellular messenger in cell signaling. It is involved in the regulation of many important cell functions, such as secretion, excitation–contraction, gene transcription, motility, enzyme activity

and transport, and state of protein phosphorylation, as well as in various forms of cell death (Carafoli, 2002). Why has Ca^{2+} been chosen to perform a vast range of intracellular messenger functions throughout evolution? Although no conclusive answer can be given, the choice appears to be driven by the necessity to bind the messenger tightly and specifically to proteins. Monovalent ions seem less suitable for this role because of their large ionic radii and low charge. This also appears to be true for large polyatomic anions such as bicarbonate and phosphate. What about other divalent cations? For instance, Mg^{2+} is significantly smaller than Ca^{2+} and this imposes difficulties for its strong binding to proteins. Assembling a small octahedral cavity with the protein's coordinating oxygen atoms (usually six) causes constraints due to insufficient flexibility. Thus, Mg^{2+} frequently needs water oxygen atoms to fulfill its coordination requirements, resulting in a reduction of its binding strength to proteins. In contrast, the larger radius of Ca^{2+} allows a wider margin for the coordination number (six to eight), maintaining tight binding with smaller physical constraints on the protein. The interplay between ionic radius, charge density, protein conformation, and reversible binding has evolutionarily selected Ca^{2+} as the most versatile intracellular messenger (Williams, 2002).

Specific sensor proteins regulate and detect the concentration of $[\text{Ca}^{2+}]_i$, reversibly binding it and thereafter signaling on to other targets (Carafoli *et al.*, 2001). The transduction process relies on specific conformational changes in the sensor proteins. EF hand proteins, a family of hundreds of members, are able to perform these tasks because they contain a Ca^{2+} -binding loop with 12 precisely positioned amino acids between highly structured α -helical coils. This helix-loop-helix motif is repeated 2–12 times. Ca^{2+} is coordinated to side-chain oxygen atoms of conserved residues at positions 1, 3, 5, and 12 of the loop, and to the carbonyl oxygen of a more variable residue at the seventh position. Calmodulin (CaM) and troponin C are among the best characterized EF hand proteins (Lewit-Bentley and Rety, 2000). The surface of these proteins becomes more hydrophobic on Ca^{2+} binding, increasing their affinity for specific targets. Although there are other proteins that decode Ca^{2+} signals, such as the annexins (Gerke and Moss, 2002), EF hand proteins are the most important. They may be part of an enzyme such as calpain (Goll *et al.*, 2003), a subunit of an individual protein, or a protein such as CaM that reversibly interacts with others (i.e., ion channels, kinases, phosphatases, and hydrolases), regulating their activity (Saimi and Kung, 2002). Calsequestrin and calreticulin are two other Ca^{2+} -buffering proteins with high Ca^{2+} -binding capacity (up to 50 Ca^{2+} per molecule) (Beard *et al.*, 2004). They were originally found in the intracellular Ca^{2+} stores, where they allow extensive Ca^{2+} accumulation without formation of Ca^{2+} phosphate precipitates. It is now known that calsequestrin can also regulate ryanodine receptors (RyRs) (Beard *et al.*, 2004; Corbett and

Michalak, 2000) and calreticulin can function as a lectin-like chaperone (Corbett and Michalak, 2000).

Furthermore, $[Ca^{2+}]_i$ is directly regulated by membrane transporters, which do not necessarily transduce its message. These proteins are found in the plasma and organelle membranes, where they have specific functions in the regulation of cellular Ca^{2+} homeostasis. In general, cells contain about 1 mM total Ca^{2+} , a concentration similar to that found outside. At rest, the level of ionized “free” Ca^{2+} in the cytoplasm is ~ 100 nM, thousands of times less than the concentration outside and the total concentration inside (Hille, 2001). Why is free Ca^{2+} in the cytosol maintained at such low levels? It is believed that low $[Ca^{2+}]_i$ is a prerequisite for the extensive use of phosphate-containing compounds as energy sources, as the high concentrations of inorganic phosphates generated during metabolic energy conversions would be incompatible with high $[Ca^{2+}]_i$ (Carafoli, 1987). In addition, the enormous Ca^{2+} gradient from the outside to the inside can be used as an efficient driving force for signaling events. It is thus understandable that a set of Ca^{2+} transporters has evolved with spatial and temporal characteristics to suit the specific functions of distinct cell types.

How do cells manage to keep a Ca^{2+} gradient of three orders of magnitude between the cytoplasm and the outside? As mentioned earlier, the cell expends a significant fraction of its energy as ATP, to keep various ATPases pumping ions against their gradient. The plasma membrane has pumps to extrude Ca^{2+} and Na^+ (Ca^{2+} -ATPase, Na^+/K^+ -ATPase) from the cytoplasm to the extracellular medium. The sarco/endoplasmic reticulum has pumps that sequester cytosolic Ca^{2+} into their lumen; such (SERCA) pumps are also present in the Golgi apparatus and the nuclear envelope. Cells have mainly two types of Na^+/Ca^{2+} exchangers (NCX) that use the ATP-driven Na^+ gradient to extrude Ca^{2+} : one type in the plasma membrane and another in the mitochondria. The mitochondrial NCX removes Ca^{2+} that entered the mitochondria by a still ill-defined transport system (Berridge *et al.*, 2003; Carafoli, 2002).

Cells at rest have their ion gradients ready to respond to external or internal cues and they express a distinct set of Ca^{2+} -signaling components tailored to their function (Fig. 1B). Ca^{2+} signals are generated mainly from two sources: the extracellular medium or from internal stores. Ca^{2+} transients with differential spatial and temporal properties frequently encode these signals. Various classes of Ca^{2+} channels in the plasma membrane allow the movement of this cation from the external medium into the cytoplasm. These channels can be regulated by voltage, ligands, pressure, or depletion of internal stores. The internal stores, principally the endo/sarcoplasmic reticulum, release Ca^{2+} through channels modulated by Ca^{2+} itself, or by other second messengers such as IP_3 , cyclic ADP ribose, nicotinic acid adenine dinucleotide phosphate (NAADP), and sphingosine 1-phosphate (Berridge *et al.*, 2003).

B. Main Types of Ca²⁺-Permeable Channels

1. Voltage-Gated Ca²⁺ Channels

The major function of the voltage-sensitive Ca²⁺ (Ca_v) channels is to convert changes in membrane potential into a Ca²⁺ signal. The Ca_v channel permeation pathway is formed by its α_1 subunit, which is encoded by a family of at least 10 genes. The structure of this subunit is based on four repeated transmembrane domains (I–IV) that contain six transmembrane α helices (S1–S6) surrounding a central pore (Catterall, 2000; Catterall *et al.*, 2003) (Fig. 2). Ca_v channels fall into two major functional classes: high voltage- and low voltage-activated channels (HVA and LVA, respectively).

HVA channels open after strong depolarizations and have been classified according to the biophysical and pharmacological characteristics of the currents into L-, N-, P/Q-, and R-type (Table I). This class of channels is encoded by seven members of the α_1 family: Ca_v1.1 to Ca_v1.4 and Ca_v2.1 to Ca_v2.3 (Catterall, 2000; Catterall *et al.*, 2003). The current through HVA channels may be modulated by alternative splicing of the α_1 subunit mRNA, by the presence of auxiliary subunits (which also represent gene families and may be subject to alternative splicing), and by posttranslational modifications (Arikkath and Campbell, 2003; Catterall, 2000). The functional consequences of these structural modifications, coupled with the selective targeting of channels to cell surface domains, provide a mechanism for the fine control of [Ca²⁺]_i.

Transcripts encoding Ca_v1.2, Ca_v1.4, Ca_v2.1, and Ca_v2.3 HVA channels have been identified by reverse transcription-polymerase chain reaction (RT-PCR) in spermatogenic cells (Espinosa *et al.*, 1999; Liévano *et al.*, 1996; Son *et al.*, 2002), while Ca_v2.2, Ca_v2.3 (Park *et al.*, 2003), and several members of the Ca_v1 family were reported in mature sperm (Goodwin *et al.*, 2000; Park *et al.*, 2003) (Fig. 1B). Likewise, Ca_v1.2 and Ca_v2.1 proteins have been documented in spermatogenic cells (Serrano *et al.*, 1999a) and the protein products for all genes of the Ca_v1 and Ca_v2 subfamilies, with the exception of Ca_v1.1 and Ca_v1.4, have been immunolocalized in mature sperm (Treviño *et al.*, 2004; Wennemuth *et al.*, 2000; Westenbroek and Babcock, 1999). Although significant HVA Ca²⁺ currents have not been detected in male germ cells, the use of HVA channel antagonists affects certain sperm Ca²⁺ responses (Wennemuth *et al.*, 2000) and the AR (Benoff, 1998a; Goodwin *et al.*, 1997). These data suggest that HVA channels may be inserted in the male germ cell membrane in a functionally inactive state and activated in mature sperm possibly by posttranslational modifications. Furthermore, it has been reported that specific spliced transcripts for α_1 subunits encoding HVA channels, particularly of the Ca_v1.2 type, are expressed in sperm (Goodwin *et al.*, 1998, 2000). The presence of these alternate splicing variants

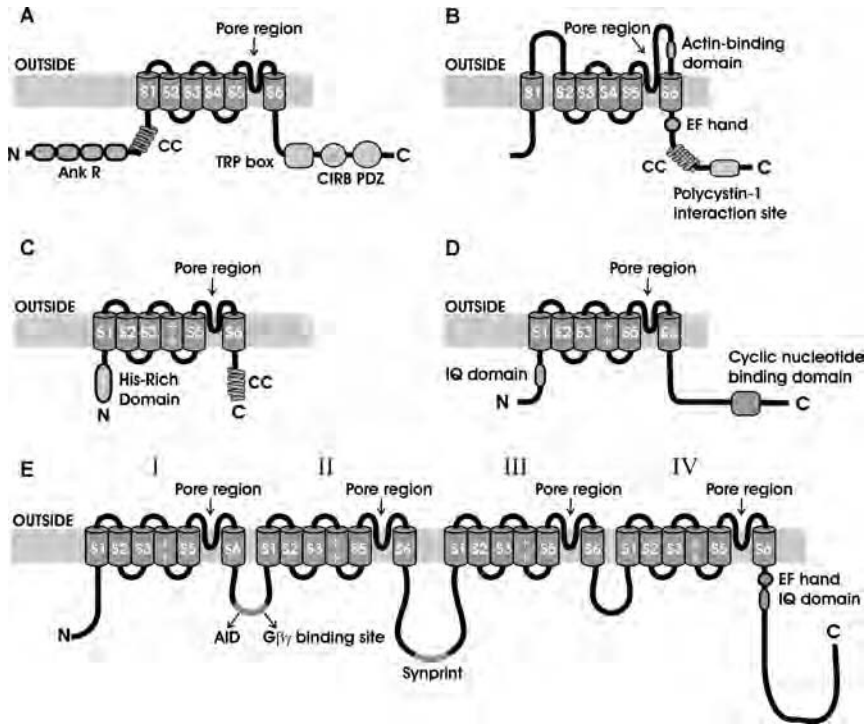


FIG. 2 Structural models of various Ca^{2+} -permeable channels expressed in sperm. (A) Cation channels of the transient receptor potential canonical (TRPC) family. Six transmembrane-spanning segments (S1–S6) are linked by short extracellular or intracellular domains. The putative pore region is formed by a hydrophilic region between S5 and S6. The intracellular N terminus contains four ankyrin-like repeats (AnkR) and a coiled-coil (CC) domain. Apparently, these are sites where TRPC channels interact with other proteins. CIRB is the putative calmodulin (CaM)- and IP_3R -binding domain, and PDZ is the region that binds PDZ domains in other proteins. The TRP box in TRPC is EWKFAR, and the topology of the functional channel may be tetrameric. (B) The topology of the polycystin-2 channel is also determined by the paradigmatic six putative transmembrane domains of the Ca^{2+} -permeable channels. Its carboxyl terminus includes consensus binding regions for Ca^{2+} , CaM, and cytoskeletal proteins. (C) The sperm cation channel, CatSper, is also a six transmembrane-spanning repeat protein. Its S4 domain has positively charged residues (lysine/arginine) that function as the putative voltage sensor of the channel. CatSper1 contains many histidine residues in its amino terminus, possibly involved in pH regulation of sperm motility. (D) The cyclic nucleotide-gated (CNG) channel. S1–S6 are the putative transmembrane domains. The cyclic nucleotide-binding site has been defined by homology to the sequences of cAMP- and cGMP-binding proteins. A putative CaM-binding domain (IQ domain) is labeled. (E) The pore-forming subunits (α_1) of voltage-gated (Ca_v) channels have four repeats of the six transmembrane-spanning domains. Some key regions of Ca_v channel regulation include the following: the α_1 subunit interaction domain (AID) in the I–II loop, where the auxiliary β subunit binds, which partially overlaps with the binding site for the G protein $\beta\gamma$ dimer; the Synprint domain on the II–III linker for SNARE protein interactions; and binding regions for Ca^{2+} (EF hand) and CaM (IQ domain).

TABLE I
Physiology and Pharmacology of Ca_v Channels

Current type	Channel name	Distribution/function	Antagonist(s)
L	Ca _v 1.1 (formerly α _{1S})	Skeletal muscle, E–C coupling	DHPs, PAA, BTZ; mibefradil (IC ₅₀ ~25 μM)
L	Ca _v 1.2 (formerly α _{1C})	Heart, smooth muscle, neurons, endocrine cells, sperm, E–S coupling, regulation of transcription, synaptic integration	DHPs, PAA, BTZ; calciseptine; mibefradil (IC ₅₀ ~25 μM)
L	Ca _v 1.3 (formerly α _{1D})	Neurons, endocrine cells, E–S coupling, regulation of transcription, synaptic integration	DHPs, PAA, BTZ
L	Ca _v 1.4 (formerly α _{1F})	Retina, E–S coupling	Not established
P	Ca _v 2.1 (formerly α _{1A})	Neurons, endocrine cells, sperm, E–S coupling	ω-Agatoxin IVA (IC ₅₀ ~2 nM); ω-conotoxin MVIIC (<100 nM)
Q	Ca _v 2.1 (formerly α _{1A})	Neurons, endocrine cells, E–S coupling	ω-Agatoxin IVA (IC ₅₀ ~200 nM)
N	Ca _v 2.2 (formerly α _{1B})	Neurons, endocrine cells, sperm, E–S coupling	ω-Conotoxin GVIA; ω-conotoxin MVIIC (>100 nM)
R	Ca _v 2.3 (formerly α _{1E})	Neurons, endocrine cells, sperm, repetitive firing	SNX-482
T	Ca _v 3.1 (formerly α _{1G})	Neurons, heart, sperm, pacemaking, repetitive firing	No specific inhibitors; mibefradil (IC ₅₀ ~5 μM); ethosuximide; amiloride; kurtoxin; Ni ²⁺ (IC ₅₀ ~250 μM)
T	Ca _v 3.2 (formerly α _{1H})	Kidney, liver, heart, brain, sperm, pacemaking, repetitive firing	No specific inhibitors; mibefradil (IC ₅₀ ~5 μM); ethosuximide; amiloride; kurtoxin; Ni ²⁺ (IC ₅₀ ~15 μM)
T	Ca _v 3.3 (formerly α _{1I})	Neurons, sperm, pacemaking, repetitive firing	No specific inhibitors; ethosuximide; Ni ²⁺ (IC ₅₀ ~220 μM)

Abbreviations: E–C, excitation–contraction; E–S, excitation–secretion; DHPs, dihydropyridines; PAA, phenylalkylamines; BTZ, benzothiazepines.

could affect the electrophysiological characteristics of the Ca^{2+} currents in sperm (Benoff, 1998b).

LVA channels open after weak depolarizations and are encoded by the Ca_v3 subfamily of genes ($\text{Ca}_v3.1$ to $\text{Ca}_v3.3$) (Perez-Reyes, 2003). In contrast to HVA channels, which function as oligomeric complexes, the recombinant $\text{Ca}_v3 \alpha_1$ subunits alone express typical T-type Ca^{2+} channels in heterologous systems. Interestingly, evidence suggests that the auxiliary subunits of the HVA channels may modulate the cell surface expression of Ca_v3 channels (Dolphin *et al.*, 1999; Dubel *et al.*, 2004). This contention remains controversial because there are other studies reporting no effects of the Ca_v auxiliary subunits on the activity and/or the expression of LVA channels (Lacinova *et al.*, 1999; Lambert *et al.*, 1997; Leuranguer *et al.*, 1998).

Patch-clamp studies have documented the presence of LVA currents in spermatogenic cells (Arnoult *et al.*, 1996a; Hagiwara and Kawa, 1984; Liévano *et al.*, 1996; Santi *et al.*, 1996). These currents share many of the cardinal features of somatic cell LVA currents, including low voltage thresholds for activation and inactivation; near-equivalent Ba^{2+} selectivity relative to Ca^{2+} ; and inhibition by amiloride, pimozone, mibefradil, kurtoxin, and low concentrations of Ni^{2+} (Arnoult *et al.*, 1998; Olamendi-Portugal *et al.*, 2002; Treviño *et al.*, 2004) (Table I). In addition, nifedipine and related 1,4-dihydropyridines (DHPs) inhibit these currents in male germ cells. Although these agents are typically considered L-type HVA channel antagonists, at micromolar concentrations they also block sperm T-type currents (Arnoult *et al.*, 1998; Santi *et al.*, 1996) (Table I). Likewise, T-type channels in male germ cells appear to be regulated by protein kinases (Arnoult *et al.*, 1997) and by CaM (Lopez-Gonzalez *et al.*, 2001). Growing evidence suggests that the channels that produce LVA currents in spermatogenic cells may be constructed from Ca_v3 subunits, as expression of all three genes and the corresponding proteins has been reported in these cells and mature sperm (Espinosa *et al.*, 1999; Jagannathan *et al.*, 2002a; Park *et al.*, 2003; Serrano *et al.*, 1999a; Son *et al.*, 2000; Treviño *et al.*, 2004; Westenbroek and Babcock, 1999) (Table I and Fig. 1B).

Ca_v1 (L-type) channels are the target of organic agents including DHPs, some of which act allosterically, shifting the channel toward the open state whereas others shift it toward a nonconducting state (Catterall *et al.*, 2003; Doering and Zamponi, 2003). Members of the Ca_v2 family of channels are insensitive to DHPs but are blocked by peptide toxins (Catterall *et al.*, 2003; Doering and Zamponi, 2003). $\text{Ca}_v2.1$ channels are blocked by ω -agatoxin IVA from funnel web spider venom (McDonough *et al.*, 1997; Mintz *et al.*, 1992) whereas $\text{Ca}_v2.2$ channels are sensitive to ω -conotoxin GVIA and related cone snail toxins (Boland *et al.*, 1994; McDonough *et al.*, 2002). $\text{Ca}_v2.3$ channels are blocked by the synthetic peptide toxin SNX-482 (Bourinet *et al.*, 2001; Newcomb *et al.*, 1998). Ca_v3 channels are insensitive

to both the DHPs and the peptide toxins that block Ca_v2 channels (Table I). However, there are some compounds that are relatively selective for these channels (Catterall *et al.*, 2003; Perez-Reyes, 2003). These antagonists include mibefradil (Arnoult *et al.*, 1998; Gomora *et al.*, 2002; Martin *et al.*, 2000; Todorovic and Lingle, 1998), amiloride (Arnoult *et al.*, 1998; Santi *et al.*, 1996; Todorovic and Lingle, 1998), ethosuximide, methylphenylsuccinimide (Gomora *et al.*, 2001; Todorovic and Lingle, 1998), and pimoziide and penfluridol (Arnoult *et al.*, 1998; Enyeart *et al.*, 1992). In addition, Ni^{2+} is somewhat selective for T versus other types of Ca^{2+} currents, although only $\text{Ca}_v3.2$ channels are blocked by low micromolar concentrations of NiCl_2 (Lee *et al.*, 1999c). Last, the peptide kurtoxin is a potent inhibitor of native and recombinant Ca_v3 channels (Chuang *et al.*, 1998; Lopez-Gonzalez *et al.*, 2003).

Ca_v channels are substrates for phosphorylation by cAMP-dependent protein kinase (PKA) and a number of other protein kinases (Catterall, 2000). Single-channel recordings suggest that phosphorylation by PKA can increase the channel open time (Bean *et al.*, 1984; Yue *et al.*, 1990). Molecular studies indicate that $\text{Ca}_v1.1$, $\text{Ca}_v1.2$, $\text{Ca}_v2.1$, and $\text{Ca}_v2.3$ channels are phosphorylated by PKA (Catterall, 2000; Hell *et al.*, 1993, 1995). In addition, protein kinase C (PKC) can also modulate Ca_v channels, although its effects on Ca^{2+} currents vary depending on the type of receptor activated and the preparation under study (Lacerda *et al.*, 1988; McHugh *et al.*, 2000; Shistik *et al.*, 1998). PKC can (1) regulate Ca_v1 channels differentially, (2) increase the activity of Ca_v2 channels directly (Herlitze *et al.*, 2001; Stea *et al.*, 1995; Yang and Tsien, 1993), and (3) reverse G protein inhibition of Ca_v2 channels (Swartz, 1993) by phosphorylating sites in the intracellular loop connecting domains I and II in the α_1 subunit (Hamid *et al.*, 1999; Zamponi *et al.*, 1997).

Ca_v channels may also participate in regulatory pathways initiated by G protein-coupled neurotransmitters and hormones (Dascal, 2001). This modulation can be indirect, via second messengers and/or by protein kinases, or direct, via physical interactions between the G protein and channel subunits (Dascal, 2001; Dolphin, 2003). Functional studies have established a reversible inhibition of neuronal non-L-type (Ca_v2) channels by a direct interaction of $\text{G}\beta\gamma$ (Herlitze *et al.*, 1996; Ikeda, 1996) with two sites in the linker region connecting their domains I and II (De Waard *et al.*, 1997; Zamponi *et al.*, 1997). It has been shown that LVA channels can be inhibited by activation of G protein-coupled receptors. In the case of $\text{Ca}_v3.2$ channels, $\text{G}\beta\gamma$ subunits can bind to the intracellular loop connecting domains II and III (Wolfe *et al.*, 2003). This region in the $\text{Ca}_v3.2$ channel seems to be crucial, because its replacement abolishes inhibition, and its transfer to nonmodulated $\text{Ca}_v3.1$ channels confers $\text{G}\beta\gamma$ sensitivity (Wolfe *et al.*, 2003).

Ca^{2+} ions control inactivation of Ca_v channels by associating with a CaM molecule tethered to the channel (Lee *et al.*, 1999a; Peterson *et al.*, 1999; Qin

et al., 1999; Zuhlke *et al.*, 1999). The Ca^{2+} -CaM complex has been implicated in the regulation of $\text{Ca}_v1.2$ (Peterson *et al.*, 1999; Qin *et al.*, 1999; Zuhlke and Reuter, 1998) and $\text{Ca}_v2.1$ (Lee *et al.*, 1999a) channels. Ca^{2+} -CaM binding to the channels causes an initial Ca^{2+} -dependent facilitation and, on a longer time scale, Ca^{2+} -dependent channel inactivation (Lee *et al.*, 1999a, 2003). There is evidence that CaM mutants incapable of binding Ca^{2+} interact with Ca_v channels, suggesting that Ca^{2+} -free CaM (apoCaM) might be constitutively associated with Ca_v channels (Erickson *et al.*, 2003). On the other hand, Ca_v3 channels seem to be regulated by Ca^{2+} -CaM through the activity of the Ca^{2+} -CaM-dependent protein kinase II (Barrett *et al.*, 2000; Welsby *et al.*, 2003; Wolfe *et al.*, 2002), although a direct interaction between CaM and these channels cannot be ruled out (Lopez-Gonzalez *et al.*, 2001).

Finally, numerous studies indicate a tight association of syntaxin and synaptotagmin with $\text{Ca}_v2.1$ and $\text{Ca}_v2.2$ channels, implicating both types of channels as components of the exocytotic vesicle docking/fusion machinery (Atlas, 2001; Catterall, 1999). These interactions are shown to be mediated by a binding domain (called synprint) in the domain II-III linker. In addition, this region in the domain II-III linker of $\text{Ca}_v1.2$ channels also binds SNAP-25 and syntaxin 1A, albeit with reduced affinity (Wiser *et al.*, 1999).

2. TRP Channels

Transient receptor potential (TRP) channels comprise a growing superfamily of cation channels that display a remarkable diversity of function. With the inclusion of the PKD autosomal dominant polycystic kidney disease (ADPKD) family of channels, the family has expanded its ranks to comprise 30 different genes. They were first identified in *Drosophila* as a mutation (*trp*) that causes blindness in bright light, due to disruption of a TRP channel-mediated visual signal transduction mechanism (Minke, 1977; Montell *et al.*, 1985). They have since been found in most cells tested. The TRP superfamily can be divided into seven subgroups (Wissenbach *et al.*, 2004) according to their sequence similarity (largely because their functions are diverse and frequently unknown): (1) TRPC (canonical), which is the most closely related to the *Drosophila* TRP and comprises seven members; (2) TRPV (vanilloid) with six members; (3) TRPM (melastatin) with eight members, and four other, more distantly related subgroups classified into the same superfamily (Wissenbach *et al.*, 2004); (4) TRPP, which includes ADPKD protein, polycystin-2 (PC2), and two PC-like proteins; (5) TRPML, which includes three members related to the mucopolysaccharidosis proteins; (6) TRPA with only one member found in mammals; and (7) TRPN (not yet identified in mammals), including the *Drosophila* NOMPC mechanosensory transduction channels.

The structure of TRP channels consists of six transmembrane segments (S1–S6) and a loop between S5 and S6 that constitutes the pore, with the N and C termini located intracellularly. The overall structure is similar to that of voltage-gated and cyclic nucleotide-gated (CNG) channels (Fig. 2), except that the S4 domain does not carry a sequence of positive residues, and therefore TRP channels are only weakly voltage dependent. Most TRP members contain a TRP box, which is an invariant sequence (EWKFAR), conserved from *Drosophila* to mammalian TRP channels. An interesting feature of three members of the TRPM subfamily is the presence of an enzymatic activity linked to the C terminus; one channel exhibits an ADP-ribose pyrophosphatase and two more contain an atypical protein kinase (Montell, 2003). The physiological relevance for the combination of channel and enzymatic activity in the same protein is still unknown. A functional channel is composed of a homo- or heterotetramer of subunits, and the association between proteins of different subgroups (TRPC1 and TRPC2) has also been reported (Tsiokas *et al.*, 1999). However, it has not been proved that expression of every TRP generates a functional channel, and some subunits might function as auxiliary subunits that by themselves may not constitute part of a channel. Most TRPs function as relatively nonselective Ca^{2+} channels, having a $P_{\text{Ca}}/P_{\text{Na}} < 10$, with the notable exceptions of TRPM4 and TRPM5, which are monovalent selective and do not permeate Ca^{2+} . In contrast, TRPV5 and TRPV6 are highly Ca^{2+} selective, with a $P_{\text{Ca}}/P_{\text{Na}} > 100$ (Clapham, 2003).

How TRP channels are activated, and what their functions might be, are complex and as yet still open questions. Several theories have been forwarded to explain TRP channel activation (Clapham, 2003). In the first of these, the “receptor-operated theory,” phospholipase C (PLC) activation via G proteins produces second messengers that open the TRP channels. G protein receptor-mediated PLC activation generates several signaling molecules and the task has been to identify a receptor-activated messenger that directly opens TRP channels. Phosphatidylinositol 4,5-bisphosphate (PIP_2) is a candidate for this function, because it can regulate several ion channels (Hilgemann *et al.*, 2001) and its concentration depends partially on PLC activity. A second theory, or “cell sensory theory,” derives from the fact that different members of the TRP superfamily are involved in sensing stimuli such as heat, cold, touch, taste, osmolarity, and mechanical stretching. TRP channels are found widely on ciliated structures and cells involved in mechanosensation, such as those involved in flow sensing and hearing, and are also found in taste- and odorant-sensing cells. Temperature is known to affect the activation of a number of TRP channels, such as TRPVs 1–4 and TRPM 8. The mechanism by which these diverse mechanical forces, temperature, and intracellular second messenger-mediated stimuli translate into TRP channel gating is still to be uncovered (Clapham, 2003).

A third theory, and arguably the most relevant to the role of TRP channels in sperm, is the “store-operated Ca^{2+} entry theory.” TRP channels are good candidates to be the so-called store-operated (SOC) or capacitative Ca^{2+} channels. In this case, the opening of TRP channels occurs after the classic activation of PLC by receptor-activated G proteins or receptor tyrosine kinases, the subsequent production of IP_3 , and the release of Ca^{2+} from intracellular stores.

The precise mechanism linking the emptying of the internal Ca^{2+} stores with the opening of Ca^{2+} channels in the plasma membrane is not yet resolved, although given the potential relevance to sperm physiology, it is worth elaborating on the three main hypotheses (Zitt *et al.*, 2002):

1. A cytosolic influx factor (CIF), an as yet unidentified diffusible molecule released on Ca^{2+} store depletion, acts as a direct activator of TRP channels (Parekh *et al.*, 1993; Randriamampita and Tsien, 1993). A novel mechanism for store-operated Ca^{2+} influx involving CIF was proposed (Smani *et al.*, 2004). It suggests that CIF displaces CaM from the Ca^{2+} -independent phospholipase A_2 , activating the enzyme and initiating production of lysophospholipids that directly activate SOC channels in a limited membrane region.

2. A protein–protein interaction between the plasma membrane TRP channels and the IP_3 receptors (IP_3Rs) present in Ca^{2+} stores (Kiselyov *et al.*, 1998), similar to that observed in skeletal muscle between the DHP receptor (DHPR) and the RyR (Chavis *et al.*, 1996; Marty *et al.*, 1994).

3. A secretory vesicle model, in which vesicles containing channels fuse with the plasma membrane on an appropriate signal (Yao *et al.*, 1999).

There is limited evidence to support each of the three theories and they are not necessarily mutually exclusive. However, not all TRP channels are activated by emptying of Ca^{2+} stores; several other channel activators have been found, such as diacylglycerol and other lipids.

TRP channels have now been implicated in several functions such as nociception, visual transduction, and fertilization (Geldziler *et al.*, 2004). Various members of this family have been identified in spermatogenic cells and sperm. RT-PCR experiments detected the mRNAs for *trpc* 1–7 and *trpc* 1, 3, 6, and 7 in mouse and human spermatogenic cells, respectively (Castellano *et al.*, 2003; Treviño *et al.*, 2001) (Table II). In mature mouse sperm TRPC 1, 2, 3 and 6 were immunolocalized predominantly in the flagella whereas TRPC 2 localizes to the overlying region of the acrosome (Jungnickel *et al.*, 2001; Treviño *et al.*, 2001) (Fig. 1B). TRPC proteins are also present in human sperm; TRPC 1, 3, 4, and 6 were detected mainly in flagella, suggesting these channels may participate in sperm motility in both species (Castellano *et al.*, 2003; Treviño *et al.*, 2001). Interestingly, three TRP genes are found in *Caenorhabditis elegans* (Minke and Cook, 2002). Animals

TABLE II
Ca²⁺-Permeable Channels Expressed in Male Germ Cells and Sperm

Channel family	Species	Spermatogenic cells	Sperm	Sperm localization	Possible role	Refs. ^a
Voltage-dependent calcium channels						
Ca _v 1.2 (α1C)	h, m, r	ICC, RT-PCR	ICC, WB	Head, flagellum		1-4
Ca _v 2.1 (α1A)	m, r	ICC, RT-PCR	ICC, WB	Head, flagellum		3-5
Ca _v 2.2 (α1B)	h, m, r	RT-PCR	ICC, WB	Head, flagellum		2-6
Ca _v 2.3 (α1E)	h, m, r	RT-PCR	ICC, WB	Head, flagellum	Motility	2, 4, 5
Ca _v 3.1 (α1G)	h, m	ICC, RT-PCR	ICC	Head, flagellum	AR	2, 7-9
Ca _v 3.2 (α1H)	h, m	ICC, RT-PCR	ICC	Head, flagellum	AR	2, 7-11
Ca _v 3.3 (α1I)	h, m	ICC, ISH, RT-PCR	ICC	Flagellum		2, 9
TRP channels						
TRPC1	h, m	ICC, RT-PCR	ICC	Midpiece		12, 13
TRPC2	b, m	ICC, RT-PCR	ICC	Head	AR	13-15
TRPC3	h, m	ICC, RT-PCR	ICC	Principal piece		12, 13
TRPC4	h, m	RT-PCR	ICC	Head, flagellum		12, 13
TRPC5	m	RT-PCR				13
TRPC6	h, m	ICC, RT-PCR	ICC	Connecting piece		12, 13
TRPC7	h, m	RT-PCR				12, 13
Intracellular Ca channels						
Ryanodine receptor 1	m	ICC, RT-PCR				16

Ryanodine receptor 2	m	RT-PCR				16
Ryanodine receptor 3	m	ICC, RT-PCR	ICC	Head, flagellum		16
IP ₃ receptor I	b, d, h, ha, m, r, s	RT-PCR	ICC, ^b WB	Head, connecting piece	AR, HA	16-20
IP ₃ receptor II	m	RT-PCR				16
IP ₃ receptor III	m	RT-PCR				16
CNG channels						
A3	b	Cloning	ICC	Flagellum		21,22
B1	b	Cloning	ICC	Principal piece		22,23
B3	m	NB				24
Catsper channels						
Catsper 1	h, m	Cloning	ICC	Principal piece	HA	25
Catsper 2	h, m, r	Cloning, ISH	ICC	Principal piece (flagellum)	HA	26,27
Catsper 3	h, m	ISA, RT-PCR				28,29
Catsper 4	h, m	ISA, RT-PCR				29

^aReferences: (1) Goodwin *et al.*, 2000; (2) Park *et al.*, 2003; (3) Serrano *et al.*, 1999a; (4) Westenbroek and Babcock, 1999; (5) Liévano *et al.*, 1996; (6) Wennemuth *et al.*, 2000; (7) Espinosa *et al.*, 1999; (8) Jagannathan *et al.*, 2002b; (9) Treviño *et al.*, 2004; (10) Son *et al.*, 2002; (11) Son *et al.*, 2000; (12) Castellano *et al.*, 2003; (13) Treviño *et al.*, 2001; (14) Jungnickel *et al.*, 2001; (15) Wissenbach *et al.*, 1998; (16) Treviño *et al.*, 1998; (17) Ho and Suarez, 2003; (18) Naaby-Hansen *et al.*, 2001; (19) Walensky *et al.*, 1995; (20) Zapata *et al.*, 1997; (21) Weyand *et al.*, 1994; (22) Wiesner *et al.*, 1998; (23) Biel *et al.*, 1996; (24) Gerstner *et al.*, 2000; (25) Ren *et al.*, 2001; (26) Quill *et al.*, 2001; (27) Quill *et al.*, 2003; (28) Arias *et al.*, 2003; (29) Lobley *et al.*, 2003.

^bIsoform specificity of antibodies used for ICC is not clear.

Abbreviations: b, bull; d, dog; ha, hamster; h, human; m, mouse; r, rat; s, sea urchin; ICC, immunocytochemistry; ISA, *in silico* analysis; ISH, *in situ* hybridization; NB, Northern blotting; WB, Western blotting; AR, acrosome reaction; HA, hyperactivation.

lacking a functional *trpc3* gene are infertile; their sperm cannot fuse with the egg although they are motile and can bind to it. Initially, *trpc 3* is localized in intracellular vesicles, which fuse with the plasma membrane during sperm activation. This process enhances store-operated and receptor-operated Ca^{2+} influx, allowing sperm to fertilize (Xu and Sternberg, 2003).

3. Ca^{2+} Release Channels

There are two known classes of Ca^{2+} release channels: RyR and IP_3R . In both cases the functional channel is a tetrameric complex. There are three different genes for each receptor and further variety is observed due to the presence of splicing isoforms. IP_3Rs and RyRs can both be present in the same cell, providing a scenario for intricate interactions and signaling mechanisms. The intracellular messengers Ca^{2+} itself, cADPR, NAADP, and IP_3 modulate these Ca^{2+} release channels. cADPR is synthesized by ADP-ribosyl cyclase, a putative NAD^+ sensor. Because NAD^+ is a product of intermediary metabolism, it is likely that production of cADPR is linked to metabolic activity (Zhang *et al.*, 2004). The role of NAD^+ and NADP^+ in signaling cascades by enzyme-catalyzed transformations has been recognized (Broetto-Biazon *et al.*, 2004). IP_3 is generated via the activation of a G protein- or tyrosine kinase-coupled receptor, which in turn activates a PLC with the subsequent cleavage of PIP_2 to produce IP_3 and diacylglycerol (DAG).

Mammals express three types of RyRs: RyR1 and RyR2, found predominantly in skeletal muscle and heart, respectively; and RyR3, which shows a more ubiquitous expression pattern. RyR channels are formed by four subunits of approximately 560 kDa each; the C-terminal portion of the protein presents the highest degree of conservation and also constitutes the pore of the channel. The N terminus is a large cytoplasmic portion of the protein that contains regulatory and ligand-binding domains. RyR channels are cation selective, with high conductance for mono- and divalent ions. In skeletal muscle a direct coupling mechanism for opening has been proposed in which RyR1 is physically coupled with the DHPR (a Ca_v) (Meissner, 2004). In contrast, RyR2 (present in cardiac muscle) and RyR3 open via a Ca^{2+} -induced Ca^{2+} release mechanism (Wellman and Nelson, 2003). RyRs are strongly regulated by Ca^{2+} with a bimodal dependence suggesting the presence of low- and high-affinity Ca^{2+} -binding sites (Kotlikoff, 2003). Other endogenous effectors include ATP, Mg^{2+} , CaM, NADH, and phosphorylation (Meissner, 2004). Exogenous agents include ryanodine, ruthenium red, and caffeine (Sutko *et al.*, 1997).

Likewise, there are three genes encoding the IP_3 channels and there are also splicing isoforms. The channel is composed of four subunits (each about 2700 amino acid residues) with a single binding site for IP_3 in each subunit.

The C terminus forms the pore of the channel. IP_3 and Ca^{2+} are required for channel opening, although the precise mode of action and the interdependence between these two modulators are still not clearly resolved (Bootman *et al.*, 2002; Taylor and Laude, 2002). The effects of IP_3 and Ca^{2+} are both stimulatory and inhibitory, depending on their concentration and also on the microenvironment of the cell (Galione and Churchill, 2002). It has been suggested that the G protein β subunit can also modulate IP_3R directly after its dissociation from the G_i protein (Zeng *et al.*, 2003).

Because Ca^{2+} release from intracellular stores is involved in several important processes, it is under tight control. One of the most important modulators of this release is CaM, either directly on Ca^{2+} -releasing channels or through a complex combination of different effectors. CaM can inhibit or stimulate RyR1 depending on Ca^{2+} concentration. At $\sim 1 \mu M$ Ca^{2+} , CaM has a stimulatory effect, whereas at about 50–100 μM Ca^{2+} , it inhibits the channel (Balshaw *et al.*, 2002). RyR2 is also inhibited at a high Ca^{2+} concentration but little or no effect was seen at low Ca^{2+} concentrations (Balshaw *et al.*, 2002). RyR3 is regulated by CaM in a manner similar to RyR1. IP_3Rs also bind CaM, but with lower affinity than RyRs. CaM has an inhibitory effect on all IP_3R isoforms (Adkins *et al.*, 2000). How CaM regulates IP_3R is uncertain because of contradictory evidence. Apparently, there is a complex interaction between IP_3Rs and CaM, in which apoCaM would be anchored by one end of its dumbbell structure to the N terminus of the IP_3R . When the other end of CaM binds Ca^{2+} , this new conformation can bind to another site of the IP_3R , causing inhibition (Taylor and Laude, 2002). It is also proposed that IP_3Rs are gated by direct physical interaction with TRP channels (Kiselyov *et al.*, 1999), in the same way as RyR1 is physically coupled to the DHPR (Lee *et al.*, 2004). In the case of TRPC3, it has been shown that this interaction is established through CaM. The proposal is that the IP_3R activates TRPC3 by displacing CaM from a common binding site (Zhu and Tang, 2004). The protein Homer has been identified as another molecule that links TRP channels and IP_3R . In this case the trimer TRPC1–Homer– IP_3R forms an inactive complex; the emptying of Ca^{2+} stores triggers the dissociation of TRPC1–Homer from IP_3R and activates TRPC1 channels at the plasma membrane; and the refilling of the stores causes the interaction with Homer to be reestablished, thus ceasing Ca^{2+} influx through the TRP channel (Yuan *et al.*, 2003).

IP_3Rs are present in the sea urchin and the mammalian sperm acrosomal membrane (Kuroda *et al.*, 1999; Naaby-Hansen *et al.*, 2001; Treviño *et al.*, 1998; Walensky and Snyder, 1995; Zapata *et al.*, 1997) (Table II). The three mRNAs for this receptor were detected in mouse spermatogenic cells (Treviño *et al.*, 1998). Furthermore, the three known genes encoding RyRs are also expressed at all stages of spermatogenesis, even though immunocytochemical studies indicated that only types I and III are present

in spermatogenic cells. In addition, only RyR3 was detected in mature sperm (Treviño *et al.*, 1998) (Table II).

4. CNG Channels

Cyclic nucleotide-gated (CNG) channels are nonselective cation channels first identified in retinal photoreceptors (Kaupp *et al.*, 1989) and olfactory sensory neurons (Ludwig *et al.*, 1990). They are composed of six transmembrane segments having a cyclic nucleotide-binding domain in their cytoplasmic C terminus (Fig. 2). Six different genes (A1, A2, A3, A4, B1, and B3) have been cloned in mammals. Although A (formerly α) subunits can form a functional channel as a homotetramer in a heterologous expression system, in a variety of tissues the native channels are composed of a heterotetramer of A and B subunits (in a 3:1 ratio) (Kaupp and Seifert, 2002). Direct binding of cyclic nucleotides, cAMP and cGMP, opens CNG channels. There is no desensitization (inactivation) of CNG channels by ligand binding; channels are downregulated by Ca^{2+} -CaM, and because CNG channels conduct Ca^{2+} (Dzeja *et al.*, 1999), Ca^{2+} influx through CNG channels negatively regulates channel activity. In all known native CNG channels, cGMP is a more potent ligand than cAMP, whereas the latter is the natural ligand in olfactory sensory neurons.

In 1994, the A3 subunit was cloned from bovine testis as a new subunit for CNG channels (Weyand *et al.*, 1994). Later studies revealed that this subunit forms part of a CNG channel in cone photoreceptors (Biel *et al.*, 1994; Bonigk *et al.*, 1993) that are responsible for color recognition. Electrophysiological analysis of the heterologously expressed A3 subunits cloned from testis demonstrated that cGMP has 200-fold higher ligand activity than cAMP; the concentration required for half-maximum channel activity is $8.3 \mu\text{M}$ for cGMP and $1720 \mu\text{M}$ for cAMP (Weyand *et al.*, 1994). Afterward, expression of the B1 (Biel *et al.*, 1996; Wiesner *et al.*, 1998) and B3 (Gerstner *et al.*, 2000) subunits was confirmed in mammalian testis. Immunocytochemical analyses revealed that the A1 subunit is distributed along the entire flagellum in bovine sperm, whereas the B1 subunit is localized only to the principal piece (Wiesner *et al.*, 1998) (Fig. 1B and Table II). Cyclic nucleotides induce Ca^{2+} influx in bovine and mouse sperm (Kobori *et al.*, 2000; Wiesner *et al.*, 1998) and cGMP is more effective than cAMP in both species, consistent with the ligand selectivity of the CNG channel. Given that CNG channels are capable of conducting Ca^{2+} under physiological conditions (Dzeja *et al.*, 1999), the $[\text{Ca}^{2+}]_i$ increases induced by cyclic nucleotides were originally attributed to Ca^{2+} influx through the sperm CNG channel. However, experiments with CatSper1 null sperm (see below), in which the $[\text{Ca}^{2+}]_i$ increase induced by cyclic nucleotides was abolished (Ren *et al.*, 2001), have

raised doubts about the role of CNG channels in this Ca^{2+} entry pathway. Furthermore, targeted disruption of the CNG A3 subunit did not cause male infertility, whereas the mutant mice were colorblind as anticipated (Biel *et al.*, 1999), questioning the importance of the CNG channel in sperm function. Nevertheless, it is not known how cyclic nucleotides activate CatSper channels, as their amino acid sequences do not contain known cyclic nucleotide-binding sites. Furthermore, staurosporine, a nonselective kinase inhibitor, did not affect the cyclic nucleotide-induced $[\text{Ca}^{2+}]_i$ increase in sperm from wild-type mice (Ren *et al.*, 2001), suggesting that phosphorylation is not involved in this signal cascade. Therefore, further careful experiments, particularly using CNG A3 null sperm, are required to resolve this issue.

5. CatSper Channels

A novel class of Ca^{2+} channel was identified and named the CatSper family (Cation channel of Sperm). Thus far, two members of this family, CatSper1 and CatSper2, are the only two candidate Ca^{2+} channels known to be required for male fertility (Quill *et al.*, 2003; Ren *et al.*, 2001), and they exert this effect through regulation of sperm motility (Carlson *et al.*, 2003; Quill *et al.*, 2003).

The first member of the CatSper family to be identified, CatSper1, was discovered by searching expressed sequence tag (EST) databases for sequences with similarity to known Ca_v channels (Ren *et al.*, 2001). Soon after a second family member, CatSper2, was identified by analysis of genes exclusively expressed in male germ cells, using a signal peptide trap strategy, which can select genes encoding secreted and membrane-bound proteins (Quill *et al.*, 2001). More recently the family was expanded further by the discovery of CatSper3 and CatSper4 (Arias *et al.*, 2003; Lobley *et al.*, 2003). All four family members are expressed almost exclusively in the testis, and when present in other tissues, transcript levels are low. CatSper1–4 share a similar structure of six transmembrane segments, a motif found among voltage-gated K^+ channels, and also in a single repeat of the four-repeat structure of voltage-gated Ca^{2+} and Na^+ channels (Fig. 2). The S4 transmembrane domain of the CatSper family members is similar in sequence to the voltage-sensing domain in other species of voltage-gated ion channels, and the S5–linker–S6 CatSper domain has strong sequence similarity to the pore-forming domain of Ca_v channels. These similarities have led to a model being proposed whereby four CatSper proteins combine to form a homo- or heteromeric tetramer that functions as a Ca_v channel. Direct evidence for this model is lacking, as all attempts to express functional CatSper channels in model systems such as *Xenopus* oocytes have

thus far failed, hampering the characterization of their precise biophysical properties. Indirect evidence of the function of CatSper has been limited to comparing Ca^{2+} responses in normal sperm with those of CatSper1 null sperm, which has shown that these putative Ca^{2+} channels may be regulated by membrane potential (Carlson *et al.*, 2003) and cyclic nucleotides (Ren *et al.*, 2001). As no known consensus cyclic nucleotide-binding domain is present in CatSper sequences, this latter result implies a role for accessory proteins in regulating CatSper channels, possibly through a C-terminal coiled-coil domain present in all four family members (Lobley *et al.*, 2003). Intriguingly, an *in silico* comparative study of CatSper1 diversity among primates found remarkable “indels” (in-frame deletion or insertion of nucleotides) in an N-terminal region of the gene (Podlaha and Zhang, 2003). The high rate of appearance of indels among recently separated species suggests that the N-terminal region of CatSper1 is subject to strong positive selection. A proposed role for this region of CatSper1 in a “ball and chain” inactivation mechanism, similar to that characterized in Shaker voltage-gated K^+ channels (to which the CatSper channels are relatively closely phylogenetically related) (Podlaha and Zhang, 2003), remains to be experimentally demonstrated.

The testis-specific expression of members of the CatSper family suggested a role in fertility for these putative Ca^{2+} channels and, indeed, male CatSper1 or CatSper2 knockout mice are infertile (Quill *et al.*, 2003; Ren *et al.*, 2001). Otherwise these male mice appear normal, and female CatSper1 or CatSper2 knockout mice remain fertile. Mating behavior, spermatogenesis, sperm morphology, and the activation of sperm motility are normal in CatSper1 or CatSper2 null males. Yet sperm from knockout mice do not undergo the transition to hyperactivated motility, and this appears to prevent sperm penetrating the zona pellucida (ZP) that surrounds the egg (Carlson *et al.*, 2003; Quill *et al.*, 2003; Ren *et al.*, 2001). The inability to undergo hyperactivation was correlated with a failure to increase $[\text{Ca}^{2+}]_i$ in response to membrane depolarization. Further evidence for a role in motility regulation is provided by immunolocalization experiments showing that CatSper1 and CatSper2 localize to the principal piece of the sperm flagella (Carlson *et al.*, 2003; Quill *et al.*, 2003; Ren *et al.*, 2001).

A systematic gene expression analysis of the ascidian *Ciona intestinalis* (Inaba *et al.*, 2002) led to the discovery of CatSper homologs expressed in a testis EST library (personal communication with K. Inaba). Because this ascidian is an excellent animal with which to study sperm chemotaxis (Yoshida *et al.*, 2002) and is also considered a suitable model for future genetics (Sasakura *et al.*, 2003), further examination of CatSper in *Ciona* might contribute to our understanding of the biophysical properties and physiological functions of this channel.

C. Alternative Approaches to Study Sperm Ion Channels

1. Ion-Sensitive Fluorescent Dyes

Understanding the finely choreographed processes of cell biology has become increasingly dependent on the quantification and visualization of signaling events and molecules with high spatial and temporal resolution within cells. The exploitation of ion- and E_m -sensitive fluorescent dyes has enabled the identification and quantification of many of the most important ionic changes that cells undergo in response to their environment and to other cells. It is now possible to detect Ca^{2+} , pH, Mg^{2+} , Na^+ , Cl^- , and E_m inside cells in populations or individually. These dyes enable researchers to perform measurements in organelles and in cells that are too small to allow the use of microelectrodes (Tsien, 1989). Furthermore, in combination with evolving high-sensitivity imaging techniques, these dyes are being employed to measure local ionic variations involved in cell signaling (Dong *et al.*, 2003). Newly engineered green fluorescent proteins have been designed to respond to an increased variety of biological events and signals, and can be targeted to specific subcellular compartments, expanding our capacity to explore the inner workings of cells (Zhang *et al.*, 2002). Unfortunately, this latter development cannot easily be applied to sperm, but progress in developing *in vitro* spermatogenesis systems could surmount the present difficulties. Some examples of the use of fluorescent probes in live sperm are as follows:

1. $[Ca^{2+}]_i$ and pH_i: Arnoult *et al.* (1999), Babcock *et al.* (1983), Baldi *et al.* (1991), Blackmore (1993), Florman *et al.* (1989, 1992), Fukami *et al.* (2003), Guerrero and Darszon (1989a,b), Lee (1984), Meizel *et al.* (1997), Sase *et al.* (1995), Schackmann and Chock (1986), Wood *et al.* (2003), and Zeng *et al.* (1996).
2. E_m : Arnoult *et al.* (1996b, 1999), Babcock *et al.* (1992), Demarco *et al.* (2003), Garcia-Soto *et al.* (1987), Gonzalez-Martinez and Darszon (1987), Gonzalez-Martinez (2003), Gonzalez-Martinez *et al.* (2002), and Lee and Garbers (1986).
3. $[Na^+]_i$: Patrat *et al.* (2000) and Rodriguez and Darszon (2003).
4. $[Cl^-]_i$: Garcia and Meizel (1999).

2. Spermatogenic Cells

It has proved difficult to directly record sperm ion channels *in situ*. The conventional electrophysiological methods employed to study ion channel function in many cells cannot be readily applied to sperm because of their morphological complexity and prohibitively small size (see Fig. 1A). In

addition, the reduction of total cell water during differentiation (Sprando and Russell, 1987; Suzuki-Toyota *et al.*, 1999) further limits the application of intracellular electrodes (Lindemann and Rikmenspoel, 1971; Polcz *et al.*, 1997) and results in a rigidified plasma membrane that limits the success of patch-clamp techniques (Espinosa *et al.*, 1998; Guerrero *et al.*, 1987). Furthermore, molecular techniques, such as RNA interference (Downward, 2004) or antisense knockdown methods (Inouye, 1988), which have been of great value in associating certain gene products with specific ion currents in many cell types, cannot be applied to sperm, in which transcription and translation have been terminated (Hecht, 1998).

The fact that the channels used by mature sperm must be synthesized by the larger spermatogenic immature cells during spermatogenesis, brought these latter cells to the attention of electrophysiologists (Arnoult *et al.*, 1996a; Hagiwara and Kawa, 1984; Liévano *et al.*, 1996; Santi *et al.*, 1996). Spermatogenic cells can be readily examined by electrophysiological methods and because they actively synthesize proteins they are suitable subjects for standard molecular biology strategies. Combining electrophysiological and molecular biological approaches in these cells has been instrumental in the study of sperm physiology in general and in the characterization of Ca_v channel activity in particular (Felix *et al.*, 2004). Although, as mentioned previously, several members of the HVA Ca_v family have been detected in mouse and human spermatogenic cells (Table II), mainly T-type currents are observed in these cells (Arnoult *et al.*, 1996a; Hagiwara and Kawa, 1984; Jagannathan *et al.*, 2002a,b; Liévano *et al.*, 1996; Santi *et al.*, 1996). Furthermore, molecular studies indicate that all Ca_v3 isoforms are present in these cells (Jagannathan *et al.*, 2002a; Park *et al.*, 2003; Son *et al.*, 2000; Treviño *et al.*, 2004).

Spermatogenic cells can be obtained without difficulty from mammalian testes (Espinosa *et al.*, 1999; Hagiwara and Kawa, 1984; Santi *et al.*, 1996) by a combination of mechanical and enzymatic dissociation of the seminiferous tubules. Once the cells are collected and resuspended in an appropriate buffer, they remain healthy for hours. When mature mice are used, the suspension contains spermatogenic cells, and connected aggregates of them called synplasts, mainly at three different stages of differentiation: pachytene spermatocytes, round spermatids, and condensing spermatids. These cell types can be used routinely for electrophysiological recordings. Systematic analysis in rodent male germ cells has shown that, as in somatic cells, T-type currents begin to activate above -60 mV and reach a peak at about -25 mV. A hallmark of these T-type currents is that they are transient, that is, currents reach a peak and then decay rapidly due to inactivation (Arnoult *et al.*, 1996a; Espinosa *et al.*, 2000; Felix *et al.*, 2003; Lopez-Gonzalez *et al.*, 2001, 2003; Santi *et al.*, 1996). This is interesting because heterologously expressed cloned T-type channels show that $Ca_v3.1$ and

Ca_v3.2 exhibit fast inactivation, whereas Ca_v3.3 channels inactivate slowly (Klockner *et al.*, 1999; Kozlov *et al.*, 1999; Lee *et al.*, 1999b; Perez-Reyes, 2003). In spite of different experimental conditions used to determine the steady state voltage dependence of inactivation of T-type Ca_v channels in spermatogenic cells, the inactivation midpoint potential is in the range of -70 to -60 mV (Arnoult *et al.*, 1996a; Espinosa *et al.*, 2000; Lopez-Gonzalez *et al.*, 2003). Recombinant Ca_v3 channels show values between -80 and -60 mV (Frazier *et al.*, 2001; Gomora *et al.*, 2002; Klockner *et al.*, 1999; Lee *et al.*, 1999b; Serrano *et al.*, 1999b). In addition, recovery from inactivation is exponential with a voltage-dependent time constant (τ). In mouse spermatogenic cells τ is ~ 370 ms at -80 mV and ~ 110 ms at -110 mV (Santi *et al.*, 1996; Stambouljian *et al.*, 2004). The characteristics of this recovery process vary depending on the type of Ca_v recombinant channel investigated. Of the three isoforms, Ca_v3.1 channels recover the fastest, with a τ of ~ 100 – 150 ms from short pulses at -90 mV (Klockner *et al.*, 1999; Serrano *et al.*, 1999b), whereas Ca_v3.3 channels show a slower time course with a τ of ~ 260 ms from long pulses (500 ms) at -100 mV (Gomora *et al.*, 2002).

Although T-type currents were first recorded almost 3 decades ago (Hagiwara *et al.*, 1975) their study has been hindered by the absence of specific channel antagonists (Yunker, 2003). Despite this, their pharmacological profile has been used as a tool to probe the participation of these currents in sperm physiology (Arnoult *et al.*, 1996a, 1999; Espinosa *et al.*, 1999; Lopez-Gonzalez *et al.*, 2001) (Table I). Inorganic divalent and trivalent cations have a limited use as T-type channel antagonists because many of them attenuate Ca²⁺ currents through both T-type and HVA Ca_v channels. Ni²⁺ is the exception; T-type currents are unusually sensitive to it, particularly Ca_v3.2 (IC₅₀ of 12 μ M) (Lee *et al.*, 1999c). The IC₅₀ with which Ni²⁺ blocks T-type currents in mouse spermatogenic cells is ~ 21 – 34 μ M, consistent with the possibility that Ca_v3.2 is the predominant isoform functionally expressed (Arnoult *et al.*, 1996a, 1998; Stambouljian *et al.*, 2004; Treviño *et al.*, 2004). This agrees with recordings of these currents in a Ca_v3.1 null mutant (Stambouljian *et al.*, 2002).

As indicated earlier, DHPs have been instrumental in the study of L-type channels (Triggle, 2003). However, later studies demonstrated that native T-type channels in different cell types including mouse male germ cells were antagonized by DHPs (Yunker, 2003). PN200-110 (Arnoult *et al.*, 1996a, 1998) and nifedipine (Liévano *et al.*, 1996; Santi *et al.*, 1996), two DHP antagonists of somatic L-type channels, block the spermatogenic cell T current with IC₅₀ values of ~ 40 nM and 5 μ M, respectively. Inhibition is only partially reversible and due to reduced peak Ca²⁺ current, without effects on either channel activation or inactivation kinetics (Arnoult *et al.*, 1996a; Santi *et al.*, 1996). The DHP agonist BAYK 8644 did not significantly affect Ca²⁺ currents in spermatogenic cells (Arnoult *et al.*, 1996a; Santi *et al.*,

1996). In addition, low concentrations of the diuretic amiloride inhibit T-type channels in mouse spermatogenic cells with an IC_{50} of about $245 \mu M$ (Arnoult *et al.*, 1996a; Santi *et al.*, 1996). Like most T-type channel blockers, the pharmacological profile of amiloride is not ideal, as higher concentrations ($>300 \mu M$) also attenuate HVA currents (Yunker, 2003). Interestingly, recombinant $Ca_v3.1$ channels are quite resistant to the drug (Lacinova *et al.*, 2000), suggesting that amiloride-sensitive T-type currents in spermatogenic cells are more likely to be carried through $Ca_v3.2$ and/or $Ca_v3.3$ channels. Diphenylbutylpiperidine derivatives such as pimozone are drugs used to treat psychiatric disorders. Notably, the Ca^{2+} current in spermatogenic cells is inhibited by pimozone with an IC_{50} of $0.47 \mu M$ (Arnoult *et al.*, 1996a, 1998). Likewise, the phenylalkylamine verapamil, which is a commonly used HVA Ca_v channel antagonist, as it preferentially attenuates L-type currents, can also reduce T-type currents from different cell types including male germ cells (IC_{50} of $70 \mu M$) (Arnoult *et al.*, 1998). Similarly, mibefradil (Ro 40-5967), a novel tetralol derivative similar in structure to verapamil, inhibits the T-type Ca^{2+} current recorded in spermatogenic cells (IC_{50} of $4.70 \mu M$) (Arnoult *et al.*, 1998). Unfortunately, at higher concentrations ($>20 \mu M$) mibefradil also blocks HVA Ca_v channels, limiting its experimental use. Last, ZD7288, a blocker of hyperpolarization-activated and cyclic nucleotide-gated (HCN) channels, has been found to inhibit the T-type Ca^{2+} current in mouse spermatogenic cells with an IC_{50} of $\sim 100 \mu M$. This blockade was more effective at voltages producing low levels of inactivation, suggesting a differential affinity of ZD7288 for different channel conformations (Felix *et al.*, 2003).

Invertebrate toxins have been useful in the study of HVA channels (Doering and Zamponi, 2003) (Table I). Disappointingly, most peptide toxins do not affect T-type channels. However, kurtoxin, a toxin isolated from scorpion venom (Olamendi-Portugal *et al.*, 2002), antagonizes T-type currents conducted by recombinant (Chuang *et al.*, 1998) and native T-type channels from spermatogenic cells (Lopez-Gonzalez *et al.*, 2003). Saturating concentrations of the toxins inhibited at most $\sim 70\%$ of the whole-cell Ca^{2+} current, suggesting the presence of a toxin-resistant component of the current in mouse male germ cells. As anticipated, kurtoxin is able to inhibit the mouse sperm AR (Lopez-Gonzalez *et al.*, 2003). Unluckily, this toxin can also affect HVA channels (Sidach and Mintz, 2002).

3. Planar Bilayers

The availability of large quantities of sperm allows the isolation and characterization of plasma membrane fractions from the different regions of the cell. This is particularly true for sperm from marine organisms such as sea urchins and starfish. The first single-channel recordings, produced from

bilayers formed at the tip of patch-clamp pipettes from monolayers generated from a mixture of lipid vesicles and isolated sea urchin sperm flagellar membranes, detected the presence of three discrete types of cation channels (Guerrero *et al.*, 1987). This planar bilayer formation strategy is sometimes referred to as tip-dip and is a modification of the Montal–Muller method, in which solvent-free monolayers are apposed to each other on a partition (Montal *et al.*, 1981). Two Ca^{2+} channels were documented, using these tip-dip bilayers formed from liposomes containing boar sperm plasma membranes. The channel with the smaller conductance was reported to be sensitive to nitrendipine and completely blocked by 0.5 mM La^{3+} (Cox and Peterson, 1989; Tiwari-Woodruff and Cox, 1995).

The most successful reconstitution system to study ion channels has been the black lipid bilayer (BLM) combined with a vesicle fusion strategy (Miller, 1986). BLMs are spontaneously assembled when phospholipids dispersed in a nonvolatile solvent, usually decane, are deposited into a small hole on a hydrophobic partition of a chamber separating two aqueous compartments. One of the compartments is connected to a voltage generator, and the other to virtual ground through a high-gain current–voltage transducer. The fusion strategy provides a simple procedure to insert ion channels present in membrane fractions (of different degrees of purification) into planar bilayers and study their electrophysiological characteristics under a variety of well-defined experimental conditions (Darszon *et al.*, 1994; Miller, 1986). BLMs containing mouse sperm plasma membranes displayed the presence of an anion channel, a cation-selective channel ($P_{\text{Na}^+}/P_{\text{K}^+} = 2.5$) with two modes of gating, and a high-conductance Ca^{2+} -selective channel ($P_{\text{Ca}^{2+}}/P_{\text{Na}^+} = 4$) (Labarca *et al.*, 1995). This latter channel has properties similar to those recorded from sea urchin sperm plasma membranes, both being blocked by micromolar concentrations of ruthenium red, an inhibitor of the AR (Liévano *et al.*, 1990). Using this strategy, two Ca^{2+} channels with different conductance were reported after human sperm membrane fusion. One was voltage dependent, increasing its open probability on depolarization, and the other was not. Both were blocked by nifedipine, but with a different potency (Chan *et al.*, 1997; Shi and Ma, 1998). Tetraethylammonium (TEA)-sensitive K^+ channels and tetrodotoxin (TTX)-sensitive Na^+ channels were also recorded, using this preparation. Unfortunately, the purity of the membrane preparation used was not examined in detail.

An interesting alternative strategy to circumvent the size restrictions of sperm is the transfer of ion channels from live sperm directly to BLMs (Beltrán *et al.*, 1994). Notably, the AR increases the probability of ion channel incorporation, both in sea urchin and in mouse sperm. In sea urchin sperm this may be due to the post-AR presence of the fusogenic protein bindin in the plasma membrane, an 18-amino acid portion of which has been shown to promote the relatively nonspecific fusion of lipid vesicles *in vitro*

(Glabe, 1985a,b; Miraglia and Glabe, 1993; Ulrich *et al.*, 1998, 1999). A Ba^{2+} -permeable channel resembling the multiconductance channels mentioned above was studied. This approach allows, in principle, the study of cell–cell interactions, such as sperm–egg fusion (Beltrán *et al.*, 1994).

4. Smart Patch

As indicated above, the small size and complex morphology of sperm have precluded the extensive characterization of their ion channels by traditional patch-clamping. In the case of sea urchin sperm, osmotic swelling improves the success rate of gigaseal formation (Babcock *et al.*, 1992; Sanchez *et al.*, 2001), although it is not possible to do this with mammalian sperm. Furthermore, conventional cell-attached seals on swollen sea urchin sperm last only minutes, and obtaining inside-out patches has proved difficult (Sanchez *et al.*, 2001). Alternatively, studying sperm ion channels in spermatogenic cells has the disadvantage that these proteins may redistribute or disappear during the last stages of spermatogenesis (Munoz-Garay *et al.*, 2001; Serrano *et al.*, 1999a). A newer approach has emerged to facilitate gigaseal formation directly on mature sperm, called “high-resolution patch-clamping” or smart patch-clamping (Gorelik *et al.*, 2002). This new strategy has enormous potential to determine ion channel type, position, and modes of regulation in conventionally “difficult-to-patch” cells such as sperm (Gu *et al.*, 2002).

The smart patch-clamp is a combination of scanning ion conductance microscopy (SICM) and patch-clamp recording with a single glass nanopipette probe. Cell surface topography is acquired by the patch-clamp electrode and utilized to facilitate single-channel recordings from small cells and submicron cellular structures that are inaccessible by conventional methods (Gorelik *et al.*, 2002). The equipment used is similar to a patch-clamp setup but includes a mechanism for coordinating optical and scanned images, through a video camera. A computer-driven three-axis piezo translation stage is employed to control the pipette position. A patch pipette held perpendicularly to the sample is first used to scan the cell surface. The ion current through the pipette is strongly influenced by the position of the tip relative to the sample surface, providing the feedback signal to control the vertical position of the tip (Korchev *et al.*, 1997, 2000). The SICM feedback control maintains a constant tip–cell surface separation. This process makes the physical approach of the pipette straightforward and safe, preventing the patch from touching the cell membrane until seal formation is desired.

This technique allowed the recording of a voltage-dependent multistate Ca^{2+} channel with a high main-state conductance (Gorelik *et al.*, 2002) that is similar to the multistate conductance channel documented in planar

bilayers (Liévano *et al.*, 1990). It is possible that this channel could participate in the uptake of Ca^{2+} required for the AR (Liévano *et al.*, 1990).

It is hoped that the smart patch technique will allow whole sperm patch-clamp recordings either directly or by the perforated patch technique. Success in this approach would generate a quantum leap in our understanding of how sperm channels participate in the most important sperm functions that lead to fertilization: motility and the AR.

5. Other Techniques

The ongoing development of genomic and proteomic analysis techniques will assist in the identification of genes and proteins that play important roles during each phase of spermatogenesis. Several research groups have been performing large-scale expression profile analyses with mammalian male germ cells undergoing mitosis, meiosis, and differentiation (Rossi *et al.*, 2004; Schlecht and Primig, 2003). A set of unique transcripts was identified at every stage. These results provide valuable information to identify and unravel the roles of ion channels and other proteins involved in the process of spermatogenesis that eventually could serve as targets for male contraceptives.

A major problem in studying the participation of ion channels during differentiation is to achieve cell survival and differentiation *in vitro*. However, certain parameters important for this process have been identified, such as temperature (scrotal temperature is below modal body temperature in many mammals), oxygen concentration, and the presence of substances such as pyruvate, glutamine, and vitamins, to promote cell viability. The timing of cellular events *in vitro* should match those *in vivo* (Parks *et al.*, 2003). In addition, the association of germ cells and Sertoli cells for survival and proliferation has been recognized (Kierszenbaum, 1994) and cocultures of these two cell types have been a common denominator for several *in vitro* cultures attempts. Development of chambers that allow cell polarization and maintain testicular cellular associations has also helped to improve culture conditions. The development of a germ cell line was reported (Feng *et al.*, 2002). These cells have the morphology of type-A spermatogonia and retain germ cell-specific markers; addition of the murine stem factor promotes differentiation up to primary spermatocytes, and further treatment with this factor allow cells to complete meiosis and form haploid spermatids. The process can be completed in the absence of supporting cells, providing a simple but powerful model to study spermatogenesis. In addition, Hong and co-workers reported success in generating from medaka fish a cell line that can differentiate to form motile sperm *in vitro* (Hong *et al.*, 2004). This result is an important step in establishing the necessary conditions to recapitulate the process of spermatogenesis *in vitro*.

Other modern approaches have been used to learn about gametogenesis. Advances include the utilization of embryonic stem (ES) cells to generate cell lines or specific tissues for implantation or to improve certain human health conditions with the use of ES cell therapy. Three independent groups have succeeded in obtaining gamete-like cells from ES cells. There are still several ethical issues to address, but the possibility exists to produce the cells required for fertilization *in vitro*. Another popular model for studies of vertebrate development is the zebra fish. It possesses several useful characteristics, including ease of manipulation and drug administration, prolific fecundity, and compatibility with techniques such as *in vivo* morpholino application to interrupt mRNA translation, forward genetic screens, *in vivo* chemical screens, and so on (Trede *et al.*, 2004). Last, a unique technique being used to study germ cell development is spermatogonial stem cell transplantation in different animal species. One group has been successful in autologously transplanting bovine spermatogonial stem cells, resulting in a complete regeneration of spermatogenesis (Izadyar *et al.*, 2003).

Proteomics is a promising new area of research that deals with the integral analysis of gene expression by a combination of techniques to resolve, identify, quantitate, and characterize proteins, as well as to store, communicate, and interlink protein and forthcoming DNA sequence and mapping information from genome projects (Celis *et al.*, 1998). To achieve its goal, this strategy utilizes a variety of techniques including high-resolution two-dimensional polyacrylamide gel electrophoresis (2-D PAGE), degradation peptide sequencing, mass spectrometry, Western blotting, and computer analysis (Brewis, 1999; Celis *et al.*, 1998). The combination of these different approaches has resulted in progress toward obtaining a complete proteome of mammalian sperm (Brewis, 1999). Initially, by analyzing a sperm membrane vesicle extract, it was estimated that motile mature sperm contained >600 proteins (Xu *et al.*, 1994). More recently, it has been shown that this number is actually larger (~1400) and that at least 100 are localized to the cell surface (Naaby-Hansen *et al.*, 1997) and about 250 are axonemal proteins (Luck, 1984).

One of the current aims in applying proteomics to sperm is the identification of novel specific target proteins for diagnostics, therapeutics of infertility (Bohring and Krause, 2003; Lefevre *et al.*, 2003; Rajeev and Reddy, 2004; Shibahara *et al.*, 2002; Utleg *et al.*, 2003), and contraception (Chauhan and Naz, 2001; Naaby-Hansen *et al.*, 1997; Shetty *et al.*, 1999, 2001). In addition, this technology can be used to assay the participation of particular proteins such as ion channels in sperm physiology; their expression during spermatogenesis can be monitored (Cossio *et al.*, 1997; Guillaume *et al.*, 2001), as well as their involvement in posttesticular sperm maturation (Dacheux *et al.*, 1998; Starita-Geribaldi *et al.*, 2001). The phosphorylation state of these proteins is an attractive characteristic to track during important functional

transitions such as hyperactivation, capacitation, and the AR (Ficarro *et al.*, 2003; Naaby-Hansen *et al.*, 2002; Peterson *et al.*, 1991). The availability of sperm databanks containing complementary information on nucleic acid and protein sequences, genome mapping, diseases, protein structure and localization, signaling pathways, and so on, has already significantly enhanced our capacity to better understand sperm function and fertilization.

IV. Sperm Motility

Sperm are highly specialized cells that have evolved to perform a single fundamental task—the delivery of their genetic material to the female of their species. Inherent in this function is the requirement for sperm to be motile. The central importance of Ca^{2+} in regulating sperm motility has long been recognized although not fully understood. There are at least two principal roles played by Ca^{2+} in sperm motility. The first is in the initiation of motility when sperm encounter the appropriate environmental cues such as an ionic (or osmotic) change or specific molecules from the egg (Morisawa, 1994). In many species initiation of motility is induced by a PKA-dependent phosphorylation of axonemal proteins, triggered by an increase in $[\text{Ca}^{2+}]_i$ required for activation of the cAMP cascade (Inaba, 2003; Morisawa, 1994). In other species, Ca^{2+} initiates sperm motility in a cAMP-independent manner (Krasznai *et al.*, 2000). The second crucial role of Ca^{2+} is to modulate sperm flagellar bending patterns. Once sperm motility has started, apparently Ca^{2+} is no longer necessary to maintain movement, as long as the energy source, ATP, is supplied. However, Ca^{2+} can alter flagellar bending forms; namely, they are relatively symmetric in low Ca^{2+} ($<100 \text{ nM}$) and become asymmetric (a high amplitude wave) in high Ca^{2+} ($>1 \mu\text{M}$) (Brokaw, 1979; Ho *et al.*, 2002). Because changes in flagellar form strongly affect sperm swimming trajectory, regulation of $[\text{Ca}^{2+}]_i$ is fundamental for sperm chemotaxis and mammalian sperm hyperactivation, as described in detail below.

A. Marine Sperm

Sperm from a number of diverse marine species possess two useful properties that make them attractive models for recording and investigating sperm motility. First, their flagella beat in near-planar waves, confining them at water–glass (and water–air) interfaces, for example, at the surface of a glass coverslip (Cosson *et al.*, 2003). Second, an inherent asymmetry in the planar waveform, in relation to the long axis of the head, causes the sperm to swim

in circles. These two combined properties confine swimming sperm to a two-dimensional plane immediately above the coverslip surface, where they remain circling for extended periods. This situation is ideal for microscopic examination of sperm motile behavior.

B. Chemotaxis

The extensive work of Miller has provided conclusive evidence that oocytes and/or their associated somatic cells can produce molecules to attract homologous sperm (Miller, 1985). This phenomenon is termed chemotaxis, and this strategy has been observed across various taxonomic phyla as a means to augment the success rate of fertilization. Although the strategy may have been well conserved, the structures of the known chemoattractant molecules in different species are diverse (Eisenbach, 1999).

There are two main lines of evidence that link Ca^{2+} to chemotaxis. Since Brokaw found that extracellular Ca^{2+} is essential for chemotactic behavior of bracken fern sperm (Brokaw, 1974), this same requirement has been demonstrated in a variety of species (Cosson, 1990). This probably stems from the ability of Ca^{2+} to directly alter the shape of flagella, as demonstrated in experiments whereby detergent-demembrated flagella (supplemented with ATP) were induced to beat with increased asymmetry in the presence of high concentrations of Ca^{2+} (greater than micromolar) (Brokaw, 1979). A common feature of chemotaxis in sperm from a number of marine (and non-marine) species is the presence of characteristic abrupt turns, named chemotactic turns (Kaupp *et al.*, 2003; Miller, 1985; Yoshida *et al.*, 2002). Miller elegantly demonstrated, using *Tubularia* (hydrozoa) (Miller and Brokaw, 1970) and *Styela* (ascidians) (Miller, 1982), that flagellar asymmetry increases during such episodes of chemotactic turning. Morisawa's group demonstrated that in *Ciona* a similar pattern of flagellar asymmetry could be induced by a purified chemoattractant, a sulfated steroid (Yoshida *et al.*, 2002). Therefore it is likely that the link between Ca^{2+} and chemotaxis lies in its ability to increase flagellar asymmetry to produce chemotactic turns, although direct experimental evidence is still lacking.

The second line of evidence for the role of Ca^{2+} in chemotaxis is the effect of chemoattractant compounds on sperm $[\text{Ca}^{2+}]_i$. As mentioned above, the presence of extracellular Ca^{2+} is a prerequisite for chemotaxis and, not surprisingly, chemoattractant compounds from the eggs of some marine species have been shown to elevate $[\text{Ca}^{2+}]_i$ after application to homologous sperm (Cook *et al.*, 1994; Matsumoto *et al.*, 2003; Schackmann and Chock, 1986). The intracellular effects of chemoattractants on sperm from marine animals are best characterized in echinoderms. The outer investments of echinoderm eggs and oocytes, called the egg jelly, contain short peptides

that dramatically alter the metabolic rate and motility of homologous sperm. More than 100 different sperm-activating peptides (SAPs) have been identified to date, and may be classified into 7 different groups according to cross-reactivity among species (Nishigaki *et al.*, 1996; Suzuki, 1995). Speract (SAP I), the first SAP to be identified, was purified from the egg jelly of the sea urchin *Strongylocentrotus purpuratus* (Hansbrough and Garbers, 1981; Suzuki *et al.*, 1981). It binds to a receptor in the flagellum of *S. purpuratus* sperm (Cardullo *et al.*, 1994), triggering increases in metabolic rate (Hansbrough and Garbers, 1981), $[Ca^{2+}]_i$ (Babcock *et al.*, 1992; Schackmann and Chock, 1986), the concentration of cyclic nucleotides (Hansbrough and Garbers, 1981), pH_i (Lee and Garbers, 1986), and changes in E_m (Babcock *et al.*, 1992; Cook and Babcock, 1993b) (Fig. 3).

These intracellular effects of speract binding have been studied intensively, but speract has not been demonstrated clearly to act as a chemoattractant (Cook *et al.*, 1994). On the other hand, a SAP purified from the sea urchin

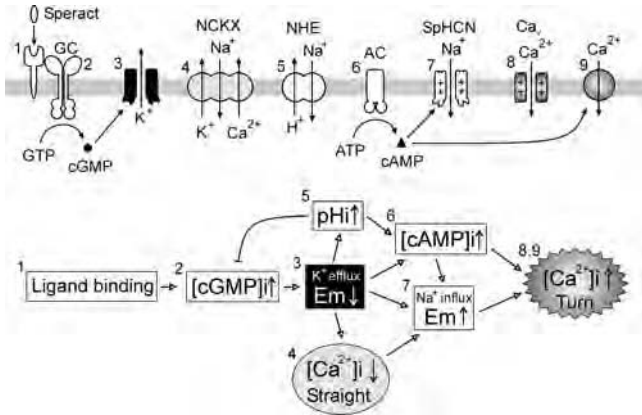


FIG. 3 A speract signaling model. Proteins involved in speract signaling and their relationship are shown: 1, speract receptor; 2, guanylyl cyclase (GC); 3, cGMP-regulated K^+ channel; 4, K^+ -dependent Na^+/Ca^{2+} exchanger (NCKX); 5, Na^+/H^+ exchanger (NHE); 6, adenylyl cyclase (AC); 7, sperm HCN channel (SpHCN); 8, voltage-gated Ca^{2+} channel; 9, cAMP-regulated Ca^{2+} transporter. Depending on the rate of speract binding to its receptor, which is determined by the speract concentration gradient and the sperm swimming direction, one of these pathways may be reversibly dominant. Because GC is inactivated by pH_i -dependent dephosphorylation and cGMP is rapidly hydrolyzed by phosphodiesterases, the opening of the cGMP-regulated K^+ channel is transient. E_m hyperpolarization facilitates the Ca^{2+} extrusion activity of NCKX. Sperm NHE and AC are known to be activated by hyperpolarization. HCN (hyperpolarization-activated and cyclic nucleotide-gated) channels open when E_m hyperpolarizes and intracellular cAMP elevates, which contributes to E_m depolarization by Na^+ influx. E_m hyperpolarization followed by depolarization is favorable to activate voltage-gated Ca^{2+} channels. Cyclic AMP activates a poorly characterized Ca^{2+} influx pathway, which may contribute to the $[Ca^{2+}]_i$ increase in the head.

Arbacia punctulata, named resact (SAP IIA), has been shown to possess clear chemotactic activity (Ward *et al.*, 1985). In general, the signaling cascades for speract and resact are similar although the structures of their respective receptors are different. Speract binds to a cysteine-rich protein that interacts with a membrane-bound guanylyl cyclase (GC) (Dangott and Garbers, 1984; Dangott *et al.*, 1989) whereas the resact receptor has intrinsic GC activity (Singh *et al.*, 1988). In either case, binding of SAPs to their respective receptors has the same initial effect, namely, activation of GC (Ramarao and Garbers, 1985) and an increase in cGMP concentration (Hansbrough and Garbers, 1981; Suzuki *et al.*, 1984). This in turn induces a membrane hyperpolarization, through the opening of K^+ channels (Babcock *et al.*, 1992; Cook and Babcock, 1993b; Lee and Garbers, 1986). Although there is evidence indicating that cGMP may directly activate a K^+ -selective channel (Galindo *et al.*, 2000), the molecular link between cGMP and K^+ channels still must be established. These two early events constitute the essential initial steps in the speract signaling pathway, as increasing $[K^+]_e$ between 2- and 5-fold (and thus inhibiting the K^+ -dependent hyperpolarization) inhibits all stages of the speract signaling cascade (Fig. 3), with the exception of the increase in cGMP (Babcock *et al.*, 1992; Cook and Babcock, 1993b; Harumi *et al.*, 1992).

Currently known events occurring after the membrane hyperpolarization include activation of Na^+/H^+ exchange activity leading to an increase in pH_i (Lee and Garbers, 1986); activation of a $Na^+/K^+ - Ca^{2+}$ exchanger resulting in a decrease in $[Ca^{2+}]_i$ (Nishigaki *et al.*, 2004; Su and Vacquier, 2002); activation of adenylyl cyclase (AC) causing an increase in cAMP (Beltrán *et al.*, 1996; Hansbrough and Garbers, 1981); membrane depolarization (Lee and Garbers, 1986); and, ultimately, after a 150- to 200-ms delay from SAP binding (Nishigaki *et al.*, 2001), a increase in $[Ca^{2+}]_i$ that is dependent on extracellular Ca^{2+} (Schackmann and Chock, 1986). It is not known how the hyperpolarization activates the sperm AC. If it is also modulated by HCO_3^- , as is the mammalian soluble AC (sAC) (Buck *et al.*, 1999), there could be a link between E_m , HCO_3^- transport, and sperm motility modulation. The speract-induced pH_i increase also causes GC dephosphorylation and reduction of its activity (Garbers, 1989; Ward *et al.*, 1986). The role and origin of the pH_i increase have been questioned (Solzin *et al.*, 2004). However, the fact that high external K^+ inhibits all the speract responses, but not the cGMP increase (Harumi *et al.*, 1992), suggests the pH_i is caused by a K^+ -dependent hyperpolarization and not by the metabolism of cGMP, as proposed lately (Solzin *et al.*, 2004).

As a result of the hyperpolarization and the cAMP increase, it is likely that a cation channel named SpHCN is activated (Gauss *et al.*, 1998). So far this is the only sea urchin sperm ion channel that has been cloned. SpHCN belongs to the hyperpolarization-activated and cyclic nucleotide-gated K^+ channel

(HCN) family (Gauss *et al.*, 1998). This family includes pacemaker channels that modulate periodicity in neural networks, control heart beat, regulate rhythmic firing in individual neurons, and contribute to E_m (Kaupp and Seifert, 2001). SpHCN displays poor K^+ selectivity ($P_{K^+}/P_{Na^+} = \sim 5$), therefore allowing Na^+ influx under physiological conditions and possibly contributing to the re- or depolarization of sperm. Because SpHCN is present mainly in the flagellum, in principle it could be involved in chemotaxis (Kaupp and Seifert, 2001). Channels with similar characteristics have been described in planar bilayers containing flagellar sperm plasma membranes (Labarca *et al.*, 1996) and by patch-clamp techniques in swollen sea urchin sperm (Sanchez *et al.*, 2001).

Of all the SAP-stimulated changes, the increase in $[Ca^{2+}]_i$ is probably the most relevant in the context of the regulation of chemotaxis, for the reasons already outlined, namely the absolute requirement for extracellular Ca^{2+} during chemotaxis and the apparent ability of Ca^{2+} to regulate flagellar form. Because of this it is worth examining the mechanisms underlying this crucial intracellular event in more detail. Sea urchin sperm $[Ca^{2+}]_i$ has been successfully measured with fluorescent Ca^{2+} indicators indo-1 (Schackmann and Chock, 1986), fura-2 (Guerrero and Darszon, 1989b), and fluo-3 and -4 (Kaupp *et al.*, 2003; Nishigaki *et al.*, 2001; Wood *et al.*, 2003). However, little is known of the route by which extracellular Ca^{2+} enters the sperm. Cook and Babcock (1993a) proposed that at least part of the Ca^{2+} entry pathway is mediated by cAMP. In addition, it was discovered using a caged derivative of cAMP, that $[Ca^{2+}]_i$ increases occur after liberation of cAMP inside *S. purpuratus* sperm in high $[K^+]_e$ (Nishigaki *et al.*, 2004). On the other hand, Kaupp and co-workers used stopped-flow fluorometry and caged cyclic nucleotides and reactant derivatives to measure the kinetics of the $[Ca^{2+}]_i$ increase in *A. punctulata* sperm (Kaupp *et al.*, 2003). These increases were found to be biphasic and named "early" and "late" phases. The authors proposed that the sperm have at least two Ca^{2+} entry pathways, with the early phase mediated by cGMP, and the late phase mediated by cAMP. Single-cell imaging of speract-induced $[Ca^{2+}]_i$ changes produced insights into the variation in Ca^{2+} signaling between cellular compartments (Wood *et al.*, 2003). It was discovered that $[Ca^{2+}]_i$ increases in the flagella were composed of a repeating sequence of large-amplitude fluctuations (up to $4 s^{-1}$) of uneven period, superimposed over a tonic $[Ca^{2+}]_i$ increase of longer duration (up to 45 s). In the head, the longer duration tonic elevation comprised the majority of the $[Ca^{2+}]_i$ signal, with superimposed fluctuations of relatively smaller amplitude. The superimposed fluctuations could be blocked by treatment with Ni^{2+} , a blocker of Ca_v channels, and by removal of $[K^+]_e$. Their period and amplitude could be modified drastically by niflumic acid, an inhibitor of anion channels. The authors proposed that the Ca^{2+} fluctuations are mediated by repeated opening of Ca_v channels, probably

through a membrane potential-dependent mechanism, and that the tonic $[Ca^{2+}]_i$ increase is probably mediated through a cAMP-dependent mechanism. It was also proposed that the Ca^{2+} fluctuations play a role in regulating some aspect of motility, as they were generated in the flagellum and propagated into the head.

These compartmentalized, multiphasic increases in $[Ca^{2+}]_i$ almost certainly play a part in regulating an important aspect of sperm physiology, but as yet there is no direct evidence of a role in regulating chemotactic motility. As might be expected from the intracellular response to a molecule that mediates a long-distance sperm-egg interaction, the sensitivity of the sperm to speract is remarkable, with graded increases in $[Ca^{2+}]_i$ observed after peptide additions over three orders of magnitude of concentration, beginning in the picomolar range (Cook *et al.*, 1994). It is noteworthy that the delay between SAP binding and the increase in $[Ca^{2+}]_i$ is roughly equivalent to the delay between SAP binding and the initiation of chemotactic turning in *A. punctulata* (Kaupp *et al.*, 2003). During this delay, $[Ca^{2+}]_i$ decreases in the head and flagella (Nishigaki *et al.*, 2004), which might play a role in regulating some aspect of chemotactic motility. This Ca^{2+} decrease is stimulated by membrane hyperpolarization, and prolonged hyperpolarization leading to a more linear swimming trajectory was at the center of a proposed model for chemotaxis (Cook *et al.*, 1994). Chemotactic motility in many species is composed of a succession of turns, interspersed with periods of more linear swimming, and it is tempting to speculate that a repetitive sequence of chemotactic turns could be stimulated by a repetitive sequence of increases in $[Ca^{2+}]_i$, such as those observed in single *S. purpuratus* sperm. Interestingly, an article that compared measured patterns of chemotactic motility in two separate species with those obtained through modeling of cellular responses to gradients of chemoattractant found that the natural patterns of chemotactic motility could be adequately reproduced by simulating the oscillation of $[Ca^{2+}]_i$ levels within the modeled system (Ishikawa *et al.*, 2004). Despite being highly suggestive of an intimate role for dynamic $[Ca^{2+}]_i$ changes in regulating chemotactic motility, these inferences and correlations will remain speculative until techniques are developed that permit the direct observation of Ca^{2+} changes in individual swimming sperm.

C. Mammalian Sperm Motility

Reaching and fertilizing the oocyte deep inside the female body is not an easy task. It is necessary to deposit thousands, or even millions, of sperm to achieve this precious goal. Sperm must adequately deal with environmental changes and signaling exchanges with the egg for fertilization to be successful.

Mammalian sperm initiate motility with a symmetrical flagellar beat, called sperm activation, when released into the female reproductive tract (Yanagimachi, 1994). To ensure this process, sperm need to mature properly in the epididymis, because testicular sperm do not have this capacity. The molecular basis of sperm maturation in the epididymis is a mystery. However, an antimicrobial peptide (Bin1b, a member of the β -defensin family of cationic pore-forming peptides) exclusively expressed in rat epididymis (Li *et al.*, 2001; Zanich *et al.*, 2003) was discovered to be important for sperm maturation (Zhou *et al.*, 2004). The heads of sperm from caput, corpus, and cauda epididymis have varied patterns of immunoreactivity toward anti-Bin1b antibody. Interestingly, Bin1b induces increases in $[Ca^{2+}]_i$ and progressive motility in immature sperm from the initial segment of the epididymis. L-type Ca_v channel blockers nifedipine and verapamil reduce the Bin1b-induced $[Ca^{2+}]_i$ increase and sperm activation, suggesting that it is not the peptide itself that generates a pore in the plasma membrane. Once sperm motility is initiated, neither anti-Bin1b antibody nor nifedipine has prominent effects, indicating that this peptide is important only for the acquisition of sperm motility during the process of sperm maturation in the epididymis. It has long been known that PKA-dependent axonemal protein phosphorylation is essential for sperm motility initiation (Morisawa, 1994).

Sperm AC has been known as a unique enzyme because it is directly activated by bicarbonate (Okamura *et al.*, 1985) and is not regulated by G proteins. It was cloned by Buck *et al.* (1999) as a cytosolic enzyme called sAC, distinct from other G protein-coupled transmembrane forms (tmACs). Using recombinant sAC, it was confirmed that sAC is directly activated by bicarbonate (Chen *et al.*, 2000) and Ca^{2+} (Jaiswal and Conti, 2003; Litvin *et al.*, 2003), which are crucial elements that regulate sperm motility and capacitation as discussed below. The increase in $[Ca^{2+}]_i$ induced by Bin1b could stimulate sAC and the cAMP signaling pathway. As anticipated, a transgenic mouse lacking sAC (and therefore deficient in PKA regulation) is infertile and its sperm are unable to swim progressively (Esposito *et al.*, 2004). In addition to sAC, several tmACs have also been immunodetected (Baxendale and Fraser, 2003; Gautier-Courteille *et al.*, 1998; Wade *et al.*, 2003), but their role in sperm physiology is unknown.

D. Hyperactivation

In some mammals, it has been shown that sperm are stored until ovulation in the initial segment of the oviduct (Suarez, 1998), owing to certain proteins on the sperm surface recognizing and binding to sugar ligands on the epithelium lining the oviduct (DeMott *et al.*, 1995; Ignotz *et al.*, 2001). This temporal

storage could function to regulate the numbers of sperm that reach the oocyte. Mammalian sperm have been isolated in an hyperactivated state from the oviduct (Katz and Yanagimachi, 1980; Suarez and Osman, 1987). A distinct feature of hyperactivated sperm motility is an increase in flagellar bend amplitude and beat asymmetry. This mode of swimming may allow sperm to escape from their temporal stop in the initial segment of the oviduct, to progress in mucous, highly viscous medium, and to penetrate the oocyte ZP (Ho and Suarez, 2001a).

There is evidence that Ca^{2+} is elevated in the flagella of hyperactivated sperm above the levels seen in active sperm (Suarez and Dai, 1995; Suarez *et al.*, 1993). Demembranated bull sperm flagella reactivated in ATP-containing medium undergo hyperactivation when Ca^{2+} is elevated from 50 to 400 nM, whereas cAMP has no effect on flagellar curvature (Ho *et al.*, 2002). Although the physiological signal for hyperactivation is unknown, it may be artificially induced by several compounds such as pentoxifylline, a phosphodiesterase inhibitor (Mbizvo *et al.*, 1993; Nassar *et al.*, 1998; Tesarik *et al.*, 1992), and procaine (Mujica *et al.*, 1994). Some of these compounds can induce hyperactivation without increasing $[\text{Ca}^{2+}]_i$ (Nassar *et al.*, 1998) or in the absence of external Ca^{2+} (Mujica *et al.*, 1994). Thapsigargin, caffeine, and thimerosal, three reagents that release Ca^{2+} from internal stores, can immediately induce hyperactivated motility in bovine sperm (Ho and Suarez, 2001b). Ca^{2+} imaging revealed that the increase in $[\text{Ca}^{2+}]_i$ was initiated at the neck region of sperm, and immunocytochemical studies indicated the existence of IP_3 receptors at this region (Ho and Suarez, 2001b; Walensky and Snyder, 1995). This flagellar store has been identified as a portion of the redundant nuclear envelope (RNE) (Fig. 1), a reticular structure constituted by nuclear membranes left over from spermatogenesis and thought to have no physiological function (Baccetti and Afzelius, 1976). Notably, the RNE is asymmetrically located between the plasma membrane and the flagellar base, just where the flagella initiate principal and reverse bend propagation (Ho and Suarez, 2003). Ca^{2+} imaging using mouse sperm also demonstrated that the progesterone-induced $[\text{Ca}^{2+}]_i$ increase is propagated from the same region (Fukami *et al.*, 2003).

All this information emphasizes the importance of understanding how Ca^{2+} enters the sperm flagellum to regulate motility. The relevance of this matter became even clearer with the discovery of a putative Ca^{2+} channel, CatSper, as its disruption resulted in male infertility, as described earlier (Ren *et al.*, 2001). CatSper (either 1 or 2) null sperm are morphologically normal and able to undergo AR, but lack the ability to initiate hyperactivated motility (Carlson *et al.*, 2003; Quill *et al.*, 2003). The $[\text{Ca}^{2+}]_i$ elevation caused by cyclic nucleotides is disrupted in sperm from CatSper1 null mice (Ren *et al.*, 2001). Bicarbonate, an activator of sAC, facilitates sperm $[\text{Ca}^{2+}]_i$ increases induced by depolarization with high $[\text{K}^+]_e$ (Wennemuth *et al.*,

2003), a response also absent in CatSper1 null sperm (Carlson *et al.*, 2003). These findings suggest that CatSper mediates the Ca^{2+} influx that is essential for hyperactivation and that cyclic nucleotides may be involved in the signaling cascade, although it is still fundamental to demonstrate that CatSper functions as, or forms part of, a Ca^{2+} channel.

Further evidence of the close interrelations between pH_i , cyclic nucleotides, and $[\text{Ca}^{2+}]_i$ comes after the discovery that male mice lacking a sperm-specific Na^+/H^+ exchanger are infertile (Wang *et al.*, 2003). The sperm from these null mice have severely compromised motility, although membrane-permeant cAMP analogs rescue the swimming defect of the mutant sperm. Do other channels such as CNGs, TRPs, SOCs, or Ca_v channels participate in the regulation of hyperactivation? The localization of various types of Ca^{2+} -permeable channels in the flagellum (Fig. 1B) suggests their possible participation in sperm motility (Castellano *et al.*, 2003; Treviño *et al.*, 2001, 2004; Wiesner *et al.*, 1998). It is worth considering that different signaling cascades may operate to achieve hyperactivation depending on the region and/or events, for instance, to detach from the oviduct reservoir, to progress along the mucous lumen of the oviduct, or to penetrate the oocyte ZP. Further studies are required to answer these questions.

E. Mammalian Sperm Chemotaxis

In marine species and ferns the occurrence of sperm chemotaxis has long been known. Until relatively recently, the presence of similar mechanisms acting on mammalian sperm has been the subject of much debate. The unequivocal identification of chemotaxis in mammalian sperm was hampered by the wide variety of experimental designs employed, and qualifying criteria applied, to the analysis of sperm behavior (Eisenbach, 1999). Although a role for chemotaxis in mammalian reproduction is now generally accepted, most of its details, such as the identity of the natural chemoattractant, the molecular events inside the sperm triggered by the chemoattractant, and how these events then translate into modified swimming behavior, are as yet unanswered.

It was observed in the 1950s that mammalian sperm accumulated around dissociated follicular cells (Moricard and Bossu, 1951) and in follicular and other egg-associated fluids (Schwartz *et al.*, 1958). These, and other more contemporary observations, were interpreted as evidence for chemotaxis. However, these early studies made no distinction between chemotaxis (defined as the modification of the direction of motility in response to a gradient of chemoattractant) and two other processes that may lead to sperm accumulation: chemokinesis (whereby the chemostimulus produces a change in the speed of swimming irrespective of any gradient direction) and

trapping (whereby net motility is greatly reduced or lost in response to a chemostimulus). Therefore, accumulation of sperm at or around the source of a stimulus does not necessarily imply a chemotactic mechanism. For example, Villanueva-Diaz and colleagues (1995) observed that progesterone causes human sperm accumulation, and suggested that this hormone was the chemoattractant in follicular fluid. Other studies showed that the concentration of progesterone was not important for this effect (Ralt *et al.*, 1991), and that it was caused by trapping of the sperm close to the progesterone source through its capacity to induce hyperactivated motility (Jaiswal *et al.*, 1999). Sperm exposed to progesterone swam vigorously yet nonprogressively, as is characteristic of the hyperactivated state, and did not change direction in response to a gradient of progesterone. Distinguishing between the three mechanisms requires careful experimental design, the most useful of which involve establishing ascending, descending, and neutral gradients of the putative chemoattractant and assessing the sperm behavior in each, preferably by analysis of the video-recorded trajectories of individual sperm. Eisenbach (1999) has compared the various methods employed to assess chemotaxis in mammalian sperm.

The function of chemotaxis in marine fertilization is relatively simple to understand; by releasing factors that advertise its presence, the egg increases its effective size manifold, guiding sperm toward it and enhancing the probability of its fertilization. In most marine species fertilization occurs externally, and both male and female gametes are exposed to near-infinite dilution factors. In mammalian fertilization, large quantities of sperm are deposited inside the female, where similar limitations of dilution do not apply. If this is the case, why does the mammalian egg need to guide sperm toward it at all? The probable answer lies in the fact that not all postejaculate sperm are equal. Although thousands of sperm may leave the uterus and enter the oviducts, in many mammals sperm become attached to the oviduct walls in a structure known as the oviductal isthmus (Suarez, 1998). Here, a continuous turnover of sperm between precapacitated, capacitated, and finally postcapacitated states probably occurs, such that in humans, a low percentage of sperm are capacitated at any given point (Cohen-Dayag *et al.*, 1995). On ovulation, capacitated sperm enter a high-motility state, detach from the oviduct walls, and progress further along the oviduct to the site of fertilization (Barratt and Cooke, 1991; Lefebvre and Suarez, 1996; Smith and Yanagimachi, 1991). In this manner, only a relatively low number of sperm that are capable of undergoing the AR (and thus fertilizing the egg) arrive. Indeed, in most mammals, seldom is more than one sperm observed in the vicinity of an egg at the moment of gamete fusion (Hunter, 1993). Is the signal that stimulates the capacitated sperm to leave the storage site the same as the chemoattractant component of follicular fluid? This is yet to be resolved, but it has been shown *in vitro* that chemotactic responsiveness to

follicular fluid is restricted to capacitated sperm, and is not present in both pre- and postcapacitated sperm (Cohen-Dayag *et al.*, 1995; Fabro *et al.*, 2002).

The identity of a candidate chemoattractant molecule in mammals has remained elusive, although growing evidence now links chemotaxis in mammalian sperm to an olfactory receptor-mediated mechanism. A specific subset of olfactory receptors is known to be expressed in male germ cells (Parmentier *et al.*, 1992; Vanderhaeghen *et al.*, 1997), and antibody staining showed that at least some of these olfactory receptors were localized to the midpiece of the flagellum (Vanderhaeghen *et al.*, 1993; Walensky *et al.*, 1995), hinting at a potential role in regulating sperm motility. Spehr *et al.* (2003) cloned and expressed one of the human testis-specific olfactory receptors (hOR17-4) in HEK cells, and discovered that this receptor is activated most strongly by a range of organic molecules containing a *para*-substituted aromatic ring linked by a two- to four-carbon chain to an aldehyde group. These same compounds were able to evoke $[Ca^{2+}]_i$ increases in human sperm at concentrations down to $10^{-8}M$. These $[Ca^{2+}]_i$ increases were dependent on the presence of extracellular Ca^{2+} , and on the activity of AC, although the route of Ca^{2+} entry remains to be determined. Computer-assisted analyses of the trajectories of sperm exposed to gradients of the aromatic aldehyde bourgeonal demonstrated that this compound can act as a chemoattractant *in vitro*. This chemotactic response also depends on $[Ca^{2+}]_e$.

Some questions do remain, such as the apparent ability of these compounds to increase $[Ca^{2+}]_i$ in noncapacitated sperm, which contrasts with the ability of the natural chemoattractant to selectively attract capacitated sperm. And as yet, no one has demonstrated that follicular fluid contains bourgeonal or its related aromatic aldehydes, although the presence of a corresponding receptor in sperm suggests a role for these compounds in some aspect of mammalian reproduction. Nevertheless, they remain strong candidates for the role of chemoattractant; it was shown that both human and rabbit sperm respond chemotactically to any one of human, rabbit, and bovine follicular fluid (Sun *et al.*, 2003). This suggests either a remarkable degree of evolutionary conservation for the receptor of the chemotactic agent, or that this receptor may respond to a range of possibly closely structurally related stimuli, as observed with the olfactory receptor analyzed in the study by Spehr and co-workers (2003). Interestingly, it was also observed that the hOR17-4 olfactory receptor is strongly inhibited by the aliphatic alcohol undecanal, even in the presence of equimolar concentrations of bourgeonal (Spehr *et al.*, 2003). Does the newly fertilized egg release undecanal (or a related compound) to inhibit chemotaxis and prevent further sperm from fusing with it? Intriguingly, just such a mechanism was proposed to explain how, in animals that release multiple eggs at ovulation (such as mice, rats, and pigs), each egg is visited by a single sperm, rather than one egg

attracting many, and others receive none as might be expected if the process were random (Eisenbach, 1999; Hunter, 1993). That sperm should be so selective in choosing unfertilized eggs suggests that the eggs rapidly lose their attractiveness once fertilized.

V. Sperm Capacitation and the Acrosome Reaction

A. Capacitation

Fully differentiated mammalian sperm acquire their ability to move forward during maturation in the epididymis. However, they must reside for some time in the female reproductive tract before they acquire the ability to fertilize the egg (Yanagimachi, 1994). The molecular, biochemical, and physiological changes that sperm acquire while inside the female tract are collectively named capacitation (Austin, 1952; Chang, 1951; Yanagimachi, 1994). This maturational process is associated with the development of a distinctive motility pattern, termed hyperactivation. This mode of swimming is characterized by a vigorous beating pattern of the sperm flagellum, and occurs in all mammalian species investigated. Several lines of evidence indicate that hyperactivation and capacitation, although occurring in parallel, are regulated by independent mechanisms (Suarez and Ho, 2003).

The molecular mechanisms involved in sperm capacitation are not well understood. Transit through the female tract exposes sperm to significant changes in ion concentrations, osmolarity, and environmental milieu. Caudal epididymal sperm are stored in a medium containing high K^+ , low Na^+ , and very low HCO_3^- concentrations (Brooks, 1983; Setchell, 1994; Yanagimachi, 1994). The ionic environment changes after ejaculation in the seminal fluid and then in the female tract; while $[K^+]_e$ is reduced, $[Na^+]_e$ and $[HCO_3^-]_e$ are significantly increased. These drastic shifts in external ion concentrations after ejaculation result in sperm E_m alterations (Arnoult *et al.*, 1999; Munoz-Garay *et al.*, 2001). In addition, capacitation involves cholesterol removal from the plasma membrane (Cross, 2004; Travis and Kopf, 2002; Visconti *et al.*, 2002), increases in pH_i (Galantino-Homer *et al.*, 2004; Parrish *et al.*, 1989) and $[Ca^{2+}]_i$ (Baldi *et al.*, 1991; DasGupta *et al.*, 1993), and activation of second-messenger cascades, mainly involving cAMP (Breitbart, 2003; De Lamirande *et al.*, 1997; Olds-Clarke, 2003) (Fig. 4).

Sperm capacitation can be accomplished *in vitro* by incubating ejaculated sperm in defined medium containing appropriate concentrations (close to those in the oviductal fluid) of three key elements: Ca^{2+} , HCO_3^- , and serum albumin (Visconti *et al.*, 1995; Yanagimachi, 1994). $[Ca^{2+}]_e$ in the range of 100–200 μM is required for mouse sperm capacitation (Fraser, 1987;

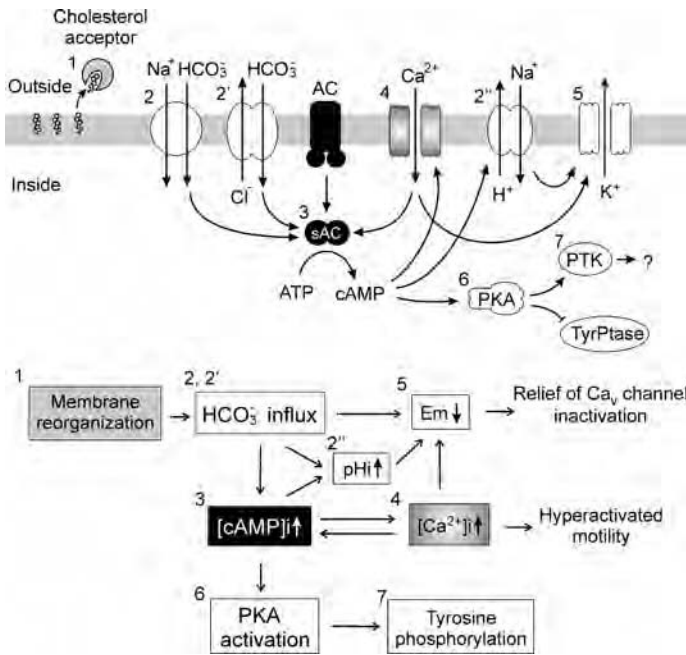


FIG. 4 A signaling model for mammalian sperm capacitation. Proteins involved in capacitation and their relationship are illustrated: 1, cholesterol acceptor (such as albumin); 2, electrogenic $\text{Na}^+/\text{HCO}_3^-$ cotransporter; 2', $\text{Cl}^-/\text{HCO}_3^-$ exchanger; 2'', Na^+/H^+ exchanger; 3, soluble adenylyl cyclase (sAC); 4, Ca^{2+} transporters (such as CNG and CatSper channels); 5, K^+ channels (Kir and Ca^{2+} -activated channels); 6, cAMP-dependent protein kinase (PKA); 7, protein tyrosine kinase (PTK). Capacitation and hyperactivation are distinct events. However, they may share several steps in the signaling cascade. Bicarbonate and Ca^{2+} are essential extracellular elements for both events. Protein tyrosine phosphorylation is a useful tool with which to monitor capacitation, but its physiological significance has not been established yet.

Marin-Briggiler *et al.*, 2003). *In vitro* studies have shown that sperm plasma membrane fluidity is altered as a result of cholesterol removal by albumin from the female reproductive tract (Cross, 2003; Travis and Kopf, 2002; Visconti *et al.*, 2002). If serum albumin is preloaded with cholesterol, it does not permit *in vitro* capacitation (Osheroff *et al.*, 1999; Visconti *et al.*, 1999). Cholesterol removal, with a resultant change in sperm plasma membrane fluidity and/or organization, could modulate Ca^{2+} and/or HCO_3^- ion fluxes, leading to the activation of AC and changes in cAMP levels (Visconti *et al.*, 2002) (Fig. 4).

It has been proposed that one of the earliest steps in capacitation is an externalization of phosphatidylethanolamine and phosphatidylserine that results in a rapid collapse of phospholipid plasma membrane asymmetry

(Gadella and Harrison, 2000; Harrison *et al.*, 1996; Harrison and Miller, 2000). Increases in membrane disorder due to cholesterol removal have also been reported (Cross, 2003). Likewise, major increases in protein tyrosine phosphorylation take place during sperm capacitation. This process is mediated by cAMP and PKA, as first noted in the mouse (Visconti *et al.*, 1995), and later demonstrated in a wide range of species (Galantino-Homer *et al.*, 1997; Leclerc *et al.*, 1996; Visconti *et al.*, 1999) (Fig. 4).

As mentioned in Section V.B, sperm from GalT I null mice are fertile (Lu and Shur, 1997). Interestingly, capacitation seems accelerated in sperm from these mice, apparently because of their inability to bind epididymal glycoconjugates that normally maintain sperm in an uncapacitated state. When measured in terms of the ability to undergo an ionophore-induced AR, capacitation of GalT I null sperm does not depend on albumin, Ca^{2+} , and HCO_3^- . Binding of sperm to ZP (another marker for capacitation) is also independent of Ca^{2+} and HCO_3^- in these sperm, but albumin is required. Thus, the downstream targets of Ca^{2+} and HCO_3^- may be constitutively active in GalT I null sperm. As anticipated, these sperm have increased levels of cAMP but, surprisingly, their protein tyrosine phosphorylation kinetics and capacitated sperm motility develop at the same rate as in wild-type sperm during *in vitro* capacitation. The authors suggest that GalT I may function as a negative regulator of sperm capacitation (Rodeheffer and Shur, 2004b).

Besides activating sAC (Litvin *et al.*, 2003), new results indicate that HCO_3^- flux through the mouse sperm plasma membrane hyperpolarizes the cell in an $[\text{Na}^+]_e$ -dependent manner (Demarco *et al.*, 2003). Ion substitution experiments suggest that an electrogenic $\text{Na}^+/\text{HCO}_3^-$ cotransporter is present in mouse sperm and is coupled to events regulating capacitation. In addition, HCO_3^- uptake may contribute to the known pH_i increase observed during sperm capacitation (Parrish *et al.*, 1989; Zeng *et al.*, 1996).

The mouse sperm E_m becomes more negative (hyperpolarizes) during capacitation and the K^+ gradient influences this change (Arnoult *et al.*, 1999; Munoz-Garay *et al.*, 2001; Zeng *et al.*, 1995). Biochemical and molecular biology data suggest the presence of various K^+ channels in mammalian testis and sperm (Jacob *et al.*, 2000; Salvatore *et al.*, 1999; Schreiber *et al.*, 1998) as well as in male germ cells (Felix *et al.*, 2002; Munoz-Garay *et al.*, 2001). Notably, the participation of a pH-regulated, inward rectifier, K^+ channel has been suggested in the capacitation-associated hyperpolarization (Munoz-Garay *et al.*, 2001). The addition of Ba^{2+} to the capacitating medium blocks these inwardly rectifying (Kir) channels and inhibits membrane hyperpolarization and, partially, the sperm AR. Likewise, an elevation in pH_i , as it occurs during capacitation, may increase the open probability of these channels, permitting K^+ ions to flow out of the sperm, driving the potential toward the K^+ equilibrium potential and hyperpolarizing the cell (Munoz-Garay *et al.*, 2001). Alternatively, the opening of Ca^{2+} -activated

K^+ channels during sperm capacitation could also hyperpolarize them. Injection of RNAs from rat spermatogenic cells into *Xenopus* oocytes resulted in the expression of currents that show similarity to maxi-K channels, the Ca^{2+} -activated K^+ channels of somatic cells (Chan *et al.*, 1998; So *et al.*, 1998; Wu *et al.*, 1998). Immunolocalization and RT-PCR assays showed that these channels are present in spermatogenic cells and sperm (Wu *et al.*, 1998). Such channels may activate when $[Ca^{2+}]_i$ increases on capacitation. However, whether the opening of Ca^{2+} -activated K^+ channels indeed contributes to capacitation and is upstream or parallel to the activation of Kir channels is not presently known (Fig. 4).

The capacitation-associated hyperpolarization is thought to release Ca_v channels from inactivation such that they become competent to respond to the ZP signal, allowing mouse sperm to undergo the AR. This hypothesis is consistent with the presence of T-type Ca_v channels in spermatogenic cells (Arnoult *et al.*, 1996a; Liévano *et al.*, 1996; Santi *et al.*, 1996) and in mature sperm (Park *et al.*, 2003; Treviño *et al.*, 2004). A signature property of T-type Ca_v channels is a low threshold for voltage-dependent inactivation, which means that these channels are inactive even at the relatively negative E_m values observed before capacitation (Arnoult *et al.*, 1996a; Liévano *et al.*, 1996; Santi *et al.*, 1996). Thus, if T-type Ca_v channels are involved in the regulation of the AR, sperm must remain hyperpolarized during the early stages of interaction with the egg. Indeed, during capacitation sperm E_m changes by tens of millivolts, reaching values that can remove inactivation from T-type Ca_v channels (Arnoult *et al.*, 1999; Munoz-Garay *et al.*, 2001). However, although mouse germ cells display mainly T-type Ca^{2+} currents (Arnoult *et al.*, 1996a; Liévano *et al.*, 1996; Santi *et al.*, 1996), the expression of different HVA Ca_v channels has also been documented in spermatogenic cells and sperm, and therefore the hyperpolarization could also prime these channels.

The increase in $[Ca^{2+}]_i$ that occurs during capacitation (Fig. 4) could result from (1) reduced Ca^{2+} efflux caused by inhibition of the Ca^{2+} -ATPase and/or the Na^+/Ca^{2+} exchanger or from (2) increased Ca^{2+} influx due to the activation of unidentified channels resulting from cholesterol removal and/or increases in cAMP (Jagannathan *et al.*, 2002a). Ca_v channels are candidates for a role in the latter proposal. In spermatogenic cells, serum albumin induces an increase in the Ca^{2+} window current of T-type Ca_v channels by shifting the voltage dependence of both steady state activation and inactivation (Espinosa *et al.*, 2000). Because these channels are present in mature sperm (Arnoult *et al.*, 1999; Treviño *et al.*, 2004) serum albumin could facilitate an increase in Ca^{2+} entry, a prerequisite to capacitation.

There are still many fundamental questions unanswered about the complex process of capacitation, some of which are as follows: (1) What is the identity of the transport system(s) responsible for the $[Ca^{2+}]_i$ and pH_i ;

increases? (2) Which of the proteins that change their phosphorylation state are important? (3) Are some of them ion channels? (4) Does the pH_i increase only modulate Kirs, or are other activities regulated? (5) What exactly are decapacitation factors and what is their mode of action? (6) What are the regulatory targets of the lipid changes?

B. Acrosome Reaction

The acrosome is a membrane-delimited organelle that overlies the sperm nucleus (Fig. 1A). In response to the physiological egg inducer or to appropriate pharmacological stimuli, the outer acrosomal membrane and the overlying plasma membrane fuse and vesiculate, leading to exposure of the acrosomal contents and modified plasma membrane to the extracellular medium (Yanagimachi, 1994). The resulting sperm membrane elements are required for egg coat penetration and for fusion with the egg plasma membrane. This exocytotic process, named the AR, is required for fertilization in all sperm species possessing an acrosome. Molecules of the egg extracellular envelope species-specifically activate homospecific sperm and induce the AR. The egg envelope is not only a protective layer but also an essential component of the gamete recognition and signaling process. External Ca^{2+} is needed for the AR (Dan, 1954) and certain ion channel blockers inhibit it, indicating the preponderant role of these transporters in the process (Darszon *et al.*, 2001; Florman *et al.*, 1998; Publicover and Barratt, 1999). Like other known exocytotic processes, the AR requires soluble *N*-ethylmaleimide-sensitive attachment protein receptors (SNARE) proteins. SNAREs have been detected in sea urchin (Schulz *et al.*, 1997, 1998) and mammalian sperm (Ramalho-Santos *et al.*, 2000). Their role in the AR has been investigated in permeabilized human sperm (Diaz *et al.*, 1996; Michaut *et al.*, 2000; Yunes *et al.*, 2000), where the requirement for the SNARE-associated proteins Rab3A (Michaut *et al.*, 2000) and *N*-ethylmaleimide-sensitive factor (Yunes *et al.*, 2000) was shown. Reconstitution experiments using recombinant SNARE proteins incorporated into liposomes, suggest that a complex of membranes, SNAREs, and synaptotagmin I forms the minimal core for Ca^{2+} -triggered exocytosis (Tucker *et al.*, 2004). It is interesting that synaptotagmins I, VI, and VIII are present in the mouse sperm head, where they could be participating in the AR (Hutt *et al.*, 2002; Michaut *et al.*, 2001; Ramalho-Santos *et al.*, 2000).

1. Marine Sperm

Sperm from marine organisms with external fertilization undergo the AR on encountering the outer investment of the egg called egg jelly (EJ) (Dan, 1952). Usually the AR-inducing factor is a species-specific sulfated polysaccharide,

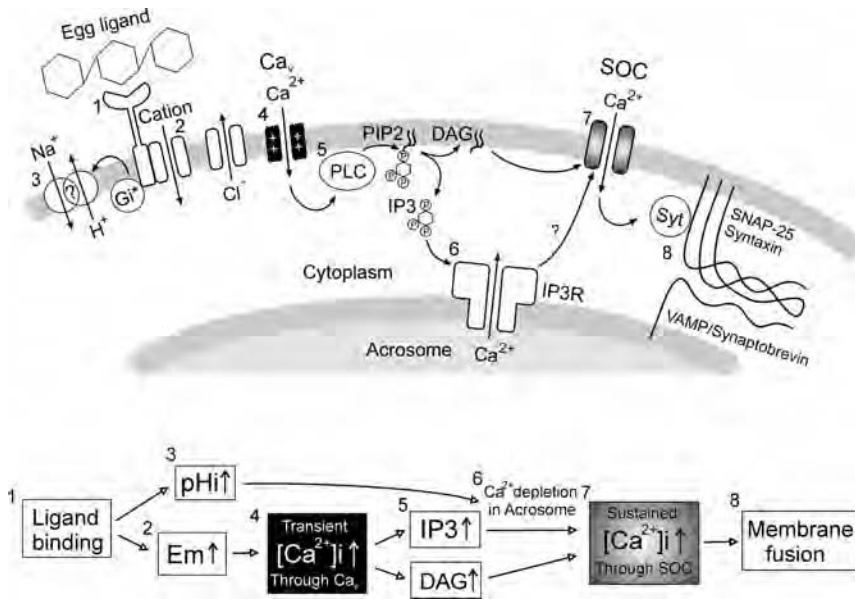


FIG. 5 A general model for the sperm AR signaling cascade. Proteins involved in the AR and their relationship are depicted: 1, receptor for AR-inducing egg ligand (such as egg jelly or ZP); 2, cation channel (PC²⁺?); 3, H⁺ efflux pathway (Na⁺/H⁺ exchanger, etc.); 4, voltage-gated Ca²⁺ channel (Ca_v); 5, phospholipase C (PLC); 6, IP₃ receptor; 7, store-operated Ca²⁺ channels (SOCs, TRP channels); 8, a putative Ca²⁺ sensor synaptotagmin (Syt) and SNAREs. There are differences in the signaling cascades between sea urchin and mammalian sperm. A pertussis toxin-sensitive G protein (G_i, marked with an asterisk) is known to be involved in the pHi increase in mammalian sperm. An E_m hyperpolarization, possibly due to Ca²⁺-induced K⁺ efflux, is essential for the pHi increase in sea urchin sperm. The molecular identity of the ion transporter(s) responsible for the pHi increase is not clear in both cases.

which is a major component of the EJ (Fig. 5). Among different sea urchins, the species specificity of the fucose sulfate polymer (FSP) is determined by the glycosidic linkage of the polymer and the sulfation pattern of the sugar residues (Alves *et al.*, 1998; Hirohashi and Vacquier, 2002c; Hirohashi *et al.*, 2002; Vacquier and Moy, 1997; Vilela-Silva *et al.*, 2002). On the other hand, in *Echinometra lucunter* (Alves *et al.*, 1997) the AR is triggered by a galactose sulfate polymer (sulfated galactan), whereas a pentasaccharide repeat containing xylose, sulfated fucose, and galactose is the AR inducer in the starfish *Asterias amurensis* (Kawamura *et al.*, 2002; Koyota *et al.*, 1997). Thus in marine animals, subtle differences in the structure of the EJ sulfated polysaccharides determine the species specificity of fertilization.

Morphologically, the AR comprises the exocytosis of the acrosomal vesicle and the pHi-dependent polymerization of actin, which leads to the extension of the acrosomal tubule (Tilney *et al.*, 1978). As indicated above, sea

urchin sperm SNAREs are most likely involved in the AR (Schulz *et al.*, 1998). The acrosomal tubule exposes a new bindin-covered membrane (Vacquier and Moy, 1977; Zigler and Lessios, 2003), which will fuse specifically through a receptor to the homologous egg (Barre *et al.*, 2003; Kamei and Glabe, 2003).

FSP binding to its *S. purpuratus* sea urchin sperm receptor, a 210-kDa membrane glycoprotein named suREJ1, triggers Ca^{2+} and Na^+ influx, and K^+ and H^+ efflux (Garbers, 1989; Garbers and Kopf, 1980; Garcia-Soto *et al.*, 1987; Schackmann, 1989; Schackmann *et al.*, 1978), leading to changes in E_m (Gonzalez-Martinez and Darzson, 1987; Gonzalez-Martinez *et al.*, 1992), and increases in $[\text{Ca}^{2+}]_i$ (Guerrero and Darzson, 1989a,b; Hirohashi and Vacquier, 2002c), pH_i (Guerrero and Darzson, 1989b; Lee *et al.*, 1983), $[\text{Na}^+]_i$ (Rodriguez and Darzson, 2003), $[\text{cAMP}]$ (Garbers, 1989; Garbers and Kopf, 1980), and IP_3 (Domino and Garbers, 1988). In addition, FSP stimulates PKA (Garbers *et al.*, 1980; Garcia-Soto *et al.*, 1991; Porter and Vacquier, 1986), phospholipase D (Domino and Garbers, 1989), and nitric oxide synthase (Kuo *et al.*, 2000) activities. Although cAMP levels increase considerably during AR, their precise role in this reaction is not known. Sperm AC activity is regulated by PKA and possibly CaM (Bookbinder *et al.*, 1991), pH_i and $[\text{Ca}^{2+}]_i$ (Cook and Babcock, 1993a), and cell hyperpolarization (Beltrán *et al.*, 1996), but not by G proteins (Garbers, 1989; Hildebrandt *et al.*, 1985).

Three of the sea urchin sperm receptors for egg jelly (suREJ) have been cloned and sequenced. suREJ1 has one transmembrane segment and binds to the fucose sulfate polymer of egg jelly to induce the sperm AR (Moy *et al.*, 1996). suREJ2 (Galindo *et al.*, 2004) has two transmembrane segments; it is present in the entire sperm plasma membrane and is concentrated over the sperm mitochondrion. This distribution led the authors to suggest that a possible function of suREJ2 could be to anchor the mitochondrion to the plasma membrane, maintaining its position as the sperm cytoplasm shrinks and the nucleus becomes triangular (Galindo *et al.*, 2004). suREJ3, with 11 putative transmembrane segments, shares several features with latrophilins, G protein-coupled receptors involved in exocytosis (Mengerink *et al.*, 2002). suREJ1 as well as suREJ3 localize to the plasma membrane over the acrosomal vesicle. Apparently suREJ2 is not exposed to the extracellular face of the plasma membrane, so it is an intracellular plasma membrane protein (Galindo *et al.*, 2004).

The three suREJ proteins possess a “REJ module” of >900 amino acids, shared by the ADPKD protein, polycystin-1 (PC1), and PCREJ, a testis-specific protein in mammals whose function is unknown. ADPKD is a common lethal genetic disorder characterized by progressive development of fluid-filled cysts in the kidney and other target organs. ADPKD is caused by mutations in the *PKD1* and *PKD2* genes, encoding the transmembrane

proteins PC1 and PC2, respectively (Arnaout, 2001; Igarashi and Somlo, 2002). PC2, a distant member of the TRP superfamily of proteins (Birnbaumer *et al.*, 2003), has amino acid sequence similarity to Ca_v and other cation channels, especially within their S3–S6 segments and the loop between S5 and S6 (Nomura *et al.*, 1998). This protein itself forms Ca^{2+} -permeable nonselective channels (Gonzalez-Perrett *et al.*, 2001; Hanaoka *et al.*, 2000; Ikeda and Guggino, 2002; Vassilev *et al.*, 2001). Considering the Ig-like fold of this sequence, it has been suggested that it could be involved in ligand binding (Bycroft *et al.*, 1999). In mammals PC1 and PC2 associate to form unique nonselective cation channels (Hanaoka *et al.*, 2000; Xu *et al.*, 2003). In humans, hPC1 modulates the activity of hPC2 (Newby *et al.*, 2002; Tsiokas *et al.*, 1997).

It is interesting that suREJ3 (Mengerink *et al.*, 2002) includes the C-terminal transmembrane region that is homologous to Ca_v channels and that has been implicated in associations with PC2 (Qian *et al.*, 1997; Xu *et al.*, 2003). Furthermore, sea urchin sperm possess a PC2 homolog (suPC2) (Fig. 2), and suREJ3 and suPC2 are physically associated in the sperm plasma membrane (Neill *et al.*, 2004). Both suREJ3 and suPC2 localize exclusively as a thin band on the plasma membrane overlying the acrosomal vesicle (Mengerink *et al.*, 2002; Neill *et al.*, 2004). The REJ proteins could be subunits of a ligand-gated channel that triggers AR in sea urchin sperm or regulators of a Ca^{2+} channel that induces this reaction (Mengerink and Vacquier, 2001, 2004; Vacquier and Moy, 1997) (Fig. 5). Notably, a high-conductance Ca^{2+} -permeable channel, whose properties resemble some of those displayed by the polycystin-L (PCL) and PC1–PC2 channels, has been recorded in BLMs containing sea urchin and mouse sperm plasma membranes (Beltrán *et al.*, 1994; Liévano *et al.*, 1990). The sea urchin sperm channel has a 170-pS main conductance state in 50 mM CaCl_2 and discriminates poorly between monovalent and divalent cations ($P_{\text{Ca}^{2+}}/P_{\text{Na}^+} = \sim 5$) (Liévano *et al.*, 1990). This evidence suggests that REJ and PC proteins may be involved in the ion fluxes that follow binding of FSP and lead to the AR. Notably, TRP channels are present in mouse sperm, where they seem to participate in the AR (Jungnickel *et al.*, 2001; Treviño *et al.*, 2001).

$[\text{Ca}^{2+}]_i$ determinations with fluorescent probes indicate the participation of two different Ca^{2+} channels in the sea urchin sperm AR (Guerrero and Darszon, 1989a,b; Schackmann, 1989). Verapamil and DHPs, both Ca_v channel blockers (Table I), inhibit the AR (Schackmann, 1989) and block a Ca^{2+} -selective channel that is transiently opened on FSP binding to REJ. Five seconds later, a second channel, insensitive to the latter blockers, activates and leads to the sperm AR. The second channel does not inactivate, is permeable to Mn^{2+} , and is pH_i dependent (Guerrero and Darszon, 1989b). It seems that the second channel allows Na^+ influx, because Ni^{2+} almost completely blocks the increase in $[\text{Na}^+]_i$ triggered by FSG. Ca^{2+} uptake

precedes the changes in pH_i and $[\text{Na}^+]_i$ (Rodriguez and Darszon, 2003). The two Ca^{2+} channels are somehow linked, because blocking the first channel inhibits the second, and inhibition of the FSP-induced pH_i increase associated with the AR prevents activation of the second channel and AR. Apparently the second channel can also be opened by a lower molecular mass (~ 60 kDa) hydrolyzed form of FSP (hFSP), which although it increases pH_i , cannot induce the AR by itself (Hirohashi and Vacquier, 2002c).

Findings in sea urchin sperm suggest that the second channel opened during the AR could be a SOC (Gonzalez-Martinez *et al.*, 2001), as proposed earlier for mammalian sperm (Jungnickel *et al.*, 2001; O'Toole *et al.*, 2000; Santi *et al.*, 1998). Hirohashi and Vacquier (2003) showed that the activity of the SOC results in the exocytosis of the acrosomal vesicle in the absence of polymerization of acrosomal actin, confirming the previous results. This may be important in the AR of many species (Darszon *et al.*, 2001; O'Toole *et al.*, 2000).

The increase in IP_3 (Domino and Garbers, 1988) that occurs in response to FSP, coupled with the fact that IP_3 receptors have been detected in sea urchin sperm (Zapata *et al.*, 1997), suggests that this signaling system may function during the AR. IP_3 -mediated release of Ca^{2+} from intracellular stores is a crucial step in store-operated Ca^{2+} entry (Putney *et al.*, 2001). Although sperm lack an endoplasmic reticulum, it has been suggested that the acrosomal vesicle may be acting as the intracellular Ca^{2+} store (Gonzalez-Martinez *et al.*, 2001). This has been shown to be true for mammalian sperm (De Blas *et al.*, 2002). In sea urchin sperm, SOC opening alone is sufficient to trigger acrosomal exocytosis, but not the polymerization of acrosomal actin (Hirohashi and Vacquier, 2003).

Other egg jelly components such as sialoglycan (SG, a polysialic acid), which causes an increase in pH_i , and speract, which contributes to the rise in pH_i in low-pH seawater (pH 7.6), can potentiate the FSP-induced AR (Hirohashi and Vacquier, 2002a). Neither nifedipine nor high $[\text{K}^+]_e$ can block the SG-induced pH_i rise, unlike the FSP-induced rise in pH_i . Therefore, the pathways by which FSP and SG induce pH_i increases are different; the receptor for SG remains unknown (Hirohashi and Vacquier, 2002b). Although the physiological relevance of such potentiation in today's seawater (pH 8.0) is not clear, it has been suggested that speract may have played a more important role in the induction of the AR in the paleo-ocean of pH 7.4 (Hirohashi and Vacquier, 2002a). Sea urchin sperm can become irreversibly refractory to FSP or EJ (Guerrero *et al.*, 1998). This process, named acrosome reaction inactivation (ARI), has also been described in starfish (Matsui *et al.*, 1986). It is triggered by EJ and requires a $[\text{Ca}^{2+}]_i$ increase. However, artificially elevating $[\text{Ca}^{2+}]_i$ does not trigger ARI, indicating that a rise in $[\text{Ca}^{2+}]_i$ alone is not sufficient to trigger ARI. The ionic requirements for ARI and the AR are different; therefore, the mechanisms involved in the two

processes differ. ARI requires egg jelly receptor activation and is probably due to uncoupling of the EJ receptor from Ca^{2+} channels, and also from the mechanism that elevates pH_i during AR. A better understanding of this interesting process will probably reveal the workings of a transduction complex, which includes the receptor, and some of the key ion transporters involved in the AR.

It is remarkable that the sea urchin sperm AR is so sensitive to external K^+ and that in *S. purpuratus* it can be inhibited by TEA, a K^+ channel blocker (Schackmann, 1989). Seawater contains 10 mM KCl; raising its concentration to 30–50 mM inhibits the AR and the increase in $[\text{Ca}^{2+}]_i$ and pH_i associated with the reaction (Darszon *et al.*, 1999). These observations suggest that K^+ channels may participate in the AR. Indeed, binding of FSP to *L. pictus* sperm induces a fast K^+ -dependent hyperpolarization that precedes and probably leads to the activation of a Ca^{2+} -dependent Na^+/H^+ exchange that in turn increases pH_i (Gonzalez-Martinez *et al.*, 1992). This hyperpolarization may also remove inactivation from Ca_v channels (Gonzalez-Martinez and Darszon, 1987; Liévano *et al.*, 1990).

Interestingly, TEA-sensitive K^+ channels have been recorded in planar bilayers with incorporated *S. purpuratus* sea urchin sperm plasma membranes (Gonzalez-Martinez *et al.*, 1992; Labarca *et al.*, 1996; Liévano *et al.*, 1985). Such reconstitution experiments have also documented the presence of Ca^{2+} and Cl^- channels in sea urchin sperm membranes. 4,4'-Diisothiocyanatostilbene-2,2'-disulfonic acid (DIDS), an inhibitor of anion channels and transporters, blocks the sea urchin sperm AR (Morales *et al.*, 1993; Ohta *et al.*, 2000). It will be interesting to examine the relationship between Cl^- transport and bicarbonate, because of the sensitivity of sAC to this latter anion (see below). The fact that some of the ion channels recorded in planar bilayers are sensitive to inhibitors of the AR (Darszon *et al.*, 1999) again emphasizes that the AR is an ion channel-regulated event.

Plasma membrane microdomains, or lipid rafts, have been isolated from sea urchin sperm (Ohta *et al.*, 2000). These lipid microdomains have been implicated in membrane trafficking and cell morphogenesis, as well as in signal transduction in mammalian cells (Edidin, 2003; Simons and Ikonen, 1997). Low-density Triton X-100-insoluble complexes isolated from *S. purpuratus* sea urchin sperm were found to contain suREJ1, the speract receptor, a 63-kDa glycosylphosphatidylinositol (GPI)-anchored protein, G_s , AC, GC, and PKA (Ohta *et al.*, 2000). Coimmunoprecipitation experiments with isolated lipid rafts indicate that the speract receptor, G_s , and the GPI-anchored protein are functionally associated in the plasma membrane. This led the authors to suggest that lipid microdomains may be involved in speract–speract receptor interactions and in the subsequent signal transduction cascades regulating sperm respiration and motility (Ohta *et al.*, 2000). Possibly suREJ1, AC, GC, and PKA may interact in different

microdomains and also cross-talk with ionic channels (Ostrom *et al.*, 2004). PKA (Burgos *et al.*, 2004) as well as ionic channels (Martens *et al.*, 2004) and receptors (Oshikawa *et al.*, 2003) have been found in lipid rafts in mammalian systems, where they form part of signaling complexes. The functional characterization of signal transduction microdomains will, no doubt, contribute to our understanding of the mechanisms that mediate the AR and, in general, to sperm physiology.

2. Mammalian Sperm

The main physiological mediator of the mammalian sperm AR is the ZP, the extracellular matrix of the egg. Up to four sulfated glycoproteins constitute the ZP (ZP1–ZP4), depending on the species (Dean, 2004; Sinowatz *et al.*, 2001; Wassarman, 2002). Murine ZP3 displays most of the sperm binding and AR-inducing activity of unfertilized eggs. This activity lies, at least in part, in its coordinated oligosaccharides (Bleil and Wassarman, 1988; Wassarman *et al.*, 2001). Genetic data in mice suggest that the three-dimensional structure of ZP is important in determining sperm binding (Hoodbhoy and Dean, 2004). The species specificity of gamete interactions, including AR induction, suggests the presence of specialized sperm receptors for ZP (Primakoff and Myles, 2002). Several candidates have been proposed as ZP3 receptors, among them β 1,4-galactosyltransferase 1 (Shi *et al.*, 2001) and SED1, a mouse homolog of p47 (Ensslin and Shur, 2003). However, their physiological relevance is still a matter of debate because knockout mice for either candidate are fertile or subfertile (Baba *et al.*, 2002; Rodeheffer and Shur, 2004b; Wassarman and Litscher, 2001). For example, GalT I null mice, unable to bind ZP3 or undergo a ZP3-induced AR, can bind to the egg coat and fertilize eggs *in vitro*, although with low efficiency (Lu and Shur, 1997). These findings indicate there are GalT–ZP3-independent interactions (Rodeheffer and Shur, 2004a). It is possible that manifold, concerted, and cooperative interactions between ZP proteins and several sperm surface receptors are required to trigger the AR (Ensslin and Shur, 2003; McLeskey *et al.*, 1998; Primakoff and Myles, 2002).

In addition to ZP3, other ligands are able to induce the AR, such as progesterone (Baldi *et al.*, 2000; Blackmore *et al.*, 1990; Meizel *et al.*, 1997; Thomas and Meizel, 1989), γ -aminobutyric acid (GABA) (Meizel, 1997; Shi *et al.*, 1997; Wistrom and Meizel, 1993), glycine (Sato *et al.*, 2000a,b), epidermal growth factor (EGF) (Lax *et al.*, 1994), ATP (Foresta *et al.*, 1996; Luria *et al.*, 2002), platelet-activating factor (PAF) (Huo and Yang, 2000; Kordan *et al.*, 2003; Sengoku *et al.*, 1996), and acetylcholine (Son and Meizel, 2003). The physiological importance of these “alternative” agonists is not well understood. As in the case of progesterone, they may facilitate capacitation (Barboni *et al.*, 1995), potentiate the ZP-induced AR (Roldan

et al., 1994), promote sperm hyperactivation (Suarez and Ho, 2003), or they may induce chemotaxis (Eisenbach, 1999). Some of these ligands may trigger transduction mechanisms that could be vestiges from previous differentiation stages.

External Ca^{2+} is essential for triggering the AR with ZP, ionophores, and most ligands (Darszon *et al.*, 1999; Yanagimachi, 1994). In addition to elevating $[\text{Ca}^{2+}]_i$ and pH_i (Florman and First, 1988; Florman *et al.*, 1989), ZP causes changes in E_m (Arnoult *et al.*, 1996b) of mature capacitated sperm, which lead to acrosomal exocytosis. Single-cell measurements with fluorescent ion indicators have revealed that ZP increases sperm $[\text{Ca}^{2+}]_i$ before exocytosis occurs (Florman, 1994; Florman *et al.*, 1989; Storey *et al.*, 1992). Pertussis toxin (PTX), a specific antagonist of the G_i class of heterotrimeric G proteins, inhibits the ZP-induced AR and its associated ion fluxes in mouse, bovine, and human sperm (Endo *et al.*, 1987, 1988; Florman *et al.*, 1989; Lee *et al.*, 1992). In agreement with these findings, several G proteins have been identified in mammalian sperm, such as G_i and G_z (Glassner *et al.*, 1991), and ZP activates G_{i1} and G_{i2} in mouse sperm (Ward *et al.*, 1994). Although, as indicated earlier (see Section III.B.1.a), Ca^{2+} channels can be regulated by G proteins (Dolphin, 2003), it is believed that the PTX-sensitive step is the ZP-induced pH_i increase necessary for the AR (Arnoult *et al.*, 1996b). However, the molecular identity of the transporter and the targets of pH_i regulation that trigger AR are unknown.

Alterations in the phosphorylation state of various mammalian sperm proteins and in phospholipid and cAMP metabolism have been shown to occur during the induction of the AR by ZP, progesterone, and other agents (Baxendale and Fraser, 2003; Breitbart, 2003; O'Toole *et al.*, 1996; Thomas and Meizel, 1989; Yuan *et al.*, 2003). PKC and PKA activation leading to protein phosphorylation during the AR has been proposed (Baldi *et al.*, 2002; Doherty *et al.*, 1995; Mendoza *et al.*, 1995). PKC α and PKC β II were immunolocalized to the equatorial segment of human sperm (Rotem *et al.*, 1992). The kinetics of the ZP-triggered AR and the cell distribution of PKC are altered by biologically active phorbol diesters and diacylglycerols (Endo *et al.*, 1991; Lax *et al.*, 1997; Lee *et al.*, 1987). Like the AR, the progesterone- and ZP-induced Ca^{2+} permeability changes are also influenced either by PKC inhibitors in human sperm (Foresta *et al.*, 1995) or by PKC and PKA inhibitors in plasma membrane vesicles, and in isolated acrosomes of bovine sperm (Breitbart and Spungin, 1997; Spungin and Breitbart, 1996).

Protein tyrosine kinases are present in mammalian sperm and their inhibitors can block the ZP-induced (Leyton *et al.*, 1992; Pukazhenthil *et al.*, 1998), progesterone-induced (Kirkman-Brown *et al.*, 2002a; Luconi *et al.*, 1995; Meizel and Turner, 1996; Tesarik *et al.*, 1993b), and thapsigargin-induced (Leclerc and Goupil, 2002) AR. Using streptolysin O (SLO)-permeabilized human sperm, a report documents Ca^{2+} -induced tyrosine phosphorylation

and proposes that both tyrosine kinases and phosphatases play a central role in the sperm AR (Tomes *et al.*, 2004). These observations altogether indicate that $[Ca^{2+}]_i$ increases can stimulate these kinases during intermediate steps of the physiologically relevant AR, which requires further study.

Several findings point out the participation of Ca_v channels in the mammalian AR (Darszon *et al.*, 1999) (Fig. 5). Many mammalian sperm species undergo a depolarization and $[Ca^{2+}]_i$ increases when $[K^+]_e$ is elevated. These changes depend on external pH and Ca^{2+} and can lead to the AR (Arnoult *et al.*, 1996b; Babcock and Pfeiffer, 1987; Brandelli *et al.*, 1996; Florman *et al.*, 1992; Linares-Hernandez *et al.*, 1998). In some species these changes are inhibited by blockers of Ca_v1 channels such as DHPs, benzothiazepine, phenylalkylamines, and Ni^{2+} (Darszon *et al.*, 1999). Mouse and bull sperm possess binding sites of moderate affinity (micromolar) for such inhibitors (e.g., PN-200-110) (Florman *et al.*, 1992). Because most of these antagonists were considered Ca_v1 (L-type) channel blockers at the time, initially it was thought that this type of channel was involved in the AR. Now it is known that at the tested concentrations these blockers can also inhibit T-type Ca_v3 channels (Arnoult *et al.*, 1996a, 1997; Liévano *et al.*, 1996; Santi *et al.*, 1996). Furthermore, as detailed above, mouse and human pachytene spermatocytes and round spermatids essentially display only T-type Ca^{2+} currents (Darszon *et al.*, 2001; Publicover and Barratt, 1999). In mouse, equivalent micromolar concentrations of DHPs, pimozide, and Ni^{2+} block the T-type channels from spermatogenic cells and inhibit both the sperm AR and its associated increase in $[Ca^{2+}]_i$ (Arnoult *et al.*, 1996a).

These findings indicate that T-type Ca^{2+} channels participate in the ZP3-induced $[Ca^{2+}]_i$ increase in mouse sperm, which results in the AR (Darszon *et al.*, 1999; Florman *et al.*, 1998). Other studies determining the pharmacological profile of depolarization-evoked $[Ca^{2+}]_i$ increases in epididymal sperm, and patch-clamp recordings in spermatogenic cells, have suggested that Ca_v2 (N-type) channels contribute to the observed activity. Immunodetection in rodent sperm membranes confirmed the presence of α_{1B} ($Ca_v2.2$) subunits (Wennemuth *et al.*, 2000), although messenger detection is as yet unavailable. It has been shown that CatSper 1 null mouse sperm are unable to undergo $[Ca^{2+}]_i$ increases induced by high $[K^+]_e$ in alkaline medium (Carlson *et al.*, 2003). This unexpected finding questions the nature of the channels assayed under these conditions, because the lack of CatSper 1 does not apparently modify the presence or location of $Ca_v1.2$, $Ca_v2.2$, and $Ca_v2.3$ channels. Although the involvement of Ca_v3 channels was not investigated, these observations led the authors to propose that the channels previously studied using alkaline K^+ -induced depolarizations might be one or more members of the CatSper family (Carlson *et al.*, 2003). However, it is still unknown whether CatSper are indeed functional voltage-dependent Ca^{2+} channels.

In mouse sperm fluorescent Ca^{2+} -sensitive dyes reveal two phases of the ZP3-induced $[\text{Ca}^{2+}]_i$ increase: (1) a fast transient $[\text{Ca}^{2+}]_i$ elevation starting a few seconds after diffusion of ZP3, which reaches its peak ($\sim 10 \mu\text{M}$) within 50 ms and relaxes to basal levels within ~ 200 ms (Arnoult *et al.*, 1999), and (2) a much slower and sustained elevation in $[\text{Ca}^{2+}]_i$ following the ZP3-induced fast transitory response, which may last for many seconds to minutes. The AR occurs only after a high, sustained $[\text{Ca}^{2+}]_i$ level is reached (Arnoult *et al.*, 1996b, O'Toole *et al.*, 2000).

a. Fast ZP-Induced Transient Increase in $[\text{Ca}^{2+}]_i$ The transient increase in mouse sperm $[\text{Ca}^{2+}]_i$ is inhibited by PN200-110, pimozide, and Ni^{2+} at concentrations that block the AR and Ca^{2+} currents in spermatogenic cells. Furthermore, the kinetics of activation and inactivation of this transient are compatible with the properties of Ca_v3 T-type channels (Arnoult *et al.*, 1999). It is worth noting that Ca^{2+} extrusion systems may also contribute to the $[\text{Ca}^{2+}]_i$ descending phase. It has been reported that the sperm plasma membrane Ca^{2+} -ATPase pump is mainly responsible for Ca^{2+} extrusion in the final stages of recovery from $[\text{Ca}^{2+}]_i$ increases caused by depolarization with high $[\text{K}^+]_e$ (Wennemuth *et al.*, 2003). This ATPase is found in the proximal principal piece of the flagellum. $\text{Na}^+/\text{Ca}^{2+}$ plasma membrane exchangers also contribute to Ca^{2+} clearance on $[\text{Ca}^{2+}]_i$ elevations. In addition, pharmacological dissection indicates that a carbonyl cyanide *m*-chlorophenylhydrazone (CCCP)-sensitive component, probably the mitochondria, participates in Ca^{2+} removal from the cytoplasm (Wennemuth *et al.*, 2003). The role of Ca^{2+} extrusion systems in sperm physiology merits further analysis.

Two important questions arise at this point: (1) What is the molecular identity of the Ca_v3 channels in spermatogenic cells? (2) Are these the exact same channels that participate in the AR? All three Ca_v3 isoforms are present in mouse spermatogenic cells and in the sperm head (Treviño *et al.*, 2004) (Fig. 1B); therefore, they might participate in the AR. However, the slow kinetics of $\text{Ca}_v3.3$ channels, the blocking profile of Ni^{2+} toward the T-type Ca^{2+} currents in spermatogenic cells, and the more prevailing presence of $\text{Ca}_v3.2$ in the sperm head suggest that $\text{Ca}_v3.2$ is the main contributor to T-type Ca^{2+} currents in spermatogenic cells and to the mouse sperm AR (Treviño *et al.*, 2004) (Table II). In agreement with this contention, $\text{Ca}_v3.1$ knockout mice are fertile and their spermatogenic cells display T-type currents that are apparently similar to those of wild-type animals (Stamboulian *et al.*, 2004). Surprisingly, $\text{Ca}_v3.2$ knockout mice are also fertile (Chen *et al.*, 2003). Do spermatogenic cells compensate for the lack of $\text{Ca}_v3.1$ or $\text{Ca}_v3.2$? The double $\text{Ca}_v3.1$ – $\text{Ca}_v3.2$ knockout mouse will, it is hoped, be helpful in settling this matter. It must be said, however, that thus far none of the single-null mutants of Ca_v channels have been found to be infertile (Chen *et al.*,

2003; Kim *et al.*, 2001; Sakata *et al.*, 2002). Is redundancy the explanation for this, or are we missing something important?

T-type Ca^{2+} currents inactivate at potentials more positive than -55 mV (Perez-Reyes, 2004) and this holds true for these channels in spermatogenic cells (Arnoult *et al.*, 1996a; Santi *et al.*, 1996). Some time ago it was proposed that a hyperpolarization detected on AR induction in *L. pictus* sperm could serve to remove inactivation from Ca^{2+} channels, allowing their opening on subsequent depolarization (Gonzalez-Martinez and Darszon, 1987; Gonzalez-Martinez *et al.*, 1992). Noncapacitated sperm have an E_m of about -55 mV (Espinosa and Darszon, 1995; Zeng *et al.*, 1995), thus (among other reasons) they require capacitation to hyperpolarize to about -65 mV and allow their T-type channels to become ready for opening during the AR (Arnoult *et al.*, 1999).

How does ZP open sperm Ca_v3 channels once they are primed? Although it occurs slowly, bovine and mouse sperm depolarize by ~ 30 mV when exposed to homologous ZP or ZP3. A nonselective, cation channel appears to mediate this depolarization (Arnoult *et al.*, 1996b). Poorly selective mammalian sperm cation channels documented in planar bilayer (Chan *et al.*, 1997; Labarca *et al.*, 1995) and patch-clamp studies (Espinosa *et al.*, 1998) are candidates to cause this depolarization. PCREJ, a mammalian homolog of suREJ, is expressed only in the testis of human and mouse, in a pattern that coincides with sperm maturation (Hughes *et al.*, 1999). The transcript shares sequence similarity with the membrane-associated region of PC1. The PCREJ protein does not contain the lectins found in REJ and thus its interaction with ZP is unclear, yet it could be part of the channel machinery that initiates the AR, possibly by depolarizing sperm.

Because the Cl^- equilibrium potential in human sperm is estimated to be within -17 to -30 mV (Garcia and Meizel, 1999), opening of anion channels would depolarize the sperm. Patch-clamp studies have detected niflumic acid-sensitive anion channels both in mouse spermatogenic cells and in sperm (Espinosa *et al.*, 1998, 1999). As stated above, GABA and glycine can induce the AR in mammalian sperm (Meizel, 1997). Ionotropic receptors to these neurotransmitters have been detected in mammalian sperm (Erdo and Wekerle, 1990; Llanos *et al.*, 2001; Sato *et al.*, 2000b). These multisubunit protein complexes contain a Cl^- channel that opens when the ligand binds (Rabow *et al.*, 1995) and their antagonists inhibit the neurotransmitter-induced AR (Meizel, 1997). Furthermore, it has been reported that glycine receptors are involved in the AR induced by recombinant human ZP3 because the reaction is inhibited by strychnine, an antagonist of this receptor (Bray *et al.*, 2002). A null mutant of the glycine receptor is subfertile and cannot undergo the ZP-induced AR (Sato *et al.*, 2000b).

b. Slow Sustained $[Ca^{2+}]_i$ Elevation Induced by ZP After the T-type Ca^{2+} channels open transiently, how do sperm manage to keep $[Ca^{2+}]_i$ elevated for minutes? Initial clues came from studies with compounds known to release Ca^{2+} from internal stores, such as thapsigargin, which inhibits SERCA pumps (Berridge *et al.*, 2003). This compound induces the AR in human, mouse, and hamster sperm, but requires external Ca^{2+} to do so (Blackmore, 1993; Llanos, 1998; Meizel and Turner, 1993; Walensky and Snyder, 1995). Thapsigargin and IP_3 prevent ATP-dependent $^{45}Ca^{2+}$ uptake into permeabilized sperm, as well as in isolated acrosomes (Spungin and Breitbart, 1996; Walensky and Snyder, 1995). Because H89, a PKA inhibitor, blocks IP_3 -induced Ca^{2+} release from isolated acrosomes, it was suggested that the IP_3R is regulated by kinases (Breitbart and Spungin, 1997). Indeed, IP_3R s are present in mature mammalian sperm in the acrosomal cap, the acrosome, the postacrosomal region, and in some species along the tail (Dragileva *et al.*, 1999; Ho and Suarez, 2003; Treviño *et al.*, 1998; Walensky and Snyder, 1995). Furthermore, mammalian sperm undergo thapsigargin-induced Ca^{2+} uptake (Blackmore, 1993).

There is also strong evidence for the role of SOCs in this sustained $[Ca^{2+}]_i$ elevation. Mouse spermatogenic cells and immotile testicular sperm possess a pH_i -sensitive Ca^{2+} channel that could correspond to an SOC (Santi *et al.*, 1998). $[Ca^{2+}]_i$ measurements in single mouse sperm revealed that thapsigargin releases Ca^{2+} from internal stores (O'Toole *et al.*, 2000) and, on doing so, it activates the uptake of external Ca^{2+} . The similarity between the kinetics and sensitivity to Ni^{2+} of this thapsigargin-mediated uptake with those displayed during the second phase of Ca^{2+} influx induced by ZP3 indicates that SOCs mediate this process (O'Toole *et al.*, 2000). It has been shown that the acrosomal vesicle is indeed a Ca^{2+} store and that the efflux of this cations is important for the AR (De Blas *et al.*, 2002). Furthermore, as mentioned in Section III.B.2, it is believed that some members of this family may be SOCs, and TRPC1, TRPC2, and TRPC6 are present in mouse and human sperm head (Jungnickel *et al.*, 2001; Treviño *et al.*, 2001). An antibody to TRPC2 was shown to inhibit the ZP3-induced mouse sperm AR (Jungnickel *et al.*, 2001), although the TRPC2 null mouse is fertile (Leypold *et al.*, 2002; Stowers *et al.*, 2002). The results, taken together, strongly suggest that some of the sperm TRPCs are responsible for the sustained Ca^{2+} increase necessary to achieve the AR. However, the molecular identity of this SOC has yet to be established.

In summary, ZP3-induced sustained $[Ca^{2+}]_i$ elevation appears to result from the release of Ca^{2+} from an IP_3 -sensitive intracellular store (Walensky and Snyder, 1995) by a signaling pathway requiring prior Ca^{2+} influx through Ca_v channels (Fig. 5). ZP3 indeed stimulates IP_3 production in sperm (Tomes *et al.*, 1996) and there is good evidence indicating that

phospholipase C δ 4 is involved (Fukami *et al.*, 2001, 2003). The PLC δ 4 isoenzyme is the most sensitive to Ca $^{2+}$, and a null mutant of this enzyme is infertile and unable to undergo the ZP3-induced AR, although all other parameters tested were normal. The PLC δ 4-mediated production of IP $_3$ would empty Ca $^{2+}$ from the acrosome and activate sustained Ca $^{2+}$ entry through SOCs, finally leading to the AR. It is worth noting that LVA Ca $^{2+}$ channel blockers (that block the initial Ca $^{2+}$ transient) added before ZP3 also inhibit the sustained [Ca $^{2+}$] $_i$ elevation, manifesting the necessary link between these two channels (Arnoult *et al.*, 1996a; O'Toole *et al.*, 2000).

Although there is substantial evidence for the role of T-type Ca $^{2+}$ channels in the mouse AR, the situation in human sperm is unclear. As discussed earlier, transcripts for Ca $_v$ 3.1, Ca $_v$ 3.2, and Ca $_v$ 3.3 are present in human spermatogenic cells and sperm, and T-type Ca $^{2+}$ currents have been detected in spermatogenic cells (Jagannathan *et al.*, 2002b; Park *et al.*, 2003; Treviño *et al.*, 2004). Yet, establishing their participation in the ZP-induced AR has been difficult in part because of ZP availability difficulties. Several groups have now reported the production of active recombinant ZP3, which should allow studies to advance faster (Bray *et al.*, 2002; Brewis *et al.*, 1998; Dong *et al.*, 2001; van Duin *et al.*, 1994). Alternatively, neoglycoproteins such as α -d-mannose-BSA have been used as analogs of ZP3 (Benoff *et al.*, 1999; Sakata *et al.*, 2002). T-type Ca $^{2+}$ channels have been reported to participate in the AR triggered by neoglycoproteins but not by progesterone (Blackmore and Eisoldt, 1999; Brandelli *et al.*, 1996). However, human sperm experiments measuring [Ca $^{2+}$] $_i$ and E_m simultaneously, and depolarizing with high [K $^+$] $_e$, did not detect T-type channels but rather [Ca $^{2+}$] $_i$ changes characteristic of R-type Ca $^{2+}$ channels. This was the case even though E_m was hyperpolarized to make sure that Ca $_v$ 3 channel inactivation was removed (Linares-Hernandez *et al.*, 1998). Clearly, further studies are needed to define the molecular identity of the Ca $_v$ channels that participate in the ZP-induced AR in human sperm.

Progesterone is produced in the cumulus (Osman *et al.*, 1989), in the vicinity of the egg, at concentrations that may trigger the AR and Ca $^{2+}$ uptake into sperm. This, and the difficulties of counting with sufficient quantities of human ZP3, have led to the extensive use of this steroid to trigger the AR (Baldi *et al.*, 2002; Kirkman-Brown *et al.*, 2002b). As mentioned before, the progesterone-induced AR is accompanied by a large [Ca $^{2+}$] $_i$ increase that depends on [Ca $^{2+}$] $_e$ (Aitken *et al.*, 1996; Baldi *et al.*, 1991; Blackmore *et al.*, 1990; Guzman-Grenfell and Gonzalez-Martinez, 2004; Thomas and Meizel, 1989) and Cl $^-$ efflux (Meizel, 1997; Meizel and Turner, 1996; Turner and Meizel, 1995). There are contradictory reports regarding the influence of tyrosine kinase inhibitors in the progesterone-induced [Ca $^{2+}$] $_i$ increase (Kirkman-Brown *et al.*, 2002a; Rathi *et al.*, 2003). Bonaccorsi and co-workers (2001) documented that these inhibitors do

not affect the rising phase but decrease the plateau. In contrast, Mendoza *et al.* (1995) found that genistein, a tyrosine kinase inhibitor, had no effect on $[Ca^{2+}]_i$ changes induced by progesterone. The progesterone-induced $[Ca^{2+}]_i$ rise and AR are insensitive to PTX, implying signaling events different from those involved in the ZP-triggered AR (Baldi *et al.*, 2002; Murase and Roldan, 1996; Tesarik *et al.*, 1993a).

VI. Single-Cell Measurements in Sperm Physiology

Our knowledge of the intracellular signaling events that occur inside the sperm during various physiological processes has come mainly from measurements taken from populations of cells. These have usually been biochemical assays on cell preparations, or fluorescence measurements made in spectrofluorimeters. These experiments have given valuable insights into the role of agonists to stimulate changes in a host of intracellular parameters and signaling molecules, including cyclic nucleotides, pH, E_m , Ca^{2+} , Na^+ , IP_3 , and so on. All these techniques are limited, however, to reporting the averaged response across all cells in the population, which to a large degree limits any interpretation to an assumption of uniform behavior within that population. Yet heterogeneity has often been reported for a number of sperm responses, from the small number of mammalian sperm that are chemotactically responsive at any one time in the female uterine tract (Cohen-Dayag *et al.*, 1994; Giojalas and Rovasio, 1998; Oliveira *et al.*, 1999), to resting $[Ca^{2+}]_i$ levels observed in individual sea urchin sperm (Wood *et al.*, 2003). Another limitation to the interpretation of population results is the assumption that measured changes are occurring throughout the cell. Sperm are highly specialized and polarized cells, and there is evidence from cell fractionation and immunolocalization studies that components of signal transduction pathways may not be evenly distributed throughout the cell (Cardullo *et al.*, 1994; Castellano *et al.*, 2003; Garcia-Soto *et al.*, 1988; Toowicharanont and Shapiro, 1988). Similarly, fluorescent dyes may not distribute evenly throughout all cell compartments, and even if they do, the difference in the cytoplasmic volume between large and small compartments may mask or swamp signals from the latter. For example, it was reported that approximately 85% of the fluorescent signal of fluo-4 loaded into sea urchin sperm originates in the head (Wood *et al.*, 2003), which hinders meaningful interpretation of Ca^{2+} measurements gained in sperm populations in terms of events that may involve the flagellum, such as chemotaxis. Another assumption implicit in the interpretation of population measurements is that the response to the agonist or stimulus occurs synchronously throughout the whole sample. Such measurements are open

to misinterpretation if, for example, an asynchronous and transient response were to become averaged into a sustained and elevated signal.

One solution to such limitations is to record intracellular changes in single cells (Fig. 6). Despite the growing popularity of this approach in other cell systems, as yet only a handful of studies have reported measurements from individual sperm. Part of the reason for this is undoubtedly their small size, which limits the amount of signal that can be collected during an experiment. Measuring such tiny signals requires the use of highly sensitive and hitherto expensive cameras and recording devices. And this sensitivity limitation has for the most part restricted measurements to being made with the most sensitive and efficient class of fluorescent sensors, the Ca^{2+} -sensing dyes, although pH_i and E_m have also been measured in single bovine, mouse, and starfish sperm (Arnoult *et al.*, 1996b, 1999; Sase *et al.*, 1995). Nevertheless,

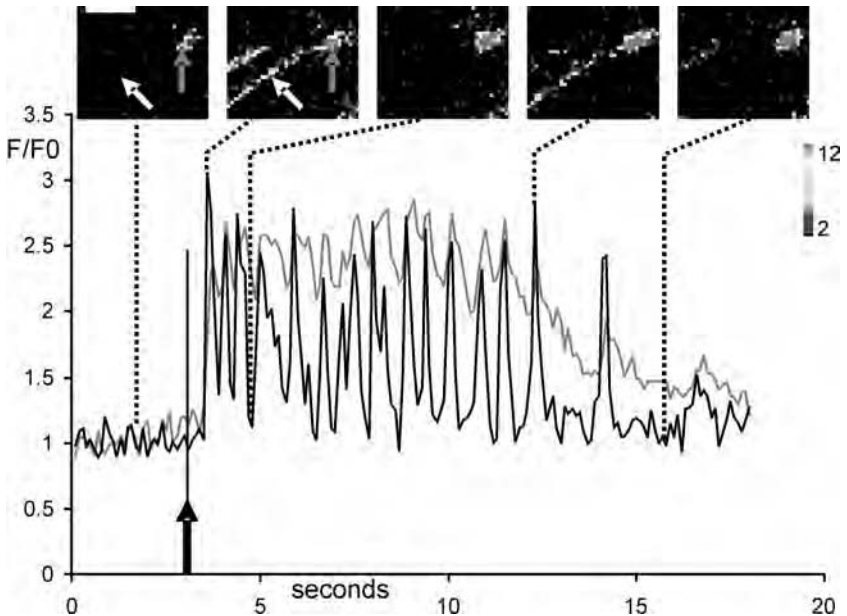


FIG. 6 Spermact-induced $[\text{Ca}^{2+}]_i$ fluctuations in single *S. purpuratus* sea urchin sperm. A sperm loaded with fluo-4 and immobilized on a poly-L-lysine-coated coverslip undergoes a biphasic increase in $[\text{Ca}^{2+}]_i$ on addition of 100 nM spermact. The increase is composed of large $[\text{Ca}^{2+}]_i$ fluctuations (up to 4 s^{-1}) superimposed over a longer tonic $[\text{Ca}^{2+}]_i$ elevation. The graph shows the ratio increase (F/F_0) of fluo-4 fluorescence in the head (red) and flagellum (black) of the single sperm shown in the fluorescence images above the graph. The black arrow on the graph marks the addition of spermact to a final concentration of 100 nM. Red and white arrows in the images mark the position of head and flagellum, respectively. Scale bar: $10 \mu\text{m}$. Images were collected every 100 ms. The color bar shows fluorescence intensity after background subtraction. (See also color insert.)

these reports demonstrate the usefulness of single-cell recordings, having revealed a number of interesting phenomena occurring at the single-cell level.

Most of the studies published with data from individual cells have been performed in mammalian sperm as investigations into $[Ca^{2+}]_i$ changes during the ZP-induced AR. The first studies in bovine sperm identified sperm that displayed two types of Ca^{2+} response: a sustained and elevated increase that spread globally throughout all regions of the sperm, and a more localized, transient increase that was confined to the head (Florman, 1994). Acrosomal exocytosis was associated almost exclusively with the former subpopulation. A later study in hamster sperm was conducted by imaging at much higher spatial and temporal resolution (Shirakawa and Miyazaki, 1999). This showed that the initial ZP-stimulated increase in $[Ca^{2+}]_i$ originated in the equatorial region of the head, spreading rapidly to the postacrosomal compartment, and finally elevating in the flagella region. The authors also noted that the initial Ca^{2+} transient was composed of more than one component, and that one of these components was sensitive to the Ca_v channel inhibitor nifedipine. Application of nifedipine truncated the initial Ca^{2+} transient, which subsequently inhibited acrosomal exocytosis. A more recent study in mouse sperm reported essentially similar results, in that ZP stimulated an initial increase in Ca^{2+} in the acrosomal region, which spread first to the equatorial segment and then on to the rest of the head (Fukami *et al.*, 2003). Progesterone, an agonist of the AR, induced a different pattern of Ca^{2+} increase, which began in the postacrosomal region and spread throughout the head. Both patterns of Ca^{2+} increase were reduced significantly in $PLC\delta 4^{-/-}$ mice, although the ZP-stimulated increase was the greater affected. Thus by careful examination of the spatiotemporal dynamics of Ca^{2+} increases, the authors concluded that two separate agonists, both capable of inducing the AR, may do so through separate (although probably overlapping) signaling pathways.

The progesterone-induced increase in $[Ca^{2+}]_i$ appears to follow a slightly different subcellular pattern in individual human sperm compared with mouse sperm, as the increases seem to initiate in the equatorial segment of the head, subsequently spreading as a wave to other head regions (Meizel *et al.*, 1997). Regarding the kinetics of these progesterone-induced Ca^{2+} changes, an early study noted that they occur as an initial, transient peak, followed by a second transient peak that terminates abruptly, probably at the moment of the AR (Tesarik *et al.*, 1996). This result differs from the patterns observed in spectrofluorimetric experiments, which show an initial Ca^{2+} transient increase, followed by a slower, more ramplike increase (Bonaccorsi *et al.*, 1995; Yang *et al.*, 1994). In a later study, a pattern of Ca^{2+} increase similar to that observed in sperm populations was recorded in single cells (Kirkman-Brown *et al.*, 2000), which the authors attributed to using modified dye-loading procedures that probably prevented the dye from

becoming compartmentalized to the acrosome. Similar to the effect on ZP-stimulated Ca^{2+} increases in hamster sperm (Shirakawa and Miyazaki, 1999), it was found that treatment of human sperm with nifedipine truncated the initial progesterone-induced Ca^{2+} transient, which subsequently inhibited both the second, sustained Ca^{2+} increase and the AR (Kirkman-Brown *et al.*, 2003). Such detailed dissections of the role of Ca^{2+} in triggering the AR would be difficult in population studies, where subtle variations in the kinetics of the Ca^{2+} changes could be obscured by slight differences in the synchronicity of the response. A development that has improved the synchronicity of certain stimulus responses has been the use of caged compounds. These are usually derivatives of signaling molecules or ligands that have all or part of their binding activity masked by the presence of an ultraviolet (UV)-labile caging group. Uncaging of these compounds is nearly instantaneous on application of a UV flash, which allows simultaneous application of a ligand, or release of a signaling intermediate, onto or inside cells. This approach has more commonly been applied to sperm populations (Kaupp *et al.*, 2003; Matsumoto *et al.*, 2003; Tatsu *et al.*, 2002), although in one report caged derivatives of cGMP and cAMP were uncaged inside bovine sperm, resulting in different patterns of $[\text{Ca}^{2+}]_i$ increase in multiple regions of the sperm depending on which cyclic nucleotide was released (Wiesner *et al.*, 1998).

Another aspect of $[\text{Ca}^{2+}]_i$ regulation that has been observed in mammalian sperm is the presence of regular slow and repetitive fluctuations in $[\text{Ca}^{2+}]_i$ that have a period of about 1–4 min. Both progesterone, and to a lesser extent ZP, were able to induce fluctuating Ca^{2+} responses of extended duration (Fukami *et al.*, 2003; Kirkman-Brown *et al.*, 2000, 2004; Meizel *et al.*, 1997). Such responses were present in a subset of the overall population, and it is not known whether they serve any physiological function. Fluctuations of a much more frequent period were measured in swimming hamster sperm, in a pioneering study by Suarez *et al.* (1993). Using the ratiometric Ca^{2+} dye indo-1, and two cameras to measure the two emission wavelengths simultaneously, changes in $[\text{Ca}^{2+}]_i$ were monitored in swimming hyperactivated sperm. Sperm in this state have the advantage of swimming in wide circles, maintaining them in a microscopic field-of-view for long periods and permitting extended recording of images. The authors found that, in approximately half the sperm tested, $[\text{Ca}^{2+}]_i$ levels fluctuate with a period equal to the flagellar beat frequency (2–4.5 Hz). The correlation was greatest for $[\text{Ca}^{2+}]_i$ changes in the proximal flagellar midpiece, although fluctuations were also measured in the acrosomal, postacrosomal, and distal flagellar midpiece regions. It was suggested that $[\text{Ca}^{2+}]_i$ fluctuations correlated with the frequency of the flagellar beat cycle are also present in nonhyperactivated sperm, although the lower level of $[\text{Ca}^{2+}]_i$ present in such sperm, together with a higher beat frequency, prevented reliable determination. These

fluctuations in the flagellar midpiece persist even after sperm have undergone the AR (with its consequent requirement for high sustained $[Ca^{2+}]_i$ in the head) (Suarez and Dai, 1995), implying that the sperm is able to simultaneously decode and respond to varying Ca^{2+} signals in different cell compartments to produce separate physiological outcomes (hyperactivated motility and the AR).

To date, only one published study presents Ca^{2+} measurements in individual sea urchin sperm. Wood *et al.* (2003) measured $[Ca^{2+}]_i$ changes in response to the SAP speract, and discovered differences in $[Ca^{2+}]_i$ increases in the head and flagellar compartments (Fig. 6). Both compartments displayed a biphasic pattern of Ca^{2+} increase, composed of a sustained, tonic increase that lasted for upward of 30 s, which had a second, shorter, phasic fluctuation superimposed on it. The tonic component made up the majority of the $[Ca^{2+}]_i$ change in the head, and the phasic fluctuations made up the majority in the tail. Detailed kinetic analysis showed that each Ca^{2+} fluctuation originated in the tail, and progressed from there through the head in a wavelike manner. This observation led the authors to propose a model whereby localized signaling events in the flagellum, initiated by speract binding to its receptor, which is localized to this region, generate pulses of a signaling molecule that diffuses outward into the head to create the measured wavelike pattern. Mathematical modeling of the $[Ca^{2+}]_i$ changes provided some support for this simple source–sink diffusion model. It was also found that the amplitude of the tonic increase showed a dose dependency on the speract concentration, as did the frequency of the phasic fluctuations, which were irregular, and varied in number from one to four per second. This graded response to speract possibly indicates a role for the tonic or phasic (or both) $[Ca^{2+}]_i$ fluctuations in a putative chemotactic response to a SAP, given the chemotactic properties of the related SAP resact, the requirement for extracellular Ca^{2+} in chemotactic responses of diverse species, and the ability of Ca^{2+} to mediate flagellar form. Further progress toward elucidating the role of these different patterns of intracellular Ca^{2+} increase requires measurement of $[Ca^{2+}]_i$ in swimming sea urchin sperm, a considerable technical challenge because of their relatively small size compared with mammalian sperm.

VII. Concluding Remarks

Ion channels are the leading instruments of the finely tuned orchestra that plays the song of fertilization. They modulate sperm maturation, motility, the acrosome reaction, and, in the end, the miracle of life. Our capacity to unravel the participation of ion channels in the sperm–egg dialogue is already

expanding because of new developments in cell imaging, electrophysiology, and genomic and proteomic informatics. The establishment of *in vitro* systems for spermatogenesis seems imminent; they will be of paramount importance to explore the use of interference strategies to understand the role of ion channels in differentiation and their molecular identity in mature sperm.

Acknowledgments

This work was supported by CONACyT (A.D., C.B., R.F., and C.W.), FIRCA (A.D.), The Wellcome Trust (A.D. and C.W.), and DGAPA/UNAM (A.D., C.T., C.B., and T.N.). We thank G. Gasque, J. J. Acevedo, I. Mendoza, L. Castellano, and I. López for comments and suggestions.

References

- Adkins, C. E., Morris, S. A., De Smedt, H., Sienaert, I., Torok, K., and Taylor, C. W. (2000). Ca^{2+} -calmodulin inhibits Ca^{2+} release mediated by type-1, -2 and -3 inositol trisphosphate receptors. *Biochem. J.* **345**, 357–363.
- Aitken, R. J., Buckingham, D. W., and Irvine, D. S. (1996). The extragenomic action of progesterone on human spermatozoa: Evidence for a ubiquitous response that is rapidly down-regulated. *Endocrinology* **137**, 3999–4009.
- Alves, A. P., Mulloy, B., Diniz, J. A., and Mourao, P. A. (1997). Sulfated polysaccharides from the egg jelly layer are species-specific inducers of acrosomal reaction in sperms of sea urchins. *J. Biol. Chem.* **272**, 6965–6971.
- Alves, A. P., Mulloy, B., Moy, G. W., Vacquier, V. D., and Mourao, P. A. (1998). Females of the sea urchin *Strongylocentrotus purpuratus* differ in the structures of their egg jelly sulfated fucans. *Glycobiology* **8**, 939–946.
- Arias, J. M., Murbartian, J., and Perez-Reyes, E. (2003). Cloning of a novel one-repeat calcium channel-like gene. *Biochem. Biophys. Res. Commun.* **303**, 31–36.
- Arikkath, J., and Campbell, K. P. (2003). Auxiliary subunits: Essential components of the voltage-gated calcium channel complex. *Curr. Opin. Neurobiol.* **13**, 298–307.
- Arnaut, M. A. (2001). Molecular genetics and pathogenesis of autosomal dominant polycystic kidney disease. *Annu. Rev. Med.* **52**, 93–123.
- Arnault, C., Cardullo, R. A., Lemos, J. R., and Florman, H. M. (1996a). Activation of mouse sperm T-type Ca^{2+} channels by adhesion to the egg zona pellucida. *Proc. Natl. Acad. Sci. USA* **93**, 13004–13009.
- Arnault, C., Zeng, Y., and Florman, H. M. (1996b). ZP3-dependent activation of sperm cation channels regulates acrosomal secretion during mammalian fertilization. *J. Cell Biol.* **134**, 637–645.
- Arnault, C., Lemos, J. R., and Florman, H. M. (1997). Voltage-dependent modulation of T-type calcium channels by protein tyrosine phosphorylation. *EMBO J.* **16**, 1593–1599.
- Arnault, C., Villaz, M., and Florman, H. M. (1998). Pharmacological properties of the T-type Ca^{2+} current of mouse spermatogenic cells. *Mol. Pharmacol.* **53**, 1104–1111.
- Arnault, C., Kazam, I. G., Visconti, P. E., Kopf, G. S., Villaz, M., and Florman, H. M. (1999). Control of the low voltage-activated calcium channel of mouse sperm by egg ZP3 and by membrane hyperpolarization during capacitation. *Proc. Natl. Acad. Sci. USA* **96**, 6757–6762.

- Atlas, D. (2001). Functional and physical coupling of voltage-sensitive calcium channels with exocytotic proteins: Ramifications for the secretion mechanism. *J. Neurochem.* **77**, 972–985.
- Austin, C. R. (1952). The capacitation of the mammalian sperm. *Nature* **170**, 326.
- Baba, D., Kashiwabara, S., Honda, A., Yamagata, K., Wu, Q., Ikawa, M., Okabe, M., and Baba, T. (2002). Mouse sperm lacking cell surface hyaluronidase PH-20 can pass through the layer of cumulus cells and fertilize the egg. *J. Biol. Chem.* **277**, 30310–30314.
- Babcock, D. F., and Pfeiffer, D. R. (1987). Independent elevation of cytosolic $[Ca^{2+}]$ and pH of mammalian sperm by voltage-dependent and pH-sensitive mechanisms. *J. Biol. Chem.* **262**, 15041–15047.
- Babcock, D. F., Rufo, G. A., Jr., and Lardy, H. A. (1983). Potassium-dependent increases in cytosolic pH stimulate metabolism and motility of mammalian sperm. *Proc. Natl. Acad. Sci. USA* **80**, 1327–1331.
- Babcock, D. F., Bosma, M. M., Battaglia, D. E., and Darszon, A. (1992). Early persistent activation of sperm K^+ channels by the egg peptide speract. *Proc. Natl. Acad. Sci. USA* **89**, 6001–6005.
- Baccetti, B., and Afzelius, B. A. (1976). The biology of the sperm cell. *Monogr. Dev. Biol.* **10**, 1–254.
- Baker, M. A., and Aitken, R. J. (2004). The importance of redox regulated pathways in sperm cell biology. *Mol. Cell. Endocrinol.* **216**, 47–54.
- Baldi, E., Casano, R., Falsetti, C., Krausz, C., Maggi, M., and Forti, G. (1991). Intracellular calcium accumulation and responsiveness to progesterone in capacitating human spermatozoa. *J. Androl.* **12**, 323–330.
- Baldi, E., Luconi, M., Muratori, M., and Forti, G. (2000). A novel functional estrogen receptor on human sperm membrane interferes with progesterone effects. *Mol. Cell. Endocrinol.* **161**, 31–35.
- Baldi, E., Luconi, M., Bonaccorsi, L., and Forti, G. (2002). Signal transduction pathways in human spermatozoa. *J. Reprod. Immunol.* **53**, 121–131.
- Balshaw, D. M., Yamaguchi, N., and Meissner, G. (2002). Modulation of intracellular calcium-release channels by calmodulin. *J. Membr. Biol.* **185**, 1–8.
- Barboni, B., Mattioli, M., and Seren, E. (1995). Influence of progesterone on boar sperm capacitation. *J. Endocrinol.* **144**, 13–18.
- Barratt, C. L., and Cooke, I. D. (1991). Sperm transport in the human female reproductive tract: A dynamic interaction. *Int. J. Androl.* **14**, 394–411.
- Barre, P., Zschornig, O., Arnold, K., and Huster, D. (2003). Structural and dynamical changes of the bindin B18 peptide upon binding to lipid membranes: A solid-state NMR study. *Biochemistry* **42**, 8377–8386.
- Barrett, P. Q., Lu, H. K., Colbran, R., Czernik, A., and Pancrazio, J. J. (2000). Stimulation of unitary T-type Ca^{2+} channel currents by calmodulin-dependent protein kinase II. *Am. J. Physiol. Cell Physiol.* **279**, C1694–C1703.
- Baxendale, R. W., and Fraser, L. R. (2003). Evidence for multiple distinctly localized adenylyl cyclase isoforms in mammalian spermatozoa. *Mol. Reprod. Dev.* **66**, 181–189.
- Bean, B. P., Nowycky, M. C., and Tsien, R. W. (1984). β -Adrenergic modulation of calcium channels in frog ventricular heart cells. *Nature* **307**, 371–375.
- Beard, N. A., Laver, D. R., and Dulhunty, A. F. (2004). Calsequestrin and the calcium release channel of skeletal and cardiac muscle. *Prog. Biophys. Mol. Biol.* **85**, 33–69.
- Beltrán, C., Darszon, A., Labarca, P., and Liévano, A. (1994). A high-conductance voltage-dependent multistate Ca^{2+} channel found in sea urchin and mouse spermatozoa. *FEBS Lett.* **338**, 23–26.
- Beltrán, C., Zapata, O., and Darszon, A. (1996). Membrane potential regulates sea urchin sperm adenylyl cyclase. *Biochemistry* **35**, 7591–7598.

- Benoff, S. (1998a). Modelling human sperm-egg interactions *in vitro*: Signal transduction pathways regulating the acrosome reaction. *Mol. Hum. Reprod.* **4**, 453–471.
- Benoff, S. (1998b). Voltage dependent calcium channels in mammalian spermatozoa. *Front. Biosci.* **3**, D1220–D1240.
- Benoff, S., Cooper, G. W., Paine, T., Hurley, I. R., Napolitano, B., Jacob, A., Scholl, G. M., and Hershlag, A. (1999). Numerical dose-compensated *in vitro* fertilization inseminations yield high fertilization and pregnancy rates. *Fertil. Steril.* **71**, 1019–1028.
- Benoff, S., Jacob, A., and Hurley, I. R. (2000). Male infertility and environmental exposure to lead and cadmium. *Hum. Reprod. Update* **6**, 107–121.
- Berridge, M. J., Bootman, M. D., and Roderick, H. L. (2003). Calcium signalling: Dynamics, homeostasis and remodelling. *Nat. Rev. Mol. Cell Biol.* **4**, 517–529.
- Biel, M., Zong, X., Distler, M., Bosse, E., Klugbauer, N., Murakami, M., Flockerzi, V., and Hofmann, F. (1994). Another member of the cyclic nucleotide-gated channel family, expressed in testis, kidney, and heart. *Proc. Natl. Acad. Sci. USA* **91**, 3505–3509.
- Biel, M., Zong, X., Ludwig, A., Sautter, A., and Hofmann, F. (1996). Molecular cloning and expression of the modulatory subunit of the cyclic nucleotide-gated cation channel. *J. Biol. Chem.* **271**, 6349–6355.
- Biel, M., Seeliger, M., Pfeifer, A., Kohler, K., Gerstner, A., Ludwig, A., Jaissle, G., Fauser, S., Zrenner, E., and Hofmann, F. (1999). Selective loss of cone function in mice lacking the cyclic nucleotide-gated channel CNG3. *Proc. Natl. Acad. Sci. USA* **96**, 7553–7557.
- Birnbaumer, L., Yidirim, E., and Abramowitz, J. (2003). A comparison of the genes coding for canonical TRP channels and their M, V and P relatives. *Cell Calcium* **33**, 419–432.
- Blackmore, P. F. (1993). Rapid non-genomic actions of progesterone stimulate Ca^{2+} influx and the acrosome reaction in human sperm. *Cell. Signal.* **5**, 531–538.
- Blackmore, P. F., and Eisoldt, S. (1999). The neoglycoprotein mannose-bovine serum albumin, but not progesterone, activates T-type calcium channels in human spermatozoa. *Mol. Hum. Reprod.* **5**, 498–506.
- Blackmore, P. F., Beebe, S. J., Danforth, D. R., and Alexander, N. (1990). Progesterone and 17α -hydroxyprogesterone: Novel stimulators of calcium influx in human sperm. *J. Biol. Chem.* **265**, 1376–1380.
- Bleil, J. D., and Wassarman, P. M. (1988). Galactose at the nonreducing terminus of O-linked oligosaccharides of mouse egg zona pellucida glycoprotein ZP3 is essential for the glycoprotein's sperm receptor activity. *Proc. Natl. Acad. Sci. USA* **85**, 6778–6782.
- Bohring, C., and Krause, W. (2003). Immune infertility: Towards a better understanding of sperm (auto)-immunity. The value of proteomic analysis. *Hum. Reprod.* **18**, 915–924.
- Boland, L. M., Morrill, J. A., and Bean, B. P. (1994). ω -Conotoxin block of N-type calcium channels in frog and rat sympathetic neurons. *J. Neurosci.* **14**, 5011–5027.
- Bonaccorsi, L., Luconi, M., Forti, G., and Baldi, E. (1995). Tyrosine kinase inhibition reduces the plateau phase of the calcium increase in response to progesterone in human sperm. *FEBS Lett.* **364**, 83–86.
- Bonaccorsi, L., Forti, G., and Baldi, E. (2001). Low-voltage-activated calcium channels are not involved in capacitation and biological response to progesterone in human sperm. *Int. J. Androl.* **24**, 341–351.
- Bonigk, W., Altenhofen, W., Muller, F., Dose, A., Illing, M., Molday, R. S., and Kaupp, U. B. (1993). Rod and cone photoreceptor cells express distinct genes for cGMP-gated channels. *Neuron* **10**, 865–877.
- Bookbinder, L. H., Moy, G. W., and Vacquier, V. D. (1991). *In vitro* phosphorylation of sea urchin sperm adenylate cyclase by cyclic adenosine monophosphate-dependent protein kinase. *Mol. Reprod. Dev.* **28**, 150–157.
- Bootman, M. D., Berridge, M. J., and Roderick, H. L. (2002). Calcium signalling: More messengers, more channels, more complexity. *Curr. Biol.* **12**, R563–R565.

- Bourinet, E., Stotz, S. C., Spaetgens, R. L., Dayanithi, G., Lemos, J., Nargeot, J., and Zamponi, G. W. (2001). Interaction of SNX482 with domains III and IV inhibits activation gating of α_{1E} ($Ca_v 2.3$) calcium channels. *Biophys. J.* **81**, 79–88.
- Brandelli, A., Miranda, P. V., and Tezon, J. G. (1996). Voltage-dependent calcium channels and G_i regulatory protein mediate the human sperm acrosomal exocytosis induced by *N*-acetylglucosaminyl/mannosyl neoglycoproteins. *J. Androl.* **17**, 522–529.
- Bray, C., Son, J. H., Kumar, P., Harris, J. D., and Meizel, S. (2002). A role for the human sperm glycine receptor/ Cl^- channel in the acrosome reaction initiated by recombinant ZP3. *Biol. Reprod.* **66**, 91–97.
- Breitbart, H. (2003). Signaling pathways in sperm capacitation and acrosome reaction. *Cell. Mol. Biol. (Noisy-le-grand)* **49**, 321–327.
- Breitbart, H., and Spungin, B. (1997). The biochemistry of the acrosome reaction. *Mol. Hum. Reprod.* **3**, 195–202.
- Brewis, I. A. (1999). Proteomics in reproductive research: The potential importance of proteomics to research in reproduction. *Hum. Reprod.* **14**, 2927–2929.
- Brewis, I. A., Clayton, R., Browes, C. E., Martin, M., Barratt, C. L., Hornby, D. P., and Moore, H. D. (1998). Tyrosine phosphorylation of a 95 kDa protein and induction of the acrosome reaction in human spermatozoa by recombinant human zona pellucida glycoprotein 3. *Mol. Hum. Reprod.* **4**, 1136–1144.
- Broetto-Biazon, A. C., Bracht, A., Ishii-Iwamoto, E. L., de Moraes Silva, V., and Kelmer-Bracht, A. M. (2004). The action of extracellular NAD^+ on Ca^{2+} efflux, hemodynamics and some metabolic parameters in the isolated perfused rat liver. *Eur. J. Pharmacol.* **484**, 291–301.
- Brokaw, C. J. (1974). Calcium and flagellar response during the chemotaxis of bracken spermatozooids. *J. Cell. Physiol.* **83**, 151–158.
- Brokaw, C. J. (1979). Calcium-induced asymmetrical beating of triton-demembrated sea urchin sperm flagella. *J. Cell Biol.* **82**, 401–411.
- Brooks, D. E. (1983). Epididymal functions and their hormonal regulation. *Aust. J. Biol. Sci.* **36**, 205–221.
- Buck, J., Sinclair, M. L., Schapal, L., Cann, M. J., and Levin, L. R. (1999). Cytosolic adenyllyl cyclase defines a unique signaling molecule in mammals. *Proc. Natl. Acad. Sci. USA* **96**, 79–84.
- Burgos, P. V., Klattenhoff, C., de la Fuente, E., Rigotti, A., and Gonzalez, A. (2004). Cholesterol depletion induces PKA-mediated basolateral-to-apical transcytosis of the scavenger receptor class B type I in MDCK cells. *Proc. Natl. Acad. Sci. USA* **101**, 3845–3850.
- Bycroft, M., Bateman, A., Clarke, J., Hamill, S. J., Sandford, R., Thomas, R. L., and Chothia, C. (1999). The structure of a PKD domain from polycystin-1: Implications for polycystic kidney disease. *EMBO J.* **18**, 297–305.
- Calamita, G., Mazzone, A., Cho, Y. S., Valenti, G., and Svelto, M. (2001). Expression and localization of the aquaporin-8 water channel in rat testis. *Biol. Reprod.* **64**, 1660–1666.
- Carafoli, E. (1987). Intracellular calcium homeostasis. *Annu. Rev. Biochem.* **56**, 395–433.
- Carafoli, E. (2002). Calcium signaling: A tale for all seasons. *Proc. Natl. Acad. Sci. USA* **99**, 1115–1122.
- Carafoli, E., Santella, L., Branca, D., and Brini, M. (2001). Generation, control, and processing of cellular calcium signals. *Crit. Rev. Biochem. Mol. Biol.* **36**, 107–260.
- Cardullo, R. A., Herrick, S. B., Peterson, M. J., and Dangott, L. J. (1994). Speract receptors are localized on sea urchin sperm flagella using a fluorescent peptide analog. *Dev. Biol.* **162**, 600–607.
- Carlson, A. E., Westenbroek, R. E., Quill, T., Ren, D., Clapham, D. E., Hille, B., Garbers, D. L., and Babcock, D. F. (2003). CatSper1 required for evoked Ca^{2+} entry and control of flagellar function in sperm. *Proc. Natl. Acad. Sci. USA* **100**, 14864–14868.

- Castellano, L. E., Treviño, C. L., Rodriguez, D., Serrano, C. J., Pacheco, J., Tsutsumi, V., Felix, R., and Darszon, A. (2003). Transient receptor potential (TRPC) channels in human sperm: Expression, cellular localization and involvement in the regulation of flagellar motility. *FEBS Lett.* **541**, 69–74.
- Catterall, W. A. (1999). Interactions of presynaptic Ca^{2+} channels and snare proteins in neurotransmitter release. *Ann. N.Y. Acad. Sci.* **868**, 144–159.
- Catterall, W. A. (2000). Structure and regulation of voltage-gated Ca^{2+} channels. *Annu. Rev. Cell. Dev. Biol.* **16**, 521–555.
- Catterall, W. A., Striessnig, J., Snutch, T. P., and Perez-Reyes, E. (2003). International Union of Pharmacology. XL. Compendium of voltage-gated ion channels: Calcium channels. *Pharmacol. Rev.* **55**, 579–581.
- Celis, J. E., Ostergaard, M., Jensen, N. A., Gromova, I., Rasmussen, H. H., and Gromov, P. (1998). Human and mouse proteomic databases: Novel resources in the protein universe. *FEBS Lett.* **430**, 64–72.
- Chan, H. C., Zhou, T. S., Fu, W. O., Wang, W. P., Shi, Y. L., and Wong, P. Y. (1997). Cation and anion channels in rat and human spermatozoa. *Biochim. Biophys. Acta* **1323**, 117–129.
- Chan, H. C., Wu, W. L., Sun, Y. P., Leung, P. S., Wong, T. P., Chung, Y. W., So, S. C., Zhou, T. S., and Yan, Y. C. (1998). Expression of sperm Ca^{2+} activated K^{+} channels in *Xenopus* oocytes and their modulation by extracellular ATP. *FEBS Lett.* **438**, 177–182.
- Chang, M. C. (1951). Fertilizing capacity of spermatozoa deposited into the fallopian tubes. *Nature* **168**, 697–698.
- Chauhan, S. C., and Naz, R. K. (2001). Effect of antibodies to sperm-specific recombinant contraceptive vaccinogen (rCV) on murine fertilization: Search for an animal model to examine its contraceptive potential. *Mol. Reprod. Dev.* **60**, 425–432.
- Chavis, P., Fagni, L., Lansman, J. B., and Bockaert, J. (1996). Functional coupling between ryanodine receptors and L-type calcium channels in neurons. *Nature* **382**, 719–722.
- Chen, C. C., Lamping, K. G., Nuno, D. W., Barresi, R., Prouty, S. J., Lavoie, J. L., Cribbs, L. L., England, S. K., Sigmund, C. D., Weiss, R. M., Williamson, R. A., Hill, J. A., and Campbell, K. P. (2003). Abnormal coronary function in mice deficient in α_{1H} T-type Ca^{2+} channels. *Science* **302**, 1416–1418.
- Chen, Y., Cann, M. J., Litvin, T. N., Iourgenko, V., Sinclair, M. L., Levin, L. R., and Buck, J. (2000). Soluble adenylyl cyclase as an evolutionarily conserved bicarbonate sensor. *Science* **289**, 625–628.
- Cho, B. S., Schuster, T. G., Zhu, X., Chang, D., Smith, G. D., and Takayama, S. (2003). Passively driven integrated microfluidic system for separation of motile sperm. *Anal. Chem.* **75**, 1671–1675.
- Chuang, R. S., Jaffe, H., Cribbs, L., Perez-Reyes, E., and Swartz, K. J. (1998). Inhibition of T-type voltage-gated calcium channels by a new scorpion toxin. *Nat. Neurosci.* **1**, 668–674.
- Clapham, D. E. (2003). TRP channels as cellular sensors. *Nature* **426**, 517–524.
- Cohen-Dayag, A., Ralt, D., Tur-Kaspa, I., Manor, M., Makler, A., Dor, J., Mashiach, S., and Eisenbach, M. (1994). Sequential acquisition of chemotactic responsiveness by human spermatozoa. *Biol. Reprod.* **50**, 786–790.
- Cohen-Dayag, A., Tur-Kaspa, I., Dor, J., Mashiach, S., and Eisenbach, M. (1995). Sperm capacitation in humans is transient and correlates with chemotactic responsiveness to follicular factors. *Proc. Natl. Acad. Sci. USA* **92**, 11039–11043.
- Cook, S. P., and Babcock, D. F. (1993a). Activation of Ca^{2+} permeability by cAMP is coordinated through the pHi increase induced by speract. *J. Biol. Chem.* **268**, 22408–22413.
- Cook, S. P., and Babcock, D. F. (1993b). Selective modulation by cGMP of the K^{+} channel activated by speract. *J. Biol. Chem.* **268**, 22402–22407.
- Cook, S. P., Brokaw, C. J., Muller, C. H., and Babcock, D. F. (1994). Sperm chemotaxis: Egg peptides control cytosolic calcium to regulate flagellar responses. *Dev. Biol.* **165**, 10–19.

- Corbett, E. F., and Michalak, M. (2000). Calcium, a signaling molecule in the endoplasmic reticulum? *Trends Biochem. Sci.* **25**, 307–311.
- Cossio, G., Sanchez, J. C., Wettstein, R., and Hochstrasser, D. F. (1997). Spermatocytes and round spermatids of rat testis: The difference between *in vivo* and *in vitro* protein patterns. *Electrophoresis* **18**, 548–552.
- Cosson, J., Huitorel, P., and Gagnon, C. (2003). How spermatozoa come to be confined to surfaces. *Cell Motil. Cytoskeleton* **54**, 56–63.
- Cosson, M. P. (1990). Sperm chemotaxis. In “Controls of Sperm Motility: Biology and Clinical Aspects” (C. Gagnon, Ed.), pp. 103–135. CRC Press, Boca Raton, FL.
- Cox, T., and Peterson, R. N. (1989). Identification of calcium conducting channels in isolated boar sperm plasma membranes. *Biochem. Biophys. Res. Commun.* **161**, 162–168.
- Cross, N. L. (2003). Decrease in order of human sperm lipids during capacitation. *Biol. Reprod.* **69**, 529–534.
- Cross, N. L. (2004). Reorganization of lipid rafts during capacitation of human sperm. *Biol. Reprod.* **71**, 1367–1371.
- Dacheux, J. L., Druart, X., Fouchecourt, S., Syntin, P., Gatti, J. L., Okamura, N., and Dacheux, F. (1998). Role of epididymal secretory proteins in sperm maturation with particular reference to the boar. *J. Reprod. Fertil. Suppl.* **53**, 99–107.
- Dan, J. C. (1952). Studies on the acrosome. I. Reaction to egg-water and other stimuli. *Biol. Bull.* **103**, 54–66.
- Dan, J. C. (1954). Studies on the acrosome. III. Effect of calcium deficiency. *Biol. Bull.* **107**, 335–349.
- Dangott, L. J., and Garbers, D. L. (1984). Identification and partial characterization of the receptor for speract. *J. Biol. Chem.* **259**, 13712–13716.
- Dangott, L. J., Jordan, J. E., Bellet, R. A., and Garbers, D. L. (1989). Cloning of the mRNA for the protein that crosslinks to the egg peptide speract. *Proc. Natl. Acad. Sci. USA* **86**, 2128–2132.
- Darszon, A., Labarca, P., Beltrán, C., Garcia-Soto, J., and Liévano, A. (1994). Sea urchin sperm: An ion channel reconstitution study case. *Methods* **6**, 37–50.
- Darszon, A., Labarca, P., Nishigaki, T., and Espinosa, F. (1999). Ion channels in sperm physiology. *Physiol. Rev.* **79**, 481–510.
- Darszon, A., Beltrán, C., Felix, R., Nishigaki, T., and Treviño, C. L. (2001). Ion transport in sperm signaling. *Dev. Biol.* **240**, 1–14.
- Dascal, N. (2001). Ion-channel regulation by G proteins. *Trends Endocrinol. Metab.* **12**, 391–398.
- DasGupta, S., Mills, C. L., and Fraser, L. R. (1993). Ca²⁺-related changes in the capacitation state of human spermatozoa assessed by a chlortetracycline fluorescence assay. *J. Reprod. Fertil.* **99**, 135–143.
- Dean, J. (2004). Reassessing the molecular biology of sperm-egg recognition with mouse genetics. *Bioessays* **26**, 29–38.
- De Blas, G., Michaut, M., Treviño, C. L., Tomes, C. N., Yunes, R., Darszon, A., and Mayorga, L. S. (2002). The intracrosomal calcium pool plays a direct role in acrosomal exocytosis. *J. Biol. Chem.* **277**, 49326–49331.
- De Lamirande, E., Leclerc, P., and Gagnon, C. (1997). Capacitation as a regulatory event that primes spermatozoa for the acrosome reaction and fertilization. *Mol. Hum. Reprod.* **3**, 175–194.
- Demarco, I. A., Espinosa, F., Edwards, J., Sosnik, J., De La Vega-Beltrán, J. L., Hockensmith, J. W., Kopf, G. S., Darszon, A., and Visconti, P. E. (2003). Involvement of a Na⁺/HCO₃⁻ cotransporter in mouse sperm capacitation. *J. Biol. Chem.* **278**, 7001–7009.
- DeMott, R. P., Lefebvre, R., and Suarez, S. S. (1995). Carbohydrates mediate the adherence of hamster sperm to oviductal epithelium. *Biol. Reprod.* **52**, 1395–1403.

- De Waard, M., Liu, H., Walker, D., Scott, V. E., Gurnett, C. A., and Campbell, K. P. (1997). Direct binding of G-protein $\beta\gamma$ complex to voltage-dependent calcium channels. *Nature* **385**, 446–450.
- Diaz, A., Dominguez, L., Fornes, M. W., Burgos, M. H., and Mayorga, L. S. (1996). Acrosome content release in streptolysin O permeabilized mouse spermatozoa. *Andrologia* **28**, 21–26.
- Doering, C. J., and Zamponi, G. W. (2003). Molecular pharmacology of high voltage-activated calcium channels. *J. Bioenerg. Biomembr.* **35**, 491–505.
- Doherty, C. M., Tarchala, S. M., Radwanska, E., and De Jonge, C. J. (1995). Characterization of two second messenger pathways and their interactions in eliciting the human sperm acrosome reaction. *J. Androl.* **16**, 36–46.
- Dolphin, A. C. (2003). β Subunits of voltage-gated calcium channels. *J. Bioenerg. Biomembr.* **35**, 599–620.
- Dolphin, A. C., Wyatt, C. N., Richards, J., Beattie, R. E., Craig, P., Lee, J. H., Cribbs, L. L., Volsen, S. G., and Perez-Reyes, E. (1999). The effect of $\alpha 2\text{-}\delta$ and other accessory subunits on expression and properties of the calcium channel $\alpha 1\text{G}$. *J. Physiol.* **519**, 35–45.
- Domino, S. E., and Garbers, D. L. (1988). The fucose–sulfate glycoconjugate that induces an acrosome reaction in spermatozoa stimulates inositol 1,4,5-trisphosphate accumulation. *J. Biol. Chem.* **263**, 690–695.
- Domino, S. E., and Garbers, D. L. (1989). Stimulation of phospholipid turnover in isolated sea urchin sperm heads by the fucose–sulfate glycoconjugate that induces an acrosome reaction. *Biol. Reprod.* **41**, 133–141.
- Dong, C. Y., French, T., So, P. T., Buehler, C., Berland, K. M., and Gratton, E. (2003). Fluorescence-lifetime imaging techniques for microscopy. *Methods Cell Biol.* **72**, 431–464.
- Dong, K. W., Chi, T. F., Juan, Y. W., Chen, C. W., Lin, Z., Xiang, X. Q., Mahony, M., Gibbons, W. E., and Oehninger, S. (2001). Characterization of the biologic activities of a recombinant human zona pellucida protein 3 expressed in human ovarian teratocarcinoma (PA-1) cells. *Am. J. Obstet. Gynecol.* **184**, 835–843; discussion, 843–844.
- Downward, J. (2004). RNA interference. *BMJ* **328**, 1245–1248.
- Dragileva, E., Rubinstein, S., and Breitbart, H. (1999). Intracellular Ca^{2+} - Mg^{2+} -ATPase regulates calcium influx and acrosomal exocytosis in bull and ram spermatozoa. *Biol. Reprod.* **61**, 1226–1234.
- Dubel, S. J., Altier, C., Chaumont, S., Lory, P., Bourinet, E., and Nargeot, J. (2004). Plasma membrane expression of T-type calcium channel α_1 subunits is modulated by HVA auxiliary subunits. *J. Biol. Chem.* **279**, 29263–29269.
- Dzeja, C., Hagen, V., Kaupp, U. B., and Frings, S. (1999). Ca^{2+} permeation in cyclic nucleotide-gated channels. *EMBO J.* **18**, 131–144.
- Edidin, M. (2003). The state of lipid rafts: From model membranes to cells. *Annu. Rev. Biophys. Biomol. Struct.* **32**, 257–283.
- Eisenbach, M. (1999). Sperm chemotaxis. *Rev. Reprod.* **4**, 56–66.
- Elkjaer, M. L., Nejsum, L. N., Gresz, V., Kwon, T. H., Jensen, U. B., Frokiaer, J., and Nielsen, S. (2001). Immunolocalization of aquaporin-8 in rat kidney, gastrointestinal tract, testis, and airways. *Am. J. Physiol. Renal Physiol.* **281**, F1047–F1057.
- Endo, Y., Lee, M. A., and Kopf, G. S. (1987). Evidence for the role of a guanine nucleotide-binding regulatory protein in the zona pellucida-induced mouse sperm acrosome reaction. *Dev. Biol.* **119**, 210–216.
- Endo, Y., Lee, M. A., and Kopf, G. S. (1988). Characterization of an islet-activating protein-sensitive site in mouse sperm that is involved in the zona pellucida-induced acrosome reaction. *Dev. Biol.* **129**, 12–24.
- Endo, Y., Komatsu, S., Hirai, M., Suzuki, S., and Shimizu, N. (1991). Protein kinase C activity and protein phosphorylation in mouse sperm. *Nippon Sanka Fujinka Gakkai Zasshi* **43**, 109–116.

- Ensslin, M. A., and Shur, B. D. (2003). Identification of mouse sperm SED1, a bimotif EGF repeat and discoidin-domain protein involved in sperm-egg binding. *Cell* **114**, 405–417.
- Enyeart, J. J., Biagi, B. A., and Mlinar, B. (1992). Preferential block of T-type calcium channels by neuroleptics in neural crest-derived rat and human C cell lines. *Mol. Pharmacol.* **42**, 364–372.
- Erdo, S. L., and Wekerle, L. (1990). GABAA type binding sites on membranes of spermatozoa. *Life Sci.* **47**, 1147–1151.
- Erickson, M. G., Liang, H., Mori, M. X., and Yue, D. T. (2003). FRET two-hybrid mapping reveals function and location of L-type Ca^{2+} channel CaM preassociation. *Neuron* **39**, 97–107.
- Espinosa, F., and Darszon, A. (1995). Mouse sperm membrane potential: Changes induced by Ca^{2+} . *FEBS Lett.* **372**, 119–125.
- Espinosa, F., de la Vega-Beltrán, J. L., Lopez-Gonzalez, I., Delgado, R., Labarca, P., and Darszon, A. (1998). Mouse sperm patch-clamp recordings reveal single Cl^- channels sensitive to niflumic acid, a blocker of the sperm acrosome reaction. *FEBS Lett.* **426**, 47–51.
- Espinosa, F., Lopez-Gonzalez, I., Serrano, C. J., Gasque, G., de la Vega-Beltrán, J. L., Treviño, C. L., and Darszon, A. (1999). Anion channel blockers differentially affect T-type Ca^{2+} currents of mouse spermatogenic cells, α_{1E} currents expressed in *Xenopus* oocytes and the sperm acrosome reaction. *Dev. Genet.* **25**, 103–114.
- Espinosa, F., Lopez-Gonzalez, I., Munoz-Garay, C., Felix, R., De la Vega-Beltrán, J. L., Kopf, G. S., Visconti, P. E., and Darszon, A. (2000). Dual regulation of the T-type Ca^{2+} current by serum albumin and β -estradiol in mammalian spermatogenic cells. *FEBS Lett.* **475**, 251–256.
- Esposito, G., Jaiswal, B. S., Xie, F., Krajnc-Franken, M. A., Robben, T. J., Strik, A. M., Kuil, C., Philipsen, R. L., van Duin, M., Conti, M., and Gossen, J. A. (2004). Mice deficient for soluble adenylyl cyclase are infertile because of a severe sperm-motility defect. *Proc. Natl. Acad. Sci. USA* **101**, 2993–2998.
- Fabro, G., Rovasio, R. A., Civalero, S., Frenkel, A., Caplan, S. R., Eisenbach, M., and Giojalas, L. C. (2002). Chemotaxis of capacitated rabbit spermatozoa to follicular fluid revealed by a novel directionality-based assay. *Biol. Reprod.* **67**, 1565–1571.
- Felix, R., Serrano, C. J., Treviño, C. L., Munoz-Garay, C., Bravo, A., Navarro, A., Pacheco, J., Tsutsumi, V., and Darszon, A. (2002). Identification of distinct K^+ channels in mouse spermatogenic cells and sperm. *Zygote* **10**, 183–188.
- Felix, R., Sandoval, A., Sanchez, D., Gomora, J. C., De la Vega-Beltrán, J. L., Treviño, C. L., and Darszon, A. (2003). ZD7288 inhibits low-threshold Ca^{2+} channel activity and regulates sperm function. *Biochem. Biophys. Res. Commun.* **311**, 187–192.
- Felix, R., Lopez-Gonzalez, I., Munoz-Garay, C., and Darszon, A. (2004). Ion channels and sperm function. “Molecular and Cellular Insights to Ion Channel Biology,” pp. 407–431. Elsevier, San Diego, CA.
- Feng, L. X., Chen, Y., Dettin, L., Pera, R. A., Herr, J. C., Goldberg, E., and Dym, M. (2002). Generation and *in vitro* differentiation of a spermatogonial cell line. *Science* **297**, 392–395.
- Ficarro, S., Chertihin, O., Westbrook, V. A., White, F., Jayes, F., Kalab, P., Marto, J. A., Shabanowitz, J., Herr, J. C., Hunt, D. F., and Visconti, P. E. (2003). Phosphoproteome analysis of capacitated human sperm: Evidence of tyrosine phosphorylation of a kinase-anchoring protein 3 and valosin-containing protein/p97 during capacitation. *J. Biol. Chem.* **278**, 11579–11589.
- Florman, H. M. (1994). Sequential focal and global elevations of sperm intracellular Ca^{2+} are initiated by the zona pellucida during acrosomal exocytosis. *Dev. Biol.* **165**, 152–164.
- Florman, H. M., and First, N. L. (1988). Regulation of acrosomal exocytosis. II. The zona pellucida-induced acrosome reaction of bovine spermatozoa is controlled by extrinsic positive regulatory elements. *Dev. Biol.* **128**, 464–473.

- Florman, H. M., Tombes, R. M., First, N. L., and Babcock, D. F. (1989). An adhesion-associated agonist from the zona pellucida activates G protein-promoted elevations of internal Ca^{2+} and pH that mediate mammalian sperm acrosomal exocytosis. *Dev. Biol.* **135**, 133–146.
- Florman, H. M., Corron, M. E., Kim, T. D., and Babcock, D. F. (1992). Activation of voltage-dependent calcium channels of mammalian sperm is required for zona pellucida-induced acrosomal exocytosis. *Dev. Biol.* **152**, 304–314.
- Florman, H. M., Arnoult, C., Kazam, I. G., Li, C., and O'Toole, C. M. (1998). A perspective on the control of mammalian fertilization by egg-activated ion channels in sperm: A tale of two channels. *Biol. Reprod.* **59**, 12–16.
- Foresta, C., Rossato, M., and Di Virgilio, F. (1995). Differential modulation by protein kinase C of progesterone-activated responses in human sperm. *Biochem. Biophys. Res. Commun.* **206**, 408–413.
- Foresta, C., Rossato, M., Chiozzi, P., and Di Virgilio, F. (1996). Mechanism of human sperm activation by extracellular ATP. *Am. J. Physiol.* **270**, C1709–C1714.
- Fraser, L. R. (1987). Minimum and maximum extracellular Ca^{2+} requirements during mouse sperm capacitation and fertilization *in vitro*. *J. Reprod. Fertil.* **81**, 77–89.
- Frazier, C. J., Serrano, J. R., George, E. G., Yu, X., Viswanathan, A., Perez-Reyes, E., and Jones, S. W. (2001). Gating kinetics of the α_{1I} T-type calcium channel. *J. Gen. Physiol.* **118**, 457–470.
- Fukami, K., Nakao, K., Inoue, T., Kataoka, Y., Kurokawa, M., Fissore, R. A., Nakamura, K., Katsuki, M., Mikoshiba, K., Yoshida, N., and Takenawa, T. (2001). Requirement of phospholipase C δ 4 for the zona pellucida-induced acrosome reaction. *Science* **292**, 920–923.
- Fukami, K., Yoshida, M., Inoue, T., Kurokawa, M., Fissore, R. A., Yoshida, N., Mikoshiba, K., and Takenawa, T. (2003). Phospholipase C δ 4 is required for Ca^{2+} mobilization essential for acrosome reaction in sperm. *J. Cell Biol.* **161**, 79–88.
- Gadella, B. M., and Harrison, R. A. (2000). The capacitating agent bicarbonate induces protein kinase A-dependent changes in phospholipid transbilayer behavior in the sperm plasma membrane. *Development* **127**, 2407–2420.
- Galantino-Homer, H. L., Visconti, P. E., and Kopf, G. S. (1997). Regulation of protein tyrosine phosphorylation during bovine sperm capacitation by a cyclic adenosine 3', 5'-monophosphate-dependent pathway. *Biol. Reprod.* **56**, 707–719.
- Galantino-Homer, H. L., Florman, H. M., Storey, B. T., Dobrinski, I., and Kopf, G. S. (2004). Bovine sperm capacitation: Assessment of phosphodiesterase activity and intracellular alkalization on capacitation-associated protein tyrosine phosphorylation. *Mol. Reprod. Dev.* **67**, 487–500.
- Galindo, B. E., Beltrán, C., Cragoe, E. J., Jr., and Darzon, A. (2000). Participation of a K^+ channel modulated directly by cGMP in the speract-induced signaling cascade of stronglycentrotus purpuratus sea urchin sperm. *Dev. Biol.* **221**, 285–294.
- Galindo, B. E., Moy, G. W., and Vacquier, V. D. (2004). A third sea urchin sperm receptor for egg jelly module protein, suREJ2, concentrates in the plasma membrane over the sperm mitochondrion. *Dev. Growth Differ.* **46**, 53–60.
- Galione, A., and Churchill, G. C. (2002). Interactions between calcium release pathways: Multiple messengers and multiple stores. *Cell Calcium* **32**, 343–354.
- Garbers, D. L. (1989). Molecular basis of fertilization. *Annu. Rev. Biochem.* **58**, 719–742.
- Garbers, D. L., and Kopf, G. S. (1980). The regulation of spermatozoa by calcium cyclic nucleotides. *Adv. Cyclic Nucleotide Res.* **13**, 251–306.
- Garbers, D. L., Tubb, D. J., and Kopf, G. S. (1980). Regulation of sea urchin sperm cyclic AMP-dependent protein kinases by an egg associated factor. *Biol. Reprod.* **22**, 526–532.

- Garcia, M. A., and Meizel, S. (1999). Progesterone-mediated calcium influx and acrosome reaction of human spermatozoa: Pharmacological investigation of T-type calcium channels. *Biol. Reprod.* **60**, 102–109.
- Garcia-Soto, J., Gonzalez-Martinez, M., de De la Torre, L., and Darszon, A. (1987). Internal pH can regulate Ca^{2+} uptake and the acrosome reaction in sea urchin sperm. *Dev. Biol.* **120**, 112–120.
- Garcia-Soto, J., Mourelle, M., Vargas, I., de De la Torre, L., Ramirez, E., Lopez-Colome, A. M., and Darszon, A. (1988). Sea urchin sperm head plasma membranes: Characteristics and egg jelly induced Ca^{2+} and Na^{+} uptake. *Biochem. Biophys. Acta* **944**, 1–12.
- Garcia-Soto, J., Araiza, L. M., Barrios, M., Darszon, A., and Luna-Arias, J. P. (1991). Endogenous activity of cyclic nucleotide-dependent protein kinase in plasma membranes isolated from *Strongylocentrotus purpuratus* sea urchin sperm. *Biochem. Biophys. Res. Commun.* **180**, 1436–1445.
- Gauss, R., Seifert, R., and Kaupp, U. B. (1998). Molecular identification of a hyperpolarization-activated channel in sea urchin sperm. *Nature* **393**, 583–587.
- Gautier-Courteille, C., Salanova, M., and Conti, M. (1998). The olfactory adenylyl cyclase III is expressed in rat germ cells during spermiogenesis. *Endocrinology* **139**, 2588–2599.
- Geldziler, B., Kadandale, P., and Singson, A. (2004). Molecular genetic approaches to studying fertilization in model systems. *Reproduction* **127**, 409–416.
- Gerke, V., and Moss, S. E. (2002). Annexins: From structure to function. *Physiol. Rev.* **82**, 331–371.
- Gerstner, A., Zong, X., Hofmann, F., and Biel, M. (2000). Molecular cloning and functional characterization of a new modulatory cyclic nucleotide-gated channel subunit from mouse retina. *J. Neurosci.* **20**, 1324–1332.
- Giojalas, L. C., and Rovasio, R. A. (1998). Mouse spermatozoa modify their motility parameters and chemotactic response to factors from the oocyte microenvironment. *Int. J. Androl.* **21**, 201–206.
- Glabe, C. G. (1985a). Interaction of the sperm adhesive protein, bindin, with phospholipid vesicles. I. Specific association of bindin with gel-phase phospholipid vesicles. *J. Cell Biol.* **100**, 794–799.
- Glabe, C. G. (1985b). Interaction of the sperm adhesive protein, bindin, with phospholipid vesicles. II. Bindin induces the fusion of mixed-phase vesicles that contain phosphatidylcholine and phosphatidylserine *in vitro*. *J. Cell Biol.* **100**, 800–806.
- Glassner, M., Jones, J., Kligman, I., Woolkalis, M. J., Gerton, G. L., and Kopf, G. S. (1991). Immunocytochemical and biochemical characterization of guanine nucleotide-binding regulatory proteins in mammalian spermatozoa. *Dev. Biol.* **146**, 438–450.
- Goll, D. E., Thompson, V. F., Li, H., Wei, W., and Cong, J. (2003). The calpain system. *Physiol. Rev.* **83**, 731–801.
- Gomora, J. C., Daud, A. N., Weiergraber, M., and Perez-Reyes, E. (2001). Block of cloned human T-type calcium channels by succinimide antiepileptic drugs. *Mol. Pharmacol.* **60**, 1121–1132.
- Gomora, J. C., Murbartian, J., Arias, J. M., Lee, J. H., and Perez-Reyes, E. (2002). Cloning and expression of the human T-type channel $\text{Ca}_v3.3$: Insights into prepulse facilitation. *Biophys. J.* **83**, 229–241.
- Gonzalez-Martinez, M., and Darszon, A. (1987). A fast transient hyperpolarization occurs during the sea urchin sperm acrosome reaction induced by egg jelly. *FEBS Lett.* **218**, 247–250.
- Gonzalez-Martinez, M. T. (2003). Induction of a sodium-dependent depolarization by external calcium removal in human sperm. *J. Biol. Chem.* **278**, 36304–36310.
- Gonzalez-Martinez, M. T., Guerrero, A., Morales, E., de De La Torre, L., and Darszon, A. (1992). A depolarization can trigger Ca^{2+} uptake and the acrosome reaction when preceded by a hyperpolarization in *L. pictus* sea urchin sperm. *Dev. Biol.* **150**, 193–202.

- Gonzalez-Martinez, M. T., Galindo, B. E., de De La Torre, L., Zapata, O., Rodriguez, E., Florman, H. M., and Darszon, A. (2001). A sustained increase in intracellular Ca^{2+} is required for the acrosome reaction in sea urchin sperm. *Dev. Biol.* **236**, 220–229.
- Gonzalez-Martinez, M. T., Bonilla-Hernandez, M. A., and Guzman-Grenfell, A. M. (2002). Stimulation of voltage-dependent calcium channels during capacitation and by progesterone in human sperm. *Arch. Biochem. Biophys.* **408**, 205–210.
- Gonzalez-Perrett, S., Kim, K., Ibarra, C., Damiano, A. E., Zotta, E., Batelli, M., Harris, P. C., Reisin, I. L., Arnaout, M. A., and Cantiello, H. F. (2001). Polycystin-2, the protein mutated in autosomal dominant polycystic kidney disease (ADPKD), is a Ca^{2+} permeable nonselective cation channel. *Proc. Natl. Acad. Sci. USA* **98**, 1182–1187.
- Goodwin, L. O., Leeds, N. B., Hurley, I., Mandel, F. S., Pergolizzi, R. G., and Benoff, S. (1997). Isolation and characterization of the primary structure of testis-specific L-type calcium channel: Implications for contraception. *Mol. Hum. Reprod.* **3**, 255–268.
- Goodwin, L. O., Leeds, N. B., Hurley, I., Cooper, G. W., Pergolizzi, R. G., and Benoff, S. (1998). Alternative splicing of exons in the alpha subunit of the rat testis L-type voltage-dependent calcium channel generates germ line-specific dihydropyridine binding sites. *Mol. Hum. Reprod.* **4**, 215–226.
- Goodwin, L. O., Karabinus, D. S., Pergolizzi, R. G., and Benoff, S. (2000). L-type voltage-dependent calcium channel α -1C subunit mRNA is present in ejaculated human spermatozoa. *Mol. Hum. Reprod.* **6**, 127–136.
- Gorelik, J., Gu, Y., Spohr, H. A., Shevchuk, A. I., Lab, M. J., Harding, S. E., Edwards, C. R., Whitaker, M., Moss, G. W., Benton, D. C., Sanchez, D., Darszon, A., Vodyanoy, I., Klenerman, D., and Korchev, Y. E. (2002). Ion channels in small cells and subcellular structures can be studied with a smart patch-clamp system. *Biophys. J.* **83**, 3296–3303.
- Gu, Y., Gorelik, J., Spohr, H. A., Shevchuk, A., Lab, M. J., Harding, S. E., Vodyanoy, I., Klenerman, D., and Korchev, Y. E. (2002). High-resolution scanning patch-clamp: New insights into cell function. *FASEB J.* **16**, 748–750.
- Guerrero, A., and Darszon, A. (1989a). Egg jelly triggers a calcium influx which inactivates and is inhibited by calmodulin antagonists in the sea urchin sperm. *Biochem. Biophys. Acta* **980**, 109–116.
- Guerrero, A., and Darszon, A. (1989b). Evidence for the activation of two different Ca^{2+} channels during the egg jelly-induced acrosome reaction of sea urchin sperm. *J. Biol. Chem.* **264**, 19593–19599.
- Guerrero, A., Sanchez, J. A., and Darszon, A. (1987). Single-channel activity in sea urchin sperm revealed by the patch-clamp technique. *FEBS Lett.* **220**, 295–298.
- Guerrero, A., Garcia, L., Zapata, O., Rodriguez, E., and Darszon, A. (1998). Acrosome reaction inactivation in sea urchin sperm. *Biochem. Biophys. Acta* **1401**, 329–338.
- Guillaume, E., Evrard, B., Com, E., Moertz, E., Jegou, B., and Pineau, C. (2001). Proteome analysis of rat spermatogonia: Reinvestigation of stathmin spatio-temporal expression within the testis. *Mol. Reprod. Dev.* **60**, 439–445.
- Guzman-Grenfell, A. M., and Gonzalez-Martinez, M. T. (2004). Lack of voltage-dependent calcium channel opening during the calcium influx induced by progesterone in human sperm: Effect of calcium channel deactivation and inactivation. *J. Androl.* **25**, 117–122.
- Hagiwara, S., and Kawa, K. (1984). Calcium and potassium currents in spermatogenic cells dissociated from rat seminiferous tubules. *J. Physiol.* **356**, 135–149.
- Hagiwara, S., Ozawa, S., and Sand, O. (1975). Voltage clamp analysis of two inward current mechanisms in the egg cell membrane of a starfish. *J. Gen. Physiol.* **65**, 617–644.
- Hamid, J., Nelson, D., Spaetgens, R., Dubel, S. J., Snutch, T. P., and Zamponi, G. W. (1999). Identification of an integration center for cross-talk between protein kinase C and G protein modulation of N-type calcium channels. *J. Biol. Chem.* **274**, 6195–6202.

- Hanaoka, K., Qian, F., Boletta, A., Bhunia, A. K., Piontek, K., Tsiokas, L., Sukhatme, V. P., Guggino, W. B., and Germino, G. G. (2000). Co-assembly of polycystin-1 and -2 produces unique cation-permeable currents. *Nature* **408**, 990–994.
- Hansbrough, J. R., and Garbers, D. L. (1981). Spermact: Purification and characterization of a peptide associated with eggs that activates spermatozoa. *J. Biol. Chem.* **256**, 1447–1452.
- Harrison, R. A., and Miller, N. G. (2000). cAMP-dependent protein kinase control of plasma membrane lipid architecture in boar sperm. *Mol. Reprod. Dev.* **55**, 220–228.
- Harrison, R. A., Ashworth, P. J., and Miller, N. G. (1996). Bicarbonate/CO₂, an effector of capacitation, induces a rapid and reversible change in the lipid architecture of boar sperm plasma membranes. *Mol. Reprod. Dev.* **45**, 378–391.
- Harumi, T., Hoshino, K., and Suzuki, N. (1992). Effects of sperm-activating peptide I on *Hemicentrotus pulcherrimus* spermatozoa in high potassium sea water. *Dev. Growth Differ.* **34**, 163–172.
- Hecht, N. B. (1998). Molecular mechanisms of male germ cell differentiation. *Bioessays* **20**, 555–561.
- Hell, J. W., Yokoyama, C. T., Wong, S. T., Warner, C., Snutch, T. P., and Catterall, W. A. (1993). Differential phosphorylation of two size forms of the neuronal class C L-type calcium channel α 1 subunit. *J. Biol. Chem.* **268**, 19451–19457.
- Hell, J. W., Yokoyama, C. T., Breeze, L. J., Chavkin, C., and Catterall, W. A. (1995). Phosphorylation of presynaptic and postsynaptic calcium channels by cAMP-dependent protein kinase in hippocampal neurons. *EMBO J.* **14**, 3036–3044.
- Herlitz, S., Garcia, D. E., Mackie, K., Hille, B., Scheuer, T., and Catterall, W. A. (1996). Modulation of Ca²⁺ channels by G-protein $\beta\gamma$ subunits. *Nature* **380**, 258–262.
- Herlitz, S., Zhong, H., Scheuer, T., and Catterall, W. A. (2001). Allosteric modulation of Ca²⁺ channels by G proteins, voltage-dependent facilitation, protein kinase C, and Ca_v β subunits. *Proc. Natl. Acad. Sci. USA* **98**, 4699–4704.
- Hildebrandt, J. D., Codina, J., Tash, J. S., Kirchick, H. J., Lipschultz, L., Sekura, R. D., and Bimbaumer, L. (1985). The membrane-bound spermatozoal adenylyl cyclase system does not share coupling characteristics with somatic cell adenylyl cyclases. *Endocrinology* **116**, 1357–1366.
- Hilgemann, D. W., Feng, S., and Nasuhoglu, C. (2001). The complex and intriguing lives of PIP₂ with ion channels and transporters. *Sci. STKE* **2001**, RE19.
- Hille, B. (2001). “Ion Channels of Excitable Membranes.” Sinauer Associates, Sunderland, MA.
- Hirohashi, N., and Vacquier, V. D. (2002a). Egg fucose sulfate polymer, sialoglycan, and spermact all trigger the sea urchin sperm acrosome reaction. *Biochem. Biophys. Res. Commun.* **296**, 833–839.
- Hirohashi, N., and Vacquier, V. D. (2002b). Egg sialoglycans increase intracellular pH and potentiate the acrosome reaction of sea urchin sperm. *J. Biol. Chem.* **277**, 8041–8047.
- Hirohashi, N., and Vacquier, V. D. (2002c). High molecular mass egg fucose sulfate polymer is required for opening both Ca²⁺ channels involved in triggering the sea urchin sperm acrosome reaction. *J. Biol. Chem.* **277**, 1182–1189.
- Hirohashi, N., and Vacquier, V. D. (2003). Store-operated calcium channels trigger exocytosis of the sea urchin sperm acrosomal vesicle. *Biochem. Biophys. Res. Commun.* **304**, 285–292.
- Hirohashi, N., Vilela-Silva, A. C., Mourao, P. A., and Vacquier, V. D. (2002). Structural requirements for species-specific induction of the sperm acrosome reaction by sea urchin egg sulfated fucan. *Biochem. Biophys. Res. Commun.* **298**, 403–407.
- Ho, H. C., and Suarez, S. S. (2001a). Hyperactivation of mammalian spermatozoa: Function and regulation. *Reproduction* **122**, 519–526.

- Ho, H. C., and Suarez, S. S. (2001b). An inositol 1,4,5-triphosphate receptor-gated intracellular Ca^{2+} store is involved in regulating sperm hyperactivated motility. *Biol. Reprod.* **65**, 1606–1615.
- Ho, H. C., and Suarez, S. S. (2003). Characterization of the intracellular calcium store at the base of the sperm flagellum that regulates hyperactivated motility. *Biol. Reprod.* **68**, 1590–1596.
- Ho, H. C., Granish, K. A., and Suarez, S. S. (2002). Hyperactivated motility of bull sperm is triggered at the axoneme by Ca^{2+} and not cAMP. *Dev. Biol.* **250**, 208–217.
- Hong, Y., Liu, T., Zhao, H., Xu, H., Wang, W., Liu, R., Chen, T., Deng, J., and Gui, J. (2004). Establishment of a normal medakafish spermatogonial cell line capable of sperm production *in vitro*. *Proc. Natl. Acad. Sci. USA* **101**, 8011–8016.
- Hoodbhoy, T., and Dean, J. (2004). Insights into the molecular basis of sperm–egg recognition in mammals. *Reproduction* **127**, 417–422.
- Hughes, J., Ward, C. J., Aspinwall, R., Butler, R., and Harris, P. C. (1999). Identification of a human homologue of the sea urchin receptor for egg jelly: A polycystic kidney disease-like protein. *Hum. Mol. Genet.* **8**, 543–549.
- Hunter, R. H. (1993). Sperm:egg ratios and putative molecular signals to modulate gamete interactions in polytocous mammals. *Mol. Reprod. Dev.* **35**, 324–327.
- Huo, L. J., and Yang, Z. M. (2000). Effects of platelet activating factor on capacitation and acrosome reaction in mouse spermatozoa. *Mol. Reprod. Dev.* **56**, 436–440.
- Hutt, D. M., Cardullo, R. A., Baltz, J. M., and Ngsee, J. K. (2002). Synaptotagmin VIII is localized to the mouse sperm head and may function in acrosomal exocytosis. *Biol. Reprod.* **66**, 50–56.
- Igarashi, P., and Somlo, S. (2002). Genetics and pathogenesis of polycystic kidney disease. *J. Am. Soc. Nephrol.* **13**, 2384–2398.
- Ignatz, G. G., Lo, M. C., Perez, C. L., Gwathmey, T. M., and Suarez, S. S. (2001). Characterization of a fucose-binding protein from bull sperm and seminal plasma that may be responsible for formation of the oviductal sperm reservoir. *Biol. Reprod.* **64**, 1806–1811.
- Ikeda, M., and Guggino, W. B. (2002). Do polycystins function as cation channels? *Curr. Opin. Nephrol. Hypertens.* **11**, 539–545.
- Ikeda, S. R. (1996). Voltage-dependent modulation of N-type calcium channels by G-protein $\beta\gamma$ subunits. *Nature* **380**, 255–258.
- Inaba, K. (2003). Molecular architecture of the sperm flagella: molecules for motility and signaling. *Zool. Sci.* **20**, 1043–1056.
- Inaba, K., Padma, P., Satouh, Y., Shin, I. T., Kohara, Y., Satoh, N., and Satou, Y. (2002). EST analysis of gene expression in testis of the ascidian *Ciona intestinalis*. *Mol. Reprod. Dev.* **62**, 431–445.
- Inouye, M. (1988). Antisense RNA: Its functions and applications in gene regulation—a review. *Gene* **72**, 25–34.
- Ishibashi, K., Kuwahara, M., Gu, Y., Kageyama, Y., Tohsaka, A., Suzuki, F., Marumo, F., and Sasaki, S. (1997). Cloning and functional expression of a new water channel abundantly expressed in the testis permeable to water, glycerol, and urea. *J. Biol. Chem.* **272**, 20782–20786.
- Ishikawa, M., Tsutsui, H., Cosson, J., Oka, Y., and Morisawa, M. (2004). Strategies for sperm chemotaxis in the siphonophores and ascidians: A numerical simulation study. *Biol. Bull.* **206**, 95–102.
- Izadyar, F., Den Ouden, K., Stout, T. A., Stout, J., Coret, J., Lankveld, D. P., Spoormakers, T. J., Colenbrander, B., Oldenbroek, J. K., Van der Ploeg, K. D., Woelders, H., Kal, H. B., and De Rooij, D. G. (2003). Autologous and homologous transplantation of bovine spermatogonial stem cells. *Reproduction* **126**, 765–774.

- Jacob, A., Hurley, I. R., Goodwin, L. O., Cooper, G. W., and Benoff, S. (2000). Molecular characterization of a voltage-gated potassium channel expressed in rat testis. *Mol. Hum. Reprod.* **6**, 303–313.
- Jagannathan, S., Publicover, S. J., and Barratt, C. L. (2002a). Voltage-operated calcium channels in male germ cells. *Reproduction* **123**, 203–215.
- Jagannathan, S., Punt, E. L., Gu, Y., Arnoult, C., Sakkas, D., Barratt, C. L., and Publicover, S. J. (2002b). Identification and localization of T-type voltage-operated calcium channel subunits in human male germ cells: Expression of multiple isoforms. *J. Biol. Chem.* **277**, 8449–8456.
- Jaiswal, B. S., and Conti, M. (2003). Calcium regulation of the soluble adenylyl cyclase expressed in mammalian spermatozoa. *Proc. Natl. Acad. Sci. USA* **100**, 10676–10681.
- Jaiswal, B. S., Tur-Kaspa, I., Dor, J., Mashiach, S., and Eisenbach, M. (1999). Human sperm chemotaxis: Is progesterone a chemoattractant? *Biol. Reprod.* **60**, 1314–1319.
- Jungnickel, M. K., Marrero, H., Birnbaumer, L., Lemos, J. R., and Florman, H. M. (2001). Trp2 regulates entry of Ca^{2+} into mouse sperm triggered by egg ZP3. *Nat. Cell Biol.* **3**, 499–502.
- Kageyama, Y., Ishibashi, K., Hayashi, T., Xia, G., Sasaki, S., and Kihara, K. (2001). Expression of aquaporins 7 and 8 in the developing rat testis. *Andrologia* **33**, 165–169.
- Kamei, N., and Glabe, C. G. (2003). The species-specific egg receptor for sea urchin sperm adhesion is EBR1, a novel ADAMTS protein. *Genes Dev.* **17**, 2502–2507.
- Katz, D. F., and Yanagimachi, R. (1980). Movement characteristics of hamster spermatozoa within the oviduct. *Biol. Reprod.* **22**, 759–764.
- Kaupp, U. B., and Seifert, R. (2001). Molecular diversity of pacemaker ion channels. *Annu. Rev. Physiol.* **63**, 235–257.
- Kaupp, U. B., and Seifert, R. (2002). Cyclic nucleotide-gated ion channels. *Physiol. Rev.* **82**, 769–824.
- Kaupp, U. B., Nüdome, T., Tanabe, T., Terada, S., Bonigk, W., Stuhmer, W., Cook, N. J., Kangawa, K., Matsuo, H., Hirose, T., Miyata, T., and Numa, S. (1989). Primary structure and functional expression from complementary DNA of the rod photoreceptor cyclic GMP-gated channel. *Nature* **342**, 762–766.
- Kaupp, U. B., Solzin, J., Hildebrand, E., Brown, J. E., Helbig, A., Hagen, V., Beyermann, M., Pampaloni, F., and Weyand, I. (2003). The signal flow and motor response controlling chemotaxis of sea urchin sperm. *Nat. Cell Biol.* **5**, 109–117.
- Kawamura, M., Matsumoto, M., and Hoshi, M. (2002). Characterization of the sperm receptor for acrosome reaction-inducing substance of the starfish, *Asterias amurensis*. *Zool. Sci.* **19**, 435–442.
- Kierszenbaum, A. L. (1994). Mammalian spermatogenesis *in vivo* and *in vitro*: A partnership of spermatogenic and somatic cell lineages. *Endocr. Rev.* **15**, 116–134.
- Kim, D., Song, I., Keum, S., Lee, T., Jeong, M. J., Kim, S. S., McEnery, M. W., and Shin, H. S. (2001). Lack of the burst firing of thalamocortical relay neurons and resistance to absence seizures in mice lacking α_{1G} T-type Ca^{2+} channels. *Neuron* **31**, 35–45.
- Kirkman-Brown, J. C., Bray, C., Stewart, P. M., Barratt, C. L., and Publicover, S. J. (2000). Biphasic elevation of $[\text{Ca}^{2+}]_i$ in individual human spermatozoa exposed to progesterone. *Dev. Biol.* **222**, 326–335.
- Kirkman-Brown, J. C., Lefievre, L., Bray, C., Stewart, P. M., Barratt, C. L., and Publicover, S. J. (2002a). Inhibitors of receptor tyrosine kinases do not suppress progesterone-induced $[\text{Ca}^{2+}]_i$ signalling in human spermatozoa. *Mol. Hum. Reprod.* **8**, 326–332.
- Kirkman-Brown, J. C., Punt, E. L., Barratt, C. L., and Publicover, S. J. (2002b). Zona pellucida and progesterone-induced Ca^{2+} signaling and acrosome reaction in human spermatozoa. *J. Androl.* **23**, 306–315.

- Kirkman-Brown, J. C., Barratt, C. L., and Publicover, S. J. (2003). Nifedipine reveals the existence of two discrete components of the progesterone-induced $[Ca^{2+}]_i$ transient in human spermatozoa. *Dev. Biol.* **259**, 71–82.
- Kirkman-Brown, J. C., Barratt, C. L., and Publicover, S. J. (2004). Slow calcium oscillations in human spermatozoa. *Biochem. J.* **378**, 827–832.
- Kiselyov, K., Xu, X., Mozhayeva, G., Kuo, T., Pessah, I., Mignery, G., Zhu, X., Birnbaumer, L., and Muallem, S. (1998). Functional interaction between $InsP_3$ receptors and store-operated Htrp3 channels. *Nature* **396**, 478–482.
- Kiselyov, K., Mignery, G. A., Zhu, M. X., and Muallem, S. (1999). The N-terminal domain of the IP_3 receptor gates store-operated hTrp3 channels. *Mol. Cell* **4**, 423–429.
- Klockner, U., Lee, J. H., Cribbs, L. L., Daud, A., Hescheler, J., Pereverzev, A., Perez-Reyes, E., and Schneider, T. (1999). Comparison of the Ca^{2+} currents induced by expression of three cloned α_1 subunits, α_{1G} , α_{1H} , and α_{1I} , of low-voltage-activated T-type Ca^{2+} channels. *Eur. J. Neurosci.* **11**, 4171–4178.
- Kobori, H., Miyazaki, S., and Kuwabara, Y. (2000). Characterization of intracellular Ca^{2+} increase in response to progesterone and cyclic nucleotides in mouse spermatozoa. *Biol. Reprod.* **63**, 113–120.
- Korchev, Y. E., Bashford, C. L., Milovanovic, M., Vodyanoy, I., and Lab, M. J. (1997). Scanning ion conductance microscopy of living cells. *Biophys. J.* **73**, 653–658.
- Korchev, Y. E., Negulyaev, Y. A., Edwards, C. R., Vodyanoy, I., and Lab, M. J. (2000). Functional localization of single active ion channels on the surface of a living cell. *Nat. Cell Biol.* **2**, 616–619.
- Kordan, W., Strzerek, J., and Fraser, L. (2003). Functions of platelet activating factor (PAF) in mammalian reproductive processes: A review. *Pol. J. Vet. Sci.* **6**, 55–60.
- Kotlikoff, M. I. (2003). Calcium-induced calcium release in smooth muscle: The case for loose coupling. *Prog. Biophys. Mol. Biol.* **83**, 171–191.
- Koyota, S., Wimalasiri, K. M., and Hoshi, M. (1997). Structure of the main saccharide chain in the acrosome reaction-inducing substance of the starfish, *Asterias amurensis*. *J. Biol. Chem.* **272**, 10372–10376.
- Kozlov, A. S., McKenna, F., Lee, J. H., Cribbs, L. L., Perez-Reyes, E., Feltz, A., and Lambert, R. C. (1999). Distinct kinetics of cloned T-type Ca^{2+} channels lead to differential Ca^{2+} entry and frequency-dependence during mock action potentials. *Eur. J. Neurosci.* **11**, 4149–4158.
- Krasznai, Z., Marian, T., Izumi, H., Damjanovich, S., Balkay, L., Tron, L., and Morisawa, M. (2000). Membrane hyperpolarization removes inactivation of Ca^{2+} channels, leading to Ca^{2+} influx and subsequent initiation of sperm motility in the common carp. *Proc. Natl. Acad. Sci. USA* **97**, 2052–2057.
- Kuo, R. C., Baxter, G. T., Thompson, S. H., Stricker, S. A., Patton, C., Bonaventura, J., and Epel, D. (2000). NO is necessary and sufficient for egg activation at fertilization. *Nature* **406**, 633–663.
- Kuroda, Y., Kaneko, S., Yoshimura, Y., Nozawa, S., and Mikoshiba, K. (1999). Influence of progesterone and GABAA receptor on calcium mobilization during human sperm acrosome reaction. *Arch. Androl.* **42**, 185–191.
- Labarca, P., Zapata, O., Beltrán, C., and Darszon, A. (1995). Ion channels from the mouse sperm plasma membrane in planar lipid bilayers. *Zygote* **3**, 199–206.
- Labarca, P., Santi, C., Zapata, O., Morales, E., Beltrán, C., Liévano, A., and Darszon, A. (1996). A cAMP regulated K^+ -selective channel from the sea urchin sperm plasma membrane. *Dev. Biol.* **174**, 271–280.
- Lacerda, A. E., Rampe, D., and Brown, A. M. (1988). Effects of protein kinase C activators on cardiac Ca^{2+} channels. *Nature* **335**, 249–251.
- Lacinova, L., Klugbauer, N., and Hofmann, F. (1999). Absence of modulation of the expressed calcium channel α_{1G} subunit by $\alpha_{2\delta}$ subunits. *J. Physiol.* **516**, 639–645.

- Lacinova, L., Klugbauer, N., and Hofmann, F. (2000). Regulation of the calcium channel α_{1G} subunit by divalent cations and organic blockers. *Neuropharmacology* **39**, 1254–1266.
- Lambert, R. C., Maulet, Y., Mouton, J., Beattie, R., Volsen, S., De Waard, M., and Feltz, A. (1997). T-type Ca^{2+} current properties are not modified by Ca^{2+} channel β subunit depletion in nodosus ganglion neurons. *J. Neurosci.* **17**, 6621–6628.
- Lax, Y., Rubinstein, S., and Breitbart, H. (1994). Epidermal growth factor induces acrosomal exocytosis in bovine sperm. *FEBS Lett.* **339**, 234–238.
- Lax, Y., Rubinstein, S., and Breitbart, H. (1997). Subcellular distribution of protein kinase C α and βI in bovine spermatozoa, and their regulation by calcium and phorbol esters. *Biol. Reprod.* **56**, 454–459.
- Leclerc, P., and Goupil, S. (2002). Regulation of the human sperm tyrosine kinase c-yes: Activation by cyclic adenosine 3',5'-monophosphate and inhibition by Ca^{2+} . *Biol. Reprod.* **67**, 301–307.
- Leclerc, P., De Lamirande, E., and Gagnon, C. (1996). Cyclic adenosine 3',5'-monophosphate-dependent regulation of protein tyrosine phosphorylation in relation to human sperm capacitation and motility. *Biol. Reprod.* **55**, 684–692.
- Lee, A., Wong, S. T., Gallagher, D., Li, B., Storm, D. R., Scheuer, T., and Catterall, W. A. (1999a). Ca^{2+} calmodulin binds to and modulates P/Q-type calcium channels. *Nature* **399**, 155–159.
- Lee, J. H., Daud, A. N., Cribbs, L. L., Lacerda, A. E., Pereverzev, A., Klockner, U., Schneider, T., and Perez-Reyes, E. (1999b). Cloning and expression of a novel member of the low voltage-activated T-type calcium channel family. *J. Neurosci.* **19**, 1912–1921.
- Lee, J. H., Gomora, J. C., Cribbs, L. L., and Perez-Reyes, E. (1999c). Nickel block of three cloned T-type calcium channels: Low concentrations selectively block α_{1H} . *Biophys. J.* **77**, 3034–3042.
- Lee, A., Zhou, H., Scheuer, T., and Catterall, W. A. (2003). Molecular determinants of Ca^{2+} /calmodulin-dependent regulation of $\text{Ca}_v2.1$ channels. *Proc. Natl. Acad. Sci. USA* **100**, 16059–16064.
- Lee, E. H., Lopez, J. R., Li, J., Protasi, F., Pessah, I. N., Kim do, H., and Allen, P. D. (2004). Conformational coupling of DHPR and RyR1 in skeletal myotubes is influenced by long-range allostereism: Evidence for a negative regulatory module. *Am. J. Physiol. Cell Physiol.* **286**, C179–C189.
- Lee, H. C. (1984). A membrane potential-sensitive $\text{Na}^+\text{-H}^+$ exchange system in flagella isolated from sea urchin spermatozoa. *J. Biol. Chem.* **259**, 15315–15319.
- Lee, H. C., and Garbers, D. L. (1986). Modulation of the voltage-sensitive $\text{Na}^+\text{/H}^+$ exchange in sea urchin spermatozoa through membrane potential changes induced by the egg peptide speract. *J. Biol. Chem.* **261**, 16026–16032.
- Lee, H. C., Johnson, C., and Epel, D. (1983). Changes in internal pH associated with initiation of motility and acrosome reaction of sea urchin sperm. *Dev. Biol.* **95**, 31–45.
- Lee, M. A., Kopf, G. S., and Storey, B. T. (1987). Effects of phorbol esters and a diacylglycerol on the mouse sperm acrosome reaction induced by the zona pellucida. *Biol. Reprod.* **36**, 617–627.
- Lee, M. A., Check, J. H., and Kopf, G. S. (1992). A guanine nucleotide-binding regulatory protein in human sperm mediates acrosomal exocytosis induced by the human zona pellucida. *Mol. Reprod. Dev.* **31**, 78–86.
- Lefebvre, R., and Suarez, S. S. (1996). Effect of capacitation on bull sperm binding to homologous oviductal epithelium. *Biol. Reprod.* **54**, 575–582.
- Lefievre, L., Barratt, C. L., Harper, C. V., Conner, S. J., Flesch, F. M., Deeks, E., Moseley, F. L., Pixton, K. L., Brewis, I. A., and Publicover, S. J. (2003). Physiological and proteomic approaches to studying prefertilization events in the human. *Reprod. Biomed. Online* **7**, 419–427.

- Leuranguer, V., Bourinet, E., Lory, P., and Nargeot, J. (1998). Antisense depletion of β -subunits fails to affect T-type calcium channels properties in a neuroblastoma cell line. *Neuropharmacology* **37**, 701–708.
- Levit-Bentley, A., and Rety, S. (2000). EF-hand calcium-binding proteins. *Curr. Opin. Struct. Biol.* **10**, 637–643.
- Leybold, B. G., Yu, C. R., Leinders-Zufall, T., Kim, M. M., Zufall, F., and Axel, R. (2002). Altered sexual and social behaviors in *trp2* mutant mice. *Proc. Natl. Acad. Sci. USA* **99**, 6376–6381.
- Leyton, L., LeGuen, P., Bunch, D., and Saling, P. M. (1992). Regulation of mouse gamete interaction by a sperm tyrosine kinase. *Proc. Natl. Acad. Sci. USA* **89**, 11692–11695.
- Li, P., Chan, H. C., He, B., So, S. C., Chung, Y. W., Shang, Q., Zhang, Y. D., and Zhang, Y. L. (2001). An antimicrobial peptide gene found in the male reproductive system of rats. *Science* **291**, 1783–1785.
- Liévano, A., Sanchez, J. A., and Darzon, A. (1985). Single-channel activity of bilayers derived from sea urchin sperm plasma membranes at the tip of a patch-clamp electrode. *Dev. Biol.* **112**, 253–257.
- Liévano, A., Vega-SaenzdeMiera, E. C., and Darzon, A. (1990). Ca^{2+} channels from the sea urchin sperm plasma membrane. *J. Gen. Physiol.* **95**, 273–296.
- Liévano, A., Santi, C. M., Serrano, C. J., Treviño, C. L., Bellve, A. R., Hernandez-Cruz, A., and Darzon, A. (1996). T-type Ca^{2+} channels and α_{1E} expression in spermatogenic cells, and their possible relevance to the sperm acrosome reaction. *FEBS Lett.* **388**, 150–154.
- Linares-Hernandez, L., Guzman-Grenfell, A. M., Hicks-Gomez, J. J., and Gonzalez-Martinez, M. T. (1998). Voltage-dependent calcium influx in human sperm assessed by simultaneous optical detection of intracellular calcium and membrane potential. *Biochim. Biophys. Acta* **1372**, 1–12.
- Lindemann, C., and Rikmenspoel, R. (1971). Intracellular potentials in bull spermatozoa. *J. Physiol.* **219**, 127–138.
- Litvin, T. N., Kamenetsky, M., Zarifyan, A., Buck, J., and Levin, L. R. (2003). Kinetic properties of “soluble” adenylyl cyclase: Synergism between calcium and bicarbonate. *J. Biol. Chem.* **278**, 15922–15926.
- Llanos, M. N. (1998). Thapsigargin stimulates acrosomal exocytosis in hamster spermatozoa. *Mol. Reprod. Dev.* **51**, 84–91.
- Llanos, M. N., Ronco, A. M., Aguirre, M. C., and Meizel, S. (2001). Hamster sperm glycine receptor: Evidence for its presence and involvement in the acrosome reaction. *Mol. Reprod. Dev.* **58**, 205–215.
- Lobley, A., Pierron, V., Reynolds, L., Allen, L., and Michalovich, D. (2003). Identification of human and mouse *CatSper3* and *CatSper4* genes: Characterisation of a common interaction domain and evidence for expression in testis. *Reprod. Biol. Endocrinol.* **1**, 53.
- Lopez-Gonzalez, I., De La Vega-Beltrán, J. L., Santi, C. M., Florman, H. M., Felix, R., and Darzon, A. (2001). Calmodulin antagonists inhibit T-type Ca^{2+} currents in mouse spermatogenic cells and the zona pellucida-induced sperm acrosome reaction. *Dev. Biol.* **236**, 210–219.
- Lopez-Gonzalez, I., Olamendi-Portugal, T., De la Vega-Beltrán, J. L., Van der Walt, J., Dyason, K., Possani, L. D., Felix, R., and Darzon, A. (2003). Scorpion toxins that block T-type Ca^{2+} channels in spermatogenic cells inhibit the sperm acrosome reaction. *Biochem. Biophys. Res. Commun.* **300**, 408–414.
- Lu, Q., and Shur, B. D. (1997). Sperm from $\beta 1,4$ -galactosyltransferase-null mice are refractory to ZP3-induced acrosome reactions and penetrate the zona pellucida poorly. *Development* **124**, 4121–4131.
- Luck, D. J. (1984). Genetic and biochemical dissection of the eucaryotic flagellum. *J. Cell Biol.* **98**, 789–794.

- Luconi, M., Bonaccorsi, L., Krausz, C., Gervasi, G., Forti, G., and Baldi, E. (1995). Stimulation of protein tyrosine phosphorylation by platelet-activating factor and progesterone in human spermatozoa. *Mol. Cell. Endocrinol.* **108**, 35–42.
- Ludwig, J., Margalit, T., Eismann, E., Lancet, D., and Kaupp, U. B. (1990). Primary structure of cAMP-gated channel from bovine olfactory epithelium. *FEBS Lett.* **270**, 24–29.
- Luria, A., Rubinstein, S., Lax, Y., and Breitbart, H. (2002). Extracellular adenosine triphosphate stimulates acrosomal exocytosis in bovine spermatozoa via P2 purinoceptor. *Biol. Reprod.* **66**, 429–437.
- Marin-Briggiler, C. I., Gonzalez-Echeverria, F., Buffone, M., Calamera, J. C., Tezon, J. G., and Vazquez-Levin, M. H. (2003). Calcium requirements for human sperm function *in vitro*. *Fertil. Steril.* **79**, 1396–1403.
- Martens, J. R., O'Connell, K., and Tamkun, M. (2004). Targeting of ion channels to membrane microdomains: Localization of KV channels to lipid rafts. *Trends Pharmacol. Sci.* **25**, 16–21.
- Martin, R. L., Lee, J. H., Cribbs, L. L., Perez-Reyes, E., and Hanck, D. A. (2000). Mibefradil block of cloned T-type calcium channels. *J. Pharmacol. Exp. Ther.* **295**, 302–308.
- Marty, I., Robert, M., Villaz, M., De Jongh, K., Lai, Y., Catterall, W. A., and Ronjat, M. (1994). Biochemical evidence for a complex involving dihydropyridine receptor and ryanodine receptor in triad junctions of skeletal muscle. *Proc. Natl. Acad. Sci. USA* **91**, 2270–2274.
- Matsui, T., Nishiyama, I., Hino, A., and Hoshi, M. (1986). Acrosome reaction-inducing substance purified from the egg jelly inhibits the jelly-induced acrosome reaction in starfish: An apparent contradiction. *Dev. Growth Differ.* **28**, 349–357.
- Matsumoto, M., Solzin, J., Helbig, A., Hagen, V., Ueno, S., Kawase, O., Maruyama, Y., Ogiso, M., Godde, M., Minakata, H., Kaupp, U. B., Hoshi, M., and Weyand, I. (2003). A sperm-activating peptide controls a cGMP-signaling pathway in starfish sperm. *Dev. Biol.* **260**, 314–324.
- Mbizvo, M. T., Johnston, R. C., and Baker, G. H. (1993). The effect of the motility stimulants, caffeine, pentoxifylline, and 2-deoxyadenosine on hyperactivation of cryopreserved human sperm. *Fertil. Steril.* **59**, 1112–1117.
- McDonough, S. I., Boland, L. M., Mintz, I. M., and Bean, B. P. (2002). Interactions among toxins that inhibit N-type and P-type calcium channels. *J. Gen. Physiol.* **119**, 313–328.
- McDonough, S. I., Mintz, I. M., and Bean, B. P. (1997). Alteration of P-type calcium channel gating by the spider toxin ω -Aga-IVA. *Biophys. J.* **72**, 2117–2128.
- McHugh, D., Sharp, E. M., Scheuer, T., and Catterall, W. A. (2000). Inhibition of cardiac L-type calcium channels by protein kinase C phosphorylation of two sites in the N-terminal domain. *Proc. Natl. Acad. Sci. USA* **97**, 12334–12338.
- McLaren, A. (1998). Germ cells and germ cell transplantation. *Int. J. Dev. Biol.* **42**, 855–860.
- McLeskey, S. B., Dowds, C., Carballada, R., White, R. R., and Saling, P. M. (1998). Molecules involved in mammalian sperm-egg interaction. *Int. Rev. Cytol.* **177**, 57–113.
- Meissner, G. (2004). NADH, a new player in the cardiac ryanodine receptor? *Circ. Res.* **94**, 418–419.
- Meizel, S. (1997). Amino acid neurotransmitter receptor/chloride channels of mammalian sperm and the acrosome reaction. *Biol. Reprod.* **56**, 569–574.
- Meizel, S., and Turner, K. O. (1993). Initiation of the human sperm acrosome reaction by thapsigargin. *J. Exp. Zool.* **267**, 350–355.
- Meizel, S., and Turner, K. O. (1996). Chloride efflux during the progesterone-initiated human sperm acrosome reaction is inhibited by lavendustin A, a tyrosine kinase inhibitor. *J. Androl.* **17**, 327–330.
- Meizel, S., Turner, K. O., and Nuccitelli, R. (1997). Progesterone triggers a wave of increased free calcium during the human sperm acrosome reaction. *Dev. Biol.* **182**, 67–75.

- Mendoza, C., Soler, A., and Tesarik, J. (1995). Nongenomic steroid action: Independent targeting of a plasma membrane calcium channel and a tyrosine kinase. *Biochem. Biophys. Res. Commun.* **210**, 518–523.
- Mengerink, K. J., and Vacquier, V. D. (2001). Glycobiology of sperm–egg interactions in deuterostomes. *Glycobiology* **11**, 37R–43R.
- Mengerink, K. J., and Vacquier, V. D. (2004). Isolation of sea urchin sperm plasma membranes. *Methods Mol. Biol.* **253**, 141–150.
- Mengerink, K. J., Moy, G. W., and Vacquier, V. D. (2002). suREJ3, a polycystin-1 protein, is cleaved at the GPS domain and localizes to the acrosomal region of sea urchin sperm. *J. Biol. Chem.* **277**, 943–948.
- Michaut, M., Tomes, C. N., De Blas, G., Yunes, R., and Mayorga, L. S. (2000). Calcium-triggered acrosomal exocytosis in human spermatozoa requires the coordinated activation of Rab3A and *N*-ethylmaleimide-sensitive factor. *Proc. Natl. Acad. Sci. USA* **97**, 9996–10001.
- Michaut, M., De Blas, G., Tomes, C. N., Yunes, R., Fukuda, M., and Mayorga, L. S. (2001). Synaptotagmin VI participates in the acrosome reaction of human spermatozoa. *Dev. Biol.* **235**, 521–529.
- Miller, C. (1986). “Ion Channel Reconstitution.” Plenum Press, New York.
- Miller, R. L. (1982). Sperm chemotaxis in ascidians. *Am. Zool.* **22**, 827–840.
- Miller, R. L. (1985). Sperm chemo-orientation in the metazoa. In “Biology of Fertilization” (C. B. Metz and A. Monroy, Eds.), pp. 275–337. Academic Press, New York.
- Miller, R. L., and Brokaw, C. J. (1970). Chemotactic turning behaviour of *Tubularia* spermatozoa. *J. Exp. Biol.* **52**, 699–706.
- Minke, B. (1977). *Drosophila* mutant with a transducer defect. *Biophys. Struct. Mech.* **3**, 59–64.
- Minke, B., and Cook, B. (2002). TRP channel proteins and signal transduction. *Physiol. Rev.* **82**, 429–472.
- Mintz, I. M., Venema, V. J., Swiderek, K. M., Lee, T. D., Bean, B. P., and Adams, M. E. (1992). P-type calcium channels blocked by the spider toxin ω -Aga-IVA. *Nature* **355**, 827–829.
- Miraglia, S. J., and Glabe, C. G. (1993). Characterization of the membrane-associating domain of the sperm adhesive protein, bindin. *Biochim. Biophys. Acta* **1145**, 191–198.
- Montal, M., Darzon, A., and Schindler, H. (1981). Functional reassembly of membrane proteins in planar lipid bilayers. *Q. Rev. Biophys.* **14**, 1–79.
- Montell, C. (2003). The venerable inveterate invertebrate TRP channels. *Cell Calcium* **33**, 409–417.
- Montell, C., Jones, K., Hafen, E., and Rubin, G. (1985). Rescue of the *Drosophila* photo-transduction mutation *trp* by germline transformation. *Science* **230**, 1040–1043.
- Morales, E., de la Torre, L., Moy, G. W., Vacquier, V. D., and Darzon, A. (1993). Anion channels in the sea urchin sperm plasma membrane. *Mol. Reprod. Dev.* **36**, 174–182.
- Moricard, R., and Bossu, J. (1951). Arrival of fertilizing sperm at the follicular cell of the secondary oocyte. *Fertil. Steril.* **2**, 260–266.
- Morisawa, M. (1994). Cell signaling mechanisms for sperm motility. *Zool. Sci.* **11**, 647–662.
- Moy, G. W., Mendoza, L. M., Schulz, J. R., Swanson, W. J., Glabe, C. G., and Vacquier, V. D. (1996). The sea urchin sperm receptor for egg jelly is a modular protein with extensive homology to the human polycystic kidney disease protein, PKD1. *J. Cell Biol.* **133**, 809–817.
- Mujica, A., Neri-Bazan, L., Tash, J. S., and Uribe, S. (1994). Mechanism for procaine-mediated hyperactivated motility in guinea pig spermatozoa. *Mol. Reprod. Dev.* **38**, 285–292.
- Munoz-Garay, C., De la Vega-Beltrán, J. L., Delgado, R., Labarca, P., Felix, R., and Darzon, A. (2001). Inwardly rectifying K^+ channels in spermatogenic cells: Functional expression and implication in sperm capacitation. *Dev. Biol.* **234**, 261–274.

- Murase, T., and Roldan, E. R. (1996). Progesterone and the zona pellucida activate different transducing pathways in the sequence of events leading to diacylglycerol generation during mouse sperm acrosomal exocytosis. *Biochem. J.* **320**, 1017–1023.
- Naaby-Hansen, S., Flickinger, C. J., and Herr, J. C. (1997). Two-dimensional gel electrophoretic analysis of vectorially labeled surface proteins of human spermatozoa. *Biol. Reprod.* **56**, 771–787.
- Naaby-Hansen, S., Wolkowicz, M. J., Klotz, K., Bush, L. A., Westbrook, V. A., Shibahara, H., Shetty, J., Coonrod, S. A., Reddi, P. P., Shannon, J., Kinter, M., Sherman, N. E., Fox, J., Flickinger, C. J., and Herr, J. C. (2001). Co-localization of the inositol 1,4,5-trisphosphate receptor and calreticulin in the equatorial segment and in membrane bounded vesicles in the cytoplasmic droplet of human spermatozoa. *Mol. Hum. Reprod.* **7**, 923–933.
- Naaby-Hansen, S., Mandal, A., Wolkowicz, M. J., Sen, B., Westbrook, V. A., Shetty, J., Coonrod, S. A., Klotz, K. L., Kim, Y. H., Bush, L. A., Flickinger, C. J., and Herr, J. C. (2002). CABYR, a novel calcium-binding tyrosine phosphorylation-regulated fibrous sheath protein involved in capacitation. *Dev. Biol.* **242**, 236–254.
- Nassar, A., Mahony, M., Blackmore, P., Morshedi, M., Ozgur, K., and Oehninger, S. (1998). Increase of intracellular calcium is not a cause of pentoxifylline-induced hyperactivated motility or acrosome reaction in human sperm. *Fertil. Steril.* **69**, 748–754.
- Neill, A. T., and Vacquier, V. D. (2004). Ligands and receptors mediating signal transduction in sea urchin spermatozoa. *Reproduction* **127**, 141–149.
- Neill, A. T., Moy, G. W., and Vacquier, V. D. (2004). Polycystin-2 associates with the polycystin-1 homolog, suREJ3, and localizes to the acrosomal region of sea urchin spermatozoa. *Mol. Reprod. Dev.* **67**, 472–477.
- Newby, L. J., Streets, A. J., Zhao, Y., Harris, P. C., Ward, C. J., and Ong, A. C. (2002). Identification, characterization, and localization of a novel kidney polycystin-1–polycystin-2 complex. *J. Biol. Chem.* **277**, 20763–20773.
- Newcomb, R., Szoke, B., Palma, A., Wang, G., Chen, X., Hopkins, W., Cong, R., Miller, J., Urge, L., Tarczy-Hornoch, K., Loo, J. A., Dooley, D. J., Nadasdi, L., Tsien, R. W., Lemos, J., and Miljanich, G. (1998). Selective peptide antagonist of the class E calcium channel from the venom of the tarantula *Hysteroecrates gigas*. *Biochemistry* **37**, 15353–15362.
- Nishigaki, T., Chiba, K., Miki, W., and Hoshi, M. (1996). Structure and function of asterosaps, sperm-activating peptides from the jelly coat of starfish eggs. *Zygote* **4**, 237–245.
- Nishigaki, T., Zamudio, F. Z., Possani, L. D., and Darszon, A. (2001). Time-resolved sperm responses to an egg peptide measured by stopped-flow fluorometry. *Biochem. Biophys. Res. Commun.* **284**, 531–535.
- Nishigaki, T., Wood, C. D., Tatsu, Y., Yumoto, N., Furuta, T., Eliza, D., Shiba, K., Baba, S. A., and Darszon, A. (2004). A sea urchin egg jelly peptide induces cGMP-mediated decrease in sperm intracellular Ca^{2+} before its increase. *Dev. Biol.* **272**, 376–388.
- Nomura, H., Turco, A. E., Pei, Y., Kalaydjieva, L., Schiavello, T., Weremowicz, S., Ji, W., Morton, C. C., Meisler, M., Reeders, S. T., and Zhou, J. (1998). Identification of PKDL, a novel polycystic kidney disease 2-like gene whose murine homologue is deleted in mice with kidney and retinal defects. *J. Biol. Chem.* **273**, 25967–25973.
- Ohta, K., Sato, C., Matsuda, T., Toriyama, M., Vacquier, V. D., Lennarz, W. J., and Kitajima, K. (2000). Co-localization of receptor and transducer proteins in the glycosphingolipid-enriched, low density, detergent-insoluble membrane fraction of sea urchin sperm. *Glycoconj. J.* **17**, 205–214.
- Okamura, N., Tajima, Y., Soejima, A., Masuda, H., and Sugita, Y. (1985). Sodium bicarbonate in seminal plasma stimulates the motility of mammalian spermatozoa through direct activation of adenylate cyclase. *J. Biol. Chem.* **260**, 9699–9705.
- Olamendi-Portugal, T., Garcia, B. I., Lopez-Gonzalez, I., Van Der Walt, J., Dyason, K., Ulens, C., Tytgat, J., Felix, R., Darszon, A., and Possani, L. D. (2002). Two new scorpion toxins

- that target voltage-gated Ca^{2+} and Na^{+} channels. *Biochem. Biophys. Res. Commun.* **299**, 562–568.
- Olds-Clarke, P. (2003). Unresolved issues in mammalian fertilization. *Int. Rev. Cytol.* **232**, 129–184.
- Oliveira, R. G., Tomasi, L., Rovasio, R. A., and Giojalas, L. C. (1999). Increased velocity and induction of chemotactic response in mouse spermatozoa by follicular and oviductal fluids. *J. Reprod. Fertil.* **115**, 23–27.
- Osheroff, J. E., Visconti, P. E., Valenzuela, J. P., Travis, A. J., Alvarez, J., and Kopf, G. S. (1999). Regulation of human sperm capacitation by a cholesterol efflux-stimulated signal transduction pathway leading to protein kinase A-mediated up-regulation of protein tyrosine phosphorylation. *Mol. Hum. Reprod.* **5**, 1017–1026.
- Oshikawa, J., Toya, Y., Fujita, T., Egawa, M., Kawabe, J., Umemura, S., and Ishikawa, Y. (2003). Nicotinic acetylcholine receptor $\alpha 7$ regulates cAMP signal within lipid rafts. *Am. J. Physiol. Cell Physiol.* **285**, C567–C574.
- Osman, R. A., Andria, M. L., Jones, A. D., and Meizel, S. (1989). Steroid induced exocytosis: The human sperm acrosome reaction. *Biochem. Biophys. Res. Commun.* **160**, 828–833.
- Ostrom, R. S., Bunday, R. A., and Insel, P. A. (2004). Nitric oxide inhibition of adenylyl cyclase type 6 activity is dependent upon lipid rafts and caveolin signaling complexes. *J. Biol. Chem.* **279**, 19846–19853.
- O'Toole, C. M., Roldan, E. R., and Fraser, L. R. (1996). Protein kinase C activation during progesterone-stimulated acrosomal exocytosis in human spermatozoa. *Mol. Hum. Reprod.* **2**, 921–927.
- O'Toole, C. M., Arnoult, C., Darszon, A., Steinhardt, R. A., and Florman, H. M. (2000). Ca^{2+} entry through store-operated channels in mouse sperm is initiated by egg ZP3 and drives the acrosome reaction. *Mol. Biol. Cell* **11**, 1571–1584.
- Parekh, A. B., Terlau, H., and Stuhmer, W. (1993). Depletion of InsP_3 stores activates a Ca^{2+} and K^{+} current by means of a phosphatase and a diffusible messenger. *Nature* **364**, 814–818.
- Park, J. Y., Ahn, H. J., Gu, J. G., Lee, K. H., Kim, J. S., Kang, H. W., and Lee, J. H. (2003). Molecular identification of Ca^{2+} channels in human sperm. *Exp. Mol. Med.* **35**, 285–292.
- Parks, J. E., Lee, D. R., Huang, S., and Kaproth, M. T. (2003). Prospects for spermatogenesis *in vitro*. *Theriogenology* **59**, 73–86.
- Parmentier, M., Libert, F., Schurmans, S., Schiffmann, S., Lefort, A., Eggerickx, D., Ledent, C., Mollereau, C., Gerard, C., Perret, J., *et al.* (1992). Expression of members of the putative olfactory receptor gene family in mammalian germ cells. *Nature* **355**, 453–455.
- Parrish, J. J., Susko-Parrish, J. L., and First, N. L. (1989). Capacitation of bovine sperm by heparin: Inhibitory effect of glucose and role of intracellular pH. *Biol. Reprod.* **41**, 683–699.
- Patrat, C., Serres, C., and Jouannet, P. (2000). The acrosome reaction in human spermatozoa. *Biol. Cell* **92**, 255–266.
- Perez-Reyes, E. (2003). Molecular physiology of low-voltage-activated T-type calcium channels. *Physiol. Rev.* **83**, 117–161.
- Perez-Reyes, E. (2004). Paradoxical role of T-type calcium channels in coronary smooth muscle. *Mol. Intervent.* **4**, 16–18.
- Peterson, B. Z., DeMaria, C. D., Adelman, J. P., and Yue, D. T. (1999). Calmodulin is the Ca^{2+} sensor for Ca^{2+} -dependent inactivation of L-type calcium channels. *Neuron* **22**, 549–558.
- Peterson, R. N., Campbell, P., Hunt, W. P., and Bozzola, J. J. (1991). Two-dimensional polyacrylamide gel electrophoresis characterization of APz, a sperm protein involved in zona binding in the pig and evidence for its binding to specific zona glycoproteins. *Mol. Reprod. Dev.* **28**, 260–271.
- Podlaha, O., and Zhang, J. (2003). Positive selection on protein-length in the evolution of a primate sperm ion channel. *Proc. Natl. Acad. Sci. USA* **100**, 12241–12246.

- Polcz, T. E., Olive, D. L., and Jones, E. E. (1997). Improving the intracytoplasmic sperm injection technique by transmembrane electric potential monitoring. *Fertil. Steril.* **68**, 735–738.
- Porter, D. C., and Vacquier, V. D. (1986). Phosphorylation of sperm histone H1 is induced by the egg jelly layer in the sea urchin *Strongylocentrotus purpuratus*. *Dev. Biol.* **116**, 203–212.
- Primakoff, P., and Myles, D. G. (2002). Penetration, adhesion, and fusion in mammalian sperm–egg interaction. *Science* **296**, 2183–2185.
- Publicover, S. J., and Barratt, C. L. (1999). Voltage-operated Ca^{2+} channels and the acrosome reaction: Which channels are present and what do they do? *Hum. Reprod.* **14**, 873–879.
- Pukazhenthii, B. S., Long, J. A., Wildt, D. E., Ottinger, M. A., Armstrong, D. L., and Howard, J. (1998). Regulation of sperm function by protein tyrosine phosphorylation in diverse wild felid species. *J. Androl.* **19**, 675–685.
- Putney, J. W., Jr., Broad, L. M., Braun, F. J., Lievremont, J. P., and Bird, G. S. (2001). Mechanisms of capacitative calcium entry. *J. Cell Sci.* **114**, 2223–2229.
- Qian, F., Germino, F. J., Cai, Y., Zhang, X., Somlo, S., and Germino, G. G. (1997). PKD1 interacts with PKD2 through a probable coiled-coil domain. *Nat. Genet.* **16**, 179–183.
- Qin, N., Olcese, R., Bransby, M., Lin, T., and Birnbaumer, L. (1999). Ca^{2+} -induced inhibition of the cardiac Ca^{2+} channel depends on calmodulin. *Proc. Natl. Acad. Sci. USA* **96**, 2435–2438.
- Quill, T. A., Ren, D., Clapham, D. E., and Garbers, D. L. (2001). A voltage-gated ion channel expressed specifically in spermatozoa. *Proc. Natl. Acad. Sci. USA* **98**, 12527–12531.
- Quill, T. A., Sugden, S. A., Rossi, K. L., Doolittle, L. K., Hammer, R. E., and Garbers, D. L. (2003). Hyperactivated sperm motility driven by CatSper2 is required for fertilization. *Proc. Natl. Acad. Sci. USA* **100**, 14869–14874.
- Rabow, L. E., Russek, S. J., and Farb, D. H. (1995). From ion currents to genomic analysis: Recent advances in GABAA receptor research. *Synapse* **21**, 189–274.
- Rajeev, S. K., and Reddy, K. V. (2004). Sperm membrane protein profiles of fertile and infertile men: Identification and characterization of fertility-associated sperm antigen. *Hum. Reprod.* **19**, 234–242.
- Ralt, D., Goldenberg, M., Fetterolf, P., Thompson, D., Dor, J., Mashiach, S., Garbers, D. L., and Eisenbach, M. (1991). Sperm attraction to a follicular factor(s) correlates with human egg fertilizability. *Proc. Natl. Acad. Sci. USA* **88**, 2840–2844.
- Ramalho-Santos, J., Moreno, R. D., Sutovsky, P., Chan, A. W., Hewitson, L., Wessel, G. M., Simerly, C. R., and Schatten, G. (2000). SNAREs in mammalian sperm: Possible implications for fertilization. *Dev. Biol.* **223**, 54–69.
- Ramarao, C. S., and Garbers, D. L. (1985). Receptor-mediated regulation of guanylate cyclase activity in spermatozoa. *J. Biol. Chem.* **260**, 8390–8396.
- Randriamampita, C., and Tsien, R. Y. (1993). Emptying of intracellular Ca^{2+} stores releases a novel small messenger that stimulates Ca^{2+} influx. *Nature* **364**, 809–814.
- Rathi, R., Colenbrander, B., Stout, T. A., Bevers, M. M., and Gadella, B. M. (2003). Progesterone induces acrosome reaction in stallion spermatozoa via a protein tyrosine kinase dependent pathway. *Mol. Reprod. Dev.* **64**, 120–128.
- Ren, D., Navarro, B., Perez, G., Jackson, A. C., Hsu, S., Shi, Q., Tilly, J. L., and Clapham, D. E. (2001). A sperm ion channel required for sperm motility and male fertility. *Nature* **413**, 603–609.
- Rodeheffer, C., and Shur, B. D. (2004a). Characterization of a novel ZP3-independent sperm-binding ligand that facilitates sperm adhesion to the egg coat. *Development* **131**, 503–512.
- Rodeheffer, C., and Shur, B. D. (2004b). Sperm from $\beta 1,4$ -galactosyltransferase 1-null mice exhibit precocious capacitation. *Development* **131**, 491–501.
- Rodriguez, E., and Darszon, A. (2003). Intracellular sodium changes during the speract response and the acrosome reaction in sea urchin sperm. *J. Physiol.* **546**, 89–100.

- Roldan, E. R., Murase, T., and Shi, Q. X. (1994). Exocytosis in spermatozoa in response to progesterone and zona pellucida. *Science* **266**, 1578–1581.
- Rossi, P., Dolci, S., Sette, C., Capolunghi, F., Pellegrini, M., Loiarro, M., Di Agostino, S., Paronetto, M. P., Grimaldi, P., Merico, D., Martegani, E., and Geremia, R. (2004). Analysis of the gene expression profile of mouse male meiotic germ cells. *Gene Expr. Patterns* **4**, 267–281.
- Rotem, R., Paz, G. F., Homonnai, Z. T., Kalina, M., Lax, J., Breitbart, H., and Naor, Z. (1992). Ca^{2+} -independent induction of acrosome reaction by protein kinase C in human sperm. *Endocrinology* **131**, 2235–2243.
- Saimi, Y., and Kung, C. (2002). Calmodulin as an ion channel subunit. *Annu. Rev. Physiol.* **64**, 289–311.
- Sakata, Y., Saegusa, H., Zong, S., Osanai, M., Murakoshi, T., Shimizu, Y., Noda, T., Aso, T., and Tanabe, T. (2002). $\text{Ca}_v2.3 \alpha_{1E} \text{Ca}^{2+}$ channel participates in the control of sperm function. *FEBS Lett.* **516**, 229–233.
- Salvatore, L., D'Adamo, M. C., Polishchuk, R., Salmona, M., and Pessia, M. (1999). Localization and age-dependent expression of the inward rectifier K^+ channel subunit Kir 5.1 in a mammalian reproductive system. *FEBS Lett.* **449**, 146–152.
- Sanchez, D., Labarca, P., and Darzson, A. (2001). Sea urchin sperm cation-selective channels directly modulated by cAMP. *FEBS Lett.* **503**, 111–115.
- Santi, C. M., Darzson, A., and Hernandez-Cruz, A. (1996). A dihydropyridine-sensitive T-type Ca^{2+} current is the main Ca^{2+} current carrier in mouse primary spermatocytes. *Am. J. Physiol.* **271**, C1583–C1593.
- Santi, C. M., Santos, T., Hernandez-Cruz, A., and Darzson, A. (1998). Properties of a novel pH-dependent Ca^{2+} permeation pathway present in male germ cells with possible roles in spermatogenesis and mature sperm function. *J. Gen. Physiol.* **112**, 33–53.
- Sasakura, Y., Awazu, S., Chiba, S., and Satoh, N. (2003). Germ-line transgenesis of the Tc1/mariner superfamily transposon Minos in *Ciona intestinalis*. *Proc. Natl. Acad. Sci. USA* **100**, 7726–7730.
- Sase, I., Okinaga, T., Hoshi, M., Feigenson, G. W., and Kinoshita, K., Jr. (1995). Regulatory mechanisms of the acrosome reaction revealed by multiview microscopy of single starfish sperm. *J. Cell Biol.* **131**, 963–973.
- Sato, Y., Son, J. H., and Meizel, S. (2000a). The mouse sperm glycine receptor/chloride channel: Cellular localization and involvement in the acrosome reaction initiated by glycine. *J. Androl.* **21**, 99–106.
- Sato, Y., Son, J. H., Tucker, R. P., and Meizel, S. (2000b). The zona pellucida-initiated acrosome reaction: Defect due to mutations in the sperm glycine receptor/ Cl^- channel. *Dev. Biol.* **227**, 211–218.
- Sato, Y., Tucker, R. P., and Meizel, S. (2002). Detection of glycine receptor/ Cl^- channel β subunit transcripts in mouse testis. *Zygote* **10**, 105–108.
- Schackmann, R. W. (1989). Ionic regulation of the sea urchin sperm acrosome reaction and stimulation by egg-derived peptides. In “The Cell Biology of Fertilization” (H. Schatte and G. Schatten, Eds.), pp. 3–28. Academic Press, San Diego, CA.
- Schackmann, R. W., and Chock, P. B. (1986). Alteration of intracellular $[\text{Ca}^{2+}]$ in sea urchin sperm by the egg peptide speract: Evidence that increased intracellular Ca^{2+} is coupled to Na^+ entry and increased intracellular pH. *J. Biol. Chem.* **261**, 8719–8728.
- Schackmann, R. W., Eddy, E. M., and Shapiro, B. M. (1978). The acrosome reaction of *Strongylocentrotus purpuratus* sperm: Ion requirements and movements. *Dev. Biol.* **65**, 483–495.
- Schlecht, U., and Primig, M. (2003). Mining meiosis and gametogenesis with DNA microarrays. *Reproduction* **125**, 447–456.

- Schreiber, M., Wei, A., Yuan, A., Gaut, J., Saito, M., and Salkoff, L. (1998). Slo3, a novel pH-sensitive K^+ channel from mammalian spermatozoa. *J. Biol. Chem.* **273**, 3509–3516.
- Schulz, J. R., Wessel, G. M., and Vacquier, V. D. (1997). The exocytosis regulatory proteins syntaxin and VAMP are shed from sea urchin sperm during the acrosome reaction. *Dev. Biol.* **191**, 80–87.
- Schulz, J. R., Sasaki, J. D., and Vacquier, V. D. (1998). Increased association of synaptosome-associated protein of 25kDa with syntaxin and vesicle-associated membrane protein following acrosomal exocytosis of sea urchin sperm. *J. Biol. Chem.* **273**, 24355–24359.
- Schwartz, R., Brooks, W., and Zinsser, H. H. (1958). Evidence of chemotaxis as a factor in sperm motility. *Fertil. Steril.* **9**, 300–308.
- Sengoku, K., Tamate, K., Takuma, N., Takaoka, Y., Yoshida, T., Nishiwaki, K., and Ishikawa, M. (1996). Involvement of protein kinases in platelet activating factor-induced acrosome reaction of human spermatozoa. *Mol. Hum. Reprod.* **2**, 401–404.
- Serrano, C. J., Treviño, C. L., Felix, R., and Darszon, A. (1999a). Voltage-dependent Ca^{2+} channel subunit expression and immunolocalization in mouse spermatogenic cells and sperm. *FEBS Lett.* **462**, 171–176.
- Serrano, J. R., Perez-Reyes, E., and Jones, S. W. (1999b). State-dependent inactivation of the α_{1G} T-type calcium channel. *J. Gen. Physiol.* **114**, 185–201.
- Setchell, B. P. (1994). Possible physiological bases for contraceptive techniques in the male. *Hum. Reprod.* **9**, 1081–1087.
- Shetty, J., Naaby-Hansen, S., Shibahara, H., Bronson, R., Flickinger, C. J., and Herr, J. C. (1999). Human sperm proteome: Immunodominant sperm surface antigens identified with sera from infertile men and women. *Biol. Reprod.* **61**, 61–69.
- Shetty, J., Diekman, A. B., Jayes, F. C., Sherman, N. E., Naaby-Hansen, S., Flickinger, C. J., and Herr, J. C. (2001). Differential extraction and enrichment of human sperm surface proteins in a proteome: Identification of immunocontraceptive candidates. *Electrophoresis* **22**, 3053–3066.
- Shi, Q. X., Yuan, Y. Y., and Roldan, E. R. (1997). γ -Aminobutyric acid (GABA) induces the acrosome reaction in human spermatozoa. *Mol. Hum. Reprod.* **3**, 677–683.
- Shi, X., Amindari, S., Paruchuru, K., Skalla, D., Burkin, H., Shur, B. D., and Miller, D. J. (2001). Cell surface β -1,4-galactosyltransferase-I activates G protein-dependent exocytotic signaling. *Development* **128**, 645–654.
- Shi, Y. L., and Ma, X. H. (1998). Ion-channels reconstituted into lipid bilayer from human sperm plasma membrane. *Mol. Reprod. Dev.* **50**, 354–360.
- Shibahara, H., Sato, I., Shetty, J., Naaby-Hansen, S., Herr, J. C., Wakimoto, E., and Koyama, K. (2002). Two-dimensional electrophoretic analysis of sperm antigens recognized by sperm immobilizing antibodies detected in infertile women. *J. Reprod. Immunol.* **53**, 1–12.
- Shirakawa, H., and Miyazaki, S. (1999). Spatiotemporal characterization of intracellular Ca^{2+} rise during the acrosome reaction of mammalian spermatozoa induced by zona pellucida. *Dev. Biol.* **208**, 70–78.
- Shistik, E., Ivanina, T., Blumenstein, Y., and Dascal, N. (1998). Crucial role of N terminus in function of cardiac L-type Ca^{2+} channel and its modulation by protein kinase C. *J. Biol. Chem.* **273**, 17901–17909.
- Sidach, S. S., and Mintz, I. M. (2002). Kurtoxin, a gating modifier of neuronal high- and low-threshold Ca channels. *J. Neurosci.* **22**, 2023–2034.
- Simons, K., and Ikonen, E. (1997). Functional rafts in cell membranes. *Nature* **387**, 569–572.
- Singh, S., Lowe, D. G., Thorpe, D. S., Rodriguez, H., Kuang, W. J., Dangott, L. J., Chinkers, M., Goettel, D. V., and Garbers, D. L. (1988). Membrane guanylate cyclase is a cell-surface receptor with homology to protein kinases. *Nature* **334**, 708–712.
- Sinowatz, F., Kolle, S., and Topfer-Petersen, E. (2001). Biosynthesis and expression of zona pellucida glycoproteins in mammals. *Cells Tissues Organs* **168**, 24–35.

- Smani, T., Zakharov, S. I., Csutora, P., Leno, E., Trepakova, E. S., and Bolotina, V. M. (2004). A novel mechanism for the store-operated calcium influx pathway. *Nat. Cell Biol.* **6**, 113–120.
- Smith, T. T., and Yanagimachi, R. (1991). Attachment and release of spermatozoa from the caudal isthmus of the hamster oviduct. *J. Reprod. Fertil.* **91**, 567–573.
- So, S. C., Wu, W. L., Grima, J., Leung, P. S., Chung, Y. W., Cheng, C. Y., Wong, P. Y., Yan, Y. C., and Chan, H. C. (1998). Functional expression of sperm angiotensin II type I receptor in *Xenopus* oocyte: Modulation of a sperm Ca^{2+} activated K^+ channel. *Biochim. Biophys. Acta* **1415**, 261–265.
- Solzin, J., Helbig, A., Van, Q., Brown, J. E., Hildebrand, E., Weyand, I., and Kaupp, U. B. (2004). Revisiting the role of H^+ in chemotactic signaling of sperm. *J. Gen. Physiol.* **124**, 115–124.
- Son, J. H., and Meizel, S. (2003). Evidence suggesting that the mouse sperm acrosome reaction initiated by the zona pellucida involves an $\alpha 7$ nicotinic acetylcholine receptor. *Biol. Reprod.* **68**, 1348–1353.
- Son, W. Y., Lee, J. H., and Han, C. T. (2000). Acrosome reaction of human spermatozoa is mainly mediated by α_{1H} T-type calcium channels. *Mol. Hum. Reprod.* **6**, 893–897.
- Son, W. Y., Han, C. T., Lee, J. H., Jung, K. Y., Lee, H. M., and Choo, Y. K. (2002). Developmental expression patterns of α_{1H} T-type Ca^{2+} channels during spermatogenesis and organogenesis in mice. *Dev. Growth Differ.* **44**, 181–190.
- Spehr, M., Gisselmann, G., Poplawski, A., Riffell, J. A., Wetzell, C. H., Zimmer, R. K., and Hatt, H. (2003). Identification of a testicular odorant receptor mediating human sperm chemotaxis. *Science* **299**, 2054–2058.
- Sprando, R. L., and Russell, L. D. (1987). Comparative study of cytoplasmic elimination in spermatids of selected mammalian species. *Am. J. Anat.* **178**, 72–80.
- Spungin, B., and Breitbart, H. (1996). Calcium mobilization and influx during sperm exocytosis. *J. Cell Sci.* **109**, 1947–1955.
- Stamboulian, S., De Waard, M., Villaz, M., and Arnoult, C. (2002). Functional interaction between mouse spermatogenic LVA and thapsigargin-modulated calcium channels. *Dev. Biol.* **252**, 72–83.
- Stamboulian, S., Kim, D., Shin, H. S., Ronjat, M., De Waard, M., and Arnoult, C. (2004). Biophysical and pharmacological characterization of spermatogenic T-type calcium current in mice lacking the $\text{CaV}3.1$ (α_{1G}) calcium channel: $\text{CaV}3.2$ (α_{1H}) is the main functional calcium channel in wild-type spermatogenic cells. *J. Cell. Physiol.* **200**, 116–124.
- Starita-Geribaldi, M., Poggioli, S., Zucchini, M., Garin, J., Chevallier, D., Fenichel, P., and Pointis, G. (2001). Mapping of seminal plasma proteins by two-dimensional gel electrophoresis in men with normal and impaired spermatogenesis. *Mol. Hum. Reprod.* **7**, 715–722.
- Stea, A., Soong, T. W., and Snutch, T. P. (1995). Determinants of PKC-dependent modulation of a family of neuronal calcium channels. *Neuron* **15**, 929–940.
- Storey, B. T., Hourani, C. L., and Kim, J. B. (1992). A transient rise in intracellular Ca^{2+} is a precursor reaction to the zona pellucida-induced acrosome reaction in mouse sperm and is blocked by the induced acrosome reaction inhibitor 3-quinuclidinyl benzilate. *Mol. Reprod. Dev.* **32**, 41–50.
- Stowers, L., Holy, T. E., Meister, M., Dulac, C., and Koentges, G. (2002). Loss of sex discrimination and male–male aggression in mice deficient for TRP2. *Science* **295**, 1493–1500.
- Su, Y. H., and Vacquier, V. D. (2002). A flagellar K^+ -dependent $\text{Na}^+/\text{Ca}^{2+}$ exchanger keeps Ca^{2+} low in sea urchin spermatozoa. *Proc. Natl. Acad. Sci. USA* **99**, 6743–6748.
- Suarez, S. S. (1998). The oviductal sperm reservoir in mammals: Mechanisms of formation. *Biol. Reprod.* **58**, 1105–1107.

- Suarez, S. S., and Dai, X. (1995). Intracellular calcium reaches different levels of elevation in hyperactivated and acrosome-reacted hamster sperm. *Mol. Reprod. Dev.* **42**, 325–333.
- Suarez, S. S., and Ho, H. C. (2003). Hyperactivated motility in sperm. *Reprod. Domest. Anim.* **38**, 119–124.
- Suarez, S. S., and Osman, R. A. (1987). Initiation of hyperactivated flagellar bending in mouse sperm within the female reproductive tract. *Biol. Reprod.* **36**, 1191–1198.
- Suarez, S. S., Varosi, S. M., and Dai, X. (1993). Intracellular calcium increases with hyperactivation in intact, moving hamster sperm and oscillates within the flagellar beat cycle. *Proc. Natl. Acad. Sci. USA* **90**, 4660–4664.
- Sun, F., Giojalas, L. C., Rovasio, R. A., Tur-Kaspa, I., Sanchez, R., and Eisenbach, M. (2003). Lack of species-specificity in mammalian sperm chemotaxis. *Dev. Biol.* **255**, 423–427.
- Sutko, J. L., Airey, J. A., Welch, W., and Ruest, L. (1997). The pharmacology of ryanodine and related compounds. *Pharmacol. Rev.* **49**, 53–98.
- Suzuki, N. (1995). Structure, function and biosynthesis of sperm-activating peptides and fucose sulfate glycoconjugate in the extracellular coat of sea urchin eggs. *Zool. Sci.* **12**, 13–27.
- Suzuki, N., Nomura, K., Ohtake, H., and Isaka, S. (1981). Purification and the primary structure of sperm-activity peptides from the jelly coat of sea urchin eggs. *Biochem. Biophys. Res. Commun.* **99**, 1238–1244.
- Suzuki, N., Shimomura, H., Radany, E. W., Ramarao, C. S., Ward, G. E., Bentley, J. K., and Garbers, D. L. (1984). A peptide associated with eggs causes a mobility shift in a major plasma membrane protein of spermatozoa. *J. Biol. Chem.* **259**, 14874–14879.
- Suzuki-Toyota, F., Ishibashi, K., and Yuasa, S. (1999). Immunohistochemical localization of a water channel, aquaporin 7 (AQP7), in the rat testis. *Cell Tissue Res.* **295**, 279–285.
- Swartz, K. J. (1993). Modulation of Ca^{2+} channels by protein kinase C in rat central and peripheral neurons: Disruption of G protein-mediated inhibition. *Neuron* **11**, 305–320.
- Tatsu, Y., Nishigaki, T., Darszon, A., and Yumoto, N. (2002). A caged sperm-activating peptide that has a photocleavable protecting group on the backbone amide. *FEBS Lett.* **525**, 20–24.
- Taylor, C. W., and Laude, A. J. (2002). IP_3 receptors and their regulation by calmodulin and cytosolic Ca^{2+} . *Cell Calcium* **32**, 321–334.
- Tesarik, J., Thebault, A., and Testart, J. (1992). Effect of pentoxifylline on sperm movement characteristics in normozoospermic and asthenozoospermic specimens. *Hum. Reprod.* **7**, 1257–1263.
- Tesarik, J., Carreras, A., and Mendoza, C. (1993a). Differential sensitivity of progesterone- and zona pellucida-induced acrosome reactions to pertussis toxin. *Mol. Reprod. Dev.* **34**, 183–189.
- Tesarik, J., Moos, J., and Mendoza, C. (1993b). Stimulation of protein tyrosine phosphorylation by a progesterone receptor on the cell surface of human sperm. *Endocrinology* **133**, 328–335.
- Tesarik, J., Carreras, A., and Mendoza, C. (1996). Single cell analysis of tyrosine kinase dependent and independent Ca^{2+} fluxes in progesterone induced acrosome reaction. *Mol. Hum. Reprod.* **2**, 225–232.
- Thomas, P., and Meizel, S. (1989). Phosphatidylinositol 4,5-bisphosphate hydrolysis in human sperm stimulated with follicular fluid or progesterone is dependent upon Ca^{2+} influx. *Biochem. J.* **264**, 539–546.
- Tilney, L. G., Kiehart, D. P., Sardet, C., and Tilney, M. (1978). Polymerization of actin. IV. Role of Ca^{++} and H^+ in the assembly of actin and in membrane fusion in the acrosomal reaction of echinoderm sperm. *J. Cell Biol.* **77**, 536–550.
- Tiwari-Woodruff, S. K., and Cox, T. C. (1995). Boar sperm plasma membrane Ca^{2+} -selective channels in planar lipid bilayers. *Am. J. Physiol.* **268**, C1284–C1294.

- Todorovic, S. M., and Lingle, C. J. (1998). Pharmacological properties of T-type Ca^{2+} current in adult rat sensory neurons: Effects of anticonvulsant and anesthetic agents. *J. Neurophysiol.* **79**, 240–252.
- Tomes, C. N., McMaster, C. R., and Saling, P. M. (1996). Activation of mouse sperm phosphatidylinositol-4,5 bisphosphate-phospholipase C by zona pellucida is modulated by tyrosine phosphorylation. *Mol. Reprod. Dev.* **43**, 196–204.
- Tomes, C. N., Roggero, C. M., De Blas, G., Saling, P. M., and Mayorga, L. S. (2004). Requirement of protein tyrosine kinase and phosphatase activities for human sperm exocytosis. *Dev. Biol.* **265**, 399–415.
- Toowicharanont, P., and Shapiro, B. M. (1988). Regional differentiation of the sea urchin sperm plasma membrane. *J. Biol. Chem.* **263**, 6877–6883.
- Travis, A. J., and Kopf, G. S. (2002). The role of cholesterol efflux in regulating the fertilization potential of mammalian spermatozoa. *J. Clin. Invest.* **110**, 731–736.
- Trede, N. S., Langenau, D. M., Traver, D., Look, A. T., and Zon, L. I. (2004). The use of zebrafish to understand immunity. *Immunity* **20**, 367–379.
- Treviño, C. L., Santi, C. M., Beltrán, C., Hernandez-Cruz, A., Darszon, A., and Lomeli, H. (1998). Localisation of inositol triphosphate and ryanodine receptors during mouse spermatogenesis: Possible functional implications. *Zygote* **6**, 159–172.
- Treviño, C. L., Serrano, C. J., Beltrán, C., Felix, R., and Darszon, A. (2001). Identification of mouse *trp* homologs and lipid rafts from spermatogenic cells and sperm. *FEBS Lett.* **509**, 119–125.
- Treviño, C. L., Felix, R., Castellano, L. E., Gutierrez, C., Rodriguez, D., Pacheco, J., Lopez-Gonzalez, I., Gomora, J. C., Tsutsumi, V., Hernandez-Cruz, A., Fiordeliso, T., Scaling, A. L., and Darszon, A. (2004). Expression and differential cell distribution of low-threshold Ca^{2+} channels in mammalian male germ cells and sperm. *FEBS Lett.* **563**, 87–92.
- Triggie, D. J. (2003). 1,4-Dihydropyridines as calcium channel ligands and privileged structures. *Cell. Mol. Neurobiol.* **23**, 293–303.
- Tsien, R. Y. (1989). Fluorescent probes of cell signaling. *Annu. Rev. Neurosci.* **12**, 227–253.
- Tsiokas, L., Kim, E., Arnould, T., Sukhatme, V. P., and Walz, G. (1997). Homo- and heterodimeric interactions between the gene products of PKD1 and PKD2. *Proc. Natl. Acad. Sci. USA* **94**, 6965–6970.
- Tsiokas, L., Arnould, T., Zhu, C., Kim, E., Walz, G., and Sukhatme, V. P. (1999). Specific association of the gene product of PKD2 with the TRPC1 channel. *Proc. Natl. Acad. Sci. USA* **96**, 3934–3939.
- Tucker, W. C., Weber, T., and Chapman, E. R. (2004). Reconstitution of Ca^{2+} -regulated membrane fusion by synaptotagmin and SNAREs. *Science* **304**, 435–438.
- Turner, K. O., and Meizel, S. (1995). Progesterone-mediated efflux of cytosolic chloride during the human sperm acrosome reaction. *Biochem. Biophys. Res. Commun.* **213**, 774–780.
- Ulrich, A. S., Otter, M., Glabe, C. G., and Hoekstra, D. (1998). Membrane fusion is induced by a distinct peptide sequence of the sea urchin fertilization protein bindin. *J. Biol. Chem.* **273**, 16748–16755.
- Ulrich, A. S., Tichelaar, W., Forster, G., Zschornig, O., Weinkauff, S., and Meyer, H. W. (1999). Ultrastructural characterization of peptide-induced membrane fusion and peptide self-assembly in the lipid bilayer. *Biophys. J.* **77**, 829–841.
- Utleg, A. G., Yi, E. C., Xie, T., Shannon, P., White, J. T., Goodlett, D. R., Hood, L., and Lin, B. (2003). Proteomic analysis of human prostasomes. *Prostate* **56**, 150–161.
- Vacquier, V. D. (1998). Evolution of gamete recognition proteins. *Science* **281**, 1995–1998.
- Vacquier, V. D., and Moy, G. W. (1977). Isolation of bindin: The protein responsible for adhesion of sperm to sea urchin eggs. *Proc. Natl. Acad. Sci. USA* **74**, 2456–2460.

- Vacquier, V. D., and Moy, G. W. (1997). The fucose sulfate polymer of egg jelly binds to sperm REJ and is the inducer of the sea urchin sperm acrosome reaction. *Dev. Biol.* **192**, 125–135.
- Vanderhaeghen, P., Schurmans, S., Vassart, G., and Parmentier, M. (1993). Olfactory receptors are displayed on dog mature sperm cells. *J. Cell Biol.* **123**, 1441–1452.
- Vanderhaeghen, P., Schurmans, S., Vassart, G., and Parmentier, M. (1997). Specific repertoire of olfactory receptor genes in the male germ cells of several mammalian species. *Genomics* **39**, 239–246.
- van Duin, M., Polman, J. E., De Breet, I. T., van Ginneken, K., Bunschoten, H., Grootenhuis, A., Brindle, J., and Aitken, R. J. (1994). Recombinant human zona pellucida protein ZP3 produced by Chinese hamster ovary cells induces the human sperm acrosome reaction and promotes sperm–egg fusion. *Biol. Reprod.* **51**, 607–617.
- Vassilev, P. M., Guo, L., Chen, X. Z., Segal, Y., Peng, J. B., Basora, N., Babakhanlou, H., Cruger, G., Kanazirska, M., Ye, C., Brown, E. M., Hediger, M. A., and Zhou, J. (2001). Polycystin-2 is a novel cation channel implicated in defective intracellular Ca^{2+} homeostasis in polycystic kidney disease. *Biochem. Biophys. Res. Commun.* **282**, 341–350.
- Vilela-Silva, A. C., Castro, M. O., Valente, A. P., Biermann, C. H., and Mourao, P. A. (2002). Sulfated fucans from the egg jellies of the closely related sea urchins *Strongylocentrotus droebachiensis* and *Strongylocentrotus pallidus* ensure species-specific fertilization. *J. Biol. Chem.* **277**, 379–387.
- Villanueva-Diaz, C., Arias-Martinez, J., Bermejo-Martinez, L., and Vellido-Ortega, F. (1995). Progesterone induces human sperm chemotaxis. *Fertil. Steril.* **64**, 1183–1188.
- Visconti, P. E., Moore, G. D., Bailey, J. L., Leclerc, P., Connors, S. A., Pan, D., Olds-Clarke, P., and Kopf, G. S. (1995). Capacitation of mouse spermatozoa. II. Protein tyrosine phosphorylation and capacitation are regulated by a cAMP-dependent pathway. *Development* **121**, 1139–1150.
- Visconti, P. E., Galantino-Homer, H., Ning, X., Moore, G. D., Valenzuela, J. P., Jorgez, C. J., Alvarez, J. G., and Kopf, G. S. (1999). Cholesterol efflux-mediated signal transduction in mammalian sperm: β -Cyclodextrins initiate transmembrane signaling leading to an increase in protein tyrosine phosphorylation and capacitation. *J. Biol. Chem.* **274**, 3235–3242.
- Visconti, P. E., Westbrook, V. A., Chertihin, O., Demarco, I., Sleight, S., and Diekman, A. B. (2002). Novel signaling pathways involved in sperm acquisition of fertilizing capacity. *J. Reprod. Immunol.* **53**, 133–150.
- Wade, M. A., Roman, S. D., Jones, R. C., and Aitken, R. J. (2003). Adenylyl cyclase isoforms in rat testis and spermatozoa from the cauda epididymidis. *Cell Tissue Res.* **314**, 411–419.
- Walensky, L. D., and Snyder, S. H. (1995). Inositol 1,4,5-trisphosphate receptors selectively localized to the acrosomes of mammalian sperm. *J. Cell Biol.* **130**, 857–869.
- Walensky, L. D., Roskams, A. J., Lefkowitz, R. J., Snyder, S. H., and Ronnett, G. V. (1995). Odorant receptors and desensitization proteins colocalize in mammalian sperm. *Mol. Med.* **1**, 130–141.
- Wang, D., King, S. M., Quill, T. A., Doolittle, L. K., and Garbers, D. L. (2003). A new sperm-specific Na^+/H^+ exchanger required for sperm motility and fertility. *Nat. Cell Biol.* **5**, 1117–1122.
- Ward, C. R., Storey, B. T., and Kopf, G. S. (1994). Selective activation of $Gi1$ and $Gi2$ in mouse sperm by the zona pellucida, the egg's extracellular matrix. *J. Biol. Chem.* **269**, 13254–13258.
- Ward, G. E., Brokaw, C. J., Garbers, D. L., and Vacquier, V. D. (1985). Chemotaxis of *Arbacia punctulata* spermatozoa to resact, a peptide from the egg jelly layer. *J. Cell Biol.* **101**, 2324–2329.
- Ward, G. E., Moy, G. W., and Vacquier, V. D. (1986). Phosphorylation of membrane-bound guanylate cyclase of sea urchin spermatozoa. *J. Cell Biol.* **103**, 95–101.

- Wassarman, P. M. (2002). Sperm receptors and fertilization in mammals. *Mt. Sinai J. Med.* **69**, 148–155.
- Wassarman, P. M., and Litscher, E. S. (2001). Towards the molecular basis of sperm and egg interaction during mammalian fertilization. *Cells Tissues Organs* **168**, 36–45.
- Wassarman, P. M., Jovine, L., and Litscher, E. S. (2001). A profile of fertilization in mammals. *Nat. Cell Biol.* **3**, E59–E64.
- Wellman, G. C., and Nelson, M. T. (2003). Signaling between SR and plasmalemma in smooth muscle: Sparks and the activation of Ca²⁺-sensitive ion channels. *Cell Calcium* **34**, 211–229.
- Welsby, P. J., Wang, H., Wolfe, J. T., Colbran, R. J., Johnson, M. L., and Barrett, P. Q. (2003). A mechanism for the direct regulation of T-type calcium channels by Ca²⁺/calmodulin-dependent kinase II. *J. Neurosci.* **23**, 10116–10121.
- Wennemuth, G., Westenbroek, R. E., Xu, T., Hille, B., and Babcock, D. F. (2000). Cav2.2 and Cav2.3 (N- and R-type) Ca²⁺ channels in depolarization-evoked entry of Ca²⁺ into mouse sperm. *J. Biol. Chem.* **275**, 21210–21217.
- Wennemuth, G., Carlson, A. E., Harper, A. J., and Babcock, D. F. (2003). Bicarbonate actions on flagellar and Ca²⁺-channel responses: Initial events in sperm activation. *Development* **130**, 1317–1326.
- Westenbroek, R. E., and Babcock, D. F. (1999). Discrete regional distributions suggest diverse functional roles of calcium channel α_1 subunits in sperm. *Dev. Biol.* **207**, 457–469.
- Weyand, I., Godde, M., Frings, S., Weiner, J., Muller, F., Altenhofen, W., Hatt, H., and Kaupp, U. B. (1994). Cloning and functional expression of a cyclic-nucleotide-gated channel from mammalian sperm. *Nature* **368**, 859–863.
- Wiesner, B., Weiner, J., Middendorff, R., Hagen, V., Kaupp, U. B., and Weyand, I. (1998). Cyclic nucleotide-gated channels on the flagellum control Ca²⁺ entry into sperm. *J. Cell Biol.* **142**, 473–484.
- Williams, R. J. (2002). Calcium. *Methods Mol. Biol.* **172**, 21–49.
- Wiser, O., Trus, M., Hernandez, A., Renstrom, E., Barg, S., Rorsman, P., and Atlas, D. (1999). The voltage sensitive Lc-type Ca²⁺ channel is functionally coupled to the exocytotic machinery. *Proc. Natl. Acad. Sci. USA* **96**, 248–253.
- Wissenbach, U., Schroth, G., Philipp, S., and Flockerzi, V. (1998). Structure and mRNA expression of a bovine *trp* homologue related to mammalian *trp2* transcripts. *FEBS Lett.* **429**, 61–66.
- Wissenbach, U., Niemeyer, B. A., and Flockerzi, V. (2004). TRP channels as potential drug targets. *Biol. Cell* **96**, 47–54.
- Wistrom, C. A., and Meizel, S. (1993). Evidence suggesting involvement of a unique human sperm steroid receptor/Cl⁻ channel complex in the progesterone-initiated acrosome reaction. *Dev. Biol.* **159**, 679–690.
- Wolfe, J. T., Wang, H., Perez-Reyes, E., and Barrett, P. Q. (2002). Stimulation of recombinant Ca_v3.2, T-type, Ca²⁺ channel currents by CaMKII γ_C . *J. Physiol.* **538**, 343–355.
- Wolfe, J. T., Wang, H., Howard, J., Garrison, J. C., and Barrett, P. Q. (2003). T-type calcium channel regulation by specific G-protein betagamma subunits. *Nature* **424**, 209–213.
- Wood, C. D., Darszon, A., and Whitaker, M. (2003). Speract induces calcium oscillations in the sperm tail. *J. Cell Biol.* **161**, 89–101.
- Wu, W. L., So, S. C., Sun, Y. P., Zhou, T. S., Yu, Y., Chung, Y. W., Wang, X. F., Bao, Y. D., Yan, Y. C., and Chan, H. C. (1998). Functional expression of a Ca²⁺-activated K⁺ channel in *Xenopus* oocytes injected with RNAs from the rat testis. *Biochim. Biophys. Acta* **1373**, 360–365.
- Xu, C., Rigney, D. R., and Anderson, D. J. (1994). Two-dimensional electrophoretic profile of human sperm membrane proteins. *J. Androl.* **15**, 595–602.

- Xu, G. M., Gonzalez-Perrett, S., Essafi, M., Timpanaro, G. A., Montalbetti, N., Arnaout, M. A., and Cantiello, H. F. (2003). Polycystin-1 activates and stabilizes the polycystin-2 channel. *J. Biol. Chem.* **278**, 1457–1462.
- Xu, X. Z., and Sternberg, P. W. (2003). A *C. elegans* sperm TRP protein required for sperm–egg interactions during fertilization. *Cell* **114**, 285–297.
- Yanagimachi, R. (1994). Mammalian fertilization. In “The Physiology of Reproduction” (E. Knobil and J. D. Neill, Eds.), Vol. 1, pp. 189–317. Raven Press, New York.
- Yang, J., and Tsien, R. W. (1993). Enhancement of N- and L-type calcium channel currents by protein kinase C in frog sympathetic neurons. *Neuron* **10**, 127–136.
- Yang, J., Serres, C., Philibert, D., Robel, P., Baulieu, E. E., and Jouannet, P. (1994). Progesterone and RU486: Opposing effects on human sperm. *Proc. Natl. Acad. Sci. USA* **91**, 529–533.
- Yao, Y., Ferrer-Montiel, A. V., Montal, M., and Tsien, R. Y. (1999). Activation of store-operated Ca^{2+} current in *Xenopus* oocytes requires SNAP-25 but not a diffusible messenger. *Cell* **98**, 475–485.
- Yoshida, M., Murata, M., Inaba, K., and Morisawa, M. (2002). A chemoattractant for ascidian spermatozoa is a sulfated steroid. *Proc. Natl. Acad. Sci. USA* **99**, 14831–14836.
- Yoshida, M., Ishikawa, M., Izumi, H., De Santis, R., and Morisawa, M. (2003). Store-operated calcium channel regulates the chemotactic behavior of ascidian sperm. *Proc. Natl. Acad. Sci. USA* **100**, 149–154.
- Yuan, J. P., Kiselyov, K., Shin, D. M., Chen, J., Shcheynikov, N., Kang, S. H., Dehoff, M. H., Schwarz, M. K., Seeburg, P. H., Muallem, S., and Worley, P. F. (2003). Homer binds TRPC family channels and is required for gating of TRPC1 by IP_3 receptors. *Cell* **114**, 777–789.
- Yue, D. T., Herzig, S., and Marban, E. (1990). β -Adrenergic stimulation of calcium channels occurs by potentiation of high-activity gating modes. *Proc. Natl. Acad. Sci. USA* **87**, 753–757.
- Yunes, R., Michaut, M., Tomes, C., and Mayorga, L. S. (2000). Rab3A triggers the acrosome reaction in permeabilized human spermatozoa. *Biol. Reprod.* **62**, 1084–1089.
- Yunker, A. M. (2003). Modulation and pharmacology of low voltage-activated (“T-type”) calcium channels *J. Bioenerg. Biomembr.* **35**, 577–598.
- Zamponi, G. W., Bourinet, E., Nelson, D., Nargeot, J., and Snutch, T. P. (1997). Crosstalk between G proteins and protein kinase C mediated by the calcium channel α_1 subunit. *Nature* **385**, 442–446.
- Zanich, A., Pascall, J. C., and Jones, R. (2003). Secreted epididymal glycoprotein 2D6 that binds to the sperm’s plasma membrane is a member of the β -defensin superfamily of pore-forming glycopeptides. *Biol. Reprod.* **69**, 1831–1842.
- Zapata, O., Ralston, J., Beltrán, C., Parys, J. B., Chen, J. L., Longo, F. J., and Darszon, A. (1997). Inositol triphosphate receptors in sea urchin sperm. *Zygote* **5**, 355–364.
- Zeng, W., Mak, D. O., Li, Q., Shin, D. M., Foskett, J. K., and Muallem, S. (2003). A new mode of Ca^{2+} signaling by G protein-coupled receptors: Gating of IP_3 receptor Ca^{2+} release channels by $\text{G}\beta\gamma$. *Curr. Biol.* **13**, 872–876.
- Zeng, Y., Clark, E. N., and Florman, H. M. (1995). Sperm membrane potential: Hyperpolarization during capacitation regulates zona pellucida-dependent acrosomal secretion. *Dev. Biol.* **171**, 554–563.
- Zeng, Y., Oberdorf, J. A., and Florman, H. M. (1996). pH regulation in mouse sperm: Identification of Na^+ -, Cl^- -, and HCO_3^- -dependent and arylaminobenzoate-dependent regulatory mechanisms and characterization of their roles in sperm capacitation. *Dev. Biol.* **173**, 510–520.
- Zhang, A. Y., Yi, F., Teggatz, E. G., Zou, A. P., and Li, P. L. (2004). Enhanced production and action of cyclic ADP-ribose during oxidative stress in small bovine coronary arterial smooth muscle. *Microvasc. Res.* **67**, 159–167.

- Zhang, J., Campbell, R. E., Ting, A. Y., and Tsien, R. Y. (2002). Creating new fluorescent probes for cell biology. *Nat. Rev. Mol. Cell. Biol.* **3**, 906–918.
- Zhou, C. X., Zhang, Y. L., Xiao, L., Zheng, M., Leung, K. M., Chan, M. Y., Lo, P. S., Tsang, L. L., Wong, H. Y., Ho, L. S., Chung, Y. W., and Chan, H. C. (2004). An epididymis-specific β -defensin is important for the initiation of sperm maturation. *Nat. Cell. Biol.* **6**, 458–464.
- Zhu, M. X., and Tang, J. (2004). TRPC channel interactions with calmodulin and IP₃ receptors. *Novartis Found. Symp.* **258**, 44–58; discussion 58–62, 98–102, 263–266.
- Zigler, K. S., and Lessios, H. A. (2003). Evolution of bindin in the pantropical sea urchin *Tripneustes*: Comparisons to bindin of other genera. *Mol. Biol. Evol.* **20**, 220–231.
- Zitt, C., Halaszovich, C. R., and Luckhoff, A. (2002). The TRP family of cation channels: Probing and advancing the concepts on receptor-activated calcium entry. *Prog. Neurobiol.* **66**, 243–264.
- Zuhlke, R. D., and Reuter, H. (1998). Ca²⁺-sensitive inactivation of L-type Ca²⁺ channels depends on multiple cytoplasmic amino acid sequences of the α_{1c} subunit. *Proc. Natl. Acad. Sci. USA* **95**, 3287–3294.
- Zuhlke, R. D., Pitt, G. S., Deisseroth, K., Tsien, R. W., and Reuter, H. (1999). Calmodulin supports both inactivation and facilitation of L-type calcium channels. *Nature* **399**, 159–162.

Genomic Imprinting: *Cis*-Acting Sequences and Regional Control

Bonnie Reinhart and J. Richard Chaillet

Department of Molecular Genetics and Biochemistry, University of Pittsburgh,
Pittsburgh, Pennsylvania 15208

This review explores the features of imprinted loci that have been uncovered by genetic experiments in the mouse. Imprinted genes are expressed from one parental allele and often contain parent-specific differences in DNA methylation within genomic regions known as differentially methylated domains (DMDs). The precise erasure, establishment, and propagation of methylation on the alleles of imprinted genes during development suggest that parental differences in methylation at DMD sequences are a fundamental distinguishing feature of imprinted loci. Furthermore, targeted mutations of many DMDs have shown that they are essential for the imprinting of single genes or large gene clusters. An essential role of DNA methylation in genomic imprinting is also shown by studies of methyltransferase-deficient embryos. Many of the DMDs known to be required for imprinting contain imprinted promoters, tandem repeats, and CpG-rich regions that may be important for regulating parent-specific gene expression.

KEY WORDS: Epigenetics, Genomic imprinting, DNA methylation, Differentially methylated domain (DMD), Tandem repeats, Chromatin. © 2005 Elsevier Inc.

I. Introduction

Normal mammalian development requires fertilization of an oocyte by a sperm to form a zygote. Each haploid gamete contributes almost an equal half of the genetic information to the developing offspring, with unequal sex chromosome contribution in male offspring being a notable exception. This

simplified view of parental inheritance suggests that the maternal and paternal genomes are equivalent, providing essentially identical information to their offspring. However, this notion has changed with the discovery of imprinted genes. Imprinted genes are recognized by a difference in expression between the maternal and paternal alleles. In the model imprinted locus, one parental allele is always expressed, while the opposite parental allele is always silenced. Because of the parent-specific expression of imprinted genes, the maternal and paternal genomes are not equivalent, even if the DNA sequences of the parental autosomes are the same.

The first observation of inequality between the parental chromosomes of a mammalian species arose during studies of the T^{hp} (hairpin-tail) allele in the mouse (Johnson, 1974). T^{hp} is a deletion within the T locus region of chromosome 17. Paternal inheritance of the T^{hp} allele led to decreased litter sizes, and adult mice inheriting the paternal T^{hp} allele had short or bent tails. In contrast, maternal inheritance of the T^{hp} allele was lethal and embryos inheriting the maternal T^{hp} allele were edematous with shortened, kinked tails. This disparity in phenotypes suggested that the T^{hp} allele behaved differently when inherited from the sperm or from the egg. A simple explanation for this observation is that the maternal allele of a gene within the T^{hp} region is expressed and the paternal allele of the same gene is silent. A gene with this difference in expression is now known as an imprinted gene.

Pronuclear transfer experiments performed in the early 1980s supported the existence of imprinted genes such as the one predicted to reside within the T^{hp} region of chromosome 17 (McGrath and Solter, 1984; Surani *et al.*, 1984). Pronuclear transfer between mouse zygotes before fusion of the maternal and paternal pronuclei allows the generation of zygotes containing two maternal pronuclei or two paternal pronuclei. Gynogenetic embryos that contained two maternal pronuclei were typically small and were able to develop to only the 25-somite stage. The extraembryonic tissues of gynogenetic embryos also developed poorly. In contrast, androgenetic embryos that contained two paternal pronuclei developed to only the eight-somite stage and showed enhanced extraembryonic tissue development. These experiments illustrated that an embryo must receive one pronucleus from each parent in order to be viable, and suggested that what is contributed to the embryo by the maternal pronucleus is different from what is contributed to the embryo by the paternal pronucleus. One likely reason for this difference is that some chromosomes provided by each parent are not equivalent in their developmental functions, even if their DNA sequences are identical. Some chromosomes are likely to contain imprinted genes that are required for embryonic development and are expressed from only one parental allele.

It could not be determined from the pronuclear transfer experiments where the presumed differences between the parental pronuclei resided, although the chromosomes were thought to contain the important parent-specific

differences. A series of elegant experiments that analyzed the phenotypes of mice with uniparental disomies of different autosomes clarified this issue (Cattanach and Kirk, 1985). For example, Cattanach and colleagues analyzed the phenotypes of mice with uniparental disomies of chromosome 11 or chromosome 13 [produced by intercrossing mice heterozygous for the Robertsonian translocation Rb(11.13)4Bnr]. Mice with a uniparental disomy of chromosome 13 were phenotypically normal, irrespective of the parental origin of the chromosome. In contrast, mice with a uniparental disomy of chromosome 11 had abnormal phenotypes. If both homologous chromosomes were inherited maternally (mUPD), mice were smaller than their littermates. In contrast, if both homologous chromosomes were inherited paternally (pUPD), mice were larger than their littermates. Importantly, uniparental disomies of many chromosomes were associated with abnormal phenotypes, including embryonic lethality. In many cases, mice with an mUPD had an abnormal phenotype different from that of mice with a pUPD of the same chromosome. These data identified the chromosomes as the location of the parent-specific pronuclear effect seen in pronuclear transfer experiments. Furthermore, the data supported the existence of imprinted genes, and narrowed the location of these genes to specific chromosomes or subchromosomal regions.

Many of the chromosomes predicted to contain imprinted genes on the basis of studies of chromosomal imbalances have since been shown to contain imprinted genes (Bartolomei *et al.*, 1991; Cattanach *et al.*, 1992; Kaneko-Ishino *et al.*, 1995). For example, the *Grb10* (*growth factor receptor-bound protein 10*) gene is located on proximal chromosome 11 and is maternally expressed (Miyoshi *et al.*, 1998). Disruption of *Grb10* on the maternal chromosome led to overgrowth of the embryo and placenta and resulted in mice that were larger than their littermates (Charalambous *et al.*, 2003). This result indicated that loss of expression of the imprinted *Grb10* gene may contribute to the overgrowth phenotype observed in mice inheriting two paternal copies of chromosome 11 (Cattanach and Kirk, 1985). More than 50 other imprinted genes have been identified in the mouse. A summary of many of the known imprinted genes can be found at <http://www.mgu.har.mrc.ac.uk/imprinting/imprinting.html>. These imprinted genes are expressed at a variety of different times, in different locations in the embryo, and frequently in extraembryonic tissues (Lucifero *et al.*, 2004).

The strict parent-specific expression of genes during fetal development indicates that the maternal and paternal alleles of imprinted genes remember whether they were derived from the egg or from the sperm. This suggests that imprints are established in the gametes, a time during development when the two parental genomes are found in different cells and are likely to be treated differently. Imprints established in the oocyte and sperm must then be perpetuated during each stage of postzygotic development, while the two

genomes reside in the same nucleus. This unique mode of inheritance also requires that imprints present on the maternal and paternal genomes be erased to allow the correct parent-specific information to be set up in the gametes. For instance, imprints passed from a mother to her son must be erased in his immature germ cells and paternal imprints must then be established in his gametes.

On the basis of this reasoning, there are constraints on the imprinting mechanism: parent-specific imprints must be erased in primordial germ cells (PGCs), established in the germ line, inherited through all postzygotic cell divisions, and influence gene expression. The continual need to erase and establish imprints through successive generations requires that the parental alleles of an imprinted locus be distinguished by an epigenetic modification that does not alter the DNA sequence. These types of modifications can include DNA cytosine methylation and histone modifications such as acetylation, phosphorylation, and methylation. Many lines of evidence indicate that DNA methylation is an excellent candidate for such a mark. This review highlights the important regulatory features of genomic imprinting with emphasis on the involvement of DNA methylation in this process.

II. Genomic Imprinting and DNA Methylation

A. Expectations of Methylation Imprints

For many imprinted genes, DNA methylation distinguishes the parental alleles. Parent-specific differences in DNA methylation at imprinted loci are located in genomic regions termed differentially methylated domains (DMDs). Methylation of mammalian DNA occurs at the 5-position of cytosine, almost exclusively within CpG dinucleotides (Fig. 1) (Bestor, 2000). Within a DMD most of the CpGs on one parental allele are methylated, and in the same region on the opposite allele most of the CpGs are unmethylated (Shemer *et al.*, 1997; Stoger *et al.*, 1993; Tremblay *et al.*, 1995). Outside of the DMD equivalent patterns of methylation are present on both parental alleles. The parent-specific methylation that is found at many imprinted loci suggests that differential DNA methylation may direct parent-specific imprinted expression.

Two essential requirements of genomic imprinting are fulfilled by the enzymatic reactions whereby DNA methylation patterns are created and maintained. DNA methylation in mammals occurs at a cytosine immediately 5' of a guanine (Bestor, 2000). A CpG dinucleotide on one DNA strand is base-paired with a CpG dinucleotide on the complementary strand of a duplex. This arrangement of methylatable CpG dinucleotides permits the

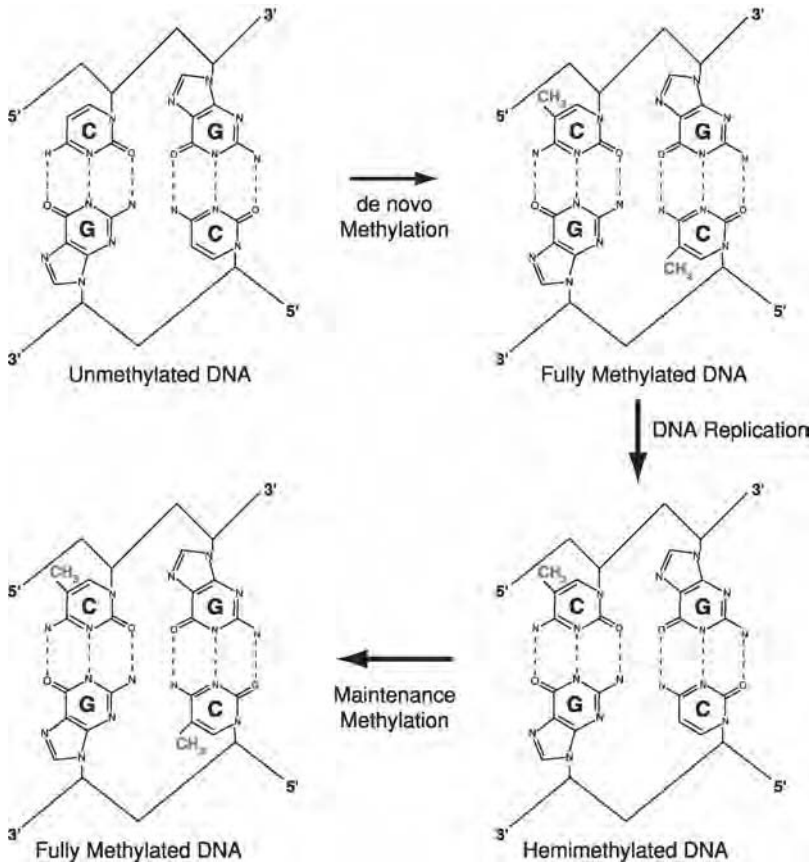


FIG. 1 *De novo* and maintenance methylation of cytosine in mammalian DNA. *De novo* methylation of unmethylated DNA (top left) occurs at the 5-position of cytosine, 5' of guanine (CpG dinucleotide), on both strands of the DNA double helix (fully methylated DNA, top right). After passage of the replication fork during DNA replication the newly synthesized DNA strand is unmethylated while the template strand of DNA is methylated (hemimethylated DNA, bottom right). The methylated DNA strand within the hemimethylated duplex serves as a template for maintenance methylation after DNA replication to form a fully methylated DNA duplex (bottom left). After successive rounds of replication without maintenance methylation the DNA is passively demethylated. (See also color insert.)

precise perpetuation of a methylation mark after semiconservative DNA replication. It is, therefore, an effective and accurate way of successively transmitting epigenetic information during all cell divisions, starting from the gametes and continuing indefinitely.

This sequence of enzymatic reactions begins with the establishment of cytosine methylation on unmethylated CpG dinucleotides through a process

termed *de novo* methylation (Fig. 1). *De novo* methylation occurs so that the CpG dinucleotides on both strands of the DNA duplex are methylated (fully methylated DNA). After passage of the replication machinery through a methylated region, the cytosines on the parent strand are methylated while the cytosines on the newly synthesized progeny strand are unmethylated (hemimethylated DNA). The methylated CpG dinucleotides on the parent strand can be used as a template to direct the methylation of the corresponding CpG dinucleotides on the unmethylated progeny strand. This process has been termed maintenance methylation (Wigler, 1981; Wigler *et al.*, 1981). Dnmt1 is the predominant methyltransferase protein in mammals. Dnmt1 preferentially methylates hemimethylated DNA *in vitro* and is localized to replication foci in mouse cells (Flynn *et al.*, 1996; Leonhardt *et al.*, 1992). These data are consistent with a requirement for Dnmt1 methyltransferase activity to maintain methylation on the hemimethylated DNA generated by DNA replication.

Another essential requirement of genomic imprinting is that parent-specific imprints are removed at some point in early germ cell development, before new parent-specific imprints are established in the male and female gametes. In principle, genomic DNA methylation could be removed by either an active or a passive mechanism. Active DNA demethylation describes the removal of methyl groups from cytosine bases by a demethylating enzyme or enzymes. Passive demethylation describes the loss of methylation that occurs by failing to maintain methylation after DNA replication. Genomic cytosine methylation is known to be lost in primordial germ cells (Kafri *et al.*, 1992; Monk *et al.*, 1987). This methylation loss may occur by passive demethylation because primordial germ cells undergo multiple cell divisions as they migrate to the genital ridge and populate the nascent germ lineage. However, it is not known whether the demethylation process in primordial germ cells is passive, active, or a combination of active and passive processes.

A final expectation of an epigenetic mark required for genomic imprinting is that it is able to influence gene expression. Inherited methylation on promoter sequences is commonly associated with inhibition of transcription. A simple view of what may occur at an imprinted locus is that one parental allele is methylated during gametogenesis, remains methylated in the embryo, and is consequently silenced. The opposite parental allele is not methylated during gametogenesis, remains unmethylated in the embryo, and is expressed. Predictably, for a given imprinted gene the presence of both an expressed allele and a silenced allele is lost in embryos with a uniparental disomy of the chromosome that contains the gene, in androgenetic embryos, and in gynogenetic embryos. In these cases the two resident alleles show no differences in expression or DNA methylation.

B. Differential Methylation at Imprinted Loci

To determine whether the DNA methylation of imprinted genes fulfills the aforementioned expectations of an epigenetic imprint the progression of DNA methylation on DMD sequences was measured during gametogenesis and embryogenesis. In primordial germ cells methylation is erased on all DMD sequences examined, regardless of whether it is maternal or paternal allele methylation. Analysis of methylation at the *Kcnq1*, *Peg3*, *Snrpn*, and *H19* genes showed that DMDs were demethylated in PGCs between days 10.5 and 13.5 (Davis *et al.*, 2000; Hajkova *et al.*, 2002; Sato *et al.*, 2003). Methylation on the maternally methylated *Igf2r* DMD was completely erased by day 11.5, and methylation on the paternally methylated *H19* DMD was completely erased by day 13.5 (Davis *et al.*, 2000; Sato *et al.*, 2003). Consistent with these findings, cloned embryos derived from single PGC nuclei possessed different developmental potentials (Lee *et al.*, 2002). Embryos generated with nuclei from PGCs on day 11.5, which retained most parental imprints, showed more advanced development than those generated with nuclei from day 12.5 or 13.5 PGCs, which showed loss of imprinting. The observation that parent-specific methylation is lost in PGCs supports the proposal that methylation at DMD sequences is erased in order to place parent-specific methylation patterns in the gametes.

Differential DNA methylation has been observed on many DMD sequences in mature gametes. For example, the DMDs of the endogenous *Igf2r* and *Snrpn* loci and the imprinted *RSVlgmyc* transgene were all highly methylated in mature oocytes and unmethylated in sperm (Chaillet *et al.*, 1991; Lucifero *et al.*, 2002). In contrast, the DMD of the *H19* locus was highly methylated in sperm and unmethylated in oocytes (Lucifero *et al.*, 2002; Tremblay *et al.*, 1995). The presence of parent-specific DMD methylation in mature germ cells lends support to the notion that gamete-specific methylation is completed at this time in order to mark the alleles of an imprinted gene just before their transmission to sons and daughters. The establishment of imprints must, therefore, occur between the loss of previous imprints in PGCs and the formation of gametes.

The exact time of maternal imprint establishment has been investigated by two different, rigorous approaches: the detailed measurement of DMD methylation patterns during oocyte growth, and the manipulation of the genome of parthenogenetic embryos. Experiments have shown that the *Snrpn* DMD is unmethylated in primary oocytes, 25% methylated in oocytes of 10-day-old mice, and completely methylated in mature MII oocytes (Lucifero *et al.*, 2002). These data suggest that acquisition of maternal-specific methylation occurs near the end of oocyte maturation, possibly in fully grown oocytes.

The observation that DMD methylation occurs by the time oocyte maturation is completed complemented observations from earlier studies that examined functional imprinting in parthenogenetic embryos. Parthenogenetic embryos that contained two genomes from fully grown oocytes died before day 10 of gestation (Kono *et al.*, 1996). These embryos lacked expression of the *Snrpn*, *Peg3*, *Peg1*, and *Igf2* imprinted genes, all normally paternally expressed. In contrast, embryos generated with one genome from a fully grown oocyte, and one genome from a less mature oocyte from a 10-day-old mouse, developed to day 13.5 and expressed the *Snrpn*, *Peg3*, *Peg1* genes (Kono *et al.*, 1996; Obata *et al.*, 1998). These studies suggest that the nongrowing oocyte genome is more "paternal-like" than the fully grown oocyte genome. The paternal-like phenotype of nongrowing oocytes is likely due to the absence of maternal imprints or, more specifically, the absence of DMD methylation on genes such as *Snrpn*, *Peg3*, and *Peg1*.

If gametic methylation patterns are epigenetic imprints they should be inherited after fertilization. Consistent with this hypothesis, DMD methylation patterns at several imprinted loci have been shown to be perpetuated in preimplantation embryos, during fetal development, and in the somatic tissues of the adult animal. Paternal-specific methylation at the *H19* locus was present in sperm and throughout embryonic development (Tremblay *et al.*, 1997; Warnecke *et al.*, 1998). Likewise, maternal-specific methylation at the *RSVlgmyc* transgene locus was detected after fertilization, during embryogenesis, and in the adult animal (Chaillet *et al.*, 1991). The maintenance of gamete-specific DMD methylation throughout development suggests that continually maintaining DMD methylation with each cell division is important to specify the identity of the maternal and paternal alleles on an imprinted gene. The maintenance of DMD methylation is significant when compared with the changing levels of genomic methylation observed on other DNA sequences (Fig. 2A).

The maintenance or persistence of DMD methylation contrasts with the general rearrangement of methylation patterns that occurs on the majority of genomic DNA. Importantly, after fertilization, during preimplantation development, global methylation levels of the mouse genome decrease dramatically (Kafri *et al.*, 1992; Monk *et al.*, 1987). Evidence indicates that the postzygotic loss of methylation from the paternal genome occurs rapidly, by a replication-independent mechanism, while the demethylation of the maternal genome occurs more slowly and likely by a passive process (Oswald *et al.*, 2000). By the preimplantation blastocyst stage of development genomic methylation levels are low. After implantation of the blastocyst stage embryo, high levels of methylation are once again established throughout the genome. The maintenance of DMD methylation during preimplantation

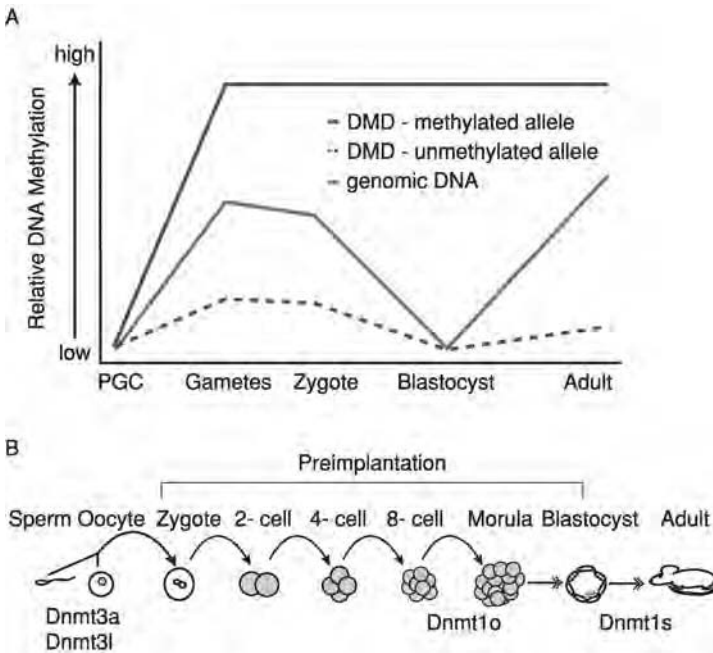


FIG. 2 Methylation levels throughout mouse development. (A) Relative genomic methylation (*y* axis) during various stages of mouse development (*x* axis). Red line indicates changes in global genomic methylation. Blue lines indicate changes in methylation at the DMDs of imprinted loci. The solid blue line indicates the methylated allele of the DMD and the dashed blue line indicates the unmethylated allele of the DMD. The methylated allele of the DMD is maintained during preimplantation development while the bulk of the genome undergoes demethylation. (B) The methyltransferases known to be required for *de novo* or maintenance methylation of imprinted gene methylation during mouse development are indicated. The methyltransferase proteins necessary for many stages of mouse preimplantation development remain unknown. (See also color insert.)

development, coincident with the rearrangement of methylation on the remainder of the genome, supports a role for DMD methylation in the perpetuation of an imprint.

The tight association between DMD methylation and genomic imprinting is strengthened by the effect of loss of DNA methylation on imprinted gene expression. A mutation in the *Dnmt1* methyltransferase gene resulted in drastically reduced genomic methylation in homozygous embryos (Li *et al.*, 1992). Loss of genomic DNA methylation in homozygous embryos led to a loss of imprinting at all loci tested, before the death of the embryos on embryonic day 9.5 (E9.5) (Li *et al.*, 1993). Loss of imprinting refers to

equivalent transcriptional behavior of maternal and paternal alleles, and can be due to activation of normally silenced alleles, or to silencing of normally active alleles at an imprinted locus. Although not shown in these experiments, a loss of methylation on DMD sequences at imprinted genes most likely occurred. The strong correlation between loss of methylation and loss of imprinting suggested that DMD methylation is absolutely essential for genomic imprinting.

C. Establishing and Maintaining Methylation Imprints

The establishment and continued perpetuation of DMD methylation should require the activity of methyltransferase proteins during gametogenesis and after each round of DNA synthesis (Fig. 2B). The Dnmt3a, Dnmt3b, and Dnmt3l proteins are expressed in the ovary and testis, and the expression levels of Dnmt3a and Dnmt3l increase at times coincident with establishment of methylation at DMDs during gametogenesis (La Salle *et al.*, 2004). The Dnmt3a and Dnmt3b proteins exhibit *de novo* methyltransferase activity and are prime candidates for the enzymes that establish methylation on DMD sequences (Hsieh, 1999; Okano *et al.*, 1999). Although the Dnmt3l protein (Dnmt3-like) does not possess methyltransferase activity, it colocalizes with Dnmt3a and Dnmt3b in transfected cells and stimulates the activity of Dnmt3a in a cell culture system (Aapola *et al.*, 2000, 2001; Chedin *et al.*, 2002; Hata *et al.*, 2002). These observations suggest that the Dnmt3 proteins may interact to regulate *de novo* methylation of DNA target sites.

The Dnmt3a methyltransferase enzyme and the Dnmt3l protein are required to establish maternal DMD methylation patterns during oogenesis (Bourc'his *et al.*, 2001; Hata *et al.*, 2002; Kaneda *et al.*, 2004). Homozygous *Dnmt3a*^{-/-} mice died at approximately 4 weeks of age and *Dnmt3l*^{-/-} mice were viable. To investigate a requirement for Dnmt3a in establishing genomic methylation, ovaries of a *Dnmt3a*^{-/-}, *Dnmt3b*^{+/-} female mouse were transplanted into a wild-type recipient and embryos were obtained (Hata *et al.*, 2002). These embryos exhibited loss of maternal methylation at several imprinted genes and maintained wild-type patterns of paternal methylation. Embryos derived from *Dnmt3l*^{-/-} homozygous female mice died at approximately E10.5, probably because of the absence of maternal imprints (Bourc'his *et al.*, 2001; Hata *et al.*, 2002). Maternal imprints were absent and paternal imprints were normal in embryos derived from *Dnmt3l*^{-/-} female mice. These experiments illustrate that Dnmt3a and Dnmt3l work together to establish methylation at the DMDs of maternally methylated imprinted genes.

Another approach has been taken to examine the requirement for Dnmt3a in imprint establishment. A conditional Dnmt3a mutant allele was generated (*Dnmt3a*^{2lox}). Cre-mediated deletion resulted in the elimination of all active Dnmt3a isoforms (*Dnmt3a*^{1lox}). This targeted mutation was used to investigate a requirement for Dnmt3a in establishment of maternal and paternal methylation at imprinted loci. To specifically eliminate Dnmt3a activity in primordial germ cells *Dnmt3a*^{2lox} mice were crossed to mice that expressed the Cre recombinase in primordial germ cells from E9.5 to late gestation [(TNAP)-Cre]. *Dnmt3a*^{2lox/1lox}, TNAP-Cre conditional mutant male and female mice showed efficient Cre-mediated deletion by E14.5. E10.5 embryos derived from conditional mutant female mice showed loss of maternal imprints at the *Snrpn*, *Igf2r*, and *Peg1* loci and retained imprints at the *H19* and *Rasgrf1* loci (Kaneda *et al.*, 2004). These results are consistent with the *Dnmt3a*^{-/-}, *Dnmt3b*^{+/-} ovary transplant experiments and confirm that the Dnmt3a methyltransferase is required for maternal imprint establishment.

The Dnmt3a and Dnmt3l proteins are also required for spermatogenesis and for the establishment of paternal methylation at certain DMDs. Homozygous *Dnmt3l*^{-/-} mutant male mice were viable but infertile, with reduced numbers of spermatogonia and no evidence of entry of these spermatogonia into meiosis (Aapola *et al.*, 2001; Bourc'his *et al.*, 2001; Hata *et al.*, 2002). *Dnmt3a*^{2lox/1lox}, TNAP-Cre conditional mutant male mice had reduced numbers of spermatogonia and no spermatids or spermatozoa (Kaneda *et al.*, 2004). Methylation at DMD sequences was examined in spermatogonia from *Dnmt3a* conditional mutant males and from *Dnmt3l*^{-/-} mutant males isolated by laser microdissection from histological sections of testes (Kaneda *et al.*, 2004). *Dnmt3a* conditional mutant males showed loss of methylation at the *H19* DMD and at the *Dlk1-Gtl2* IG-DMR. However, the *Rasgrf1* DMD remained normally methylated. The *Dnmt3l*^{-/-} mutant males also showed loss of methylation at *H19*, although wild-type levels of methylation were observed at both the *Dlk1-Gtl2* and *Rasgrf1* genes. The requirement for Dnmt3a and Dnmt3l is apparently gene specific in the male germ line, as different imprinted genes lose methylation in the two mutants. These data conclusively show that both Dnmt3a and Dnmt3l are required to establish the complete array of DMD methylation during spermatogenesis.

It has been well established that the Dnmt1 methyltransferase protein is the predominant maintenance methyltransferase in mammals (Flynn *et al.*, 1996; Leonhardt *et al.*, 1992). The Dnmt1s isoform of the Dnmt1 protein is present after implantation of the blastocyst stage embryo and is required for maintenance of methylation in somatic cells (Leonhardt *et al.*, 1992; Li *et al.*, 1992; Mertineit *et al.*, 1998). Dnmt1s is required for maintenance of

methylation at many genomic locations, including imprinted loci (Section II.B). However, because Dnmt1s is required for maintenance of general genomic methylation, the loss of this protein in embryos provides little information about how imprinted DMD methylation patterns are maintained. In contrast, the Dnmt1o isoform of the Dnmt1 protein is expressed in preimplantation embryos, and has been shown to have maintenance methyltransferase activity specific to DMDs (Howell *et al.*, 2001; Mertineit *et al.*, 1998).

The *Dnmt1*^{Δ1o} mutation specifically eliminates the oocyte-specific isoform of the Dnmt1 protein. Homozygous *Dnmt1*^{Δ1o/Δ1o} mutant mice were phenotypically normal. However, embryos derived from Dnmt1o-deficient oocytes (*Dnmt1*^{Δ1o/Δ1o}) died during the last third of gestation with the exception of an occasional surviving mouse (Howell *et al.*, 2001). Embryos generated from Dnmt1o-deficient oocytes showed no differences in the levels of global genomic methylation when compared with wild-type embryos. Interestingly, in E10.5 embryos half of the normally methylated alleles of imprinted genes were completely unmethylated. Loss of methylation was seen at DMDs that were normally maternally methylated and at DMDs that were normally paternally methylated. However, DMD methylation was established normally in Dnmt1o-deficient oocytes. These data demonstrate that the Dnmt1o methyltransferase is essential for maintenance of DMD methylation during preimplantation development.

Dnmt1o protein is synthesized in the oocyte but is localized to the nucleus only at the eight-cell stage of preimplantation development (Mertineit *et al.*, 1998). At every other preimplantation stage Dnmt1o is located in the cytoplasm. The unique pattern of methylation loss seen in Dnmt1o-deficient embryos and the unique nuclear-cytoplasmic trafficking of Dnmt1o during preimplantation development suggest that the protein is active only during the fourth S phase of preimplantation development. Absence of Dnmt1o maintenance methyltransferase activity at one cell cycle would result in the observed loss of methylation from half of the normally methylated alleles of imprinted genes. This evidence suggests that Dnmt1o is active only at the fourth S phase of preimplantation development; however, no candidate methyltransferase enzymes have been identified for the maintenance of methylation at the other preimplantation stages.

The experiments described above suggest that specific DNA methyltransferase proteins are required at different times in development to establish and maintain methylation at the DMDs of imprinted loci. Loss of DNA methyltransferase activity resulted in loss of DNA methylation at DMDs and corresponded to a loss of imprinting (activation of normally silenced alleles, or silencing of normally active alleles) at the imprinted loci tested. These data illustrate that establishment and maintenance of methylation are essential components of the imprinting mechanism.

III. Regional Control at Imprinted Gene Clusters

A. Imprinting at the Human Prader–Willi Syndrome Region

The Prader–Willi syndrome (PWS) is caused by disruption of wild-type gene expression in a defined region of human chromosome 15. This region is approximately 2 mb in size and contains several paternally expressed imprinted genes. Loss of paternal gene expression can be brought about in several ways including maternal UPD of chromosome 15 or paternal deletions on chromosome 15 (Nicholls and Knepper, 2001; Nicholls *et al.*, 1989). The shortest region of overlap (SRO) of many chromosome 15 deletions is a 4.3-kb genomic region that includes the promoter and first exon of the *SNRPN* gene (Ohta *et al.*, 1999). The PWS-SRO is essential for expression of the paternal allele of the *SNRPN* gene, and also for the expression of several other imprinted genes within this chromosomal domain. Accordingly, the 4.3-kb SRO has been termed the Prader-Willi syndrome-imprinting center (PWS-IC).

The PWS-IC overlaps a DMD within the *SNRPN* gene. The *SNRPN* DMD shows maternal-specific methylation in oocytes and in somatic cells (Geuns *et al.*, 2003; Glenn *et al.*, 1996). Overlap between the PWS-IC and the *SNRPN* DMD suggests that differential methylation patterns are involved in the regulation of imprinted gene expression. This idea is supported by studies showing that PWS patients can exhibit abnormal methylation at the imprinting center on the paternal allele without having identifiable deletions or mutations (Buiting *et al.*, 2003). The requirement of the PWS-IC (DMD) sequences for imprinting of multiple genes on human chromosome 15 highlights the importance of DMD sequences in genomic imprinting.

B. Primary and Secondary DMDs at Imprinted Gene Clusters

More than 50 imprinted genes exist in the mouse and are distributed among 12 different chromosomes. Much like the tight linkage of imprinted genes in the human PWS region, many imprinted genes in the mouse are arranged in clusters of two or more genes. This arrangement suggests the possibility of coordinate regulation of imprinted gene expression within a cluster, governed by IC and DMD sequences. When other imprinted gene clusters are carefully examined DMDs are indeed found. Frequently more than one DMD is found within one gene cluster. What are the roles of the multiple DMDs within an imprinted gene cluster? Do they represent distinct ICs, each controlling the expression of part of the cluster?

DMDs that possess an IC function also possess one important feature: they are established in the parental germ lines. Specifically, these DMDs show allele-specific methylation in the gametes and in somatic tissues and are referred to as primary DMDs. Establishment of a primary DMD in the germ line would allow for strict parent-of-origin specific gene expression. Other DMDs found within a gene cluster acquire their methylation postfertilization (secondary DMDs) (Hanel and Wevrick, 2001; Tremblay *et al.*, 1997). Methylation at secondary DMDs is often tightly linked to methylation at primary DMDs, and may develop during embryogenesis as a consequence of a *cis*-directed interaction with a primary DMD.

An example of an imprinted locus that contains multiple DMDs is the mouse *Igf2r* locus. *Igf2r* is maternally expressed and contains two clearly delineated differentially methylated domains (Stoger *et al.*, 1993). A paternally methylated DMD (DMD1) is located in the 5' region of the gene and contains the *Igf2r* promoter. A maternally methylated DMD (DMD2) is found within the second intron of the *Igf2r* gene. Analysis of DNA methylation at both DMDs has illustrated that maternal-specific methylation of DMD2 is established in the gametes (Stoger *et al.*, 1993). Paternal-specific methylation of DMD1 is not established until later in development. Moreover, it was found that DMD2 is required for maternal-specific expression of *Igf2r* and that the existence of DMD1 depends on the presence of DMD2 (Wutz *et al.*, 2001; Zwart *et al.*, 2001) (described in Section III.D). These findings illustrate that methylation of DMD1 and DMD2 may be connected and that there may be a distinction between primary and secondary DMDs that relates to their role in regulating gene expression.

Evidence obtained from studies of the mouse *H19* and *Igf2* loci also suggests that the methylation of primary and secondary DMDs may be connected. *H19* is maternally expressed and contains a paternally methylated DMD -2 to -4 kb 5' of its transcription start site (Bartolomei *et al.*, 1991; Tremblay *et al.*, 1997). Paternal-specific methylation in this region is established in the germ line. The paternally expressed *Igf2* gene is located 90 kb from *H19* and has not been shown to contain a primary DMD. Targeted deletion studies have demonstrated that the *H19* DMD is required for maternal-specific *H19* expression and for paternal-specific expression of the *Igf2* gene (Thorvaldsen *et al.*, 1998) (Section III.D). Interestingly, it has been shown that the *H19* DMD may be required for the acquisition of methylation at two paternally methylated secondary DMDs within the *Igf2* locus (Lopes *et al.*, 2003). In the absence of the *H19* DMD, the *Igf2* DMDs were no longer clearly differentially methylated. These data suggest that establishment of methylation at a primary DMD is necessary to establish methylation at a secondary DMD, and that these secondary epigenetic changes in turn are required for gene expression.

Secondary changes in DNA methylation may exist at other imprinted gene clusters. For example, at the *Dlk1-Gtl2* imprinted gene cluster a paternally methylated DMD (IG-DMR) upstream of the *Gtl2* gene is established in the gametes. At the same gene cluster a paternally methylated DMD within the *Dlk1* gene does not become methylated until later in development, in the embryo (Takada *et al.*, 2002). The *Gtl2* and *Dlk1* genes are located approximately 80 kb apart on mouse chromosome 12 and are regulated by the primary DMD upstream of *Gtl2* (Lin *et al.*, 2003) (described in Section III.D). Interestingly, methylation of the *Dlk1* DMD is abolished in the absence of the *Gtl2* DMD. These observations raise the possibility that the expression of genes within a cluster is coordinately regulated through one primary DMD and related secondary DMDs.

C. Structural Features of DMDs

The connection between DMDs and imprinted genes has been elucidated, in part, by genetic experiments in the mouse. The well-defined primary DMDs in the mouse genome are described in Table I. These DMDs were identified by the presence of clear differences in methylation in somatic cells and in the germ line. Many of these DMD sequences have been deleted by targeted mutagenesis in the mouse and these experiments have confirmed that DMDs are an important element in the control of genomic imprinting.

DMDs can be broadly separated into two categories: those that are methylated on the maternal allele and those that are methylated on the paternal allele. The sequences within both types of DMDs have several possible functions at imprinted genes. They may be required to establish differential methylation in the germ line, maintain their differential methylation during development, or regulate gene expression. To identify the DMD sequences involved in these, and possibly other, imprinting events, it is first important to compare DMDs from a number of imprinted genes of a given species to uncover similar structural features.

The mouse *Snrpn*, *Kcnq1*, and *Igf2r* loci contain primary DMDs, in all of which methylation is established in the germ line and then inherited (Table I) (Shemer *et al.*, 1997; Smilnich *et al.*, 1999; Stoger *et al.*, 1993). Interestingly, there is no apparent similarity in DNA sequence among the DMDs of these genes. Nevertheless, they do possess many common features (Fig. 3A–C). For instance, the *Snrpn*, *Kcnq1*, and *Igf2r* DMDs each contain a paternally expressed promoter. The *Snrpn* DMD contains the promoter for the paternally expressed *Snrpn* gene (Shemer *et al.*, 1997). The *Igf2r* DMD2 is located within the second intron of the maternally expressed *Igf2r* gene, and contains the promoter for the *Air* untranslated RNA. *Air* is synthesized in the opposite direction to transcription of the normal *Igf2r* transcript (Stoger

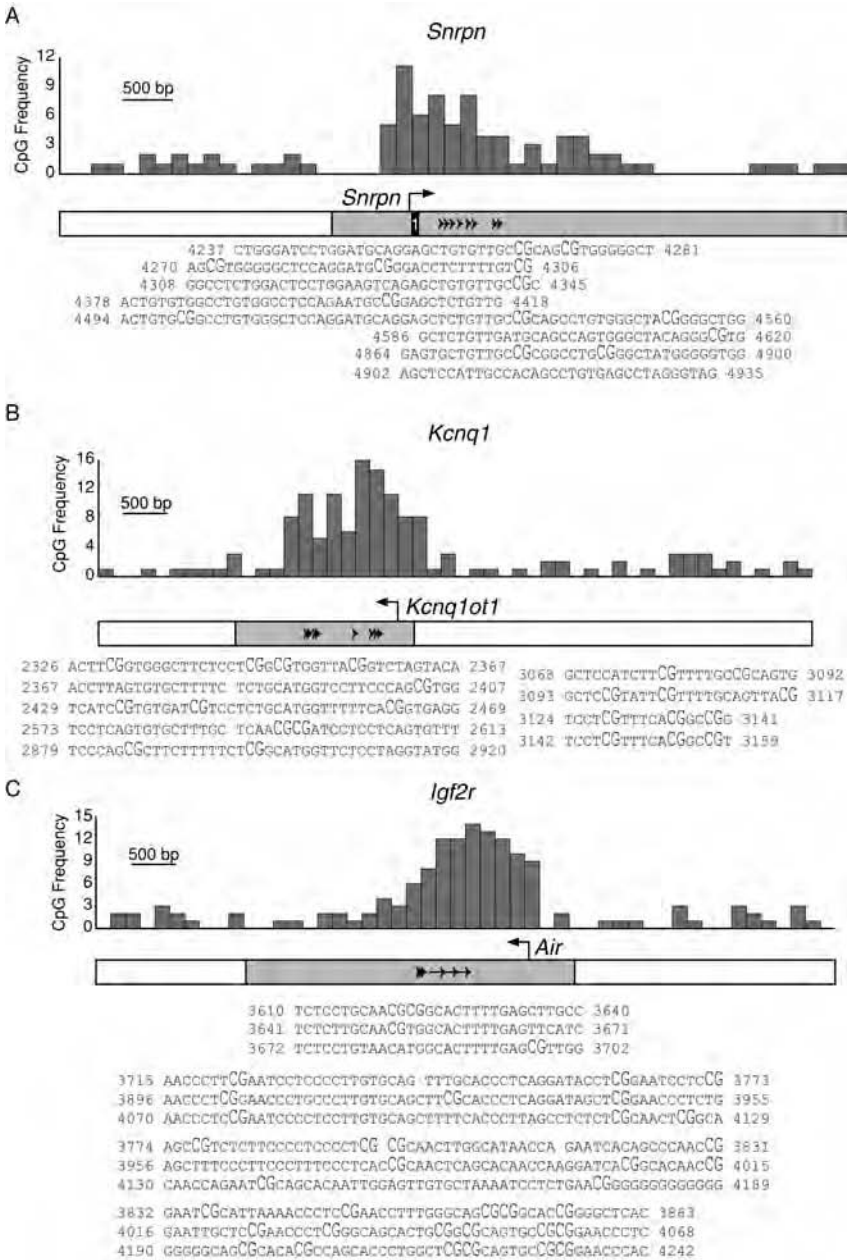


FIG. 3 Features of the *Snrpn*, *Igf2r*, and *Kcnq1* maternally methylated DMDs. For each panel the schematic represents the genomic region of each locus [(A) *Snrpn*; (B) *Kcnq1*; (C) *Igf2r*] as an open rectangle; the DMD within the sequence is shown as a shaded rectangle. Tandem repeats

et al., 1993; Wutz *et al.*, 1997). Finally, the *Kcnq1* DMD is located within intron 10 of the maternally expressed *Kcnq1* gene and contains the promoter for the *Kcnq1ot1* untranslated RNA. *Kcnq1ot1* is paternally expressed and is synthesized in the opposite direction of normal *Kcnq1* transcription (Smilnich *et al.*, 1999). The presence of an imprinted promoter within each DMD suggests that transcription originating within the DMD is required for imprinting.

TABLE I
Primary Differentially Methylated Domains

Primary DMD ^a	Gamete-specific methylation	DMD deletion ^b	Ref. ^c
<i>Snrpn</i>	Maternal	LOI <i>Snrpn</i> , <i>Ipw</i> , <i>Ndn</i>	1–3
<i>Kcnq1</i>	Maternal	LOI <i>Kcnq1</i> , <i>Tssc3</i> , <i>Slc22a11</i> , <i>Tssc4</i> , <i>Ascl2</i> , <i>Kcnq1ot1</i> , <i>Cdkn1c</i>	4, 5
<i>Igf2r</i>	Maternal	LOI <i>Igf2r</i> , <i>Air</i> , <i>Slc22a2</i> , <i>Slc22a3</i>	3, 6, 7
<i>H19</i>	Paternal	LOI <i>H19</i> , <i>Igf2</i>	3, 8, 9
<i>Rasgrf1</i>	Paternal	LOI <i>Rasgrf1</i>	10, 11
<i>Gtl2-Dlk1</i>	Paternal	LOI <i>Gtl2</i> , <i>Dlk1</i> , <i>Dio3</i> , <i>Rtl1</i>	12, 13
<i>Gnas</i>	Maternal	ND	14
<i>Nest-as-Gnasx1</i>	Maternal	ND	15
<i>Peg3</i>	Maternal	ND	3
<i>Peg1/Mest</i>	Maternal	ND	3, 16
<i>Peg10</i>	Maternal	ND	17

^aDifferentially methylated domains (DMDs) are indicated by the closest imprinted gene.

^bDeletions include DMD sequences and, in some cases, surrounding genomic sequence. Effects described refer to inheritance of the DMD deletion on the unmethylated parental chromosome (LOI, loss of imprinting).

^cReferences: (1) Bielinska *et al.*, 2000; (2) Shemer *et al.*, 1997; (3) Lucifero *et al.*, 2002; (4) Fitzpatrick *et al.*, 2002; (5) Smilnich *et al.*, 1999; (6) Stoger *et al.*, 1993; (7) Wutz *et al.*, 2001; (8) Thorvaldsen *et al.*, 1998; (9) Tremblay *et al.*, 1995; (10) Shibata *et al.*, 1998; (11) Yoon *et al.*, 2002; (12) Lin *et al.*, 2003; (13) Takada *et al.*, 2002; (14) Liu *et al.*, 2000; (15) Coombes *et al.*, 2003; (16) Lefebvre *et al.*, 1997; (17) Ono *et al.*, 2003.

are shown as black arrowheads and the sequence of each unit copy of the repeat is listed below (numbers are based on the beginning of the pictured sequence and CpG dinucleotides are raised compared with the rest of the sequence). Arrows indicate transcription start sites. The graph above each schematic depicts the CpG frequency (y axis) across the genomic sequence (x axis); each bar represents the number of CpGs in 1/50th of the sequence.

Another feature that is common to all three maternally methylated DMDs is the prominent presence of tandem repeats (Gabriel *et al.*, 1998; Neumann *et al.*, 1995; Smilnich *et al.*, 1999). The tandem repeats within the three DMDs do not share sequence similarity, but they do share other distinct similarities. The repeats are imperfect repeats, with the unit copies ranging in size from 18 to 170 bp. In addition, each unit copy of a tandem repeat contains one or more CpGs that have higher average methylation on maternal alleles than on paternal alleles. Interestingly, each tandem repeat region is located within an intron, downstream of at least one imprinted promoter. The *Igf2r* and *Kcnq1* repeats are also located downstream of an oppositely imprinted promoter. The presence of tandem repeats within each DMD suggests that these sequences are required for a specific imprinting function.

When compared with the surrounding gene sequence the *Snrpn*, *Kcnq1*, and *Igf2r* DMDs all include sequences rich in CpGs that can be defined as CpG islands. In each DMD the CpG-rich region includes the promoter and tandem repeat sequences described above. The CpGs within these regions are targets of methylation on the maternal allele and are protected from methylation on the paternal allele. The CpG-rich sequences may perform a direct function in methylation acquisition and maintenance, or they may be merely carriers of the requisite methylation.

The paternally methylated DMDs of the *H19* and *Dlk1-Gtl2* loci do not share many common features with the maternally methylated DMDs described above (Fig. 4A and B). First, their DMDs do not contain imprinted promoters. In fact, both DMDs are located some distance 5' of the closest imprinted promoter. The *H19* DMD is located 2 to 4 kb upstream of the transcription start site of the *H19* promoter (Tremblay *et al.*, 1997). The DMD of the *Dlk1-Gtl2* imprinted region (IG-DMR) is located 10 to 15 kb 5' of the *Gtl2* locus (Takada *et al.*, 2002). This is clearly one structural difference between the two types of DMDs and this difference may suggest that promoter activity may be necessary to generate a maternally imprinted gene.

Also, the presence of tandem repeats is not consistently found within paternally methylated DMDs. The *Dlk1-Gtl2* DMD contains tandem repeats. Like the tandem repeats seen at the maternally methylated DMDs, the tandem repeats within the *Dlk1-Gtl2* DMD are 25–40 bp in size and contain multiple CpG dinucleotides. The *H19* DMD does not contain tandem repeats. However, a 30-bp repeated sequence is found 5' of the DMD and a G-rich repetitive element is located 3' of the DMD. One notable difference between the repeats 5' of the *H19* DMD and the repeats within the DMDs described above is that the repeats associated with the *H19* DMD do not contain many CpG dinucleotides. These differences in DMD organization may indicate functional differences in the way imprinting is regulated among different paternally methylated imprinted genes. This

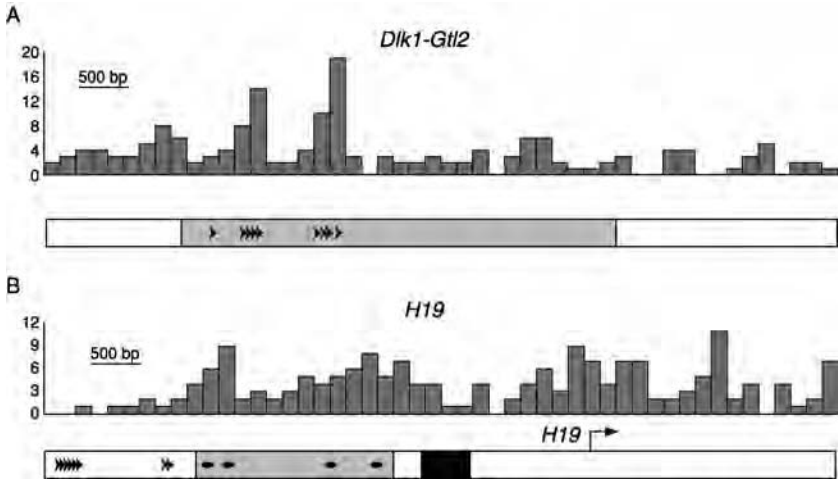


FIG. 4 Features of the *Dlk1-Gtl2* and *H19* paternally methylated DMDs. Schematic representations of the *Dlk1-Gtl2* (A) and *H19* (B) genomic regions. Descriptions are as in Fig. 3, with the addition of a G-rich repetitive region (solid rectangle) and CTCF-binding sites (solid ovals) in (B).

idea is supported by the variation in methylation loss seen among the *H19*, *Rasgrf1*, and *Gtl2* paternally methylated imprinted genes examined in spermatogonia of *Dnmt3a* and *Dnmt3l* mutant male mice (Kaneda *et al.*, 2004).

Like the maternally methylated DMDs described above, the *H19* and *Dlk1-Gtl2* DMDs each have regions rich in CpG dinucleotides. As seen at the maternally methylated DMDs, the CpG-rich region of the *Dlk1-Gtl2* DMD overlaps with its repetitive sequences. The CpG-rich region of the *H19* DMD has no apparent direct repeats. Four CTCF (CCCTC-binding factor) protein-binding sites are present within the CpG-rich region of the *H19* DMD, but at scattered locations rather than tandemly repeated (Hark *et al.*, 2000). These CTCF-binding sites are known to be involved in methylation-dependent imprinted gene expression (Section III.D). Every CpG within the CpG-rich DMD region is targeted for methylation on the paternal allele during specific times in development.

Two general types of experiments can test the role of DMDs or selected DMD sequences in genomic imprinting. Deletion experiments targeted at endogenous imprinted loci can test the requirement of specific sequences within a DMD for genomic imprinting. Mouse transgenes provide the ability to test DMD sequences for imprinting functions outside of their endogenous genomic context. Together these types of studies have begun to shed light on the requirement for specific DMD sequences in the imprinting process.

D. DMD Sequences Required for Imprinted Gene Expression

The PWS gene cluster on human chromosome 15 contains an IC that is essential for the imprinting of a 2-mb gene cluster, and corresponds to the DMD of the *SNRPN* gene (Section III.A). The arrangement of genes within the PWS gene cluster is conserved in a region on mouse chromosome 7. Several paternally expressed imprinted genes are located in the mouse PWS cluster. The mouse *Snrpn* gene contains a maternally methylated DMD that is differentially methylated in the gametes and in somatic cells (Section II.B). This DMD includes the promoter and first exon of the *Snrpn* gene. Because of the similarities observed in organization of this gene cluster in the mouse and in the human, numerous mutations have been generated in the vicinity of the mouse *Snrpn* locus to gain a better understanding of the regulation of imprinted genes in this region (Fig. 5A).

Studies have shown that removal of specific genomic sequence from the *Snrpn* locus alters *Snrpn* expression and expression of other imprinted genes within the same cluster. For example, a 42-kb deletion, encompassing 23 kb of sequence upstream of the *Snrpn* transcription start site and exons 1 through 6 of the *Snrpn* gene, altered the expression of several imprinted genes (Yang *et al.*, 1998). The *Snrpn*, *Zfp127*, *Ndn*, and *Ipw* genes, all normally paternally expressed, were silenced when the deletion was inherited

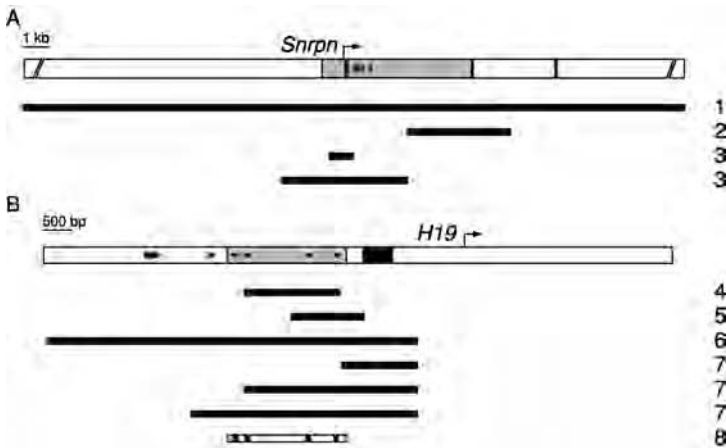


FIG. 5 Mutational analyses at the *Snrpn* and *H19* imprinted mouse loci. The schematics of the *Snrpn* (A) and *H19* (B) loci are enlargements of those shown in Figs. 3 and 4, respectively. Solid bars below each diagram represent the genomic regions targeted for mutation in the references listed to the right (list is not all-inclusive). References: (1) Yang *et al.*, 1998; (2) Tsai *et al.*, 1999; (3) Bressler *et al.*, 2001; (4) Thorvaldsen *et al.*, 1998; (5) Drewell *et al.*, 2000; (6) Srivastava *et al.*, 2000; (7) Thorvaldsen *et al.*, 2002; (8) Schoenherr *et al.*, 2003.

through the paternal germ line. Furthermore, loss of expression of the *Zfp127* and *Ndn* genes was associated with altered methylation at the secondary DMDs of each gene (Bielinska *et al.*, 2000). Thus, deletion of the 5' region of the *Snrpn* gene, including the primary DMD, abolished imprinting of genes located over a 2-mb region.

Additional information regarding the sequences required to imprint the *Snrpn* cluster has been obtained by small deletions within the 5' region of the *Snrpn* gene. Deletion of the 3' end of the DMD and exon 2 of the *Snrpn* gene resulted in loss of expression of the full-length *Snrpn* transcript, but was not an imprinting mutation (Tsai *et al.*, 1999). Also, experiments suggest that the *Snrpn* promoter is not required for imprinting. Deletion of a 900-bp region that contained the *Snrpn* promoter did not alter imprinting (Bressler *et al.*, 2001). However, a 4.8-kb deletion that contained the *Snrpn* promoter and tandem repeats altered imprinted gene expression within the cluster. The 4.8-kb deletion resulted in a loss of imprinting after inheritance through the paternal germ line (Bressler *et al.*, 2001). Inheritance of the same deletion through the maternal germ line had no effect. That is, maternal alleles of imprinted genes remained silent. Taken together, these experiments suggest that whereas the promoter sequences are dispensable for imprinting, the tandem repeat sequences within the DMD may be functionally important to imprint the gene cluster.

Deletion of primary DMD sequences at other imprinted gene clusters has been shown to affect expression of imprinted genes. The mouse *Igf2r* gene is located within an imprinted gene cluster on chromosome 17 (Zwart *et al.*, 2001). The *Igf2r* gene contains a maternally methylated DMD within its second intron (DMD2) that is methylated in the oocyte and unmethylated in sperm (Sections II.B and III.B). The DMD houses the promoter for the untranslated *Air* RNA that shows paternal-specific gene expression. The *Igf2r*, *Slc22a2*, and *Slc22a3* genes in the same imprinted gene cluster all show maternal-specific gene expression (Wutz *et al.*, 2001; Zwart *et al.*, 2001). Deletion of DMD2 from the normally unmethylated paternal chromosome abolished imprinting, whereas deletion of DMD2 from the normally methylated maternal chromosome did not affect imprinting (Wutz *et al.*, 2001). Specifically, the paternal deletion of DMD2 resulted in loss of *Air* expression and in biallelic expression of *Igf2r*, *Slc22a2*, and *Slc22a3*. Similar to what was seen at the *Snrpn* cluster, these data suggest that DMD sequences are essential for imprinting.

The *Igf2r* DMD2 contains both the promoter for the *Air* transcript and tandem repeats. The *Air* transcript overlaps the *Igf2r* transcript and may be involved in regulation of *Igf2r* imprinting. To address the requirement for the antisense transcript in genomic imprinting, the *Air* transcript was truncated at the downstream border of the DMD (Sleutels *et al.*, 2002). Inheritance of the altered allele on the expressed paternal chromosome resulted in a loss

of imprinting. The *Igf2r*, *Slc22a2*, and *Slc22a3* genes were no longer paternally silenced on the altered chromosome. In contrast, the mutation did not affect imprinting of the *Air* transcript. The *Air* transcript remained silent and the DMD2 sequences remained maternally methylated. These experiments indicate that complete and normal transcription from the *Air* promoter is required for long-range regulation of imprinted gene expression. However, these experiments also suggest that the full-length antisense transcript is not required to establish or maintain *Air* differential methylation or expression.

Another cluster of genes appears to be regulated in a manner similar to those within the *Igf2r* gene cluster. The *Kcnq1* gene has a maternally methylated DMD that contains the *Kcnq1ot1* antisense promoter and tandem repeats (Smilnich *et al.*, 1999). *Kcnq1* is located on mouse chromosome 7 in a large gene cluster containing at least six other imprinted genes. Deletion of the *Kcnq1* DMD, including the *Kcnq1ot1* promoter and tandem repeats, abolished imprinting at the gene cluster (Fitzpatrick *et al.*, 2002). Paternal inheritance of the DMD deletion resulted in loss of *Kcnq1ot1* expression and biallelic expression of the other genes within the cluster. The same deletion inherited on the maternal chromosome had no effect on gene expression. As seen with *Snrpn* and *Igf2r* deletion studies, these data suggest a function for DMD sequences (including the promoter and tandem repeats) in genomic imprinting.

The paternally expressed *Dlk1* gene and the maternally expressed noncoding RNA *Gtl2* are located approximately 80 kb apart within a 1-mb gene cluster on mouse chromosome 12 that also includes the paternally expressed *Rtl1* and *Dio3* genes (Schmidt *et al.*, 2000). The 5-kb DMD located between the two genes includes a CpG-rich region and tandem repeats. This region is highly methylated in sperm and unmethylated in oocytes (Takada *et al.*, 2002). Experiments have shown that the 5-kb primary DMD 5' of *Gtl2* is required for imprinting at this gene cluster (Lin *et al.*, 2003). Inheritance of 4.5-kb DMD deletion through the maternal germ line was lethal after embryonic day 16. Embryos inheriting the deletion on the maternal chromosome did not express *Gtl2* and biallelically expressed *Dlk1*, *Rtl1*, and *Dio3*. In contrast, inheritance of the same deletion on the paternal chromosome had no effect. Thus, removal of the primary DMD from the normally unmethylated parental chromosome eliminated imprinting for genes in a 1-mb gene region. The deleted region contained the CpG-rich tandem repeats of the DMD and had similar effects to those observed after deletion of the maternally methylated DMDs described above.

The experiments described above highlight the existence of coordinate imprinted gene expression within gene clusters and suggest that DMD sequences are an essential component of the imprinting mechanism. Deletion of the unmethylated DMD sequence had an effect on gene expression, but removal of the methylated DMD sequence did not affect gene expression.

These data suggest that the unmethylated sequences have a particular function and that methylation is normally present on one allele of the DMD to abrogate that function. In each case the effect of DMD deletion or methylation on gene expression at each gene cluster is different. This suggests that each gene cluster has a unique way in which its DMD influences gene expression. Exactly how DMD sequences are involved in directing imprinted gene expression, and how the removal of such small sequences can affect the expression of genes several hundred kilobases away, remain to be clarified.

The maternally expressed *H19* gene is located on chromosome 7, 90 kb from the paternally expressed *Igf2* gene. Both genes share enhancers located 3' of both *H19* and *Igf2* (Leighton *et al.*, 1995). Proceeding in the 5' direction away from the *H19* transcribed region there is a 461-bp G-rich repetitive element (-1.2 to -1.7 kb), a paternally methylated DMD containing four CTCF-binding sites (-2 to -4 kb), and multiple copies of a tandem repeat (-5 to -6 kb) (Fig. 5B). Extensive targeted deletion studies have demonstrated that among these different elements it is the 2-kb DMD that is required for maternal-specific *H19* expression and for paternal-specific expression of the *Igf2* gene.

A deletion from 2.1 to 3.7 kb 5' of the *H19* transcription start site resulted in a loss of imprinting (Thorvaldsen *et al.*, 1998). This deletion removed 1.6 kb of the 2-kb DMD, including three of the four CTCF-binding sites. When inherited through the paternal germ line this deletion led to 60% activation of the normally silent *H19* allele and 66% reduction in expression of the normally active *Igf2* allele. Inheritance of the same deletion through the maternal germ line led to 50% reduction in *H19* expression from the normally active allele and 33% activation of the normally silent *Igf2* allele. In a follow-up experiment all four CTCF-binding sites were removed. The addition of extra sequence to the deleted region did not enhance the effect of the DMD deletion on gene expression (Thorvaldsen *et al.*, 2002). Also, deletion of the G-rich repetitive element did not affect imprinted expression from the two genes, and deletion of both the DMD and the G-rich repetitive element had no increased effect. These data illustrate the coordinate expression of *H19* and *Igf2* and show that removal of the DMD, including the CTCF-binding sites, but not the G-rich repetitive element, eliminates monoallelic expression of both genes.

A more extensive deletion was generated to conditionally delete the sequence located 7 to 0.8 kb 5' of the *H19* transcription start site (Srivastava *et al.*, 2000). This deletion includes the entire DMD, G-rich repetitive element, and the 5' tandem repeats. If this region was deleted in the germ line and inherited paternally the normally silent paternal *H19* allele was expressed. This result is similar to the result observed with the smaller DMD deletion. If the deletion occurred in the zygote and was inherited paternally the normally silent paternal *H19* allele was expressed. However,

H19 expression was not affected if the sequences were deleted from the paternal allele in terminally differentiated skeletal and cardiac muscle cells. Interestingly, deletion of the DMD in somatic cells late in development still resulted in loss of *Igf2* imprinting. These experiments showed that increasing the size of the deletion did not affect the extent of the expression differences seen for *H19* and *Igf2*. However, the timing of the deletion was critical for its effect. The DMD must be present in the germ line and zygote for proper imprinting. However, if the DMD is removed late in development monoallelic *H19* expression still occurs, but monoallelic *Igf2* expression is lost.

Other targeted deletions of portions of the *H19* DMD have shown different effects. A deletion that removed sequences 1.7 to 2.9 kb 5' of the *H19* transcription start site had specific effects on *H19* expression, but did not affect *Igf2* expression (Drewell *et al.*, 2000). This region includes two CTCF-binding sites at the 3' end of the DMD. Paternal inheritance of this deletion resulted in 50% activation of the normally silent *H19* allele, while maternal inheritance showed wild-type expression. Importantly, this deletion did not affect paternal-specific methylation of the DMD and did not affect *Igf2* expression. These data suggest that this sequence acts as a silencer specific to *H19*. These data also illustrate that although imprinted expression is coordinated between the two genes, specific sequences are required for precise expression of each gene individually.

The functional importance of CTCF binding for *H19* and *Igf2* imprinting has been investigated. Binding of CTCF to sites in the *H19* DMD was shown to be methylation sensitive. Furthermore, when the *H19* DMD was artificially positioned between an enhancer and a promoter, CTCF binding to the DMD blocked the enhancer from activating the promoter (Bell and Felsenfeld, 2000; Hark *et al.*, 2000). The CTCF-binding sites within the *H19* DMD are located between enhancers downstream of *H19* and the promoter of the *Igf2* gene. The methylation-sensitive enhancer-blocking properties of CTCF suggest that CTCF, when bound to the unmethylated *H19* DMD on the maternal chromosome, acts as a boundary element, blocking the *Igf2* promoter from enhancers downstream of *H19* and silencing gene expression. Consistent with this hypothesis, the absence of the *H19* DMD (and therefore the CTCF-binding sites) on the maternal chromosome activated the normally silent *Igf2* allele. These studies illustrate that regulation of imprinted expression at the *H19* and *Igf2* loci requires the presence of differential methylation and CTCF-binding sites found within the DMD.

The importance of the CTCF-binding sites in the control of imprinting has been more closely scrutinized. Point mutations were generated at all four CTCF-binding sites that precluded CTCF binding (Schoenherr *et al.*, 2003). When the four CTCF-binding sites were mutated on the maternal allele *Igf2* silencing and *H19* expression were both disrupted. Interestingly, in neonatal

tissues the mutated maternal allele showed increased DNA methylation. The mutant DMD was not methylated in oocytes and showed little methylation in blastocysts heterozygous for the maternal mutation. No disturbances were noted in methylation on the mutated paternal allele. This suggests that CTCF is not only involved in imprinting at the level of gene expression, but is also involved in regulation of differential methylation after preimplantation. CTCF-binding sites are required to maintain an unmethylated state on the maternal allele after the preimplantation blastocyst stage of development.

E. Study of DMD Sequences Using Mouse Transgenes

Targeted deletion experiments at endogenous imprinted loci clearly illustrate that small DNA sequence elements can be identified at imprinted loci that are required for genomic imprinting (Section III.D). These elements include the gamete-derived DMDs of many imprinted loci. Moreover, such studies suggest that specific features (including CTCF-binding sites or tandem repeat sequences) may be required for distinct functions in the imprinting process. However, these studies cannot easily define what combination of features is sufficient to generate an imprinted locus. Mouse transgenes have been used to address these issues.

To determine the minimal sequence information needed to create an imprint, transgenes have been designed using combinations of endogenous sequences in an attempt to generate an imprinted locus. These experiments shared several common findings. One important conclusion was that DMD sequences alone were not imprinted. For example, a transgene composed of the *H19* DMD and 4 kb of genomic flanking sequence was not imprinted and a 3-kb transgene containing only the *Igf2r* DMD2 was not imprinted (Cranston *et al.*, 2001; Wutz *et al.*, 1997). However, transgenes composed of larger amounts of genomic sequence were more often imprinted. Transgenes containing 14 to 16 kb of *H19* genomic sequence, including the DMD, were imprinted although not in an entirely consistent way (Cranston *et al.*, 2001; Elson and Bartolomei, 1997). When transgenes were constructed with large regions of genomic sequence surrounding an endogenous imprinted locus, consistent transgene imprinting resulted. A transgene composed of 130 kb of genomic sequence surrounding the *H19* DMD was consistently imprinted and a 300-kb transgene containing the *Igf2r* DMD was imprinted (Ainscough *et al.*, 1997; Wutz *et al.*, 1997). Interestingly, a 4-kb deletion containing DMD2 abolished imprinting of the 300-kb *Igf2r* transgene. These experiments suggest that a large contiguous genomic sequence, or multiple elements within and surrounding an endogenous imprinted locus, are essential for imprinting. Also, they confirm the requirement for a DMD in

genomic imprinting. Unfortunately, the inability to generate small, consistently imprinted transgenes makes a fine-scale analysis of *cis*-acting sequences difficult.

Valuable information about genomic imprinting has been gained from the *RSVlgmyc* imprinted transgene. The *RSVlgmyc* mouse transgene was the first gene identified that exhibited the characteristics of an imprinted locus (Swain *et al.*, 1987). The *RSVlgmyc* transgene is composed of pBR322 vector sequences, Rous sarcoma virus (RSV) long terminal repeat (LTR) sequences, and a fusion gene from the S107 mouse plasmacytoma cell line (translocation of the *c-myc* gene into the *immunoglobulin α heavy chain* locus). Expression of a transgene-specific *c-myc* transcript was observed after paternal inheritance of *RSVlgmyc*. No expression was detected from the same transgene after maternal inheritance. Correspondingly, *RSVlgmyc* was highly methylated when inherited through the maternal germ line, and undermethylated when inherited through the paternal germ line. Parent-specific expression and methylation of the transgene were observed at all sites of integration (Chaillet *et al.*, 1995). The consistent imprinting of the transgene illustrates that its imprinting is controlled by sequence elements contained within the transgene and that its imprinting is not dependent on flanking genomic sequence.

The consistent imprinting and small size (16 kb) of the *RSVlgmyc* transgene make it suitable for deletion and methylation analyses designed to determine the sequence requirements for generating an imprinted gene. The *RSVlgmyc* transgene contained a 2.5-kb DMD composed of pBR322 and RSV sequences that was methylated just on the maternal allele (Reinhart *et al.*, 2002). Removal of the transgene DMD abolished imprinting. Furthermore, a transgene composed of the DMD alone was not imprinted and deletion of any other single sequence element from *RSVlgmyc* did not affect its imprinting (Chaillet *et al.*, 1995; Reinhart *et al.*, 2002). These data suggest that the DMD is a critical component of the imprinting mechanism. They also suggest that the DMD works in conjunction with other transgene sequences to generate an imprint. The common requirement for DMD sequences among many imprinted loci suggests that DMDs share a common function.

The ability of endogenous DMD sequences to perform the same function in different genomic locations was tested with derivatives of the *RSVlgmyc* transgene. Removal of the DMD from the imprinted *RSVlgmyc* transgene generated the nonimprinted *Ig/myc* transgene. If DMD sequences have a common function, then it should be possible to replace the transgene DMD with an endogenous DMD and restore transgene imprinting. The ability of endogenous DMDs to functionally replace the transgene DMD was assayed by restoration of maternal-specific transgene methylation. Interestingly, specific sequences from endogenous imprinted gene DMDs were able to restore imprinting to the transgene.

Replacing the DMD of the *RSVlgmyc* transgene with DMD sequences from the endogenous *Igf2r* locus generated an imprinted transgene (Reinhart *et al.*, 2002). The CpGs within the DMD were methylated on each maternal allele and unmethylated on each paternal allele. More specifically, sequences from the tandem repeat region within the *Igf2r* DMD2 restored imprinting to the *Ig/myc* transgene. The *Igf2r* DMD2 includes three copies of a 30-bp repeat (TR1) and three copies of a 170-bp repeat (TR2+3). A transgene containing the TR1 repeats and 2.5 copies of the TR2+3 repeat was able to functionally replace the DMD of the *RSVlgmyc* transgene. In fact, 2.5 copies of the TR2+3 repeats alone were able to restore imprinting to the *Ig/myc* transgene, whereas the TR1 repeats alone were not. Similar experiments showed that the promoter and first exon of *Snrpn* were not able to functionally replace the *RSVlgmyc* transgene DMD (Reinhart *et al.*, 2002). These experiments suggest that sequences (possibly tandem repeats) within maternally methylated DMDs share a common, interchangeable function in establishing and maintaining a maternal methylation mark.

F. Possible Functions for Tandem Repeats

Genomic imprinting presumably requires several sequences from within the DMD to perform a variety of functions. The DMD must attract methylation in the appropriate gamete, while ensuring that the same sequences do not acquire methylation in the opposite gamete. This process undoubtedly requires DNA methyltransferases and methyltransferase-like proteins, sequences within the DMD, and possibly germ line-specific factors. After fertilization the patterns of methylation that have been established on the methylated allele must be maintained in the somatic cells of embryonic and adult mice. Presumably this process also requires sequences within the DMD, the same ones as required in the germ line or distinct ones, and protein factors including DNA methyltransferases. On the other hand, the unmethylated allele must be protected from acquiring methylation after implantation of the blastocyst-stage embryo. Again, this process must depend on specific proteins and DNA sequences. Apart from the maintenance of a germ line imprint during development, the DMD sequences are involved in governing the monoallelic expression of genes over a large genomic distance. Yet again, this gene regulatory function requires the presence of the DMD, either utilizing the same sequences needed for persistence of methylation, or still different sequences within the DMD.

The establishment and maintenance of a DMD is an essential feature common to all imprinted gene clusters. However, the elaborate gene regulatory requirements of each gene cluster are markedly different. The elements required to establish and maintain a DMD are therefore more likely conserved among DMD sequences than those needed for long-distance

regulation of transcription. Notably, the DMDs described above share several common features including a CpG-rich region that encompasses an imprinted promoter and tandem repeats. The studies described here suggest that the tandem repeat sequences are an essential element of the imprinting process. First, deletion of DMD sequences that contain tandem repeats abolished imprinting at several imprinted loci (specific to deletion on the unmethylated, paternal alleles). Second, the tandem repeat sequences of the *Igf2r* DMD were able to establish and maintain differential methylation of a hybrid transgene outside of their endogenous location. In contrast, a requirement for promoter sequences in imprinting is not as clear. Deletion of the *Snrpn* promoter did not affect imprinting within the gene cluster. In addition, unlike the *Igf2r* DMD repeats, the *Snrpn* promoter sequences, within the DMD but excluding the tandem repeats, were not able to establish and maintain differential methylation of a hybrid transgene. These experiments are consistent with the notion that tandem repeats are needed to establish and maintain differential methylation throughout preimplantation and postimplantation development.

Tandem repeats may be required to target a DMD for *de novo* methylation in the gametes and to ensure that methylation is maintained during preimplantation development. During this period of development specific methyltransferases are known to be required for establishing and maintaining imprints. Dnmt3A and Dnmt3L are needed in oocytes and spermatogonia to establish imprints and Dnmt1o is needed at the fourth S phase of embryogenesis to maintain all imprints. Tandem repeats may function to attract necessary DNA-binding proteins or methyltransferase proteins to the DMD in the gametes, preimplantation, or postimplantation embryos. However, the tandem repeats for each gene cluster are not perfect repeats. This may argue against a function for the repeats in attracting a common sequence-specific binding protein. A requirement may exist purely for repetitiveness. However, the presence of a repeated sequence alone does not seem sufficient to attract differential methylation. In experiments with *Ig/myc* hybrid transgenes the TR2+3 repeats of the *Igf2r* locus were able to function as a DMD; however, neither the TR1 repeats nor the repeated sequences within the LTR of an IAP (intracisternal A particle) element served the same function. Consequently, a function specific to these imperfect tandem repeats within DMDs is most likely.

G. Chromatin and Imprinted Gene Expression

Imprinted genes are located within large chromosomal domains that include maternally expressed genes, paternally expressed genes, and biallelically expressed genes. Several studies have shown that a DMD deletion inherited

on the normally unmethylated parental chromosome resulted in a loss of imprinting at genes located a long distance from the DMD. These data suggest that DMDs, and possibly DNA methylation, have far-reaching effects on gene expression. However, how parent-specific gene expression is regulated within the context of a large chromosomal domain is not well understood.

It is important to take into account that the activation or silencing of gene expression within an imprinted gene cluster occurs on a genomic DNA template that is packaged into chromatin. The extent of gene expression at an imprinted locus is due in part to the relative accessibility of the DNA template to proteins required to activate or repress transcription. Within regions of loosely packaged chromatin the DNA is easily accessed and actively transcribed, whereas within regions of tightly packaged chromatin the DNA is less accessible and not transcribed. The basic components of chromatin are nucleosomes that consist of 147 bp of genomic DNA wrapped around a core histone octamer. The histone octamer is composed of two copies of each of the four histone proteins H3, H4, H2A, and H2B. The core histone proteins contain N-terminal tails with amino acid residues that are subject to modification by acetylation, methylation, and phosphorylation. The covalent modification of histone tails, as well as the methylation of DNA, can alter the structure of chromatin and thereby alter gene expression. In addition, DNA and histone modifications can recruit or repel proteins that in turn alter gene activity. The combination of modifications present within an imprinted domain would ultimately influence the parental allele-specific expression of genes.

1. Histone Modifications

The N-terminal tails of the core histone proteins are subject to acetylation and methylation at specific lysine (K) residues. Similarly, serine (S) and threonine (T) residues can be phosphorylated. It has become apparent that covalent modifications of histones affect gene expression (Fischle *et al.*, 2003). It is well accepted that hyperacetylated histones are associated with actively transcribed genes, whereas hypoacetylated histones are associated with inactive genes. Histone methylation can be associated with repression or activation of transcription, depending on the specific histone tail residues that are modified. The acetylation of Lys-9 in the N-terminal tail of histone H3 (H3-K9) is often associated with active transcription, as is methylation of Lys-4 on histone H3 (H3-K4). In contrast, methylated H3-K9 is often associated with gene repression. Other histone modifications are also correlated with gene activity. These definitions are by no means absolute, as an individual histone modification may have different effects when present in combination with other modifications on the same, or different, histone tails.

Therefore, it is the combination of modifications present on chromatin that leads to alterations in gene expression.

Many proteins have been identified that add or remove histone modifications. Histone acetyltransferases (HATs) and histone deacetylases (HDACs) acetylate histones or deacetylate histones, respectively (Kuo and Allis, 1998). Histone methyltransferases (HMTases) have been characterized that add methyl groups to histone tails (Rice and Allis, 2001). Many proteins have been described that interact with modified histones. In general, proteins that interact with acetylated histones contain a conserved bromodomain, and proteins that interact with methylated histones contain a chromodomain. Interactions between proteins containing chromodomains or bromodomains and modified histones can alter promoter activity or facilitate the propagation of specific histone modifications. For example, the mammalian Suv39h1 and Suv39h2 proteins are HMTases that specifically methylate H3-K9. Methylated H3-K9 creates a binding site for the chromodomain protein heterochromatin protein 1 (HP1) (Lachner *et al.*, 2001). HP1 in turn interacts with Suv39h1 and Suv39h2 and it is thought that this interaction may facilitate the spreading or perpetuation of histone methylation within a region of chromatin. Similar interactions exist between acetylated histone tails and recruitment of bromodomain-containing HAT proteins. These types of interactions would allow the propagation of active or repressive histone modifications in specific gene regions.

2. Histone Modifications at Imprinted Loci

The levels of acetylation or methylation on histone tails have been examined in the genomic regions surrounding many imprinted genes. A primary focus of these experiments has been to identify differences in histone acetylation or methylation within the DMD regions already shown to be required for imprinting. In embryonic stem (ES) cells and in the adult liver the *Snrpn* DMD was acetylated on the paternal (expressed) allele. In comparison, the silent (maternal) allele was less acetylated (Gregory *et al.*, 2001). Similar studies showed that the paternal allele of the *Snrpn* DMD had a higher level of methylation at Lys-4 of H3 than did the maternal allele, and the maternal allele had a higher level of methylation at Lys-9 of H3 than did the paternal allele (Fournier *et al.*, 2002). These observed histone modifications are consistent with paternal-specific expression from the *Snrpn* locus. These observations point to a correlation between differential histone modifications and differential expression of imprinted genes.

Several studies have examined histone methylation and acetylation within the DMD1 and DMD2 regions of the *Igf2r* locus (Fournier *et al.*, 2002; Yang *et al.*, 2003). DMD1 displays paternal-specific DNA methylation and contains the maternally expressed *Igf2r* promoter. DMD2 displays

maternal-specific DNA methylation and contains the paternally expressed *Air* promoter. The maternal allele of DMD1 was shown to be enriched in acetylated histones H3 and H4 and in histone H3 methylated at Lys-4. In contrast, the paternal allele of DMD1 was underacetylated, and lacked histone H3 methylated at Lys-4. In addition, the paternal allele of DMD2 was shown to be hyperacetylated when compared with the maternal allele. These studies strengthen the correlation between the extent of histone acetylation or methylation at the maternal and paternal alleles of an imprinted locus and the promoter activity of each allele. In these examples differential chromatin modifications occur in regions originally defined by parental allele specific differences in DNA methylation.

The previously described experiments suggest that histone modifications are likely to be involved in the regulation of transcription from both parental alleles at an imprinted locus. In fact, it is likely that modified histones are important for the regulation of gene expression within large, coordinately regulated, gene clusters. However, it is more difficult to envision that these modifications provide a straightforward mechanism to establish and continually maintain the identity of the parental alleles at an imprinted locus. Details concerning the timing of specific epigenetic modifications, interactions among these modifications, and, importantly, their absolute requirement for genomic imprinting remain to be clarified.

3. Connections Between Histone Modifications and DNA Methylation

Differential histone modifications are associated with many imprinted promoters and coincide with both primary and secondary DMDs. It has been demonstrated that many DMDs are created in the germ line and continuously maintained. However, next to nothing is known about the developmental stage at which areas of differential histone methylation or histone acetylation are acquired. Such differences may be established in the germ line or acquired after fertilization. Interactions among many different proteins have been described that may connect DNA methylation with histone acetylation or methylation at imprinted loci.

Many proteins bind methylated CpG dinucleotides via a DNA-binding domain termed a methyl-binding domain (MBD). MBD proteins are often associated with transcription regulation via interactions with single proteins or multiprotein complexes (Cross *et al.*, 1997; Jorgensen and Bird, 2002; Nan *et al.*, 1997). The MeCP2 protein, a component of the Sin3a/HDAC histone deacetylase complex, interacts with the histone methyltransferase proteins (Fuks *et al.*, 2003; Jones *et al.*, 1998; Nan *et al.*, 1998). The MBD1 protein is involved in transcriptional repression via associations with histone deacetylases and the Suv39h1-HP1 heterochromatic complex (Fujita *et al.*, 2003; Ng

et al., 2000). In addition, the MBD2 protein binds methylated CpGs as a part of the MeCP1/NuRD complex that has been shown to remodel and deacetylate chromatin templates (Feng and Zhang, 2001; Ng *et al.*, 1999). Interestingly, the mammalian HMTase ESET (ERG-associated protein with SET domain) also contains a methyl CpG-binding domain, suggesting that histone-modifying proteins may directly interact with methylated DNA (Bird, 2001; Blackburn *et al.*, 2003). Interactions between MBD proteins and proteins involved in regulating histone modifications provide an obvious connection between DNA methylation and histone modifications. These interactions suggest that differential DNA methylation in a defined region can recruit proteins to modulate promoter activity and to modify nearby histones.

It has also been suggested that histone modifications can direct DNA methylation. An association between DNA methylation and histone methylation at the major satellite repeats of pericentric heterochromatin was suggested in one study. In ES cell extracts Dnmt3b coimmunoprecipitated with HP1 α , HP1 β , and with H3-K9 HMTase activity (Lehnertz *et al.*, 2003). Also, both HP1 and histone H3 trimethylated at Lys-9 localize to heterochromatin in ES cells. The Dnmt1 and Dnmt3b DNA methyltransferases are also enriched in these regions. However, in ES cells that lack the Suv39h HMTase proteins no trimethylated pericentric heterochromatin was observed. Correspondingly, the HP1 proteins do not bind to these domains. The Dnmt3b and MeCP2 proteins were also specifically depleted from these regions. In addition, methylation of major satellite DNA was impaired in mutant ES cells. In contrast, mutations in the DNA methyltransferase proteins did not affect localization of H3-K9 trimethylation or HP1 α to regions of pericentric heterochromatin. These experiments suggest that histone modifications can target CpG methylation to certain DNA regions.

4. Involvement of the PcG Protein Eed in Imprinting

Evidence indicates that proteins required for chromatin modification are also involved in the regulation of imprinted gene expression. The polycomb group (PcG) and trithorax group (TrxG) proteins are involved in both long- and short-term regulation of developmentally regulated gene expression as part of multiprotein complexes. PcG complexes typically repress expression and TrxG complexes typically activate expression of developmentally regulated and cell-cycle related genes (Orlando, 2003). The mammalian Eed and Ezh2 proteins are part of a PcG protein complex that is homologous to the *Drosophila* ESC-E(z) complex. The Eed/Ezh2 complex possesses histone methyltransferase activity and interacts with HDACs, interactions that indicate that regulation of gene expression by the complex is controlled by altering histone modifications (Cao and Zhang, 2004).

The Eed/Ezh2 complex is essential for mammalian development. Mutations in the Eed protein are lethal, causing gastrulation and anterior–posterior patterning defects. A hypomorphic mutation in the Eed protein led to altered expression patterns of specific *Hox* genes and anterior-to-posterior skeletal transformation along the entire anterior–posterior axis (Wang *et al.*, 2002). Null mutations of the *eed* gene were midgestation lethal and homozygous null *eed*^{-/-} mutants gastrulated but failed to differentiate an embryo proper (Morin-Kensicki *et al.*, 2001). Mutations of the Eed protein were also shown to cause defects in primary and secondary trophoblast giant cells in females and in imprinted X inactivation (Wang *et al.*, 2001). The *eed*^{-/-} mutation leads to reactivation of genes on the imprinted X chromosome in extraembryonic tissues.

Importantly, the Eed protein was shown to be required for correct expression of imprinted genes (Mager *et al.*, 2003). Imprinted gene expression was analyzed in *eed*^{-/-} mutant embryos compared with wild-type embryos on E7.5. Loss of the Eed protein resulted in a loss of imprinting specific to a few imprinted genes. The maternally expressed genes *Cdkn1c*, *Ascl2*, *Grb10*, and *Meg3*, found on three different mouse chromosomes, were all biallelically expressed in mutant embryos on E7.5. In contrast, 10 other imprinted genes retained their normal monoallelic expression pattern. Methylation analysis of genomic DNA from E7.5 embryos showed that four different imprinted gene DMDs remained normally methylated in mutant embryos when compared with wild-type embryos. Only slight differences in methylation were noted. For example, the *Grb10* gene, which is normally maternally methylated, showed a sporadic gain of methylation on paternal alleles. In contrast, the *Snrpn* gene showed no changes in methylation at the promoter and first exon. Overall, certain genes that were normally paternally silenced in wild-type embryos were inappropriately activated in mutant embryos. These changes showed no correlation to changes in DNA methylation. In addition, no changes were observed in the expression or methylation of primary DMDs that are part of large imprinted gene clusters. These results suggest that changes in chromatin modifications act downstream of methylation marks needed for imprinted expression.

5. Chromatin Insulators

As previously discussed, the *H19* gene has been well studied by both DNA methylation analysis and by targeted mutations. From these studies it is evident that differential DNA methylation and the CTCF protein are required for *H19* and *Igf2* imprinting. A possible role for histone modifications in *H19* and *Igf2* imprinting has been examined. In a mouse fibroblast cell line the expressed, maternal allele of the *H19* locus was hyperacetylated in the vicinity of the promoter (Grandjean *et al.*, 2001; Pedone *et al.*, 1999). It was

also shown that the coordinately regulated *Igf2* gene contained a region of differential acetylation in the vicinity of its promoter (Grandjean *et al.*, 2001). However, the DMD required to regulate both genes does not show parent-specific differences in histone acetylation (Grandjean *et al.*, 2001).

While it is not entirely clear that the DMD of the *H19* locus contains any differential histone modifications, it is known to contain binding sites for the methylation-sensitive binding of CTCF. Methylation-sensitive binding of CTCF is thought to control gene expression by blocking access of the *Igf2* promoter to enhancer elements downstream of *H19* when bound at the unmethylated DMD. CTCF enhancer-blocking activity is thought to be mediated by formation of a chromatin boundary that prevents the *Igf2* promoter from interacting with required enhancers. Similarly, CTCF was identified as a protein with enhancer-blocking activity at an insulator element 5' of the chicken β -globin locus (Recillas-Targa *et al.*, 2002). Both elements show enhancer-blocking activity when located between a promoter and an enhancer (Burgess-Beusse *et al.*, 2002). In this way, insulators can block cross-talk between closely located promoters and enhancers when gene expression is not required.

IV. Concluding Remarks

The experiments described in this review illustrate the requirement for gamete-specific DNA methylation marks to distinguish the parental alleles of imprinted genes. This requirement suggests that distinct processes operate in oocytes and in sperm to target methylation to the appropriate allele of an imprinted gene. Subsequently, gamete-specific methylation is recognized during preimplantation development and maintained during periods of significant loss of genomic DNA methylation. This process requires the coordinate activity of specific DNA methyltransferase proteins to establish and maintain methylation. Also, this process would presumably be directed by *cis*-acting sequences within the genomic region of the imprinted locus. Importantly, the proteins and sequences necessary to maintain differential methylation at each stage of development are not yet clear.

The Dnmt3a and Dnmt3l proteins are required to establish imprinted gene methylation during oogenesis and spermatogenesis. The Dnmt3a protein is a *de novo* methyltransferase. The function of Dnmt3l is not fully understood, although it probably interacts with Dnmt3a to control the specificity of methylation acquisition in the gametes. After the establishment of methylation, the Dnmt1o protein is required to maintain methylation at the fourth S phase of preimplantation development. The enzymes required for maintenance methylation at the other preimplantation stages remain to be

identified. In addition, little is known about the proteins or sequences required to protect the unmethylated allele of the DMD from acquiring methylation in the germ line and during embryonic development. Obviously, a large amount of work remains to be done to clarify what *cis*-acting sequences are involved in these processes.

Targeted deletion studies at many genomic locations have clearly illustrated that the DMD sequences that carry the differential methylation are required for genomic imprinting. Deletion of the DMD sequence from the normally unmethylated parental chromosome resulted in a loss of imprinting. Importantly, this loss of imprinting affected genes located several kilobases to several megabases away from the DMD. Evidence suggests that the coordinate regulation of imprinted gene expression may involve secondary epigenetic changes such as the establishment of secondary DMDs or regions of differential histone acetylation or methylation. If and how the primary DMD is related to any secondary epigenetic modifications within a gene cluster is unknown.

The sequences required to create an imprinted gene continue to be investigated with imprinted transgenes. Studies of transgenes composed of sequences from endogenous loci have confirmed that DMD sequences are required for imprinting. Comparative sequence analysis and experiments with imprinted transgenes suggest that tandem repeat sequences are involved in the establishment and/or perpetuation of methylation at an imprinted locus. Whether these sequences are the same or different from those that are required for the long-distance regulation of imprinted gene expression is not known. However, it seems possible that while the mechanism needed to create a DMD at an imprinted locus may be the same among gene clusters, the intricate mechanism needed to control specific patterns of gene expression may be drastically different.

References

- Aapola, U., Kawasaki, K., Scott, H. S., Ollila, J., Vihinen, M., Heino, M., Shintani, A., Minoshima, S., Krohn, K., Antonarakis, S. E., Shimizu, N., Kudoh, J., and Peterson, P. (2000). Isolation and initial characterization of a novel zinc finger gene, *DNMT3L*, on 21q22.3, related to the cytosine-5-methyltransferase 3 gene family. *Genomics* **65**, 293–298.
- Aapola, U., Lyle, R., Krohn, K., Antonarakis, S. E., and Peterson, P. (2001). Isolation and initial characterization of the mouse *Dnmt3l* gene. *Cytogenet. Cell Genet.* **92**, 122–126.
- Ainscough, J. F., Koide, T., Tada, M., Barton, S., and Surani, M. A. (1997). Imprinting of *Igf2* and *H19* from a 130 kb YAC transgene. *Development* **124**, 3621–3632.
- Bartolomei, M. S., Zemel, S., and Tilghman, S. M. (1991). Parental imprinting of the mouse *H19* gene. *Nature* **351**, 153–155.
- Bell, A. C., and Felsenfeld, G. (2000). Methylation of a CTCF-dependent boundary controls imprinted expression of the *Igf2* gene. *Nature* **405**, 482–485.

- Bestor, T. H. (2000). The DNA methyltransferases of mammals. *Hum. Mol. Genet.* **9**, 2395–2402.
- Bielinska, B., Blaydes, S. M., Buiting, K., Yang, T., Krajewska-Walasek, M., Horsthemke, B., and Brannan, C. I. (2000). *De novo* deletions of *SNRPN* exon 1 in early human and mouse embryos result in a paternal to maternal imprint switch. *Nat. Genet.* **25**, 74–78.
- Bird, A. (2001). Molecular biology: Methylation talk between histones and DNA. *Science* **294**, 2113–2115.
- Blackburn, M. L., Chansky, H. A., Zielinska-Kwiatkowska, A., Matsui, Y., and Yang, L. (2003). Genomic structure and expression of the mouse *ESET* gene encoding an ERG-associated histone methyltransferase with a SET domain. *Biochim. Biophys. Acta* **1629**, 8–14.
- Bourc'his, D., Xu, G. L., Lin, C. S., Bollman, B., and Bestor, T. H. (2001). Dnmt3L and the establishment of maternal genomic imprints. *Science* **294**, 2536–2539.
- Bressler, J., Tsai, T. F., Wu, M. Y., Tsai, S. F., Ramirez, M. A., Armstrong, D., and Beaudet, A. L. (2001). The SNRPN promoter is not required for genomic imprinting of the Prader-Willi/Angelman domain in mice. *Nat. Genet.* **28**, 232–240.
- Buiting, K., Gross, S., Lich, C., Gillissen-Kaesbach, G., el-Maarri, O., and Horsthemke, B. (2003). Epimutations in Prader-Willi and Angelman syndromes: A molecular study of 136 patients with an imprinting defect. *Am. J. Hum. Genet.* **72**, 571–577.
- Burgess-Beusse, B., Farrell, C., Gaszner, M., Litt, M., Mutskov, V., Recillas-Targa, F., Simpson, M., West, A., and Felsenfeld, G. (2002). The insulation of genes from external enhancers and silencing chromatin. *Proc. Natl. Acad. Sci. USA* **99**(Suppl. 4), 16433–16437.
- Cao, R., and Zhang, Y. (2004). The functions of E(Z)/EZH2-mediated methylation of lysine 27 in histone H3. *Curr. Opin. Genet. Dev.* **14**, 155–164.
- Cattanach, B. M., and Kirk, M. (1985). Differential activity of maternally and paternally derived chromosome regions in mice. *Nature* **315**, 496–498.
- Cattanach, B. M., Barr, J. A., Evans, E. P., Burtenshaw, M., Beechey, C. V., Leff, S. E., Brannan, C. I., Copeland, N. G., Jenkins, N. A., and Jones, J. (1992). A candidate mouse model for Prader-Willi syndrome which shows an absence of *Snrpn* expression. *Nat. Genet.* **2**, 270–274.
- Chaillet, J. R., Vogt, T. F., Beier, D. R., and Leder, P. (1991). Parental-specific methylation of an imprinted transgene is established during gametogenesis and progressively changes during embryogenesis. *Cell* **66**, 77–83.
- Chaillet, J. R., Bader, D. S., and Leder, P. (1995). Regulation of genomic imprinting by gametic and embryonic processes. *Genes Dev.* **9**, 1177–1187.
- Charalambous, M., Smith, F. M., Bennett, W. R., Crew, T. E., Mackenzie, F., and Ward, A. (2003). Disruption of the imprinted *Grb10* gene leads to disproportionate overgrowth by an *Igf2*-independent mechanism. *Proc. Natl. Acad. Sci. USA* **100**, 8292–8297.
- Chedin, F., Lieber, M. R., and Hsieh, C. L. (2002). The DNA methyltransferase-like protein DNMT3L stimulates *de novo* methylation by Dnmt3a. *Proc. Natl. Acad. Sci. USA* **99**, 16916–16921.
- Coombes, C., Arnaud, P., Gordon, E., Dean, W., Coar, E. A., Williamson, C. M., Feil, R., Peters, J., and Kelsey, G. (2003). Epigenetic properties and identification of an imprint mark in the Nesp-Gnasxl domain of the mouse *Gnas* imprinted locus. *Mol. Cell. Biol.* **23**, 5475–5488.
- Cranston, M. J., Spinka, T. L., Elson, D. A., and Bartolomei, M. S. (2001). Elucidation of the minimal sequence required to imprint *H19* transgenes. *Genomics* **73**, 98–107.
- Cross, S. H., Meehan, R. R., Nan, X., and Bird, A. (1997). A component of the transcriptional repressor MeCP1 shares a motif with DNA methyltransferase and HRX proteins. *Nat. Genet.* **16**, 256–259.
- Davis, T. L., Yang, G. J., McCarrey, J. R., and Bartolomei, M. S. (2000). The *H19* methylation imprint is erased and re-established differentially on the parental alleles during male germ cell development. *Hum. Mol. Genet.* **9**, 2885–2894.

- Drewell, R. A., Brenton, J. D., Ainscough, J. F., Barton, S. C., Hilton, K. J., Arney, K. L., Dandolo, L., and Surani, M. A. (2000). Deletion of a silencer element disrupts *H19* imprinting independently of a DNA methylation epigenetic switch. *Development* **127**, 3419–3428.
- Elson, D. A., and Bartolomei, M. S. (1997). A 5' differentially methylated sequence and the 3'-flanking region are necessary for *H19* transgene imprinting. *Mol. Cell. Biol.* **17**, 309–317.
- Feng, Q., and Zhang, Y. (2001). The MeCP1 complex represses transcription through preferential binding, remodeling, and deacetylating methylated nucleosomes. *Genes Dev.* **15**, 827–832.
- Fischle, W., Wang, Y., and Allis, C. D. (2003). Histone and chromatin cross-talk. *Curr. Opin. Cell Biol.* **15**, 172–183.
- Fitzpatrick, G. V., Soloway, P. D., and Higgins, M. J. (2002). Regional loss of imprinting and growth deficiency in mice with a targeted deletion of *KvDMR1*. *Nat. Genet.* **32**, 426–431.
- Flynn, J., Glickman, J. F., and Reich, N. O. (1996). Murine DNA cytosine-C5 methyltransferase: Pre-steady- and steady-state kinetic analysis with regulatory DNA sequences. *Biochemistry* **35**, 7308–7315.
- Fournier, C., Goto, Y., Ballestar, E., Delaval, K., Hever, A. M., Esteller, M., and Feil, R. (2002). Allele-specific histone lysine methylation marks regulatory regions at imprinted mouse genes. *EMBO J.* **21**, 6560–6570.
- Fujita, N., Watanabe, S., Ichimura, T., Tsuruzoe, S., Shinkai, Y., Tachibana, M., Chiba, T., and Nakao, M. (2003). Methyl-CpG binding domain 1 (MBD1) interacts with the Suv39h1–HP1 heterochromatic complex for DNA methylation-based transcriptional repression. *J. Biol. Chem.* **278**, 24132–24138.
- Fuks, F., Hurd, P. J., Wolf, D., Nan, X., Bird, A. P., and Kouzarides, T. (2003). The methyl-CpG-binding protein MeCP2 links DNA methylation to histone methylation. *J. Biol. Chem.* **278**, 4035–4040.
- Gabriel, J. M., Gray, T. A., Stubbs, L., Saitoh, S., Ohta, T., and Nicholls, R. D. (1998). Structure and function correlations at the imprinted mouse *Snrpn* locus. *Mamm. Genome.* **9**, 788–793.
- Geuns, E., De Rycke, M., Van Steirteghem, A., and Liebaers, I. (2003). Methylation imprints of the imprint control region of the SNRPN-gene in human gametes and preimplantation embryos. *Hum. Mol. Genet.* **12**, 2873–2879.
- Glenn, C. C., Saitoh, S., Jong, M. T., Filbrandt, M. M., Surti, U., Driscoll, D. J., and Nicholls, R. D. (1996). Gene structure, DNA methylation, and imprinted expression of the human SNRPN gene. *Am. J. Hum. Genet.* **58**, 335–346.
- Grandjean, V., O'Neill, L., Sado, T., Turner, B., and Ferguson-Smith, A. (2001). Relationship between DNA methylation, histone H4 acetylation, and gene expression in the mouse imprinted *Igf2–H19* domain. *FEBS Lett.* **488**, 165–169.
- Gregory, R. I., Randall, T. E., Johnson, C. A., Khosla, S., Hatada, I., O'Neill, L. P., Turner, B. M., and Feil, R. (2001). DNA methylation is linked to deacetylation of histone H3, but not H4, on the imprinted genes *Snrpn* and *U2af1-rs1*. *Mol. Cell. Biol.* **21**, 5426–5436.
- Hajkova, P., Erhardt, S., Lane, N., Haaf, T., El-Maarri, O., Reik, W., Walter, J., and Surani, M. A. (2002). Epigenetic reprogramming in mouse primordial germ cells. *Mech. Dev.* **117**, 15–23.
- Hanel, M. L., and Wevrick, R. (2001). Establishment and maintenance of DNA methylation patterns in mouse *Ndn*: Implications for maintenance of imprinting in target genes of the imprinting center. *Mol. Cell. Biol.* **21**, 2384–2392.
- Hark, A. T., Schoenherr, C. J., Katz, D. J., Ingram, R. S., Levorse, J. M., and Tilghman, S. M. (2000). CTCF mediates methylation-sensitive enhancer-blocking activity at the *H19/Igf2* locus. *Nature* **405**, 486–489.
- Hata, K., Okano, M., Lei, H., and Li, E. (2002). Dnmt3L cooperates with the Dnmt3 family of *de novo* DNA methyltransferases to establish maternal imprints in mice. *Development* **129**, 1983–1993.

- Howell, C. Y., Bestor, T. H., Ding, F., Latham, K. E., Mertineit, C., Trasler, J. M., and Chaillet, J. R. (2001). Genomic imprinting disrupted by a maternal effect mutation in the *Dnmt1* gene. *Cell* **104**, 829–838.
- Hsieh, C. L. (1999). *In vivo* activity of murine *de novo* methyltransferases, Dnmt3a and Dnmt3b. *Mol. Cell. Biol.* **19**, 8211–8218.
- Johnson, D. R. (1974). Hairpin-tail: A case of post-reductional gene action in the mouse egg. *Genetics* **76**, 795–805.
- Jones, P. L., Veenstra, G. J., Wade, P. A., Vermaak, D., Kass, S. U., Landsberger, N., Strouboulis, J., and Wolffe, A. P. (1998). Methylated DNA and MeCP2 recruit histone deacetylase to repress transcription. *Nat. Genet.* **19**, 187–191.
- Jorgensen, H. F., and Bird, A. (2002). MeCP2 and other methyl-CpG binding proteins. *Ment. Retard. Dev. Disabil. Res. Rev.* **8**, 87–93.
- Kafri, T., Ariel, M., Brandeis, M., Shemer, R., Urven, L., McCarrey, J., Cedar, H., and Razin, A. (1992). Developmental pattern of gene-specific DNA methylation in the mouse embryo and germ line. *Genes Dev.* **6**, 705–714.
- Kaneda, M., Okano, M., Hata, K., Sado, T., Tsujimoto, N., Li, E., and Sasaki, H. (2004). Essential role for *de novo* DNA methyltransferase Dnmt3a in paternal and maternal imprinting. *Nature* **429**, 900–903.
- Kaneko-Ishino, T., Kuroiwa, Y., Miyoshi, N., Kohda, T., Suzuki, R., Yokoyama, M., Viville, S., Barton, S. C., Ishino, F., and Surani, M. A. (1995). Peg1/Mest imprinted gene on chromosome 6 identified by cDNA subtraction hybridization. *Nat. Genet.* **11**, 52–59.
- Kono, T., Obata, Y., Yoshimizu, T., Nakahara, T., and Carroll, J. (1996). Epigenetic modifications during oocyte growth correlates with extended parthenogenetic development in the mouse. *Nat. Genet.* **13**, 91–94.
- Kuo, M. H., and Allis, C. D. (1998). Roles of histone acetyltransferases and deacetylases in gene regulation. *Bioessays* **20**, 615–626.
- Lachner, M., O'Carroll, D., Rea, S., Mechtler, K., and Jenuwein, T. (2001). Methylation of histone H3 lysine 9 creates a binding site for HP1 proteins. *Nature* **410**, 116–120.
- La Salle, S., Mertineit, C., Taketo, T., Moens, P. B., Bestor, T. H., and Trasler, J. M. (2004). Windows for sex-specific methylation marked by DNA methyltransferase expression profiles in mouse germ cells. *Dev. Biol.* **268**, 403–415.
- Lee, J., Inoue, K., Ono, R., Ogonuki, N., Kohda, T., Kaneko-Ishino, T., Ogura, A., and Ishino, F. (2002). Erasing genomic imprinting memory in mouse clone embryos produced from day 11.5 primordial germ cells. *Development* **129**, 1807–1817.
- Lefebvre, L., Viville, S., Barton, S. C., Ishino, F., and Surani, M. A. (1997). Genomic structure and parent-of-origin-specific methylation of Peg1. *Hum. Mol. Genet.* **6**, 1907–1915.
- Lehnertz, B., Ueda, Y., Derijck, A. A., Braunschweig, U., Perez-Burgos, L., Kubicek, S., Chen, T., Li, E., Jenuwein, T., and Peters, A. H. (2003). Suv39h-mediated histone H3 lysine 9 methylation directs DNA methylation to major satellite repeats at pericentric heterochromatin. *Curr. Biol.* **13**, 1192–1200.
- Leighton, P. A., Saam, J. R., Ingram, R. S., Stewart, C. L., and Tilghman, S. M. (1995). An enhancer deletion affects both H19 and Igf2 expression. *Genes Dev.* **9**, 2079–2089.
- Leonhardt, H., Page, A. W., Weier, H. U., and Bestor, T. H. (1992). A targeting sequence directs DNA methyltransferase to sites of DNA replication in mammalian nuclei. *Cell* **71**, 865–873.
- Li, E., Bestor, T. H., and Jaenisch, R. (1992). Targeted mutation of the DNA methyltransferase gene results in embryonic lethality. *Cell* **69**, 915–926.
- Li, E., Beard, C., and Jaenisch, R. (1993). Role for DNA methylation in genomic imprinting. *Nature* **366**, 362–365.
- Lin, S. P., Youngson, N., Takada, S., Seitz, H., Reik, W., Paulsen, M., Cavaille, J., and Ferguson-Smith, A. C. (2003). Asymmetric regulation of imprinting on the maternal and

- paternal chromosomes at the *Dlk1-Gtl2* imprinted cluster on mouse chromosome 12. *Nat. Genet.* **35**, 97–102.
- Lopes, S., Lewis, A., Hajkova, P., Dean, W., Oswald, J., Forne, T., Murrell, A., Constancia, M., Bartolomei, M., Walter, J., and Reik, W. (2003). Epigenetic modifications in an imprinting cluster are controlled by a hierarchy of DMRs suggesting long-range chromatin interactions. *Hum. Mol. Genet.* **12**, 295–305.
- Lucifero, D., Mertineit, C., Clarke, H. J., Bestor, T. H., and Trasler, J. M. (2002). Methylation dynamics of imprinted genes in mouse germ cells. *Genomics* **79**, 530–538.
- Lucifero, D., Chaillet, J. R., and Trasler, J. M. (2004). Potential significance of genomic imprinting defects for reproduction and assisted reproductive technology. *Hum. Reprod. Update* **10**, 3–18.
- Mager, J., Montgomery, N. D., de Villena, F. P., and Magnuson, T. (2003). Genome imprinting regulated by the mouse Polycomb group protein Eed. *Nat. Genet.* **33**, 502–507.
- McGrath, J., and Solter, D. (1984). Completion of mouse embryogenesis requires both the maternal and paternal genomes. *Cell* **37**, 179–183.
- Mertineit, C., Yoder, J. A., Taketo, T., Laird, D. W., Trasler, J. M., and Bestor, T. H. (1998). Sex-specific exons control DNA methyltransferase in mammalian germ cells. *Development* **125**, 889–897.
- Miyoshi, N., Kuroiwa, Y., Kohda, T., Shitara, H., Yonekawa, H., Kawabe, T., Hasegawa, H., Barton, S. C., Surani, M. A., Kaneko-Ishino, T., and Ishino, F. (1998). Identification of the *Meg1/Grb10* imprinted gene on mouse proximal chromosome 11, a candidate for the Silver–Russell syndrome gene. *Proc. Natl. Acad. Sci. USA* **95**, 1102–1107.
- Monk, M., Boubelik, M., and Lehnert, S. (1987). Temporal and regional changes in DNA methylation in the embryonic, extraembryonic and germ cell lineages during mouse embryo development. *Development* **99**, 371–382.
- Morin-Kensicki, E. M., Faust, C., LaMantia, C., and Magnuson, T. (2001). Cell and tissue requirements for the gene eed during mouse gastrulation and organogenesis. *Genesis* **31**, 142–146.
- Nan, X., Campoy, F. J., and Bird, A. (1997). MeCP2 is a transcriptional repressor with abundant binding sites in genomic chromatin. *Cell* **88**, 471–481.
- Nan, X., Ng, H. H., Johnson, C. A., Laherty, C. D., Turner, B. M., Eisenman, R. N., and Bird, A. (1998). Transcriptional repression by the methyl-CpG-binding protein MeCP2 involves a histone deacetylase complex. *Nature* **393**, 386–389.
- Neumann, B., Kubicka, P., and Barlow, D. P. (1995). Characteristics of imprinted genes. *Nat. Genet.* **9**, 12–13.
- Ng, H. H., Zhang, Y., Hendrich, B., Johnson, C. A., Turner, B. M., Erdjument-Bromage, H., Tempst, P., Reinberg, D., and Bird, A. (1999). MBD2 is a transcriptional repressor belonging to the MeCP1 histone deacetylase complex. *Nat. Genet.* **23**, 58–61.
- Ng, H. H., Jeppesen, P., and Bird, A. (2000). Active repression of methylated genes by the chromosomal protein MBD1. *Mol. Cell. Biol.* **20**, 1394–1406.
- Nicholls, R. D., and Knepper, J. L. (2001). Genome organization, function, and imprinting in Prader-Willi and Angelman syndromes. *Annu. Rev. Genomics Hum. Genet.* **2**, 153–175.
- Nicholls, R. D., Knoll, J. H., Butler, M. G., Karam, S., and Lalonde, M. (1989). Genetic imprinting suggested by maternal heterodisomy in nondeletion Prader-Willi syndrome. *Nature* **342**, 281–285.
- Obata, Y., Kaneko-Ishino, T., Koide, T., Takai, Y., Ueda, T., Domeki, I., Shiroishi, T., Ishino, F., and Kono, T. (1998). Disruption of primary imprinting during oocyte growth leads to the modified expression of imprinted genes during embryogenesis. *Development* **125**, 1553–1560.
- Ohta, T., Gray, T. A., Rogan, P. K., Buiting, K., Gabriel, J. M., Saitoh, S., Muralidhar, B., Bilienska, B., Krajewska-Walasek, M., Driscoll, D. J., Horsthemke, B., Butler, M. G., and

- Nicholls, R. D. (1999). Imprinting-mutation mechanisms in Prader-Willi syndrome. *Am. J. Hum. Genet.* **64**, 397–413.
- Okano, M., Bell, D. W., Haber, D. A., and Li, E. (1999). DNA methyltransferases Dnmt3a and Dnmt3b are essential for *de novo* methylation and mammalian development. *Cell* **99**, 247–257.
- Ono, R., Shiura, H., Aburatani, H., Kohda, T., Kaneko-Ishino, T., and Ishino, F. (2003). Identification of a large novel imprinted gene cluster on mouse proximal chromosome 6. *Genome Res.* **13**, 1696–1705.
- Orlando, V. (2003). Polycomb, epigenomes, and control of cell identity. *Cell* **112**, 599–606.
- Oswald, J., Engemann, S., Lane, N., Mayer, W., Olek, A., Fundele, R., Dean, W., Reik, W., and Walter, J. (2000). Active demethylation of the paternal genome in the mouse zygote. *Curr. Biol.* **10**, 475–478.
- Pedone, P. V., Pikaart, M. J., Cerrato, F., Vernucci, M., Ungaro, P., Bruni, C. B., and Riccio, A. (1999). Role of histone acetylation and DNA methylation in the maintenance of the imprinted expression of the *H19* and *Igf2* genes. *FEBS Lett.* **458**, 45–50.
- Recillas-Targa, F., Pikaart, M. J., Burgess-Beusse, B., Bell, A. C., Litt, M. D., West, A. G., Gaszner, M., and Felsenfeld, G. (2002). Position-effect protection and enhancer blocking by the chicken β -globin insulator are separable activities. *Proc. Natl. Acad. Sci. USA* **99**, 6883–6888.
- Reinhart, B., Eljanne, M., and Chaillet, J. R. (2002). Shared role for differentially methylated domains of imprinted genes. *Mol. Cell. Biol.* **22**, 2089–2098.
- Rice, J. C., and Allis, C. D. (2001). Histone methylation versus histone acetylation: New insights into epigenetic regulation. *Curr. Opin. Cell Biol.* **13**, 263–273.
- Sato, S., Yoshimizu, T., Sato, E., and Matsui, Y. (2003). Erasure of methylation imprinting of *Igf2r* during mouse primordial germ-cell development. *Mol. Reprod. Dev.* **65**, 41–50.
- Schmidt, J. V., Matteson, P. G., Jones, B. K., Guan, X. J., and Tilghman, S. M. (2000). The *Dlk1* and *Gtl2* genes are linked and reciprocally imprinted. *Genes Dev.* **14**, 1997–2002.
- Schoenherr, C. J., Levorse, J. M., and Tilghman, S. M. (2003). CTCF maintains differential methylation at the *Igf2/H19* locus. *Nat. Genet.* **33**, 66–69.
- Shemer, R., Birger, Y., Riggs, A. D., and Razin, A. (1997). Structure of the imprinted mouse *Snrpn* gene and establishment of its parental-specific methylation pattern. *Proc. Natl. Acad. Sci. USA* **94**, 10267–10272.
- Shibata, H., Yoda, Y., Kato, R., Ueda, T., Kamiya, M., Hiraiwa, N., Yoshiki, A., Plass, C., Pearsall, R. S., Held, W. A., Muramatsu, M., Sasaki, H., Kusakabe, M., and Hayashizaki, Y. (1998). A methylation imprint mark in the mouse imprinted gene *Grfl/Cdc25Mm* locus shares a common feature with the *U2 afbp-rs* gene: An association with a short tandem repeat and a hypermethylated region. *Genomics* **49**, 30–37.
- Sleutels, F., Zwart, R., and Barlow, D. P. (2002). The non-coding Air RNA is required for silencing autosomal imprinted genes. *Nature* **415**, 810–813.
- Smilnich, N. J., Day, C. D., Fitzpatrick, G. V., Caldwell, G. M., Lossie, A. C., Cooper, P. R., Smallwood, A. C., Joyce, J. A., Schofield, P. N., Reik, W., Nicholls, R. D., Weksberg, R., Driscoll, D. J., Maher, E. R., Shows, T. B., and Higgins, M. J. (1999). A maternally methylated CpG island in *KvLQT1* is associated with an antisense paternal transcript and loss of imprinting in Beckwith–Wiedemann syndrome. *Proc. Natl. Acad. Sci. USA* **96**, 8064–8069.
- Srivastava, M., Hsieh, S., Grinberg, A., Williams-Simons, L., Huang, S. P., and Pfeifer, K. (2000). *H19* and *Igf2* monoallelic expression is regulated in two distinct ways by a shared *cis* acting regulatory region upstream of *H19*. *Genes Dev.* **14**, 1186–1195.
- Stoger, R., Kubicka, P., Liu, C. G., Kafri, T., Razin, A., Cedar, H., and Barlow, D. P. (1993). Maternal-specific methylation of the imprinted mouse *Igf2r* locus identifies the expressed locus as carrying the imprinting signal. *Cell* **73**, 61–71.
- Surani, M. A., Barton, S. C., and Norris, M. L. (1984). Development of reconstituted mouse eggs suggests imprinting of the genome during gametogenesis. *Nature* **308**, 548–550.

- Swain, J. L., Stewart, T. A., and Leder, P. (1987). Parental legacy determines methylation and expression of an autosomal transgene: A molecular mechanism for parental imprinting. *Cell* **50**, 719–727.
- Takada, S., Paulsen, M., Tevendale, M., Tsai, C. E., Kelsey, G., Cattanaach, B. M., and Ferguson-Smith, A. C. (2002). Epigenetic analysis of the *Dlk1-Gtl2* imprinted domain on mouse chromosome 12: Implications for imprinting control from comparison with *Igf2-H19*. *Hum. Mol. Genet.* **11**, 77–86.
- Thorvaldsen, J. L., Duran, K. L., and Bartolomei, M. S. (1998). Deletion of the *H19* differentially methylated domain results in loss of imprinted expression of *H19* and *Igf2*. *Genes Dev.* **12**, 3693–3702.
- Thorvaldsen, J. L., Mann, M. R., Nwoko, O., Duran, K. L., and Bartolomei, M. S. (2002). Analysis of sequence upstream of the endogenous *H19* gene reveals elements both essential and dispensable for imprinting. *Mol. Cell. Biol.* **22**, 2450–2462.
- Tremblay, K. D., Saam, J. R., Ingram, R. S., Tilghman, S. M., and Bartolomei, M. S. (1995). A paternal-specific methylation imprint marks the alleles of the mouse *H19* gene. *Nat. Genet.* **9**, 407–413.
- Tremblay, K. D., Duran, K. L., and Bartolomei, M. S. (1997). A 5' 2-kilobase-pair region of the imprinted mouse *H19* gene exhibits exclusive paternal methylation throughout development. *Mol. Cell. Biol.* **17**, 4322–4329.
- Tsai, T. F., Jiang, Y. H., Bressler, J., Armstrong, D., and Beaudet, A. L. (1999). Paternal deletion from *Snrpn* to *Ube3a* in the mouse causes hypotonia, growth retardation and partial lethality and provides evidence for a gene contributing to Prader-Willi syndrome. *Hum. Mol. Genet.* **8**, 1357–1364.
- Wang, J., Mager, J., Chen, Y., Schneider, E., Cross, J. C., Nagy, A., and Magnuson, T. (2001). Imprinted X inactivation maintained by a mouse Polycomb group gene. *Nat. Genet.* **28**, 371–375.
- Wang, J., Mager, J., Schnedier, E., and Magnuson, T. (2002). The mouse PcG gene *eed* is required for *Hox* gene repression and extraembryonic development. *Mamm. Genome.* **13**, 493–503.
- Warnecke, P. M., Mann, J. R., Frommer, M., and Clark, S. J. (1998). Bisulfite sequencing in preimplantation embryos: DNA methylation profile of the upstream region of the mouse imprinted *H19* gene. *Genomics* **51**, 182–190.
- Wigler, M., Levy, D., and Perucho, M. (1981). The somatic replication of DNA methylation. *Cell* **24**, 33–40.
- Wigler, M. H. (1981). The inheritance of methylation patterns in vertebrates. *Cell* **24**, 285–286.
- Wutz, A., Smrzka, O. W., Schweifer, N., Schellander, K., Wagner, E. F., and Barlow, D. P. (1997). Imprinted expression of the *Igf2r* gene depends on an intronic CpG island. *Nature* **389**, 745–749.
- Wutz, A., Theussl, H. C., Dausman, J., Jaenisch, R., Barlow, D. P., and Wagner, E. F. (2001). Non-imprinted *Igf2r* expression decreases growth and rescues the *Tme* mutation in mice. *Development* **128**, 1881–1887.
- Yang, T., Adamson, T. E., Resnick, J. L., Leff, S., Wevrick, R., Francke, U., Jenkins, N. A., Copeland, N. G., and Brannan, C. I. (1998). A mouse model for Prader-Willi syndrome imprinting-centre mutations. *Nat. Genet.* **19**, 25–31.
- Yang, Y., Li, T., Vu, T. H., Ulaner, G. A., Hu, J. F., and Hoffman, A. R. (2003). The histone code regulating expression of the imprinted mouse *Igf2r* gene. *Endocrinology* **144**, 5658–5670.
- Yoon, B. J., Herman, H., Sikora, A., Smith, L. T., Plass, C., and Soloway, P. D. (2002). Regulation of DNA methylation of *Rasgrfl*. *Nat. Genet.* **30**, 92–96.
- Zwart, R., Sleutels, F., Wutz, A., Schinkel, A. H., and Barlow, D. P. (2001). Bidirectional action of the *Igf2r* imprint control element on upstream and downstream imprinted genes. *Genes Dev.* **15**, 2361–2366.

Insulin-Like Growth Factor Signaling in Fish

Antony W. Wood,^{*} Cunming Duan,^{*,†} and Howard A. Bern[§]

^{*}Department of Molecular, Cellular, and Developmental Biology, University of Michigan—Ann Arbor, Ann Arbor, Michigan 48109

[§]Department of Integrative Biology and Cancer Research Laboratory, University of California, Berkeley, California 94720

The insulin-like growth factor (IGF) system plays a central role in the neuroendocrine regulation of growth in all vertebrates. Evidence from studies in a variety of vertebrate species suggest that this growth factor complex, composed of ligands, receptors, and high-affinity binding proteins, evolved early during vertebrate evolution. Among nonmammalian vertebrates, IGF signaling has been studied most extensively in fish, particularly teleosts of commercial importance. The unique life history characteristics associated with their primarily aquatic existence has fortuitously led to the identification of novel functions of the IGF system that are not evident from studies in mammals and other tetrapod vertebrates. Furthermore, the emergence of the zebrafish as a preferred model for development genetics has spawned progress in determining the requirements for IGF signaling during vertebrate embryonic development. This review is intended as a summary of our understanding of IGF signaling, as revealed through research into the expression, function, and evolution of IGF ligands, receptors, and binding proteins in fish.

KEY WORDS: IGF, Fish, Growth factors, Development, Receptors, Binding proteins, Evolution. © 2005 Elsevier Inc.

I. Introduction

It has long been recognized that the growth hormone/insulin-like growth factor axis plays an integral role in the neuroendocrine regulation of vertebrate growth. As outlined in the current “somatomedin hypothesis,” tissue

[†]Corresponding author. E-mail: cduan@umich.edu.

secretions of insulin-like growth factors (IGFs) mediate the growth-promoting actions of pituitary growth hormone (GH) by way of endocrine, paracrine, and/or autocrine mechanisms (Le Roith *et al.*, 2001). At the cellular level, IGF signaling can trigger a variety of biological responses including, but not limited to, growth, proliferation, survival, migration, and differentiation. The specific cellular responses are ultimately dependent on local interactions among the ligands, receptors, IGF-binding proteins (IGFBPs), specific proteases, extracellular matrix proteins, and intracellular signal transduction pathways (Clemmons, 2001; Duan, 2002; Firth and Baxter, 2002). At the whole animal level, it is the coordination of these cellular responses among different tissues and cell types that ultimately determines the global pattern of organismal growth. Although our appreciation for the complexity of IGF-mediated growth and development has increased exponentially, discoveries suggesting additional functions for the IGF system (e.g., life span determination; Holzenberger *et al.*, 2003) clearly indicate that our understanding of the intricacies of IGF signaling remains incomplete.

Studies in lower vertebrates, including fish, have yielded many insightful perspectives on the evolution of the IGF system, and its role in the neuroendocrine regulation of animal growth and development. This review is intended to provide the reader with a modern, and, it is hoped, unique, perspective on the past, present, and future of IGF research, viewed primarily through the lens of piscine endocrinology.

II. General Background

A. Discovery of the IGFs

After the identification of growth hormone in the 1940s (Li and Evans, 1944), considerable debate emerged regarding the mechanistic basis of its growth-promoting actions. One of the major obstacles to progress in this area was the lack of concordance between the observed effects of GH *in vivo* and *in vitro*. For example, hypophysectomy markedly decreased protein synthesis in cultured explants of epiphyseal cartilage, as indicated by $^{35}\text{SO}_4$ uptake (sulfation), whereas GH injection restored cartilage sulfation activities. However, when added directly to cultured cartilage explants, GH exerted negligible effects (Denko and Bergenstal, 1955). A significant breakthrough occurred in 1957, on the observation that addition of normal rat serum, or serum from hypophysectomized rats injected with GH, significantly stimulated sulfate uptake in cartilage explants, whereas culture medium containing only purified GH had no effect (Salmon and Daughaday, 1957). Because the

serum of hypophysectomized rats was virtually inactive, it was proposed that the growth-promoting actions of GH were mediated by an unidentified substance in the serum, subsequently named "sulfation factor." It later became evident that sulfation factor could elicit a broad spectrum of biological effects, including the stimulation of both DNA and protein synthesis (Daughaday and Mariz, 1962; Hall, 1970; Hall and Uthne, 1971; Salmon and Du Vall, 1970a,b). Sulfation factor was subsequently renamed "somatomedin" (SM), to reflect its general mediation of GH actions on somatic growth (Daughaday *et al.*, 1972).

Ongoing efforts to purify SM by a variety of procedures and bioassay systems led to the identification of three SM variants: a neutral polypeptide (SM-A), an acidic polypeptide (SM-B), and a basic polypeptide (SM-C) (Hall and Uthne, 1971; Van Wyk *et al.*, 1974). SM-B was later identified as epidermal growth factor (EGF), and is no longer considered to be a member of the SM family (Heldin *et al.*, 1981). SM-A and SM-C, meanwhile, were both shown to exhibit insulin-like activities (Hall and Uthne, 1971; Underwood *et al.*, 1972).

The concurrent work of two other research groups eventually converged with the work of Daughaday *et al.*, yielding a new paradigm in our understanding of IGF biology. In investigating the effects of serum insulin-like activity (ILA) on adipocyte metabolism, Froesch *et al.* (1963) reported that a proportion of the ability of serum ILA to stimulate glucose uptake could not be suppressed with antiserum raised against insulin (Froesch *et al.*, 1963). This activity, referred to as nonsuppressible insulin-like activity (NSILA), was found to be regulated independently of insulin, and was thus concluded to be a unique factor with insulin-like properties. Meanwhile, Temin (1967) reported that virus-infected chick embryo fibroblast cells grew faster and reached a higher saturation density than uninfected cells when cultured in medium containing limited levels of serum. He concluded that both normal and infected cells required a serum factor for proliferation, but infected cells needed less of this factor. Insulin could partially replace this serum factor, but only at concentrations approximately 100 times greater than normal levels of insulin in the circulation, leading to the suggestion that some "insulin-like activity" might be involved in stimulating cell proliferation. A few years later, Pierson and Temin (1972) demonstrated that a fraction of calf serum ["multiplication-stimulating activity" (MSA), so called for its ability to stimulate cell proliferation and DNA synthesis] exhibited significant insulin-like activity on rat adipocytes. The inability to suppress MSA with antiserum raised against insulin led to the suggestion that MSA and NSILA were the same molecule.

These three lines of independent research merged when the biologically active molecules were purified, and their primary structures were determined. In 1978, the primary structures of NSILA I and II were reported, and shown

to be highly similar to insulin and its precursor, proinsulin (Rinderknecht and Humbel, 1978a,b); the two peptides were therefore renamed “insulin-like growth factors” (IGF-1 and -2), and both were subsequently shown to potently stimulate cartilage sulfation activity *in vitro* (Zapf *et al.*, 1978). Further purification and structural analyses led to the eventual clarification of the relationships between SMs, IGFs, and MSAs: SM-C is identical to IGF-1 (SM-A is a deaminated form of SM-C/IGF-1) and MSA is identical to IGF-2 (Klapper *et al.*, 1983; Marquardt *et al.*, 1981). IGF-1 and IGF-2 are now recognized as the primary ligands of the insulin-like growth factor (IGF) family.

B. IGF System in Mammals

It is now well established that the IGFs are components of a remarkably complex hormone system that also includes specific cell surface receptors and a family of high-affinity ligand-binding proteins. In the interests of brevity, we provide in this section only brief descriptions of the primary components of this system as described in mammals (Fig. 1). Readers are referred elsewhere for more comprehensive reviews of the mammalian IGF system (Clemmons, 2001; Firth and Baxter, 2002; Jones and Clemmons, 1995; Le Roith *et al.*, 2001; Nakae *et al.*, 2001).

1. Ligands

Mature human IGF-1 (70 amino acids) and IGF-2 (67 amino acids) are single-chain polypeptides structurally similar to proinsulin. The mature IGF peptides contain four biochemically distinct domains (B-C-A-D); the presence of the carboxyl-terminal D domain distinguishes mature IGFs from proinsulin, which contains only the B, C, and A domains. As with all known insulin-like peptides, the IGFs are synthesized as prohormones, and targeted for secretion by hydrophobic signal peptides. Removal of the signal peptide yields prohormones containing carboxyl-terminus extensions (E domains) of 25 (pro-IGF-1) and 89 (pro-IGF-2) amino acids; these are proteolytically removed to generate the four-domain mature IGF peptides (Fig. 2).

The central importance of the IGFs to prenatal and postnatal growth is illustrated by the severe growth-retarded phenotype (dwarfism) exhibited by mice in which the IGF-1, IGF-2, and/or IGF-1 receptor genes have been inactivated by homologous gene targeting. Independently targeting either IGF gene induced intermediate growth retardation, whereas knockout of both genes, or the IGF-1 receptor gene, yielded neonates less than half normal size that died shortly after birth (Baker *et al.*, 1993; DeChiara *et al.*, 1990; Liu *et al.*, 1993; Nakae *et al.*, 2001). The importance of IGFs as

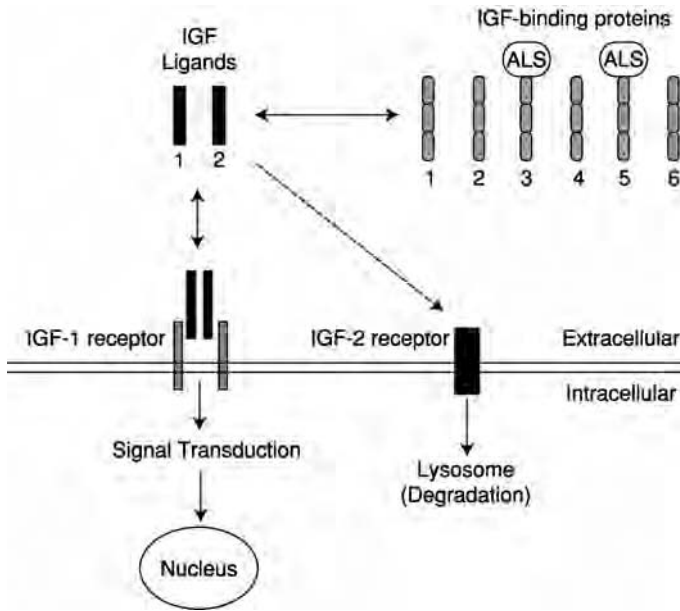


FIG. 1 The mammalian insulin-like growth factor (IGF) system. IGF ligands signal through the IGF-1 receptor, a receptor tyrosine kinase. The IGF-2 receptor preferentially binds IGF-2, but targets the ligand to degradation. The IGF-binding proteins (IGFBPs) modulate the bioavailability of IGFs in the extracellular environment, thereby influencing ligand–receptor interactions. IGFBP-3 and -5 can form ternary complexes with IGFs and the acid-labile subunit (ALS); most serum IGFs are in such a complex with IGFBP-3.

regulators of human growth is similarly indicated by the severe dwarfism observed in a human patient with a natural truncation mutation in the IGF-1 gene (Woods *et al.*, 1996).

Although originally thought to be synthesized and secreted exclusively by the liver under the regulation of GH, it is now well established that both IGFs are also synthesized in many, if not all, nonhepatic tissues (Daughaday and Rotwein, 1989; Jones and Clemmons, 1995). Importantly, extrahepatic sources of IGF-1 can compensate for a complete absence of hepatic IGF-1 production (Yakar *et al.*, 1999), an observation that underlies modern revisions to the original somatomedin hypothesis (Le Roith *et al.*, 2001). Furthermore, it is now well established that IGF-1 synthesis and secretion is GH independent during early development, and this independence may extend to specific organs (e.g., gonads) during later development (Nakae *et al.*, 2001).

Efforts to determine the precise functional requirements for the dual IGF ligands have been complicated by the variations in IGF-signaling dynamics among species and developmental stages. In the mouse, homologous gene

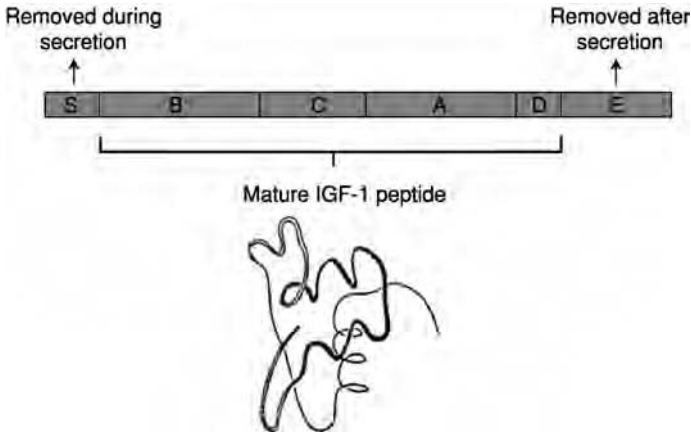


FIG. 2 Schematic diagram illustrating the primary structure of the mammalian insulin-like growth factor 1 (IGF-1) preprohormone (*top*) and the tertiary structure of mature IGF-1 (*bottom*). The signal peptide (S) is removed during secretion, to yield a prohormone (proIGF-1) containing five domains (B-C-A-D-E). The E domain is removed from the secreted prohormone to yield the four-domain mature IGF-1 peptide. (IGF-1 tertiary structure image courtesy of Chan and Steiner, 2000.)

targeting revealed that paternally inherited IGF-2 is the primary growth-promoting ligand between embryonic days 11.5 and 13.5. Effects of deletion were not observed before this period (Baker *et al.*, 1993; DeChiara *et al.*, 1990), suggesting IGF-independent growth during early embryogenesis, despite molecular expression data indicating otherwise (Heyner *et al.*, 1989, 1993). Both ligands, however, are clearly necessary to regulate fetal growth in mice, and postnatal growth in mice seems largely dependent on IGF-1.

In humans, both IGF ligands are required for normal growth throughout fetal and postnatal development. Moreover, IGF-2 cannot fully compensate for an absence of IGF-1 expression during postnatal development, indicating nonredundant functions for the two ligands (Nakae *et al.*, 2001). The absence of significant fetal growth restriction in GH and GH receptor knockout mice also suggests that the growth-promoting actions of IGFs are GH independent during fetal development (Le Roith *et al.*, 2001).

The biological responses to IGF signaling were initially broadly classified as either metabolic (insulin-like), or anabolic. Metabolic effects ascribed to IGF signaling include the stimulation of glucose uptake and oxidation, glycogen synthesis, amino acid uptake, and lipogenesis (Binoux, 1995). These effects are thought to be mediated primarily through binding to the insulin receptor, which exhibits considerable structural similarity to IGF receptors. The anabolic actions of IGFs include stimulation of cell proliferation, protein synthesis, and nucleic acid (RNA and DNA) synthesis, and the suppression

of protein degradation; these actions are mediated primarily through activation of its cognate (IGF-1) receptor. However, there is genetic evidence suggesting that some of the mitogenic effects of IGF-2 in the mammalian fetus may be mediated through alternatively spliced insulin receptor variants, which are expressed during fetal development despite an absence of insulin expression (Nakae *et al.*, 2001).

Recognition that the biological actions of IGFs are not limited to tissue growth or intermediary metabolism has spawned widespread interest in the study of IGF signaling. IGF signaling has been shown to stimulate cell proliferation, cell growth, differentiation, and migration; inhibit apoptosis; modulate steroid hormone and cytokine production; and activate specific genes involved in cell cycle progression (Le Roith *et al.*, 2001). The remarkably diverse effects of IGF signaling in multiple cell types argue for the central importance of this growth factor system as a regulator of animal growth and development.

2. Receptors

In mammals, there are two classes of receptors that bind IGFs with high affinity. The type I (or IGF-1) receptor is a member of the tyrosine kinase superfamily of transmembrane receptors, and is recognized as the definitive mediator of IGF signaling in mammals. It is synthesized as a single polypeptide chain, posttranslationally modified by removal of a 30-residue signal peptide, and bisected into a 710-residue α subunit and a 627-residue β subunit. The α and β subunits are subsequently linked by disulfide bonds to form an $\alpha\beta$ hemireceptor, which hybridizes to another $\alpha\beta$ hemireceptor to form the mature $\alpha_2\beta_2$ holoreceptor (Fig. 3). The extracellular α subunits contain the ligand-binding domain, whereas the intracellular catalytic (e.g., tyrosine kinase) domains are located within the β subunits (Butler *et al.*, 1998).

Ligand binding triggers tyrosine phosphorylation of the β domain, leading to recruitment of multiple endogenous substrates (e.g., insulin-receptor substrate, IRS) to specific phosphotyrosine-docking sites within the β subunit. The recruitment of IRS and other substrate molecules initiates a cascade of further phosphorylation events involving multiple second-messenger molecules; for example, recruitment of SH2 domain-containing proteins can activate the monomeric G protein Ras, triggering activation of the mitogen-activated protein kinase (MAPK) signaling pathway. Alternatively, receptor phosphorylation can activate the phosphoinositol-3-kinase (PI3-kinase) or protein kinase B (PKB/Akt) signal transduction pathways. These signaling pathways ultimately induce alterations in target gene expression, the precise nature of which is dependent on cell type and cellular context.

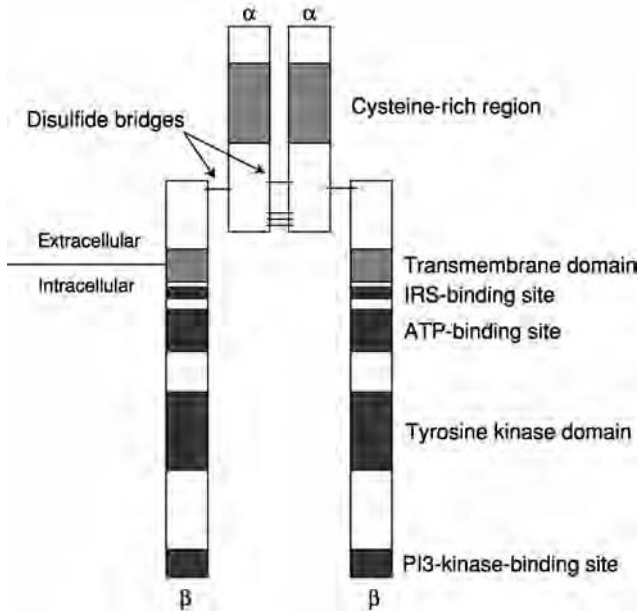


FIG. 3 The heterotetrameric type 1 IGF receptor in mammals. The holoreceptor is composed of two dimeric $\alpha\beta$ hemireceptors; the α subunits are bound by disulfide bridges to form the ligand-binding site in the extracellular region. Tyrosine kinase activity is conferred by the β subunits, which span the cell membrane. The β subunits also contain an insulin receptor substrate (IRS)-binding site, an ATP-binding site, and a PI3-kinase-binding site.

The IGF-1 receptor shows significant structural similarity to the insulin receptor. Although there is evidence for heterologous binding between insulin and IGFs, and their respective receptors, the IGF-1 receptor exhibits 100- to 1000-fold greater affinity for its cognate ligand. As noted above, however, IGF-2 can bind to insulin receptor variants in fetal mammals, and this binding was shown to partially rescue the growth defects induced by targeted deletion of the IGF-1 receptor gene (Nakae *et al.*, 2001). Hybrid insulin/IGF-1 receptors, consisting of an IGF-1 α/β subunit linked to an insulin α/β subunit, have also been identified in mammalian cells (Moxham *et al.*, 1989; Soos *et al.*, 1993); although it has been shown that these hybrid receptors bind IGF-1 preferentially over insulin (Soos *et al.*, 1993), it remains unclear whether hybrid receptors have distinct physiological functions *in vivo*.

The type II IGF receptor identified in mammals is identical to one of the known cation-independent mannose 6-phosphate receptors (MPR 300), generally associated with lysosomal targeting of extracellular molecules (e.g., bacterial toxins). This monomeric transmembrane receptor has a molecular mass of approximately 250 kDa, and exhibits greater affinity for IGF-2 than

for IGF-1 (Tong *et al.*, 1988). The absence of any recognizable catalytic domains suggests that the type II receptor does not activate conventional signal transduction pathways. Rather, binding of IGF-2 to the type II receptor has been shown to result in internalization and degradation of the ligand, a process that may be under the regulation of extracellular insulin (Oka *et al.*, 1985). These observations have led to the suggestion that IGF-2 receptor binding (and ligand degradation) may have evolved as a means to modulate cross-talk between insulin and IGFs, and their respective tyrosine kinase receptors.

3. Binding Proteins

The majority of the IGFs present in extracellular fluids of mammals are found in complex with specific, high-affinity insulin-like growth factor-binding proteins (IGFBPs). To date, six distinct IGFBPs have been characterized in humans and other mammals. Designated IGFBP-1 through IGFBP-6, these secreted proteins exhibit distinct structural and biochemical properties, despite relatively high amino acid sequence similarities among family members (Clemmons, 2001; Clemmons *et al.*, 1998).

All mammalian IGFBPs are synthesized as propeptides with a hydrophobic leader sequence, removal of which yields a mature protein composed of 3 recognizable domains of similar size (~80 residues): an N-terminal domain, typically with 12 conserved cysteine residues (10 in IGFBP-6); a C-terminal domain with 6 conserved cysteine residues; and a central L-domain, thought to act as a hinge between the N and C domains (Fig. 4). The N and C domains are required for high-affinity ligand binding, and are consequently the most highly conserved among family members, and across species (Firth and Baxter, 2002). All mammalian IGFBPs also contain a thyroglobulin type 1 (TY) motif in the C-terminal region; TY motifs are common to a number of other proteins (e.g., teleost oocyte protease inhibitors; Wood *et al.*, 2004), and may confer antiproteolytic properties to the IGFBPs (Fowles *et al.*, 1997), as seen for other proteins containing this domain (Molina *et al.*, 1996). Further insights into the functional requirements for specific domains, discrete domain regions, and individual amino acid residues, have emerged using site-directed mutagenesis; this topic has been comprehensively reviewed (Clemmons, 2001).

It was initially thought that the role of IGFBPs was to form biologically inactive complexes with IGFs, primarily to prevent the hypoglycemic effects resulting from nonspecific activation of the insulin receptor. More recently, a series of intriguing observations has led to additional hypothesized roles for IGFBPs. For example, IGFBPs have been suggested (1) to mediate the efflux of IGFs from the vascular space to the cell surface, thereby modulating interactions between the ligands and receptors, and (2) to prevent proteolytic

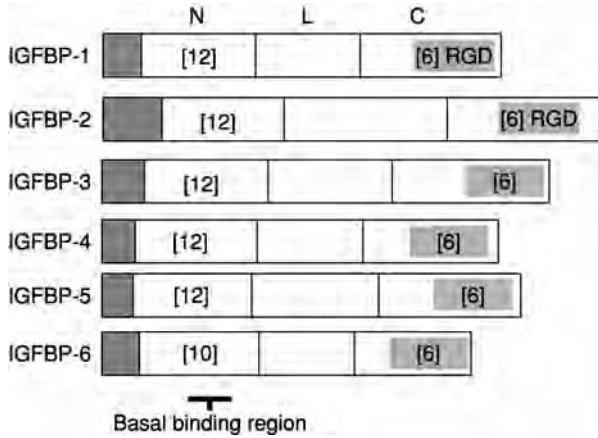


FIG. 4 Schematic representation of the primary structures of the human insulin-like growth factor-binding proteins (IGFBP-1 through IGFBP-6). All IGFBPs contain a signal peptide, and three distinct domains (N-L-C) in the mature (secreted) peptide. Numbers in brackets indicate the number of cysteine residues within the indicated domain. Binding to IGFs requires specific residues in a defined region of the N-terminal domain (basal binding region), while residues in the C domain confer high binding affinity. The L domain serves as a hinge between the N and C domains. Each shaded box indicates the relative position of a thyroglobulin type 1 motif, found in all six IGFBP sequences; IGFBP-1 and IGFBP-2 also contain an Arg/Lys/Asp (RGD) sequence, which may facilitate cell surface binding.

degradation of IGFs, thereby prolonging their half-lives in serum (Clemmons, 2001; Duan, 2002; Firth and Baxter, 2002). Because IGFBPs have also been shown to bind to IGFs with higher affinities than those of the IGF receptors, they may also provide a means of spatially coordinating the delivery of IGFs to specific target cells.

IGFBPs have hence been proposed as primary integrators of IGF signaling, whose overall functions are to modulate interactions between IGFs and their cell surface receptors (Clemmons, 2001; Firth and Baxter, 2002; Jones and Clemmons, 1995). Intriguingly, an additional level of complexity in IGFBP function has emerged: IGF-independent biological actions have now been documented for selected IGFBP family members (Andress and Birnbaum, 1992; Clemmons, 2001; Firth and Baxter, 2002; Jones *et al.*, 1993; Oh *et al.*, 1993). Elucidating the IGF-independent functions of IGFBPs is currently the focus of considerable research interest (Duan, 2002; Firth and Baxter, 2002).

In adult rats, approximately 80% of circulating IGFs are bound within a 150-kDa ternary complex consisting of ligand (IGF-1 or -2), IGFBP-3, and an 88-kDa non-IGF-binding glycoprotein termed the acid-labile subunit (ALS; Baxter and Martin, 1989; Firth and Baxter, 2002; Leong *et al.*,

1992). As part of the 150-kDa complex, IGFs do not readily leave the vascular compartment, and their half-lives can be prolonged for up to 12–15 h, in comparison with the exceptionally short (<10 min) half-life of free IGFs in circulation (Guler *et al.*, 1989; Hodgkinson *et al.*, 1987). IGFs are released from the ternary complex to target tissues as required, either as free IGF or as a membrane-permeable binary complex with IGFBP-3. Evidence indicates that IGFBP-3 proteolysis may underlie the mobilization of IGFs from the circulating reservoir, thereby facilitating precise delivery of the ligand to target tissues (Lee and Rechler, 1995, 1996). Of interest, there is also evidence that IGFBP-5 can also form a 130-kDa ternary complex with IGF-1 and the ALS (Twigg *et al.*, 1998).

Lesser quantities of IGFs form binary complexes with IGFBP-3, or one of three other lower molecular weight IGFBPs (IGFBP-1, IGFBP-2, or IGFBP-4). In general, low levels of IGFBP-5 and IGFBP-6 are detected in rat serum, although more recent studies have indicated that IGFBP-5 may exert biological effects in a variety of cell types by way of specific, paracrine and/or intracrine mechanisms (Xu *et al.*, 2004). Overall, the different binding proteins show distinct patterns of expression and regulation, suggesting independent physiological roles for the individual family members.

Several peptides have been identified that exhibit sequence and structural similarities to mammalian IGFBPs (Oh *et al.*, 1996). The identification of these “IGFBP-related peptides” (IGFBP-rPs) led to the proposed designation of an IGFBP superfamily, characterized primarily by the presence of clustered cysteine-rich regions in their terminal domains (Hwa *et al.*, 1999). Despite *in vitro* evidence of binding between IGFs and IGFBP-rPs, it is now generally acknowledged that IGFBP-rPs have low affinities for IGFs, and are unlikely to function as conventional IGF-binding proteins *in vivo*.

C. Evidence of IGFs in Fish

The existence of an IGF signaling system in fish was uncertain until the late 1980s and early 1990s. Initial efforts to detect IGFs in fish, using heterologous (i.e., mammalian) IGF immunoassay reagents, yielded mixed results (Bautista *et al.*, 1990; Drakenberg *et al.*, 1989; Funkenstein *et al.*, 1989; Furlanetto *et al.*, 1977; Lindahl *et al.*, 1985; Wilson and Hintz, 1982); these were generally attributed to the limited sensitivity of mammalian antibodies for fish IGFs. Furthermore, it became apparent that IGFBPs, particularly abundant in fish serum, could interfere with the detection and measurement of IGFs. Despite the ambiguous results of heterologous assays, strong evidence for the existence of IGFs in fish was obtained through classic physiological studies. For instance, IGF activity was detected in the serum of both teleosts and elasmobranchs, using a porcine cartilage sulfation bioassay

(Shapiro and Pimstone, 1977). These results were later confirmed in a study showing that sulfate uptake in rainbow trout (*Oncorhynchus mykiss*) gill arch cartilage could be stimulated by coincubation with liver slices from normal, but not from hypophysectomized, fish (Komourdjian and Idler, 1978). Duan and Innui (1990a,b) subsequently reported a GH-dependent sulfation factor in the serum of Japanese eel (*Anguilla japonica*), and demonstrated that human IGF-1 could stimulate sulfate uptake in cultured explants of eel gill arch (Duan and Hirano, 1990). These studies clearly suggested the existence of IGF-like activity, and putative IGF receptors, in teleosts and other fish, providing convincing evidence for the importance of IGF signaling throughout vertebrate evolution. The advent of recombinant DNA technology has greatly promoted further interest and progress in describing the evolution and function of IGF signaling in all vertebrates, including fish.

D. Evolution of the IGF System: Ligands, Receptors, and Binding Proteins

Evidence for a functional IGF system (ligands, receptors, and IGF-BPs) in all known vertebrate groups, including fish, indicates a relatively long evolutionary history for this growth factor complex (Bern *et al.*, 1991; Chan and Steiner, 1994, 2000; Chen *et al.*, 1994; Duan, 1997, 1998; Kelley *et al.*, 2002; Moriyama *et al.*, 2000; Navarro *et al.*, 1999; Plisetskaya, 1998; Reinecke and Collet, 1998; Siharath and Bern, 1993; Upton *et al.*, 1998). The origins of this signaling system, however, can be traced much earlier, to an ancestral insulin-like signaling system that likely arose near the dawn of metazoan evolution (Skorokhod *et al.*, 1999).

Vertebrate IGFs (IGF-1 and IGF-2) are derived members of the insulin superfamily, characterized by a common "insulin-like" tertiary structure conferred by conserved cysteine residues and a hydrophobic core (Chan and Steiner, 2000). In addition to insulin and the IGFs, this superfamily has been proposed to include relaxin, placentin, and other insulin-like peptides (ILPs) in vertebrates (Chan and Steiner, 2000; Kasik *et al.*, 2000); insulin, relaxin, and IGF-like and hybrid insulin/IGF-like peptides in protochordates (Chan and Steiner, 2000; Chan *et al.*, 1990; Georges and Schwabe, 1999; McRory and Sherwood, 1997; Reinecke *et al.*, 1999); and numerous ILPs characterized in invertebrates (Brogiolo *et al.*, 2001; Krieger *et al.*, 2004; Lagueux *et al.*, 1990; Nagasawa *et al.*, 1986; Pierce *et al.*, 2001b; Smit *et al.*, 1988). To date, IGF-like molecules have not been identified in any invertebrate, whereas distinct insulin and IGF-like genes have been shown to exist in urochordates (McRory and Sherwood, 1997; Reinecke *et al.*, 1999), suggesting that the original "IGF-like" gene diverged from its insulin-like ancestor

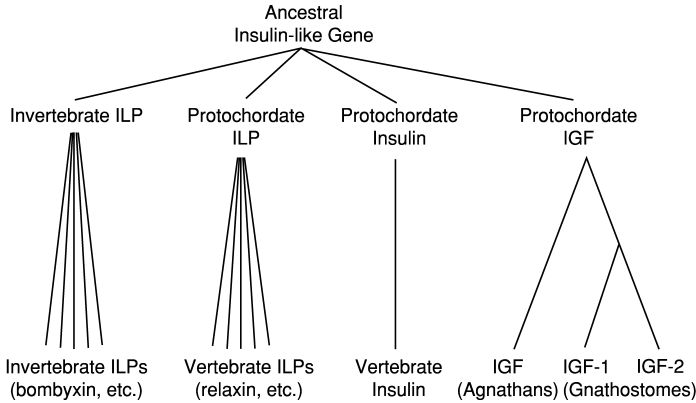


FIG. 5 Evolutionary origins of the insulin-like growth factors (IGFs). The IGFs are derived from an ancestral insulin-like gene that has duplicated and diverged many times throughout metazoan evolution, yielding vertebrate insulin and the IGFs, in addition to a number of insulin-like peptides (ILPs) in both vertebrates and invertebrates. IGF-like genes have not been described in an invertebrate species, suggesting that appearance of the IGFs postdated divergence of the vertebrates from their invertebrate ancestors.

after divergence of the protochordates from their invertebrate ancestor, but before the appearance of vertebrates (Fig. 5).

IGF signaling is mediated primarily by the type I IGF receptor (IGF-1R), which exhibits structural homology to the insulin receptor (InsR), and likely evolved from a common ancestral gene. The InsR and the IGF-1R are heterotetrameric transmembrane receptor tyrosine kinases; this family also includes the vertebrate InsR-related receptor, a number of InsR homologs in invertebrates (e.g., Fernandez *et al.*, 1995), and insulin receptor-like tyrosine kinases identified in marine sponges (Skorokhod *et al.*, 1999). Thus, the presence of both insulin-like peptides and insulin receptor-like tyrosine kinases throughout the metazoans suggests that the evolution of insulin-like signaling may have coincided with the evolution of multicellularity.

The structural similarities between the InsR and the IGF-1R, and their respective ligands, provide the possibility for heterologous ligand–receptor interactions, a phenomenon that has been observed experimentally (Nakae *et al.*, 2001). This potential for cross-activation has been proposed to explain the origin and evolution of the IGF-binding proteins (IGFBPs), secreted peptides in the serum of vertebrates that exhibit high affinity for IGFs, but little affinity for insulin (Kelley *et al.*, 2002). According to this model, the binding characteristics of IGFBPs provide a secondary mechanism by which the cellular responses to IGF signaling can be specified. In addition, some IGFBPs appear to have evolved (or retained) additional ligand-independent functions (Duan, 2002).

Although a partial sequence for an IGFBP-like molecule has been identified in amphioxus (GenBank accession no. AB080316), and biochemical evidence supports the existence of IGFbps in agnathans, the evolutionary origins of the IGFbps remain largely unresolved at this time. Multiple models have been proposed to explain the evolutionary origins of IGFbps and other IGFBP-related proteins. A summary of these is beyond the scope of this review; readers are therefore referred to other reviews of this topic (Hwa *et al.*, 1999; Kelley *et al.*, 2002).

III. IGFs of Fish

A. IGF-1

1. Primary Structure

a. Teleosts Full-length IGF-1 cDNA sequences have been published for coho salmon (*Oncorhynchus kisutch*; Cao *et al.*, 1989; Duguay *et al.*, 1992), rainbow trout (Shamblott and Chen, 1992), Atlantic salmon (*Salmo salar*; Duguay *et al.*, 1992), chinook salmon (*Oncorhynchus tshawytscha*; Wallis and Devlin, 1993), chum salmon (*Oncorhynchus keta*; Kavsan *et al.*, 1993), broad-head catfish (*Clarias macrocephalus*; McRory and Sherwood, 1994), gilthead seabream (*Sparus aurata*; Duguay *et al.*, 1996), carp (*Cyprinus carpio*; Liang *et al.*, 1996), tilapia (*Oreochromis mossambicus*; Reinecke *et al.*, 1997), daddy sculpin (*Cottus scorpius*; Loffing-Cueni *et al.*, 1998), barramundi (*Lates calcarifer*; Stahlbom *et al.*, 1999), rabbitfish (*Siganus guttatus*; Ayson *et al.*, 2002), zebrafish (Maures *et al.*, 2002), turbot (*Psetta maxima*; Duval *et al.*, 2002), and four-spine sculpin (*Cottus kazika*; Inoue *et al.*, 2003). Partial or complete IGF-1 cDNA sequence information is also available from public genome databases (GenBank) for additional teleost species, although at the time of writing, these had not been published in the primary literature. These include sequences for yellow perch (*Perca flavescens*), channel catfish (*Ictalurus punctatus*), orange-spotted grouper (*Epinephelus coioides*), European perch (*Perca fluviatilis*), mud carp (*Cirrhinus molitorella*), Korean rockfish (*Sebastes schlegeli*), grass carp (*Ctenopharyngodon idella*), goldfish (*Carassius auratus*), bluntnout bream (*Megalobrama amblycephala*), triangular bream (*Megalobrama terminalis*), black seabream (*Acanthopagrus schlegeli*), and Japanese flounder (*Paralichthys olivaceus*).

As seen with other vertebrates, teleost IGF-1 cDNA sequences are predicted to encode preprohormones, ranging between 159 and 193 amino acids in length. All contain a putative signal peptide, removed during secretion to yield the IGF-1 prohormone composed of five distinct domains (B-C-A-D-E) as seen for mammalian IGFs. Subsequent proteolytic removal of the E

domain yields the mature IGF-1 peptide (domains B-C-A-D), containing either 68 or 70 amino acids, depending on the species. The difference in length among species is due specifically to the presence/absence of two amino residues in the C domain, a divergence that occurs at the ordinal level within the teleost lineage. Specifically, mature IGF-1 peptides in cypriniforms (carp), salmoniforms (salmon), and siluriforms (catfish) possess histidine and asparagine residues at positions 39 and 40, respectively (position 1 is designated as the first residue of the mature peptide). In *Xenopus* and chicken IGF-1, these respective positions are occupied by histidine residues, and in mammals they are occupied by a proline and a glutamine. In contrast, these residues are absent from the C domains of IGF-1 in those perciforms (perch), scorpaeniforms (scorpionfishes) and pleuronectiforms (flatfishes) so far examined; the functional consequences of this distinct sequence divergence are unknown. Overall, mature teleost IGF-1 peptides exhibit 72–81% identity with mature human IGF-1, confirming that the structure of the functional IGF-1 peptide has been well conserved throughout vertebrate evolution.

b. Elasmobranchs To our knowledge, IGF-1 has been cloned from only a single elasmobranch species, the spiny dogfish shark (*Squalus acanthias*; Duguay *et al.*, 1995). The shark IGF-1 cDNA encodes a 126-amino acid preprohormone, containing a signal peptide (24 residues) somewhat shorter than the signal sequence of IGF-1 in teleosts and other vertebrates, but similar to the length of signal peptides in other secreted proteins. The primary structure of the secreted prohormone is consistent with that of other vertebrates, being composed of five domains (B-C-A-D-E). Proteolytic removal of the E domain yields a mature peptide of 70 amino acids; interestingly, its identity with mature human IGF-1 (72%) is higher than its identity with the known teleost IGF-1 peptides (62–70%). The pro-IGF-1 E domain is composed of 32 amino acids, slightly shorter than the typical 35 amino acids seen in other vertebrates. Most of the sequence variability between mature IGF-1 of shark and that of other vertebrates is evident in the C and D domains.

c. Agnathans Agnathans (jawless fishes) represent a class of vertebrates whose lineage diverged from the ancestors of jawed vertebrates (gnathostomes) approximately 550 million years ago. Sequence information from extant agnathans (lampreys and hagfishes) thus has the potential to offer valuable insights into vertebrate genome evolution. Complementary DNAs encoding prepro-IGFs have been cloned from two representative agnathans, the Atlantic hagfish (*Myxine glutinosa*; Nagamatsu *et al.*, 1991), and the sea lamprey (*Petromyzon marinus*; Kawauchi *et al.*, 2002). The deduced amino acid sequences of these prepro-IGFs are similar to vertebrate prepro-IGFs, possessing relatively long signal peptides, and the typical five-domain

structure. To date, only a single IGF-like molecule has been identified in species of this class; it exhibits highest similarity to IGF-1 in gnathostomes, particularly in the A and B domains. The known coexistence of an agnathan insulin gene (Chan *et al.*, 1981) suggests that divergence of the insulin and IGF genes predated divergence of the agnathan lineage, but that duplication and divergence of the IGF precursor into two subtypes (IGF-1 and IGF-2; see below) occurred within the gnathostome lineage after divergence from the agnathans. Importantly, characterization of hagfish prepro-IGF has revealed that specific residues necessary for maintaining tertiary structure and biological activity have been highly conserved in IGF family peptides for more than 550 million years of vertebrate evolution (Nagamatsu *et al.*, 1991).

2. Genes and mRNAs

There are distinct differences between the gene structures of IGF-1 in mammals and fish. For example, human IGF-1 is encoded by a single gene of six exons spanning more than 100 kilobases of genomic DNA, whereas the IGF-1 genes of zebrafish (Chen *et al.*, 2001), salmon (Kavsan *et al.*, 1993, 1994), and flounder (Tanaka *et al.*, 1998) are composed of five exons, spanning approximately 15, 22, and 17.5 kb, respectively. Wallis and Devlin (1993) furthermore demonstrated that coho salmon possess two nonallelic IGF-1 genes, a finding that was subsequently confirmed in chum salmon (Kavsan *et al.*, 1993, 1994). The presence of duplicate IGF-1 genes was not unexpected in salmonids, because of their pseudotetraploid nature (Allendorf and Thorgaard, 1984); a similar finding was reported in the tetraploid *Xenopus laevis* (Shuldinger *et al.*, 1990). However, more recent evidence suggests the presence of duplicate IGF-1 genes in the zebrafish (Chen *et al.*, 2001), although transcriptional activity remains to be confirmed for both genes. Nagamatsu *et al.* (1991) provided evidence that hagfish likely have a single copy of the IGF gene; to our knowledge, the number of IGF-1 genes has not been determined in any elasmobranch species. A single copy is expected in light of evidence suggesting that the genome duplication in fish occurred subsequent to divergence of the bony fish from their cartilaginous ancestors (Allendorf and Thorgaard, 1984).

In mammals, separate leader exons of the IGF-1 gene can be differentially transcribed to yield two distinct IGF-1 mRNA transcripts. By several complicated mechanisms, multiple mRNA transcripts are subsequently generated, but these ultimately yield either of two IGF-1 prohormones (pro-IGF-1A and pro-IGF-1B). These are identical in the region corresponding to the mature IGF-1 peptide, but differ in the carboxyl-terminal E domain (Daughaday and Rotwein, 1989).

Using Northern hybridization, IGF-1 mRNA transcripts were detected as a single band in coho and chinook salmon (approximately 4.0 kb; Cao *et al.*,

1989; Duan and Hirano, 1992). Subsequent studies using reverse transcription-polymerase chain reaction (RT-PCR) and RNase protection assay, however, revealed the presence of at least four distinct splice variants, designated Ea-1 to Ea-4 (Duguay *et al.*, 1992, 1994). The Ea-1 transcript encodes a prohormone with highest identity to mammalian pro-IGF-1A; Ea-2 is similar to Ea-1, but contains a 36-bp insertion in the E domain encoding region; Ea-3 contains this 36-bp insertion in addition to an 81-bp insertion in the E-domain region; Ea-4 contains the 81-bp insertion without the 36-bp insertion.

Determination of the genomic sequences of IGF-1 genes in salmonids revealed the complicated origins of these splice variants (Shamblott and Chen, 1993; Wallis and Devlin, 1993). The genomic region encoding the E domain of chinook salmon IGF-1 spans three exons (Fig. 6). The 81-bp E-domain insertions in Ea-3 and Ea-4 are derived from a span of 81 nucleotides contiguous with exon 3, whereas the 36-bp insertion of Ea-2 and Ea-3 is encoded entirely by exon 4. The most highly conserved variant (Ea-1) is generated by removal of the 81-bp insert of exon 3 and the entire fourth exon, thereby encoding an E domain of 35 amino acids. Inclusion of the fourth exon, but removal of the terminal 81 bp of exon 3, yields Ea-2, encoding an E domain of 47 amino acids. The longest splice variant of chinook salmon pro-IGF-1 (Ea-3) includes both the terminal 81 bp of exon 3

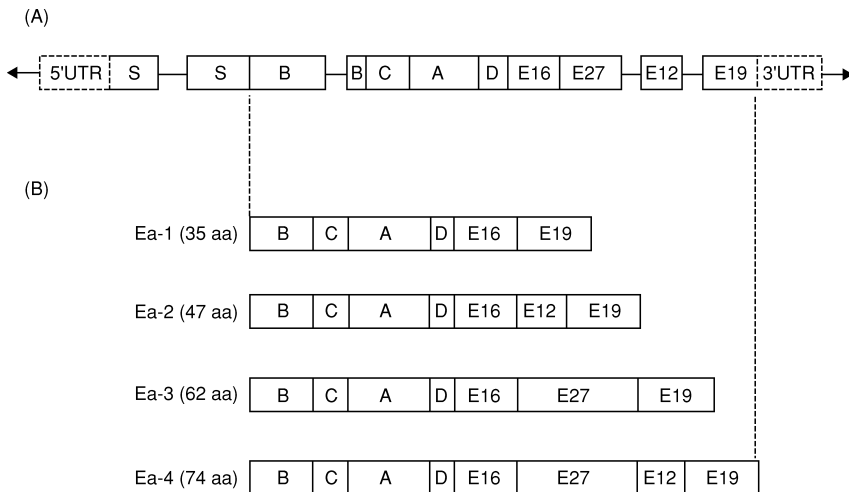


FIG. 6 Schematic diagram illustrating the splice variants of the salmon IGF-1 gene. Differential splicing of the gene (A) yields multiple pro-IGF-1 variants (B) that differ in the length and composition of their respective E domains. (A) Solid boxes indicate gene exons, solid lines indicate introns, and hatched boxes indicate untranslated regions (UTRs). S, signal peptide-encoding region. E-domain numbering (e.g., E16) indicates the number of amino acid residues encoded by the respective gene segment (A) or contained in the pro-IGF-1 peptide (B).

and exon 4, encoding an E domain of 74 amino acids, whereas removal of exon 4 alone yields an E domain (Ea-4) of 62 amino acids. The physiological functions of the various splice variants have not been fully investigated, although data suggesting tissue specificity, and differential hormone responsiveness, of the different pro-IGF-1 transcripts indicate considerable complexity in the regulation of IGF-1 signaling in fish. Intriguingly, evidence has also suggested independent biological activities for specific IGF-1 E-domain peptides (Chen *et al.*, 2002; Tian *et al.*, 1999).

Multiple IGF-1 mRNA transcripts have since been demonstrated in a number of nonsalmonid fish, including tilapia (Schmid *et al.*, 1999), carp (Hashimoto *et al.*, 1997), Japanese flounder (Tanaka *et al.*, 1998), and barramundi (Stahlbom *et al.*, 1999). The mRNA species detected in flounder and barramundi are highly similar to salmonid Ea-2 and Ea-4, with the latter being more abundantly expressed in hepatic tissues. In the flounder, however, the two detected mRNA transcripts (2.9 and 4.7 kb) were predicted to arise from alternative polyadenylation sites in the 3' untranslated region.

Although evidence derived from PCR-based cloning suggests the existence of duplicate IGF-1 genes in zebrafish, only one (designated IGF-1a) has been characterized to date. The exon/intron structure of zebrafish IGF-1a is similar to that of salmonid IGF-1 genes, but is devoid of the 81-bp insertion at the 3' end of exon 3, yielding a pro-IGF-1 with an E domain (Ea-2) of 47 amino acids. By RT-PCR, this was revealed to be the sole variant of pro-IGF-1 detectably expressed in zebrafish embryos and adult tissues (Chen *et al.*, 2001); it remains to be established whether zebrafish IGF-1b is a pseudogene.

The mature IGF-1 peptide in salmon is encoded by portions of exons 2 and 3, as seen for both mammalian and chicken IGF-1 genes. Multiple putative transcription initiation sites have been identified in the IGF-1 genes of chum salmon (Kavsan *et al.*, 1993; Koval *et al.*, 1994), zebrafish (Chen *et al.*, 2001) and tilapia (Chen *et al.*, 1998). Koval *et al.* (1994) furthermore showed that a 385-bp fragment preceding the ATG start codon in the chum salmon possesses basal promoter activity; however, no TATA box- or CAAT box-like sequences were identified. A further comparison of the salmon, chicken, and mammalian IGF-1 genes revealed considerable identity between their 5' flanking regions (Kavsan *et al.*, 1993), an unusual and intriguing finding that suggests potential regulatory functions for this region.

3. Expression Patterns of IGF-1

In accordance with the somatomedin hypothesis, most early studies of IGFs in fish focused on the regulation of hepatic IGF-1 expression in juveniles and adults, its response to specific hormones (e.g., GH), and the

effects of interactions of these factors on somatic growth. However, evidence derived from studies in model vertebrates suggests (1) an important role for nonhepatic sites of IGF-1 expression and localization (Yakar *et al.*, 1999), and (2) a possible role for IGF-1 signaling during early embryonic development, before development of a GH-IGF axis. Evidence from molecular studies in fish clearly indicates that the IGF-1 gene is transcriptionally active throughout all stages of fish development, including embryogenesis; the significance of these findings is discussed in greater detail below (see Section VI: Biological Actions of the IGF System in Fish).

a. IGF-1 mRNA Duguay *et al.* (1992) were among the first to demonstrate that IGF-1 mRNA is detectably expressed in teleost (salmonid) embryos. IGF-1 mRNA expression was subsequently demonstrated in unfertilized eggs, fertilized embryos, and larvae of gilthead seabream (Duguay *et al.*, 1996; Funkenstein *et al.*, 1996; Perrot *et al.*, 1999), zebrafish (Maures *et al.*, 2002), and rainbow trout (Gabillard *et al.*, 2003a; Greene and Chen, 1997), and in larvae of barramundi (Stahlbom *et al.*, 1999), silver seabream (*Sparus sarba*; Deane *et al.*, 2003), and rabbitfish (Ayson *et al.*, 2002). Using *in situ* hybridization, Maures *et al.* (2002) demonstrated ubiquitous tissue distribution of IGF-1 mRNA transcripts in zebrafish embryos from the eight-cell stage through to hatched larvae (72 h), whereas in larval shi drum (*Umbrina cirrosa*), IGF-1 mRNA expression was more specific, being first detected in developing myomeres 1 day posthatching (Radaelli *et al.*, 2003b). Although IGF-1 mRNA was not detected in eggs or pre-hatch embryos of the latter species, its detection in unfertilized eggs of most species suggests a maternal origin for zygotic transcripts, a finding that is in agreement with observations made in *Xenopus*, chickens and mice (Doherty *et al.*, 1994; Scavo *et al.*, 1989, 1991).

More recently, Chen *et al.* (1998) fused a reporter gene (green fluorescent protein, GFP) to the putative promoter region of the tilapia IGF-1 gene; injection of this construct into zebrafish embryos resulted in detectable GFP expression by the 1000-cell stage of development. The delayed onset of GFP expression may reflect the transition from maternal to zygotic gene expression; it remains to be determined whether and when maternal IGF mRNA transcripts are translated to functional proteins during embryonic development in fish.

A number of studies have demonstrated IGF-1 mRNA expression in multiple tissues of juvenile salmonids, including muscle, spleen, fat, intestine, liver, heart, testes, ovary, kidney, pituitary, and brain (Biga *et al.*, 2004; Duan and Plisetskaya, 1993; Duguay *et al.*, 1992; Shamblott and Chen, 1993). A similarly wide distribution of IGF-1 mRNA expression has been reported in juvenile carp (Vong *et al.*, 2003) and juvenile four-spine sculpin (Inoue *et al.*, 2003).

IGF-1 mRNA expression has also been demonstrated in both hepatic and nonhepatic tissues of adult teleosts, including salmonids (Duan and Plisetskaya, 1993; Duan *et al.*, 1993a; Duguay *et al.*, 1992, 1994; Plisetskaya *et al.*, 1993; Sakamoto and Hirano, 1993), daddy sculpin (Loffing-Cueni *et al.*, 1998), tilapia (Reinecke *et al.*, 1997), and goldfish (Otteson *et al.*, 2002). Schmid *et al.* (1999) further investigated the expression of IGF-1 mRNA in the developing tilapia ovary; using *in situ* hybridization, they demonstrated moderate expression of IGF-1 mRNA in the ooplasm of young oocytes, and higher levels of expression in somatic follicle cells (granulosa and theca) of oocytes at the yolk globule stages.

Few studies have investigated the tissue distribution of IGF-1 mRNA in agnathans. Nagamatsu *et al.* (1991) detected hagfish IGF-like transcripts in brain, heart, liver, skeletal muscle, and the islet organ, and Kawauchi *et al.* (2002) demonstrated IGF-1 mRNA expression in sea lamprey liver. These data indicate that wide distribution of IGF-1 mRNA expression has been well conserved throughout vertebrate evolution.

Quantitative estimations of IGF-1 mRNA abundance generally indicate that the liver exhibits the highest levels of expression in fish (e.g., Inoue *et al.*, 2003; Vong *et al.*, 2003), as seen in other vertebrates. One explanation for this may be the presence of a liver-specific, or liver-enriched, IGF-1 transcription factor. In support of this hypothesis, a hepatocyte nuclear factor 1 (HNF-1)-binding element was identified in the promoter region of a salmon IGF-1 gene (Kulik *et al.*, 1995); HNF-1 was furthermore shown to bind to this element and stimulate transcriptional activity. The sequence of this HNF-1-binding site is conserved in all known mammalian, avian, amphibian, and fish species, suggesting that HNF-1 may be responsible for the high levels of IGF-1 gene expression observed in hepatic tissues of vertebrates.

b. IGF-1 Protein Owing to the secretory nature of IGFs, most studies of IGF-1 protein have focused on measurements of its abundance in serum in relation to various physiological or environmental parameters. As noted above, early efforts in this regard were somewhat limited by the reliance on heterologous immunoassay methods. The development of a homologous immunoassay for salmon IGF-1 (Moriyama *et al.*, 1993, 1994) was a significant step toward improved sensitivity and precision in this regard. Homologous immunoassay methods have since been successfully used to quantify serum levels of IGF-1 in coho, Atlantic, chinook and amago salmon (Beckman *et al.*, 1998; Moriyama, 1995; Moriyama *et al.*, 1997a; McCormick *et al.*, 1998).

The detection of IGF-1 protein by immunocytochemical methods can provide additional insight into sites of hormone synthesis, binding, or activity, although much of the available data were generated with heterologous antibodies, and must therefore be interpreted with caution. IGF-1 protein

was immunocytochemically detected in various tissues of larval and/or juvenile shi drum (Radaelli *et al.*, 2003b), turbot (Berwert *et al.*, 1995), and gilthead seabream (Perrot *et al.*, 1999); in follicular epithelial cells of red seabream (*Pagrus major*) ovarian follicles (Kagawa *et al.*, 1995); and in multiple tissues of adult tilapia, including somatic and germ cells of the gonads, in addition to pancreatic cells, gastroentero-endocrine cells, renal proximal tubule cells, interrenal cells, gill chondrocytes, chloride cells, and neurons (Reinecke *et al.*, 1997; Schmid *et al.*, 1999).

Reinecke and colleagues have investigated the tissue localization of IGF peptides in various fish species, with particular attention to their pancreatic localization relative to other metabolic peptides. For example, IGF-1 and insulin immunoreactivity in adult daddy sculpin was colocalized in Brockman bodies and small islets of the pancreas (Loffing-Cueni *et al.*, 1998); in carp, IGF-1 was detected in islet cells exhibiting immunoreactivity for glucagons, pancreatic polypeptide, and somatostatin; and in goldfish and eel, IGF-1 protein was detected primarily in somatostatin-positive cells (Reinecke *et al.*, 1993). IGF-1 immunoreactivity has also been demonstrated in various tissues of two elasmobranchs [thornback ray (*Raja clavata*) and spiny dogfish shark; Reinecke *et al.*, 1992], and one agnathan (hagfish; Reinecke *et al.*, 1991, 1993).

4. Regulation of IGF-1 Expression

a. Hormones There is abundant evidence that growth hormone (GH) is the primary regulator of IGF-1 synthesis and/or secretion in juvenile and adult fishes. For example, GH injections were shown to increase hepatic IGF-1 mRNA levels in coho salmon (Cao *et al.*, 1989; Duan *et al.*, 1993a; Duguay *et al.*, 1994), rainbow trout (Sakamoto and Hirano, 1993; Shambloott *et al.*, 1995), gilthead seabream (Duguay *et al.*, 1996), tilapia (Kajimura *et al.*, 2001; Shepherd *et al.*, 1997), zebrafish (Maures *et al.*, 2002), carp (Hashimoto *et al.*, 1997), and goldfish (Vong *et al.*, 2003). Furthermore, plasma or serum levels of IGF-1, and/or tissue responsiveness to IGF-1, were shown to be GH dependent in a number of teleost species, including tilapia (Funkenstein *et al.*, 1989; Kajimura *et al.*, 2001; Shepherd *et al.*, 1997), eel (Duan and Hirano, 1992; Duan and Inui, 1990a,b), longjaw mudsucker (*Gillichthys mirabilis*; Gray and Kelley, 1991), goldfish (Marchant and Moroz, 1993), and various salmonids (Moriyama, 1995; Moriyama *et al.*, 1994; Niu *et al.*, 1993; Skyrud *et al.*, 1989). Binding studies have, in addition, confirmed the presence of high-affinity GH-binding sites (receptors) in hepatic tissues of teleosts (Gray *et al.*, 1992; Shepherd *et al.*, 1997).

The existence of a functional (bidirectional) GH-IGF axis in fish is further supported by a number of *in vivo* and *in vitro* studies. For example, GH stimulation of IGF-1 mRNA expression was shown to be dose dependent in

primary hepatocyte cultures of coho salmon (Duan *et al.*, 1993b; Pierce *et al.*, 2004) and rainbow trout (Shablott *et al.*, 1995). Conversely, administration of IGF-1 suppressed GH secretion in rainbow trout *in vivo* (Blaise *et al.*, 1995), from cultured tilapia pituitaries (Kajimura *et al.*, 2002), and from isolated pituitary cells of a variety of fish species (Blaise *et al.*, 1995; Fruchtmann *et al.*, 2000, 2001, 2002; Perez-Sanchez *et al.*, 1992; Weil *et al.*, 1999), suggesting the presence of classic negative feedback regulation within the GH-IGF axis of fish.

Although most studies have focused on GH regulation of hepatic IGF-1 expression, the stimulatory responses of GH are not necessarily limited to the liver. For example, GH injection was shown to increase IGF-1 mRNA levels in retina, brain, gill, and intestine of goldfish (Otteson *et al.*, 2002; Vong *et al.*, 2003), in gill and kidney of rainbow trout (Sakamoto and Hirano, 1993), and in tilapia muscle (Kajimura *et al.*, 2001). High-affinity, saturable GH-binding sites have furthermore been identified in many nonhepatic fish tissues (Yao *et al.*, 1991).

Despite abundant evidence supporting a relationship between GH and IGF-1 expression, not all tissues are responsive to GH in terms of IGF-1 expression. For example, GH injections that stimulated hepatic IGF-1 mRNA expression in coho salmon failed to elicit a similar response in heart, fat, brain, ovary, or spleen (Duan *et al.*, 1993a; Duguay *et al.*, 1994). Similarly in rainbow trout, GH injections failed to stimulate IGF-1 expression in the pyloric caeca, kidney, or gill, despite stimulating IGF-1 expression in the liver and IGF-2 expression in pyloric caeca (Shablott *et al.*, 1995). Last, GH injections that stimulated IGF-1 mRNA expression in liver and muscle of tilapia failed to stimulate IGF-1 mRNA expression in gill tissues (Kajimura *et al.*, 2001).

These observations may be explained by the differential tissue distributions of the different pro-IGF-1 mRNAs expressed in teleosts. For example, expression of Ea-1 and Ea-3 isoforms of pro-IGF-1 was restricted to the liver in coho salmon, whereas expression of the Ea-4 isoform was generally more widespread. Duguay *et al.* (1994) showed that GH treatment specifically increased the expression of Ea-1 and Ea-3 transcripts, whereas the Ea-4 transcript was GH resistant. This finding was confirmed in cultured salmon hepatocytes (Duan *et al.*, 1994), suggesting that different pro-IGF-1 isoforms may vary in both tissue distribution and responsiveness to GH. The presence or absence of GH-responsive transcripts (Ea-1 and Ea-3) in other species has not been rigorously studied.

Data from other studies have provided additional evidence for the inherent complexity of the GH-IGF axis in fish. For example, four-spine sculpin reared in saltwater exhibit faster growth than freshwater-reared fish; the accelerated growth of saltwater fish was shown to be associated with elevated hepatic IGF-1 mRNA, but similar pituitary GH mRNA levels (Inoue *et al.*,

2003). A reverse pattern was observed in coho salmon, for which premature seawater transfer is observed to induce growth retardation (stunting): hepatic IGF-1 mRNA levels in stunted fish were significantly lower than in fish maintained in freshwater, whereas plasma GH levels showed an opposite trend (Duan *et al.*, 1995). Similar patterns of expression were observed in salmon subjected to nutritional deprivation (Duan and Plisetskaya, 1993), indicating GH resistance in growth-stunted salmonids. The influence of nutritional status on hepatic (IGF) responsiveness to GH in fish and other vertebrates has been well described; the phenomenon of GH resistance in fish is described in greater detail below.

Evidence from studies in salmonids suggests that insulin may influence hepatic synthesis and/or release of IGF-1. For example, injection of streptozotocin, a drug that destroys insulin-producing beta cells in the pancreas, reduced both circulating insulin levels and IGF-1 levels in coho salmon and brook trout (Banos *et al.*, 1999; Moriyama *et al.*, 1994), and hepatic IGF-1 mRNA levels in coho salmon (Plisetskaya and Duan, 1994). Similarly, in the longjaw mudsucker, experimental induction of diabetes mellitus by surgical removal of the pancreatic islet organ resulted in significant growth retardation (Kelley *et al.*, 1993) and subsequent reductions in IGF-1-like (cartilage sulfation) activity *in vitro*. However, in contrast to mammals, GH injections in diabetic fish restored cartilage sulfation activity levels, and cartilage explants from diabetic fish exhibited high sulfation activities in response to IGF-1 treatment. These observations suggest that in teleosts, abrogated insulin synthesis may not compromise tissue responsiveness to GH or IGF-1, as has been reported in mammals.

Glucocorticoids have been associated with reductions in serum IGFs in a variety of species and circumstances. For example, stressors (e.g., osmotic shock, handling, and confinement) that elicited an increase in serum cortisol resulted in concomitant declines in serum IGF-1 concentrations in Atlantic salmon, Southern bluefin tuna (*Thunnus maccoyii*), silver perch (*Bidyanus bidyanus*), and black bream (*Acanthopagrus butcheri*) (Dyer *et al.*, 2004). Likewise, intraperitoneal injections of cortisol suppressed both plasma IGF-1 and hepatic IGF-1 mRNA expression in tilapia (Kajimura *et al.*, 2003). The absence of any effects of cortisol injections on plasma or pituitary GH levels suggests that corticosteroids may act at the level of the liver to downregulate the abundance or responsiveness of GH receptors, thereby inducing GH resistance.

There is also evidence from fish that sex steroid hormones may influence the GH-IGF axis. This has been shown in sexually dimorphic tilapia, among which females exhibit reduced somatic growth, lower plasma levels of IGF-1, and higher plasma levels of GH than their male counterparts. Injection of 17 β -estradiol into males resulted in a GH-IGF profile more closely resembling that of female fish, whereas administering dihydrotestosterone to

female fish elicited a serum GH-IGF profile resembling that of males (Riley *et al.*, 2002a). Similarly, administration of methyltestosterone to tilapia stimulated both plasma IGF-1 levels and somatic growth (Riley *et al.*, 2002b). These data are in agreement with those of an earlier study showing that plasma IGF-1 levels markedly decline in precociously maturing amago salmon, *Oncorhynchus masou ishikawai*, whereas plasma IGF-1 remained elevated in their immature siblings (Moriyama *et al.*, 1997a). These observations suggest cross-talk between sex steroid hormones and the GH-IGF axis, possibly at the level of hepatic GH receptors; GH resistance induced by sex steroids may thus contribute to the developmental switch between somatic and reproductive development associated with sexual maturation in fishes.

Last, bioactive thyroid hormone (3,5,3'-triiodothyronine, T₃) was reported to stimulate IGF-1 expression in cultured tilapia hepatocytes *in vitro*, and injection of T₃ into adult tilapia resulted in significant increases in hepatic IGF-1 mRNA levels (Schmid *et al.*, 2003). Whereas the stimulatory effects of T₃ on pituitary GH expression were well described in mammals (Koenig *et al.*, 1987), these data provided the first evidence that T₃ may directly influence IGF-1 gene expression in teleost hepatic tissues. Furthermore, they complemented previous data demonstrating the presence of T₃ receptors in rainbow trout liver (Bres and Eales, 1986; MacLatchy and Eales, 1992).

b. Nutrition Nutritional status is clearly an important determining factor in the expression and secretion of metabolic hormones such as insulin family peptides. For example, prolonged starvation generally results in suppressed body growth, with concomitant reductions in the levels of circulating IGF-1. The reduced circulating IGF-1 levels are paradoxically associated with increased plasma GH levels, likely resulting from the absence of negative feedback on pituitary somatotropes (Thissen *et al.*, 1994).

Studies on juvenile and adult teleosts have confirmed a similar relationship between nutritional status and circulating IGF-1 in fish. For example, food consumption and circulating IGF-1 levels have been shown to correlate in many teleosts (Beckman *et al.*, 2004; Duan and Plisetskaya, 1993; Komourdjian and Idler, 1978; Larsen *et al.*, 2001; Moriyama *et al.*, 1994; Niu *et al.*, 1993; Pierce *et al.*, 2001a; Sumpter *et al.*, 1991; Uchida *et al.*, 2003). It was further shown that plasma IGF-1 levels are responsive to both dietary protein content and ration size in seabream (Perez-Sanchez *et al.*, 1994, 1995).

The mechanisms underlying the relationship between nutrition and plasma IGF-1 levels have been explored in a number of species. For example, Duan and Hirano (1992) showed that hepatic IGF-1 mRNA levels were significantly lower in fasted eels compared with fed controls. Similar observations were made in coho salmon (Duan and Plisetskaya, 1993), barramundi (Matthews *et al.*, 1997), and tilapia (Méton *et al.*, 2000; Uchida *et al.*, 2003), although neither diet composition nor ration size were observed to

influence hepatic IGF-1 mRNA levels in the latter species (Méton *et al.*, 2000). Increases in IGF-1 mRNA levels were also observed in coho salmon liver (Duan and Plisetskaya, 1993) and rainbow trout muscle (Chauvigné *et al.*, 2003) after resumption of feeding after a prolonged fasting period. Collectively, these data suggest that nutritional status can regulate circulating IGF-1 levels, in part by modulating transcriptional activity of the IGF-1 gene, although other regulatory mechanisms (e.g., effects on serum binding proteins) have not been ruled out at this time.

In contrast to rats, a relatively long period of fasting is required to induce significant alterations to plasma IGF-1 levels in fish. In rats, 3 days of starvation caused a significant decrease in IGF-1 levels, and 2 days of refeeding partially restored IGF-1 levels (Thissen *et al.*, 1994). In salmon, significant changes in hepatic IGF-1 mRNA or serum IGF-1 protein levels were detected only after 3 to 4 weeks of fasting, and 2 weeks of refeeding were necessary to restore them (Duan and Plisetskaya, 1993). The delayed responses in salmon may reflect metabolic adaptations to a cold-water existence, a carnivorous diet, or the prolonged fasting periods experienced during the complex salmonid life history.

Interestingly, nutritional status may exert differential effects on IGF-1 mRNA splice variants. In coho salmon, nutritional status correlated with the expression of Ea-1 and Ea-3 transcripts, whereas no changes were observed in Ea-4 transcripts (Duan *et al.*, 1994). This variant-specific response to nutritional status is similar to patterns observed after injection of GH or streptozotocin, again suggesting precise mechanisms by which the expression of individual splice variants are regulated in a tissue-specific manner.

c. Development IGF-1 expression exhibits both temporal and spatial variability during the early stages of fish development, although the factors influencing IGF expression levels during these stages have only more recently become a topic of investigation. In zebrafish embryos, IGF-1 mRNA levels remained relatively constant from fertilization through 60 h after fertilization, but were detectably enriched in hepatic and testicular tissues of adults (Maurus *et al.*, 2002). In both seabream and rainbow trout, whole body IGF-1 mRNA levels were relatively low throughout the embryonic period, but increased during the larval phase (Duguay *et al.*, 1996; Gabillard *et al.*, 2003a; Perrot *et al.*, 1999). Particularly robust increases in expression were observed in anterior (head) regions of rainbow trout at the onset of larval development (Gabillard *et al.*, 2003a). There may again be developmental differences in the expression of specific IGF-1 mRNA splice variant(s): in rainbow trout, Ea-1 and Ea-3 mRNA transcripts were detectably expressed in unfertilized eggs; Ea-4 transcripts were detected only after activation of the zygotic genome, whereas Ea-2 transcripts were undetected throughout embryonic development (Greene and Chen, 1997).

d. Environment Seasonal, photoperiodic, temperature, and diurnal variations have all been linked with fluctuating serum IGF-1 levels in fish (Beckman *et al.*, 1998; Dickhoff *et al.*, 1997; Larsen *et al.*, 2001; Méton *et al.*, 2000; Mingarro *et al.*, 2002), although the causative mechanisms underlying these fluctuations remain a source of continued investigation. Future studies will undoubtedly shed further light on this issue, which remains of central importance to those interested in the endocrine control of vertebrate growth.

B. IGF-2

1. Primary Structure

Although early biochemical studies failed to detect IGF-2-like peptides in fish (Daughaday *et al.*, 1985), there is now substantial evidence supporting the existence of IGF-2-like peptides in nearly all vertebrate groups (Reinecke *et al.*, 1995), agnathans being the only exception. As noted above, a single IGF-like gene was identified in agnathans, exhibiting highest identity to other vertebrate forms of IGF-1, but with features similar to both IGF-1 and IGF-2. These observations have been taken as evidence that the IGF-like molecule in agnathans is a descendant of the ancestral molecule that later duplicated to yield IGF-1 and IGF-2, after divergence of the gnathostome lineage (Nagamatsu *et al.*, 1991).

The first piscine IGF-2 cDNA to be cloned was that of rainbow trout (Shambloott and Chen, 1992); since then, IGF-2 has been wholly or partially cloned in multiple species, including teleosts and elasmobranchs. Published gene and/or cDNA sequences for IGF-2 are now available for seabream (Duguay *et al.*, 1996), barramundi (Collet *et al.*, 1997), tilapia (Chen *et al.*, 1997), daddy sculpin (Loffing-Cueni *et al.*, 1999), zebrafish (Maures *et al.*, 2002), rabbitfish (Ayson *et al.*, 2002), turbot (Duval *et al.*, 2002), carp (Tse *et al.*, 2002), chum salmon (Palamarchuk *et al.*, 2002), and the dogfish shark (Duguay *et al.*, 1995). In addition, partial and/or complete IGF-2 sequences are available in GenBank for orange spotted grouper, rainbow krib (*Pelvicachromis pulcher*), bastard halibut, Atlantic salmon, and pufferfish (*Fugu rubripes*).

IGF-2 is synthesized as a prohormone with a signal peptide that varies in length among species. Removal of the leader sequence during secretion yields the prohormone, pro-IGF-2, containing a five-domain structure (B-C-A-D-E) similar to that of IGF-1. Subsequent removal of the E domain yields the mature peptide; mature IGF-2 contains 67 amino acids in humans, 70 amino acids in teleosts, and 68 amino acids in the dogfish shark. The difference in peptide length between teleosts and humans is due to the

presence/absence of residues in the C domain; in mammals, this domain contains 8 residues, whereas in most teleosts, this domain contains 11 residues. An exception to this pattern is the C domain of zebrafish IGF-2b (a putative IGF-2 paralog), which contains nine residues. The C domain of dogfish shark IGF-2 contains eight residues as seen in mammals, although the overall identity between human and shark IGF-2 is only 66%, whereas sequence identities between human IGF-2 and teleost orthologs range between 70 and 75%. Among the known teleost IGF-2 sequences, identities range between 85 and 100%.

The A and B domains of IGF-2 are highly conserved among vertebrates, with sequence identities generally between 70 and 90%. The first five N-terminal residues of the B domain differ somewhat markedly between fish and mammals, although the functional consequences of this divergence are unknown. The pattern of variability in vertebrate D domains differs between IGF-1 and IGF-2; in contrast to the highly variable D domain of IGF-1, the D domain of IGF-2 appears to be well conserved among fish and other vertebrates, with five of six residues exhibiting complete identity between humans and teleosts (e.g., Loffing-Cueni *et al.*, 1999). The E domains of IGF-2 prohormones are also generally longer than those of IGF-1, containing as many as 98 residues (Ayson *et al.*, 2002); no alternative splicing has been reported in IGF-2 of vertebrate species.

A number of distinctive features in mature IGF-2 peptides have been conserved in vertebrates, including fish: the first residue (Glu) of the A domain is unique and conserved among all known IGF-2 sequences; the Glu-Thr-Leu-Cys-Gly sequence found in all IGF B domains is preceded by two amino acids in IGF-1, but by four or five residues in all known IGF-2 sequences, and the A domain of IGF-1 contains a highly basic motif consisting of Leu/Phe-Arg-Arg-Leu⁵⁷, whereas the homologous region in IGF-2 contains two hydrophobic residues. The functional consequences of these sequence characters are not fully understood, but have clearly retained importance throughout vertebrate evolution.

2. Genes and mRNAs

The human IGF-2 gene is relatively complex, being composed of nine exons distributed across approximately 30 kb of genomic DNA. Four of the exons are preceded by distinct promoter sites; combinations of these four promoter-exons with either of two polyadenylation signals yield a complex array of mRNA transcripts of different sizes (Rotwein, 1991). However, as seen with IGF-1, all variants are ultimately modified to yield an identical mature IGF-2 peptide. In rodents, the IGF-2 gene is somewhat less complex, being composed of six exons with three distinct promoter regions, spread across 12–15 kb of DNA.

The structure of the IGF-2 gene was determined for three species of teleosts: chum salmon (Palamarchuk *et al.*, 2002), barramundi perch (Collet *et al.*, 1997) and pufferfish (GenBank accession no. AL021880). In comparison with mammalian IGF-2 genes, those of the teleosts are markedly less complex. The chum salmon, barramundi, and pufferfish IGF-2 genes are composed of four exons and three introns, spanning approximately 7.9, 5.5, and 4.2 kb of genomic DNA, respectively. Despite efforts to identify a duplicate IGF-2 gene in the (tetraploid) chum salmon, none was detected (Palamarchuk *et al.*, 2002). This was somewhat surprising, in light of the evidence for a duplicate IGF-2 gene (IGF-2b) in the zebrafish (GenBank accession no. AY049027). Mature zebrafish IGF-2b is 68% identical to human IGF-2, but shares only 65–68% identity with other fish orthologs; interestingly, its paralog (zebrafish IGF-2a) is at the lower end of this spectrum (65%), suggesting an ancient duplication of the IGF-2 gene in this species.

Expression of multiple IGF-2 mRNA transcripts has been demonstrated in a number of fish species. For example, three mRNA transcripts were detected by Northern hybridization in tilapia (Schmid *et al.*, 1999), and two in both seabream (Perrot *et al.*, 2000) and common carp (Tse *et al.*, 2002). By contrast, only a single transcript was detected in whole larval seabream (Radaelli *et al.*, 2003a) and in retinal tissues of the cichlid (*Haplochromis burtoni*; Mack *et al.*, 1995). These inconsistencies may be explained by tissue- and/or developmental stage-specific patterns of IGF-2 mRNA expression, or by differences in detection limits among studies; as shown in tilapia, different mRNA transcripts can vary significantly in abundance (Schmid *et al.*, 1999). The variation in size among different mRNA transcripts in common carp may result from differential utilization of multiple polyadenylation signals (Tse *et al.*, 2002), although there is evidence for two transcription initiation sites in the chum salmon IGF-2 gene (Palamarchuk *et al.*, 2002). Variable-length E domains, such as those seen in vertebrate proIGF-1 peptides, have not been reported for IGF-2 in any vertebrate species.

3. Expression Patterns of IGF-2

Evidence from the mouse model has suggested that IGF-2 may play an important role in regulating fetal growth; IGF-2 expression has also been reported to precede the onset of IGF-1 expression in mice (Rotwein, 1991). Studies suggest a similar pattern of IGF-2 expression in many fish species. For example, IGF-2 mRNA was detected in unfertilized rabbitfish eggs, and its abundance exceeded that of IGF-1 mRNA throughout early development (Ayson *et al.*, 2002). Similar patterns in the relative abundances of IGF-1 and IGF-2 mRNA transcripts were reported in embryonic rainbow trout (Gabillard *et al.*, 2003a; Greene and Chen, 1999a) and gilthead seabream

(Perrot *et al.*, 1999), although a reverse pattern was detected in common carp (Tse *et al.*, 2002). Chen *et al.* (1998) showed that a reporter gene (enhanced green fluorescent protein, eGFP) fused to the tilapia IGF-2 promoter region exhibited detectable mRNA expression in zebrafish embryos at the 32-cell stage, well in advance of IGF-1 promoter-driven reporter gene expression. These data suggest that IGF-2 may be expressed at earlier stages and at relatively higher levels than IGF-1 in fish.

Considerable interspecies variations in IGF-2 expression patterns are observed during postnatal development in vertebrates. For example, IGF-2 mRNA is abundantly expressed in fetal rats, but declines after birth in most tissues, with the exception of the choroid plexus and meninges, in which high expression is maintained (Bondy *et al.*, 1990; Nilsson *et al.*, 1996). In contrast, IGF-2 mRNA levels in humans and guinea pigs remain high in most adult tissues, including the liver (Rotwein, 1991). The IGF-2 gene has been shown to be abundantly expressed in both hepatic and nonhepatic tissues of juvenile and adult teleosts, including common carp (Tse *et al.*, 2002; Vong *et al.*, 2003), rainbow trout (Aegerter *et al.*, 2004; Bobe *et al.*, 2003; Chauvigné *et al.*, 2003; Gabillard *et al.*, 2003b), zebrafish (Maures *et al.*, 2002), daddy sculpin (Loffing-Cueni *et al.*, 1999), tilapia (Caelers *et al.*, 2003; Schmid *et al.*, 1999), seabream (Perrot *et al.*, 2000; Radaelli *et al.*, 2003a), and rabbitfish (Ayson *et al.*, 2002). Interestingly, particularly abundant expression has been demonstrated in brain tissues of tilapia (Caelers *et al.*, 2003), particularly the choroid plexus, suggesting conservation of tissue expression patterns across species. It is clearly evident that IGF-2 retains importance during posthatching development in teleosts, possibly as a local paracrine/autocrine regulator of tissue growth.

4. Regulation of IGF-2 Expression

a. Hormones The hormonal factors involved in the regulation of IGF-2 expression are less well defined in fish as compared with mammals, and less well studied overall in comparison with IGF-1. The available evidence suggests that the fish IGF-2 gene may be responsive to GH, although less so than IGF-1. For example, GH treatment increased IGF-2 mRNA content in hepatic and intestinal tissues (*in vivo*) and cultured hepatocytes (*in vitro*) of rainbow trout (Shamblott *et al.*, 1995), and in brain, gill, intestine, kidney, liver, and muscle of common carp (Tse *et al.*, 2002; Vong *et al.*, 2003). Other studies, however, offer contradictory evidence: GH treatment did not induce a detectable increase in IGF-2 mRNA levels in any somatic tissues of seabream (Duguay *et al.*, 1996), nor was IGF-2 expression detectably responsive to GH treatment in zebrafish (Maures *et al.*, 2002), whereas IGF-1 was responsive in both instances. A study in humans provides evidence that IGF-2 gene activity may be regulated by GH in a promoter-specific manner:

Two of the four human IGF-2 promoters (P2 and P4) were responsive to GH treatment both *in vivo* and *in vitro*, whereas the P1 promoter was unresponsive in all tests (von Horn *et al.*, 2002). Although multiple promoters have not been identified in fish IGF-2 genes, additional studies are clearly required to understand more fully the hormonal regulation of IGF-2 synthesis, secretion, and function in fish.

b. Nutrition In juvenile rainbow trout refed after a prolonged fasting period, IGF-2 mRNA levels in myotomal muscle tissues were observed to increase in time-dependent fashion for at least 34 days of refeeding (Chauvigné *et al.*, 2003). IGF-2 mRNA levels in refed fish were detectably higher (~1.7-fold) than levels in fasted fish after 34 days, although this response was much less robust than that seen with IGF-1 mRNA expression. The abundance of IGF-1 mRNA increased rapidly in refed animals, reaching levels nearly 15-fold higher than those in fasted animals, after only 12 days of resumed feeding. Thus, in juvenile rainbow trout, nutritional status is observed to affect IGF-2 mRNA levels, although expression may be influenced less than IGF-1 mRNA expression under similar conditions.

IV. IGF Receptors and IGF-Binding Proteins

A. IGF Receptors

1. Type I IGF Receptors

The presence of receptors with properties (e.g., binding specificity, enzyme activities) similar to those of the mammalian IGF-1 receptor has been demonstrated by biochemical methods in teleosts (carp, brown trout, coho salmon, sockeye salmon, Atlantic salmon, rainbow trout, barramundi perch, and daddy sculpin), cartilaginous fish (thornback ray), and the Atlantic hagfish (Drakenberg *et al.*, 1993, 1997; Gutierrez *et al.*, 1993; Leibush *et al.*, 1996; Loir and Le Gac, 1994; Maestro *et al.*, 1997a; Parrizas *et al.*, 1995a,b). In a comparison of receptor-binding affinities between mammals and fish, recombinant teleost IGF-1 (salmon and barramundi) and recombinant hagfish IGF exhibited relatively lower affinities than human IGF-1 for the rat IGF-1 receptor (IGF-1R) in mammalian cells, whereas salmon and human IGF-1 peptides competed equally for the IGF-1R in piscine cells (Pozios *et al.*, 2001; Upton *et al.*, 1997, 1998). Although data derived from heterologous systems are difficult to interpret, the evolutionary conservation of IGF receptors is further supported by functional studies demonstrating equal potency of salmon and human IGF-1 in stimulating sulfation

activity in fish cartilage and DNA synthesis in zebrafish embryonic cells (Moriyama *et al.*, 1993; Pozios *et al.*, 2001; Upton *et al.*, 1998), and by the demonstrated presence of tyrosine kinase activity in IGF-1 receptor preparations from various teleosts (e.g., Gutierrez *et al.*, 1995; Maestro *et al.*, 1997a; Parrizas *et al.*, 1995a). The biochemical aspects of IGF-1R activation are discussed in further detail below (see Section IV.A.1.b, Signal Transduction Pathways).

a. Primary Structure The application of molecular cloning approaches has confirmed the expression of IGF-1R mRNA in a variety of fish, at all stages of development. Full-length cDNAs encoding IGF-1Rs have been reported in turbot (Elies *et al.*, 1999), zebrafish (Maures *et al.*, 2002), and Japanese flounder (Nakao *et al.*, 2002). In addition, partial IGF-1R cDNAs have been reported for seabream (Perrot *et al.*, 1999), turbot (Elies *et al.*, 1998a,b), rainbow trout (Greene and Chen, 1999b), goldfish (Otterson *et al.*, 2002), zebrafish (Ayaso *et al.*, 2002), and Arctic charr (Tao and Boulding, 2003). Partial IGF-1R cDNA sequences are also available in GenBank for white perch, white bass, striped bass, Atlantic salmon, tilapia, and coho salmon.

To date, the duplicate IGF-1R receptor pairs (IGF-1Ra and IGF-1Rb) in flounder and zebrafish are the only fish cDNAs to be fully sequenced; only those of zebrafish have been biochemically confirmed to encode functional (IGF-binding) receptors (Maures *et al.*, 2002). Affinity cross-linking studies with ^{125}I -labeled IGF-1 ($[^{125}\text{I}]\text{IGF-1}$) also indicated the presence of putative IGF receptors in zebrafish lysates, with molecular masses (~ 400 kDa) near to those of predicted heterotetrameric ($\alpha_2\beta_2$) IGF-1R receptors. These findings were concordant with previous studies indicating a molecular mass of approximately 350 kDa for putative IGF-1Rs of trout and carp (Leibush *et al.*, 1996; Parrizas *et al.*, 1995b). Furthermore, affinity cross-linking assays indicated the presence of proteins corresponding to the molecular masses of dimeric ($\alpha\beta$) receptor complexes (~ 200 kDa) and single α subunits (~ 125 kDa) in zebrafish embryonic (ZF-4) cells (Pozios *et al.*, 2001).

The available evidence indicates that the dual IGF-1R cDNAs detected in teleosts (e.g., zebrafish, turbot, and salmonids) are derived from nonallelic gene duplicates, as opposed to alternative splicing or allelic variation of a single gene. Zebrafish IGF-1Ra and IGF-1Rb have 1405 and 1380 amino acids, respectively, share 63.2 and 59.6% identity with human IGF-1R, respectively, and have high overall structural similarity (Fig. 7). The surprisingly low (69.8%) amino acid identity between the paralogous pair, however, suggests an ancient duplication of the ancestral IGF-1R gene. Interestingly, the IGF-1R receptors in zebrafish ZF-4 cells exhibited similar binding affinities for IGF-1 and IGF-2 (Pozios *et al.*, 2001); this differs from what has been reported in mammals, and deserves further investigation, particularly in light of the limited evidence for functional IGF-2 receptors in fish.

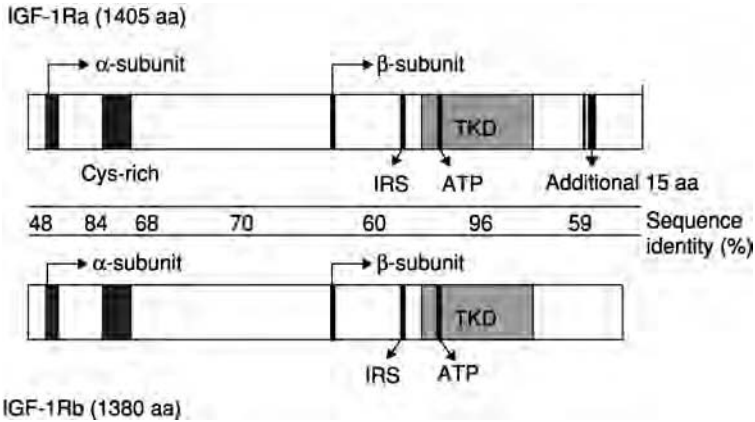


FIG. 7 Schematic diagram of the type I IGF receptors in zebrafish. The α domains of both receptors contain conserved cysteine-rich (Cys-rich) regions; the β domains of both contain insulin receptor substrate (IRS)-binding sites, ATP-binding sites, and tyrosine-kinase domains (TKDs). The β domain of IGF-1Ra contains an insertion of 15 contiguous amino acids not found in IGF-1Rb. (Modified from Maures *et al.*, 2002.)

Similar results have been reported in other fish species (Fruchtman *et al.*, 2002).

Ongoing studies are being performed to elucidate the functional divergence of these gene duplicates. For example, heterosynchronous expression patterns have been demonstrated in the embryonic zebrafish (Maures *et al.*, 2002). Unique functions for the duplicate receptors are further suggested by studies employing antisense gene knockdown approaches; these are discussed in greater detail below (see Section V.B, Embryonic Development).

b. Signal Transduction Pathways A number of studies have provided evidence that the signal transduction pathways mediating IGF signaling through the IGF-1R are conserved in fish. For example, tyrosine kinase activity was demonstrated in IGF-1Rs purified from carp and a number of salmonids (Gutierrez *et al.*, 1993, 1995; Leibush *et al.*, 1996; Maestro *et al.*, 1997a, 1998; Mendez *et al.*, 2001b; Parrizas *et al.*, 1995a,b). The presence of tyrosine kinase domains in the β subunits of IGF-1R cDNAs has been confirmed by molecular cloning in zebrafish, rainbow trout, turbot, and flounder (Chan *et al.*, 1997; Elies *et al.*, 1999; Greene and Chen, 1999b; Maures *et al.*, 2002; Nakao *et al.*, 2002). In zebrafish, the tyrosine kinase domains of both IGF-1Rs were predicted to contain a number of conserved functional elements, including a putative ATP-binding site, a cluster of three tyrosine residues corresponding to the tyrosine phosphorylation site in the mammalian IGF-1R, and an insulin receptor substrate 1-binding motif known to be required for IGF-1R signaling in mammals (Fig. 7).

Further *in vitro* evidence indicates that the biological effects of IGF-1R activation are transduced by MAPK and PI3-kinase signal transduction pathways, as described in mammals. For example, treatment of ZF-4 cells with IGFs dose dependently stimulated phosphorylation of p44/42 MAPK, PKB/Akt, and putative IGF-1R β subunits (Pozios *et al.*, 2001). Furthermore, specific inhibitors of MAPK and PKB/Akt attenuated the mitogenic effects of IGFs in these cells. Similarly, treatment of hybrid striped bass pituitary cells with inhibitors of MAPK and PI3-kinase was shown to block the stimulatory (prolactin) and suppressive (GH) effects of IGF-1 on hormone secretion (Fruchtman *et al.*, 2000, 2001). Collectively, these data suggest that the intrinsic biological responses to IGF-1R activation are conserved in fish; as with all vertebrates, it remains to be clearly demonstrated how the cellular responses to IGF signaling in fish are specified, considering the known expression of other growth factor receptor tyrosine kinases (Goishi *et al.*, 2003).

c. Expression and Regulation Because of the primary importance of IGF signaling as a mediator of somatic growth, it is not surprising that IGF-1R mRNA is widely expressed in vertebrate tissues. In fish, nearly ubiquitous distribution of IGF-1R mRNA was demonstrated in embryonic and adult zebrafish (Ayaso *et al.*, 2002; Maures *et al.*, 2002), rainbow trout (Aegerter *et al.*, 2004; Biga *et al.*, 2004; Chauvigné *et al.*, 2003; Gabillard *et al.*, 2003a,b; Greene and Chen, 1999a,b), and seabream (Perrot *et al.*, 1999, 2000). A widespread distribution of IGF-1R mRNA expression has also been demonstrated in adult turbot (Elies *et al.*, 1998a, 1999), Japanese flounder (Nakao *et al.*, 2002), goldfish (Otteson *et al.*, 2002), and salmon (Chan *et al.*, 1997).

Determining the tissue distribution of IGF-1R peptides generally involves competitive binding approaches, using labeled ligands (IGF-1 or IGF-2) as a tracer. With these methods, IGF receptors were detected in goldfish retina (Boucher and Hitchcock, 1998a), skeletal and cardiac muscle of carp and various salmonids (Gutierrez *et al.*, 1995; Moon *et al.*, 1996; Parrizas *et al.*, 1995b), ovarian tissues of carp, brown trout (*Salmo trutta fario*), and coho salmon (Gutierrez *et al.*, 1993; Maestro *et al.*, 1997a,b, 1999), and brain tissues of rainbow trout, brown trout, carp, daddy sculpin, thornback ray, and Atlantic hagfish (Blaise *et al.*, 1995; Drakenberg *et al.*, 1993; Leibush *et al.*, 1996). Although generally effective, these approaches must be interpreted carefully, as results can be confounded by interactions with IGF-BPs, whose affinity for IGF ligands may equal or exceed that of the receptors, and that may exhibit localized expression in the pericellular environment.

The expression of IGF-1 receptors in fish may be influenced by a variety of factors, including hormones, temperature, and metabolic status. For

example, IGF-1 elicited a decline in IGF-1R abundance in cultured trout cardiomyocytes (Moon *et al.*, 1996), suggesting that receptor abundance may be regulated by binding with its cognate ligand. Insulin, which can bind the IGF-1R with reduced affinity, may also regulate IGF-1R abundance. For example, acute hyperinsulinemia induced by intraperitoneal arginine injections provoked a rapid downregulation of IGF-1R abundance in red muscle of rainbow trout and carp (Banos *et al.*, 1997), and exposure of cardiomyocytes to insulin *in vitro* reduced IGF-1R abundance (Moon *et al.*, 1996). Paradoxically, prolonged exposure of rainbow trout to a carbohydrate-enriched diet led to chronically elevated plasma insulin levels, but a concomitant increase in the abundance of receptors for both insulin and IGF-1; these data may suggest longer term metabolic adjustments to chronic carbohydrate enrichment (Banos *et al.*, 1998).

More recently, it was shown that rainbow trout refed after a prolonged fasting period may exhibit rapid increases in IGF-1 mRNA expression, but reduced or unchanged IGF-1R mRNA levels, suggesting that the abundance of growth-promoting ligands may be the limiting factor during short-term compensatory growth events (Chauvigné *et al.*, 2003). Consistent with this, rainbow trout reared at various temperatures exhibited no differences in IGF-1R mRNA expression, although receptor binding in red muscle was inversely proportional to rearing temperature, suggesting the receptor turnover (i.e., degradation) may be enhanced in fish reared at higher temperatures (Gabillard *et al.*, 2003b).

2. Type II IGF Receptors

In mammals, two mannose 6-phosphate receptors (MPRs) have been described, both of which target the delivery of extracellular proteins to a prelysosomal compartment. One of these (MPR 300) is a multifunctional protein with a high-affinity binding site for IGF-2, and has thus been alternatively termed a type II (or IGF-2) receptor. Although both MPRs are structurally and functionally conserved in fish (Nadimpalli *et al.*, 1999; Yerramalla *et al.*, 2000), binding experiments using human IGFs as ligands failed to demonstrate the presence of an IGF-2-like receptor in fish (Drakenberg *et al.*, 1993). This finding was in agreement with studies in other nonmammalian vertebrates: for example, MPR preparations from chicken and *Xenopus* were unable to bind to IGF-2 (Canfield and Kornfeld, 1989; Clairmont and Czech, 1989; Yang *et al.*, 1991).

More recently, the presence of an MPR with high affinity for IGF-2 was demonstrated in rainbow trout embryos (Mendez *et al.*, 2001a). The purified protein was similar in size to mammalian MPR 300, could be immunoprecipitated with an antibody against the rat MPR, and was devoid of tyrosine

kinase activity. The molecular identity and function of this putative trout type II IGF receptor remain unknown.

B. Fish IGF-Binding Proteins

1. Biochemical Evidence

One or more circulating serum proteins with binding affinity and specificity for IGFs have been identified in multiple teleosts, including coho and chinook salmon, rainbow trout, striped bass, longjaw mudsucker, tilapia, barramundi, channel catfish, and golden perch (*Macquaria ambigua*) (Anderson *et al.*, 1993; Beckman *et al.*, 2004; Degger *et al.*, 2000; Fukazawa *et al.*, 1995; Johnson *et al.*, 2003; Kajimura *et al.*, 2003; Kelley *et al.*, 1992; Niu and Le Bail, 1993; Niu *et al.*, 1993; Park *et al.*, 2000; Shimizu *et al.*, 1999, 2003a,b; Siharath *et al.*, 1996). IGFbps have furthermore been identified in at least one agnathan species (pouched lamprey, *Geotria australis*), suggesting an early origin of this gene family during vertebrate evolution (Upton *et al.*, 1993). *In vitro* studies have confirmed the secretion of putative IGFbps from cultured organ tissues of striped bass (Fukazawa *et al.*, 1995; Siharath *et al.*, 1995a) and coho salmon (Moriyama *et al.*, 1997b), and from hepatoma cells of rainbow trout (Bauchat *et al.*, 2001). Although the presence of putative IGFbps in the serum of teleosts and more primitive fish suggests a central role for this protein family as an integrator of IGF signaling throughout vertebrate evolution (Kelley *et al.*, 1996, 2001), the specific identity, regulation, and function of the individual binding proteins in fish have been a source of considerable debate and confusion for many years.

In most fish studied, IGF-1 is observed to bind most abundantly to a protein of 40–45 kDa (Shimizu *et al.*, 1999), similar in size to the binding protein (IGFBP-3) to which the majority of IGFs are bound in mammals (Firth and Baxter, 2002). Serum levels of this binding protein in fish increase in response to GH treatment, and decrease during fasting, further suggesting similarity to mammalian IGFBP-3 (Beckman *et al.*, 2004; Johnson *et al.*, 2003; Kelley *et al.*, 1992; Shimizu *et al.*, 2003a).

Other IGFbps detected in fish serum exhibit similarities in size to mammalian IGFBP-1 (29–31 kDa), IGFBP-2 (30–32 kDa), and IGFBP-4 (21–24 kDa). There is no evidence for a tertiary complex (IGF-1 with IGFBP-3 or -5, and ALS), although there is evidence for an ALS-like molecule in zebrafish (C. Duan, unpublished data). A high molecular weight protein (~80–90 kDa) with affinity for IGFs has been described in some fish and birds, but its identity remains unknown at this time (Fukazawa *et al.*, 1995; Johnson *et al.*, 2003). Molecular cloning efforts have at last begun to confirm the identity of IGFbps in fish, and to clarify their relationship with IGFbps in other vertebrates.

2. Primary Structures

Full-length cDNA sequences have now been reported for zebrafish IGFBP-1, -2, and -5 (Ding and Duan, 2004; Duan *et al.*, 1999; Maures and Duan, 2002), seabream IGFBP-2 (Funkenstein *et al.*, 2002), and zebrafish IGFBP-3 (Chen *et al.*, 2003); partial sequences for longjaw mudsucker IGFBP-1 (Gracey *et al.*, 2001) and a chinook salmon IGFBP (Shimizu *et al.*, 2003a) have also been reported, although the identity of the latter remains unclear. Partial cDNA sequences are also available in GenBank for medaka IGFBP-2 and tilapia IGFBP-3. To our knowledge, IGFBPs have not yet been cloned in any elasmobranch or agnathan species.

The cDNA sequences for seabream and zebrafish IGFBP-2 are predicted to encode secreted proteins of ~280 residues; removal of the hydrophobic leader sequence (22 residues) from each sequence yields a mature peptide with the three-domain structure (N-L-C) typical of IGFBPs in other vertebrates. Although the mature peptides share only moderate identities with their putative orthologs in other species ($\leq 52\%$ with human IGFBP-2), most of the variability can be attributed to the central hinge region (L domain), which is highly variable among all known vertebrate orthologs. The cysteine residues in the N and C domains (12 and 6 residues, respectively) of human IGFBP-2 are present in both fish sequences, as is an Arg-Gly-Asp (RGD) sequence in the C domain. A putative heparin-binding motif (PKKXRP), present in all mammalian and avian IGFBP-2 sequences, is partially conserved in seabream (PKKTRL), but only marginally conserved in the zebrafish (PK—AP).

The peptide encoded by the zebrafish IGFBP-1 cDNA shares 40% identity with human IGFBP-1 and 39% identity with human IGFBP-4 (Maures and Duan, 2002), and the 18 cysteine residues in the N and C domains are present in zebrafish sequence. More recent analysis of the putative promoter and intronic region of the zebrafish IGFBP-1 gene has demonstrated the presence of specific transcriptional regulatory elements (e.g., glucocorticoid response elements) previously reported in mammalian IGFBP-1 genes (Kajimura *et al.*, 2004), suggesting that transcriptional regulation of IGFBP-1 has been evolutionarily conserved among the vertebrates. However, the RGD sequence found in most vertebrate orthologs, thought to promote associations between IGFBPs and extracellular matrix proteins, is not evident in zebrafish IGFBP-1.

3. Biochemical Properties

Recombinant expression of zebrafish IGFBP-2 in Chinese hamster ovary (CHO) cells yielded secretion of a protein of approximately 30 kDa, similar to the predicted size for IGFBP-2 (Duan *et al.*, 1999). The secreted protein

bound to human IGF-1 and IGF-2 with high affinity and specificity, but showed negligible binding affinity for insulin or Des(1–3)IGF-1, an IGF variant with reduced affinity for IGF-BPs. Overexpression of this recombinant protein inhibited the mitogenic actions of IGFs in CHO cells and zebrafish (ZF-4) cells, suggesting that zebrafish IGF-BP-2 may be a growth-inhibitory IGF-binding protein in this species.

Similarly, the 30-kDa peptide secreted by rainbow trout hepatoma cells was shown to bind IGFs with high affinity and specificity, but showed negligible affinity for insulin or Des(1–3)IGF-1. N-terminal sequencing of this peptide revealed highest similarity with mammalian IGF-BP-1, although complete sequencing is required to positively confirm its identity. The purified protein also potently inhibited IGF-1-induced cell proliferation in both human SYSY-5Y neuroblastoma cells and ZF-4 cells (Bauchat *et al.*, 2001).

As noted above, the 41-kDa binding protein identified in the serum of salmonids (e.g., chinook salmon) was shown to exhibit properties similar to those of its presumed mammalian homolog (IGFBP-3). Although sequencing of the N-terminal region of this protein revealed highest identity with the deduced amino acid sequences of zebrafish and seabream IGF-BP-2 (Shimizu *et al.*, 2003b), the high similarities among N domains of IGF-BPs precluded its positive identification. Further efforts to determine the identity of fish IGF-BPs through molecular cloning approaches are required to clarify these issues.

4. Expression and Localization

IGFBP-1 mRNA was detected by RT-PCR in whole zebrafish homogenates throughout the embryonic period [0–96 h postfertilization (hpf)], although expression levels were below the detection limits of Northern hybridization (Maures and Duan, 2002). By *in situ* hybridization, IGF-BP-1 mRNA was readily detectable beyond 24 hpf, primarily in anterior (cranial) regions. The absence of detected expression by *in situ* and Northern hybridization before 24 hpf suggests that IGF-BP-1 is likely expressed at low levels during early development. Beyond 48 hpf, IGF-BP-1 mRNA was detected by *in situ* hybridization in mandibular arches, pharyngeal arches and otic vesicles, although expression was again reduced to undetectable levels beyond 96 hpf. In adult zebrafish, IGF-BP-1 mRNA expression was detected exclusively in the liver, albeit at low levels. Subjecting fish to hypoxia greatly increased the mRNA content of IGF-BP-1 in both embryos and adults (Kajimura *et al.*, 2004; Maures and Duan, 2002); similar elevations in IGF-BP-1 mRNA were also reported in response to nutritional deprivation (Kelley *et al.*, 2001; Maures *et al.*, 2002) and stress (Kelley *et al.*, 2001, 2002) in different teleosts.

IGFBP-2 mRNA expression was detected in zebrafish (Duan *et al.*, 1999; Wood and Duan, 2004) and seabream (Funkenstein *et al.*, 2002) throughout

the embryonic period, although at relatively low levels. Using *in situ* hybridization, IGFBP-2 mRNA in zebrafish embryos was first detected in anterior regions at ~18 hpf, and became localized to the optic region by approximately 20 h of development. Between 48 and 72 hpf, mRNA was predominantly detected at the midbrain–hindbrain boundary in close association with vascular tracts, whereas at the termination of embryogenesis, highest expression was detected in the liver (Wood and Duan, 2004). A single (1.8 kb) IGFBP-2 mRNA transcript was detected by Northern hybridization in the liver of adult zebrafish; lower levels of this transcript were detected by Northern hybridization in many nonhepatic tissues, including brain, eye, intestine, muscle, and fin (Duan *et al.*, 1999).

In adult seabream, two IGFBP-2 mRNA transcripts were detected by Northern analysis; RT-PCR analysis revealed mRNA expression in multiple tissues, including gonad, eye, spleen, kidney, gill, intestine, skin, heart, gut, muscle, pituitary, and liver (Funkenstein *et al.*, 2002). These data support the notion that IGFbps play important paracrine and/or autocrine roles in the constitutive regulation of IGF signaling; the specific requirements for IGFBP-2 during development are discussed in further detail below.

In embryonic zebrafish, IGFBP-5 mRNA expression was first detected in somites and branchial mesenchyme around 24 hpf. By 48 hpf, expression became restricted to newly forming craniofacial cartilage tissue regions, and this pattern of expression persisted into the larval stages (Ding and Duan, 2004).

In vitro tissue culture methods have been used to study IGFBP secretion in some teleosts. In striped bass, a 30- to 33-kDa binding protein (putatively IGFBP-2) was secreted from spleen, kidney, hindbrain, pituitary, and liver, while the liver also secreted a 29-kDa isoform (putatively IGFBP-1; Siharath *et al.*, 1995a). Secretion of two isoforms (23 and 29 kDa) was also shown in primary hepatocyte cultures from coho salmon (Moriyama *et al.*, 1997b), although conditioned media from other sources (e.g., gonad, gill filaments, ceratobranchial cartilage, ceratobranchial bone, heart, muscle, and gut) gave inconsistent results. In general, these data are consistent with mRNA expression patterns in other fish and higher vertebrates, suggesting that most, if not all, vertebrate tissues synthesize and secrete IGFbps.

5. Regulation

The hypothesized importance of IGFbps as regulators of IGF ligand–receptor interactions predicts that physiological regulation of IGFBP levels is an important aspect of IGF signaling. In accordance, a number of factors have been associated with variations in IGFBP levels in fish, including hormones, metabolic status, developmental status, and environmental conditions (e.g., temperature and oxygen availability).

a. Hormones At the present time, it is somewhat difficult to clearly summarize the hormonal regulation of IGFbps in fish, particularly considering the difficulty in identifying fish IGFbps on the basis of molecular weights. Furthermore, individual IGFBP family members are differentially responsive to specific hormones, and the responses of a given IGFBP to a specific hormone may vary among species, or even within an individual under different metabolic circumstances.

Coho salmon and tilapia exhibited increases in serum content of 41-kDa IGFBP after GH injection (Park *et al.*, 2000; Shimizu *et al.*, 1999, 2003a), similar to responses seen with mammalian IGFBP-3. By contrast, GH treatment had no detectable effects on a suite of IGFbps in striped bass serum (Siharath *et al.*, 1995b), and elicited a decline in the serum content of multiple IGFbps in channel catfish (Johnson *et al.*, 2003). The data become more clear in the case of IGFbps that have been positively identified through cloning. For example, GH treatment elicited a marked decline in IGFBP-2 mRNA levels in zebrafish (Duan *et al.*, 1999), but had no detectable effect on IGFBP-2 mRNA levels in seabream (Funkenstein *et al.*, 2002).

Hypophysectomy is generally seen to induce a decline in the serum content of the binding protein most similar in size to IGFBP-3, although levels of binding proteins presumed (by size) to be IGFBP-1 or -2 increased, or remained unchanged. Subsequent injection of GH restored IGFBP-3 levels, but had variable effects on other binding proteins, depending on the species (Park *et al.*, 2000; Siharath *et al.*, 1995b). Cortisol injections were also reported to rapidly increase the serum content of at least four IGFBP-isoforms (24, 28, 30, and 32 kDa) in tilapia (Kajimura *et al.*, 2003). Collectively, these data suggest that in fish, growth-inhibitory binding proteins (e.g., IGFBP-1 and IGFBP-2) may be upregulated in catabolic circumstances, whereas IGFBP-3 levels correlate positively with growth, and may be directly regulated by circulating GH.

Results from studies in a teleost with induced diabetes (via isletectomy) are concordant with these interpretations, and further suggest that insulin may influence IGFBP synthesis and/or secretion in teleosts (Banos *et al.*, 1997, 1998, 1999; Kelley *et al.*, 1993). For example, surgical removal of the islet organ in longjaw mudsucker resulted in increased levels of 24- and 30-kDa IGFbps, and insulin replacement therapy abrogated these effects (Kelley *et al.*, 2001).

b. Metabolic Status In mammals, physiological shifts toward a catabolic state (e.g., stress and starvation) are generally associated with declines in serum IGFs and IGFBP-3, and concomitant increases in serum levels of growth-inhibitory IGFbps (e.g., Ooi *et al.*, 1990; Orłowski *et al.*, 1990). These physiological responses presumably evolved as a means to divert resources away from energetically expensive growth processes under adverse

conditions (Kelley *et al.*, 2001). A similar response to nutritional deprivation has been described in a number of fish. For example, serum levels of low molecular mass IGFbps (<30 kDa) were increased in longjaw mudsucker (Kelley *et al.*, 2001; Siharath *et al.*, 1996) and catfish (Peterson and Small, 2004) subjected to prolonged fasting, and IGFBP-1 and IGFBP-2 mRNA levels were increased in fasted zebrafish (Duan *et al.*, 2002). In all three species, a return to prefasted IGFBP-1 levels was observed on refeeding. In contrast, serum levels of two other IGFbps (35 and 45 kDa) were unchanged with fasting in catfish, whereas serum levels of 41 kDa IGFBP (IGFBP-3) were positively correlated with feeding rate in coho salmon (Beckman *et al.*, 2004).

V. Biological Actions of the IGF System in Fish

The IGF system is generally associated with the neuroendocrine regulation of somatic growth in vertebrates, although accumulating evidence suggests broader functions for these peptide growth factors in a diversity of vertebrates. In fish, additional functions include osmoregulatory acclimation, reproductive development, and tissue regeneration. Here, we review the biological functions of IGFs as reported in fish; where possible, the putative mechanisms underlying these pleiotropic actions are discussed.

A. Growth

Although an early *in vivo* attempt to examine the effects of exogenously elevated IGF-1 in brook trout led unexpectedly to reduced growth and increased mortality (Skyrud *et al.*, 1989), there is now incontrovertible evidence that IGF-1 plays a central role in mediating somatic growth in fish. For example, direct administration of IGF-1 through implanted miniosmotic pumps was shown to increase juvenile coho salmon body size (McCormick *et al.*, 1992a). Furthermore, IGF-1 levels have been positively correlated with growth in a variety of species (Beckman *et al.*, 1998, 2001; Duan *et al.*, 1995; Mingarro *et al.*, 2002), and respond predictably to changes in serum GH levels during normal development (Cao *et al.*, 1989; Funkenstein *et al.*, 1989; Gray and Kelley, 1991).

The critical role of IGF-1 as a primary regulator of somatic growth in fish is well illustrated by the stunted growth model. Transfer of yearling salmon from freshwater to seawater before physiological completion of smoltification results in significant growth retardation (stunting) in a fraction of the population (Clarke and Nagahama, 1977). Stunted fish exhibit elevated

levels of serum GH compared with normally growing fish (Bolton *et al.*, 1987; Duan *et al.*, 1995), but a lower abundance of hepatic GH-binding sites (Gray *et al.*, 1992). The reduced abundance of hepatic GH-binding sites in stunted fish is associated with reduced expression of hepatic IGF-1 mRNA, and reduced levels of circulating IGF-1 protein (Duan *et al.*, 1995). Collectively, these data suggest that stunted fish are GH resistant and IGF-1 deficient, implicating the latter as the primary regulator of somatic growth in fish.

The modulatory roles of IGFbps in the regulation of fish growth appear largely consistent with the observed roles of homologous peptides in higher vertebrates, and are consistent with the modern somatomedin hypothesis. For example, the serum abundance of a binding protein similar in size to mammalian IGFbp-3 is increased in anabolic circumstances, whereas lower molecular weight IGFbps (putatively IGFbp-1, -2, and -4) are detectably upregulated in catabolic circumstances (e.g., fasting) (Kelley *et al.*, 2001). Thus, while no tertiary complex with an ALS-like molecule has been demonstrated in fish, the homolog to mammalian IGFbp-3 appears to facilitate IGF signaling in teleosts, perhaps by prolonging the half-life of IGFs, while lower molecular weight IGFbps are thought to suppress IGF-mediated growth by inhibiting activation of the IGF-1R. What follows is a summary of the reported biological effects of IGF signaling in fish at tissue, cellular and molecular levels.

1. Cartilage Sulfation

One of the original *in vitro* assays for IGF-1 activity is based on measurements of $^{35}\text{SO}_4$ incorporation (sulfation) into cultured cartilage explants, indicating cartilage (skeletal) growth. Using this approach, it was shown that mammalian IGF-1 and IGF-2 stimulated sulfation in branchial cartilage explants of Japanese eel, with IGF-1 being the more potent (Duan and Hirano, 1990, 1992; Duan *et al.*, 1992). Similar effects of IGFs were subsequently reported in other teleost species, including longjaw mudsucker (Gray and Kelley, 1991; Kelley *et al.*, 1993), tilapia (Datuin *et al.*, 2001; Ng *et al.*, 2001), coho salmon (Chan *et al.*, 1997; McCormick *et al.*, 1992b; Moriyama *et al.*, 1997b; Tsai *et al.*, 1994), goldfish (Marchant and Moroz, 1993), carp (Cheng and Chen, 1995), and rainbow trout (Takagi and Bjornsson, 1996), and in two elasmobranch species (*Raja eglanteria* and *Raja porosa* Gunther; Fan *et al.*, 2003; Gelsleichter and Musick, 1999).

The production and characterization of recombinant IGF peptides has shed further light on the anabolic actions of IGFs in fish. Recombinant IGFs characterized include IGF-1 from coho salmon (Moriyama *et al.*, 1993), seabream (Fine *et al.*, 1997), barramundi (Degger *et al.*, 2000), and turbot (Duval *et al.*, 2002); IGF-2 from barramundi (Degger *et al.*, 2001), rainbow

trout (Gentil *et al.*, 1996), turbot (Duval *et al.*, 2002), tilapia (Chen *et al.*, 1997; Hu *et al.*, 2004), and Atlantic salmon (Wilkinson *et al.*, 2004); and the IGF-like peptide from hagfish (Upton *et al.*, 1997). These recombinant IGFs show biological activities to similar to those of their respective mammalian orthologs. For example, human IGF-1 and recombinant teleost IGF-1 peptides exhibited equal potency in stimulating sulfation activity in cartilage explants of salmon and seabream (Fine *et al.*, 1997; Moriyama *et al.*, 1993).

2. DNA Synthesis/Cell Proliferation

IGFs have potent mitogenic effects in a variety of tissues and cell types. For example, recombinant human IGF-1 and/or IGF-2 potently stimulated [³H]thymidine incorporation in eel cartilage (Duan *et al.*, 1992), goldfish ovarian follicles (Srivastava and Van Der Kraak, 1994, 1995), rainbow trout myoblasts, spermatogonia, and spermatocytes (Loir and Le Gac, 1994; Castillo *et al.*, 2004), and zebrafish embryonic (ZF-4) cells (Duan *et al.*, 1999; Pozios *et al.*, 2001). Similar stimulatory effects of human IGF-1 were observed on goldfish retinal progenitor cells (Boucher and Hitchcock, 1998b) and ZF-4 cells (Pozios *et al.*, 2001), using bromodeoxyuridine (BrdU) incorporation as an indicator of DNA synthesis. Administration of exogenous IGF-1 was also shown to stimulate the proliferation of rod precursor cells in the cichlid retina (Mack and Fernald, 1993), and somewhat more indirectly, GH injections that stimulated IGF-1 mRNA synthesis in liver, brain, and retinal cells of goldfish were also observed to stimulate retinal cell proliferation (Otteson *et al.*, 2002).

Studies using recombinant piscine IGFs have further confirmed their mitogenic activity in both heterologous and homologous systems. For example, recombinant seabream IGF-1 stimulated proliferation of murine mammary gland-derived cells (Fine *et al.*, 1997). In addition, recombinant tilapia IGF-2 stimulated [³H]thymidine incorporation in tilapia ovary (TO-2) cells (Chen *et al.*, 1997), and cell proliferation in both teleost and mammalian cell lines (Hu *et al.*, 2004).

Somewhat intriguingly, it has been suggested that the E domains of pro-IGF peptides possess biological activity. Long considered to be inert fragments simply removed by proteolysis, it has now been demonstrated that recombinant E-domain peptides derived from rainbow trout pro-IGF-1 can stimulate mitotic activity and morphological changes in a variety of cell types (Chen *et al.*, 2002; Tian *et al.*, 1999). Considering the multiplicity and heterogeneity of the E-domain peptides of fish IGFs (Fig. 6), these findings offer the tantalizing prospect of revealing novel biological activities for peptide fragments derived from the IGF gene products.

3. Protein Synthesis

There is abundant evidence that both IGF-1 and IGF-2 stimulate protein synthesis in fish cells. For example, recombinant human IGF-1 stimulated [14 C]glycine incorporation in cultured muscle tissues of Gulf killifish (*Fundulus grandis*; Negatu and Meier, 1995), L-alanine uptake in rainbow trout myocytes (Castillo *et al.*, 2004), and both L-alanine uptake and L-leucine incorporation in brown trout cardiomyocytes (Gallardo *et al.*, 2001). Furthermore, recombinant barramundi IGF-1 and IGF-2 stimulated protein synthesis in barramundi liver *in vivo* (Degger *et al.*, 2000, 2001). Perhaps most compelling is the observation that recombinant hagfish IGF effectively stimulated protein synthesis in rat myoblasts (Upton *et al.*, 1997); although its potency was lower than the potencies of recombinant mammalian IGFs, its ability to elicit a relevant biological response clearly suggests functional conservation of the IGF system throughout millions of years of vertebrate evolution.

B. Embryonic Development

Embryogenesis is a remarkably dynamic period of development, marked by tremendous growth and a diverse spectrum of morphogenic events involving cell proliferation, growth, differentiation, migration, and apoptosis. The successful completion of embryonic development requires the coordinated integration of these diverse cellular events, many of which have independently been shown to be influenced by IGF signaling in a variety of model systems.

The physiological requirements for IGF signaling during embryogenesis have been a source of considerable debate among developmental endocrinologists (Nakae *et al.*, 2001). Whereas evidence from gene knockout studies in the mouse suggests that IGF signaling may not be required during the earliest phases of embryogenesis (Baker *et al.*, 1993), the demonstrated expression of IGF ligands and receptors in preimplantation embryos has been alternatively interpreted as evidence for functional IGF signaling during this period (Heyner and Garside, 1994; Heyner *et al.*, 1989, 1990, 1993).

There are at least two possible factors that may account for the confusion surrounding this issue: (1) early embryonic developmental is relatively difficult to study in mammals, because of the inaccessibility of the embryo during gestation; and (2) the considerable redundancy in expression patterns of IGF-related genes (e.g., IGFBPs) in rodents raises the specter of functional compensation in gene knockout animals, hampering efforts to determine independently the *in vivo* functions of individual genes. For example, increased serum levels of IGFBP-1, -3, and -4 were reported in mice after homologous gene targeting of IGFBP-2; the increase in nontargeted binding

proteins was suggested to explain the absence of growth defects hypothesized to result from deletion of the IGFBP-2 gene (Wood *et al.*, 2000).

The free-living zebrafish embryo exhibits many features that render it highly advantageous for the study of embryonic development. The embryos of this species develop rapidly, are optically transparent, and are highly versatile with respect to genetic manipulation. We have thus initiated studies to determine specifically the physiological requirements for IGF signaling during zebrafish embryonic development. To date, there are two lines of published evidence suggesting the presence of functional IGF signaling during early development in fish: (1) the reported coexpression of mRNAs encoding IGF ligands and their cognate (IGF-1) receptors in the embryos of selected species (e.g., zebrafish, Maures *et al.*, 2002), and (2) the demonstrated presence of proteins corresponding to functional IGF receptors in zebrafish embryos (Maures *et al.*, 2002), and isolated zebrafish embryonic (ZF-4) cells (Pozios *et al.*, 2001).

Our ongoing investigations are attempting to explore this issue further, using loss-of-function genetic approaches. Much of this work has employed morpholino-modified antisense oligonucleotides (MOs), which have been shown to effectively and specifically “knock down” the translation of target genes in embryonic zebrafish (Ekker, 2000; Ekker and Larson, 2001). Detailed phenotypic analysis of the “morphant” embryos can thus shed light on the physiological requirements for targeted genes.

1. IGF-1 Receptors

Targeted knockdown of the duplicate IGF-1Rs in zebrafish embryos by morpholino-modified oligonucleotides resulted in dramatic developmental perturbations and eventual death, indicating distinct requirements for IGF signaling during embryonic development in this species (Schlueter *et al.*, 2003). Morphant embryos exhibited marked growth retardation, compromised formation of many organs and tissues (e.g., eye, ear, heart, and muscle), and disorganized motor neuron formation. Independently knocking down either of the duplicate receptors resulted in similar, but less severe, phenotypes; interestingly, however, IGF-1Rb morphants failed to develop spontaneous contractile activity (coiling behavior; Saint-Amant and Drapeau, 1998), whereas contractile activity was consistently evident in IGF-1Ra morphants. These findings may indicate specific functional requirements for IGF-1Rb in zebrafish neuromuscular development.

2. IGFBP-1

As with other vertebrates, there is good evidence from studies in fish that IGFBP-1 may play a specific role in growth regulation during hypoxia.

Supporting evidence comes from the zebrafish, in which hypoxia has been shown to markedly increase IGFBP-1 mRNA levels in both embryos and adults (Maures and Duan, 2002); this induction was specific, as mRNA levels of other IGFBPs were unaffected by hypoxia (Kajimura *et al.*, 2004). The concomitant growth retardation observed in fish subjected to hypoxia could be partially rescued by MO knockdown of IGFBP-1 expression, indicating that hypoxia-induced growth retardation can be attributed in part to induced expression of IGFBP-1 (Kajimura *et al.*, 2004).

3. IGFBP-2

Targeted knockdown of IGFBP-2 in zebrafish embryos resulted in distinct-cardiovascular defects, a phenotype that is consistent with the expression patterns of IGFBP-2 during the embryonic period (Wood and Duan, 2004). IGFBP-2 morphant embryos exhibited a reduced density of circulating blood cells, hypochromic anemia, pericardial and brain ventricle edema, and ectopic pooling of blood cells in selected (e.g., ocular) regions. The mRNA expression of specific hematopoietic transcription factors (e.g., *GATA-1* and *SCL-1*) was initially normal, indicating that specification of blood and vascular precursor cells was likely not compromised. However, analysis of vascular patterning in IGFBP-2 morphant embryos, using a transgenic zebrafish line expressing a vascular-specific reporter gene (*flk1*-promoter-GFP; D. Beis, J. N. Chen, and D. Y. R. Stainier, unpublished data), revealed defects in angiogenesis in cerebral regions associated with IGFBP-2 expression. These are the first data to suggest that IGFBP-2 may facilitate IGF-1-induced cardiovascular development in vertebrate embryos.

4. IGFBP-5

Knockdown of IGFBP-5 in zebrafish embryos resulted in an abnormally curved body shape and reduced craniofacial skeletal tissues; the latter phenotype was consistent with the craniofacial expression patterns of IGFBP-5 mRNA. The effects of gene knockdown were judged to be specific because mRNA expression of *dlx-2*, a transcription factor expressed in branchial arch precursor cells, was greatly diminished in IGFBP-5 knockdown embryos. However, there were no detectable effects on mRNA expression of neuronal homeotic genes (e.g., *Emx-1* and *Rx-1*), confirming the specificity of MO-mediated IGFBP-5 knockdown. These data provide the first *in vivo* evidence that IGFBP-5 may function in a paracrine fashion to guide formation of craniofacial skeletal tissues in a model vertebrate.

C. Osmoregulation

The GH-IGF system has been long recognized as an important participant in the osmoregulatory physiology of fish (Mancera and McCormick, 1998b). The first evidence for this was derived from anadromous salmonids, which undergo a characteristic developmental transformation (smoltification) from freshwater-adapted "parr" to seawater-adapted "smolts" during the transition to a marine existence. Recognition of the involvement of the GH-IGF axis stemmed from observations that treatment with exogenous GH could facilitate seawater acclimation (Agustsson *et al.*, 2001; Clarke *et al.*, 1977; Komourdjian *et al.*, 1976). McCormick and colleagues were among the first to demonstrate that exogenous administration of IGF-1 to salmonids could also improve their ability to maintain plasma osmolality and sodium levels during seawater challenge (McCormick, 1996; McCormick *et al.*, 1991). Subsequent studies showed that IGF-1 stimulated gill Na^+, K^+ -ATPase activity, indicating a direct effect of IGF-1 on osmoregulatory organs of salmonids (Madsen and Bern, 1993; Madsen *et al.*, 1995), although IGF-1 was less effective than GH over prolonged exposure periods (McCormick, 1996). Interestingly, GH exposure in some instances was seen to enhance the osmoregulatory responsiveness of osmoregulatory tissues to IGF-1 (Madsen and Bern, 1993).

Whereas IGF-1 mRNA levels increase in liver and gill tissues during smoltification in coho salmon (Duguay *et al.*, 1994; Sakamoto *et al.*, 1995), direct transfer of rainbow trout to 80% seawater resulted in increased IGF-1 mRNA levels in gill and kidney, but not in liver (Sakamoto and Hirano, 1993). Thus, the osmoregulatory functions of the GH-IGF axis in salmonids may be mediated by the local synthesis of IGF-1 in osmoregulatory organs, and be regulated independently of the pituitary-hepatic growth axis.

The pronounced growth typically observed during salmonid smoltification has made it difficult to dissociate experimentally the osmoregulatory and anabolic actions of the GH-IGF axis. However, evidence from nonsalmonid teleosts suggests that involvement of the GH-IGF axis in osmoregulatory acclimation may indeed be independent of smoltification-associated growth (Sakamoto *et al.*, 1997). For example, administration of recombinant bovine IGF-1 enhanced the ability of mummichog (*Fundulus heteroclitus*) to maintain plasma osmolality, and stimulated gill Na^+, K^+ -ATPase activity. These effects were enhanced by coadministration with GH (Mancera and McCormick, 1998a), whereas recombinant human IGF-2 and bovine insulin had no effect. In addition, transfer of seawater-adapted tilapia to freshwater resulted in reduced growth and reduced tissue levels of GH and IGF-1 mRNAs, but increased serum levels of GH and IGF-1, suggesting that osmoregulatory stress may directly activate the GH-IGF axis with no concomitant stimulation of somatic growth (Riley *et al.*, 2003).

D. Reproduction

The IGF system has been relatively well studied within the context of mammalian reproductive development (Adashi, 1998; Gougeon, 1996). Gonadal tissues of both sexes abundantly express mRNAs for IGFs, their receptors, and binding proteins, in addition to specific proteases that modulate interactions between these molecules (Erickson and Shimasaki, 2001; Monget *et al.*, 2003). IGF-1 has been shown to enhance the stimulatory effects of follicle-stimulating hormone on steroid synthesis by ovarian follicles, and has also been identified as a potent follicle survival factor by its antiapoptotic actions (Chun *et al.*, 1994; Guthrie *et al.*, 1998). In addition, individual IGFbps have been variously implicated in the promotion or inhibition of follicular development in a number of species (Wandji *et al.*, 1998).

Fish are a convenient model in which to investigate gonadal development and function, and studies have indicated an important role for the IGF system in fish reproductive development. Fish gonads express mRNAs encoding IGFs (Duan and Plisetskaya, 1993; Duguay *et al.*, 1992, 1994; Perrot *et al.*, 2000), IGF receptors (Maires *et al.*, 2002; Perrot *et al.*, 2000), and IGFbps (Funkenstein *et al.*, 2002); IGF-1 has been immunolocalized in the developing ovary of at least one species (Kagawa *et al.*, 1995); and specific binding sites for both IGF-1 and IGF-2 have been identified in ovarian and/or testicular tissues of various fish species (Gutierrez *et al.*, 1993; Loir and Le Gac, 1994; Maestro *et al.*, 1997a,b; Mendez *et al.*, 2001a). The roles of the IGF system in reproductive development of fish have not been exhaustively investigated, but there is evidence that at least two distinct aspects of gonadal development, hormone production and oocyte maturation, are influenced by IGF actions. These may be considered as above and beyond the classic anabolic effects of IGF signaling.

1. Hormone Production

In many vertebrates, IGF signaling has been shown to influence the synthesis and/or secretion of reproductive steroid hormones from gonadal tissues (Adashi, 1998; Gougeon, 1996). Similar observations have been made in fish: for example, both human and recombinant salmon IGF-1 were shown to inhibit basal and LH-stimulated testosterone and 17α -hydroxyprogesterone production by isolated thecal-interstitial cells from coho salmon preovulatory follicles. In addition, they stimulated production of 17β -estradiol and $17,20\beta$ -progesterone ($17,20\beta$ -P) by granulosa cells from prematurational follicles, and $17,20\beta$ -P from granulosa cells of maturational follicles (Maestro *et al.*, 1997b). Similarly, culture of striped bass prematurational follicles with recombinant human IGF-1 enhanced the secretion of

17 β -estradiol and maturation-inducing steroid (MIS), and decreased testosterone secretion (Weber and Sullivan, 2000). IGF-1 was also shown to stimulate progesterone production and aromatase activity in carp ovarian follicles, effects that were accelerated and augmented by coculture with 17 β -estradiol (Behl and Pandey, 1999). Cross-talk between IGFs and ovarian steroids has similarly been observed in testicular tissues: for example, recombinant human IGF-1 alone had no stimulatory effects on spermatogenesis by Japanese eel testicular fragments, but enhanced the stimulatory effects of 11-ketotestosterone (Nader *et al.*, 1999).

Conversely, neither IGF-1 nor IGF-2 had any effect on steroid production by ovarian follicles of mummichog (Negatu *et al.*, 1998), although both ligands were biologically effective with respect to oocyte maturation (discussed below). In agreement with the latter findings, IGF-1 was shown to increase the abundance of oocyte receptors for MIS in spotted sea trout (*Cynoscion nebulosa*) follicles, with a potency equal to that of human chorionic gonadotropin (Thomas *et al.*, 2001).

IGFs have also been shown to influence the secretion of gonadotropic hormones by the pituitary gland. For example, both IGF-1 and IGF-2 increased the cell content and secretion of luteinizing hormone from European eel pituitary cells (Huang *et al.*, 1998). Similarly, prolonged incubation of dispersed coho salmon gonadotropes with IGF-1 enhanced their content and secretion of follicle-stimulating hormone (FSH). The effects in the latter study were not attributed to enhanced gonadotrope proliferation or survival, as the DNA content of cultured cells was unaffected by treatment with IGF-1 (Baker *et al.*, 2000). Although IGF-1 did not affect basal secretion of gonadotropins by rainbow trout gonadotropes, it was shown to enhance their responsiveness to gonadotropin-releasing hormone (Weil *et al.*, 1999). These observations suggest that IGFs may play an integral role during sexual development (puberty), possibly by stimulating reproductive development in lieu of somatic growth.

2. Oocyte Maturation

Multiple studies have suggested a role for IGF signaling in the regulation of oocyte maturation in fishes. As noted above, IGF-1 directly stimulated oocyte maturation in mummichog, with even greater potency than the endogenous MIS (Negatu *et al.*, 1998). Similarly, in red seabream, IGF-1 was shown to stimulate oocyte maturation (Kagawa *et al.*, 1994); interestingly, IGF-1 also stimulated the formation of gap junctions between follicular cells and the oocyte, effects coincident with an increase in oocyte maturational competence (Patiño and Kagawa, 1999). More recently, ovarian IGF-2 mRNA expression was associated with an increase in oocyte maturational

competence in rainbow trout (Bobe *et al.*, 2003, 2004), whereas both IGF-1 and IGF-2 mRNA levels were significantly higher in maturing oocytes than in maturationally incompetent oocytes (Bobe *et al.*, 2004). Collectively, these data suggest that IGF signaling influences oocyte maturation, perhaps through modulation of steroid–receptor signaling.

VI. Summary

Fish represent the most abundant group of vertebrates in the animal kingdom, with more than 28,000 described species (<http://www.fishbase.org>). Studies in extant fish, which exhibit remarkable variations in form and function across taxa, provide the opportunity for unparalleled insights into the conservation and/or diversification of genes and gene networks during vertebrate evolution.

Research has revealed that the fundamental elements of IGF signaling have been well conserved among the vertebrates. Whereas rudimentary elements of this system are evident in the most primitive fish (agnathans), a full complement of IGF ligands, receptors, and binding proteins had clearly evolved before divergence of the jawed fish from their tetrapod cousins. The functions of the IGF system furthermore appear to have been established early in the evolutionary trajectory; IGF signaling in gnathostome fish is mediated by two IGF ligands interacting with a receptor tyrosine kinase, whereas the interactions between ligands and receptors are modulated by a family of secreted, high-affinity ligand-binding proteins.

Studies of IGF-mediated growth in fish, driven largely by the tremendous commercial importance of the food fishery, clearly suggest that the modern somatomedin hypothesis serves well as a model to explain the neuroendocrine regulation of growth in all vertebrates, including fish (Fig. 8). However, the unique physiological challenges imposed by a life history spent under water have permitted the revelation of novel functions for the IGF system not directly evident from studies in tetrapod vertebrates. For example, studies in fish have revealed an important role for IGFs in the maintenance of osmoregulatory homeostasis, in part through direct stimulation of ion transporter enzymes in osmoregulatory tissues (e.g., gills).

Although the effects of the IGF system on growth, osmoregulation, and reproduction have been reasonably well described in fish, new lines of evidence indicate that IGF signaling may also be essential as a central regulator of embryonic and larval development in fish (Fig. 9). These new research directions, for which the teleost embryonic model is particularly well suited, have already begun to confirm that IGF signaling may indeed be a central feature throughout the life history of all vertebrates.

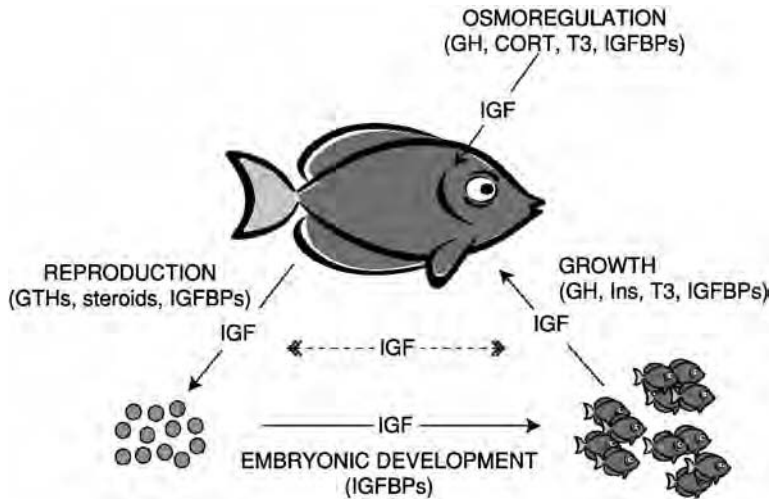


FIG. 9 Insulin-like growth factor (IGF) signaling (indicated by arrows), in association with hormones and IGF-binding proteins (IGFBPs), affects multiple aspects of fish development and physiology. Its importance for growth, osmoregulation, and reproduction has been relatively well defined; more recent studies indicate a central role for IGF signaling in embryonic growth and development. IGF signaling may also serve to facilitate the switch between reproductive and somatic development (indicated by the dashed, bidirectional arrow). Abbreviations: CORT, cortisol; GH, growth hormone; GTHs, gonadotropins; Ins, insulin; T3, triiodothyronine.

which are remarkably similar to those of humans, and directly manipulate gene expression levels using both gain-of-function and loss-of-function approaches. In addition, forward genetic screens using the zebrafish (Haffter *et al.*, 1996) have yielded hundreds of embryonic mutants, with specific defects in the formation and function of organs and tissues. The anticipated development of techniques permitting tissue- and/or organ-specific gene manipulations will undoubtedly provide even greater insights into vertebrate physiology and development; research in IGF signaling in fish is well placed to take advantage of these research methods as they emerge.

Acknowledgments

The authors thank the University of Michigan trio—Shingo Kajimura, Peter Schlueter, and Dr. Erica Crespi—for thoughtful comments on earlier drafts of this manuscript. A.W.W. was supported by a postdoctoral fellowship from the Natural Sciences and Engineering Research Council (NSERC) of Canada and by NSF grant IBN 0110864 during the preparation of this manuscript. Research in the Duan laboratory was supported by NSF grant IBN 0110864.

References

- Adashi, E. Y. (1998). The IGF family and folliculogenesis. *J. Reprod. Immunol.* **39**, 13–19.
- Aegerter, S., Jalabert, B., and Bobe, J. (2004). Messenger RNA stockpile of cyclin B, insulin-like growth factor I, insulin-like growth factor II, insulin-like growth factor receptor Ib, and p53 in the rainbow trout oocyte in relation with developmental competence. *Mol. Reprod. Dev.* **67**, 127–135.
- Agustsson, T., Sundell, K., Sakamoto, T., Johansson, V., Ando, M., and Bjornsson, B. (2001). Growth hormone endocrinology of Atlantic salmon (*Salmo salar*): Pituitary gene expression, hormone storage, secretion and plasma levels during parr–smolt transformation. *J. Endocrinol.* **170**, 227–234.
- Allendorf, F. W., and Thorgaard, G. H. (1984). Tetraploidy and the evolution of salmonid fishes. In “Evolutionary Genetics of Fishes” (B. J. Turner, Ed.), pp. 1–53. Plenum Press, New York.
- Anderson, T. A., Bennett, L. R., Conlon, M. A., and Owens, P. C. (1993). Immunoreactive and receptor-active insulin-like growth factor-I (IGF-I) and IGF-binding protein in blood plasma from the freshwater fish *Macquaria ambigua* (golden perch). *J. Endocrinol.* **136**, 191–198.
- Andress, D. L., and Birnbaum, R. S. (1992). Human osteoblast-derived insulin-like growth factor (IGF) binding protein-5 stimulates osteoblast mitogenesis and potentiates IGF action. *J. Biol. Chem.* **267**, 22467–22472.
- Ayaso, E., Nolan, C. M., and Byrnes, L. (2002). Zebrafish insulin-like growth factor-I receptor: Molecular cloning and developmental expression. *Mol. Cell Endocrinol.* **191**, 137–148.
- Ayson, F. G., de Jesus, E. G., Moriyama, S., Hyodo, S., Funkenstein, B., Gertler, A., and Kawachi, H. (2002). Differential expression of insulin-like growth factor I and II mRNAs during embryogenesis and early larval development in rabbitfish, *Siganus guttatus*. *Gen. Comp. Endocrinol.* **126**, 165–174.
- Baker, D. M., Davies, B., Dickhoff, W. W., and Swanson, P. (2000). Insulin-like growth factor I increases follicle-stimulating hormone (FSH) content and gonadotropin-releasing hormone-stimulated FSH release from coho salmon pituitary cells *in vitro*. *Biol. Reprod.* **63**, 865–871.
- Baker, J., Liu, J. P., Robertson, E. J., and Efstratiadis, A. (1993). Role of insulin-like growth factors in embryonic and postnatal growth. *Cell* **75**, 73–82.
- Banos, N., Moon, T. W., Castejon, C., Gutierrez, J., and Navarro, I. (1997). Insulin and insulin-like growth factor-I (IGF-I) binding in fish red muscle: Regulation by high insulin levels. *Regul. Pept.* **68**, 181–187.
- Banos, N., Baro, J., Castejon, C., Navarro, I., and Gutierrez, J. (1998). Influence of high-carbohydrate enriched diets on plasma insulin levels and insulin and IGF-I receptors in trout. *Regul. Pept.* **77**, 55–62.
- Banos, N., Planas, J. V., Gutierrez, J., and Navarro, I. (1999). Regulation of plasma insulin-like growth factor-I levels in brown trout (*Salmo trutta*). *Comp. Biochem. Physiol. C* **124**, 33–40.
- Bauchat, J. R., Busby, W. H. J., Garmong, A., Swanson, P., Moore, J., Lin, M., and Duan, C. (2001). Biochemical and functional analysis of a conserved IGF-binding protein isolated from rainbow trout (*Oncorhynchus mykiss*) hepatoma cells. *J. Endocrinol.* **170**, 619–628.
- Bautista, C. M., Mohan, S., and Baylink, D. J. (1990). Insulin-like growth factors I and II are present in the skeletal tissues of ten vertebrates. *Metabolism* **39**, 96–100.
- Baxter, R. C., and Martin, J. L. (1989). Structure of the M_r 140,000 growth hormone-dependent insulin-like growth factor binding protein complex: Determination by reconstitution and affinity-labeling. *Proc. Natl. Acad. Sci. USA* **86**, 6898–6902.
- Beckman, B. R., Larsen, D. A., Moriyama, S., Lee-Pawlak, B., and Dickhoff, W. W. (1998). Insulin-like growth factor-I and environmental modulation of growth during smoltification of spring chinook salmon (*Oncorhynchus tshawytscha*). *Gen. Comp. Endocrinol.* **109**, 325–335.

- Beckman, B. R., Shearer, K. D., Cooper, K. A., and Dickhoff, W. W. (2001). Relationship of insulin-like growth factor-I and insulin to size and adiposity of under-yearling chinook salmon. *Comp. Biochem. Physiol. A* **129**, 585–593.
- Beckman, B. R., Shimizu, M., Gadberry, B. A., and Cooper, K. A. (2004). Response of the somatotrophic axis of juvenile coho salmon to alterations in plane of nutrition with an analysis of the relationships among growth rate and circulating IGF-I and 41 kDa IGFBP. *Gen. Comp. Endocrinol.* **135**, 334–344.
- Behl, R., and Pandey, R. S. (1999). Effect of insulin-like growth factor-I on steroidogenesis in cultured carp ovarian follicles: Interactions with estradiol. *Indian J. Exp. Biol.* **37**, 138–142.
- Bern, H. A., McCormick, S. D., Kelley, K. M., Gray, E. S., Nishioka, R. S., Madsen, S. S., and Tsai, P. I. (1991). Insulin-like growth factors “under water”: Role in growth and function in fish and other poikilothermic vertebrates. In “Modern Concepts of Insulin-Like Growth Factors” (E. M. Spencer, Ed.), pp. 85–96. Elsevier Press, New York.
- Berwert, L., Segner, H., and Reinecke, M. (1995). Ontogeny of IGF-1 and the classical islet hormones in the turbot, *Scophthalmus maximus*. *Peptides* **16**, 113–122.
- Biga, P. R., Schelling, G. T., Hardy, R. W., Cain, K. D., Overturf, K., and Ott, T. L. (2004). The effects of recombinant bovine somatotropin (rbST) on tissue IGF-I, IGF-I receptor, and GH mRNA levels in rainbow trout, *Oncorhynchus mykiss*. *Gen. Comp. Endocrinol.* **135**, 324–333.
- Binox, M. (1995). The IGF system in metabolism regulation. *Diabetes Metab.* **21**, 330–337.
- Blaise, O., Weil, C., and LeBail, P. Y. (1995). Role of IGF-I in the control of GH secretion in rainbow trout (*Oncorhynchus mykiss*). *Growth Regul.* **5**, 142–150.
- Bobe, J., Maugars, G., Nguyen, T., Rime, H., and Jalabert, B. (2003). Rainbow trout follicular maturational competence acquisition is associated with an increased expression of follicle stimulating hormone receptor and insulin-like growth factor 2 messenger RNAs. *Mol. Reprod. Dev.* **66**, 46–53.
- Bobe, J., Nguyen, T., and Jalabert, B. (2004). Targeted gene expression profiling in the rainbow trout (*Oncorhynchus mykiss*) ovary during maturational competence acquisition and oocyte maturation. *Biol. Reprod.* **71**, 73–82.
- Bolton, J. P., Young, G., Nishioka, R. S., Hirano, T., and Bern, H. A. (1987). Plasma growth hormone levels in normal and stunted yearling coho salmon, *Oncorhynchus kisutch*. *J. Exp. Zool.* **242**, 379–382.
- Bondy, C. A., Werner, H., Roberts, C. T., Jr., and LeRoith, D. (1990). Cellular pattern of insulin-like growth factor-I (IGF-I) and type I IGF receptor gene expression in early organogenesis: Comparison with IGF-II gene expression. *Mol. Endocrinol.* **4**, 1386–1398.
- Boucher, S. E., and Hitchcock, P. F. (1998a). Insulin-like growth factor-I binds in the inner plexiform layer and circumferential germinal zone in the retina of the goldfish. *J. Comp. Neurol.* **394**, 395–401.
- Boucher, S. E., and Hitchcock, P. F. (1998b). Insulin-related growth factors stimulate proliferation of retinal progenitors in the goldfish. *J. Comp. Neurol.* **394**, 386–394.
- Bres, O., and Eales, J. G. (1986). Thyroid hormone binding to isolated trout (*Salmo gairdneri*) liver nuclei *in vitro*: Binding affinity, capacity, and chemical specificity. *J. Endocrinol.* **146**, 239–245.
- Broggiolo, W., Stocker, H., Ikeya, T., Rintelen, F., Fernandez, R., and Hafen, E. (2001). An evolutionarily conserved function of the *Drosophila* insulin receptor and insulin-like peptides in growth control. *Curr. Biol.* **11**, 213–221.
- Butler, A. A., Yakar, S., Gewolb, I. H., Karas, M., Okubo, Y., and LeRoith, D. (1998). Insulin-like growth factor-I receptor signal transduction: At the interface between physiology and cell biology. *Comp. Biochem. Physiol. B* **121**, 19–26.

- Caelters, A., Schmid, A. C., Hrusovsky, A., and Reinecke, M. (2003). Insulin-like growth factor II mRNA is expressed in neurones of the brain of the bony fish *Oreochromis mossambicus*, the tilapia. *Eur. J. Neurosci.* **18**, 355–363.
- Canfield, W. M., and Kornfeld, S. (1989). The chicken liver cation-independent mannose 6-phosphate receptor lacks the high affinity binding site for insulin-like growth factor II. *J. Biol. Chem.* **264**, 7100–7103.
- Cao, Q. P., Duguay, S. J., Plisetskaya, E., Steiner, D. F., and Chan, S. J. (1989). Nucleotide sequence and growth hormone-regulated expression of salmon insulin-like growth factor I mRNA. *Mol. Endocrinol.* **3**, 2005–2010.
- Castillo, J., Codina, M., Martinez, M. L., Navarro, I., and Gutierrez, J. (2004). Metabolic and mitogenic effects of IGF-I and insulin on muscle cells of rainbow trout. *Am. J. Physiol.* **286**, R935–R941.
- Chan, S. J., and Steiner, D. F. (1994). Structure and expression of insulin-like growth factor genes in fish. In “Fish Physiology” (W. S. Hoar and D. J. Randall, Eds.), Vol. XIII. Academic Press, New York.
- Chan, S. J., and Steiner, D. F. (2000). Insulin through the ages: Phylogeny of a growth-promoting and metabolic regulatory hormone. *Am. Zool.* **40**, 213–222.
- Chan, S. J., Emdin, S. O., Kwok, S. C., Kramer, J. M., Falkmer, S., and Steiner, D. F. (1981). Messenger RNA sequence and primary structure of preproinsulin in a primitive vertebrate, the Atlantic hagfish. *J. Biol. Chem.* **256**, 7595–7602.
- Chan, S. J., Cao, Q. P., and Steiner, D. F. (1990). Evolution of the insulin superfamily: Cloning of a hybrid insulin/insulin-like growth factor cDNA from amphioxus. *Proc. Natl. Acad. Sci. USA* **87**, 9319–9323.
- Chan, S. J., Plisetskaya, E. M., Urbinati, E., Jin, Y., and Steiner, D. F. (1997). Expression of multiple insulin and insulin-like growth factor receptor genes in salmon gill cartilage. *Proc. Natl. Acad. Sci. USA* **94**, 12446–12451.
- Chauvigné, F., Gabillard, J. C., Weil, C., and Rescan, P. Y. (2003). Effect of refeeding on IGF1, IGFII, IGF receptors, FGF2, FGF6, and myostatin mRNA expression in rainbow trout myotomal muscle. *Gen. Comp. Endocrinol.* **132**, 209–215.
- Chen, J. Y., Chang, C. Y., Chen, J. C., Shen, S. C., and Wu, J. L. (1997). Production of biologically active recombinant tilapia insulin-like growth factor-II polypeptides in *Escherichia coli* cells and characterization of the genomic structure of the coding region. *DNA Cell Biol.* **16**, 883–892.
- Chen, J. Y., Tsai, H. L., Chang, C. Y., Wang, J. I., Shen, S. C., and Wu, J. L. (1998). Isolation and characterization of tilapia (*Oreochromis mossambicus*) insulin-like growth factors gene and proximal promoter region. *DNA Cell Biol.* **17**, 359–376.
- Chen, J. Y., Chen, J. C., Huang, W. T., Liu, C. W., Hui, C. F., Chen, T. T., and Wu, J. L. (2003). Molecular cloning and tissue-specific, developmental-stage-specific, and hormonal regulation of IGFBP3 gene in zebrafish. *Mar. Biotechnol. (NY)* **6**, 1–7.
- Chen, M. H., Lin, G., Gong, H., Weng, C., Chang, C., and Wu, J. (2001). The characterization of prepro-insulin-like growth factor-1 Ea-2 expression and insulin-like growth factor-1 genes (devoid 81 bp) in the zebrafish (*Danio rerio*). *Gene* **268**, 67–75.
- Chen, M. J., Kuo, Y. H., Tian, X. C., and Chen, T. T. (2002). Novel biological activities of the fish pro-IGF-I E-peptides: Studies on effects of fish pro-IGF-I E-peptide on morphological change, anchorage-dependent cell division, and invasiveness in tumor cells. *Gen. Comp. Endocrinol.* **126**, 342–351.
- Chen, T. T., Marsh, A., Shambloott, M., Chan, K.-M., Tang, Y.-L., Cheng, C. M., and Yang, B.-Y. (1994). Structure and evolution of fish GH and insulin-like growth factor genes. In “Fish Physiology” (W. S. Hoar and D. J. Randall, Eds.), Vol. XIII, pp. 179–209. Academic Press, New York.

- Cheng, C. M., and Chen, T. T. (1995). Synergism of GH and IGF-I in stimulation of sulphate uptake by teleostean branchial cartilage *in vitro*. *J. Endocrinol.* **147**, 67–73.
- Chun, S.-Y., Billig, H., Tilly, J. L., Furuta, I., Tsafri, A., and Hsueh, A. J. W. (1994). Gonadotropin suppression of apoptosis in cultured preovulatory follicles: Mediator role of endogenous insulin-like growth factor I. *Endocrinology* **135**, 1845–1853.
- Clairmont, K. B., and Czech, M. P. (1989). Chicken and *Xenopus* mannose 6-phosphate receptors fail to bind insulin-like growth factor II. *J. Biol. Chem.* **264**, 16390–16392.
- Clarke, W. C., and Nagahama, Y. (1977). The effect of premature transfer to seawater on growth and morphology of the pituitary, thyroid, pancreas and interrenal in juvenile coho salmon (*Oncorhynchus kisutch*). *Can. J. Zool.* **55**, 1620–1630.
- Clarke, W. C., Farmer, S. W., and Hartwell, K. M. (1977). Effect of teleost pituitary growth hormone on growth of *Tilapia mossambica* and on growth and seawater adaptation of sockeye salmon (*Oncorhynchus nerka*). *Gen. Comp. Endocrinol.* **33**, 174–178.
- Clemmons, D. R. (2001). Use of mutagenesis to probe IGF-binding protein structure/function relationships. *Endocr. Rev.* **22**, 800–817.
- Clemmons, D. R., Busby, W., Clarke, J. B., Parker, A., Duan, C., and Nam, T. J. (1998). Modifications of insulin-like growth factor binding proteins and their role in controlling IGF actions. *Endocr. J. Suppl.* **45**, S1–S8.
- Collet, C., Candy, J., Richardson, N., and Sara, V. (1997). Organization, sequence, and expression of the gene encoding IGFII from Barramundi (Teleostei; *Lates calcarifer*). *Biochem. Genet.* **35**, 211–224.
- Datuin, J. P., Ng, K. P., Hayes, T. B., and Bern, H. A. (2001). Effects of glucocorticoids on cartilage growth and response to IGF-I in the tilapia (*Oreochromis mossambicus*). *Gen. Comp. Endocrinol.* **121**, 289–294.
- Daughaday, W. H., and Mariz, I. K. (1962). Conversion of proline U-C¹⁴ to labeled hydroxyproline by rat cartilage *in vitro*: Effects of hypophysectomy, growth hormone, and cortisol. *J. Lab. Clin. Med.* **59**, 741–752.
- Daughaday, W. H., Hall, K., Raben, M. S., Salmon, W. D. J., van den Brande, J. L., and van Wyk, J. J. (1972). Somatomedin: Proposed designation for sulphation factor. *Nature* **235**, 107.
- Daughaday, W. H., Kapadia, M., Yanow, C. E., Fabrick, K., and Mariz, I. K. (1985). Insulin-like growth factors I and II of nonmammalian sera. *Gen. Comp. Endocrinol.* **59**, 316–325.
- Daughaday, W. H., and Rotwein, P. (1989). Insulin-like growth factors I and II: Peptide, messenger ribonucleic acid and gene structures, serum, and tissue concentrations. *Endocr. Rev.* **10**, 68–91.
- Deane, E. E., Kelly, S. P., Collins, P. M., and Woo, N. Y. (2003). Larval development of silver sea bream (*Sparus sarba*): Ontogeny of RNA-DNA ratio, GH, IGF-I, and Na⁺-K⁺ ATPase. *Mar. Biotechnol. (NY)* **5**, 79–91.
- DeChiara, T. M., Efstratiadis, A., and Robertson, E. J. (1990). A growth-deficiency phenotype in heterozygous mice carrying an insulin-like growth factor II gene disrupted by targeting. *Nature* **345**, 78–80.
- Degger, B., Upton, Z., Soole, K., Collet, C., and Richardson, N. (2000). Comparison of recombinant barramundi and human insulin-like growth factor (IGF)-I in juvenile barramundi (*Lates calcarifer*): *In vivo* metabolic effects, association with circulating IGF-binding proteins, and tissue localisation. *Gen. Comp. Endocrinol.* **117**, 395–403.
- Degger, B., Richardson, N., Collet, C., and Upton, Z. (2001). Production, *in vitro* characterisation, *in vivo* clearance, and tissue localisation of recombinant barramundi (*Lates calcarifer*) insulin-like growth factor II. *Gen. Comp. Endocrinol.* **123**, 38–50.
- Denko, C. W., and Bergenstal, D. M. (1955). The effect of hypophysectomy and growth hormone on S35 fixation in cartilage. *Endocrinology* **57**, 76–86.

- Dickhoff, W. W., Beckman, B. R., Larsen, D. A., Duan, C., and Moriyama, S. (1997). The role of growth in endocrine regulation of salmon smoltification. *Fish Physiol. Biochem.* **17**, 231–236.
- Ding, J., and Duan, C. (2004). IGF binding protein-5 is required for pharyngeal skeleton formation *in vivo*. Society for Integrative and Comparative Biology Annual Meeting, New Orleans, LA, OR55-4 (Abstract).
- Doherty, A. S., Temeles, G. L., and Schultz, R. M. (1994). Temporal pattern of IGF-I expression during mouse preimplantation embryogenesis. *Mol. Reprod. Dev.* **37**, 21–26.
- Drakenberg, K., Sara, V. R., Lindahl, K. I., and Kewish, B. (1989). The study of insulin-like growth factors in tilapia, *Oreochromis mossambicus*. *Gen. Comp. Endocrinol.* **74**, 173–180.
- Drakenberg, K., Sara, V. R., Falkmer, S., Gammeltoft, S., Maake, C., and Reinecke, M. (1993). Identification of IGF-1 receptors in primitive vertebrates. *Regul. Pept.* **43**, 73–81.
- Drakenberg, K., Carey, G., Mather, P., Anderson, A., and Sara, V. R. (1997). Characterization of an insulin-like growth factor (IGF) receptor and the insulin-like effects of IGF-1 in the bony fish, *Lates calcarifer*. *Regul. Pept.* **69**, 41–45.
- Duan, C. (1997). The insulin-like growth factor system and its biological actions in fish. *Am. Zool.* **37**, 489–501.
- Duan, C. (1998). Nutritional and developmental regulation of insulin-like growth factors in fish. *J. Nutr.* **128**, 306S–314S.
- Duan, C. (2002). Specifying the cellular responses to IGF signals: Roles of IGF-binding proteins. *J. Endocrinol.* **175**, 41–54.
- Duan, C., and Hirano, T. (1990). Stimulation of ³⁵S-sulfate uptake by mammalian insulin-like growth factor I and II in cultured cartilages of Japanese eel, *Anguilla japonica*. *J. Exp. Zool.* **256**, 347–350.
- Duan, C., and Hirano, T. (1992). Effects of insulin-like growth factor-I and insulin on the *in vitro* uptake of sulphate by eel branchial cartilage: Evidence for the presence of independent hepatic and pancreatic sulphation factors. *J. Endocrinol.* **133**, 211–219.
- Duan, C. M., and Inui, Y. (1990a). Evidences for the presence of a somatomedin-like plasma factor(s) in the Japanese eel, *Anguilla japonica*. *Gen. Comp. Endocrinol.* **79**, 326–331.
- Duan, C. M., and Inui, Y. (1990b). Effects of recombinant eel growth hormone on the uptake of [³⁵S]sulfate by ceratobranchial cartilages of the Japanese eel, *Anguilla japonica*. *Gen. Comp. Endocrinol.* **79**, 320–325.
- Duan, C., and Plisetskaya, E. M. (1993). Nutritional regulation of insulin-like growth factor-I mRNA expression in salmon tissues. *J. Endocrinol.* **139**, 243–252.
- Duan, C., Noso, T., Moriyama, S., Kawauchi, H., and Hirano, T. (1992). Eel insulin: Isolation, characterization and stimulatory actions on [³⁵S]sulphate and [³H]thymidine uptake in the branchial cartilage of the eel *in vitro*. *J. Endocrinol.* **133**, 221–230.
- Duan, C., Duguay, S. J., and Plisetskaya, E. M. (1993a). Insulin-like growth factor I (IGF-I) mRNA expression in coho salmon, *Oncorhynchus kisutch*: Tissue distribution and effects of growth hormone/prolactin family peptides. *Fish Physiol. Biochem.* **11**, 371–379.
- Duan, C., Hanzawa, N., Takeuchi, Y., Hamada, E., Miyachi, S., and Hirano, T. (1993b). Use of primary cultures of salmon hepatocytes for the study of hormonal regulation of insulin-like growth factor I expression *in vitro*. *Zool. Sci.* **10**, 473–480.
- Duan, C., Plisetskaya, E. M., and Dickhoff, W. W. (1995). Expression of insulin-like growth factor I in normally and abnormally developing coho salmon (*Oncorhynchus kisutch*). *Endocrinology* **136**, 446–452.
- Duan, C., Ding, J., Li, Q., Tsai, W., and Pozios, K. (1999). Insulin-like growth factor binding protein 2 is a growth inhibitory protein conserved in zebrafish. *Proc. Natl. Acad. Sci. USA* **96**, 15274–15279.

- Duguay, S. J., Park, L. K., Samadpour, M., and Dickhoff, W. W. (1992). Nucleotide sequence and tissue distribution of three insulin-like growth factor I prohormones in salmon. *Mol. Endocrinol.* **6**, 1202–1210.
- Duguay, S. J., Swanson, P., and Dickhoff, W. W. (1994). Differential expression and hormonal regulation of alternatively spliced IGF-I mRNA transcripts in salmon. *J. Mol. Endocrinol.* **12**, 25–37.
- Duguay, S. J., Chan, S. J., Mommsen, T. P., and Steiner, D. F. (1995). Divergence of insulin-like growth factors I and II in the elasmobranch, *Squalus acanthias*. *FEBS Lett.* **371**, 69–72.
- Duguay, S. J., Lai-Zhang, J., Steiner, D. F., Funkenstein, B., and Chan, S. J. (1996). Developmental and tissue-regulated expression of IGF-I and IGF-II mRNAs in *Sparus aurata*. *J. Mol. Endocrinol.* **16**, 123–132.
- Duval, H., Rousseau, K., Elies, G., Le Bail, P. Y., Dufour, S., Boeuf, G., and Boujard, D. (2002). Cloning, characterization, and comparative activity of turbot IGF-I and IGF-II. *Gen. Comp. Endocrinol.* **126**, 269–278.
- Dyer, A. R., Upton, Z., Stone, D., Thomas, P. M., Soole, K. L., Higgs, N., Quinn, K., and Carragher, J. F. (2004). Development and validation of a radioimmunoassay for fish insulin-like growth factor I (IGF-I) and the effect of aquaculture related stressors on circulating IGF-I levels. *Gen. Comp. Endocrinol.* **135**, 268–275.
- Ekker, S. C. (2000). Morphants: A new systematic vertebrate functional genomics approach. *Yeast* **17**, 302–306.
- Ekker, S. C., and Larson, J. D. (2001). Morphant technology in model developmental systems. *Genesis* **30**, 89–93.
- Elies, G., Duval, H., Groigno, L., Wolff, J., Boeuf, G., and Boujard, D. (1998b). Turbot (*Psetta maxima*) IGF-I and receptor cDNAs cloning. *Bull. Fr. Pêche Piscic.* **350**, 623–634.
- Elies, G., Groigno, L., Wolff, J., Boeuf, G., and Boujard, D. (1998a). Cloning of the IGF-I receptor cDNA of turbot (*Scophthalmus maximus*): Messenger expression and polyadenylation status. *Ann. N.Y. Acad. Sci.* **839**, 513–514.
- Elies, G., Duval, H., Bonnet, G., Wolff, J., Boeuf, G., and Boujard, D. (1999). Insulin and insulin-like growth factor-1 receptors in an evolved fish, the turbot: cDNA cloning and mRNA expression. *Mol. Cell. Endocrinol.* **158**, 173–185.
- Erickson, G. F., and Shimasaki, S. (2001). The physiology of folliculogenesis: The role of novel growth factors. *Fertil. Steril.* **76**, 943–949.
- Fan, T. J., Jin, L. Y., and Wang, X. F. (2003). Initiation of cartilage cell culture from skate (*Raja porosa* Gunther). *Mar. Biotechnol. (NY)* **5**, 64–69.
- Fernandez, R., Tabarini, D., Azpiazu, N., Frasch, M., and Schlessinger, J. (1995). The *Drosophila* insulin receptor homologue: A gene essential for embryonic development encodes two receptor isoforms with different signaling potential. *EMBO J.* **14**, 101–112.
- Fine, M., Amuly, R., Sandowski, Y., Marchant, T. A., Chan, S. J., Gertler, A., and Funkenstein, B. (1997). Recombinant gilthead seabream (*Sparus aurata*) insulin-like growth factor-I: Subcloning, expression in *Escherichia coli*, purification and characterization. *J. Endocrinol.* **153**, 139–150.
- Firth, S. M., and Baxter, R. C. (2002). Cellular actions of the insulin-like growth factor binding proteins. *Endocr. Rev.* **23**, 824–854.
- Fowles, J. L., Thraikill, K. M., George-Nascimento, C., Rosenberg, C. K., and Sera, D. M. (1997). Heparin-binding, highly basic regions within the thyroglobulin type-1 repeat of insulin-like growth factor (IGF)-binding proteins (IGFBPs) -3, -5, and -6 inhibit IGFBP-4 degradation. *Endocrinology* **138**, 2280–2285.
- Froesch, E. R., Burgi, H., Ramseier, E. B., Bally, P., and Labhart, A. (1963). Antibody-suppressible and nonsuppressible insulin-like activities in human serum and their physiological significance. *J. Clin. Invest.* **42**, 1816–1834.

- Fruchtman, S., Jackson, L., and Borski, R. (2000). Insulin-like growth factor I disparately regulates prolactin and growth hormone synthesis and secretion: Studies using the teleost pituitary model. *Endocrinology* **141**, 2886–2894.
- Fruchtman, S., Gift, B., Howes, B., and Borski, R. (2001). Insulin-like growth factor-I augments prolactin and inhibits growth hormone release through distinct as well as overlapping cellular signaling pathways. *Comp. Biochem. Physiol. B* **129**, 237–242.
- Fruchtman, S., McVey, D. C., and Borski, R. J. (2002). Characterization of pituitary IGF-I receptors: Modulation of prolactin and growth hormone. *Am. J. Physiol.* **283**, R468–R476.
- Fukazawa, Y., Siharath, K., Iguchi, T., and Bern, H. A. (1995). *In vitro* secretion of insulin-like growth factor-binding proteins from liver of striped bass, *Morone saxatilis*. *Gen. Comp. Endocrinol.* **99**, 239–247.
- Funkenstein, B., Silbergeld, A., Cavari, B., and Laron, Z. (1989). Growth hormone increases plasma levels of insulin-like growth factor (IGF-I) in a teleost, the gilthead seabream (*Sparus aurata*). *J. Endocrinol.* **120**, R19–R21.
- Funkenstein, B., Shemer, R., and Cohen, I. (1996). Nucleotide sequence of the promoter region of *Sparus aurata* insulin-like growth factor I gene and expression in eggs and embryos. *Mol. Mar. Biol. Biotechnol.* **5**, 43–51.
- Funkenstein, B., Tsai, W., Maures, T., and Duan, C. (2002). Ontogeny, tissue distribution, and hormonal regulation of insulin-like growth factor binding protein-2 (IGFBP-2) in a marine fish, *Sparus aurata*. *Gen. Comp. Endocrinol.* **128**, 112–122.
- Furlanetto, R. W., Underwood, L. E., Van Wyk, J. J., and D'Ercole, A. J. (1977). Estimation of somatomedin-C levels in normals and patients with pituitary disease by radioimmunoassay. *J. Clin. Invest.* **60**, 648–657.
- Gabillard, J. C., Rescan, P. Y., Fauconneau, B., Weil, C., and Le Bail, P. Y. (2003a). Effect of temperature on gene expression of the GH/IGF system during embryonic development in rainbow trout (*Oncorhynchus mykiss*). *J. Exp. Zool.* **298**, 134–142.
- Gabillard, J. C., Weil, C., Rescan, P. Y., Navarro, I., Gutierrez, J., and Le Bail, P. Y. (2003b). Effects of environmental temperature on IGF1, IGF2, and IGF type I receptor expression in rainbow trout (*Oncorhynchus mykiss*). *Gen. Comp. Endocrinol.* **133**, 233–242.
- Gallardo, M. A., Castejon, C., Navarro, I., Blasco, J., Gutierrez, J., and Sanchez, J. (2001). L-leucine and L-alanine uptake by trout (*Salmo trutta*) cardiomyocytes: The effect of IGF-I and insulin. *Fish Physiol. Biochem.* **25**, 239–248.
- Gelsleichter, J., and Musick, J. A. (1999). Effects of insulin-like growth factor-I, corticosterone, and 3,3',5-tri-iodo-L-thyronine on glycosaminoglycan synthesis in vertebral cartilage of the clearnose skate, *Raja eglanteria*. *J. Exp. Zool.* **284**, 549–556.
- Gentil, V., Martin, P., Smal, J., and Le Bail, P. Y. (1996). Production of recombinant insulin-like growth factor-II in the development of a radioimmunoassay in rainbow trout (*Oncorhynchus mykiss*). *Gen. Comp. Endocrinol.* **104**, 156–167.
- Georges, D., and Schwabe, C. (1999). Porcine relaxin, a 500 million-year-old hormone? The tunicate *Ciona intestinalis* has porcine relaxin *FASEB J.* **13**, 1269–1275.
- Goishi, K., Lee, P., Davidson, A. J., Nishi, E., Zon, L. I., and Klagsbrun, M. (2003). Inhibition of zebrafish epidermal growth factor receptor activity results in cardiovascular defects. *Mech. Dev.* **120**, 811–822.
- Gougeon, A. (1996). Regulation of ovarian follicular development in primates: Facts and hypotheses. *Endocr. Rev.* **17**, 121–154.
- Gracey, A. Y., Troll, J. V., and Somero, G. N. (2001). Hypoxia-induced gene expression profiling in the euryoptic fish *Gillichthys mirabilis*. *Proc. Natl. Acad. Sci. USA* **98**, 1993–1998.
- Gray, E. S., and Kelley, K. M. (1991). Growth regulation in the gobiid teleost, *Gillichthys mirabilis*: Roles of growth hormone, hepatic growth hormone receptors and insulin-like growth factor-I. *J. Endocrinol.* **131**, 57–66.

- Gray, E. S., Kelley, K. M., Law, S., Tsai, R., Young, G., and Bern, H. A. (1992). Regulation of hepatic growth hormone receptors in coho salmon (*Oncorhynchus kisutch*). *Gen. Comp. Endocrinol.* **88**, 243–252.
- Greene, M. W., and Chen, T. T. (1997). Temporal expression pattern of insulin-like growth factor mRNA during embryonic development in a teleost, rainbow trout (*Oncorhynchus mykiss*). *Mol. Mar. Biol. Biotechnol.* **6**, 144–151.
- Greene, M. W., and Chen, T. T. (1999a). Quantitation of IGF-I, IGF-II, and multiple insulin receptor family member messenger RNAs during embryonic development in rainbow trout. *Mol. Reprod. Dev.* **54**, 348–361.
- Greene, M. W., and Chen, T. T. (1999b). Characterization of teleost insulin receptor family members. II. Developmental expression of insulin-like growth factor type I receptor messenger RNAs in rainbow trout. *Gen. Comp. Endocrinol.* **115**, 270–281.
- Guler, H. P., Zapf, J., Schmid, C., and Froesch, E. R. (1989). Insulin-like growth factors I and II in healthy man: Estimations of half-lives and production rates. *Acta Endocrinol. (Copenh.)* **121**, 753–758.
- Guthrie, H. D., Garrett, W. M., and Cooper, B. S. (1998). Follicle-stimulating hormone and insulin-like growth factor-I attenuate apoptosis in cultured porcine granulosa cells. *Biol. Reprod.* **58**, 390–396.
- Gutierrez, J., Parrizas, M., Carneiro, N., Maestro, J. L., Maestro, M. A., and Planas, J. (1993). Insulin and IGF-I receptors and tyrosine kinase activity in carp ovaries: Changes with reproductive cycle. *Fish Physiol. Biochem.* **11**, 247–254.
- Gutierrez, J., Parrizas, M., Maestro, M. A., Navarro, I., and Plisetskaya, E. M. (1995). Insulin and IGF-I binding and tyrosine kinase activity in fish heart. *J. Endocrinol.* **146**, 35–44.
- Haffrie, P., Granato, M., Brand, M., Mullins, M. C., Hammerschmidt, M., Kane, D. A., Odenthal, J., van Eeden, F. J., Jiang, Y. J., Heisenberg, C. P., Kelsh, R. N., Furutani-Seiki, M., Vogelsang, E., Beuchle, D., Schach, U., Fabian, C., and Nusslein-Volhard, C. (1996). The identification of genes with unique and essential functions in the development of the zebrafish, *Danio rerio*. *Development* **123**, 1–36.
- Hall, K. (1970). Quantitative determination of the sulphation factor activity in human serum. *Acta Endocrinol. (Copenh.)* **63**, 338–350.
- Hall, K., and Uthne, K. (1971). Some biological properties of purified sulfation factor (SF) from human plasma. *Acta Med. Scand.* **190**, 137–143.
- Hashimoto, H., Mikawa, S., Takayama, E., Yokoyama, Y., Toyohara, H., and Sakaguchi, M. (1997). Molecular cloning and growth hormone-regulated gene expression of carp insulin-like growth factor-I. *Biochem. Mol. Biol. Int.* **41**, 877–886.
- Heldin, C. H., Wasteson, A., Fryklund, L., and Westermarck, B. (1981). Somatomedin B: Mitogenic activity derived from contaminant epidermal growth factor. *Science* **213**, 1122–1123.
- Heyner, S., and Garside, W. T. (1994). Biological actions of IGFs in mammalian development. *Bioessays* **16**, 55–57.
- Heyner, S., Smith, R. M., and Schultz, G. A. (1989). Temporally regulated expression of insulin and insulin-like growth factors and their receptors in early mammalian development. *Bioessays* **11**, 171–176.
- Heyner, S., Farber, M., and Rosenblum, I. Y. (1990). The insulin family of peptides in early mammalian development. *Curr. Top. Dev. Biol.* **24**, 137–159.
- Heyner, S., Shi, C. Z., Garside, W. T., and Smith, R. M. (1993). Functions of the IGFs in early mammalian development. *Mol. Reprod. Dev.* **35**, 421–426.
- Hodgkinson, S. C., Davis, S. R., Burleigh, B. D., Henderson, H. V., and Gluckman, P. D. (1987). Metabolic clearance rate of insulin-like growth factor-I in fed and starved sheep. *J. Endocrinol.* **115**, 233–240.

- Hodgkinson, S. C., Davis, S. R., Moore, L. G., Henderson, H. V., and Gluckman, P. D. (1989). Metabolic clearance of insulin-like growth factor-II in sheep. *J. Endocrinol.* **123**, 461–468.
- Holzenberger, M., Dupont, J., Ducos, B., Leneuve, P., Geloën, A., Even, P. C., Cervera, P., and Le Bouc, Y. (2003). IGF-1 receptor regulates lifespan and resistance to oxidative stress in mice. *Nature* **421**, 182–187.
- Hu, S. Y., Wu, J. L., and Huang, J. H. (2004). Production of tilapia insulin-like growth factor-2 in high cell density cultures of recombinant *Escherichia coli*. *J. Biotechnol.* **107**, 161–171.
- Huang, Y. S., Rousseau, K., Le Belle, N., Vidal, B., Burzawa-Gerard, E., Marchelidon, J., and Dufour, S. (1998). Insulin-like growth factor-I stimulates gonadotrophin production from eel pituitary cells: A possible metabolic signal for induction of puberty. *J. Endocrinol.* **159**, 43–52.
- Hwa, V., Oh, Y., and Rosenfeld, R. G. (1999). The insulin-like growth factor binding protein (IGFBP) superfamily. *Endocr. Rev.* **20**, 761–787.
- Inoue, K., Iwatani, H., and Takei, Y. (2003). Growth hormone and insulin-like growth factor I of a euryhaline fish *Cottus kazika*: cDNA cloning and expression after seawater acclimation. *Gen. Comp. Endocrinol.* **131**, 77–84.
- Johnson, J., Silverstein, J., Wolters, W. R., Shimizu, M., Dickhoff, W. W., and Shepherd, B. S. (2003). Disparate regulation of insulin-like growth factor-binding proteins in a primitive, ictalurid teleost (*Ictalurus punctatus*). *Gen. Comp. Endocrinol.* **134**, 122–130.
- Jones, J. I., and Clemmons, D. R. (1995). Insulin-like growth factors and their binding proteins: Biological actions. *Endocr. Rev.* **16**, 3–34.
- Jones, J. I., Pevette, T., Gockerman, A., and Clemmons, D. R. (1993). Ligand occupancy of the $\alpha_V\beta_3$ integrin is necessary for smooth muscle cells to migrate in response to insulin-like growth factor I. *Proc. Natl. Acad. Sci. USA* **93**, 2482–2487.
- Kagawa, H., Kobayashi, M., Hasegawa, Y., and Aida, K. (1994). Insulin and insulin-like growth factors I and II induce final maturation of oocytes of red seabream, *Pagrus major*, *in vitro*. *Gen. Comp. Endocrinol.* **95**, 293–300.
- Kagawa, H., Moriyama, S., and Kawauchi, H. (1995). Immunocytochemical localization of IGF-I in the ovary of the red seabream, *Pagrus major*. *Gen. Comp. Endocrinol.* **99**, 307–315.
- Kajimura, S., Uchida, K., Yada, T., Riley, L. G., Byatt, J. C., Collier, R. J., Aida, K., Hirano, T., and Grau, E. G. (2001). Stimulation of insulin-like growth factor-I production by recombinant bovine growth hormone in Mozambique tilapia, *Oreochromis mossambicus*. *Fish Physiol. Biochem.* **25**, 221–230.
- Kajimura, S., Uchida, K., Yada, T., Hirano, T., Aida, K., and Gordon Grau, E. (2002). Effects of insulin-like growth factors (IGF-I and -II) on growth hormone and prolactin release and gene expression in euryhaline tilapia, *Oreochromis mossambicus*. *Gen. Comp. Endocrinol.* **127**, 223–231.
- Kajimura, S., Hirano, T., Visitacion, N., Moriyama, S., Aida, K., and Grau, E. G. (2003). Dual mode of cortisol action on GH/IGF-I/IGF-binding proteins in the tilapia, *Oreochromis mossambicus*. *J. Endocrinol.* **178**, 91–99.
- Kajimura, S., Aida, K., and Duan, C. (2004). Induction of insulin-like growth factor binding protein-1 (IGFBP-1) by hypoxia during zebrafish embryogenesis: Possible implications for embryonic growth. Proceedings of the 4th Congress of Asia and Oceania Society of Comparative Endocrinology, Nara, Japan. pp. 224–226.
- Kasik, J. W., Lu, C., and Menon, R. K. (2000). The expanding insulin family: Structural, genomic, and functional considerations. *Pediat. Diabetes* **1**, 169–177.
- Kavsan, V. M., Koval, A. P., Grebenjuk, V. A., Chan, S. J., Steiner, D. F., Roberts, C. T. J., and LeRoith, D. (1993). Structure of the chum salmon insulin-like growth factor I gene. *DNA Cell Biol.* **12**, 729–737.
- Kavsan, V. M., Grebenjuk, V. A., Koval, A. P., Skorokhod, A. S., Roberts, C. T. J., and LeRoith, D. (1994). Isolation of a second nonallelic insulin-like growth factor I gene from the salmon genome. *DNA Cell Biol.* **13**, 555–559.

- Kawauchi, H., Suzuki, K., Yamazaki, T., Moriyama, S., Nozaki, M., Yamaguchi, K., Takahashi, A., Youson, J., and Sower, S. A. (2002). Identification of growth hormone in the sea lamprey, an extant representative of a group of the most ancient vertebrates. *Endocrinology* **143**, 4916–4921.
- Kelley, K. M., Siharath, K., and Bern, H. A. (1992). Identification of insulin-like growth factor-binding proteins in the circulation of four teleost fish species. *J. Exp. Zool.* **263**, 220–224.
- Kelley, K. M., Gray, E. S., Siharath, K., Nicoll, C. S., and Bern, H. A. (1993). Experimental diabetes mellitus in a teleost fish. II. Roles of insulin, growth hormone (GH), insulin-like growth factor-I, and hepatic GH receptors in diabetic growth inhibition in the goby, *Gillichthys mirabilis*. *Endocrinology* **132**, 2696–2702.
- Kelley, K. M., Oh, Y., Gargosky, S. E., Gucev, Z., Matsumoto, T., Hwa, V., Ng, L., Simpson, D. M., and Rosenfeld, R. G. (1996). Insulin-like growth factor-binding proteins (IGFBPs) and their regulatory dynamics. *Int. J. Biochem. Cell Biol.* **28**, 619–637.
- Kelley, K. M., Haigwood, J. T., Perez, M., and Galima, M. M. (2001). Serum insulin-like growth factor binding proteins (IGFBPs) as markers for anabolic/catabolic condition in fishes. *Comp. Biochem. Physiol. B* **129**, 229–236.
- Kelley, K. M., Schmidt, K. E., Berg, L., Sak, K., Galima, M. M., Gillespie, C., Balogh, L., Hawayek, A., Reyes, J. A., and Jamison, M. (2002). Comparative endocrinology of the insulin-like growth factor-binding protein. *J. Endocrinol.* **175**, 3–18.
- Klapper, D. G., Svoboda, M. E., and Van Wyk, J. J. (1983). Sequence analysis of somatomedin-C: Confirmation of identity with insulin-like growth factor I. *Endocrinology* **112**, 2215–2217.
- Koenig, R. J., Brent, G. A., Warne, R. L., Larsen, P. R., and Moore, D. D. (1987). Thyroid hormone receptor binds to a site in the rat growth hormone promoter required for induction by thyroid hormone. *Proc. Natl. Acad. Sci. USA* **84**, 5670–5674.
- Komourdjian, M. P., and Idler, D. R. (1978). Hepatic mediation of hormonal and nutritional factors influencing the *in vitro* sulfur uptake by rainbow trout bone. *Gen. Comp. Endocrinol.* **36**, 33–39.
- Komourdjian, M. P., Saunders, R. L., and Fenwick, J. C. (1976). The effect of porcine somatotropin on growth, and survival in seawater of Atlantic salmon (*Salmo salar*) parr. *Can. J. Zool.* **54**, 531–535.
- Koval, A., Kulik, V., Duguay, S., Plisetskaya, E., Adamo, M. L., Roberts, C. T. J., LeRoith, D., and Kavsan, V. (1994). Characterization of a salmon insulin-like growth factor I promoter. *DNA Cell Biol.* **13**, 1057–1062.
- Krieger, M. J. B., Jahan, N., Riehle, M. A., Cao, C., and Brown, M. R. (2004). Molecular characterization of insulin-like peptide genes and their expression in the African malaria mosquito, *Anopheles gambiae*. *Insect Mol. Biol.* **13**, 305–315.
- Kulik, V. P., Kavsan, V. M., van Schaik, F. M., Nolten, L. A., Steenbergh, P. H., and Sussenbach, J. S. (1995). The promoter of the salmon insulin-like growth factor I gene is activated by hepatocyte nuclear factor I. *J. Biol. Chem.* **270**, 1068–1073.
- Lagueux, M., Lwoff, L., Meister, M., Goltzene, F., and Hoffmann, J. (1990). cDNAs from neurosecretory cells of brains of *Locusta migratoria* (Insecta, Orthoptera) encoding a novel member of the superfamily of insulins. *Eur. J. Biochem.* **187**, 249–254.
- Larsen, D. A., Beckman, B. R., and Dickhoff, W. W. (2001). The effect of low temperature and fasting during the winter on metabolic stores and endocrine physiology (insulin, insulin-like growth factor-I, and thyroxine) of coho salmon, *Oncorhynchus kisutch*. *Gen. Comp. Endocrinol.* **123**, 308–323.
- LeRoith, D., Bondy, C., Yakar, S., Liu, J. L., and Butler, A. (2001). The somatomedin hypothesis: 2001. *Endocr. Rev.* **22**, 53–74.
- Lee, C. Y., and Rechler, M. M. (1995). A major portion of the 150-kilodalton insulin-like growth factor-binding protein (IGFBP) complex in adult rat serum contains

- unoccupied, proteolytically nicked IGFBP-3 that binds IGF-II preferentially. *Endocrinology* **136**, 668–678.
- Lee, C. Y., and Rechler, M. M. (1996). Proteolysis of insulin-like growth factor (IGF)-binding protein-3 (IGFBP-3) in 150-kilodalton IGFBP complexes by a cation-dependent protease activity in adult rat serum promotes the release of bound IGF-I. *Endocrinology* **137**, 2051–2058.
- Leibush, B., Parrizas, M., Navarro, I., Lappova, Y., Maestro, M. A., Encinas, M., Plisetskaya, E. M., and Gutierrez, J. (1996). Insulin and insulin-like growth factor-I receptors in fish brain. *Regul. Pept.* **61**, 155–161.
- Leong, S. R., Baxter, R. C., Camerato, T., Dai, J., and Wood, W. I. (1992). Structure and functional expression of the acid-labile subunit of the insulin-like growth factor-binding protein complex. *Mol. Endocrinol.* **6**, 870–876.
- Li, C. H., and Evans, H. M. (1944). The isolation of pituitary growth hormone. *Science* **99**, 184–186.
- Liang, Y. H., Cheng, C. H., and Chan, K. M. (1996). Insulin-like growth factor-I Ea2 is the predominantly expressed form of IGF in common carp (*Cyprinus carpio*). *Mol. Mar. Biol. Biotechnol.* **5**, 145–152.
- Lindahl, K. I., Sara, V., Fridberg, G., and Nishimiya, T. (1985). The presence of somatomedin in the Baltic salmon, *Salmo salar*, with special reference to smoltification. *Aquaculture* **45**, 177–183.
- Liu, J. P., Baker, J., Perkins, A. S., Robertson, E. J., and Efstratiadis, A. (1993). Mice carrying null mutations of the genes encoding insulin-like growth factor I (IGF-1) and type I IGF receptor (IGF-1R). *Cell* **75**, 59–72.
- Loffing-Cueni, D., Schmid, A. C., Graf, H., and Reinecke, M. (1998). IGF-I in the bony fish *Cottus scorpius*: cDNA, expression and differential localization in brain and islets. *Mol. Cell Endocrinol.* **141**, 187–194.
- Loffing-Cueni, D., Schmid, A. C., and Reinecke, M. (1999). Molecular cloning and tissue expression of the insulin-like growth factor II prohormone in the bony fish *Cottus scorpius*. *Gen. Comp. Endocrinol.* **113**, 32–37.
- Loir, M., and Le Gac, F. (1994). Insulin-like growth factor-I and -II binding and action on DNA synthesis in rainbow trout spermatogonia and spermatocytes. *Biol. Reprod.* **51**, 1154–1163.
- Mack, A. F., and Fernald, R. D. (1993). Regulation of cell division and rod differentiation in the teleost retina. *Brain Res. Dev. Brain Res.* **76**, 183–187.
- Mack, A. F., Balt, S. L., and Fernald, R. D. (1995). Localization and expression of insulin-like growth factor in the teleost retina. *Vis. Neurosci.* **12**, 457–461.
- MacLatchy, D. L., and Eales, J. G. (1992). Intra- and extra-cellular sources of T3 binding to putative thyroid hormone receptors in liver, kidney, and gill nuclei of immature rainbow trout, *Oncorhynchus mykiss*. *J. Exp. Zool.* **262**, 22–29.
- Madsen, S. S., and Bern, H. A. (1993). *In-vitro* effects of insulin-like growth factor-I on gill Na^+ , K^+ -ATPase in coho salmon, *Oncorhynchus kisutch*. *J. Endocrinol.* **138**, 23–30.
- Madsen, S. S., Jensen, M. K., Nhr, J., and Kristiansen, K. (1995). Expression of Na^+ - K^+ -ATPase in the brown trout, *Salmo trutta*: *In vivo* modulation by hormones and seawater. *Am. J. Physiol.* **269**, R1339–R1345.
- Maestro, M. A., Méndez, E., Parrizas, M., and Gutierrez, J. (1997a). Characterization of insulin and insulin-like growth factor-I ovarian receptors during the reproductive cycle of carp (*Cyprinus carpio*). *Biol. Reprod.* **56**, 1126–1132.
- Maestro, M. A., Planas, J. V., Moriyama, S., Gutierrez, J., Planas, J., and Swanson, P. (1997b). Ovarian receptors for insulin and insulin-like growth factor I (IGF-I) and effects of IGF-I on steroid production by isolated follicular layers of the preovulatory coho salmon ovarian follicle. *Gen. Comp. Endocrinol.* **106**, 189–201.

- Maestro, M. A., Méndez, E., Bayraktaroglu, E., Banos, N., and Gutierrez, J. (1998). Appearance of insulin and insulin-like growth factor-I (IGF-I) receptors throughout the ontogeny of brown trout (*Salmo trutta fario*). *Growth Horm. IGF Res.* **8**, 195–204.
- Maestro, M. A., Méndez, E., Planas, J. V., and Gutiérrez, J. (1999). Dynamics of insulin and insulin-like growth factor-I (IGF-I) ovarian receptors during maturation in the brown trout (*Salmo trutta*). *Fish Physiol. Biochem.* **20**, 341–349.
- Mancera, J. M., and McCormick, S. D. (1998a). Evidence for growth hormone/insulin-like growth factor I axis regulation of seawater acclimation in the euryhaline teleost *Fundulus heteroclitus*. *Gen. Comp. Endocrinol.* **111**, 103–112.
- Mancera, J. M., and McCormick, S. D. (1998b). Osmoregulatory actions of the GH/IGF axis in non-salmonid teleosts. *Comp. Biochem. Physiol. B* **121**, 43–48.
- Marchant, T. A., and Moroz, B. M. (1993). *In vitro* effects of insulin-like growth factors and related peptides on the uptake of [³⁵S]-sulfate from the goldfish (*Carassius auratus* L.). *Fish Physiol. Biochem.* **11**, 393–400.
- Marquardt, H., Todaro, G. J., Henderson, L. E., and Oroszlan, S. (1981). Purification and primary structure of a polypeptide with multiplication-stimulating activity from rat liver cell cultures: Homology with human insulin-like growth factor II. *J. Biol. Chem.* **256**, 6859–6865.
- Matthews, S. J., Kihl, A. K. K., Hoeben, P., Sara, V. R., and Anderson, T. A. (1997). Nutritional regulation of insulin-like growth factor-I mRNA expression in barramundi, *Lates calcarifer*. *J. Mol. Endocrinol.* **18**, 273–276.
- Maures, T. J., and Duan, C. (2002). Structure, developmental expression, and physiological regulation of zebrafish IGF-binding protein-1. *Endocrinology* **143**, 2722–2731.
- Maures, T., Chan, S. J., Xu, B., Sun, H., Ding, J., and Duan, C. (2002). Structural, biochemical, and expression analysis of two distinct insulin-like growth factor I receptors and their ligands in zebrafish. *Endocrinology* **143**, 1858–1871.
- McCormick, S. D. (1996). Effects of growth hormone and insulin-like growth factor I on salinity tolerance and gill Na⁺, K⁺-ATPase in Atlantic salmon (*Salmo salar*): Interaction with cortisol. *Gen. Comp. Endocrinol.* **101**, 3–11.
- McCormick, S. D., Sakamoto, T., Hasegawa, S., and Hirano, T. (1991). Osmoregulatory actions of insulin-like growth factor-I in rainbow trout (*Oncorhynchus mykiss*). *J. Endocrinol.* **130**, 87–92.
- McCormick, S. D., Kelley, K. M., Young, G., Nishioka, R. S., and Bern, H. A. (1992a). Stimulation of coho salmon growth by insulin-like growth factor I. *Gen. Comp. Endocrinol.* **86**, 398–406.
- McCormick, S. D., Tsai, P. I., Kelley, K. M., Nishioka, R. S., and Bern, H. A. (1992b). Hormonal control of sulfate uptake by branchial cartilage of coho salmon: Role of IGF-I. *J. Exp. Zool.* **262**, 166–171.
- McCormick, S. D., Shrimpton, J. M., Carey, J. B., O'Dea, M. F., Sloan, K. E., Moriyama, S., and Bjornsson, B. T. (1998). Repeated acute stress reduces growth rate of Atlantic salmon parr and alters plasma levels of growth hormone, insulin-like growth factor I and cortisol. *Aquaculture* **168**, 221–235.
- McRory, J. E., and Sherwood, N. M. (1994). Catfish express two forms of insulin-like growth factor-I (IGF-I) in the brain: Ubiquitous IGF-I and brain-specific IGF-I. *J. Biol. Chem.* **269**, 18588–18592.
- McRory, J. E., and Sherwood, N. M. (1997). Ancient divergence of insulin and insulin-like growth factor. *DNA Cell Biol.* **16**, 939–949.
- Mendez, E., Planas, J. V., Castillo, J., Navarro, I., and Gutierrez, J. (2001a). Identification of a type II insulin-like growth factor receptor in fish embryos. *Endocrinology* **142**, 1090–1097.
- Mendez, E., Smith, A., Figueiredo-Garutti, M. L., Planas, J. V., Navarro, I., and Gutierrez, J. (2001b). Receptors for insulin-like growth factor-I (IGF-I) predominate over insulin

- receptors in skeletal muscle throughout the life cycle of brown trout, *Salmo trutta*. *Gen. Comp. Endocrinol.* **122**, 148–157.
- Méton, I., Caseras, A., Canto, E., Fernandez, F., and Baanante, I. V. (2000). Liver insulin-like growth factor-I mRNA is not affected by diet composition or ration size but shows diurnal variations in regularly-fed gilthead sea bream (*Sparus aurata*). *J. Nutr.* **130**, 757–760.
- Mingarro, M., Vega-Rubin de Celis, S., Astola, A., Pendon, C., Valdivia, M. M., and Perez-Sanchez, J. (2002). Endocrine mediators of seasonal growth in gilthead sea bream (*Sparus aurata*): The growth hormone and somatolactin paradigm. *Gen. Comp. Endocrinol.* **128**, 102–111.
- Molina, F., Bouanani, M., Pau, B., and Granier, C. (1996). Characterization of the type-I repeat from thyroglobulin, a cysteine-rich module found in proteins from different families. *Eur. J. Biochem.* **240**, 125–133.
- Monget, P., Mazerbourg, S., Delpuech, T., Maurel, M. C., Maniere, S., Zapf, J., Lalmanach, G., Oxvig, C., and Overgaard, M. T. (2003). Pregnancy-associated plasma protein-A is involved in insulin-like growth factor binding protein-2 (IGFBP-2) proteolytic degradation in bovine and porcine preovulatory follicles: Identification of cleavage site and characterization of IGFBP-2 degradation. *Biol. Reprod.* **68**, 77–86.
- Moon, T. W., Castejon, C., Banos, N., Maestro, M. A., Plisetskaya, E. M., Gutierrez, J., and Navarro, I. (1996). Insulin and IGF-I binding in isolated trout cardiomyocytes. *Gen. Comp. Endocrinol.* **103**, 264–272.
- Moriyama, S. (1995). Increased plasma insulin-like growth factor-I (IGF-I) following oral and intraperitoneal administration of growth hormone to rainbow trout, *Oncorhynchus mykiss*. *Growth Regul.* **5**, 164–167.
- Moriyama, S., Duguay, S. J., Conlon, J. M., Duan, C., Dickhoff, W. W., and Plisetskaya, E. M. (1993). Recombinant coho salmon insulin-like growth factor I: Expression in *Escherichia coli*, purification and characterization. *Eur. J. Biochem.* **218**, 205–211.
- Moriyama, S., Swanson, P., Nishii, M., Takahashi, A., Kawauchi, H., Dickhoff, W. W., and Plisetskaya, E. M. (1994). Development of a homologous radioimmunoassay for coho salmon insulin-like growth factor-I. *Gen. Comp. Endocrinol.* **96**, 149–161.
- Moriyama, S., Shimma, H., Tagawa, M., and Kagawa, H. (1997a). Changes in plasma insulin-like growth factor-I levels in the precociously maturing amago salmon, *Oncorhynchus masou ishikawai*. *Fish Physiol. Biochem.* **17**, 253–259.
- Moriyama, S., Kagawa, H., Duan, C., Dickhoff, W. W., and Plisetskaya, E. M. (1997b). Characterization of two forms of recombinant insulin-like growth factor-I: Activities and complexing with insulin-like growth factor-I binding proteins. *Comp. Biochem. Physiol. C* **117**, 201–206.
- Moriyama, S., Ayson, F. G., and Kawauchi, H. (2000). Growth regulation by insulin-like growth factor-I in fish. *Biosci. Biotechnol. Biochem.* **64**, 1553–1562.
- Moxham, C. P., Duronio, V., and Jacobs, S. (1989). Insulin-like growth factor I receptor β -subunit heterogeneity: Evidence for hybrid tetramers composed of insulin-like growth factor I and insulin receptor heterodimers. *J. Biol. Chem.* **264**, 13238–13244.
- Nader, M. R., Miura, T., Ando, N., Miura, C., and Yamauchi, K. (1999). Recombinant human insulin-like growth factor I stimulates all stages of 11-ketotestosterone-induced spermatogenesis in the Japanese eel, *Anguilla japonica*, *in vitro*. *Biol. Reprod.* **61**, 944–947.
- Nadimpalli, S. K., Yerramalla, U. L., Hille-Rehfeld, A., and von Figura, K. (1999). Mannose 6-phosphate receptors (MPR 300 and MPR 46) from a teleostean fish (trout). *Comp. Biochem. Physiol. B* **123**, 261–265.
- Nagamatsu, S., Chan, S. J., Falkmer, S., and Steiner, D. F. (1991). Evolution of the insulin gene superfamily: Sequence of a preproinsulin-like growth factor cDNA from the Atlantic hagfish. *J. Biol. Chem.* **266**, 2397–2402.

- Nagasawa, H., Kataoka, H., Isogai, A., Tamura, S., Suzuki, A., Mizoguchi, A., Yuko, F., Suzuki, A., Takaha, S. Y., and Ishizaki, H. (1986). Amino acid sequence of a prothoracicotropic hormone of the silkworm *Bombyx mori*. *Proc. Natl. Acad. Sci. USA* **83**, 5840–5843.
- Nakae, J., Kido, Y., and Accili, D. (2001). Distinct and overlapping functions of insulin and IGF-I receptors. *Endocr. Rev.* **22**, 818–835.
- Nakao, N., Tanaka, M., Higashimoto, Y., and Nakashima, K. (2002). Molecular cloning, identification and characterization of four distinct receptor subtypes for insulin and IGF-I in Japanese flounder, *Paralichthys olivaceus*. *J. Endocrinol.* **173**, 365–375.
- Navarro, I., Leibush, B., Moon, T. W., Plisetskaya, E. M., Banos, N., Mendez, E., Planas, J. V., and Gutierrez, J. (1999). Insulin, insulin-like growth factor-I (IGF-I) and glucagon: The evolution of their receptors. *Comp. Biochem. Physiol. B* **122**, 137–153.
- Negatu, Z., and Meier, A. H. (1995). *In vitro* incorporation of [¹⁴C]glycine into muscle protein of gulf killifish (*Fundulus grandis*) in response to insulin-like growth factor-I. *Gen. Comp. Endocrinol.* **98**, 193–201.
- Negatu, Z., Hsiao, S. M., and Wallace, R. A. (1998). Effects of insulin-like growth factor-I on final oocyte maturation and steroid production in *Fundulus hereroclitus*. *Fish Physiol. Biochem.* **19**, 13–21.
- Ng, K. P., Datuin, J. P., and Bern, H. A. (2001). Effects of estrogens *in vitro* and *in vivo* on cartilage growth in the tilapia (*Oreochromis mossambicus*). *Gen. Comp. Endocrinol.* **121**, 295–304.
- Nilsson, C., Hultberg, B. M., and Gammeltoft, S. (1996). Autocrine role of insulin-like growth factor II secretion by the rat choroid plexus. *Eur. J. Neurosci.* **8**, 629–635.
- Niu, P. D., and Le Bail, P. Y. (1993). Presence of insulin-like growth factor binding protein (IGF-BP) in rainbow trout (*Oncorhynchus mykiss*) serum. *J. Exp. Zool.* **265**, 627–636.
- Niu, P. D., Perez-Sanchez, J., and Le Bail, P. Y. (1993). Development of a protein binding assay for teleost insulin-like growth factor (IGF)-like peptide: Relationship between growth hormone (GH) and IGF-like peptide in the blood of rainbow trout (*Oncorhynchus mykiss*). *Fish Physiol. Biochem.* **11**, 381–391.
- Oh, Y., Muller, H. L., Lamson, G., and Rosenfeld, R. G. (1993). Insulin-like growth factor (IGF)-independent action of IGF-binding protein-3 in Hs578T human breast cancer cells: Cell surface binding and growth inhibition. *J. Biol. Chem.* **268**, 14964–14971.
- Oh, Y., Nagalla, S. R., Yamanaka, Y., Kim, H. S., Wilson, E., and Rosenfeld, R. G. (1996). Synthesis and characterization of insulin-like growth factor-binding protein (IGFBP)-7: Recombinant human mac25 protein specifically binds IGF-I and -II. *J. Biol. Chem.* **271**, 30322–30325.
- Oka, Y., Rozek, L. M., and Czech, M. P. (1985). Direct demonstration of rapid insulin-like growth factor II receptor internalization and recycling in rat adipocytes: Insulin stimulates ¹²⁵I-insulin-like growth factor II degradation by modulating the IGF-II receptor recycling process. *J. Biol. Chem.* **260**, 9435–9442.
- Ooi, G. T., Orłowski, C. C., Brown, A. L., Becker, R. E., Unterman, T. G., and Rechler, M. M. (1990). Different tissue distribution and hormonal regulation of messenger RNAs encoding rat insulin-like growth factor-binding proteins-1 and -2. *Mol. Endocrinol.* **4**, 321–328.
- Orłowski, C. C., Brown, A. L., Ooi, G. T., Yang, Y. W., Tseng, L. Y., and Rechler, M. M. (1990). Tissue, developmental, and metabolic regulation of messenger ribonucleic acid encoding a rat insulin-like growth factor-binding protein. *Endocrinology* **126**, 644–652.
- Otteson, D. C., Cirenza, P. F., and Hitchcock, P. F. (2002). Persistent neurogenesis in the teleost retina: Evidence for regulation by the growth-hormone/insulin-like growth factor-I axis. *Mech. Dev.* **117**, 137–149.
- Palamarchuk, A., Gritsenko, O., Holthuizen, E., Sussenbach, J., Caelers, A., Reinecke, M., and Kavsan, V. (2002). Complete nucleotide sequence of the chum salmon insulin-like growth factor II gene. *Gene* **295**, 223–230.

- Park, R., Shepherd, B. S., Nishioka, R. S., Grau, E. G., and Bern, H. A. (2000). Effects of homologous pituitary hormone treatment on serum insulin-like growth factor binding proteins (IGFBPs) in hypophysectomized tilapia, *Oreochromis mossambicus*, with special reference to a novel 20-kDa IGFBP. *Gen. Comp. Endocrinol.* **117**, 404–412.
- Parrizas, M., Plisetskaya, E. M., Planas, J., and Gutierrez, J. (1995a). Abundant insulin-like growth factor-1 (IGF-1) receptor binding in fish skeletal muscle. *Gen. Comp. Endocrinol.* **98**, 16–25.
- Parrizas, M., Maestro, M. A., Banos, N., Navarro, I., Planas, J., and Gutierrez, J. (1995b). Insulin/IGF-I binding ratio in skeletal and cardiac muscles of vertebrates: A phylogenetic approach. *Am. J. Physiol.* **269**, R1370–R1377.
- Patiño, R., and Kagawa, H. (1999). Regulation of gap junctions and oocyte maturational competence by gonadotropin and insulin-like growth factor-I in ovarian follicles of red seabream. *Gen. Comp. Endocrinol.* **115**, 454–462.
- Perez-Sanchez, J., Weil, C., and Le Bail, P. Y. (1992). Effects of human insulin-like growth factor-I on release of growth hormone by rainbow trout (*Oncorhynchus mykiss*) pituitary cells. *J. Exp. Zool.* **262**, 287–290.
- Perez-Sanchez, J., Marti-Palanca, H., and Le Bail, P. Y. (1994). Seasonal changes in circulating growth hormone (GH), hepatic GH-binding and plasma immunoreactivity in a marine fish, gilthead seabream, *Sparus aurata*. *Fish Physiol. Biochem.* **13**, 199–208.
- Perez-Sanchez, J., Marti-Palanca, H., and Kaushik, S. J. (1995). Ration size and protein intake affect circulating growth hormone concentration, hepatic growth hormone binding and plasma insulin-like growth factor-I immunoreactivity in a marine teleost, the gilthead sea bream (*Sparus aurata*). *J. Nutr.* **125**, 546–552.
- Perrot, V., Moiseeva, E. B., Gozes, Y., Chan, S. J., Ingleton, P., and Funkenstein, B. (1999). Ontogeny of the insulin-like growth factor system (IGF-I, IGF-II, and IGF-1R) in gilthead seabream (*Sparus aurata*): Expression and cellular localization. *Gen. Comp. Endocrinol.* **116**, 445–460.
- Perrot, V., Moiseeva, E. B., Gozes, Y., Chan, S. J., and Funkenstein, B. (2000). Insulin-like growth factor receptors and their ligands in gonads of a hermaphroditic species, the gilthead seabream (*Sparus aurata*): Expression and cellular localization. *Biol. Reprod.* **63**, 229–241.
- Peterson, B. C., and Small, B. C. (2004). Effects of fasting on circulating IGF-binding proteins, glucose, and cortisol in channel catfish (*Ictalurus punctatus*). *Domest. Anim. Endocrinol.* **26**, 231–240.
- Pierce, A. L., Beckman, B. R., Shearer, K. D., Larsen, D. A., and Dickhoff, W. W. (2001a). Effects of ration on somatotrophic hormones and growth in coho salmon. *Comp. Biochem. Physiol. B* **128**, 255–264.
- Pierce, A. L., Dickey, J. T., Larsen, D. A., Fukada, H., Swanson, P., and Dickhoff, W. W. (2004). A quantitative real-time RT-PCR assay for salmon IGF-I mRNA, and its application in the study of GH regulation of IGF-I gene expression in primary culture of salmon hepatocytes. *Gen. Comp. Endocrinol.* **135**, 401–411.
- Pierce, S. B., Costa, M., Wisotzkey, R., Devadhar, S., Homburger, S. A., Buchman, A. R., Ferguson, K. C., Heller, J., Platt, D. M., Pasquinelli, A. A., Liu, L. X., Doberstein, S. K., and Ruvkun, G. (2001b). Regulation of DAF-2 signaling by human insulin and *ins-1*, a member of the unusually large and diverse *C. elegans* insulin gene family. *Genes Dev.* **15**, 672–686.
- Pierson, R. W. J., and Temin, H. M. (1972). The partial purification from calf serum of a fraction with multiplication-stimulating activity for chicken fibroblasts in cell culture and with non-suppressible insulin-like activity. *J. Cell Physiol.* **79**, 319–330.
- Plisetskaya, E. M. (1998). Some of my not so favorite things about insulin and insulin-like growth factors in fish. *Comp. Biochem. Physiol. B* **121**, 3–11.
- Plisetskaya, E. M., and Duan, C. (1994). Insulin and insulin-like growth factor I in coho salmon *Oncorhynchus kisutch* injected with streptozotocin. *Am. J. Physiol.* **267**, R1408–R1412.

- Plisetzkaya, E. M., Bondareva, V. M., Duan, C., and Duguay, S. J. (1993). Does salmon brain produce insulin? *Gen. Comp. Endocrinol.* **91**, 74–80.
- Pozios, K. C., Ding, J., Degger, B., Upton, Z., and Duan, C. (2001). IGFs stimulate zebrafish cell proliferation by activating MAP kinase and PI3-kinase-signaling pathways. *Am. J. Physiol.* **280**, R1230–R1239.
- Radaelli, G., Patruno, M., Maccatrozzo, L., and Funkenstein, B. (2003a). Expression and cellular localization of insulin-like growth factor-II protein and mRNA in *Sparus aurata* during development. *J. Endocrinol.* **178**, 285–299.
- Radaelli, G., Domeneghini, C., Arrighi, S., Bosi, G., Patruno, M., and Funkenstein, B. (2003b). Localization of IGF-I, IGF-I receptor, and IGFBP-2 in developing *Umbrina cirrosa* (Pisces: Osteichthyes). *Gen. Comp. Endocrinol.* **130**, 232–244.
- Reinecke, M., and Collet, C. (1998). The phylogeny of the insulin-like growth factors. *Int. Rev. Cytol.* **183**, 1–94.
- Reinecke, M., Drakenberg, K., Falkmer, S., and Sara, V. R. (1991). Presence of IGF-1-like peptides in the neuroendocrine system of the Atlantic hagfish, *Myxine glutinosa* (Cyclostomata): Evidence derived by chromatography, radioimmunoassay and immunohistochemistry. *Histochemistry* **96**, 191–196.
- Reinecke, M., Drakenberg, K., Falkmer, S., and Sara, V. R. (1992). Peptides related to insulin-like growth factor 1 in the gastro-entero-pancreatic system of bony and cartilaginous fish. *Regul. Pept.* **37**, 155–165.
- Reinecke, M., Maake, C., Falkmer, S., and Sara, V. R. (1993). The branching of insulin-like growth factor-I and insulin: An immunohistochemical analysis during phylogeny. *Regul. Pept.* **48**, 65–76.
- Reinecke, M., Broger, I., Brun, R., Zapf, J., and Maake, C. (1995). Immunohistochemical localization of insulin-like growth factor I and II in the endocrine pancreas of birds, reptiles, and amphibia. *Gen. Comp. Endocrinol.* **100**, 385–396.
- Reinecke, M., Schmid, A., Ermatinger, R., and Loffing-Cueni, D. (1997). Insulin-like growth factor I in the teleost *Oreochromis mossambicus*, the tilapia: Gene sequence, tissue expression, and cellular localization. *Endocrinology* **138**, 3613–3619.
- Reinecke, M., Eppler, E., David, I., and Georges, D. (1999). Immunohistochemical evidence for the presence, localization and partial coexistence of insulin, insulin-like growth factor I and relaxin in the protochordate *Ciona intestinalis*. *Cell Tissue Res.* **295**, 331–338.
- Riley, L. G., Hirano, T., and Grau, E. G. (2002a). Disparate effects of gonadal steroid hormones on plasma and liver mRNA levels of insulin-like growth factor-I and vitellogenin in the tilapia, *Oreochromis mossambicus*. *Fish Physiol. Biochem.* **26**, 223–230.
- Riley, L. G., Richman, N. H., III, Hirano, T., and Grau, E. G. (2002b). Activation of the growth hormone/insulin-like growth factor axis by treatment with 17 α -methyltestosterone and seawater rearing in the tilapia, *Oreochromis mossambicus*. *Gen. Comp. Endocrinol.* **127**, 285–292.
- Riley, L. G., Hirano, T., and Grau, E. G. (2003). Effects of transfer from seawater to fresh water on the growth hormone/insulin-like growth factor-I axis and prolactin in the tilapia, *Oreochromis mossambicus*. *Comp. Biochem. Physiol. B* **136**, 647–655.
- Rinderknecht, E., and Humbel, R. E. (1978a). Primary structure of human insulin-like growth factor II. *FEBS Lett.* **89**, 283–286.
- Rinderknecht, E., and Humbel, R. E. (1978b). The amino acid sequence of human insulin-like growth factor I and its structural homology with proinsulin. *J. Biol. Chem.* **253**, 2769–2776.
- Rotwein, P. (1991). Structure, evolution, expression and regulation of insulin-like growth factors I and II. *Growth Factors* **5**, 3–18.
- Saint-Amant, L., and Drapeau, P. (1998). Time course of the development of motor behaviors in the zebrafish embryo. *J. Neurobiol.* **37**, 622–632.

- Sakamoto, T., and Hirano, T. (1993). Expression of insulin-like growth factor I gene in osmoregulatory organs during seawater adaptation of the salmonid fish: Possible mode of osmoregulatory action of growth hormone. *Proc. Natl. Acad. Sci. USA* **90**, 1912–1916.
- Sakamoto, T., Hirano, T., Madsen, S. S., Nishioka, R. S., and Bern, H. A. (1995). Insulin-like growth factor I gene expression during parr-smolt transformation of coho salmon. *Zool. Sci.* **12**, 249–252.
- Sakamoto, T., Shepherd, B. S., Madsen, S. S., Nishioka, R. S., Siharath, K., Richman, N. H. R., Bern, H. A., and Grau, E. G. (1997). Osmoregulatory actions of growth hormone and prolactin in an advanced teleost. *Gen. Comp. Endocrinol.* **106**, 95–101.
- Salmon, W. D., Jr., and Daughaday, W. H. (1957). A hormonally controlled serum factor which stimulates sulfate incorporation by cartilage *in vitro*. *J. Lab. Clin. Med.* **49**, 825–836.
- Salmon, W. D., Jr., and DuVall, M. R. (1970a). A serum fraction with “sulfation factor activity” stimulates *in vitro* incorporation of leucine and sulfate into protein-polysaccharide complexes, uridine into RNA, and thymidine into DNA of costal cartilage from hypophysectomized rats *Endocrinology* **86**, 721–727.
- Salmon, W. D., Jr., and DuVall, M. R. (1970b). *In vitro* stimulation of leucine incorporation into muscle and cartilage protein by a serum fraction with sulfation factor activity: Differentiation of effects from those of growth hormone and insulin. *Endocrinology* **87**, 1168–1180.
- Scavo, L., Alemany, J., Roth, J., and de Pablo, F. (1989). Insulin-like growth factor I activity is stored in the yolk of the avian egg. *Biochem. Biophys. Res. Commun.* **162**, 1167–1173.
- Scavo, L., Shuldiner, A. R., Serrano, J., Dashner, R., Roth, J., and de Pablo, F. (1991). Genes encoding receptors for insulin and insulin-like growth factor I are expressed in *Xenopus* oocytes and embryos. *Proc. Natl. Acad. Sci. USA* **88**, 6214–6218.
- Schlueter, P. J., Li, Y., Royer, T., Laser, B., Chan, S. J., Steiner, D. F., and Duan, C. (2003). Targeted knock-down of the two zebrafish IGF-I receptor genes reveals novel functions for IGF signaling in organ development. The Endocrine Society Annual Meeting, Philadelphia, PA, June 19–22, pp. 3–365 (Abstract).
- Schmid, A. C., Naf, E., Kloas, W., and Reinecke, M. (1999). Insulin-like growth factor-I and -II in the ovary of a bony fish, *Oreochromis mossambicus*, the tilapia: *In situ* hybridisation, immunohistochemical localisation, Northern blot and cDNA sequences. *Mol. Cell Endocrinol.* **156**, 141–149.
- Schmid, A. C., Lutz, I., Kloas, W., and Reinecke, M. (2003). Thyroid hormone stimulates hepatic IGF-I mRNA expression in a bony fish, the tilapia *Oreochromis mossambicus*, *in vitro* and *in vivo*. *Gen. Comp. Endocrinol.* **130**, 129–134.
- Shamblott, M. J., and Chen, T. T. (1992). Identification of a second insulin-like growth factor in a fish species. *Proc. Natl. Acad. Sci. USA* **89**, 8913–8917.
- Shamblott, M. J., and Chen, T. T. (1993). Age-related and tissue-specific levels of five forms of insulin-like growth factor mRNA in a teleost. *Mol. Mar. Biol. Biotechnol.* **2**, 351–361.
- Shamblott, M. J., Cheng, C. M., Bolt, D., and Chen, T. T. (1995). Appearance of insulin-like growth factor mRNA in the liver and pyloric ceca of a teleost in response to exogenous growth hormone. *Proc. Natl. Acad. Sci. USA* **92**, 6943–6946.
- Shapiro, B., and Pimstone, B. L. (1977). A phylogenetic study of sulphation factor activity in 26 species. *J. Endocrinol.* **74**, 129–135.
- Shepherd, B. S., Sakamoto, T., Nishioka, R. S., Richman, N. H., III, Mori, I., Madsen, S. S., Chen, T. T., Hirano, T., Bern, H. A., and Grau, E. G. (1997). Somatotropic actions of the homologous growth hormone and prolactins in the euryhaline teleost, the tilapia, *Oreochromis mossambicus*. *Proc. Natl. Acad. Sci. USA* **94**, 2068–2072.
- Shimizu, M., Swanson, P., and Dickhoff, W. W. (1999). Free and protein-bound insulin-like growth factor-I (IGF-I) and IGF-binding proteins in plasma of coho salmon, *Oncorhynchus kisutch*. *Gen. Comp. Endocrinol.* **115**, 398–405.

- Shimizu, M., Hara, A., and Dickhoff, W. W. (2003a). Development of an RIA for salmon 41 kDa IGF-binding protein. *J. Endocrinol.* **178**, 275–283.
- Shimizu, M., Swanson, P., Hara, A., and Dickhoff, W. W. (2003b). Purification of a 41-kDa insulin-like growth factor binding protein from serum of chinook salmon, *Oncorhynchus tshawytscha*. *Gen. Comp. Endocrinol.* **132**, 103–111.
- Shuldinger, A. R., Nirula, A., Scott, L. A., and Roth, J. (1990). Evidence that *Xenopus laevis* contains two different nonallelic insulin-like growth factor I genes. *Biochem. Biophys. Res. Commun.* **166**, 223–230.
- Siharath, K., and Bern, H. A. (1993). The physiology of insulin-like growth factor (IGF) and its binding proteins in teleost fishes. *Proc. Zool. Soc. Calcutta Haldane Commem.* **3**, 113–124.
- Siharath, K., Nishioka, R. S., and Bern, H. A. (1995a). *In vitro* production of IGF-binding proteins (IGFBP) by various organs of the striped bass, *Morone saxatilis*. *Aquaculture* **135**, 195–202.
- Siharath, K., Nishioka, R. S., Madsen, S. S., and Bern, H. A. (1995b). Regulation of IGF-binding proteins by growth hormone in the striped bass, *Morone saxatilis*. *Mol. Mar. Biol. Biotechnol.* **4**, 171–178.
- Siharath, K., Kelley, K. M., and Bern, H. A. (1996). A low-molecular-weight (25-kDa) IGF-binding protein is increased with growth inhibition in the fasting striped bass, *Morone saxatilis*. *Gen. Comp. Endocrinol.* **102**, 307–316.
- Skorokhod, A., Gamulin, V., Gundacker, D., Kavsan, V., Muller, I. M., and Muller, W. E. G. (1999). Origin of insulin receptor-like tyrosine kinases in marine sponges. *Biol. Bull.* **197**, 198–205.
- Skyrud, T., Andersen, O., Alestrom, P., and Gautvik, K. M. (1989). Effects of recombinant human growth hormone and insulin-like growth factor 1 on body growth and blood metabolites in brook trout (*Salvelinus fontinalis*). *Gen. Comp. Endocrinol.* **75**, 247–255.
- Smit, A., Vreugdenhil, E., Ebberink, R., Geraerts, W., Klootwijk, J., and Joosse, J. (1988). Growth controlling molluscan neurons produce the precursor of an insulin-related peptide. *Nature* **331**, 335–338.
- Soos, M. A., Field, C. E., and Siddle, K. (1993). Purified hybrid insulin/insulin-like growth factor-I receptors bind insulin-like growth factor-I, but not insulin, with high affinity. *Biochem. J.* **290**, 419–426.
- Srivastava, R. K., and Van Der Kraak, G. (1994). Regulation of DNA synthesis in goldfish vitellogenic ovarian follicles by hormones and growth factors. *J. Exp. Zool.* **270**, 263–272.
- Srivastava, R. K., and Van Der Kraak, G. (1995). Multifactorial regulation of DNA synthesis in goldfish ovarian follicles. *Gen. Comp. Endocrinol.* **100**, 397–403.
- Stahlbom, A. K., Sara, V. R., and Hoeben, P. (1999). Insulin-like growth factor mRNA in barramundi (*Lates calcarifer*): Alternative splicing and nonresponsiveness to growth hormone. *Biochem. Genet.* **37**, 69–93.
- Sumpter, J. P., Le Bail, P. Y., Pickering, A. D., Pottinger, T. G., and Carragher, J. F. (1991). The effect of starvation on growth and plasma growth hormone concentrations of rainbow trout, *Oncorhynchus mykiss*. *Gen. Comp. Endocrinol.* **83**, 94–102.
- Takagi, Y., and Björnsson, B. T. (1996). Regulation of cartilage glycosaminoglycan synthesis in the rainbow trout, *Oncorhynchus mykiss*, by 3,3',5-tri-iodo-L-thyronine and IGF-I. *J. Endocrinol.* **149**, 357–365.
- Tanaka, M., Taniguchi, T., Yamamoto, I., Sakaguchi, K., Yoshizato, H., Ohkubo, T., and Nakashima, K. (1998). Gene and cDNA structures of flounder insulin-like growth factor-I (IGF-I): Multiple mRNA species encode a single short mature IGF-I. *DNA Cell Biol.* **17**, 859–868.
- Tao, W. J., and Boulding, E. G. (2003). Associations between single nucleotide polymorphisms in candidate genes and growth rate in Arctic charr (*Salvelinus alpinus* L.). *Heredity* **91**, 60–69.

- Temin, H. M. (1967). Studies on carcinogenesis by avian sarcoma viruses. VI. Differential multiplication of uninfected and of converted cells in response to insulin. *J. Cell. Physiol.* **69**, 377–384.
- Thissen, J. P., Ketelslegers, J. M., and Underwood, L. E. (1994). Nutritional regulation of the insulin-like growth factors. *Endocr. Rev.* **15**, 80–101.
- Thomas, P., Pinter, J., and Das, S. (2001). Upregulation of the maturation-inducing steroid membrane receptor in spotted seatrout ovaries by gonadotropin during oocyte maturation and its physiological significance. *Biol. Reprod.* **64**, 21–29.
- Tian, X. C., Chen, M. J., Pantschenko, A. G., Yang, T. J., and Chen, T. T. (1999). Recombinant E-peptides of pro-IGF-I have mitogenic activity. *Endocrinology* **140**, 3387–3390.
- Tong, P. Y., Tollefsen, S. E., and Kornfeld, S. (1988). The cation-independent mannose 6-phosphate receptor binds insulin-like growth factor II. *J. Biol. Chem.* **263**, 2585–2588.
- Tsai, P. I., Madsen, S. S., McCormick, S. D., and Bern, H. A. (1994). Endocrine control of cartilage growth in coho salmon: GH influence *in vivo* on the response to IGF-I *in vitro*. *Zool. Sci.* **11**, 299–303.
- Tse, M. C., Vong, Q. P., Cheng, C. H., and Chan, K. M. (2002). PCR-cloning and gene expression studies in common carp (*Cyprinus carpio*) insulin-like growth factor-II. *Biochim. Biophys. Acta* **1575**, 63–74.
- Twigg, S. M., Kiefer, M. C., Zapf, J., and Baxter, R. C. (1998). Insulin-like growth factor binding protein-5 complexes with the acid-labile subunit: Role of the carboxyl-terminal domain. *J. Biol. Chem.* **273**, 28791–28798.
- Uchida, K., Kajimura, S., Riley, L. G., Hirano, T., Aida, K., and Grau, E. G. (2003). Effects of fasting on growth hormone/insulin-like growth factor I axis in the tilapia, *Oreochromis mossambicus*. *Comp. Biochem. Physiol. A* **134**, 429–439.
- Underwood, L. E., Hintz, R. L., Voina, S. J., and Van Wyk, J. J. (1972). Human somatomedin, the growth hormone dependent sulfation factor, is antilipolytic. *J. Clin. Endocrinol. Metab.* **35**, 194–198.
- Upton, Z., Chan, S. J., Steiner, D. F., Wallace, J. C., and Ballard, F. J. (1993). Evolution of insulin-like growth factor binding proteins. *Growth Regul.* **3**, 29–32.
- Upton, Z., Francis, G. L., Chan, S. J., Steiner, D. F., Wallace, J. C., and Ballard, F. J. (1997). Evolution of insulin-like growth factor (IGF) function: Production and characterization of recombinant hagfish IGF. *Gen. Comp. Endocrinol.* **105**, 79–90.
- Upton, Z., Yandell, C. A., Degger, B. G., Chan, S. J., Moriyama, S., Francis, G. L., and Ballard, F. J. (1998). Evolution of insulin-like growth factor-I (IGF-I) action: *In vitro* characterization of vertebrate IGF-I proteins. *Comp. Biochem. Physiol. B* **121**, 35–41.
- Van Wyk, J. J., Underwood, L. E., Hintz, R. L., Clemmons, D. R., Voina, S. J., and Weaver, R. P. (1974). The somatomedins: A family of insulinlike hormones under growth hormone control. *Recent Prog. Horm. Res.* **30**, 259–318.
- Vong, Q. P., Chan, K. M., and Cheng, C. H. (2003). Quantification of common carp (*Cyprinus carpio*) IGF-I and IGF-II mRNA by real-time PCR: Differential regulation of expression by GH. *J. Endocrinol.* **178**, 513–521.
- von Horn, H., Ekstrom, C., Ellis, E., Olivecrona, H., Einarsson, C., Tally, M., and Ekstrom, T. J. (2002). GH is a regulator of IGF2 promoter-specific transcription in human liver. *J. Endocrinol.* **172**, 457–465.
- Wallis, A. E., and Devlin, R. H. (1993). Duplicate insulin-like growth factor-I genes in salmon display alternative splicing pathways. *Mol. Endocrinol.* **7**, 409–422.
- Wandji, S. A., Wood, T. L., Crawford, J., Levison, S. W., and Hammond, J. M. (1998). Expression of mouse ovarian insulin growth factor system components during follicular development and atresia. *Endocrinology* **139**, 5205–5214.

- Weber, G. M., and Sullivan, C. V. (2000). Effects of insulin-like growth factor-I on *in vitro* final oocyte maturation and ovarian steroidogenesis in striped bass, *Morone saxatilis*. *Biol. Reprod.* **63**, 1049–1057.
- Weil, C., Carré, F., Blaise, O., Breton, B., and Le Bail, P. Y. (1999). Differential effect of insulin-like growth factor I on *in vitro* gonadotropin (I and II) and growth hormone secretions in rainbow trout (*Oncorhynchus mykiss*) at different stages of the reproductive cycle. *Endocrinology* **140**, 2054–2062.
- Wilkinson, R. J., Elliott, P., Carragher, J. F., and Francis, G. (2004). Expression, purification, and *in vitro* characterization of recombinant salmon insulin-like growth factor-II. *Protein Expr. Purif.* **35**, 334–343.
- Wilson, D. M., and Hintz, R. L. (1982). Inter-species comparison of somatomedin structure using immunological probes. *J. Endocrinol.* **95**, 59–64.
- Wood, A. W., and Duan, C. (2004). Targeted gene knockdown reveals an important role for insulin-like growth factor binding protein-2 in zebrafish embryonic development. Society for Integrative and Comparative Biology Annual Meeting, New Orleans, LA, OR55-3 (Abstract).
- Wood, A. W., Matsumoto, J. A., and Van Der Kraak, G. (2004). Thyroglobulin type-I domain protease inhibitors exhibit specific expression in the cortical ooplasm of vitellogenic rainbow trout oocytes. *Mol. Reprod. Dev.* **69**, 205–214.
- Wood, T. L., Rogler, L. E., Czick, M. E., Schuller, A. G., and Pintar, J. E. (2000). Selective alterations in organ sizes in mice with a targeted disruption of the insulin-like growth factor binding protein-2 gene. *Mol. Endocrinol.* **14**, 1472–1482.
- Woods, K. A., Camacho-Hubner, C., Savage, M. O., and Clark, A. J. (1996). Intrauterine growth retardation and postnatal growth failure associated with deletion of the insulin-like growth factor I gene. *N. Engl. J. Med.* **335**, 1363–1367.
- Xu, Q., Li, S., Zhao, Y., Maures, T. J., Yin, P., and Duan, C. (2004). Evidence that IGF-binding protein-5 functions as a ligand-independent transcriptional regulator in vascular smooth muscle cells. *Circ. Res.* **94**, E46–E54.
- Yakar, S., Liu, J. L., Stannard, B., Butler, A., Accili, D., Sauer, B., and LeRoith, D. (1999). Normal growth and development in the absence of hepatic insulin-like growth factor I. *Proc. Natl. Acad. Sci. USA* **96**, 7324–7329.
- Yang, Y. W., Robbins, A. R., Nissley, S. P., and Rechler, M. M. (1991). The chick embryo fibroblast cation-independent mannose 6-phosphate receptor is functional and immunologically related to the mammalian insulin-like growth factor-II (IGF-II)/man 6-P receptor but does not bind IGF-II. *Endocrinology* **128**, 1177–1189.
- Yao, K., Niu, P. D., Le Gac, F., and Le Bail, P. Y. (1991). Presence of specific growth hormone binding sites in rainbow trout (*Oncorhynchus mykiss*) tissues: Characterization of the hepatic receptor. *Gen. Comp. Endocrinol.* **81**, 72–82.
- Yerramalla, U. L., Nadimpalli, S. K., Schu, P., von Figura, K., and Hille-Rehfeld, A. (2000). Conserved cassette structure of vertebrate M_r 300kDa mannose 6-phosphate receptors: Partial cDNA sequence of fish MPR 300. *Comp. Biochem. Physiol. B* **127**, 433–441.
- Zapf, J., Schoenle, E., and Froesch, E. R. (1978). Insulin-like growth factors I and II: Some biological actions and receptor binding characteristics of two purified constituents of nonsuppressible insulin-like activity of human serum. *Eur. J. Biochem.* **87**, 285–296.

Cell Biology of Cardiac Cushion Development

Anthony D. Person,* Scott E. Klewer,*[†] and Raymond B. Runyan*

*Department of Cell Biology and Anatomy, University of Arizona School of Medicine, Tucson, Arizona 85724

[†]Department of Pediatrics, University of Arizona School of Medicine, Tucson, Arizona 85724

The valves of the heart develop in the embryo from precursor structures called endocardial cushions. After cardiac looping, endocardial cushion swellings form and become populated by valve precursor cells formed by an epithelial–mesenchymal transition (EMT). Endocardial cushions subsequently undergo directed growth and remodeling to form the valvular structures and the membranous septa of the mature heart. The developmental processes that mediate cushion formation include many prototypic cellular actions including adhesion, signaling, migration, secretion, replication, differentiation, and apoptosis. Cushion morphogenesis is unique in that these cellular processes occur in a functioning organ where the cushions act as valves even while developing into definitive valvular structures. Cardiovascular defects are the most common congenital defects, and one of the most common causes of death during infancy. Thus, there is significant interest in understanding the mechanisms that underlie this complex developmental process. In this regard, substantial progress has been made by incorporating an understanding of cardiac morphology and cell biology with the rapidly expanding repertoire of molecular mechanisms gained through human genetics and research using animal models. This article reviews cardiac morphogenesis as it relates to heart valve formation and highlights selected growth factors, intracellular signaling mediators, and extracellular matrix components involved in the creation and remodeling of endocardial cushions into mature cardiac structures.

KEY WORDS: Cell invasion, Transforming growth factor β , β -Catenin, BMP, Wnt, ErbB3, Notch, Extracellular matrix. © 2005 Elsevier Inc.

I. Introduction

The developing vertebrate heart arises from a complex set of events in the early embryo that ultimately lead to formation of a muscular four-chambered pump. The heart is the first organ to function in developing embryos and its viability is critical to subsequent organogenesis and embryogenesis. The early-stage straight heart tube consists of an outer myocardial layer and an inner endocardial cell layer. After initial heart tube formation, localized secretion of extracellular matrix by the myocardium distends the endocardium into the lumen, forming endocardial cushions. Endocardial cushions form in both the atrioventricular canal and outflow regions of the primitive tubular heart. Endocardial cushions subsequently undergo differentiation, growth, and extensive remodeling to form the mature mitral, tricuspid, aortic, and pulmonary valves in addition to forming the atrioventricular and outflow septa. Congenital heart defects are a leading cause of human birth defects, occurring in 1 in 100 live births (Hoffman, 1990), with valve and septal defects accounting for a majority these defects (Samanek *et al.*, 1989). Our understanding of cardiac valve formation has progressed from morphological descriptions to dissection of many cellular and molecular mechanisms governing these events.

II. Cardiac Morphology and Cell Biology

A. Tubular Heart Formation

Early specification of heart cell precursors has received much attention. Fate-mapping studies in the developing chicken show that epiblast cells in the anterior primitive streak at Hamburger and Hamilton (HH) stage 3 (Hamburger and Hamilton, 1951) include heart progenitors (Garcia-Martinez and Schoenwolf, 1993). The heart-forming primordia within the primitive streak involute and migrate cranially and laterally to form bilateral heart fields (the cardiac crescent) within the lateral plate mesoderm. Lineage-tracing studies in HH stage 3 chickens reveal that cells in the rostral third of the primitive streak, excluding Hensen's node, contribute to the anterior-most segments of the mature heart (right ventricle and proximal outflow tract). Cells in the caudal primitive streak contribute to the caudal inlet segments of the heart (sinus venosus and atrium) (Garcia-Martinez and Schoenwolf, 1993). At HH stage 5, cells isolated from the precardiac mesoderm can differentiate into cardiac muscle and therefore appear specified to form cardiac myocytes (Antin *et al.*, 1994; Gannon and Bader, 1995;

Gonzalez-Sanchez and Bader, 1990; Montgomery *et al.*, 1994). At HH stage 7, cardiac progenitors are present in the splanchnic mesoderm directly above the primitive foregut endoderm. At this time, a population of endocardial precursors is detectable as distinct from the premyocardium. It is currently not known whether splanchnic mesoderm differentiates into both endocardial and myocardial cells, or whether these cardiac lineages arise from separate progenitors specified earlier during development (Mikawa, 1999).

Beginning at HH stage 8 in the chick, embryonic folding brings the splanchnic mesoderm together at the midline in a rostral-to-caudal fashion. Fusion of the primitive heart and visible contractions occur by HH stage 10. The functional heart tube at stage 10 consists of an outer myocardial cell layer and an inner endocardial cell layer (Fig. 1A). Between the two cell layers is an extracellular matrix layer, called the cardiac jelly. At HH stage 12, the primary linear heart tube begins to loop to the right, at which time the external surface of the heart exhibits minor constrictions that demarcate a series of primitive cardiac segments (Fig. 1B). The cardiac segments from caudal to rostral are as follows: the sinus venosus, atrium, left ventricle, and right ventricle. The primitive atrium forms from contributions of cells from the sinus venosus, whereas the conus forms from a mesodermal secondary heart field directly dorsal to the primitive heart tube (Mjaatvedt *et al.*, 2001). The secondary heart field is a population of mesodermal cells that contribute to the outflow region of the heart after the inflow and ventricular segments of the primary heart tube have already formed (Kelly *et al.*, 2001; Mjaatvedt *et al.*, 2001; Waldo *et al.*, 2001).

B. Cardiac Cushion Formation

Localized enhanced production of cardiac jelly is observed just after the linear heart tube begins to loop. This expansion, occurring at the junctions between the atrium and left ventricle and in the outflow tract, is mediated by a poorly understood but regulated secretion of extracellular matrix (ECM) components by myocardial cells (Fig. 1C). Pulse-chase radioactive labeling showed that 95% of the ECM in the cushions is secreted by the myocardium (Krug *et al.*, 1985). Early studies investigating the composition of cardiac jelly components reported secretion of both chondroitin sulfate and hyaluronan from the myocardium (Manasek *et al.*, 1970, 1973). These glycosaminoglycans are highly charged hydrophilic molecules thought to promote swelling of the acellular space, aiding in the formation of endocardial cushions (Manasek *et al.*, 1975; Markwald *et al.*, 1972, 1977). Gene inactivation of either hyaluronan synthetase 2 (Has-2) or versican in mouse embryos results in hearts lacking endocardial cushions (Camenisch *et al.*, 2000; Mjaatvedt *et al.*, 1998; Yamamura *et al.*, 1997). These genetic models provide

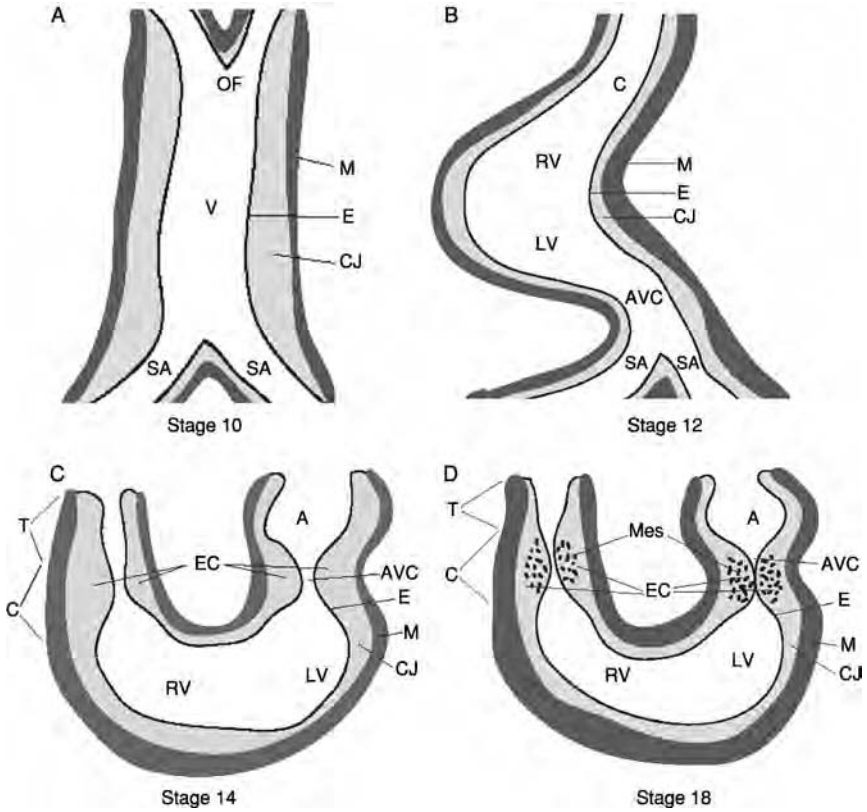


FIG. 1 Early endocardial cushion development. (A) At HH stage 10 the heart is a tubular structure with an outer myocardial cell layer (*M*) and a luminal endocardial cell layer (*E*) separated by an extracellular matrix layer called the cardiac jelly (*CJ*). At stage 10, the heart consists of the sinus arteriosus (*SA*), the primitive ventricle (*V*), and the outflow (*OF*) region. (B) The beginning of looping creates constrictions in HH stage 12 hearts, resulting in the initial formation of primitive chambers. The atrioventricular canal (*AVC*), left ventricle (*LV*), right ventricle (*RV*), and conus (*C*) become evident at HH stage 12. (C) Continued looping of the heart brings the atrium in proximity to the outflow tract at HH stage 14. At the *AVC* and conus, secretion of extracellular matrix from the myocardium displaces the endocardium away from the myocardium, creating endocardial cushions (*EC*). At HH stage 14 endothelial–mesenchyma transition (EMT) inductive signals begin to be secreted from the myocardium. (D) By HH stage 18 epithelial cells in both the AV cushions and conal cushions are undergoing EMT to create mesenchymal cells (*Mes*) that migrate into endocardial cushions. *T*, truncus arteriosus. (See also color insert.)

direct evidence that secretion of both hyaluronan and the chondroitin sulfate proteoglycan versican is essential for initial cardiac cushion formation.

Questions remain about the regulation of ECM production in endocardial cushions. Growth factors such as bone morphogenetic protein 2 (BMP-2)

and Wnt-6 are expressed specifically in the myocardium of cushion-forming regions (Lyons *et al.*, 1990; Schubert *et al.*, 2002). Zebrafish adenomatous polyposis coli (APC) mutants with hyperactive β -catenin also show expanded cardiac cushion expression domains of both Has-2 and versican. It is possible that either Wnt-6 or BMP-2 could regulate enhanced myocardial secretion of hyaluronan and Versican and thus expansion of the endocardial cushions, although this has not been directly tested.

After cushion formation, mesenchymal cells were observed in the endocardial cushions at HH stage 17–18 chickens (Figs. 1D and 2B) (Chang, 1932; Patten *et al.*, 1948). Different theories were proposed to explain the origin of this cell population. Some argued that cardiac cushion mesenchyme originated from the myocardial cell layer (Chang, 1932), whereas others believed cardiac cushion mesenchyme originated from the endocardium (Patten *et al.*, 1948). Pioneering work using video microscopy of atrioventricular (AV) canals in culture definitively showed that the mesenchymal cells originated from the endocardial cell layer by an epithelial–mesenchymal transition (EMT) (Kinsella and Fitzharris, 1980).

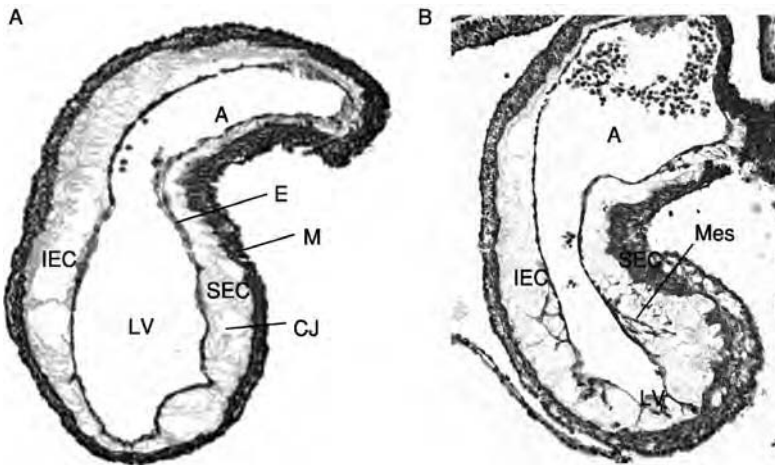


FIG. 2 Initiation of EMT in the AV canal. (A) Hematoxylin and eosin (H&E)-stained cross-section through the atrioventricular junction of an HH stage 14 chicken heart. The myocardium (*M*) and the endocardium (*E*) are separated by the acellular cardiac jelly (*CJ*). At HH stage 14, the superior endocardial cushion (*SEC*) is on the inner curvature of the looping heart while the inferior endocardial cushion (*IEC*) is on the outer curvature. Endocardial cells have not transformed into migratory mesenchymal cells at HH stage 14. *LV*, left ventricle; *A*, atrium. (B) At HH stage 17, endocardial cells are beginning to transform into mesenchymal cells (*Mes*) that migrate into the cardiac jelly in both the superior and inferior endocardial cushions separating the atrium (*A*) from the left ventricle (*LV*).

C. Epithelial–Mesenchymal Transition

EMT is an integral part of several morphogenetic processes, including gastrulation, neural crest development, formation of the epicardium, and cardiac valve development (Mikawa and Gourdie, 1996; Savagner, 2001). The biologic events that define EMT, in our view, include the loss of intercellular connections, endothelial cell hypertrophy (activation), and the acquisition of cell migratory and invasive capacity (transformation). EMT during development is believed to represent a non-cell-autonomous process that requires the activation of external stimuli through tightly regulated mechanisms (Boyer *et al.*, 2000).

D. EMT Inductive Stimuli

Efforts to investigate the mechanisms of cardiac cushion EMT were greatly facilitated by the use of a three-dimensional type I collagen gel explant system first employed by Markwald and colleagues in the early 1980s (Bernanke and Markwald, 1982). In this system, AV canals are isolated before EMT and explanted onto a collagen gel surface. The endocardium of the AV canal migrates onto the surface of the gel and a subset of endocardial cells subsequently transforms into mesenchymal cells that invade the hydrated matrix (Fig. 3). Experimentation with the collagen gel assay provided evidence that tissue interactions between the myocardium and endocardium were necessary for AV canal EMT (Mjaatvedt *et al.*, 1987; Runyan and Markwald, 1983). EMT does not take place if the myocardium is removed immediately after the pre-EMT endocardium has migrated onto the surface of the gel (Runyan and Markwald, 1983). Further studies established that only the endocardium of the AV canal is competent to undergo EMT. If endocardium from ventricular explants was incubated with AV canal myocardium, the ventricular endocardium would not undergo EMT. This is consistent with the endocardium of the AV canal, and not the ventricle, being competent to respond to EMT inductive signals. In addition, if AV canal endocardium was incubated with ventricular myocardium, EMT would also not occur (Mjaatvedt *et al.*, 1987). Taken together, these studies demonstrate that AV myocardium is unique in its capacity to secrete specific signals necessary for EMT, and only AV canal endocardium is competent to transform into heart valve primordia.

After these landmark observational studies, the focus shifted to understand the makeup of the myocardial inductive signal for EMT in AV canal endocardial cells. One approach isolated cardiac jelly from different parts of the developing heart in an effort to characterize regional differences in composition. AV canal ECM extracted with EDTA and testicular

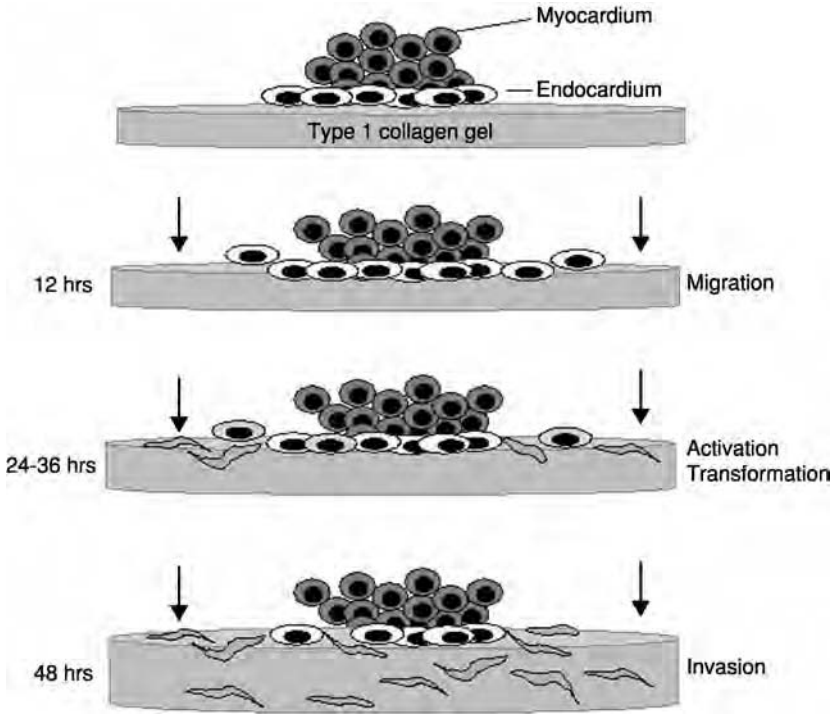


FIG. 3 *In vitro* collagen I gel explant assay. Isolated HH stage 14 AV canals are placed on a rat tail collagen I gel. After 12 h of incubation, endothelial cells migrate onto the surface of the collagen I gel, forming a confluent endothelial layer. If the myocardium is removed after 12 h, EMT will not occur. If the myocardium remains on the collagen gel, the endocardium receives inductive stimuli from the myocardium, resulting in activation of the endocardial cell layer. Activation is characterized by endothelial cell hypertrophy and cell-cell separation. Activated endothelial cells then undergo transformation into mesenchymal cells that migrate into the collagen I gel. (See also color insert.)

hyaluronidase activated competent AV endothelial monolayers, but was not sufficient for mesenchymal cell invasion (Krug *et al.*, 1985). AV canal ECM extracted with EDTA alone resulted in both activation and invasion, suggesting a functional role for either intact hyaluronan or a complex organization of the ECM during mesenchymal cell invasion (Krug *et al.*, 1987).

At approximately the same time that studies were exploring the inductive activities of the cardiac ECM, Markwald and colleagues observed that specific conditions of preparation and immunostaining revealed a particulate organization of the ECM in the AV canal (Mjaatvedt *et al.*, 1987). They identified these aggregates as "adheron like" because of similarities to adherons observed in neuron cultures (Schubert *et al.*, 1983) and utilized the properties of

the aggregates to purify an inductive fraction of the cardiac ECM. Adherons are multicomponent protein complexes that have biological function in cell–cell or cell–extracellular matrix adhesion (Schubert and LaCorbiere, 1980, 1982). Polyclonal antisera generated against the particulate AV canal ECM fraction, designated ES-1, inhibited mesenchymal cell invasion in cultured AV canal explants (Mjaatvedt *et al.*, 1991). A monoclonal antibody against adheron complexes recognizing a 130-kDa protein (ES130) also inhibited EMT in AV canal explants (Rezaee *et al.*, 1993). ES130 protein localized to the myocardium, endocardium, and mesenchymal cells before and during active mesenchymal cell formation in endocardial cushions (Krug *et al.*, 1995). The identity of the 130-kDa protein, as well as other proteins recognized by other anti-adheron antibodies, remains to be determined.

E. Mesenchymal Cell Invasion and Migration

After endocardial cells receive a myocardial-derived inductive stimulus, they hypertrophy, undergo cell–cell separation, and migrate away from the endocardial cell surface into the cardiac jelly. Scanning electron microscopy (SEM) studies demonstrate that the pre-EMT endocardium of the AV and outflow tract cushions is closely packed and displays a cobblestone luminal appearance (Markwald *et al.*, 1975). These endocardial cells possess undilated rough endoplasmic reticulum and underdeveloped Golgi complexes, consistent with limited secretory potential (Markwald *et al.*, 1975). Immediately preceding cell transformation, endocardial cells begin to swell with a concomitant dilation of the rough endoplasmic reticulum (RER) cisternae and hypertrophy of Golgi complexes. After endocardial cell hypertrophy or “activation,” SEM images reveal regions of cell–cell separation at the luminal endocardial surface (Markwald *et al.*, 1975). Molecular studies correlate this loss of endocardial cell–cell adhesion during the initial stages of EMT with downregulated expression of neural cell adhesion molecule (N-CAM), vascular endothelial (VE)-cadherin, and platelet endothelial cell adhesion molecule 1 (PECAM-1) (Baldwin *et al.*, 1994; Crossin and Hoffman, 1991; Timmerman *et al.*, 2004).

After endocardial cell separation, the transforming endocardium extends filopodia into the cardiac jelly. Mesenchymal cells with numerous filopodia then migrate into the cardiac jelly away from the endocardial cell layer (Fig. 2B). Many mitotic figures are observed in the endocardial cell layer during cell transformation (Markwald *et al.*, 1975). Although not completely understood, this heightened endocardial cell proliferation may be necessary to ensure integrity of the luminal endocardial cell layer amidst the continual loss of endocardial cells during cell transformation. By HH stage 20, numerous mesenchymal cells are observed in the cardiac jelly of the AV canal and outflow tract endocardial cushions (Fig. 4A, B).

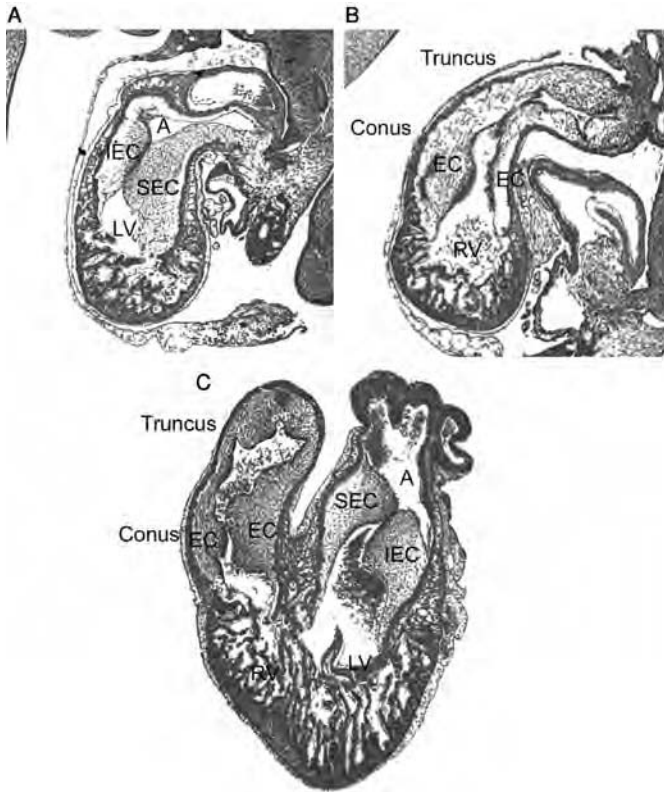


FIG. 4 Cross-sections of HH stage 20 and stage 24 chicken hearts. (A) H&E-stained cross-section through the AV canal of HH stage 20 chicken heart. The atrium (*A*) and left ventricle (*LV*) are separated by the superior endocardial cushion (*SEC*) and inferior endocardial cushion (*IEC*). Both endocardial cushions contain numerous mesenchymal cells that originated from endocardial cells that have undergone EMT. (B) H&E-stained cross-section of the outflow tract region of an HH stage 20 heart. Endocardial cushions (*EC*) in both the conus and truncus arteriosus are filled with transformed mesenchymal cells at this stage. Mesenchymal cells in the conus are thought to contribute to the mature semilunar valves whereas the mesenchymal cells in the truncus are thought to contribute to the aorticopulmonary septum. (C) H&E-stained cross-section of an HH stage 24 chicken heart, showing further development of both the AV and outflow tract cushions. Fusion of the superior and inferior cushions is beginning in the AV canal.

F. Heart Valve Remodeling and Chamber Septation

After mesenchymal cells populate the AV and outflow tract endocardial cushions, a series of differentiation events lead to the formation of valvular structures and septation of the mature heart (Anderson *et al.*, 2003a,b; Moorman *et al.*, 2003). In the AV canal, two major endocardial cushion

projections are apparent by Carnegie stage 12 in humans, embryonic day 10.5 (E10.5) in the mouse, and HH stage 17 in the chicken (Fig. 2B; see Table I for species comparison). The ventral (superior) AV endocardial cushion is associated with the inner curvature of the heart, whereas the dorsal (inferior) AV endocardial cushion is associated with the outer curvature of the heart. The inferior and superior cushions expand and become juxtaposed by HH stage 24–26 in the chicken (de la Cruz *et al.*, 1983) (Fig. 4C). Central fusion of the AV endocardial cushions divides the AV junction with separate right and left sided orifices.

After cushion fusion, the atrioventricular canal expands rightward to position the atrioventricular septum in line with the developing ventricular septum, resulting in the initial formation of a mature four-chambered heart (Fig. 5A). Fusion of the inferior and superior cushions at the midline forms the central cushion-derived mass called the septum intermedium. This septum intermedium or AV septum is positioned between the muscular

TABLE I
Human, Mouse, and Chicken Developmental Stage Comparison^{a,b}

Human (Carnegie stage/ embryonic day)	Mouse (embryonic day)	Chicken (Hamburger and Hamilton stage)
9/20	9	14
10/22	9.5	15
11/24	10	16
12/28	10.5	17
13/30	11	18
14/33	11.5	19
15/36	12	20–22
16/40	12.5	23–24
17/42	13	25–26
18/44	13.5	27–28
19/48	14	29–30
20/52	14.5	31–32
21/54	15	33–34
22/55	15.5	35
23/58	16	36

^aAdapted from Butler, H., and Juurlink, B. H. J. (1987). "An Atlas for Staging Mammalian and Chick Embryos." CRC Press, Boca Raton, FL.

^bAdapted from Camenisch, T. D., Molin, D. G., Person, A., Runyan, R. B., Gittenberger-de Groot, A. C., McDonald, J. A., and Klewer, S. E. (2002a). Temporal and distinct TGF β ligand requirements during mouse and avian endocardial cushion morphogenesis. *Dev. Biol.* **248**, 170–181.

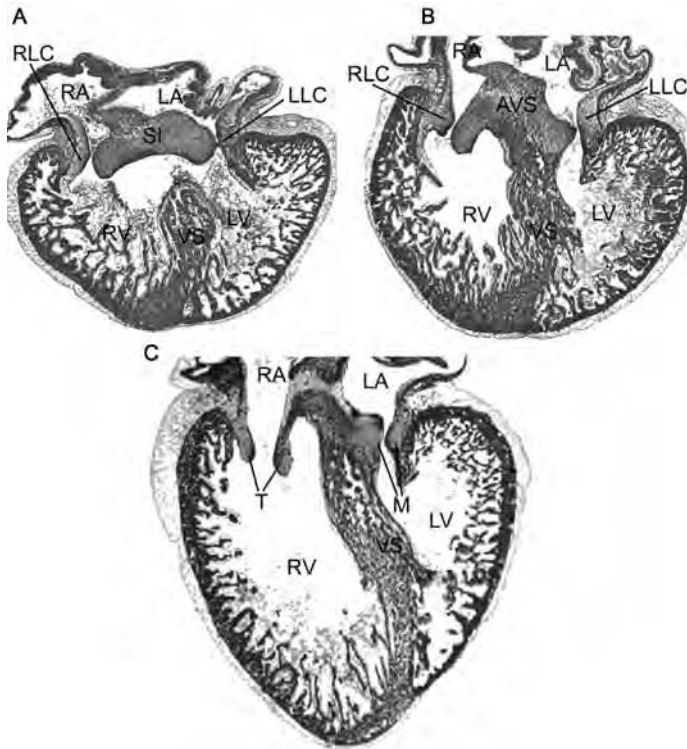


FIG. 5 Endocardial cushion remodeling into mature valves and septa. H&E-stained cross-sections of HH stage 30 (A), HH stage 33 (B), and HH stage 38 (C). (A) The superior and inferior AV cushions have completely fused, forming the septum intermedium (*SI*). Rightward shifting of the AV canal has positioned the atria directly above the ventricles. The right lateral cushion (*RLC*) and the left lateral cushion (*LLC*) begin to form in the right and left atrioventricular junctions. The ventricular septum has not met the septum intermedium at this stage. (B) At HH stage 33, the ventricular septum (*VS*) connects with the septum intermedium or atrioventricular septum (*AVS*). Lateral cushions and *AVS* projections begin to elongate to form mitral and tricuspid valve leaflets. (C) At HH stage 38, the elongated cushion projections have formed tricuspid (*T*) leaflets. The mitral (*M*) leaflets are also formed at this stage, but are slightly out of this plane of section. Abbreviations: *RA*, right atrium; *LA*, left atrium; *RV*, right ventricle; *LV*, left ventricle.

ventricular septum and the interatrial septum (Wessels and Sedmera, 2003) (Fig. 5B). Further morphogenesis of the AV septum leads to the eventual formation of the posteroinferior and septal leaflets of the tricuspid valve and the aortic leaflet of the mitral valve. During superior and inferior cushion fusion, another set of relatively small endocardial cushions begins to form on the lateral sides of the newly formed right and left AV junctions (Fig. 5A). The molecular mechanisms responsible for lateral cushion formation and subsequent development into tricuspid and mitral valve leaflets are poorly

understood (Wessels and Sedmera, 2003). Development of the endocardial cushion after the initiation of EMT is understood mainly at the level of basic morphology (Anderson *et al.*, 2003a,b; Moorman *et al.*, 2003). The molecular mechanisms governing endocardial outgrowth, superior and inferior cushion fusion, and subsequent mitral and tricuspid valve morphogenesis are just beginning to be investigated.

The outflow tract undergoes EMT beginning in the chicken at HH stage 18 and many mesenchymal cells are apparent by HH stage 20 (Fig. 4B). Cushion mesenchyme in the outflow tract contributes to the formation of the semilunar valves. A major difference between AV and outflow tract morphogenesis is the contribution of neural crest cells to the outflow tract of the heart. Neural crest cells originating from the neural tube, between the otic vesicle and the third somite, migrate through pharyngeal arches 3, 4, and 6 and into the distal outflow tract (Kirby and Waldo, 1995). The cardiac neural crest forms the spiral aorticopulmonary septum, which separates the truncus into the aorta and pulmonary arteries (Kirby and Waldo, 1995). Clinical persistent truncus arteriosus (a failure to separate the aorta and pulmonary artery) occurs after neural crest cell ablation in early avian embryos (Kirby *et al.*, 1983). Streams of neural crest cells migrate into the truncus beginning at about HH stage 18/19 in the chicken and as early as E9.5–E10.5 in the mouse (Brown *et al.*, 2001; Hutson and Kirby, 2003; Jiang *et al.*, 2000; Kirby *et al.*, 1983). Despite a significant contribution to the distal outflow tract, cardiac neural crest cells do not appear to contribute to the formation of the AV cushions (Brown *et al.*, 2001).

Research also shows that a secondary heart field contributes to the outflow tract and distal right ventricle (Kelly *et al.*, 2001; Mjaatvedt *et al.*, 2001; Waldo *et al.*, 2001). The secondary heart field is a group of cells that are medial to the primary cardiac crescent during early stages of heart formation. Cells from the secondary heart field ingress into the outflow tract from the pharyngeal mesoderm to form a substantial portion of the myocardial precursors of the developing arterial pole of the heart (Kelly *et al.*, 2001).

III. Molecular Mechanisms of Cardiac EMT and Valve Morphogenesis

A. Growth Factors and Other Molecules

1. Transforming Growth Factor β s

A major advance in the study of cardiac cushion development was a shift from using biochemical approaches to applying molecular techniques to investigate the role of specific genes during cardiac cushion formation.

An initial screen of growth factors suggested that transforming growth factor β s (TGF- β s) were components of the EMT inductive stimulus (Fig. 6). Addition of TGF- β_1 or TGF- β_2 to pre-EMT AV endocardium cultured with ventricular myocardium produced an EMT *in vitro* (Potts and Runyan, 1989). In addition, a function-blocking pan-anti-TGF- β antibody prevented EMT (Potts and Runyan, 1989). This suggested that TGF- β was an inductive component found in AV but not ventricular myocardium (Potts and Runyan, 1989). RNase protection assays showed that TGF- β_2 and TGF- β_3 were the TGF- β isoforms found in the AV canal of chickens (Potts *et al.*, 1992).

Function-blocking antibodies and antisense oligonucleotides against TGF- β_2 and TGF- β_3 were used to dissect the interplay between TGF- β isoforms in cardiac cushion development. Antisense oligonucleotides directed against TGF- β_3 inhibited EMT in chicken AV canals *in vitro* (Potts and Runyan, 1989). TGF- β_3 function-blocking antibodies inhibited EMT after cell-cell separation by preventing invasion into the collagen I matrix *in vitro* (Boyer *et al.*, 1999). Anti-TGF- β_2 function-blocking antibodies inhibited the

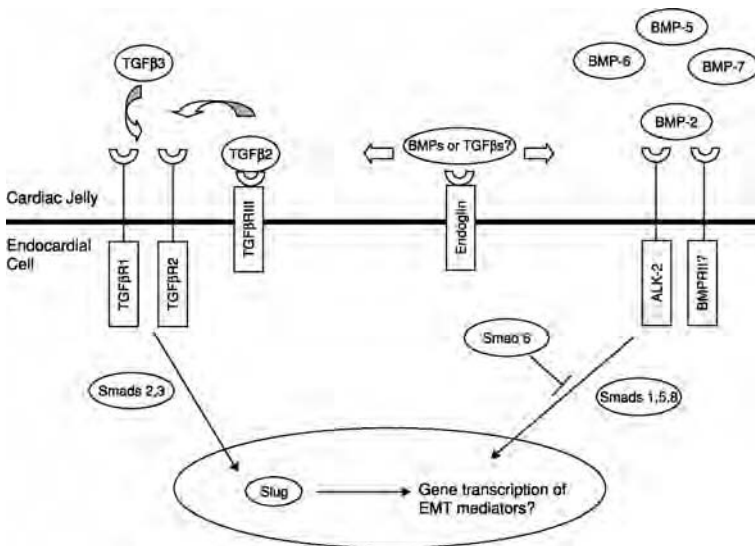


FIG. 6 TGF- β superfamily members and EMT induction. TGF- β_2 and TGF- β_3 bind to the T β R signaling complex at the cell surface of endocardial cells, resulting in the activation of Smad-2 and Smad-3 to activate expression of EMT mediators such as the transcription factor Slug. Various BMP family members bind to BMP receptors at the endocardial cell surface, resulting in Smad-1, Smad-3, and Smad-8 activation and subsequent expression of unknown EMT mediators. The inhibitory Smad, Smad-6, functions in a negative fashion to inhibit EMT and regulate mesenchymal cell numbers during cell transformation.

initial step of cell–cell separation, similar to the effect seen with the pan-specific anti-TGF- β antibody used in the previously mentioned study (Boyer *et al.*, 1999; Potts and Runyan, 1989). Therefore, in the chicken, TGF- β_2 and TGF- β_3 are necessary for endothelial cell activation and mesenchymal cell invasion respectively (Boyer *et al.*, 1999).

TGF- β_2 signaling in endocardial cushions is at least partially mediated by the transcription factor Slug. Slug is a zinc finger transcription factor expressed in various mesenchymal cell populations and is required for several EMTs throughout development (Nieto *et al.*, 1994). The Snail/Slug family of transcription factors promotes migratory phenotypes by interfering with E-cadherin-mediated cell–cell attachments. Reverse transcription-polymerase chain reaction (RT-PCR) and immunostaining revealed Slug mRNA expression and protein localization in the chicken outflow tract (OFT) and AV cardiac cushions from HH stages 14–20 (Romano and Runyan, 1999). Protein localization of Slug persists, at least until HH stage 30, primarily in the transformed mesenchyme of AV and OFT valves (Carmona *et al.*, 2000). Antisense oligonucleotides directed against *slug* inhibited EMT in AV canal explant cultures by blocking endocardial cell activation (Romano and Runyan, 1999). TGF- β_2 -blocking antibodies, known to inhibit AV canal EMT at a similar stage (Boyer *et al.*, 1999), reduced Slug expression in AV canal explants (Romano and Runyan, 2000). Overexpression of Slug rescued cell transformation in cultures treated with anti-TGF- β_2 antibodies, further arguing that Slug signals downstream of TGF- β_2 (Romano and Runyan, 2000).

Characterization of TGF- β isoform expression during development reveals temporal and spatial expression consistent with an important role for TGF- β s in endocardial cushion EMT. In the mouse, TGF- β_1 is expressed in cardiac mesoderm before initiation of EMT and later becomes localized in the endocardial cells that undergo EMT (Akhurst *et al.*, 1990). TGF- β_2 expression is detected in the myocardium of both the AV and outflow tract during EMT, with a loss of specific cushion myocardial expression after EMT in mouse hearts (Dickson *et al.*, 1993). TGF- β_3 is expressed in the heart after EMT in mouse embryos, but expression is detected in chicken cardiac cushions during EMT (Letterio *et al.*, 1994; Potts *et al.*, 1992).

Genetic mouse models using targeted inactivation of TGF- β_1 did not produce cardiac phenotypes (Shull *et al.*, 1992). These mice had defects involving the immune system and vasculogenesis (Shull *et al.*, 1992). TGF- β_2 knockout mice displayed multiple cardiac defects including atrial and septal defects, double outlet right ventricle, double inlet left ventricle, and a failure of muscularization of the developing outflow tract (Sanford *et al.*, 1997). TGF- β_2 null mice did form at least some mesenchymal cells in the cardiac cushions. This suggested that TGF- β_2 is either not necessary for EMT or there is a partial redundancy for this step by another TGF- β family

member. As normal EMT is blocked in mouse AV canal explants with pan-anti-TGF- β function-blocking antibodies (Camenisch *et al.*, 2002a), there appears to be greater potential for redundancy in the mouse. Mice null for both TGF- β_2 and TGF- β_3 have a more severe cushion phenotype than TGF- β_2 null mice alone (Dunker *et al.*, 2002). Mice null for TGF- β_3 were not embryonic lethals but rather displayed delayed pulmonary development, defective palatogenesis, and died shortly after birth (Kaartinen *et al.*, 1995). Cardiac cushion EMT was not affected in TGF- $\beta_3^{-/-}$ mice with no apparent atrial, ventricular, outflow tract, or atrioventricular defects (Kaartinen *et al.*, 1995). A complete list of human and mouse mutants with endocardial cushion-derived phenotypes is provided in Table II.

The apparent functional discrepancies on inhibition of various TGF- β isoforms in the mouse and chicken can be explained by differences in temporal expression between the two organisms. RNase protection assays using chicken heart tissue showed TGF- β_3 expression primarily in the AV canal, with greatly reduced expression in the ventricle during EMT stages (Potts *et al.*, 1992). In the mouse, TGF- β_3 expression was detected in the AV canal by *in situ* hybridization only after EMT. This lack of expression during EMT was consistent with the TGF- $\beta_3^{-/-}$ mouse not displaying defective cardiac cushion development. Direct comparisons of chicken and mouse hearts revealed distinct functional differences in TGF- β ligand function during EMT (Camenisch *et al.*, 2002a). In the chicken, both TGF- β_2 and TGF- β_3 were necessary for EMT whereas only TGF- β_2 and not TGF- β_3 was necessary for EMT in mouse cardiac cushions (Camenisch *et al.*, 2002a).

At the cellular level, TGF- β ligand activation provides another layer of complexity in TGF- β signal transduction in endocardial cushions. TGF- β_1 , TGF- β_2 , and TGF- β_3 are each individually secreted as part of latent TGF- β complexes (Annes *et al.*, 2003). These latent TGF- β complexes consist of the active TGF- β protein, a latency-associated peptide (LAP), and a latent TGF- β -binding protein (LTBP) (Gleizes *et al.*, 1997). LTBP was shown to direct the latent complex to the ECM, where the complex awaits activation. Activation occurs when LAP is dissociated from the complex by proteolysis mediated by plasmin, which releases the active TGF- β protein (Sato and Rifkin, 1989). LTBP-1 was shown to colocalize with TGF- β_1 in areas surrounding mesenchymal cells of AV canals *in vitro* (Nakajima *et al.*, 1997). Function-blocking LTBP-1 antibodies inhibited EMT in AV canal explants *in vitro*. Addition of TGF- β_1 to anti-LTBP-1 treated cultures rescued EMT. This suggested that LTBP-1 was necessary for processing of a latent TGF- β complex into an active TGF- β protein capable of EMT induction (Nakajima *et al.*, 1997).

Annexin II, a coreceptor for plasminogen and plasminogen activator, promotes cell surface production of plasmin (Cesarman *et al.*, 1994; Hajjar *et al.*, 1994). Annexin II is expressed in the endocardial cells of the AV canal

TABLE II
Endocardial Cushion-Derived Mutant Phenotypes

Gene	Expression within cushions		Phenotype	
	Location	Ref. ^a	Description	Ref. ^b
<i>TGF-β₂</i>	Myo, Endo, Mes	1	VSD, DORV, DILV	1
<i>Has-2</i>	Myo, Endo, Mes		Lack of cushion formation	2
<i>Versican</i>	Myo		Lack of cushion formation	3, 4
<i>Endoglin</i>	Endo	2	Hypocellular AV and OFT cushions	5
<i>BMP-4</i>	Myo, Endo, Mes	3	Hypo. BMP-4 expressed in Myo, AVSD	6
<i>BMP-5/BMP-7</i>	Myo, Myo, Mes	4, 5	Lack of cushion formation	7
<i>BMP-6/BMP-7</i>	Myo, Mes/Myo, Mes	5	Delayed OFT cushion formation	8
<i>Smad-6</i>	Endo, Mes		Hypercellular AV and OFT cushions	9
<i>Erbb3</i>	Endo, Mes		Hypocellular AV and OFT cushions	10
<i>BMPR2</i>	Endo, Myo, Mes	6	Hypo. BMPR2, PTA, OFT valve defects	11
<i>ALK-3</i>	Endo, Myo, Mes	7	Myo inactivation, AV and septum defects	12
<i>NFATc</i>	Endo		VSD, underdeveloped AV and OFT valves	13, 14
<i>NF-1</i>	Endo, Myo, Mes		Hypercellular AV and OFT cushions	15
<i>Sox-9</i>	Mes	8, 9	Hypocellular AV and OFT cushions	16
<i>GATA-4</i>	Myo	10	ASD, VSD, AVSD, pulmonary stenosis	17
<i>FOG-2</i>	Myo	11	AVSD, tetralogy of Fallot	18

<i>TBX-5</i>	Myo	12	ASD, ASD, tetralogy of Fallot	19–21
<i>Nkx2.5</i>	Myo	13, 14	ASD, VSD	22
<i>EGFR</i>	Endo, Myo, Mes	15	Hypo. allele, SL hyperplasia AV and SLV hyperplasia	23 24
<i>Shp-2</i>	Endo, Myo, Mes		EGFR/Hypo.shp2 mutants SL hyperplasia	23
<i>HB-EGF</i>	Endo, Myo		AV and SLV hyperplasia	24, 25
<i>TACE</i>	Endo, Myo		AV and SLV hyperplasia	24
<i>Pitx2a,b,c</i>	Myo		AVSD, DORV, PTA	26–29
<i>Pitx2c</i>	Myo		AVSD, DORV	29, 30
<i>Hey-2</i>	Endo, Myo, Mes	16	VSD and right ventricular hypertrophy	31

^aReferences: (1) Dickson *et al.*, 1993; (2) Cheifetz *et al.*, 1992; (3) Jones *et al.*, 1991; (4) Solloway and Robertson, 1999; (5) Dudley and Robertson, 1997; (6) Roelen *et al.*, 1997; (7) Dewulf *et al.*, 1995; (8) Zhao *et al.*, 1997; (9) Ng *et al.*, 1997; (10) Heikinheimo *et al.*, 1994; (11) Lu *et al.*, 1999a; (12) Chapman *et al.*, 1996; (13) Komuro and Izumo, 1993; (14) Lints *et al.*, 1993; (15) Jackson *et al.*, 2003; (16) Leimeister *et al.*, 1999.

^aReferences: (1) Sanford *et al.*, 1997; (2) Camenisch *et al.*, 2000; (3) Yamamura *et al.*, 1997; (4) Mjaatvedt *et al.*, 1998; (5) Bourdeau *et al.*, 1999; (6) Jiao *et al.*, 2003; (7) Solloway and Robertson, 1999; (8) Kim *et al.*, 2001; (9) Galvin *et al.*, 2000; (10) Erickson *et al.*, 1997; (11) Delot *et al.*, 2003; (12) Gaussin *et al.*, 2002; (13) Ranger *et al.*, 1998; (14) de la Pompa *et al.*, 1998; (15) Lakkis and Epstein, 1998; (16) Akiyama *et al.*, 2004; (17) Garg *et al.*, 2003; (18) Tevosian *et al.*, 2000; (19) Li *et al.*, 1997b; (20) Basson *et al.*, 1997; (21) Bruneau *et al.*, 2001; (22) Schott *et al.*, 1998; (23) Chen *et al.*, 2000; (24) Jackson *et al.*, 2003; (25) Iwamoto *et al.*, 2003; (26) Kitamura *et al.*, 1999; (27) Gage *et al.*, 1999; (28) Lu *et al.*, 1999b; (29) Liu *et al.*, 2001; (30) Liu *et al.*, 2002; (31) Donovan *et al.*, 2002.

Abbreviations: ASD, atrial septal defect; AV, atrioventricular; AVSD, atrioventricular septal defect; BMP, bone morphogenetic protein; BMPR, bone morphogenetic protein receptor; DILV, double inlet left ventricle; DIRV, double inlet right ventricle; DORV, double outlet right ventricle; EGFR, epidermal growth factor receptor; Endo, endocardium; Hypo., hypomorphic allele; Mes, mesenchyme; Myo, myocardium; OFT, outflow tract; PTA, persistent truncus arteriosus; SL, semilunar; SLV, semilunar valve; VSD, ventricular septal defect.

and outflow tract during EMT (Krishnan *et al.*, 2004). Anti-annexin II antibodies inhibited EMT *in vitro*, and this inhibition was rescued by addition of TGF- β_3 (Krishnan *et al.*, 2004). Western blotting analysis failed to detect active TGF- β_3 in conditioned media from EMT stage hearts cultured with anti-annexin II antibodies or α_2 -antiplasmin, a pharmacological plasmin inhibitor. Active TGF- β_3 was detected in conditioned media from control treated cultures (Krishnan *et al.*, 2004). These data suggest that annexin II mediates plasmin production that subsequently releases active TGF- β_3 from a latent complex.

Studies investigating TGF- β receptors further argue that TGF- β signaling is a major EMT inductive stimulus in cardiac cushions. TGF- β signaling is transduced via two serine-threonine kinase domain-containing transmembrane receptors T β RI and T β RII (TGF- β receptors I and II, respectively) (Wrana *et al.*, 1994). Binding of TGF- β ligands to T β RII results in phosphorylation of T β RI that in turn activates Smad intracellular signaling mediators that activate TGF- β -dependent gene transcription (Shi and Massague, 2003). T β RIII, also known as betaglycan, can bind and present TGF- β ligands to the T β RI and T β RII complex. T β RIII contains a short intracellular tail and possesses no identified intracellular signaling function (Kretschmar and Massague, 1998).

Gene inactivation of T β RII in mice did not provide insight into the role of this receptor in cardiac cushion development because T β RII^{-/-} mice die before endocardial cushion formation (Oshima *et al.*, 1996). Functional studies in the chicken showed that antisera directed against T β RII inhibited epithelial-to-mesenchymal cell transformation in AV canal explants (Brown *et al.*, 1996). T β RII is expressed throughout the endothelium of the vasculature as well as the endocardium throughout the heart (Brown *et al.*, 1996). The localized transformation event in cardiac cushions may be due to restricted expression of T β RIII in the endocardium and transformed mesenchymal cells of developing cushions (Brown *et al.*, 1999). Anti-T β RIII function-blocking antisera inhibited mesenchymal cell formation and therefore T β RIII seemed to be a necessary component for cardiac cushion EMT. Overexpression of T β RIII in ventricular explants induced ventricular explants to display enhanced EMT in the presence of TGF- β_2 (Brown *et al.*, 1999). Increased expression of T β RIII in ventricles could allow either for TGF- β_2 -mediated EMT in the ventricular endocardium, or may enhance invasion by a subset of AV endocardial cells dissected into the explant. Either way, T β RIII is functional during EMT. Efforts are still underway to explain the mechanism of T β RIII signaling during cardiac cushion EMT.

Endoglin is another TGF- β superfamily receptor that binds to TGF- β_1 and TGF- β_3 and presents these ligands to T β RII in a similar fashion as T β RIII (Cheifetz *et al.*, 1992; Letamendia *et al.*, 1998). Endoglin also binds other members of the TGF- β superfamily such as BMP-2, BMP-7, and

activin (Pece-Barbara *et al.*, 1999). Endoglin is expressed in all endothelial cells and endoglin knockout mice display global vascular defects (Bourdeau *et al.*, 1999). Importantly, the AV canal endocardial cushions failed to undergo epithelial-to-mesenchymal cell transformation, resulting in hypocellular cushions at E9.5. Endoglin null embryos died of cardiac insufficiency at E10.5 (Bourdeau *et al.*, 1999). Endoglin is necessary for EMT in the AV canal cardiac cushions but the ligand/ligands that bind endoglin in cardiac cushions have not been reported. The necessity for endoglin during EMT further argues that TGF- β superfamily members are important in directing endocardial cushion EMTs (Fig. 4).

2. Bone Morphogenetic Proteins

Other TGF- β superfamily members are also expressed in the developing cardiac cushions. BMP-2, BMP-4, BMP-5, BMP-6, and BMP-7 are expressed in the AV canal and outflow tract during the initiation of EMT. BMP-2 expression is restricted to the AV canal and outflow tract myocardium before and during EMT (Lyons *et al.*, 1990). Attempts to study the functional role for BMP-2 in cardiac cushion morphogenesis, using mouse genetics, are complicated by early embryonic lethality for BMP-2 null embryos (Zhang and Bradley, 1996). One report, using mouse AV explants, showed that BMP-2 was sufficient to induce EMT in mouse AV canal cultures in the absence of AV myocardium (Sugi *et al.*, 2004). Treatment of AV cultures with Noggin, a BMP inhibitor, inhibited mesenchymal cell formation in untreated cultures, and also inhibited BMP-2-induced EMT in AV cultures with intact AV myocardium (Sugi *et al.*, 2004). BMP-2 treatments of AV explants resulted in increased TGF- β_2 protein levels, perhaps partially explaining the mechanism of BMP-2 induction (Sugi *et al.*, 2004). BMP-4 is also expressed in the cardiac cushions during the initiation of EMT. This BMP family member is not necessary for EMT, but rather for later developmental steps necessary for valve maturation (discussed in more detail below).

BMP-5 is expressed in the myocardium before and during cardiac cushion EMT in the mouse (Solloway and Robertson, 1999). BMP-6 expression is noted primarily in the outflow tract myocardium of the mouse at the onset of EMT (Dudley and Robertson, 1997). Later in development, BMP-6 expression persists in the outflow tract myocardium and expression becomes detectable in the AV canal, but not outflow tract, cushion mesenchyme (Kim *et al.*, 2001). BMP-7 is expressed throughout the myocardium of the linear heart tube (Dudley and Robertson, 1997), and later has modest expression in AV valve mesenchyme (Kim *et al.*, 2001). Traditional gene inactivation of BMP-5, BMP-6, or BMP-7 alone does not produce cardiac defects (Dudley and Roberson, 1997; Kingsley *et al.*, 1992). Several groups have created

compound BMP knockout mouse models to further investigate the role of BMPs in cardiac cushion development. BMP-5/BMP-7 double-knockout mice do not form cardiac cushions (Sollaway and Robertson, 1999). However, the precise role(s) of BMP-5 and BMP-7 in cushion morphogenesis is complicated by a severe delay and global disorganization of development (Sollaway and Robertson, 1999). BMP-6/BMP-7 double-knockout mice show a marked delay in the formation of outflow tract cushions because of reduced cell proliferation (Kim *et al.*, 2001). Compared with the outflow tract cushions, AV canal cushions are generally less compromised by the loss of BMP-6 and BMP-7 (Kim *et al.*, 2001).

Research in chicken embryos shows that activin receptor-like kinase 2 (ALK-2) is an important TGF- β superfamily receptor in AV canal development. Polyclonal antiserum against ALK-2, but not ALK-5, resulted in reduced mesenchymal cell formation in AV canal cultures (Lai *et al.*, 2000). ALK-2 and ALK-5/T β RI are both TGF- β superfamily type I receptors that signal in combination with various TGF- β superfamily type II receptors, including type II B activin receptor (ActRII/B), antimüllerian hormone type II receptor (AMHR-II), and T β RII (Shi and Massague, 2003). Both ALK-2 and ALK-5 are localized throughout the endothelium of the heart and therefore likely do not account for the restricted EMT events in cardiac cushions (Lai *et al.*, 2000). ALK-2 could interact with either T β RII/T β RIII complexes or BMP receptors to influence cardiac cushion EMT. At this time, it is not known exactly how ALK-2 signals during cardiac cushion EMT.

Intracellular TGF- β superfamily signaling mediators also appear necessary for cell transformation in developing endocardial cushions. TGF- β superfamily ligands bind to type II receptors and activate a cascade of signaling mediators including Smad intracellular proteins. TGF- β superfamily receptor kinases directly phosphorylate and activate receptor (R) Smads. R-Smads Smad-2 and Smad-3 respond to signaling by the TGF- β subfamily whereas R-Smads Smad-1, Smad-5, and Smad-8 respond primarily to BMP signaling. Activated R-Smads from both the TGF- β and BMP pathways form heterodimers with Smad-4. These Smad-4/R-Smad heterodimer complexes translocate into the nucleus to activate gene transcription (Shi and Massague, 2003). Smad-6 negatively regulates BMP signaling by competing for Smad-1 binding of Smad-4 (Hata *et al.*, 1998). Smad-6 is expressed in the AV and outflow tract regions of the heart during development (Galvin *et al.*, 2000). Smad-6 may modulate BMP signaling in these areas of the heart because Smad-6 preferentially inhibits BMP signaling (Shi and Massague, 2003). Smad-6 homozygous knockout mice displayed hypercellular AV and outflow tract cardiac cushions (Galvin *et al.*, 2000). The hypercellular cushion phenotype in *Smad-6*^{-/-} mice is consistent with BMP mediating either EMT or subsequent mesenchymal cell proliferation within cardiac cushions (Galvin *et al.*, 2000). It would seem that BMP-induced mesenchyme

formation or proliferation is controlled by a negative feedback mechanism involving Smad-6. In the absence of negative Smad-6 regulation, mesenchymal cell numbers increase, leading to enlarged hypercellular cushions.

BMP-4 signaling does not appear to be involved in cardiac cushion EMT, but rather growth and remodeling of cushions into mature valvular and septal structures. Attempts to study the role of BMP-4 in cardiac cushions was not possible by conventional gene inactivation because of early embryonic lethality reported in the BMP-4 knockout mouse (Winnier *et al.*, 1995). However, mice harboring a conditionally inactivated hypomorphic BMP-4 allele in cardiac myocytes have defined a critical role for this factor in heart valve development (Jiao *et al.*, 2003). BMP-4 was originally thought to be involved in the induction of EMT in cardiac cushions (Markwald and Wessels, 2001), but embryos with hypomorphic myocardial BMP-4 expression produce cushion mesenchyme. Of course, one could argue that the remaining BMP-4 activity in a hypomorphic setting may be sufficient to induce cell transformation. Modest reductions in BMP-4 expression in the myocardium of the heart result in partial atrioventricular septal defects (AVSDs). More pronounced reductions in myocardial BMP-4 expression results in a complete AVSD, with a common AV valve similar to those of humans with Down syndrome. The AVSDs in these mouse models appear to result from decreased cell proliferation within the AV cardiac cushions (Jiao *et al.*, 2003).

Functional investigations of factors downstream of BMP provide additional support for a critical role of BMP signaling during endocardial cushion morphogenesis. Mice with a hypomorphic BMP receptor II allele (*Bmpr2*) die before birth as a result of cardiovascular abnormalities (Delot *et al.*, 2003). *Bmpr2* interacts with activin receptor-like kinase (ALK-3; Shi and Massague, 2003). *Bmpr2*/ALK-3 can bind BMP-2, BMP-4, or BMP-7 to activate an intracellular cascade involving Smad intracellular signaling mediators (Shi and Massague, 2003). Mice expressing hypomorphic *Bmpr2* alleles display persistent truncus arteriosus along with semilunar valve defects (Delot *et al.*, 2003). EMT is initiated in both the AV and outflow tract endocardial cushions, arguing that *Bmpr2* is not necessary for EMT. A reduced level of *Bmpr2* could be sufficient for EMT, and the question of whether *Bmpr2* is necessary for EMT could only be answered by complete removal of this receptor. Outflow tract cushions failed to develop past initial EMT events, indicating that *Bmpr2* is required for subsequent growth and maintenance of the conotruncal cushions (Delot *et al.*, 2003). Persistent truncus arteriosus can be caused by an inhibition of proper cardiac neural crest contribution to the distal outflow tract, resulting in an absence of the aorticopulmonary septum (Kirby *et al.*, 1983). At least some cardiac neural crest cells enter the outflow tract in mice expressing the hypomorphic *Bmpr2*.

This led to speculation that BMP signaling may be important in regulating the interaction between migrating neural crest and cells intrinsic to the developing outflow tract (Delot *et al.*, 2003).

Myocardial-specific gene inactivation of the *Bmpr2* signaling partner, ALK-3, also results in cardiac defects (Gaussin *et al.*, 2002). Interestingly, defects are observed in the AV junction and not in the outflow tract cushions (Delot *et al.*, 2003; Gaussin *et al.*, 2002). Initial steps of cardiac cushion development are normal in both the AV and outflow tract cushions, suggesting that ALK-3 is dispensable for EMT. However, after EMT, the cushions are reduced in size, and inferior and superior cushion fusion does not occur (Gaussin *et al.*, 2002). An increase in cell death of cardiac myocytes lacking ALK-3 may explain this abnormal AV canal phenotype. Elimination of ALK-3 also results in diminished TGF- β_2 expression in the AV canal (Gaussin *et al.*, 2002). These data supported a hypothesis that BMP signaling in the myocardium regulates TGF- β_2 expression in the AV canal (Gaussin *et al.*, 2002).

ALK-2 is involved in other aspects of heart development in addition to cardiac cushion development. Conditionally knocking out ALK-2 in the neural crest impaired normal neural crest contribution to the outflow tract, resulting in persistent truncus arteriosus and abnormalities in the aortic arch arteries (Kaartinen *et al.*, 2004). Various TGF- β superfamily ligands (TGF- β_2 , TGF- β_3 , BMP-2, BMP-4, BMP-5, BMP-6, and BMP-7) are expressed in the outflow tract at the right time to signal via ALK-2. The specific BMP ligand promoting neural crest migration into the outflow tract was not identified. TGF- β_2 null mice displayed aortic arch artery and outflow tract septation defects (Molin *et al.*, 2002; Sanford *et al.*, 1997) similar to those in the neural crest ALK-2 null mice, arguing that TGF- β_2 may be an ALK-2 ligand. Conditional ALK-2 knockouts showed a marked decrease in expression of the transcription factor *Msx-1* (a known BMP target). One of the BMPs expressed in the outflow tract could be signaling through ALK-2 (Kaartinen *et al.*, 2004). Additional studies will be required to understand the ALK-2/ligand interactions that govern cardiac cushion and cardiac neural crest cell migration.

BMPs function prominently to regulate various aspects of endocardial cushion development. BMP signal transduction components control mesenchyme formation and subsequent mesenchymal cell proliferation (Jiao *et al.*, 2003; Lai *et al.*, 2000; Sugi *et al.*, 2004). BMP signaling is also necessary for cardiac neural crest cell migration into the outflow tract (Delot *et al.*, 2003; Kaartinen *et al.*, 2004). Removing various BMP components through mouse knockout studies recapitulates heart defects including AVSD, semilunar valve hypoplasia, and persistent truncus arteriosus. Future studies will focus on how BMP pathways interact with other growth factor pathways to direct these different aspects of endocardial cushion development.

3. Heregulins and ErbB3

Heregulins (also called neuregulins) are a structurally diverse group of secreted glycoproteins that possess epidermal growth factor (EGF)-like domains (Lemke, 1996). Heregulins signal through Erb receptors, a family of tyrosine kinase transmembrane receptors of the class I EGFR family. The ErbB3 receptor is expressed in the endocardium and mesenchyme of cardiac cushions (Erickson *et al.*, 1997). Gene inactivation of ErbB3 in the mouse results in a reduction of mesenchymal cells in the AV and outflow tract cardiac cushions (Erickson *et al.*, 1997). AV and outflow tract valves are hypoplastic and underdeveloped in *ErbB3*^{-/-} mice and likely contribute to embryonic death observed by E13.5 (Erickson *et al.*, 1997). Initially, the mechanism of Erb signaling within cardiac cushions was not understood (Erickson *et al.*, 1997). More recent studies implicate an interaction between hyaluronan and Erb signaling during endocardial cushion development. Hyaluronan null hearts do not form cardiac cushions and do not undergo EMT (Camenisch *et al.*, 2000). Rescue of EMT in *Has-2* null AV canals with hyaluronan is associated with phosphorylation of ErbB3 (Camenisch *et al.*, 2002b). Addition of heregulin to *Has-2*^{-/-} AV canal cultures also activates ErbB2 and ErbB3 and rescues EMT (Camenisch *et al.*, 2002b). Specific ErbB2 or ErbB3 inhibitors block heregulin rescue of *Has-2*^{-/-} EMT (Camenisch *et al.*, 2002b). At this time, it is not known whether hyaluronan directly interacts with ErbB3 receptors or if hyaluronan activates ErbB3 by an indirect mechanism.

4. Epidermal Growth Factors and Shp-2

Humans with Noonan syndrome, an autosomal dominant condition, display thickened dysplastic heart valves and occasional hypertrophic cardiomyopathy. More than 50% of Noonan patients have mutations in the *PTPN11* gene (Tartaglia *et al.*, 2001). *PTPN11* encodes SHP2, a protein tyrosine phosphatase that acts downstream of growth factor signaling, including epidermal growth factor (EGF) (Fragale *et al.*, 2004).

Several animal models recapitulate the cardiac phenotypes observed in Noonan syndrome. Mice mutant for Shp-2 and the EGF receptor (EGFR) have thickened valves and hypertrophic cardiomyopathy (Chen *et al.*, 2000). In addition, disruption of the EGF receptor ErbB1, TACE (tumor necrosis factor- α converting enzyme; secreted activator of EGF), or HB-EGF (Heparin-binding EGF), all cause thickened semilunar and AV valves (Jackson *et al.*, 2003). These data clearly indicate that aberrations of multiple components of EGF signaling can lead to abnormal heart valve formation.

EGF signaling may control cushion morphology through modulation of BMP signaling. EGF signaling inhibits BMP-4 signaling by mitogen-activated

protein kinase (MAPK)-mediated phosphorylation and inhibition of Smad-1 (Kretzschmar *et al.*, 1997). The increase in cell proliferation in *HB-EGF*^{-/-} embryos was coupled with increased activation of Smad-1, Smad-5, and Smad-8 in endocardial cushions at E14.5 (Jackson *et al.*, 2003). Smad-1, Smad-5, and Smad-8 are known to mediate BMP signaling, so inactivation of HB-EGF likely results in increased cell proliferation via enhanced BMP signaling. These data are consistent with reduced BMP-4 expression resulting in decreased cell proliferation within endocardial cushions after EMT events (Jiao *et al.*, 2003). EGF signaling also regulates apoptosis in other contexts (Barnes *et al.*, 1982; Gill *et al.*, 1981; MacLeod *et al.*, 1986). Removal of this proapoptotic signal could result in enlarged endocardial cushions due to a lack of EGFR-directed programmed cell death (Chen *et al.*, 2000).

5. Wnts and β -Catenin

Wnt glycoproteins are secreted growth factors that direct differentiation, proliferation, specification, and migration of various cell types during embryogenesis (Miller, 2002). Wnts bind to cell surface Frizzled receptors, leading to one of three known signal transduction pathways (Pandur *et al.*, 2002). In the canonical Wnt signaling pathway, Wnt binding to Frizzled receptors activates a cascade of intracellular signaling mediators leading to the stabilization of β -catenin and activation of β -catenin-mediated gene transcription. The canonical Wnt pathway governs many developmental events and can promote cancerous cell phenotypes when unregulated (Pandur *et al.*, 2002).

Work in our laboratory demonstrates that Wnt-9a (formerly Wnt-14) expression is restricted to the endocardial cell population of AV cardiac cushions beginning at HH stage 16 in the chicken and persists at least through stage 24 (Person *et al.*, 2005). Wnt-9a activates a β -catenin-responsive reporter in AV canal cells and promotes cell proliferation when overexpressed in endocardial cushions. Cardiac cushion endocardium and transformed mesenchyme also express a secreted Wnt antagonist, Frzb (Ladher *et al.*, 2000; Person *et al.*, 2005). Wnt-9a overexpression induces cell proliferation and results in enlarged AV cardiac cushions *in ovo*. Frzb inhibits Wnt-9a-mediated cell proliferation within the developing cardiac cushions (Person *et al.*, 2005). These data support a hypothesis that Wnt-9a signals through β -catenin to activate cell proliferation in the developing cardiac cushions, which likely promotes cardiac cushion outgrowth and remodeling. Frzb appears to modulate Wnt-mediated cell proliferation and may promote mesenchymal cell differentiation after endocardial cushion EMT (Person *et al.*, 2005).

Transgenic zebrafish and mouse embryos with β -catenin-responsive reporters show active β -catenin signaling in the endocardium and newly formed

mesenchyme of cardiac cushions during EMT and later valve remodeling (Gitler *et al.*, 2003a; Hurlstone *et al.*, 2003). Adenomatous polyposis coli (APC) is a tumor suppressor gene that negatively regulates β -catenin activity (Rubinfeld *et al.*, 1993). Transgenic zebrafish embryos expressing a non-functional APC display hypercellular cardiac cushions because of enhanced β -catenin activity (Hurlstone *et al.*, 2003). Ectopic β -catenin activity and expanded expression domains for several cushion markers are seen in the hearts of APC mutant zebrafish (Hurlstone *et al.*, 2003). Cell proliferation is dramatically increased throughout the hearts of APC mutants (Hurlstone *et al.*, 2003).

β -Catenin activation also functions prominently during the cardiac cushion epithelial-to-mesenchymal cell transformation. Endothelial specific β -catenin inactivation inhibits cardiac cushion epithelial-mesenchymal cell transition both *in vitro* and *in vivo* (Liebner *et al.*, 2004). The transgenic β -catenin/T cell factor (TCF)/Lef-1 reporter construct (BAT-gal) is active in endocardial and mesenchymal cells during EMT. TGF- β_2 -induced EMT *in vitro* was strongly repressed in β -catenin null explants, although TGF- β_2 -induced Smad phosphorylation was unchanged. This suggests that β -catenin is downstream of TGF- β_2 . TGF- β_3 can upregulate Lef-1 expression during EMT in palatal development (Nawshad and Hay, 2003), and a similar TGF- β_2 activation of β -catenin signaling may also occur during endocardial cushion EMT.

6. Notch

Mutations in the Notch receptor Jagged-1 have been implicated in the rare autosomal dominant disorder called Alagille syndrome (Li *et al.*, 1997a; Oda *et al.*, 1997). People with Alagille syndrome suffer from various congenital heart defects, including peripheral pulmonic stenosis, pulmonic valve stenosis, atrial septal defects (ASDs), ventricular septal defects (VSDs), coarctation of the aorta, tricuspid atresia, and Tetralogy of Fallot (McCright *et al.*, 2002). Inactivation of Hey-2 also causes similar Alagille syndrome heart defects, implicating this transcription factor in a Notch/Jagged signaling pathway (Donovan *et al.*, 2002). Notch-1 and Notch-2 are expressed in the endocardium of the aorta, pulmonary artery, and cardiac cushions (Loomes *et al.*, 2002). Functional analysis points to a role for Notch signaling during EMT. Inhibition of Notch activity in mice and zebrafish embryos severely attenuates cardiac cushion mesenchymal cell formation. In addition, overexpression of activated Notch leads to hypercellular cardiac cushions (Timmerman *et al.*, 2004). Mutations in Notch signaling components negatively affect mesenchyme formation in endocardial cushions, leading to several defects that likely arise from primary endocardial cushion dysfunction. Other defects involving the outflow circulation may come about as a

result of aberrant Notch signaling in areas other than endocardial cushions. The predominant right-sided heart defects observed in Alagille syndrome are more likely due to inhibition of Notch function in the developing pulmonary artery.

7. Fibroblast Growth Factors

Although many studies have focused on the process of epithelial–mesenchymal cell transition during endocardial cushion development, events after EMT have been relatively unexplored. Reports have shown that fibroblast growth factor (FGF) signaling is important for growth and development of cardiac cushions after EMT (Sugi *et al.*, 2003). Myocardium, endocardium, and mesenchyme of avian cardiac cushions express FGF-4 at HH stage 25, and recombinant FGF-4 increases cell proliferation of cardiac cushion mesenchyme *in vitro* (Sugi *et al.*, 2003). Injection of a replication-defective FGF-4-containing retrovirus into the conal cushions increases mesenchymal cell proliferation and luminal expansion of the cushions (Sugi *et al.*, 2003). Expression of FGF receptors (1, 2, and 3) is detected in cardiac cushions of HH stage 22 chicken embryos, with FGFR-2 and FGFR-3 displaying restricted cardiac cushion expression. The endocardium and mesenchyme in proximity to the lumen express FGFR-2, while cushion endocardium expresses FGFR-3 (Sugi *et al.*, 2003). These data suggest that FGF-4 is a major proliferative signal directing cardiac cushion outgrowth and remodeling.

8. Vascular Endothelial Growth Factor

Embryos exposed to hypoxic conditions have an increased risk of cardiovascular malformations (Jaffee, 1974). Hypoxia stimulates vascular endothelial growth factor (VEGF) expression to induce new blood vessel formation to restore oxygen homeostasis in affected tissue (Dor and Keshet, 1997). At E10.5, VEGF is highly expressed in the myocardium of the AV canal endocardial cushions, while both VEGFR-1 and VEGFR-2 are expressed in the endocardium (Dor *et al.*, 2001). Overexpression of VEGF drastically reduces mesenchyme formation in AV endocardial cushions. In addition, hypoxia-induced EMT inhibition was rescued by overexpression with a soluble VEGFR-1 protein that specifically binds to and inhibits VEGF (Dor *et al.*, 2001). Thus, embryogenesis in hypoxic environments upregulates VEGF expression that appears to suppress EMT during early valvulogenesis.

Maternal diabetes is a well-known factor contributing to congenital heart defects, particularly AV septal defects (Loffredo *et al.*, 2001). Elevated glucose levels during development cause increases in VEGF and vascular abnormalities (Pinter *et al.*, 2001). AV canal explants in high-glucose

environments show decreases in mesenchymal cell invasion (Enciso *et al.*, 2003). *In vivo*, hyperglycemic conditions reduce VEGF expression in the AV canal myocardium. Addition of VEGF restores EMT under high-glucose conditions whereas treatment with a secreted VEGF receptor inhibits EMT. This VEGF-mediated increase in EMT is contradictory to reports of VEGF treatments causing decreases in endocardial cushion EMT (Dor *et al.*, 2001). Perhaps subtle VEGF gene dosage differences can be the difference between stimulation and inhibition of EMT. Matrix metalloprotease 2 (MMP-2) expression is also decreased in a high-glucose environment, suggesting that hyperglycemia also affects factors necessary for mesenchymal invasion (Enciso *et al.*, 2003). Hyperglycemia causes decreases in VEGF expression that negatively affect endocardial cushion development, contributing to the increased incidence of congenital heart defects in children born to diabetic mothers.

B. Transcription Factors

1. NFATc

Nuclear factor of activated T cells (NFATc) is a transcription factor with expression in the endocardium of the heart (de la Pompa *et al.*, 1998; Ranger *et al.*, 1998). NFATc is activated by the calmodulin-dependent, calcium-activated protein phosphatase calcineurin (Emmel *et al.*, 1989). Genetically engineered mice lacking NFATc have hypoplastic semilunar and AV valves and ventricular septal defects (de la Pompa *et al.*, 1998; Ranger *et al.*, 1998). Mesenchymal cells populate both the AV and conotruncal cushions in *NFATc*^{-/-} embryos, suggesting NFATc is not required for EMT. In fact, NFATc expression is lost as cells transform from endocardial cells into mesenchymal cells (de la Pompa *et al.*, 1998; Ranger *et al.*, 1998). *NFATc*^{-/-} mice also have underdeveloped semilunar and AV valves at E13.5 (de la Pompa *et al.*, 1998). These data suggest that NFATc may be critical for regulating cell proliferation in post-EMT valvuloseptal morphogenesis at the leading edges of forming valve and septum projections.

2. NF-1

NF-1 is encoded by a tumor suppressor gene associated with the genetic disorder neurofibromatosis type I (Sawada *et al.*, 1996). Ablation of NF-1 in mice results in embryonic death with cardiovascular defects that include hypercellular cardiac cushions (Lakkis and Epstein, 1998). Loss of NF-1 specifically in endocardial cells resulted in increased MAPK phosphorylation and hypercellular cardiac cushions (Gitler *et al.*, 2003b). The defects in NF-1

null mice were originally thought to be secondary to cardiac neural crest deficiencies (Lakkis and Epstein, 1998). Gene inactivation of NF-1 in neural crest cells did not result in defects similar to those seen in conventional or endocardial specific NF-1 knockout animals (Gitler *et al.*, 2003b; Lakkis and Epstein, 1998). These data are consistent with a model in which NF-1 signaling in cardiac cushions regulates Ras activity as required for mesenchymal cell proliferation and valve remodeling. Similar to Smad-6 and EGF, NF-1 negatively regulates cell proliferation to maintain a balance between growth and differentiation in developing endocardial cushions.

NF-1 and Ras appear to be upstream of NFATc in a cardiac cushion intracellular signaling pathway. Nuclear localization of NFATc increased in mice with endocardial-specific NF-1 gene inactivation as well as in heart explants overexpressing constitutively active Ras (Gitler *et al.*, 2003b). The significance of NFATc endocardial cell nuclear localization is not presently understood but may be involved in sustaining endocardial cell morphology (Akiyama *et al.*, 2004).

3. Sox-9

Sox-9 encodes a high-mobility group transcription factor that is expressed in various developmental tissues, including the cardiac cushions (Ng *et al.*, 1997; Zhao *et al.*, 1997). Heterozygous *Sox-9* mutations cause campomelic dysplasia, which is characterized by hypoplasia of the endochondrial bones, XY sex reversal, kidney and pancreas defects, as well as ventricular septal defects and the Tetralogy of Fallot (Houston *et al.*, 1983). *Sox-9* is expressed in the mesenchymal cells, but not endocardial cells, of AV and outflow tract endocardial cushions (Akiyama *et al.*, 2004). Homozygous *Sox-9* null mice die from cardiac insufficiency at about 12.5 days postcoitus (12.5dpc) and display severely underdeveloped cardiac cushions. The hypocellular cardiac cushions in *Sox-9* null mice are due, at least in part, to decreased cell proliferation. Floxed *Sox-9* mice were mated with mice harboring the *Wnt-1-Cre* transgene (neural crest specific expression) to test whether the outflow tract cushion defects are due to improper cardiac neural crest contribution. Lack of *Sox-9* in neural crest cells results in defects in the distal (truncus) but not proximal (conus) outflow tract. This demonstrates that *Sox-9* is required for cushion mesenchyme contribution from both neural crest and endocardial cells (Akiyama *et al.*, 2004).

NFATc, normally expressed only in the endocardium of the heart (de la Pompa *et al.*, 1998; Ranger *et al.*, 1998), is expressed ectopically in the mesenchyme of *Sox-9*^{-/-} embryos. In normal embryos when endocardial cells transform into mesenchyme they lose NFATc expression and activate *Sox-9* expression. In mice lacking *Sox-9*, NFATc continued to be expressed in transforming cells near the endocardial layer. This ectopic

NFATc expression indicates that Sox-9 mutants initiate EMT but subsequent differentiation into mature mesenchyme is defective (Akiyama *et al.*, 2004). Sox-9 seemingly promotes a mesenchymal cell phenotype through inhibition of NFATc transcription.

ErbB3, an epidermal growth factor receptor tyrosine kinase normally expressed in the endocardial cushion mesenchyme, was undetectable in Sox-9 homozygotes (Akiyama *et al.*, 2004). *ErbB3* null mice also have hypoplastic cardiac cushions much like those of Sox-9 mutants, implicating ErbB3 in a regulatory pathway mediated by Sox-9 in cardiac cushion mesenchyme. A potential interaction between Wnt signal transduction components and Sox-9 may also exist. Sox-9 is expressed in the highly proliferative domains of developing interstitial epithelium, similar to expression domains of Wnt signaling components. Effectors of canonical Wnt signaling are required for Sox-9 expression in epithelial cells of the intestine (Blache *et al.*, 2004). Wnt/ β -catenin may also promote cell transformation by activating Sox-9 expression in the endocardial cushions. Sox transcription factors, including Sox-9, are involved in a signaling cascade that promotes neural crest EMT (Cheung and Briscoe, 2003; Perez-Alcala *et al.*, 2004). Sox-5 overexpression in the dorsal neural tube activates the small GTPase RhoB. RhoB is important for the delamination of neural crest cells and lies downstream of Slug (del Barrio and Nieto, 2002; Liu and Jessell, 1998). Sox-9 could function in a similar way to promote mesenchymal cell formation in endocardial cushions.

4. TBX-5

TBX-5 is a transcription factor involved in cardiac septum formation. *TBX-5* mutations cause Holt-Oram syndrome, an autosomal dominant disorder characterized by skeletal and cardiac defects (Basson *et al.*, 1997; Li *et al.*, 1997b). The most frequently seen cardiac defects in Holt-Oram syndrome include atrial septal defects, ventricular septal defects, and occasionally the Tetralogy of Fallot. A mouse model harboring inactivated *TBX-5* alleles displays septal defects similar to those of humans with Holt-Oram syndrome (Bruneau *et al.*, 2001). With TBX-5 expression, throughout the myocardium, it is difficult to assess a direct functional role of TBX-5 in cushion development. Loss of TBX-5 in the myocardium could result in cardiac cushion defects secondary to myocardial dysfunction.

5. GATA-4 and Fog-2

The GATA family of transcription factors plays an important role during specification of cardiac myocardium during early heart development. Developing cardiac tissues express GATA-4, GATA-5, and GATA-6 (Parmacek

and Leiden, 1999). GATA factors physically interact with other transcription factors to regulate gene expression. Humans with GATA-4 mutations have atrial septal defects, ventricular septal defects, atrioventricular canal defects, and pulmonary valve thickening (Garg *et al.*, 2003).

Interaction of GATA-4 with FOG-2 (Friend of GATA) results in synergistic activation or repression of GATA dependent cardiac promoters (Lu *et al.*, 1999a). Embryonic and adult myocardium expresses FOG-2 (Lu *et al.*, 1999a). *FOG-2*^{-/-} embryos die during midgestation and display cardiac defects including thinned ventricular myocardium, common atrioventricular canal, and the tetralogy of Fallot (Tevosian *et al.*, 2000). The defects seen in humans with GATA-4 mutations were similar to those observed in *FOG-2*^{-/-} mouse embryos, consistent with FOG-2 and GATA-4 signaling in the same pathway during heart development. A heterozygous G296S missense mutation in GATA-4 found in all members of one family caused diminished DNA binding and activity of GATA-4. This glycine-to-serine mutation also resulted in a loss of GATA-4 binding to the transcription factor TBX-5 (Garg *et al.*, 2003). Similar to TBX-5, the myocardial expression of GATA-4 and FOG-2 suggests cardiac cushion-derived defects are likely secondary to myocardial dysfunction.

Zebrafish with the cardiofunk mutation fail to form cardiac cushions due to a point mutation in a novel sarcomeric actin (Bartman *et al.*, 2004). This point mutation inhibits actin polymerization and myocardial function. In addition, silent heart embryos lack a heartbeat because of a mutation in cardiac troponin T and do not form cardiac cushions. Myocardial dysfunction rather than a lack of blood flow seems to be the reason for this lack of endocardial cushion formation in both cardiofunk and silent heart mutants (Bartman *et al.*, 2004). Other mutations of genes expressed throughout the myocardium (*GATA-4*, *FOG-2*, and *TBX-5*) could also be affecting endocardial cushions secondary to more global problems with myocardial function.

6. Nkx2.5

The transcription factor Nkx2.5 is also involved in early myocardial lineage specification (Cleaver *et al.*, 1996). Nkx2.5 knockout mice have a range of defects including myocardial thinning and a failure to undergo cardiac looping (Lyons *et al.*, 1995). Humans with Nkx2.5 mutations display atrial septal defects, late-onset heart block, and infrequently VSDs (Schott *et al.*, 1998). Nkx2.5, GATA-4, and TBX-5 all bind to each other (Garg *et al.*, 2003) and all seem to be necessary for proper atrial and septa development. Nkx2.5 knockout mice fail to develop left atrial-restricted expression of the transcription factor E-hand. Loss of Nkx2.5 function therefore may function to specify the correct position of atrial septum formation. Atrioventricular node

abnormalities coupled with defective atrial septation suggest that compromised myocardial function is responsible for heart defects in humans with *Nkx2.5* mutations.

7. *Pitx2*

Pitx2 is a homeodomain transcription factor known to play important roles in cardiogenesis. Four *Pitx2* isoforms (a, b, c, and d) arise from alternative splicing (Schweickert *et al.*, 2000). Only *Pitx2c* has asymmetrical expression during embryogenesis (Campione *et al.*, 2001; Kitamura *et al.*, 1999; Schweickert *et al.*, 2000). *Pitx2c* is expressed in the left myocardial precursors at the tubular heart stages. *Pitx2c* expression persists in the left atrium, the medial aspect of the left ventricle, the right ventricle, and the left side of the outflow tract (Franco and Campione, 2003). Inactivation of *Pitx2c* by homologous recombination results in AVSD and double outlet right ventricle (DORV) (Liu *et al.*, 2001, 2002). Compound mutant mice harboring null alleles for *Pitx2a*, *Pitx2b*, and *Pitx2c* display cardiac defects similar to those of *Pitx2c*^{-/-} embryos and persistent truncus arteriosus (Gage *et al.*, 1999; Kitamura *et al.*, 1999; Liu *et al.*, 2001; Lu *et al.*, 1999b). AV canal cushions showed prominent growth in *Pitx2a*, *Pitx2b*, and *Pitx2c* mutants (Gage *et al.*, 1999; Kitamura *et al.*, 1999; Liu *et al.*, 2001; Lu *et al.*, 1999b). *Pitx2* expression in the myocardium of the AV junction could affect endocardial cell transformation or endocardial cushion cell proliferation (Kitamura *et al.*, 1999). Lineage-tracing experiments show that *Pitx2*-expressing cells migrate from the myocardium into the developing atrioventricular endocardial cushions; *Pitx2c* null animals lack this cellular migration (Liu *et al.*, 2002). The precise mechanism by which hypercellular cushions in *Pitx2a*, *Pitx2b*, and *Pitx2c* null embryos contribute to the common AV canal phenotype is not completely understood. Abnormal cardiac looping, including excessive rightward shifting of the AV canal and deficient leftward shifting of the outflow tract, could account for the observed AVSD and DORV.

C. Extracellular Matrix and Mesenchymal Cell Invasion

The characterization of extracellular matrix components found in endocardial cushions uncovered several substrates capable of supporting mesenchymal cell migration. The acellular layer between the myocardium and endocardium consists of glycosaminoglycans (hyaluronan and chondroitin sulfate), glycoproteins (fibronectin, laminin, vitronectin, cytotoxin, fibulin, and thrombospondin), collagens (I, III, and IV), and various proteoglycans (Little and Rongish, 1995). Immunostaining of cryopreserved chicken hearts with antibodies to fibronectin (FN), laminin, collagen IV, and heparan

sulfate proteoglycan (HSPG) reveals an organization that closely resembles that of a conventional basement membrane (Kitten *et al.*, 1987). It was proposed that the cardiac jelly is a fusion between a larger, myocardially derived basement membrane, having a lamina densa and an extended reticular lamina, and an endothelial-derived basement membrane composed of only a lamina densa (Kitten *et al.*, 1987).

Early studies investigating the composition of cardiac jelly components reported secretion of both chondroitin sulfate and hyaluronan from the myocardium (Manasek *et al.*, 1970, 1973). These glycosaminoglycans are highly charged hydrophilic molecules, the presence of which likely promotes swelling of the acellular space and creates an environment conducive for cell invasion (Manasek *et al.*, 1975; Markwald *et al.*, 1972, 1977). Radioactive labeling studies suggested that the vast majority of the extracellular matrix in cardiac cushions was produced by the myocardium (Krug *et al.*, 1985).

Expression and functional analysis point to an important role for fibronectin during cardiac cushion EMT and mesenchymal cell migration. At stages before migration, both the myocardium and endocardium of cardiac cushions express fibronectin (Ffrench-Constant and Hynes, 1988). Once mesenchymal migration begins, myocardial cells no longer synthesize fibronectin while endocardial and mesenchymal cells continue to express fibronectin (Ffrench-Constant and Hynes, 1988). Addition of RGD peptides, which disrupt integrin–fibronectin binding, produces a rounded cell morphology in AV canal explants (Loeber and Runyan, 1990). Laminins also seem important for mesenchymal cell migration. Another competitive inhibitory peptide, YIGSR, binds to the cell adhesion domain of laminin B1 and reduces mesenchyme migration in AV canal cultures (Loeber and Runyan, 1990). Fibronectin and laminins appear to provide important extracellular matrix anchors to support cell adhesion and mesenchyme cell migration. Future studies will likely focus on understanding the specific interactions between cell surface receptors (integrins) and surrounding extracellular matrix that are essential for mesenchymal cell migration.

1. Hyaluronan

The glycosaminoglycan hyaluronan (HA) is a major constituent of the cardiac cushions (Markwald *et al.*, 1978). Hyaluronidase treatments of EDTA-soluble heart ECM fractions allowed for cellular hypertrophy (activation) but not migration of cushion endothelial cells. This suggested that intact hyaluronan is not necessary for endothelial cell activation but rather for later mesenchymal cell invasion. Surprisingly, hyaluronidase treatments of EDTA-soluble heart fractions coupled with addition of exogenous hyaluronan did not completely recapitulate cushion EMT (Krug *et al.*, 1985). This was interpreted to suggest the requirement for a structural organization

or presentation of the ECM stimulus that was not replaced by the addition of exogenous hyaluronan to the heart fraction. Data demonstrate that HA provides an inductive stimulus necessary for cardiac cushion EMT. Mice null for hyaluronan synthetase 2 (Has-2), the principal synthetic enzyme for HA production in early development, completely lack cardiac cushions (Camenisch *et al.*, 2000). Cardiac cushion endocardial and mesenchymal cells express Has-2 during EMT. This restricted expression pattern of Has-2 suggests that localized HA production facilitates cell transformation and/or mesenchymal cell migration. AV canal explants from *Has-2*^{-/-} embryos fail to undergo EMT in the collagen gel explant system. Addition of exogenous hyaluronan or constitutively active Ras rescued EMT in Has-2 null AV canal explants. A dominant negative Ras construct inhibited mesenchymal cell formation in hyaluronan-rescued Has-2 null explants. These data indicate that hyaluronan is sufficient to induce EMT in *Has-2*^{-/-} embryos and that this induction may be mediated by Ras (Camenisch *et al.*, 2000). Taken together, these studies suggest that hyaluronan possesses dual functions during endocardial cushion development. Hyaluronan appears necessary for endocardial cushion formation and subsequent induction of EMT. It remains to be determined whether hyaluronan acts directly through an unidentified receptor or whether its effects on EMT are indirect.

2. Collagen VI

The majority of clinical heart defects involving abnormal AV cushion morphogenesis are diagnosed in infants with trisomy 21 (Down syndrome) (Korenberg *et al.*, 1992). Likewise, most heart defects in trisomy 21 infants are atrioventricular septal defects (AVSDs) (Adams *et al.*, 1981; Carmi *et al.*, 1992). This association has led to speculation that chromosome 21 genes are important in AV valve development. Genetic analyses have shown that variations in the collagen type VI (Col VI) locus on chromosome 21 are associated with AVSD in trisomy 21 (Davies *et al.*, 1995). A potential role for Col VI, a microfibrillar component of the ECM (Aumailley *et al.*, 1989, 1991), in AV valve morphogenesis is supported by its expression pattern in the developing heart. Col VI is expressed commensurate with cell migration within the developing AV cushions. Later in development, Col VI forms an organized extracellular network within the valve leaflets (Klewer *et al.*, 1998). In human trisomy 21 and normal fetal hearts, consistent with gene dosage predictions, Col VI is increased in trisomy 21 AV valves. Importantly, however, increased Col VI immunoreactivity is similar in trisomy 21 hearts with AVSD and those without a congenital heart defect (CHD) (Gittenberger-de Groot *et al.*, 2003). These data indicate that, although Col VI is an excellent molecular marker for cells in the developing AV valves, the clinical association between Col VI and AVSD is not direct.

Computer modeling suggests that an increase in cell adhesion would be sufficient to account for AVSD (Kurnit *et al.*, 1985). In quantitative cell adhesion assays, trisomy 21 fibroblasts display increased adhesion for Col VI compared with normal cells. Targeting integrin receptors with specific function-blocking antibodies identifies $\alpha_3\beta_1$ as the predominant integrin mediating both trisomy 21 and nontrisomic skin fibroblast adhesion on Col VI (Jongewaard *et al.*, 2002). These studies provide a cellular mechanism that is completely consistent with AVSD computer-modeling predictions.

3. Fibullins and Fibrillin-2

In an effort to define cardiac cushion specific cell surface endocardial markers, the endocardium of AV canals was used to create monoclonal antibodies. One of these antibodies, JB3, recognizes only a subset of endocardial cells in the cardiac cushions (Mjaatvedt *et al.*, 1998; Wunsch *et al.*, 1994). JB3 recognizes a protein of about 350 kDa (Wunsch *et al.*, 1994) that was later identified to be fibrillin-2 (Rongish *et al.*, 1998). Fibrillin-2 is a secreted multidomain protein that contains two RGD motifs shown to be important for binding to fibronectin (Pierschbacher and Ruoslahti, 1984). A functional role remains to be defined, but fibrillin-2 likely functions as a link between the cell surface and the local extracellular matrix scaffold to promote mesenchymal cell migration within cardiac cushions.

The calcium-binding glycoproteins, fibulins, are extracellular matrix components found specifically in endocardial cushions. Fibulin-1 is localized to the entire thickness of the cardiac cushions before EMT and subsequently becomes highly enriched on the surfaces of migratory mesenchymal cells (Spence *et al.*, 1992). Fibulin-1, as well as fibulin-2, are expressed in endocardial cushion tissues and colocalize with fibronectin (Bouchev *et al.*, 1996; Zhang *et al.*, 1995). The interaction of fibulin-1 with fibronectin (Balbona *et al.*, 1992) was shown to be important for fibulin-1 assembly into cultured cell extracellular matrices (Godyna *et al.*, 1996; Roman and McDonald, 1993). Although fibulins are spatially restricted in the cardiac cushion extracellular matrix and are likely functionally important during mesenchymal cell migration, functional analysis of fibulins during cardiac cushion development has not been reported.

4. Matrix Metalloproteinase 2

Matrix metalloproteinases (MMPs) are a family of extracellular proteinases that degrades a wide variety of extracellular matrix components. MMP activity promotes metastatic growth in several animal model systems and therefore has been an area of intense research. Many of the same factors involved in cell transformation and migration in tumor metastasis

also function during EMT in endocardial cushions. MMPs are not an exception.

Mesenchymal cell migration in cardiac cushions is facilitated by the presence of the matrix metalloprotease (MMP-2). *In situ* hybridization analysis reveals high levels of MMP-2 restricted to the cardiac cushions during EMT and subsequent mesenchymal cell migration (Alexander *et al.*, 1997). Expression of the MMP-2 activator MT-MMP is upregulated during stages of mesenchymal cell migration in quail embryos (Alexander *et al.*, 1997). This expression pattern suggests that MMP-2 activity is important for mesenchymal cell migration in cardiac cushions. Studies in other contexts show that MMP-2 localized to the surface of invasive cells types through an interaction with $\alpha_v\beta_3$ integrin (Brooks *et al.*, 1996) to create an area of controlled proteolysis that facilitates cell invasion (Deryugina *et al.*, 1997). Inhibitors of MMP-2 abrogate mesenchymal cell migration in the cardiac cushions. Additional *in vitro* studies in avian embryos showed that MMP-2 promotes cardiac cushion mesenchymal cell migration by degrading type IV collagen, a major constituent of cardiac cushions (Song *et al.*, 2000). In addition, TGF- β_3 upregulates expression of MMP-2 when overexpressed in AV canals (Song *et al.*, 2000). Increasing evidence shows that MMPs also promote tumor progression and metastatic cell migration by affecting nonmatrix factors (Coussens *et al.*, 2002). MMPs could be modulating growth factor activity levels, growth factor receptor properties, or even adhesion molecules to affect endocardial cushion mesenchymal cell migration.

5. Urokinase and Plasmin

Urokinase is a serine protease that modulates the extracellular matrix of cardiac cushions, facilitating mesenchymal cell migration (McGuire and Alexander, 1993a,b). Elevated urokinase expression and activity in the endocardial cell layer correlate with the onset of EMT in the AV and outflow tract endocardial cushions (McGuire and Alexander, 1993a,b). Inhibition of urokinase activity with phosphatidylinositol-specific phospholipase C or antisense oligonucleotides disrupt AV and outflow tract mesenchymal cell motility *in vitro* (McGuire and Alexander, 1993a).

Urokinase activity is regulated by hepatocyte growth factor (HGF) in endocardial cushions (Song *et al.*, 1999). HGF protein localizes to the myocardium of the AV and outflow tract cushions of stage 18 and stage 24 avian embryos. HGF treatment of isolated cardiac cushion endocardium results in increased mesenchymal cell motility, proliferation, and urokinase activity (Song *et al.*, 1999). Ets-2 transcription factor is expressed in endocardial cushion mesenchyme and was shown to interact with the urokinase promoter (Majka and McGuire, 1997), although it is not known whether HGF stimulates Ets-2 in the cardiac cushions. *In situ* hybridization studies

show HGF receptor expression in the endocardium of cardiac cushions. These data support a mechanism by which HGF is secreted by the cardiac cushion myocardium and binds to endocardial cells to promote cell transformation and migration (Song *et al.*, 1999). The mechanism of urokinase activation of mesenchymal cell motility is not fully understood. Urokinase cleaves inactive pro-HGF and may create a positive feedback loop during mesenchymal cell migration (Song *et al.*, 1999). Of course, urokinase may also cleave other inactive growth factors, such as latent TGF- β s.

IV. Integration of Molecular Pathways Governing Cardiac EMT

Prevalvular mesenchyme formation is a prototypical EMT event sharing similar molecular cascades responsible for other developmental EMTs, including gastrulation, neural crest cell formation, branching morphogenesis in the lung, somite development, and coronary artery development. Although EMT during development is believed to represent a non-cell-autonomous process (Boyer *et al.*, 2000), it is probable that similar pathways are also activated during cell-autonomous cell transformations that occur in cancer. Wnts, TGF- β s, BMPs, EGFs, HGFs, and Notch/Jagged all function prominently during most developmental and cancerous cell transformations. Research is beginning to integrate these pathways to create a more complete understanding of EMT.

In the endocardial cushions, many examples of pathway integration are being uncovered. For example, EGF signaling negatively regulates cell proliferation and possibly EMT in cardiac cushions (Chen *et al.*, 2000). Loss of HB-EGF results in increased phosphorylation of BMP Smads, suggesting that EGF modulates BMP-mediated proliferation or EMT (Jackson *et al.*, 2003). BMP pathways also regulate endocardial cushion TGF- β expression. Myocardial-specific inactivation of the BMP receptor ALK-3 causes diminished expression of the positive EMT stimulus, TGF- β_2 (Gaussin *et al.*, 2002). Notch signaling also seems to affect TGF- β_2 expression. Inhibition of Notch in the endocardium reduces myocardial TGF- β_2 expression. Functional Notch receptors are not expressed in the myocardium, and therefore Notch could promote a novel endocardial signal that establishes the restricted AV myocardial expression of TGF- β_2 (Timmerman *et al.*, 2004). TGF- β_2 activates EMT in the heart by inducing expression of the transcription factor Slug (Romano *et al.*, 1999). Snail, a Slug family member, is known to inhibit E-cadherin expression and to promote EMT in other developmental EMTs (Battle *et al.*, 2000; Cano *et al.*, 2000). Notch mutants show a severe reduction in endocardial cushion Slug and VE-cadherin expression, and this may occur through downregulation of TGF- β_2 expression (Timmerman *et al.*, 2004).

TGF- β_2 may also be in a molecular cascade involving Wnt/ β -catenin and Sox-9. TGF- β_2 fails to induce EMT in β -catenin null hearts despite phosphorylation of Smad-2 and Smad-3 (Liebner *et al.*, 2004). This suggests that β -catenin is downstream of Smads in an EMT induction cascade. Wnt/ β -catenin signaling is required for Sox-9 expression in the developing intestinal crypts (Blache *et al.*, 2004). Wnts and Sox-9 are also important regulators of neural crest delamination (Cheung and Briscoe, 2003; Dearnorff *et al.*, 2001). β -Catenin activity becomes apparent in the cushion endocardial cells just before they transform into mesenchymal cells expressing Sox-9. Although not directly tested yet, β -catenin likely activates Sox-9 expression during cell transformation in endocardial cushions. Sox-9 expression subsequently turns off endocardial-specific expression and turns on mesenchymal cell effectors. Sox-9 promotes mesenchymal cell formation by repressing endocardial NFATc expression and promoting mesenchymal cell ErbB3 expression (Akiyama *et al.*, 2004). Hyaluronan and EGF pathways also interact to direct mesenchymal cell formation in endocardial cushions. Heregulin activates ErbB2 and ErbB3 and rescues EMT in Has-2 null hearts. Rescue of EMT in Has-2 null hearts with hyaluronan is also associated with phosphorylation of ErbB3. These data suggest that ErbB3 receptor activation is downstream of hyaluronan in an EMT inductive pathway (Camenisch *et al.*, 2002b). Further dissections of the molecular interactions during valve formation will not only affect our knowledge of overall cushion morphogenesis but may also provide insight into basic EMT mechanisms that could be applied to other developmental and cancerous cell transformation events.

V. The Future of Cardiac Cushion Development

Many growth factors, secreted growth factor inhibitors, growth factor receptors, intracellular signaling mediators, and extracellular matrix components have been shown to play a role in endocardial cushion morphogenesis. With the advent of Cre/*lox*-mediated gene inactivation, future studies will clarify functional requirements for many of these factors in development. Studies using mouse genetics will no longer report how one gene is involved in heart development, but rather will focus on how the loss or overexpression of that gene affects expression of other genes. Mouse genetics, retroviral gene delivery, and the collagen gel explant system provide powerful tools with which to understand the interplay between different factors known to be involved in EMT and cushion morphogenesis. Integrating some of the pathways already known to direct cardiac cushion development is already underway (Akiyama *et al.*, 2004).

Significant progress has been made in understanding the molecular and cellular mechanisms directing EMT in cardiac cushion development, but much work remains to be done. Researchers are now beginning to investigate the mechanisms involved in transforming naive endocardial cushions into mature valves and septa. The proliferative forces that direct endocardial cushion expansion and remodeling are just beginning to be understood (Jiao *et al.*, 2003; Sugi *et al.*, 2003). Further investigations into tissue-specific expression and function of various factors will provide a complex multitissue understanding of later cushion development.

Acknowledgments

Anthony Person was supported by American Heart Association Predoctorate Fellowship 0215182Z. Research on heart development in the coauthor's laboratories is supported by Projects 1 and 3 of National Institutes of Health Program Project Grant 5P01HL063926.

References

- Adams, M. M., Erickson, J. D., Layde, P. M., and Oakley, G. P. (1981). Down's syndrome: Recent trends in the United States. *JAMA* **246**, 758–760.
- Akhurst, R. J., Lehnert, S. A., Faissner, A., and Duffie, E. (1990). TGF β in murine morphogenetic processes: The early embryo and cardiogenesis. *Development* **108**, 645–656.
- Akiyama, H., Chaboissier, M. C., Behringer, R. R., Rowitch, D. H., Schedl, A., Epstein, J. A., and De Crombrughe, B. (2004). Essential role of Sox9 in the pathway that controls formation of cardiac valves and septa. *Proc. Natl. Acad. Sci. USA* **101**, 6502–6507.
- Alexander, S. M., Jackson, K. J., Bushnell, K. M., and McGuire, P. G. (1997). Spatial and temporal expression of the 72-kDa type IV collagenase (MMP-2) correlates with development and differentiation of valves in the embryonic avian heart. *Dev. Dyn.* **209**, 261–268.
- Anderson, R. H., Webb, S., Brown, N. A., Lamers, W., and Moorman, A. (2003a). Development of the heart. 2. Septation of the atriums and ventricles. *Heart* **89**, 949–958.
- Anderson, R. H., Webb, S., Brown, N. A., Lamers, W., and Moorman, A. (2003b). Development of the heart. 3. Formation of the ventricular outflow tracts, arterial valves, and intrapericardial arterial trunks. *Heart* **89**, 1110–1118.
- Annes, J. P., Munger, J. S., and Rifkin, D. B. (2003). Making sense of latent TGF β activation. *J. Cell Sci.* **116**, 217–224.
- Antin, P. B., Taylor, R. G., and Yatskiyevych, T. (1994). Precardiac mesoderm is specified during gastrulation in quail. *Dev. Dyn.* **200**, 144–154.
- Aumailley, M., Mann, K., von der Mark, H., and Timpl, R. (1989). Cell attachment properties of collagen type VI and Arg-Gly-Asp dependent binding to its α_2 (VI) and α_3 (VI) chains. *Exp. Cell Res.* **181**, 463–474.
- Aumailley, M., Specks, U., and Timpl, R. (1991). Cell adhesion to type-VI collagen. *Biochem. Soc. Trans.* **19**, 843–847.
- Balbona, K., Tran, H., Godyna, S., Ingham, K. C., Strickland, D. K., and Argraves, W. S. (1992). Fibulin binds to itself and to the carboxyl-terminal heparin-binding region of fibronectin. *J. Biol. Chem.* **267**, 20120–20125.

- Baldwin, H. S., Shen, H. M., Yan, H. C., DeLisser, H. M., Chung, A., Mickanin, C., Trask, T., Kirschbaum, N. E., Newman, P. J., and Albelda, S. M. (1994). Platelet endothelial cell adhesion molecule-1 (PECAM-1/CD31): Alternatively spliced, functionally distinct isoforms expressed during mammalian cardiovascular development. *Development* **120**, 2539–2553.
- Barnes, D. W. (1982). Epidermal growth factor inhibits growth of A431 human epidermoid carcinoma in serum-free cell culture. *J. Cell Biol.* **93**, 1–4.
- Bartman, T., Walsh, E. C., Wen, K. K., McKane, M., Ren, J., Alexander, J., Rubenstein, P. A., and Stainier, D. Y. (2004). Early myocardial function affects endocardial cushion development in zebrafish. *PLoS Biol.* **2**, E129.
- Basson, C. T., Bachinsky, D. R., Lin, R. C., Levi, T., Elkins, J. A., Soultz, J., Grayzel, D., Kroumpouzou, E., Traill, T. A., Leblanc-Straceski, J., Renault, B., Kucherlapati, R., Seidman, J. G., and Seidman, C. E. (1997). Mutations in human *TBX5* [corrected] cause limb and cardiac malformation in Holt-Oram syndrome *Nat. Genet.* **15**, 30–35 [Published erratum appears in *Nat. Genet.* **15**, 411].
- Battle, E., Sancho, E., Franci, C., Dominguez, D., Monfar, M., Baulida, J., and Garcia De Herreros, A. (2000). The transcription factor snail is a repressor of E-cadherin gene expression in epithelial tumour cells. *Nat. Cell Biol.* **2**, 84–89.
- Bernanke, D. H., and Markwald, R. R. (1982). Migratory behavior of cardiac cushion tissue cells in a collagen–lattice culture system. *Dev. Biol.* **91**, 235–245.
- Blache, P., van de Wetering, M., Duluc, I., Domon, C., Berta, P., Freund, J. N., Clevers, H., and Jay, P. (2004). SOX9 is an intestine crypt transcription factor, is regulated by the Wnt pathway, and represses the CDX2 and MUC2 genes. *J. Cell Biol.* **166**, 37–47.
- Bouchey, D., Argraves, W. S., and Little, C. D. (1996). Fibulin-1, vitronectin, and fibronectin expression during avian cardiac valve and septa development. *Anat. Rec.* **244**, 540–551.
- Bourdeau, A., Dumont, D. J., and Letarte, M. (1999). A murine model of hereditary hemorrhagic telangiectasia. [see comment] *J. Clin. Invest.* **104**, 1343–1351.
- Boyer, A. S., Ayerinkas, II, Vincent, E. B., McKinney, L. A., Weeks, D. L., and Runyan, R. B. (1999). TGF β_2 and TGF β_3 have separate and sequential activities during epithelial–mesenchymal cell transformation in the embryonic heart. *Dev. Biol.* **208**, 530–545.
- Boyer, A. S., Finch, W. T., and Runyan, R. B. (2000). Trichloroethylene inhibits development of embryonic heart valve precursors *in vitro* [see comment] *Toxicol. Sci.* **53**, 109–117.
- Brooks, P. C., Stromblad, S., Sanders, L. C., von Schalscha, T. L., Aimes, R. T., Stetler-Stevenson, W. G., Quigley, J. P., and Cheresch, D. A. (1996). Localization of matrix metalloproteinase MMP-2 to the surface of invasive cells by interaction with integrin $\alpha_v\beta_3$. *Cell* **85**, 683–693.
- Brown, C. B., Boyer, A. S., Runyan, R. B., and Barnett, J. V. (1996). Antibodies to the type II TGF β receptor block cell activation and migration during atrioventricular cushion transformation in the heart. *Dev. Biol.* **174**, 248–257.
- Brown, C. B., Boyer, A. S., Runyan, R. B., and Barnett, J. V. (1999). Requirement of type III TGF- β receptor for endocardial cell transformation in the heart. *Science* **283**, 2080–2082.
- Brown, C. B., Feiner, L., Lu, M. M., Li, J., Ma, X., Webber, A. L., Jia, L., Raper, J. A., and Epstein, J. A. (2001). PlexinA2 and semaphorin signaling during cardiac neural crest development. *Development* **128**, 3071–3080.
- Bruneau, B. G., Nemer, G., Schmitt, J. P., Charron, F., Robitaille, L., Caron, S., Conner, D. A., Gessler, M., Nemer, M., Seidman, C. E., and Seidman, J. G. (2001). A murine model of Holt-Oram syndrome defines roles of the T-box transcription factor *Tbx5* in cardiogenesis and disease. *Cell* **106**, 709–721.
- Butler, H., and Juurlink, B. H. J. (1987). *An Atlas for Staging Mammalian and Chick Embryos*. CRC Press, Boca Raton, FL.
- Camenisch, T. D., Spicer, A. P., Brehm-Gibson, T., Biesterfeldt, J., Augustine, M. L., Calabro, A., Jr., Kubalak, S., Klewer, S. E., and McDonald, J. A. (2000). Disruption of hyaluronan

- synthase-2 abrogates normal cardiac morphogenesis and hyaluronan-mediated transformation of epithelium to mesenchyme. [see comment] *J. Clin. Invest.* **106**, 349–360.
- Camenisch, T. D., Molin, D. G., Person, A., Runyan, R. B., Gittenberger-de Groot, A. C., McDonald, J. A., and Klewer, S. E. (2002a). Temporal and distinct TGF β ligand requirements during mouse and avian endocardial cushion morphogenesis. *Dev. Biol.* **248**, 170–181.
- Camenisch, T. D., Schroeder, J. A., Bradley, J., Klewer, S. E., and McDonald, J. A. (2002b). Heart-valve mesenchyme formation is dependent on hyaluronan-augmented activation of ErbB2-ErbB3 receptors. *Nat. Med.* **8**, 850–855.
- Campione, M., Ros, M. A., Icardo, J. M., Piedra, E., Christoffels, V. M., Schweickert, A., Blum, M., Franco, D., and Moorman, A. F. (2001). Pitx2 expression defines a left cardiac lineage of cells: Evidence for atrial and ventricular molecular isomerism in the *iv/iv* mice. *Dev. Biol.* **231**, 252–264.
- Cano, A., Perez-Moreno, M. A., Rodrigo, I., Locascio, A., Blanco, M. J., del Barrio, M. G., Portillo, F., and Nieto, M. A. (2000). The transcription factor Snail controls epithelial–mesenchymal transitions by repressing E-cadherin expression. *Nat. Cell Biol.* **2**, 76–83.
- Carmi, R., Boughman, J. A., and Ferencz, C. (1992). Endocardial cushion defect: Further studies of “isolated” versus “syndromic” occurrence. *Am. J. Med. Genet.* **43**, 569–575.
- Carmona, R., Gonzalez-Iriarte, M., Macias, D., Perez-Pomares, J. M., Garcia-Garrido, L., and Munoz-Chapuli, R. (2000). Immunolocalization of the transcription factor Slug in the developing avian heart. *Anat. Embryol.* **201**, 103–109.
- Cesarman, G. M., Guevara, C. A., and Hajjar, K. A. (1994). An endothelial cell receptor for plasminogen/tissue plasminogen activator (t-PA). II. Annexin II-mediated enhancement of t-PA-dependent plasminogen activation. *J. Biol. Chem.* **269**, 21198–21203.
- Chang, C. (1932). On the reaction of the endocardium to the bloodstream in the embryonic heart, with special reference to the endocardial thickenings in the atrioventricular canal and the bulbus cordis. *Anat. Rec.* **5**, 253–265.
- Chapman, D. L., Garvey, N., Hancock, S., Alexiou, M., Agulnik, S. I., Gibson-Brown, J. J., Cebra-Thomas, J., Bollag, R. J., Silver, L. M., and Papaioannou, V. E. (1996). Expression of the T-box family genes, Tbx1-Tbx5, during early mouse development. *Dev. Dyn.* **206**, 379–390.
- Cheifetz, S., Bellon, T., Cales, C., Vera, S., Bernabeu, C., Massague, J., and Letarte, M. (1992). Endoglin is a component of the transforming growth factor- β receptor system in human endothelial cells. *J. Biol. Chem.* **267**, 19027–19030.
- Chen, B., Bronson, R. T., Klamann, L. D., Hampton, T. G., Wang, J. F., Green, P. J., Magnuson, T., Douglas, P. S., Morgan, J. P., and Neel, B. G. (2000). Mice mutant for *Egfr* and *Shp2* have defective cardiac semilunar valvulogenesis. *Nat. Genet.* **24**, 296–299.
- Cheung, M., and Briscoe, J. (2003). Neural crest development is regulated by the transcription factor Sox9. *Development* **130**, 5681–5693.
- Cleaver, O. B., Patterson, K. D., and Krieg, P. A. (1996). Overexpression of the *tinman*-related genes *XNkx-2.5* and *XNkx-2.3* in *Xenopus* embryos results in myocardial hyperplasia. *Development* **122**, 3549–3556.
- Coussens, L. M., Fingleton, B., and Matrisian, L. M. (2002). Matrix metalloproteinase inhibitors and cancer: Trials and tribulations. *Science* **295**, 2387–2392.
- Crossin, K. L., and Hoffman, S. (1991). Expression of adhesion molecules during the formation and differentiation of the avian endocardial cushion tissue. *Dev. Biol.* **145**, 277–286.
- Davies, G. E., Howard, C. M., Farrer, M. J., Coleman, M. M., Bennett, L. B., Cullen, L. M., Wyse, R. K., Burn, J., Williamson, R., and Kessling, A. M. (1995). Genetic variation in the *COL6A1* region is associated with congenital heart defects in trisomy 21 (Down’s syndrome). *Ann. Hum. Genet.* **59**, 253–269.

- Deardorff, M. A., Tan, C., Saint-Jeannet, J. P., and Klein, P. S. (2001). A role for frizzled 3 in neural crest development. *Development* **128**, 3655–3663.
- De la Cruz, M. V., Gimenez-Ribotta, M., Saravalli, O., and Cayre, R. (1983). The contribution of the inferior endocardial cushion of the atrioventricular canal to cardiac septation and to the development of the atrioventricular valves: Study in the chick embryo. *Am. J. Anat.* **166**, 63–72.
- de la Pompa, J. L., Timmerman, L. A., Takimoto, H., Yoshida, H., Elia, A. J., Samper, E., Potter, J., Wakeham, A., Marengere, L., Langille, B. L., Crabtree, G. R., and Mak, T. W. (1998). Role of the NF-ATc transcription factor in morphogenesis of cardiac valves and septum. *Nature* **392**, 182–186.
- del Barrio, M. G., and Nieto, M. A. (2002). Overexpression of Snail family members highlights their ability to promote chick neural crest formation. *Development* **129**, 1583–1593.
- Delot, E. C., Bahamonde, M. E., Zhao, M., and Lyons, K. M. (2003). BMP signaling is required for septation of the outflow tract of the mammalian heart. *Development* **130**, 209–220.
- Deryugina, E. I., Luo, G. X., Reisfeld, R. A., Bourdon, M. A., and Strongin, A. (1997). Tumor cell invasion through matrigel is regulated by activated matrix metalloproteinase-2. *Anticancer Res.* **17**, 3201–3210.
- Dewulf, N., Verschueren, K., Lonnoy, O., Moren, A., Grimsby, S., Vande Spiegle, K., Miyazono, K., Huylebroeck, D., and Ten Dijke, P. (1995). Distinct spatial and temporal expression patterns of two type I receptors for bone morphogenetic proteins during mouse embryogenesis. *Endocrinology* **136**, 2652–2663.
- Dickson, M. C., Slager, H. G., Duffie, E., Mummery, C. L., and Akhurst, R. J. (1993). RNA and protein localisations of TGF- β 2 in the early mouse embryo suggest an involvement in cardiac development. *Development* **117**, 625–639.
- Donovan, J., Kordylewska, A., Jan, Y. N., and Utset, M. F. (2002). Tetralogy of fallot and other congenital heart defects in *Hey2* mutant mice. *Curr. Biol.* **12**, 1605–1610.
- Dor, Y., and Keshet, E. (1997). Ischemia-driven angiogenesis. *Trends Cardiovasc. Med.* **7**, 289–294.
- Dor, Y., Camenisch, T. D., Itin, A., Fishman, G. I., McDonald, J. A., Carmeliet, P., and Keshet, E. (2001). A novel role for VEGF in endocardial cushion formation and its potential contribution to congenital heart defects. *Development* **128**, 1531–1538.
- Dudley, A. T., and Robertson, E. J. (1997). Overlapping expression domains of bone morphogenetic protein family members potentially account for limited tissue defects in BMP7 deficient embryos. *Dev. Dyn.* **208**, 349–362.
- Dunker, N., and Kriegstein, K. (2002). *Tgfb2^{-/-} Tgfb3^{-/-}* double knockout mice display severe midline fusion defects and early embryonic lethality. *Anat. Embryol.* **206**, 73–83.
- Emmel, E. A., Verweij, C. L., Durand, D. B., Higgins, K. M., Lacy, E., and Crabtree, G. R. (1989). Cyclosporin A specifically inhibits function of nuclear proteins involved in T cell activation. *Science* **246**, 1617–1620.
- Enciso, J. M., Gratzinger, D., Camenisch, T. D., Canosa, S., Pinter, E., and Madri, J. A. (2003). Elevated glucose inhibits VEGF-A-mediated endocardial cushion formation: Modulation by PECAM-1 and MMP-2. *J. Cell Biol.* **160**, 605–615.
- Erickson, S. L., O'Shea, K. S., Ghaboosi, N., Loverro, L., Frantz, G., Bauer, M., Lu, L. H., and Moore, M. W. (1997). ErbB3 is required for normal cerebellar and cardiac development: A comparison with ErbB2- and heregulin-deficient mice. *Development* **124**, 4999–5011.
- Ffrench-Constant, C., and Hynes, R. O. (1988). Patterns of fibronectin gene expression and splicing during cell migration in chicken embryos. *Development* **104**, 369–382.
- Fragale, A., Tartaglia, M., Wu, J., and Gelb, B. D. (2004). Noonan syndrome-associated SHP2/*PTPN11* mutants cause EGF-dependent prolonged GAB1 binding and sustained ERK2/MAPK1 activation. *Hum. Mutat.* **23**, 267–277.

- Franco, D., and Campione, M. (2003). The role of Pitx2 during cardiac development: Linking left-right signaling and congenital heart diseases. *Trends Cardiovasc. Med.* **13**, 157–163.
- Gage, P. J., Suh, H., and Camper, S. A. (1999). The bicoid-related *Pitx* gene family in development. *Mamm. Genome.* **10**, 197–200.
- Galvin, K. M., Donovan, M. J., Lynch, C. A., Meyer, R. I., Paul, R. J., Lorenz, J. N., Fairchild-Huntress, V., Dixon, K. L., Dunmore, J. H., Gimbrone, M. A. Jr., Falb, D., and Huszar, D. (2000). A role for smad6 in development and homeostasis of the cardiovascular system. *Nat. Genet.* **24**, 171–174.
- Gannon, M., and Bader, D. (1995). Initiation of cardiac differentiation occurs in the absence of anterior endoderm. *Development* **121**, 2439–2450.
- Garcia-Martinez, V., and Schoenwolf, G. C. (1993). Primitive-streak origin of the cardiovascular system in avian embryos. *Dev. Biol.* **159**, 706–719.
- Garg, V., Kathiriyai, I. S., Barnes, R., Schluterman, M. K., King, I. N., Butler, C. A., Rothrock, C. R., Eapen, R. S., Hirayama-Yamada, K., Joo, K., Matsuoka, R., Cohen, J. C., and Srivastava, D. (2003). *GATA4* mutations cause human congenital heart defects and reveal an interaction with *TBX5*. *Nature* **424**, 443–447.
- Gaussin, V., Van de Putte, T., Mishina, Y., Hanks, M. C., Zwijsen, A., Huylebroeck, D., Behringer, R. R., and Schneider, M. D. (2002). Endocardial cushion and myocardial defects after cardiac myocyte-specific conditional deletion of the bone morphogenetic protein receptor ALK3. *Proc. Natl. Acad. Sci. USA* **99**, 2878–2883.
- Gill, G. N., and Lazar, C. S. (1981). Increased phosphotyrosine content and inhibition of proliferation in EGF-treated A431 cells. *Nature* **293**, 305–307.
- Gitler, A. D., Lu, M. M., Jiang, Y. Q., Epstein, J. A., and Gruber, P. J. (2003a). Molecular markers of cardiac endocardial cushion development. *Dev. Dynam.* **228**, 643–650.
- Gitler, A. D., Zhu, Y., Ismat, F. A., Lu, M. M., Yamauchi, Y., Parada, L. F., and Epstein, J. A. (2003b). Nf1 has an essential role in endothelial cells. *Nat. Genet.* **33**, 75–79.
- Gittenberger-de Groot, A. C., Bartram, U., Oosthoek, P. W., Bartelings, M. M., Hogers, B., Poelmann, R. E., Jongewaard, I. N., and Klewer, S. E. (2003). Collagen type VI expression during cardiac development and in human fetuses with trisomy 21. *Anat. Rec.* **275A**, 1109–1116.
- Gleizes, P. E., Munger, J. S., Nunes, I., Harpel, J. G., Mazzeri, R., Noguera, I., and Rifkin, D. B. (1997). TGF- β latency: Biological significance and mechanisms of activation. *Stem Cells* **15**, 190–197.
- Godyna, S., Diaz-Ricart, M., and Argraves, W. S. (1996). Fibulin-1 mediates platelet adhesion via a bridge of fibrinogen. *Blood* **88**, 2569–2577.
- Gonzalez-Sanchez, A., and Bader, D. (1990). *In vitro* analysis of cardiac progenitor cell differentiation. *Dev. Biol.* **139**, 197–209.
- Hajjar, K. A., Jacovina, A. T., and Chacko, J. (1994). An endothelial cell receptor for plasminogen/tissue plasminogen activator. I. Identity with annexin II. *J. Biol. Chem.* **269**, 21191–21197.
- Hamburger, V., and Hamilton, H. L. (1951). A series of normal stages in the development of the chick embryo. *J. Morphol.* **88**, 49–92.
- Hata, A., Lagna, G., Massague, J., and Hemmati-Brivanlou, A. (1998). Smad6 inhibits BMP/Smad1 signaling by specifically competing with the Smad4 tumor suppressor. *Genes Dev.* **12**, 186–197.
- Heikinheimo, M., Scandrett, J. M., and Wilson, D. B. (1994). Localization of transcription factor GATA-4 to regions of the mouse embryo involved in cardiac development. *Dev. Biol.* **164**, 361–373.
- Hoffman, J. I. (1990). Congenital heart disease: Incidence and inheritance. *Pediatr. Clin. North Am.* **37**, 25–43.

- Houston, C. S., Opitz, J. M., Spranger, J. W., Macpherson, R. I., Reed, M. H., Gilbert, E. F., Herrmann, J., and Schinzel, A. (1983). The campomelic syndrome: Review, report of 17 cases, and follow-up on the currently 17-year-old boy first reported by Maroteaux *et al.* in 1971. *Am. J. Med. Genet.* **15**, 3–28.
- Hurlstone, A. F., Haramis, A. P., Wienholds, E., Begthel, H., Korving, J., Van Eeden, F., Cuppen, E., Zivkovic, D., Plasterk, R. H., and Clevers, H. (2003). The Wnt/ β -catenin pathway regulates cardiac valve formation. *Nature* **425**, 633–637.
- Hutson, M. R., and Kirby, M. L. (2003). Neural crest and cardiovascular development: A 20-year perspective. *Birth Defects Res. Part C, Embryo Today* **69**, 2–13.
- Iwamoto, R., Yamazaki, S., Asakura, M., Takashima, S., Hasuwa, H., Miyado, K., Adachi, S., Kitakaze, M., Hashimoto, K., Raab, G., Nanba, D., Higashiyama, S., Hori, M., Klagsbrun, M., and Mekada, E. (2003). Heparin-binding EGF-like growth factor and ErbB signaling is essential for heart function. *Proc. Natl. Acad. Sci. USA* **100**, 3221–3226.
- Jackson, L. F., Qiu, T. H., Sunnarborg, S. W., Chang, A., Zhang, C., Patterson, C., and Lee, D. C. (2003). Defective valvulogenesis in HB-EGF and TACE-null mice is associated with aberrant BMP signaling. *EMBO J.* **22**, 2704–2716.
- Jaffee, O. C. (1974). The effects of moderate hypoxia and moderate hypoxia plus hypercapnea on cardiac development in chick embryos. *Teratology* **10**, 275–281.
- Jiang, X., Rowitch, D. H., Soriano, P., McMahon, A. P., and Sucov, H. M. (2000). Fate of the mammalian cardiac neural crest. *Development* **127**, 1607–1616.
- Jiao, K., Kulesa, H., Tompkins, K., Zhou, Y., Batts, L., Baldwin, H. S., and Hogan, B. L. (2003). An essential role of Bmp4 in the atrioventricular septation of the mouse heart. *Genes Dev.* **17**, 2362–2367.
- Jones, C. M., Lyons, K. M., and Hogan, B. L. (1991). Involvement of bone morphogenetic protein-4 (BMP-4) and Vgr-1 in morphogenesis and neurogenesis in the mouse. *Development* **111**, 531–542.
- Jongewaard, I. N., Lauer, R. M., Behrendt, D. A., Patil, S., and Klewer, S. E. (2002). β_1 -Integrin activation mediates adhesive differences between trisomy 21 and non-trisomic fibroblasts on type VI collagen. *Am. J. Med. Genet.* **109**, 298–305.
- Kaartinen, V., Voncken, J. W., Shuler, C., Warburton, D., Bu, D., Heisterkamp, N., and Groffen, J. (1995). Abnormal lung development and cleft palate in mice lacking TGF- β_3 indicates defects of epithelial–mesenchymal interaction. *Nat. Genet.* **11**, 415–421.
- Kaartinen, V., Dudas, M., Nagy, A., Sridurongrit, S., Lu, M. M., and Epstein, J. A. (2004). Cardiac outflow tract defects in mice lacking ALK2 in neural crest cells. *Development* **131**, 3481–3490.
- Kelly, R. G., Brown, N. A., and Buckingham, M. E. (2001). The arterial pole of the mouse heart forms from Fgf10-expressing cells in pharyngeal mesoderm. *Dev. Cell* **1**, 435–440.
- Kim, R. Y., Robertson, E. J., and Solloway, M. J. (2001). Bmp6 and Bmp7 are required for cushion formation and septation in the developing mouse heart. *Dev. Biol.* **235**, 449–466.
- Kingsley, D. M., Bland, A. E., Grubber, J. M., Marker, P. C., Russell, L. B., Copeland, N. G., and Jenkins, N. A. (1992). The mouse short ear skeletal morphogenesis locus is associated with defects in a bone morphogenetic member of the TGF β superfamily. *Cell* **71**, 399–410.
- Kinsella, M. G., and Fitzharris, T. P. (1980). Origin of cushion tissue in the developing chick heart: cinematographic recordings of *in situ* formation. *Science* **207**, 1359–1360.
- Kirby, M. L., and Waldo, K. L. (1995). Neural crest and cardiovascular patterning. *Circ. Res.* **77**, 211–215.
- Kirby, M. L., Gale, T. F., and Stewart, D. E. (1983). Neural crest cells contribute to normal aorticpulmonary septation. *Science* **220**, 1059–1061.
- Kitamura, K., Miura, H., Miyagawa-Tomita, S., Yanazawa, M., Katoh-Fukui, Y., Suzuki, R., Ohuchi, H., Suehiro, A., Motegi, Y., Nakahara, Y., Kondo, S., and Yokoyama, M. (1999).

- Mouse *Pitx2* deficiency leads to anomalies of the ventral body wall, heart, extra- and periocular mesoderm and right pulmonary isomerism. *Development* **126**, 5749–5758.
- Kitten, G. T., Markwald, R. R., and Bolender, D. L. (1987). Distribution of basement membrane antigens in cryopreserved early embryonic hearts. *Anat. Rec.* **217**, 379–390.
- Klewer, S. E., Krob, S. L., Kolker, S. J., and Kitten, G. T. (1998). Expression of type VI collagen in the developing mouse heart. *Dev. Dyn.* **211**, 248–255.
- Komuro, I., and Izumo, S. (1993). *Csx*: A murine homeobox-containing gene specifically expressed in the developing heart. *Proc. Natl. Acad. Sci. USA* **90**, 8145–8149.
- Korenberg, J. R., Bradley, C., and Distèche, C. M. (1992). Down syndrome: Molecular mapping of the congenital heart disease and duodenal stenosis. *Am. J. Hum. Genet.* **50**, 294–302.
- Kretzschmar, M., and Massague, J. (1998). SMADs: Mediators and regulators of TGF- β signaling. *Curr. Opin. Genet. Dev.* **8**, 103–111.
- Kretzschmar, M., Liu, F., Hata, A., Doody, J., and Massague, J. (1997). The TGF- β family mediator *Smad1* is phosphorylated directly and activated functionally by the BMP receptor kinase. *Genes Dev.* **11**, 984–995.
- Krishnan, S., Deora, A. B., Annes, J. P., Osoria, J., Rifkin, D. B., and Hajjar, K. A. (2004). Annexin II-mediated plasmin generation activates TGF- β_3 during epithelial–mesenchymal transformation in the developing avian heart. *Dev. Biol.* **265**, 140–154.
- Krug, E. L., Runyan, R. B., and Markwald, R. R. (1985). Protein extracts from early embryonic hearts initiate cardiac endothelial cytodifferentiation. *Dev. Biol.* **112**, 414–426.
- Krug, E. L., Mjaatvedt, C. H., and Markwald, R. R. (1987). Extracellular matrix from embryonic myocardium elicits an early morphogenetic event in cardiac endothelial differentiation. *Dev. Biol.* **120**, 348–355.
- Krug, E. L., Rezaee, M., Isokawa, K., Turner, D. K., Litke, L. L., Wunsch, A. M., Bain, J. L., Riley, D. A., Capehart, A. A., and Markwald, R. R. (1995). Transformation of cardiac endothelium into cushion mesenchyme is dependent on ES/130: Temporal, spatial, and functional studies in the early chick embryo. *Cell. Mol. Biol. Res.* **41**, 263–277.
- Kurnit, D. M., Aldridge, J. F., Neve, R. L., and Matthyssse, S. (1985). Genetics of congenital heart malformations: A stochastic model. *Ann. N.Y. Acad. Sci.* **450**, 191–204.
- Ladher, R. K., Church, V. L., Allen, S., Robson, L., Abdelfattah, A., Brown, N. A., Hattersley, G., Rosen, V., Luyten, F. P., Dale, L., and Francis-West, P. H. (2000). Cloning and expression of the Wnt antagonists *Sfrp-2* and *Frzb* during chick development. *Dev. Biol.* **218**, 183–198.
- Lai, Y. T., Beason, K. B., Brames, G. P., Desgrosellier, J. S., Cleggett, M. C., Shaw, M. V., Brown, C. B., and Barnett, J. V. (2000). Activin receptor-like kinase 2 can mediate atrioventricular cushion transformation. *Dev. Biol.* **222**, 1–11.
- Lakkis, M. M., and Epstein, J. A. (1998). Neurofibromin modulation of ras activity is required for normal endocardial–mesenchymal transformation in the developing heart. *Development* **125**, 4359–4367.
- Leimeister, C., Externbrink, A., Klamt, B., and Gessler, M. (1999). *Hey* genes: A novel subfamily of *hairy*- and *Enhancer of split* related genes specifically expressed during mouse embryogenesis. *Mech. Dev.* **85**, 173–177.
- Lemke, G. (1996). Neuregulins in development. *Mol. Cell. Neurosci.* **7**, 247–262.
- Letamendia, A., Lastres, P., Botella, L. M., Raab, U., Langa, C., Velasco, B., Attisano, L., and Bernabeu, C. (1998). Role of endoglin in cellular responses to transforming growth factor- β : A comparative study with betaglycan. *J. Biol. Chem.* **273**, 33011–33019.
- Letterio, J. J., Geiser, A. G., Kulkarni, A. B., Roche, N. S., Sporn, M.B., and Roberts, A. B. (1994). Maternal rescue of transforming growth factor- β_1 null mice. *Science* **264**, 1936–1938.
- Li, L., Krantz, I. D., Deng, Y., Genin, A., Banta, A. B., Collins, C. C., Qi, M., Trask, B. J., Kuo, W. L., Cochran, J., Costa, T., Pierpont, M. E., Rand, E. B., Piccoli, D. A., Hood, L.,

- and Spinner, N. B. (1997a). Alagille syndrome is caused by mutations in human *Jagged1*, which encodes a ligand for Notch1. *Nat. Genet.* **16**, 243–251.
- Li, Q. Y., Newbury-Ecob, R. A., Terrett, J. A., Wilson, D. I., Curtis, A. R., Yi, C. H., Gebuhr, T., Bullen, P. J., Robson, S. C., Strachan, T., Bonnet, D., Lyonnet, S., Young, I. D., Raeburn, J. A., Buckler, A. J., Law, D. J., and Brook, J. D. (1997b). Holt-Oram syndrome is caused by mutations in *TBX5*, a member of the Brachyury (T) gene family. *Nat. Genet.* **15**, 21–29.
- Liebner, S., Cattelino, A., Gallini, R., Rudini, N., Iurlaro, M., Piccolo, S., and Dejana, E. (2004). β -Catenin is required for endothelial–mesenchymal transformation during heart cushion development in the mouse. *J. Cell Biol.* **166**, 359–367.
- Lints, T. J., Parsons, L. M., Hartley, L., Lyons, I., and Harvey, R. P. (1993). *Nkx-2.5*: A novel murine homeobox gene expressed in early heart progenitor cells and their myogenic descendants. *Development* **119**, 969.
- Little, C. D., and Rongish, B. J. (1995). The extracellular matrix during heart development. *Experientia* **51**, 873–882.
- Liu, C., Liu, W., Lu, M. F., Brown, N. A., and Martin, J. F. (2001). Regulation of left–right asymmetry by thresholds of *Pitx2c* activity. *Development* **128**, 2039–2048.
- Liu, C., Liu, W., Palie, J., Lu, M. F., Brown, N. A., and Martin, J. F. (2002). *Pitx2c* patterns anterior myocardium and aortic arch vessels and is required for local cell movement into atrioventricular cushions. *Development* **129**, 5081–5091.
- Liu, J. P., and Jessell, T. M. (1998). A role for rhoB in the delamination of neural crest cells from the dorsal neural tube. *Development* **125**, 5055–5067.
- Loeber, C. P., and Runyan, R. B. (1990). A comparison of fibronectin, laminin, and galactosyltransferase adhesion mechanisms during embryonic cardiac mesenchymal cell migration *in vitro*. *Dev. Biol.* **140**, 401–412.
- Loffredo, C. A., Wilson, P. D., and Ferencz, C. (2001). Maternal diabetes: An independent risk factor for major cardiovascular malformations with increased mortality of affected infants [see comment]. *Teratology* **64**, 98–106.
- Loomes, K. M., Taichman, D. B., Glover, C. L., Williams, P. T., Markowitz, J. E., Piccoli, D. A., Baldwin, H. S., and Oakey, R. J. (2002). Characterization of Notch receptor expression in the developing mammalian heart and liver. *Am. J. Med. Genet.* **112**, 181–189.
- Lu, J. R., McKinsey, T. A., Xu, H., Wang, D. Z., Richardson, J. A., and Olson, E. N. (1999a). FOG-2, a heart- and brain-enriched cofactor for GATA transcription factors. *Mol. Cell. Biol.* **19**, 4495–4502.
- Lu, M. F., Pressman, C., Dyer, R., Johnson, R. L., and Martin, J. F. (1999b). Function of Rieger syndrome gene in left–right asymmetry and craniofacial development. *Nature* **401**, 276–278.
- Lyons, I., Parsons, L. M., Hartley, L., Li, R., Andrews, J. E., Robb, L., and Harvey, R. P. (1995). Myogenic and morphogenetic defects in the heart tubes of murine embryos lacking the homeo box gene *Nkx2-5*. *Genes Dev.* **9**, 1654–1666.
- Lyons, K. M., Pelton, R. W., and Hogan, B. L. (1990). Organogenesis and pattern formation in the mouse: RNA distribution patterns suggest a role for bone morphogenetic protein-2A (BMP-2A). *Development* **109**, 833–844.
- MacLeod, C. L., Luk, A., Castagnola, J., Cronin, M., and Mendelsohn, J. (1986). EGF induces cell cycle arrest of A431 human epidermoid carcinoma cells. *J. Cell. Physiol.* **127**, 175–182.
- Majka, S. M., and McGuire, P. G. (1997). Regulation of urokinase expression in the developing avian heart: A role for the *Ets-2* transcription factor. *Mech. Dev.* **68**, 127–137.
- Manasek, F. J. (1970). Sulfated extracellular matrix production in the embryonic heart and adjacent tissues. *J. Exp. Zool.* **174**, 415–439.
- Manasek, F. J. (1975). The extracellular matrix: A dynamic component of the developing embryo. *Curr. Top. Dev. Biol.* **10**, 35–102.

- Manasek, F. J., Reid, M., Vinson, W., Seyer, J., and Johnson, R. (1973). Glycosaminoglycan synthesis by the early embryonic chick heart. *Dev. Biol.* **35**, 332–348.
- Markwald, R. R., and Smith, W. N. (1972). Distribution of mucosubstances in the developing rat heart. *J. Histochem. Cytochem.* **20**, 896–907.
- Markwald, R. R., and Wessels, A. (2001). Overview of heart development. In “Formation of the Heart and Its Regulation” (R. J. Tomanek and R. B. Runyan, Eds.), pp. 1–22. Birkhauser, Boston.
- Markwald, R. R., Fitzharris, T. P., and Smith, W. N. (1975). Structural analysis of endocardial cytodifferentiation. *Dev. Biol.* **42**, 160–180.
- Markwald, R. R., Fitzharris, T. P., and Manasek, F. J. (1977). Structural development of endocardial cushions. *Am. J. Anat.* **148**, 85–119.
- Markwald, R. R., Fitzharris, T. P., Bank, H., and Bernanke, D. H. (1978). Structural analyses on the matrical organization of glycosaminoglycans in developing endocardial cushions. *Dev. Biol.* **62**, 292–316.
- McCright, B., Lozier, J., and Gridley, T. (2002). A mouse model of Alagille syndrome: Notch2 as a genetic modifier of Jag1 haploinsufficiency. *Development* **129**, 1075–1082.
- McGuire, P. G., and Alexander, S. M. (1993a). Inhibition of urokinase synthesis and cell surface binding alters the motile behavior of embryonic endocardial-derived mesenchymal cells *in vitro*. *Development* **118**, 931–993.
- McGuire, P. G., and Alexander, S. M. (1993b). Urokinase production by embryonic endocardial-derived cells: Regulation by substrate composition. *Dev. Biol.* **155**, 442–451.
- Mikawa, T. (1999). Cardiac lineages. In “Heart Development” (R. P. Harvey and N. Rosenthal, Eds.), pp. 19–33. Academic Press, San Diego, CA.
- Mikawa, T., and Gourdie, R. G. (1996). Pericardial mesoderm generates a population of coronary smooth muscle cells migrating into the heart along with ingrowth of the epicardial organ. *Dev. Biol.* **174**, 221–232.
- Miller, J. R. (2002). The Wnts. *Genome Biol.* **3**, REVIEWS3001.
- Mjaatvedt, C. H., Lepera, R. C., and Markwald, R. R. (1987). Myocardial specificity for initiating endothelial–mesenchymal cell transition in embryonic chick heart correlates with a particulate distribution of fibronectin. *Dev. Biol.* **119**, 59–67.
- Mjaatvedt, C. H., Krug, E. L., and Markwald, R. R. (1991). An antiserum (ES1) against a particulate form of extracellular matrix blocks the transition of cardiac endothelium into mesenchyme in culture. *Dev. Biol.* **145**, 219–230.
- Mjaatvedt, C. H., Yamamura, H., Capehart, A. A., Turner, D., and Markwald, R. R. (1998). The *Cspg2* gene, disrupted in the *hdf* mutant, is required for right cardiac chamber and endocardial cushion formation. *Dev. Biol.* **202**, 56–66.
- Mjaatvedt, C. H., Nakaoka, T., Moreno-Rodriguez, R., Norris, R. A., Kern, M. J., Eisenberg, C. A., Turner, D., and Markwald, R. R. (2001). The outflow tract of the heart is recruited from a novel heart-forming field. *Dev. Biol.* **238**, 97–109.
- Molin, D. G., DeRuiter, M. C., Wisse, L. J., Azhar, M., Doetschman, T., Poelmann, R. E., and Gittenberger-de Groot, A. C. (2002). Altered apoptosis pattern during pharyngeal arch artery remodelling is associated with aortic arch malformations in *Tgfβ2* knock-out mice. *Cardiovasc. Res.* **56**, 312–322.
- Montgomery, M. O., Litvin, J., Gonzalez-Sanchez, A., and Bader, D. (1994). Staging of commitment and differentiation of avian cardiac myocytes. *Dev. Biol.* **164**, 63–71.
- Moorman, A., Webb, S., Brown, N. A., Lamers, W., and Anderson, R. H. (2003). Development of the heart. 1. Formation of the cardiac chambers and arterial trunks. *Heart* **89**, 806–814.
- Nakajima, Y., Miyazono, K., Kato, M., Takase, M., Yamagishi, T., and Nakamura, H. (1997). Extracellular fibrillar structure of latent TGF β binding protein-1: Role in TGF β -dependent endothelial–mesenchymal transformation during endocardial cushion tissue formation in mouse embryonic heart. *J. Cell Biol.* **136**, 193–204.

- Nawshad, A., and Hay, E. D. (2003). TGF β 3 signaling activates transcription of the LEF1 gene to induce epithelial-mesenchymal transformation during mouse palate development. *J. Cell Biol.* **163**, 1291-1301.
- Ng, L. J., Wheatley, S., Muscat, G. E., Conway-Campbell, J., Bowles, J., Wright, E., Bell, D. M., Tam, P. P., Cheah, K. S., and Koopman, P. (1997). SOX9 binds DNA, activates transcription, and coexpresses with type II collagen during chondrogenesis in the mouse. *Dev. Biol.* **183**, 108-121.
- Nieto, M. A., Sargent, M. G., Wilkinson, D. G., and Cooke, J. (1994). Control of cell behavior during vertebrate development by *Slug*, a zinc finger gene. *Science* **264**, 835-839.
- Oda, T., Elkahlon, A. G., Pike, B. L., Okajima, K., Krantz, I. D., Genin, A., Piccoli, D. A., Meltzer, P. S., Spinner, N. B., Collins, F. S., and Chandrasekharappa, S. C. (1997). Mutations in the human *Jagged1* gene are responsible for Alagille syndrome. *Nat. Genet.* **16**, 235-242.
- Oshima, M., Oshima, H., and Taketo, M. M. (1996). TGF- β receptor type II deficiency results in defects of yolk sac hematopoiesis and vasculogenesis. *Dev. Biol.* **179**, 297-302.
- Pandur, P., Maurus, D., and Kuhl, M. (2002). Increasingly complex: New players enter the Wnt signaling network. *Bioessays* **24**, 881-884.
- Parmacek, M. S., and Leiden, J. M. (1999). GATA transcription factors and cardiac development. In "Heart Development" (R. P. Harvey and N. Rosenthal, Eds.), pp. 291-306. Academic Press, San Diego, CA.
- Patten, B. M., Kramer, T. C., and Barry, A. (1948). Valvular action in the embryonic chick heart by localized apposition of endocardial masses. *Anat. Rec.* **102**, 299-311.
- Pece-Barbara, N., Cymerman, U., Vera, S., Marchuk, D. A., and Letarte, M. (1999). Expression analysis of four endoglin missense mutations suggests that haploinsufficiency is the predominant mechanism for hereditary hemorrhagic telangiectasia type 1. *Hum. Mol. Genet.* **8**, 2171-2181.
- Perez-Alcala, S., Nieto, M. A., and Barbas, J. A. (2004). LSox5 regulates RhoB expression in the neural tube and promotes generation of the neural crest. *Development* **131**, 4455-4465.
- Person, A. D., Garriock, R. J., Kreig, P. A., Runyan, R. B., and Klewer, S. E. (2005). Frzb modulates Wnt-9a-mediated β -catenin signaling during avian atrioventricular cardiac cushion development. *Dev. Biol.* (in press).
- Pierschbacher, M. D., and Ruoslahti, E. (1984). Cell attachment activity of fibronectin can be duplicated by small synthetic fragments of the molecule. *Nature* **309**, 30-33.
- Pinter, E., Haigh, J., Nagy, A., and Madri, J. A. (2001). Hyperglycemia-induced vasculopathy in the murine conceptus is mediated via reductions of VEGF-A expression and VEGF receptor activation [see comment] *Am. J. Pathol.* **158**, 1199-1206.
- Potts, J. D., and Runyan, R. B. (1989). Epithelial-mesenchymal cell transformation in the embryonic heart can be mediated, in part, by transforming growth factor β . *Dev. Biol.* **134**, 392-401.
- Potts, J. D., Vincent, E. B., Runyan, R. B., and Weeks, D. L. (1992). Sense and antisense TGF β 3 mRNA levels correlate with cardiac valve induction. *Dev. Dyn.* **193**, 340-345.
- Ranger, A. M., Grusby, M. J., Hodge, M. R., Gravalles, E. M., de la Brousse, F. C., Hoey, T., Mickanin, C., Baldwin, H. S., and Glimcher, L. H. (1998). The transcription factor NF-ATc is essential for cardiac valve formation. *Nature* **392**, 186-190.
- Rezaee, M., Isokawa, K., Halligan, N., Markwald, R. R., and Krug, E. L. (1993). Identification of an extracellular 130-kDa protein involved in early cardiac morphogenesis. *J. Biol. Chem.* **268**, 14404-14411.
- Roelen, B. A., Goumans, M. J., van Rooijen, M. A., and Mummery, C. L. (1997). Differential expression of BMP receptors in early mouse development. *Int. J. Dev. Biol.* **41**, 541-549.
- Roman, J., and McDonald, J. A. (1993). Fibulin's organization into the extracellular matrix of fetal lung fibroblasts is dependent on fibronectin matrix assembly. *Am. J. Respir. Cell Mol. Biol.* **8**, 538-545.

- Romano, L. A., and Runyan, R. B. (1999). Slug is a mediator of epithelial–mesenchymal cell transformation in the developing chicken heart. *Dev. Biol.* **212**, 243–254.
- Romano, L. A., and Runyan, R. B. (2000). Slug is an essential target of TGF β 2 signaling in the developing chicken heart. *Dev. Biol.* **223**, 91–102.
- Rongish, B. J., Drake, C. J., Argraves, W. S., and Little, C. D. (1998). Identification of the developmental marker, JB3-antigen, as fibrillin-2 and its *de novo* organization into embryonic microfibrillar arrays. *Dev. Dyn.* **212**, 461–471.
- Rubinfeld, B., Souza, B., Albert, I., Muller, O., Chamberlain, S. H., Masiarz, F. R., Munemitsu, S., and Polakis, P. (1993). Association of the APC gene product with β -catenin. *Science* **262**, 1731–1734.
- Runyan, R. B., and Markwald, R. R. (1983). Invasion of mesenchyme into three-dimensional collagen gels: A regional and temporal analysis of interaction in embryonic heart tissue. *Dev. Biol.* **95**, 108–114.
- Ruoslahti, E. (1984). Fibronectin in cell adhesion and invasion. *Cancer Metastasis Rev.* **3**, 43–51.
- Samaneck, M., Slavik, Z., Zborilova, B., Hrobonova, V., Voriskova, M., and Skovranek, J. (1989). Prevalence, treatment, and outcome of heart disease in live-born children: A prospective analysis of 91,823 live-born children. *Pediatr. Cardiol.* **10**, 205–211.
- Sanford, L. P., Ormsby, I., Gittenberger-de Groot, A. C., Sariola, H., Friedman, R., Boivin, G. P., Cardell, E. L., and Doetschman, T. (1997). TGF β 2 knockout mice have multiple developmental defects that are non-overlapping with other TGF β knockout phenotypes. *Development* **124**, 2659–2670.
- Sato, Y., and Rifkin, D. B. (1989). Inhibition of endothelial cell movement by pericytes and smooth muscle cells: Activation of a latent transforming growth factor- β 1-like molecule by plasmin during co-culture. *J. Cell Biol.* **109**, 309–315.
- Savagner, P. (2001). Leaving the neighborhood: Molecular mechanisms involved during epithelia–mesenchymal transition. *Bioessays* **23**, 912–923.
- Sawada, S., Florell, S., Purandare, S. M., Ota, M., Stephens, K., and Viskochil, D. (1996). Identification of NF1 mutations in both alleles of a dermal neurofibroma. *Nat. Genet.* **14**, 110–112.
- Schott, J. J., Benson, D. W., Basson, C. T., Pease, W., Silberbach, G. M., Moak, J. P., Maron, B. J., Seidman, C. E., and Seidman, J. G. (1998). Congenital heart disease caused by mutations in the transcription factor NKX2-5. *Science* **281**, 108–111.
- Schubert, D., and LaCorbiere, M. (1980). Role of a 16S glycoprotein complex in cellular adhesion. *Proc. Natl. Acad. Sci. USA* **77**, 4137–4141.
- Schubert, D., and LaCorbiere, M. (1982). The specificity of extracellular glycoprotein complexes in mediating cellular adhesion. *J. Neurosci.* **2**, 82–89.
- Schubert, D., LaCorbiere, M., Klier, F. G., and Birdwell, C. (1983). A role for adherons in neural retina cell adhesion. *J. Cell Biol.* **96**, 990–998.
- Schubert, F. R., Mootoosamy, R. C., Walters, E. H., Graham, A., Tumiotto, L., Munsterberg, A. E., Lumsden, A., and Dietrich, S. (2002). Wnt6 marks sites of epithelial transformations in the chick embryo. *Mech. Dev.* **114**, 143–148.
- Schweickert, A., Campione, M., Steinbeisser, H., and Blum, M. (2000). Pitx2 isoforms: Involvement of Pitx2c but not Pitx2a or Pitx2b in vertebrate left–right asymmetry. *Mech. Dev.* **90**, 41–51.
- Shi, Y., and Massague, J. (2003). Mechanisms of TGF- β signaling from cell membrane to the nucleus. *Cell* **113**, 685–700.
- Shull, M. M., Ormsby, I., Kier, A. B., Pawlowski, S., Diebold, R. J., Yin, M., Allen, R., Sidman, C., Proetzel, G., and Calvin, D. (1992). Targeted disruption of the mouse transforming growth factor- β 1 gene results in multifocal inflammatory disease. *Nature* **359**, 693–699.
- Solloway, M. J., and Robertson, E. J. (1999). Early embryonic lethality in Bmp5;Bmp7 double mutant mice suggests functional redundancy within the 60A subgroup. *Development* **126**, 1753–1768.

- Song, W., Majka, S. M., and McGuire, P. G. (1999). Hepatocyte growth factor expression in the developing myocardium: Evidence for a role in the regulation of the mesenchymal cell phenotype and urokinase expression. *Dev. Dyn.* **214**, 92–100.
- Song, W., Jackson, K., and McGuire, P. G. (2000). Degradation of type IV collagen by matrix metalloproteinases is an important step in the epithelial–mesenchymal transformation of the endocardial cushions. *Dev. Biol.* **227**, 606–617.
- Spence, S. G., Argraves, W. S., Walters, L., Hungerford, J. E., and Little, C. D. (1992). Fibulin is localized at sites of epithelial–mesenchymal transitions in the early avian embryo. *Dev. Biol.* **151**, 473–484.
- Sugi, Y., Ito, N., Szebenyi, G., Myers, K., Fallon, J. F., Mikawa, T., and Markwald, R. R. (2003). Fibroblast growth factor (FGF)-4 can induce proliferation of cardiac cushion mesenchymal cells during early valve leaflet formation. *Dev. Biol.* **258**, 252–263.
- Sugi, Y., Yamamura, H., Okagawa, H., and Markwald, R. R. (2004). Bone morphogenetic protein-2 can mediate myocardial regulation of atrioventricular cushion mesenchymal cell formation in mice. *Dev. Biol.* **269**, 505–518.
- Tartaglia, M., Mehler, E. L., Goldberg, R., Zampino, G., Brunner, H. G., Kremer, H., van der Burgt, I., Crosby, A. H., Ion, A., Jeffery, S., Kalidas, K., Patton, M. A., Kucherlapati, R. S., and Gelb, B. D. (2001). Mutations in *PTPN11*, encoding the protein tyrosine phosphatase SHP-2, cause Noonan syndrome. *Nat. Genet.* **29**, 465–468 [erratum appears in *Nat. Genet.* **29**, 491].
- Tevosian, S. G., Deconinck, A. E., Tanaka, M., Schinke, M., Litovsky, S. H., Izumo, S., Fujiwara, Y., and Orkin, S. H. (2000). FOG-2, a cofactor for GATA transcription factors, is essential for heart morphogenesis and development of coronary vessels from epicardium. *Cell* **101**, 729–739.
- Timmerman, L. A., Grego-Bessa, J., Raya, A., Bertran, E., Perez-Pomares, J. M., Diez, J., Aranda, S., Palomo, S., McCormick, F., Izpisua-Belmonte, J. C., and de la Pompa, J. L. (2004). Notch promotes epithelial–mesenchymal transition during cardiac development and oncogenic transformation. *Genes Dev.* **18**, 99–115.
- Waldo, K. L., Kumiski, D. H., Wallis, K. T., Stadt, H. A., Hutson, M. R., Platt, D. H., and Kirby, M. L. (2001). Conotruncal myocardium arises from a secondary heart field. *Development* **128**, 3179–3188.
- Wessels, A., and Sedmera, D. (2003). Developmental anatomy of the heart: A tale of mice and man. *Physiol. Genomics* **15**, 165–176.
- Winnier, G., Blessing, M., Labosky, P. A., and Hogan, B. L. (1995). Bone morphogenetic protein-4 is required for mesoderm formation and patterning in the mouse. *Genes Dev.* **9**, 2105–2116.
- Wrana, J. L., Attisano, L., Wieser, R., Ventura, F., and Massague, J. (1994). Mechanism of activation of the TGF- β receptor. *Nature* **370**, 341–347.
- Wunsch, A. M., Little, C. D., and Markwald, R. R. (1994). Cardiac endothelial heterogeneity defines valvular development as demonstrated by the diverse expression of JB3, an antigen of the endocardial cushion tissue. *Dev. Biol.* **165**, 585–601.
- Yamamura, H., Zhang, M., Markwald, R. R., and Mjaatvedt, C. H. (1997). A heart segmental defect in the anterior–posterior axis of a transgenic mutant mouse. *Dev. Biol.* **186**, 58–72.
- Zhang, H., and Bradley, A. (1996). Mice deficient for BMP2 are nonviable and have defects in amnion/chorion and cardiac development. *Development* **122**, 2977–2986.
- Zhang, H. Y., Chu, M. L., Pan, T. C., Sasaki, T., Timpl, R., and Ekblom, P. (1995). Extracellular matrix protein fibulin-2 is expressed in the embryonic endocardial cushion tissue and is a prominent component of valves in adult heart. *Dev. Biol.* **167**, 18–26.
- Zhao, Q., Eberspaecher, H., Lefebvre, V., and De Crombrugge, B. (1997). Parallel expression of Sox9 and Col2a1 in cells undergoing chondrogenesis. *Dev. Dyn.* **209**, 377–386.

INDEX

A

Acanthopagrus butcheri, fish IGF in, 237
Acanthopagrus schlegeli, fish IGF in, 228
Acid-labile subunit (ALS), IGF background with, 219
Activin receptor-like kinase 2 (ALK-2), BMP with, 306
Activin receptor-like kinase 3 (ALK-3), *Bmpr2* with, 308
Adenomatous polyposis coli (APC), β -catenin with, 310–311
ALK-2. *see* Activin receptor-like kinase 2
ALK-3. *see* Activin receptor-like kinase 3
Alopecia, keratin pathologies with, 56
ALS. *see* Acid-labile subunit
Amago salmon, fish IGF in, 238
 γ -aminobutyric acid (GABA), acrosome reaction with, 130
Androgen receptors
 hair keratin expression regulation of, 33–37
 hHa7 with, 33–37
Anguilla japonica, fish IGF in, 226
Annexin II, TGF- β with, 301
Antisense knockdown methods, calcium/Ca²⁺ channels studied in, 89, 102
APC. *see* Adenomatous polyposis coli
Apical matrix, nails with, 13, 15
Arbacia punctulata, SAP from, 112, 114
Asterias amurensis, acrosome reaction with, 125
Atlantic hagfish, fish IGF in, 229
Atlantic salmon, fish IGF in, 228
ATP, acrosome reaction with, 130

Atrioventricular septal defects (AVSD)
 BMP with, 307
 collagen VI with, 319–320
AVSD. *see* Atrioventricular septal defects
Axoneme, sperm physiology with, 82, 83

B

Barramundi, fish IGF in, 228
Basal cell carcinomas, hair follicle-derived tumors of, 25
Bidyanus bidyanus, fish IGF in, 237
Black lipid bilayer (BLM), sperm ion channel studies with, 105
Black seabream, fish IGF in, 228, 237
BLM. *see* Black lipid bilayer
Bluntnout bream, fish IGF in, 228
BMP. *see* Bone morphogenetic protein
BMP receptor II allele (*Bmpr2*)
 ALK-3 with, 308
 endocardial cushion morphogenesis with, 307–308
BMP2, 290–291, 305, 307, 308
BMP4, 305, 307, 308
BMP5, 305–306, 308
BMP6, 305, 308
BMP7, 305–306, 307, 308
Bone morphogenetic protein (BMP)
 ALK-2 with, 306
 AVSD with, 307, 308
 BMP2, 290–291, 305, 307, 308
 BMP4, 305, 307, 308
 BMP5, 305–306, 308
 BMP6, 305, 308
 BMP7, 305–306, 307, 308

- Bone morphogenetic protein (BMP)
 (*continued*)
Bmpr2 with, 307–308
 cardiac cushion development with,
 290–291, 305–308
 cardiac EMT with, 305–308
 EMT with, 322
 hair keratin expression regulation of, 38–39
 mouse, 305–307
 signaling with, 306–307
 Broadhead catfish, fish IGF in, 228

C

- Calcium/Ca²⁺ channels, 79–174
 acrosome reaction with, 124–137
Asterias amurensis, 125
 ATP induction of, 130
Echinometra lucunter, 125
 EGF induction of, 130
 FSP in, 125–126, 128
 GABA induction of, 130
 mammalian sperm, 130–137
 marine sperm, 124–130
 PAF induction of, 130
 progesterone induction of, 130, 131,
 136, 139, 140
S. purpuratus, 126
 slow sustained [Ca²⁺]_i elevation in,
 135–137
 SNARE proteins needed for,
 124, 125, 126
 suREJ in, 126–127
 transient increase in [Ca²⁺]_i in, 133–135
 ZP mediation of, 130–131, 133–137,
 139, 140
 alternative sperm ion channel studies for,
 101–109
 antisense knockdown methods in, 102
 BLM in, 105
 DHP in, 103
 ES cells in, 108
 HCN channels in, 104
 invertebrate toxins in, 104
 ion-sensitive fluorescent dyes in, 101
 L-type currents in, 103
 other techniques in, 107–109
 patch-clamp studies in, 102, 106
 planar bilayers in, 104–106
 proteomics in, 108–109
 SICM in, 106
 smart patch clamp in, 106–107
 spermatogenic cells in, 101–104
 T-type currents in, 103, 104
 vesicle fusion strategy in, 105
 calcium's role in
 Ca²⁺ intracellular messaging with,
 83–84
 calreticulin regulating, 84
 calsequestrin regulating, 84
 CaM regulating, 84
 cellular ion gradient with, 85
 EF hand proteins regulating, 84
 membrane transporters regulating, 85
 Mg²⁺ v., 84
 regulation of cell function by, 83–84
 sensor proteins regulating, 84
 troponin C regulating, 84
 concluding remarks on, 141–142
 intracellular signaling events with,
 137–138
 introduction to, 79
 main types of, 86–109
 Ca²⁺ release channels as, 96–98
 CatSper channels as, 87, 94–95, 99–100
 Ca_v1/Ca_v2/Ca_v3 channels as,
 88, 89–91, 94
 Ca_v3 channels as, 88, 89–91, 94
Ciona intestinalis with, 100
 CNG channels as, 87, 94–95, 98–99
 DHP sensitivity of, 88, 89–90
Drosophila with, 91–92
 HVA channels as, 86, 89
 IP₃R release channels as, 96–97
 LVA channels as, 86, 89, 90
 patch-clamp studies on, 89
 protein kinase phosphorylation with, 90
 regulatory pathways with, 90
 RyR release channels as, 96–98
 synaptotagmin associated with, 91
 syntaxin associated with, 91
 TRP channels as, 87, 91–96
 voltage-gated Ca²⁺ channels as, 86–91,
 94–95
Xenopus with, 99
 single-cell measurements with,
 137–141
 [Ca²⁺]_i fluctuations in, 140–141
 cell populations v., 137–138
 source-sink diffusion model from, 141
Strongylocentrotus purpuratus with, 138

- sperm capacitation with, 120–124
 - hyperpolarization in, 122, 123
 - mammalian, 121–122
 - molecular mechanisms in, 120
 - mouse, 122–123
 - signaling model for, 121–122
 - unanswered questions about, 123–124
- sperm motility with, 109–120
 - Arbacia punctulata* having, 112, 114
 - bracken fern sperm with, 110
 - chemoattractant compounds with, 110–114, 111
 - chemotaxis in, 110–114, 117–120
 - hyperactivation in, 115–117
 - mammalian, 114–115, 117–120
 - marine, 109–110
 - membrane hyperpolarization with, 112
 - SAP with, 111–114
 - speract signaling with, 111–112
 - SpHCN activated in, 112–113
 - Strongylocentrotus purpuratus* having, 111, 113
 - two roles of Ca^{2+} in, 109
- sperm physiology background and, 79–83
- sperm physiology characteristics with, 82, 83
 - axoneme in, 82, 83
 - Ca^{2+} channel distribution in, 82
 - flagellum in, 82, 83
 - head in, 82, 83
 - microtubules in, 83
 - mitochondria in, 82, 83
- spermatogenesis with, 79–83
 - three phases of, 81
- Carassius auratus*, fish IGF in, 228
- Cardiac cushion development
 - cell biology of, 287–324
 - BMP in, 290–291, 305–308
 - chamber septation in, 295–298
 - cushion formation in, 289–291
 - ECM in, 289–290, 317–322
 - heart valve remodeling in, 295–298
 - mesenchymal cell invasion/migration in, 294–295, 317–322
 - N-CAM in, 294
 - PECAM-1 in, 294
 - RER in, 294
 - SEM studies on, 294
 - species developmental stage comparison for, 296
 - tubular heart formation in, 288–289, 290
 - EMT in, 290, 291–294, 295, 298–322, 322–324
 - inductive stimuli with, 292–294
 - integrating molecular pathways governing, 322–323
 - molecular mechanisms of, 298–322
 - extracellular matrix in, 317–322
 - collagen VI with, 319–320
 - fibullins with, 320
 - hyaluronan with, 318–319
 - matrix metalloproteinase 2 with, 320–321
 - plasma with, 321–322
 - urokinase with, 321–322
 - future of, 323–324
 - growth factors/other molecules in, 298–313
 - bone morphogenic proteins as, 305–308
 - β -catenin as, 310–311
 - epidermal growth factors as, 309–310
 - ErbB3 as, 309
 - fibroblast growth factors as, 312
 - heregulins as, 309
 - notch as, 311–312
 - Shp-2 as, 309–310
 - transforming growth factor β as, 298–305
 - vascular endothelial growth factor as, 312–313
 - Wnt as, 291, 310–311
 - introduction to, 288
 - mesenchymal cell invasion with, 317–322
 - morphology of, 287, 288–298
 - transcription factors with, 313–317
 - Fog-2 as, 315–316
 - GATA-4 as, 315–316
 - NF-1 as, 313–314
 - NFATc as, 313
 - Nkx2.5 as, 316–317
 - Pitx2 as, 317
 - Sox-9 as, 314–315
 - TBX-5 as, 315
 - valve morphogenesis in, 298–322
- Carp, fish IGF in, 228
- β -catenin
 - APC with, 310–311
 - cardiac cushion development with, 310–311
 - hair keratin expression regulation of, 29–30

- CatSper channels
Ciona intestinalis with, 100
 sperm physiology with, 87, 94–95, 99–100
Xenopus with, 99
- CCAAT displacement protein (CDP), hair follicle regulatory process with, 60–61, 62
- CDP. *see* CCAAT displacement protein
- Cell fate determination, hair follicles with, 53, 54
- Cell sensory theory, TRP channels with, 92
- Channel catfish, fish IGF in, 228
- Chemotaxis
 bracken fern sperm with, 110
 chemoattractant compounds with, 110–114
 mammalian sperm, 117–120
 chemoattractant molecule in, 119
 membrane hyperpolarization with, 112
 SAP with, 111–114
 speract signaling with, 111–112
 sperm motility with, 110–114, 117–120
- Chinook salmon, fish IGF in, 228
- Chum salmon, fish IGF in, 228
- CIF. *see* Cytosolic influx factor
- Ciona intestinalis*, CatSper channels with, 100
- Cirrhinus molitorella*, fish IGF in, 228
- CL. *see* Companion layer
- Clarias macrocephalus*, fish IGF in, 228
- CNG channels. *see* Cyclic nucleotide-gated channels
- Coho salmon, fish IGF in, 228
- Collagen VI
 AVSD with, 319–320
 cardiac cushion development ECM with, 319–320
- Companion layer (CL)
 epithelial keratins of, 41–45, 54
Flügelzellen with, 48
 IIF studies for, 43, 44
 IRS with, 3
 K6hf in, 43–45, 57
 K16 in, 43, 44
 K17 in, 43–45
 keratin pathologies of, 55–60
 ORS with, 41–42
 regulatory processes in, 60–62
 type II keratin gene with, 43
- Cottus kazika*, fish IGF in, 228
- Cottus scorpius*, fish IGF in, 228
- Ctenopharyngodon idella*, fish IGF in, 228
- Cyclic nucleotide-gated channels (CNG channels)
 cAMP binding with, 98
 cGMP binding with, 98
 ligand binding with, 98
 sperm physiology with, 87, 94–95, 98–99
- Cyprinus carpio*, fish IGF in, 228
- Cytosine, DNA methylation in, 176–178
- Cytosolic influx factor (CIF), TRP channels with, 93
- ## D
- Daddy sculpin, fish IGF in, 228
- Desmoplastic trichoepitheliomas, hair follicle-derived tumors of, 25
- Differentially methylated domain (DMD)
 chromatin in gene expression with, 200–206
 HAT with, 202
 HDAC with, 202
 histone modifications with, 201–203
 HMTase with, 202
 insulators of, 205–206
 PcG protein with, 204–205
 TrxG protein with, 204
- concluding remarks on, 206–207
- genomic imprinting with,
 173, 176–178, 179–207
- DMD sequences required for,
 192–197
- DNA methylation and,
 173, 176–178, 179
- mouse transgenes in study of, 197–199
- regional control of, 185–206
- primary/secondary, 185–187
- structural features of, 187–191
- tandem repeats with, 173, 199–200
- DMD. *see* Differentially methylated domain
- Dnmt3a, DNA methylation with, 182–183
- Dnmt3b, DNA methylation with, 182
- Dnmt3l, DNA methylation with, 182–184
- Drosophila*, TRP channels with, 91–92
- ## E
- EBS. *see* Epidermolysis bullosa simplex
- Echinometra lucunter*, acrosome reaction with, 125

- ECM. *see* Extracellular matrix
- EGF. *see* Epidermal growth factors
- EGFP. *see* Enhanced green fluorescent protein
- Electron microscope, medulla studied with, 51
- Embryogenesis, DNA methylation with, 179
- Embryonic stem cells (ES cells), sperm ion channel studies with, 108
- EMT. *see* Epithelial-mesenchymal transition
- Endocardial cushions. *see* Cardiac cushion development
- Endoglin, TGF- β with, 304–305
- Enhanced green fluorescent protein (EGFP), ORS studied with, 42
- Epidermal growth factors (EGF)
- acrosome reaction with, 130
 - cardiac cushion development with, 309–310
 - EMT with, 322
 - IGF background with, 217
- Epidermolysis bullosa simplex (EBS), keratin pathologies with, 55
- Epinephelus coioides*, fish IGF in, 228
- Epithelial-mesenchymal transition (EMT)
- cardiac cushion development with, 290, 291–294, 295, 298–322
 - extracellular matrix with, 317–322
 - collagen VI with, 319–320
 - fibullins with, 320
 - hyaluronan with, 318–319
 - matrix metalloproteinase 2 with, 320–321
 - plasmin with, 321–322
 - urokinase with, 321–322
 - growth factors/other molecules with, 298–313, 302–303
 - bone morphogenic proteins as, 305–308
 - β -catenin as, 310–311
 - epidermal growth factors as, 309–310
 - ErbB3 as, 309
 - fibroblast growth factors as, 312
 - heregulins as, 309
 - notch as, 311–312
 - Shp-2 as, 309–310
 - transforming growth factor β as, 298–305
 - vascular endothelial growth factor as, 312–313
 - Wnt as, 291, 310–311
 - inductive stimuli with, 292–294
 - integrating molecular pathways governing, 322–323
- BMP in, 322
- EGF in, 322
- HGF in, 322
- MMP-2 in, 323
- Notch in, 322
- TGF- β in, 322
- Wnts in, 322
- transcription factors with, 313–317
- Fog-2 as, 315–316
 - GATA-4 as, 315–316
 - NF-1 as, 313–314
 - NFATc as, 313
 - Nkx2.5 as, 316–317
 - Pitx2 as, 317
 - Sox-9 as, 314–315
 - TBX-5 as, 315
- ErbB3, cardiac cushion development growth factors of, 309
- ES cells. *see* Embryonic stem cells
- European perch, fish IGF in, 228
- Extracellular matrix (ECM), cardiac cushion development with, 289–290

F

- FGF. *see* Fibroblast growth factors
- Fibroblast growth factors (FGF), cardiac cushion development with, 312
- Fibullins, cardiac cushion development ECM with, 320
- Fish
- biological actions of IGF system in, 254–263
 - cartilage sulfation from, 255–256
 - cell proliferation from, 256
 - DNA synthesis from, 256
 - embryonic development from, 257–259
 - growth from, 254–257
 - hormone production with, 261–262
 - IGF-1 receptors within, 258
 - IGFBP-1 within, 258–259
 - IGFBP-2 within, 259
 - IGFBP-5 within, 259
 - oocyte maturation with, 262–263
 - osmoregulation with, 260
 - protein synthesis from, 257
 - reproduction with, 261–263
 - IGF binding proteins for
 - biochemical evidence of, 249
 - biochemical properties of, 250–251

Fish (*continued*)

- expression of, 251–252
- hormonal regulation of, 253
- localization of, 251–252
- metabolic status of, 253–254
- primary structures of, 250
- regulation of, 252–254
- IGF in, 215, 225–226, 228–244
 - Acanthopagrus butcheri* with, 237
 - Acanthopagrus schlegeli* with, 228
 - amago salmon with, 238
 - Anguilla japonica* with, 226
 - Atlantic hagfish with, 229
 - Atlantic salmon with, 228
 - barramundi with, 228
 - Bidyanus bidyanus* with, 237
 - black seabream with, 228, 237
 - bluntnout bream with, 228
 - broadhead catfish with, 228
 - Carassius auratus* with, 228
 - carp with, 228
 - channel catfish with, 228
 - chinook salmon with, 228
 - chum salmon with, 228
 - Cirrhinus molitorella* with, 228
 - Clarias macrocephalus* with, 228
 - coho salmon with, 228
 - Cottus kazika* with, 228
 - Cottus scorpius* with, 228
 - Ctenopharyngodon idella* with, 228
 - Cyprinus carpio* with, 228
 - daddy sculpin with, 228
 - Epinephelus coioides* with, 228
 - European perch with, 228
 - evidence of, 225–226
 - four-spine sculpin with, 228
 - general background on, 215, 225–226
 - gilthead seabream with, 228
 - goldfish with, 228
 - grass carp with, 228
 - Ictalurus punctatus* with, 228
 - Japanese eel with, 226
 - Japanese flounder with, 228
 - Korean rockfish with, 228
 - Lates calcarifer* with, 228
 - Megalobrama amblycephala* with, 228
 - Megalobrama terminalis* with, 228
 - mud carp with, 228
 - Myxine glutinosa* with, 229
 - Oncorhynchus keta* with, 228
 - Oncorhynchus kisutch* with, 228

- Oncorhynchus masou ishikawai* with, 228
- Oncorhynchus mykiss* with, 226
- Oncorhynchus tshawytscha* with, 228
- orange-spotted grouper with, 228
- Oreochromis mossambicus* with, 228
- Paralichthys olivaceus* with, 228
- Perca flavescens* with, 228
- Perca fluviatilis* with, 228
- Petromyzon marinus* with, 229
- rabbit fish with, 228
- rainbow trout with, 226
- Salmo salar* with, 228
- sea lamprey with, 229
- Sebastes schlegeli* with, 228
- Siganus guttatus* with, 228
- silver perch with, 237
- Southern bluefin tuna with, 237
- Sparus aurata* with, 228
- Thunnus maccoyii* with, 237
- tilapia with, 228
- triangular bream with, 228
- turbot with, 228
- yellow perch with, 228
- zebrafish with, 228, 245, 246
- IGF-1 in, 228–240
 - agnathans, 229–230
 - development of, 239
 - elasmobranchs, 229
 - environment of, 240
 - expression patterns of, 232–235
 - expression regulation of, 235–240
 - genes of, 230–232, 321
 - GH regulation of, 235–238
 - hormones of, 235–238
 - mRNA of, 230–232, 233–234
 - nutrition with, 238–239
 - primary structure of, 228–230
 - protein of, 234–235
 - teleost, 228–229
- IGF-2 in, 240–244
 - expression patterns of, 242–243
 - expression regulation of, 243–244
 - genes of, 241–242
 - GH regulation of, 243–244
 - hormones of, 243–244
 - mRNA of, 241–242
 - nutrition with, 244
 - primary structure of, 240–241
 - summary of IGF signaling in, 263–265
- Flagellum, sperm physiology with, 82, 83

Flügelzellen

function of, 149

hair follicle IRS with, 48–49

FOG1. *see* Friend of GATA1

Fog-2, cardiac cushion development with, 315–316

Forkhead box n1 gene (Foxn1 gene)

hair keratin expression regulation of, 26–29

type I hair keratin with, 28

Four-spine sculpin, fish IGF in, 228

Foxn1 gene. *see* Forkhead box n1 gene

hair keratin expression regulation of, 26–29

Friend of GATA1 (FOG1), hair follicle regulatory process with, 61

FSP. *see* Fucose sulfate polymer

Fucose sulfate polymer (FSP), acrosome reaction with, 125–126, 128

G

GABA. *see* γ -aminobutyric acid

Gametogenesis, DNA methylation with, 179, 182

GATA-3, hair follicle regulatory process with, 61–62

GATA-4, cardiac cushion development with, 315–316

Gene expression

DNA methylation influencing, 178

hair keratins with, 26–39

androgen receptor in, 33–37

BMP signaling in, 38–39

β -catenin in, 29–30

foxn1 gene in, 27–29

hHa7 in, 33–37

HOXC13 in, 30–33, 38–39

KAP with, 30

LEF1 in, 29–30, 33, 38–39

Meis in, 33

nude mice and, 27–29

Pbx in, 33

Prep in, 33

synopsis for, 38–39

TALE in, 33

Wnt signaling with, 29–30, 39

human hair keratins in, 4–18

catalog listing, 16–18

expression characteristics with, 7–16

IIF studies with, 7, 8, 14, 16

ISH with, 7, 8

nail keratin and, 13–16

physical organization in, 5–7

pseudogenes with, 5–6, 11

Gene regulation, keratins in, 60–62

CDP with, 60–61, 62

FOG1 with, 61

GATA-3 with, 61–62

HDR with, 61

Genomic imprinting, 173–207

chromatin in expression of, 200–206

HAT with, 202

HDAC with, 202

histone modifications with, 201–203

HMTase with, 202

insulators of, 205–206

PcG protein with, 204–205

TrxG protein with, 204

concluding remarks on, 206–207

DNA methylation and, 173, 176–184

active v. passive demethylation with, 178

cytosine with, 176–178

differential, 179–182

DMD with, 173, 176–178, 179

Dnmt3a with, 182–183

Dnmt3b with, 182

Dnmt3l with, 182–184

embryogenesis with, 179

establishing imprints of, 181, 182–184

gametogenesis with, 179, 182

gene expression influenced with, 178

H19 with, 179, 186, 189, 190–191,

195–196, 197, 205–206

histone modifications with, 203–204

Igf2r with, 179, 186, 187, 188, 189, 190,

193–194, 199, 205–206

imprinted loci with, 179–182, 181

Kcnq1 with, 179, 187, 188, 189, 190, 194

maintaining imprints of, 182–184

mammalian, 176–178

methylation imprint expectations with, 176–178

mouse development with, 181

Peg3 with, 179, 180, 189

Snrpn with, 179, 180, 187, 188, 189, 193, 205

spermatogenesis with, 182

first observation of, 174

gamete establishment of, 175

Grb10 in, 175, 205

introduction to, 173–176

Genomic imprinting (*continued*)
 mouse with, 174–175
 parent-specific imprints in, 176
 PGC in, 176
 pronuclear transfer experiments with,
 174–175
 regional control of, 185–206
 DMD sequences for, 191–199
 DMD structural features with,
 187–191
 human PWS, 185
 mouse genetic experiments in, 187–191
 mouse transgene DMD sequences in,
 197–199
 primary/secondary DMDs with,
 185–187
 PWS-IC with, 185
 RSV LTR in, 198
 tandem repeats with, 173, 199–200
 GH. *see* Growth hormone
 Gilthead seabream, fish IGF in, 228
 Goldfish, fish IGF in, 228
 Grass carp, fish IGF in, 228
Grb10. *see* Growth factor receptor-bound
 protein 10
 Growth factor receptor-bound protein 10
 (*Grb10*)
 genomic imprinting of, 175, 205
 genomic imprinting with, 175
 Growth hormone (GH), IGF background
 with, 216–217

H

H19, genomic imprinting in, 179, 186, 189,
 190–191, 195–196, 197, 205–206
 HA. *see* Hyaluronan
 Hair follicle
 alopecia and, 56
 cell fate determination with, 53, 54
 CL with, 3, 41, 42–45
 epithelial keratins of, 41, 42–45
 IIF studies for, 43, 44
 K6hf in, 43–45, 57
 K16 in, 43, 44
 K17 in, 43–45
 keratin pathologies of, 55–60
 ORS and, 41–42
 regulatory processes in, 60–62
 type II keratin gene with, 43

concluding remarks on, 62–65
 EBS and, 55
 epithelial keratins of, 39–53
 hereditary disorders of,
 18–23, 20, 55–56
 41-kDa protein in, 22
 gene mutation leading to, 55–56
 monilethrix as, 19–22, 20
 mutations involved in, 20
 pili annulati as, 19
 pili trianguli et canaliculi as, 19
 spun glass hair as, 19
 truncated hair keratin hHa1-t in,
 22–23
 uncombable hair as, 19
 woolly hair as, 19
 HSS and, 56, 59
 human hair keratin gene family with,
 4–18
 catalog of, 16–18
 expression characteristics of,
 7–16
 IIF studies with, 7, 8, 14, 16
 ISH with, 7, 8
 nail keratin and, 13–16
 physical organization of, 5–7
 pseudogenes with, 5–6, 11
 introduction to, 1–4
 IRS with, 2–3, 3, 40–41, 44, 45–49, 54
 cuticle of, 3, 40
 epithelial keratins of,
 39–41, 44, 45–49, 54
Flügelzellen in, 48–49
 Henle layers of, 3, 40–41,
 44, 46–49
 Huxley layers of, 3, 40, 46–49
 IIF studies for, 44, 49
 keratin pathologies of, 55–60
 mK6irs in, 46–47, 57
 regulatory processes in, 60–62
 type I keratin gene in, 46
 keratin expression regulation of,
 26–39
 androgen receptor in, 33–37
 BMP signaling in, 38–37
 β -catenin in, 29–30
 foxn1 gene in, 27–29
 hHa7 in, 33–38
 HOXC13 in, 30–33, 38–39
 KAP with, 30
 LEF1 in, 29–30, 33, 38–39

- Meis in, 33
- nude* mice and, 27–29
- Pbx in, 33
- Prep in, 33
- synopsis for, 37–39
- TALE in, 33
- Wnt signaling with, 29–30, 39
- keratins of, 1–65
- LAH with, 57
- medulla with, 41, 49–51, 52, 53, 54
 - biochemical analyses of, 51
 - electron microscopic studies of, 51
 - IIF studies of, 51
 - K17 in, 51
 - keratin pathologies of, 55–60
 - morphology of, 51
 - regulatory processes in, 60–62
 - X-ray studies of, 51
- nomenclature of, 64–65
- ORS with, 3, 40–43, 44, 54
 - CL and, 42–43
 - EGFP studies on, 42
 - epithelial keratins of, 39–42, 44, 54
 - K6 in, 41–42
 - K15 in, 42
 - K17 in, 41–42
 - K19 in, 42
 - keratin pathologies of, 55–60
 - mouse v. human, 42
- outlook for, 62–65
- pathologies of, 18–26
- PFB with, 57, 58–59
- pilomatricoma with, 23–26
 - histopathological classification and, 25
 - malignant, 26
 - transcription factors and, 24
- regulatory process in, 60–62
 - CDP with, 60–61, 62
 - FOG1 with, 61
 - GATA-3 with, 61–62
 - HDR with, 61
- sexual, 52–53
 - hHa7 in, 52–53
 - K6hf in, 52–53
 - K17 in, 52–53
- tissue differentiation with, 53, 54
- tumors with, 23–26
 - basal cell carcinomas as, 25
 - desmoplastic trichoepitheliomas as, 25
 - pilomatricomas as, 23–26
 - trichoblastomas as, 25
 - trichoepitheliomas as, 25
- type I keratin gene with, 4–7, 8, 9–18, 28, 62–65
 - catalog of, 17–18
 - disease-related mutations in, 21
 - excess over type II of, 18
 - expression characteristics of, 7–16
 - foxn1 gene and, 29
 - gene clusters of, 6, 7
 - IRS having, 46
 - keratogenous zone of, 16
 - nomenclature of, 4–5, 64–65
- type II keratin gene with, 4–7, 9–18, 19–20, 43, 62–65
 - catalog of, 17–18
 - CL having, 43
 - excess of type I over, 18
 - expression characteristics of, 7–16
 - gene clusters of, 6, 7
 - HIM encoded in, 20
 - HTM encoded in, 20
 - keratogenous zone of, 16
 - monilethrix linked to, 19–20
 - nomenclature of, 4–5, 64–65
- HAT. *see* Histone acetyltransferases
- HCN channels. *see* Hyperpolarization-activated and cyclic nucleotide-gated channels
- HDAC. *see* Histone deacetylases
- HDR. *see* Hypoparathyroidism, deafness, and renal dysplasia syndrome
- Helix initiation motif (HIM), type II keratin gene encoding of, 20
- Helix termination motif (HTM), type II keratin gene encoding of, 20
- Henle layers
 - epithelial keratins of, 40–41, 44, 46–49
 - Flügelzellen* with, 48–49
 - IRS with, 3, 40–41, 44, 46–49
- Hepatocyte growth factor (HGF)
 - EMT with, 322
 - urokinase regulated by, 321–322
- Heregulins, cardiac cushion development growth factors of, 309
- hfh11*. *see* Forkhead box n1 gene
- HGF. *see* Hepatocyte growth factor
- HGNC. *see* Hugo Gene Nomenclature Committee

- hHa7
 hair keratin expression regulation of, 33–37
 sexual hairs, 52
- High voltage-activated channels (HVA channels), sperm physiology with, 86, 89
- HIM. *see* Helix initiation motif
- Histone acetyltransferases (HAT), genomic imprinting with, 202
- Histone deacetylases (HDAC), genomic imprinting with, 202
- Histone methyltransferases (HMTase), genomic imprinting with, 202
- HMTase. *see* Histone methyltransferases
- HOXC13, hair keratin expression regulation of, 30–33, 38–39
- HSS. *see* Hypotrichosis simplex of scalp
- HTM. *see* Helix termination motif
- Hugo Gene Nomenclature Committee (HGNC), 64–65
- Huxley layers
 epithelial keratins of, 39–41, 44, 45–49
Flügelzellen in, 48–49
 IRS with, 3, 40–41, 44, 46–49
 mK6irs in, 47
- HVA channels. *see* High voltage-activated channels
- Hyaluronan (HA), cardiac cushion development ECM with, 318–319
- Hyperpolarization-activated and cyclic nucleotide-gated channels (HCN channels), sperm ion channel studies with, 104
- Hypoparathyroidism, deafness, and renal dysplasia syndrome (HDR), hair follicle regulatory process with, 61
- Hypotrichosis simplex of scalp (HSS), keratin pathologies with, 56, 59
- I**
- Ictalurus punctatus*, fish IGF in, 228
- IGF. *see* Insulin-like growth factor
- Igf2r*, genomic imprinting in, 179, 186, 187, 188, 189, 190, 193–194, 199, 205–206
- IGFBP. *see* Insulin-like growth factor-binding proteins
- ILA. *see* Insulin-like activity
- In situ hybridization (ISH), human hair keratin gene family with, 7, 8
- Indirect immunofluorescence (IIF)
 CL studied with, 43, 44
 human hair keratin gene family studied with, 7, 8, 14, 16
 medulla studied with, 51
- Ingrown hairs. *see* Pseudofolliculitis barbae
- Inner root sheath (IRS), 2–3
 CL with, 3
 cuticle of, 3, 40
 epithelial keratins of, 39–41, 44, 45–49, 54
Flügelzellen in, 48–49
 Henle layers of, 3, 40–41, 44, 46–49
 Huxley layers of, 3, 40–41, 44, 46–49
 IIF studies for, 44, 49
 keratin pathologies of, 55–60
 mK6irs in, 46–47, 57
 regulatory processes in, 60–62
 type I keratin gene in, 46
- Insulin-like activity (ILA), IGF background with, 217
- Insulin-like growth factor (IGF)
 binding proteins of, 216, 223–225, 227–228, 249–254
 biochemical evidence of, 249
 biochemical properties of, 250–251
 expression of, 251–252
 general background on, 216, 223–225, 224, 227–228
 hormonal regulation of, 253
 localization of, 251–252
 metabolic status of, 253–254
 primary structures of, 250
 regulation of, 252–254
 biological actions on fish of, 254–263
 cartilage sulfation in, 255–256
 cell proliferation in, 256
 DNA synthesis in, 256
 embryonic development in, 257–259
 growth in, 254–257
 hormone production with, 261–262
 IGF-1 receptors within, 258
 IGFBP-1 within, 258–259
 IGFBP-2 within, 259
 IGFBP-5 within, 259
 oocyte maturation with, 262–263
 osmoregulation with, 260
 protein synthesis from, 257
 evolutionary origins of, 226–228, 227
 fish with, 215, 225–226, 228–244

- Anguilla japonica*, 226
 evidence of, 225–226
 general background on, 215, 225–226
 GH regulation in, 235–238, 243–244
 IGF-1, 228–240
 IGF-1 agnathans, 229–230
 IGF-1 development in, 239
 IGF-1 elasmobranchs, 229
 IGF-1 environment in, 240
 IGF-1 expression patterns in, 232–235
 IGF-1 expression regulation in, 235–240
 IGF-1 genes in, 230–232, 321
 IGF-1 primary structure in, 228–230
 IGF-1 protein in, 234–235
 IGF-1 teleost, 228–229
 IGF-1 with hormones in, 235–238
 IGF-1 with mRNA in, 230–232, 233–234
 IGF-1 with nutrition in, 238–239
 IGF-2 expression patterns in, 242–243
 IGF-2 expression regulation in, 243–244
 IGF-2 genes in, 241–242
 IGF-2 in, 240–244
 IGF-2 nutrition in, 244
 IGF-2 primary structure in, 240–241
 IGF-2 with hormones in, 243–244
 IGF-2 with mRNA in, 241–242
 Japanese eel, 226
Oncorhynchus mykiss, 226
 rainbow trout, 226
 general background on, 216–228
 ALS in, 219
 EGF in, 217
 evolution in, 226–228
 fetal growth regulation in, 220
 GH in, 216–217, 219
 IGF discovery in, 216–218
 IGF signaling in, 227
 IGF synthesis in, 219
 IGFBP in, 216, 223–225, 227–228
 IRS in, 221, 222
 mammalian binding proteins in, 223–225
 mammalian ligands in, 218–221
 mammalian receptors in, 221–223
 mammals in, 218–225
 MAPK in, 221
 mouse dwarfism in, 218
 MSA in, 217, 218
 severe growth-retarded phenotype in, 218
 SM in, 217, 218
 sulfation factor in, 217
 type I receptors in, 221–222
 type II receptors in, 222–223
 introduction to, 215–216
 MPR with, 248
 receptors of, 244–249, 246
 signaling in fish with, 215–265
 somatomedin hypothesis with, 215–216, 264
 summary of signaling in fish with, 263–265
 type I receptors of, 244–248
 expression with, 247–248
 primary structure for, 245–246
 regulation with, 247–248
 signal transduction pathways with, 246–247
 type II receptors of, 248–249
 Insulin-like growth factor-binding proteins (IGFBP)
 biochemical evidence of, 249
 biochemical properties of, 250–251
 evolutionary origins of, 227–228
 expression of, 251–252
 fish with, 249–254
 general background with, 216, 223–225, 227–228
 hormonal regulation of, 253
 localization of, 251–252
 metabolic status of, 253–254
 primary structures of, 250
 regulation of, 252–254
 Insulin-receptor substrate (IRS), IGF
 background with, 221
 Ion-sensitive fluorescent dyes, sperm ion channel studies with, 101
 IP₃R release channels, sperm physiology with, 96–97
 IRS. *see* Inner root sheath; Insulin-receptor substrate
 ISH. *see* In situ hybridization
- J**
- Japanese flounder, fish IGF in, 228
- K**
- K6, ORS with, 41–42
 K6hf
 CL with, 43–45

- K6hf (*continued*)
 gene defect of, 57, 58
 sexual hairs, 52
- K15, ORS with, 42
- K16, CL with, 43, 44
- K17
 CL with, 43–45
 medulla with, 51
 ORS with, 41–42
 sexual hairs, 52
- K19, ORS with, 42
- KAP. *see* Keratin-associated proteins
- Kcnq1*, genomic imprinting in,
 179, 187, 188, 189, 190, 194
- Keratin-associated proteins (KAP), hair
 keratin expression regulation of, 30
- Keratins
 alopecia and, 56
 cell fate determination with, 53, 54
 concluding remarks on, 62–65
 EBS and, 55
 epithelial, 39–53
 expression regulation of, 26–39
 androgen receptor in, 33–37
 BMP signaling in, 38–39
 β -catenin in, 29–30
foxn1 gene in, 27–29
hHa7 in, 33–37
HOXC13 in, 30–33, 38–39
 KAP with, 30
LEF1 in, 29–30, 33, 38–39
Meis in, 33
nude mice and, 27–29
Pbx in, 33
Prep in, 33
 synopsis for, 37–39
 TALE in, 33
 Wnt signaling with, 29–30, 39
 hair follicle CL with, 3, 41, 42–45, 54
 epithelial keratins of, 41, 42–45, 54
 IIF studies for, 43, 44
 K6hf in, 43–46, 57
 K16 in, 43, 44
 K17 in, 43–46
 keratin pathologies of, 55–60
 ORS and, 41–42
 regulatory processes in, 60–62
 type II keratin gene with, 43
 hair follicle IRS with, 2–3, 40–41,
 44, 45–49, 54
 cuticle of, 3, 40
 epithelial keratins of, 39–41, 44,
 45–49, 54
Flügelzellen in, 48–49
 Henle layers of, 3, 40–41, 44, 46–49
 Huxley layers of, 3, 40, 46–49
 IIF studies for, 44, 49
 keratin pathologies of, 55–60
 mK6irs in, 46–47, 57
 regulatory processes in, 60–62
 type I keratin gene in, 46
 hair follicles with, 1–65
 hereditary disorders of,
 18–23, 20, 55–56
 41-kDa protein in, 22
 gene mutation leading to, 55–56
 monilethrix as, 19–22
 mutations involved in, 20
pili annulati as, 19
pili trianguli et canaliculari as, 19
 spun glass hair as, 19
 truncated hair keratin hHa1-t in, 22–23
 uncombable hair as, 19
 woolly hair as, 19
 HSS and, 56, 59
 human hair gene family of, 4–18
 catalog listing, 16–18
 expression characteristics with, 7–16
 IIF studies with, 7, 8, 14, 16
 ISH with, 7, 8
 nail keratin and, 13–16
 physical organization in, 5–7
 pseudogenes with, 5–6, 11
 introduction to, 1–4
 LAH with, 57
 medulla with, 41, 49–51, 52, 53, 54
 biochemical analyses of, 51
 electron microscopic studies of, 51
 IIF studies of, 51
 K17 in, 51
 keratin pathologies of, 55–60
 morphology of, 51
 regulatory processes in, 60–62
 X-ray studies of, 51
 nomenclature of, 64–65
 ORS with, 3, 40–43, 44, 54
 CL and, 42–43
 EGFP studies on, 42
 epithelial keratins of, 39–43, 44, 54
 K6 in, 41–42
 K15 in, 42
 K17 in, 41–42

K19 in, 42
 keratin pathologies of, 55–60
 mouse v. human, 42
 outlook for, 62–65
 pathologies of, 18–26
 PFB with, 57, 58–59
 pilomatricoma with, 23–26
 histopathological classification and, 25
 malignant, 26
 transcription factors and, 24
 regulatory process in, 60–62
 CDP with, 60–61, 62
 FOG1 with, 61
 GATA-3 with, 61–62
 HDR with, 61
 sexual, 52–53
 hHa7 in, 52–53
 K6hf in, 52–53
 K17 in, 52–53
 tissue differentiation with, 53, 54
 tumors with, 23–26
 basal cell carcinomas as, 25
 desmoplastic trichoepitheliomas as, 25
 pilomatricomas as, 23–26
 trichoblastomas as, 25
 trichoepitheliomas as, 25
 type I gene, 4–7, 8, 9–18, 28, 62–65
 catalog of, 17–18
 disease-related mutations in, 21
 excess over type II of, 18
 expression characteristics of,
 7–16
 foxn1 gene and, 29
 gene clusters of, 6, 7
 IRS having, 46
 keratogenous zone of, 16
 nomenclature of, 4–5, 64–65
 type II gene, 4–7, 9–18, 19–20,
 43, 62–65, 64
 catalog of, 17–18
 CL having, 43
 excess of type I over, 18
 expression characteristics of, 7–16
 gene clusters of, 6, 7
 HIM encoded in, 20
 HTM encoded in, 20
 keratogenous zone of, 16
 monilethrix linked to, 19–20
 nomenclature of, 4–5, 64–65
 Keratogenous zone, nails with, 15–16
 Korean rockfish, fish IGF in, 228

L

LAH. *see* Loose anagen hair syndrome
 LAP. *see* Latency-associated peptide
 Latency-associated peptide (LAP), TGF- β
 with, 301
Lates calcarifer, fish IGF in, 228
 LEF1, hair keratin expression regulation of,
 29–30, 33, 38–39
 Long terminal repeat (LTR), genomic
 imprinting sequences with, 198, 200
 Loose anagen hair syndrome (LAH), keratin
 pathologies with, 57
 Low voltage-activated channels (LVA
 channels), sperm physiology with,
 86, 89, 90
 LTBP. *see* TGF- β binding protein
 LTR. *see* Long terminal repeat
 LVA channels. *see* Low voltage-activated
 channels

M

Mannose 6-phosphate receptors (MPR), IGF
 receptors with, 248
 MAPK. *see* Mitogen-activated protein kinase
 Matrix metalloproteinase 2 (MMP)
 cardiac cushion development ECM with,
 320–321
 EMT with, 323
 Medulla
 biochemical analyses of, 51
 electron microscopic studies of, 51
 hair follicle with, 41, 49–51, 52, 53, 54
 IIF studies of, 51
 K17 in, 51
 keratin pathologies of, 55–60
 morphology of, 51
 regulatory processes in, 60–62
 X-ray studies of, 51
Megalobrama amblycephala, fish IGF in, 228
Megalobrama terminalis, fish IGF in, 228
 Meiosis, 81
 Meis, hair keratin expression regulation of, 33
 Membrane hyperpolarization, sperm motility
 with, 112
 Mesenchymal cell, cardiac cushion
 development with, 294–295
 Microtubules, sperm physiology with, 83
 Mitochondria, sperm physiology with, 82, 83

Mitogen-activated protein kinase (MAPK), IGF background with, 221

mK6irs, hair follicle IRS with, 46–47

MMP. *see* Matrix metalloproteinase 2

Monilethrix

- hair follicle disorders of, 19–22, 20
- mutations involved in, 20

Mouse

- BMP in, 305–307
- DNA methylation in development of, 181
- dwarfism in, 218
- genetic experiments in, 187–191
- genomic imprinting in, 174–175
- hair keratin expression regulation in, 26–29
- hair keratin expression regulation of, 26–29
- human ORS v., 42
- IGF in, 218
- nude*, 27–29
- Snrpn* in, 192
- sperm capacitation with, 122–123
- TGF- β in, 300–301
- transgenes in study of, 197–199
 - RSVlgmye*, 198–199

MPR. *see* Mannose 6-phosphate receptors

MSA. *see* Multiplication-stimulating

Mud carp, fish IGF in, 228

Multiplication-stimulating (MSA), IGF background with, 217, 218

Myxine glutinosa, fish IGF in, 229

N

Nail plate, 15

Nails

- apical matrix of, 13, 15
- histology of, 15
- human hair keratin gene family and, 13–16
- keratogenous zone of, 15–16
- nail plate of, 15
- ventral matrix of, 13, 15

N-CAM. *see* Neural cell adhesion molecule

Necklace hair. *see* Monilethrix

Neural cell adhesion molecule (N-CAM), cardiac cushion development with, 294

Neuregulins. *see* Heregulins

NF-1, cardiac cushion development with, 313–314

NFATc. *see* Nuclear factor of activated T cells

Nkx2.5, cardiac cushion development with, 316–317

Notch

- cardiac cushion development with, 311–312
- EMT with, 322

Nuclear factor of activated T cells (NFATc), cardiac cushion development with, 313

Nude mice

- hair keratin expression regulation and, 26–29
- hair keratin expression regulation of, 26–29

O

Oncorhynchus keta, fish IGF in, 228

Oncorhynchus kisutch, fish IGF in, 228

Oncorhynchus masou ishikawai, fish IGF in, 238

Oncorhynchus mykiss, fish IGF in, 226

Oncorhynchus tshawytscha, fish IGF in, 228

Orange-spotted grouper, fish IGF in, 228

Oreochromis mossambicus, fish IGF in, 228

ORS. *see* Outer root sheath

Outer root sheath (ORS), 3, 40–42, 44, 54

- CL with, 42–43
- EGFP studies on, 42
- epithelial keratins of, 39–43, 44, 54
- K6 in, 41–42
- K15 in, 42
- K17 in, 41–42
- K19 in, 42
- keratin pathologies of, 55–60
- mouse v. human, 42

P

PAF. *see* Platelet-activating factor

Paralichthys olivaceus, fish IGF in, 228

Patch-clamp studies

- calcium/Ca²⁺ channels in, 89, 102
- sperm ion channel studies with, 102, 106

Pbx, hair keratin expression regulation of, 33

PcG. *see* Polycomb group

PECAM-1. *see* Platelet endothelial cell adhesion molecule 1

Peg3, genomic imprinting in, 179, 180, 189

Perca flavescens, fish IGF in, 228

Perca fluviatilis, fish IGF in, 228

Petromyzon marinus, fish IGF in, 229

PFB. *see* Pseudofolliculitis barbae

PGC. *see* Primordial germ cells
Pili annulati, hair follicle disorders of, 19
Pili incarnati. see Pseudofolliculitis barbae
Pili trianguli et canaliculi, hair follicle disorders of, 19
 Pilomatricomas, hair follicle-derived tumors of, 23–26
 Pitx2, cardiac cushion development with, 317
 Planar bilayers, sperm ion channel studies with, 104–106
 BLM in, 105
 vesicle fusion strategy in, 105
 Plasmin, cardiac cushion development ECM with, 321–322
 Platelet endothelial cell adhesion molecule 1 (PECAM-1), cardiac cushion development with, 294
 Platelet-activating factor (PAF), acrosome reaction with, 130
 Polycomb group (PcG), genomic imprinting with, 204–205
 Prader-Willi syndrome (PWS), genomic imprinting region of, 185
 Prader-Willi syndrome-imprinting center (PWS-IC), genomic imprinting with, 185
 Prep, hair keratin expression regulation of, 33
 Primordial germ cells (PGC), genomic imprinting in, 176
 Progesterone, acrosome reaction with, 130, 131, 136, 139, 140
 Proteomics, sperm ion channel studies with, 108–109
 Pseudofolliculitis barbae (PFB), keratin pathologies with, 57, 58–59
 PWS. *see* Prader-Willi syndrome
 PWS-IC. *see* Prader-Willi syndrome-imprinting center

R

Rabbit fish, fish IGF in, 228
 Rainbow trout, fish IGF in, 226
 Receptor-operated theory, TRP channels with, 92
 RER. *see* Rough endoplasmic reticulum
 Reverse transcription-polymerase chain reaction (RT-PCR), TGF- β with, 300
 Rough endoplasmic reticulum (RER), cardiac cushion development with, 294

Rous sarcoma virus (RSV), genomic imprinting with, 198
 RSV. *see* Rous sarcoma virus
RSVlgmye, 198–199
 RT-PCR. *see* Reverse transcription-polymerase chain reaction
 RyR release channels, sperm physiology with, 96–98

S

S. purpuratus. see *Strongylocentrotus purpuratus*
Salmo salar, fish IGF in, 228
 SAP. *see* Sperm-activating peptides
 Scanning electron microscopy (SEM), cardiac cushion development in, 294
 Scanning ion conductance microscopy (SICM), sperm ion channel studies with, 106
 Sea lamprey, fish IGF in, 229
 Sea urchin sperm receptors for egg jelly (suREJ), acrosome reaction with, 126–127
Sebastes schlegeli, fish IGF in, 228
 SEM. *see* Scanning electron microscopy
 Shp-2
 cardiac cushion development growth factors of, 309–310
 cardiac cushion development with, 309–310
 SICM. *see* Scanning ion conductance microscopy
Siganus guttatus, fish IGF in, 228
 Silver perch, fish IGF in, 237
 SM. *see* Somatomedin
 Smart patch clamp, sperm ion channel studies with, 106–107
 SNARE. *see* Soluble N-ethylmaleimide-sensitive attachment protein receptors
Snrpn, genomic imprinting in, 179, 180, 187, 188, 189, 193, 205
 Soluble N-ethylmaleimide-sensitive attachment protein receptors (SNARE), acrosome reaction with, 124, 125, 126
 Somatomedin (SM), IGF background with, 217, 218
 Southern bluefin tuna, fish IGF in, 237
 Sox-9, cardiac cushion development with, 314–315
Sparus aurata, fish IGF in, 228

- Speract signaling, sperm motility with, 111–112
- Sperm physiology, 79–174
- acrosome reaction with, 124–137
 - Asterias amurensis*, 125
 - ATP induction of, 130
 - Echinometra lucunter*, 125
 - EGF induction of, 130
 - FSP in, 125–126, 128
 - GABA induction of, 130
 - mammalian sperm, 130–137
 - marine sperm, 124–130
 - PAF induction of, 130
 - progesterone induction of, 130, 131, 136, 139, 140
 - S. purpuratus*, 126
 - slow sustained $[Ca^{2+}]_i$ elevation in, 135–137
 - SNARE proteins needed for, 124, 125, 126
 - suREJ in, 126–127
 - transient increase in $[Ca^{2+}]_i$ in, 133–135
 - ZP mediation of, 130–131, 133–137, 139, 140
 - alternative ion channel studies for, 101–109
 - antisense knockdown methods in, 102
 - BLM in, 105
 - DHP in, 103
 - ES cells in, 108
 - HCN channels in, 104
 - invertebrate toxins in, 104
 - ion-sensitive fluorescent dyes in, 101
 - L-type currents in, 103
 - other techniques in, 107–109
 - patch-clamp studies in, 102, 106
 - planar bilayers in, 104–106
 - proteomics in, 108–109
 - SICM in, 102, 106
 - smart patch clamp in, 106–107
 - spermatogenic cells in, 101–104
 - T-type currents in, 103, 104
 - vesicle fusion strategy in, 105
 - basic characteristics of, 82, 83
 - axoneme in, 82, 83
 - Ca^{2+} channel distribution in, 82
 - flagellum in, 82, 83
 - head in, 82, 83
 - microtubules in, 83
 - mitochondria in, 82, 83
 - calcium/ Ca^{2+} channels in, 83–109, 87, 88, 94–95
 - Ca^{2+} release channels as, 96–98
 - CatSper channels as, 87, 94–95, 99–100
 - $Ca_v1/Ca_v2/Ca_v3$ channels as, 88, 89–91, 94
 - Ciona intestinalis* with, 100
 - CNG channels as, 87, 94–95, 98–99
 - DHP sensitivity of, 88, 89–90
 - Drosophila* with, 91–92
 - HVA channels as, 86, 89
 - IP_3R release channels as, 96–97
 - LVA channels as, 86, 89, 90
 - patch-clamp studies on, 89
 - protein kinase phosphorylation with, 90
 - regulatory pathways with, 90
 - RyR release channels as, 96–98
 - synaptotagmin associated with, 91
 - syntaxin associated with, 91
 - TRP channels as, 87, 91–96
 - voltage-gated Ca^{2+} channels as, 86–91, 94–95
 - Xenopus* with, 99
 - calcium's role in
 - Ca^{2+} intracellular messaging with, 83–84
 - calreticulin regulating, 84
 - calsequestrin regulating, 84
 - CaM regulating, 84
 - cellular ion gradient with, 85
 - EF hand proteins regulating, 84
 - membrane transporters regulating, 85
 - Mg^{2+} v., 84
 - regulation of cell function by, 83–84
 - sensor proteins regulating, 84
 - troponin C regulating, 84
 - concluding remarks on, 141–142
 - general background on, 79–83
 - intracellular signaling events in, 137–138
 - introduction to, 79
 - single-cell measurements in, 137–141
 - $[Ca^{2+}]_i$ fluctuations in, 140–141
 - cell populations v., 137–138
 - source-sink diffusion model from, 141
 - Strongylocentrotus purpuratus* with, 138
 - sperm capacitation with, 120–124
 - hyperpolarization in, 122, 123
 - mammalian, 121–122
 - molecular mechanisms in, 120
 - mouse, 122–123
 - signaling model for, 121–122
 - unanswered questions about, 123–124

- sperm motility with, 109–120
 - Arbacia punctulata* having, 112, 114
 - bracken fern sperm with, 110
 - chemoattractant compounds with, 110–114
 - chemotaxis in, 110–114, 117–120
 - hyperactivation in, 115–117
 - mammalian, 114–115, 117–120
 - marine, 109–110
 - membrane hyperpolarization with, 112
 - SAP with, 111–114
 - speract signaling with, 111–112
 - SpHCN activated in, 112–113
 - Strongylocentrotus purpuratus* having, 111, 113
 - two roles of Ca^{2+} in, 109
 - spermatogenesis with, 79–83
 - three phases of, 81
 - Sperm-activating peptides (SAP), sperm motility with, 111–114
 - Spermatocytogenesis, 81
 - Spermatogenesis, 79–83
 - DNA methylation with, 182
 - mammals with, 81
 - three phases of, 81
 - meiosis in, 81
 - spermatocytogenesis in, 81
 - spermiogenesis in, 81
 - Spermatogenic cells
 - HCN channels with, 104
 - invertebrate toxins studies for, 104
 - L-type currents with, 103
 - mammalian testes with, 102
 - sperm ion channel studies with, 101–104
 - T-type currents with, 103, 104
 - Spermiogenesis, 81
 - SpHCN channel, sperm motility with, 112–113
 - Spun glass hair, hair follicle disorders of, 19
 - Store-operated Ca^{2+} entry theory, TRP channels with, 93
 - Strongylocentrotus purpuratus*
 - acrosome reaction with, 126
 - intracellular signaling events in, 138
 - SAP with, 111, 113
 - suREJ. *see* Sea urchin sperm receptors for egg jelly
 - Synaptotagmin, Ca_v2 associated with, 91
 - Syntaxin, Ca_v2 associated with, 91
- ## T
- TALE. *see* Three amino acid loop extension
 - TBX-5, cardiac cushion development with, 315
 - TGF- β . *see* Transforming growth factor β
 - TGF- β binding protein (LTBP), TGF- β with, 301
 - Three amino acid loop extension (TALE), hair keratin expression regulation of, 33
 - Thunnus maccoyii*, fish IGF in, 237
 - Tilapia, fish IGF in, 228
 - Tissue differentiation, hair follicle, 53, 54
 - Transforming growth factor β (TGF- β)
 - Annexin II with, 301
 - antisense oligonucleotides against, 299
 - cardiac cushion development with, 298–305
 - EMT induction with, 299
 - EMT with, 322
 - endoglin with, 304–305
 - function-blocking antibodies against, 299
 - LAP with, 301
 - ligand activation with, 301
 - LTBP with, 301
 - mouse with, 300–301
 - RT-PCR with, 300
 - signaling with, 304, 306
 - Transient receptor potential channels (TRP channels)
 - activation of, 92
 - cell sensory theory of, 92
 - CIF with, 93
 - Drosophila* with, 91–92
 - emptying Ca^{2+} stores in, 93
 - functions of, 92, 93
 - receptor-operated theory of, 92
 - sperm physiology with, 87, 91–96
 - store-operated Ca^{2+} entry theory of, 93
 - structure of, 92
 - Triangular bream, fish IGF in, 228
 - Trichoblastomas, hair follicle-derived tumors of, 25
 - Trichoepitheliomas, hair follicle-derived tumors of, 25
 - Trithorax group (TrxG), genomic imprinting with, 204

TRP channels. *see* Transient receptor potential channels
 TrxG. *see* Trithorax group
 Turbot, fish IGF in, 228

U

Uncombable hair, hair follicle disorders of, 19
 Urokinase
 cardiac cushion development ECM with, 321–322
 HGF regulation of, 321–322

V

Vascular endothelial growth factor (VEGF), cardiac cushion development with, 312–313
 Vascular endothelium (VE), cardiac cushion development with, 294
 VEGF. *see* Vascular endothelial growth factor
 Ventral matrix, nails with, 13, 15
 Voltage-gated Ca^{2+} channels
 $\text{Ca}_v1\text{Ca}_v2/\text{Ca}_v3$ channels as, 88, 89–91, 94
 DHP sensitivity of, 88, 89–90
 HVA channels as, 86, 89
 LVA channels as, 86, 89, 90
 patch-clamp studies on, 89
 protein kinase phosphorylation with, 90
 regulatory pathways with, 90
 sperm physiology with, 86–91, 94–95
 synaptotagmin associated with, 91
 syntaxin associated with, 91

W

whn. *see* Forkhead box n1 gene
 Winged-helix-nude. *see* Forkhead box n1 gene
 Wnts
 cardiac cushion development with, 291, 310–311
 EMT with, 322
 hair keratin expression regulation of, 29–30, 39
 signaling, 29–30, 39
 Woolly hair, hair follicle disorders of, 19

X

Xenopus, CatSper channels with, 99
 X-ray, medulla studied with, 51

Y

Yellow perch, fish IGF in, 228

Z

Zebrafish
 fish IGF in, 228, 245, 246
 IGF structure in, 245, 246
 ZP
 acrosome reaction with, 130–131, 133–137, 139, 140
 slow sustained $[\text{CA}^{2+}]_i$ elevation induced by, 135–137
 transient increase in $[\text{CA}^{2+}]_i$ induced by, 133–135